Agricultural landscape structure and biological control

Patrizia Zamberletti

THÈSE DE DOCTORAT D'AVIGNON UNIVERSITÉ

École Doctorale 536
Agrosciences et sciences

Mention de doctorat :
Biologie des populations et écologie

Unité Biostatistique et Processus Spatiaux (BioSP)- INRAE

Présentée par
Patrizia Zamberletti

STRUCTURE DU PAYSAGE AGRICOLE ET REGULATION DES RAVAGEURS

EFFET DE L'HÉTÉROGÉNÉITÉ SPATIALE DU PAYSAGE SUR LA DYNAMIQUE ÉCO-ÉVOLUTIVE D'UN SYSTÈME PRÉDATEUR-PROIE.

Soutenue publiquement le 26/11/2021 devant le jury composé de :

Frédéric Hamelin, Maître de Conférences Hors-Classe (HDR), Agrocampus-ouest, Rennes, **Rapporteur**
Kerstin Wiegand, Professor, Department of Ecosystem Modelling, University of Göttingen, **Rapporteure**
Janine Illian, Professor, School of Mathematics and Statistics, Glasgow, **Examinatrice**
Manuel Plantegenest, Professor, Agrocampus-ouest, Rennes, **Examinateur**
Edith Gabriel, Directrice de recherche, BioSP, INRAE, Avignon **Directrice de thèse**
Thomas Opitz, Chargé de recherche (HDR), BioSP, INRAE, Avignon **Co-directeur de thèse**
Julien Papaïx, Chargé de recherche, BioSP, INRAE, Avignon **Co-directeur de thèse**

Résumé

La structure du paysage agricole est définie par l'hétérogénéité spatiale de la mosaïque de parcelles cultivées et de la matrice des habitats naturels. L'oragnisation spatiale des parcelles influence fortement le fonctionnement des agro-écosystèmes en déterminant les ressources disponibles, la diversité des espèces et les interactions entre le milieu cultivé et les espaces naturels. En particulier, la structure des habitats naturels et semi-naturels peut favoriser un ensemble de services écosystémiques, tels que la lutte biologique contre les ravageurs. Si la complexité paysagère est souvent associée à une plus forte régulation des ravageurs des cultures, cette relation peut être aussi ambiguë. Les habitats semi-naturels favorisent la présence et la diversité des espèces auxiliaires mais n'induisent pas forcément par un meilleur service de régulation. En effet, les espèces auxiliaires diffèrent dans leur cycle de vie, leurs comportements et leurs stratégies de prédation, s'influençant mutuellement de manière positive ou négative. Dans le cadre de cette thèse, nous approfondissons différents aspects de la complexité du paysage et des interactions entre espèces afin de mieux comprendre leurs effets sur le contrôle biologique.

Dans une première partie nous abordons la question de la représentation de paysages agricoles réels pour permettre l'analyse structurelle du paysage et la génération de scénarios paysagers. Nous développons des outils statistiques pour représenter des paysages composés d'éléments surfaciques et linéaires. En particulier, nous nous intéressons à la distribution des catégories d'occupation du sol. Nous proposons une méthode de validation des modèles reposant sur un ensemble de métriques paysagères et nous développons un outil permettant la simulation de paysages agricoles. Les données paysagères proviennent de la basse vallée de la Durance (France). Dans une deuxième partie, nous définissons, sur les paysages simulés, un modèle proie-prédateur décrivant la dynamique de ravageurs et d'auxiliaires. Le modèle est spatialement explicite, il considère la dispersion des organismes à la fois dans les parcelles et le long des haies, ainsi que de potentiels traitements phytosanitaires. Nous démontrons que l'hétérogénéité spatiale du paysage et les traits d'histoire de vie du ravageur et de son auxiliaire jouent conjointement un rôle clé dans l'efficacité du service de contrôle du ravageur. Nous ne limitons pas notre analyse à l'échelle globale mais nous proposons aussi une nouvelle méthode pour étudier la dynamique du système à plusieurs échelles. Plus précisément, nous définissons un processus

ponctuel spatio-temporel comme méta-modèle pour étudier le lien entre la dynamique localisée des pullulations de ravageur et les caractéristiques du paysage à différentes échelles spatiales. Enfin, dans une troisième partie, nous étendons nos recherches aux aspects évolutifs en abordant deux questions. Dans une première nous étudions comment l'hétérogénéité environnementale influence la structure phénotypique d'une population dont les traits de dispersion et de croissance sont soumis à un compromis évolutif. Ce travail est basé sur un modèle de type paysage adaptatif et nous nous attachons à caractériser de façon analytique les équilibres du système. La seconde question consiste à étudier comment la présence de prédateurs, en interaction avec la structure du paysage, modifie les réponses comportementales de la proie. Pour ce faire nous complexifions le modèle développé dans la deuxième partie pour une système avec plusieurs espèces.

Dans cette thèse nous explorons et intégrons différentes échelles spatio-temporelles (éléments linéaires et surfaciques, échelles globales et locales, évolution temporelle des ravageurs et des prédateurs) et différents niveaux de biodiversité (multi-espèces, diversité comportementale et diversité génétique). De cette manière, nous enrichissons les connaissances existantes en soulignant la nécessité de méthodes intégratrices afin de mieux évaluer en quoi la complexité des paysages agricoles impacte les différentes facettes de la biodiversité.

Abstract

Agricultural landscape structure is defined by the heterogeneity arising from a mosaic of cultivated patches within a natural matrix. The spatial arrangement of these agricultural habitats strongly influences ecosystem functioning and, therefore, determines environmental resources, species diversity and interactions. Specifically, the amount and the organisation of natural and semi-natural habitats can promote a bundle of desired ecosystem services, such as biological pest control. However, the relationships among desired effects and landscape complexity can be ambiguous. Even if semi-natural area favours natural enemy species presence and diversity, this might not be directly translated into a profitable advantage for natural pest suppression. The reason is that enemy species differ in their life-cycle, their behaviours and predating strategy, influencing each other in positive or negative ways. In this thesis, we deepen various aspects of the landscape complexity, population dynamics and their relationships to better understand the effect on conservation biological control.

Firstly, we deal with the representation of real agricultural landscapes to allow for landscape structural analysis and scenario generation. We develop statistical tools to represent real landscapes composed by patches and linear elements, to capture the distribution of landscape features, and to simulate land-use category allocation. We estimate model parameters for sub-regions of the Lower Durance Valley (France), validate the model based on a diversity of landscape metrics and implement simulations of agricultural scenarios. Secondly, we couple landscape generation with population dynamics based on the landscape model through a spatially explicit predator-pest model taking into account pesticide applications, which are employed when biological control through predator efforts is not enough. We demonstrate that spatial heterogeneity, species traits and their interactions jointly play a key role for biological control outcomes. Since we recognise that integration of species traits with landscape structure at multiple scales are needed, and that the output aggregation over time and space cause information loss, we do not limit our analysis to the global scale. We propose a more parsimonious representation to take into account all the relevant information of spatially-explicit outputs to fully characterise spatio-temporal pest-predator dynamics. Specifically, we recur to meta-models based on spatio-temporal point processes. Through this multi-scale approach, we gain insights on both local and global

spatio-temporal dynamics of predator-pest systems. Finally, we extend our analyses to the assessment of genetic diversity and behavioural strategies to better represent species adaptation to different drivers like environmental conditions and different predating pressure.

During this thesis, we explore and integrate different spatio-temporal ranges (*i.e.*, linear and areal landscape elements, global and local scales, temporal pest and predator evolution) and different biodiversity levels (multi-species, behavioural diversity and genetic diversity). By focusing on different perspectives, we enrich the existing knowledge and highlight the necessity of more integrated methods and efforts to better account for the various important dimensions of biodiversity, jointly with agricultural landscape complexity.

Acknowledgements

I am deeply grateful to all members of the jury for agreeing to read the manuscript and to participate in the defense of this thesis.

I wish to express my sincere gratitude to my supervisors: Edith Gabriel, Thomas Opitz and Julien Papaïx. They guided and encouraged me through all the thesis. Without their persistent help, invaluable expertise and support, this work of thesis would not have been of such high level. Their insightful feedback pushed me to sharpen my thinking and approach to research. Collaborating with them profoundly contributed to my professional and personal growth.

I would like to thank all the members of my scientific thesis committee: Lionel Roques, Olivier Bonnefon, Katarzyna Adamczyk, Sabrina Gaba, Fabrice Vinatier, Céline Lacaux and Claire Lavigne. Their invaluable guidance and advice have greatly improved my work and enabled me to clearly develop and deepen the subject in details. I would also like to extend my gratitude to Loic Houde, who helped me a lot with all the computational troubles; Sylvie Jouslin who helped me in all the administrative tasks and was always kind and supportive.

I would like to acknowledge all PhD, Postdoc and research associate colleagues, along with my office mates, who provided stimulating discussions as well as happy distractions to rest my mind outside of my research.

I would also like to profoundly thank all the members of BioSP, who welcomed me from the first day, when I was still unable to speak French. All of them showed to me kind help, encouragement and they have made my work and life in Avignon a pleasant time.

I am profoundly thankful to my family whose constant love, presence and support keep me motivated and confident.

Lastly, I thank the PACA region (Provence-Alpes-Côtes d'Azur) and the INRAE Math-Num and SPE division for jointly funding my thesis.

Contents

List of abbreviations

- AP: Areal Photography
- BC: Biological Control
- CBC: Conservation Biological Control
- GLM: Generalised Linear Model
- GLMM Generalized Linear Mixed-Effect model
- GRF: Gaussian Random Field
- IBM: Individual Based Model
- L: Local numerical solution
- MCMC: Monte Carlo Markov Chain
- NL: Non-local numerical solution
- PDC: Population Dynamic Covariate
- PDE: Partial Differential Equation
- PRC: Pest Resistant alternative crop
- SAR: Synthetic Aperture Radar
- SC: Spatial Covariate
- SNH: Semi-Natural Habitat
- STC: Spatio-Temporal Covariate
- STPP: Spatio-Temporal Point Process

General context

Agroecosystem sustainability relies on various ecosystem services, such as crop production, nutrient cycling, flood regulation, climate regulation, biological control of pests, and aesthetic value (MEA, 2005; Zhang et al., 2007). However, the demand for increasing agricultural productivity leads to significant changes and intensification of farming practices, such as land consolidation, shortening of crop rotations, and selection of the most productive cultivars relying on agri-chemicals to protect fields from pathogens and pests (Foley et al., 2005; Poggi et al., 2021). Recent studies spotlight a dramatic decline in biodiversity, species richness and abundance as the main consequence of habitat loss and land use change driven by intensive agriculture and urbanisation, pollution, biological factors (including pathogens and introduced species), and climate change (Sánchez-Bayo and Wyckhuys, 2019). Indeed, it has been established that land use simplification, associated with a strong dependence on agro-chemical inputs, is decreasing environmental quality and is threatening biodiversity (MEA, 2005), as most ecosystem services are influenced by agricultural landscape structure (Mitchell et al., 2014; Bianchi et al., 2006; Chaplin-Kramer et al., 2011a).

Agricultural landscapes can vary from structurally simple landscapes composed by few cropping systems to a complex mosaic of different cultivated patches embedded in a natural matrix (Power, 2010). Landscape structure is defined with respect to its heterogeneity, which can be expressed through landscape configuration, referring to the size, shape, and spatio-temporal arrangement of land-use patches, and through landscape composition, referring to the number and proportion of land-use types (Martin et al., 2019). The structural complexity of these systems influences ecological responses, such as animal movements (Fahrig, 2007), population persistence (Fraterrigo et al., 2009), species interaction (Polis et al., 2004) and other ecosystem functions (Lovett et al., 2005) providing more niches and diverse ways of exploiting the environmental resources (Fahrig et al., 2011). Specifically, landscape configuration affects species movements, spillover and the colonization of neighbouring patches (Tscharntke et al., 2005; Rand et al., 2006; Blitzer et al., 2012); landscape composition affects diversity by providing complementary resources along the different stages of an organism's life cycle, by increasing species diversity, by affecting species interactions and by favouring complex trophic network relationships (Benton et al., 2003; Fahrig, 2013). Specifically, in agricultural landscapes, the amount and the organisation of natural and semi-natural habitats have the potential to promote a bundle of desired ecosystem services, such as pest

regulation and pollination, due to their influence on the community ecology at multiple spatial and temporal scales (Bianchi et al., 2006; Chaplin-Kramer et al., 2011b; Tscharntke et al., 2016a). Non-crop habitats often include woody (*e.g.*, forest and hedgerow) and herbaceous habitats (*e.g.*, field margins, road verges and meadows). These habitats are relatively undisturbed and permanent areas, and they are often a source of complementary resources and refuges. Thus, they can support more diverse and abundant natural pest enemies than simple landscapes. Thus, commonly, pest regulation is expected to be greater in complex landscapes that contain a greater proportion or diversity of semi-natural habitats, such as forest, meadows, hedgerows or ditches (Chaplin-Kramer et al., 2011a). However, despite this potentially beneficial role of semi-natural habitats for biological control, there is a tendency to favour arable fields and large field sizes allocation in modern agricultural landscapes (Rusch et al., 2016; Tscharntke et al., 2005)

The nexus among agricultural landscape structure, natural habitat presence and species trophic interactions is not trivial. There can be potentially negative, neutral, or positive consequences for biological control outcomes (Martin et al., 2013; Snyder, 2019). For example, carabids alternate between semi-natural and crop habitats as they require both during their life cycle (Kromp, 1999; Bareille et al., 2020). They reproduce in field margins and move to crops where they feed on agricultural pests, such as aphids (Kromp, 1999). In this case, the intermixing of semi-natural elements within crops positively affects carabid dynamics and, thus, positively favours the pest regulation thanks to predation by carabids (Garcia et al., 2000; Joyce et al., 1999). By contrast, natural habitat can also host a high variety of pest species such as aphids, herbivorous flies and beetles (Langer, 2001). Similarly to their predators, these pests can benefit of complementary resources, or they can use those habitats in some stages of their life cycle, and they can then inflict damages on crops (Rand et al., 2006; Tscharntke et al., 2016a).

Even if the presence of semi-natural area favours the presence and diversity of natural enemy species , this does not directly translate into a profitable advantage for natural pest regulation (Holt et al., 2001). Natural enemy species may differ in their life-cycle, their behaviours and their predating strategy, and they can therefore influence each other in positive or negative ways. Specifically, natural enemy richness is beneficial for pest regulation when species act in a complementary manner in terms of pest suppression (positive effect); by contrast, it is also possible that natural enemies are in competition and disturb each other (negative effect) (Northfield et al., 2010; Finke and Snyder, 2010). Complementary strategies can be characterised by different predating time (*e.g.*, nocturnal vs diurnal predators) or by different dispersal ability and predating strategy (*e.g.*, actively-searching vs sit-and-wait predators) (Tscharntke et al., 2005). Negative effects may occur when natural enemies show similar or identical behaviours limiting predator density or predating efficacy, such as feeding on each other (*e.g.*, intra-guild predation) (Finke and Snyder, 2010). For these reasons, functional diversity, rather than species richness per se, may often determine the

relationship between biodiversity and biological control. When species are categorised into functional groups based on their behavioural and ecological traits, species within the same group are considered as ecologically redundant, and species in different groups are complementary (Hillebrand and Matthiessen, 2009; Northfield et al., 2012). However, species richness and species functional diversity are naturally linked: having a large number of different species would likely result in a large pool of species that could potentially have different functions in the ecosystem (Tilman, 1996; Cadotte et al., 2011). Thus, it is always important to consider the correlation among species richness and functional diversity (Tilman et al., 2001). In addition, maintaining species richness and functional redundancy may be an important insurance and resilience strategy, since it provides options of composition change in response to future stressors or species loss (Tilman, 1996; Peterson et al., 1998). Specifically, species having the same function in the present environmental context may respond differently in future contexts as they may adapt their traits and behaviours in different ways to changing drivers. In addition, species in the same functional group may operate at different scales, such that they provide mutual reinforcement and contribute to the resilience of a function (Peterson et al., 1998).

Divergent organism functions and behaviours are also influenced by landscape structure and resource distribution, which, consequently, influence species interactions (Cenzer and M'Gonigle, 2019). For predators, the combination of their preferred habitat and their dispersal ability jointly determines the spatial domain where they search for the prey, and it determines the predating strategy they apply. Moreover, the predating strategy is adapted to the behaviour of preys: sit-and-wait predators are more effective at capturing actively moving prey, whereas actively moving predators are more effective at capturing sedentary prey. Thus, a change in the environmental context and species composition can result in morphological or behavioural adaptation of species to adjust their traits and strategies to match the new situation. Thus, predator–prey interactions and behavioural strategies should be considered as an *adaptive foraging games* (Schmitz et al., 2017): predator success results from the ability to capture the prey; prey success results from the ability to evade predators. For example, Start and Gilbert (2017) study how predator behaviour and density interact in structuring prey abundance, community composition and the strength of trophic cascades. They demonstrate that predator strategy can create differences in abundance of preys and in their composition (Royauté and Pruitt, 2015). Moreover, they suggest that intraspecific variation in one species can allow for the coexistence of the other species with which it interacts (Pruitt et al., 2012). They also show that active predators are more likely to cannibalise one another, and cannibalisation may become the dominant feeding strategy when they are at high density, leading to weaker predation of other prey (Rudolf, 2007). Sommer and Schmitz (2020) study how personality differences in a species of herbivore prey mediated tri-trophic interactions involving its predator and its plant resources. They show that it is insufficient to characterise a population's trophic interactions across environ-

mental contexts based on the mean trait value alone. Specifically, they noted a convergence of opposite prey personality trait values and different resource utilisation under predation risk by a sit-and-wait spider predator.

The interplay between species sorting and adaptation shapes the structure and functioning of communities based on the species' functional traits (Lavorel and Garnier, 2002; Martin et al., 2019). In recent literature, the reciprocal interactions between ecological and evolutionary processes, which enable the organisms to both shape and adapt to their environment, are called *Eco-evolutionary processes* ("eco-evo") (Becks et al., 2012; Legrand et al., 2017; Bonte and Bafort, 2018). Ecological dynamics, such as species interactions and demography, can influence evolutionary change by altering natural selection. This, in turn, can alter ecological dynamics (Burak et al., 2018). Therefore, eco-evo interactions should not be dissociated from the ecological and environmental context in which they occur (Urban et al., 2008; Hanski and Mononen, 2011; Legrand et al., 2017). This holds especially in those habitats that are currently shaped by human activities, such as agricultural practices (Legrand et al., 2017). Many phenotypic traits can be affected by spatial heterogeneity and structure, in particular those traits related to mating systems, competitive skills, movement abilities or habitat use (Legrand et al., 2017). Indeed, accounting for species traits and their role in shaping the interaction between ecological and evolutionary dynamics is crucial to understand many processes in ecology, such as evolutionary rescue (Lavigne et al., 2020), migrational meltdown (Ronce and Kirkpatrick, 2001) or biological invasion (Szűcs et al., 2019). For example, population expansion is an ecological process mainly driven by traits related to reproduction and dispersal (Turchin, 1998; Deforet et al., 2019). However, there are many examples where individuals who invest more in the development of their traits related to the dispersal strategy reduce the effort in foraging and reproduction (Bonte and Bafort, 2018; Baguette and Schtickzelle, 2006; Hanski et al., 2006). In such cases, two possible evolutionary strategies exist: dispersing faster, or growing more strongly (Deforet et al., 2019). This results in a trade-off between the species' traits that shapes the ecological and evolutionary dynamics of populations.

In this thesis, we highlight the role of agricultural landscape structure on shaping population dynamics and on influencing biological control outcomes. In order to develop a general methodology where we do not restrict our findings to a specific case study, we propose and illustrate different perspectives and approaches that are generic and flexible enough to be easily adapted to different systems.

The conceptual framework and structure of the thesis is presented in Figure 1. In the Part I of this thesis, we deal with the representation of real agricultural landscapes. We give a general overview of agricultural systems and dynamics where we highlight their complexity and open challenges (Chapter 1). Then, we present novel models we developed to

represent agricultural landscapes through computer generated-simulations where we vary representative parameters related to landscape features such as the percentage of land-cover, the habitat fragmentation, or spatial auto-correlation (Chapter 2) (Gardner, 1999; Saura and Martinez-Millan, 2000; Gardner and Urban, 2007; Sciaini et al., 2018; Langhammer et al., 2019). In this part of our research, the characterisation of virtual agricultural landscapes is performed regardless of underlying ecological or social processes (*i.e.*, neutral model-based landscape generator) (Langhammer et al., 2019). This allows deeply focusing on one or several characteristics of composition and configuration useful to simulate different, but statistically similar landscapes having features close to real ones. In Part II, we investigated the role of agricultural landscape heterogeneity on pest-predator dynamic (Chapter 3). In order to go further and explore the role of complex landscape on BC, we couple stochastic landscape models with a population dynamic model accounting for both dispersal along the hedges and within surfaces. In this way, we are able to unravel the joint influences of landscape features and species traits on BC output at global (Chapter 4) and local scale (Chapter 5).

In Part III we take into account species functional diversity by focusing on species behaviours and species traits (Chapter 6), which are able to influence species interactions. To assess traits evolution and adaptation during key ecological processes, in Chapter 7 we characterise species with a continuous space of phenotype traits describing a simplified system to focus on eco-evolutionary processes in new or changing environment. We decide to describe a simplified system: the spatial support is represented by a 1D spatial domain; and we consider a single species. We consider the expansion process driven by co-evolving species traits, where the two possible eco-evolutionary strategies involve a trade-off: growing faster (but dispersing more slowly), or dispersing faster (but growing more slowly). We explore the spreading dynamics of a consumer species exploiting a resource in a heterogeneous environment through a reaction-diffusion model. Even if this is a theoretical work; it may be placed in the context biological control to study species invasion or colonisation in an heterogeneous environment. Lastly, by using the idea and key messages of Chapter 7, we expand the pest-predator model presented in Chapter 4 towards a two-predators and two-pest system where species show opposite habits and traits. Here, we analyse how the landscape structure may play a role in shaping species optimal strategies and fitness (Chapter 8).

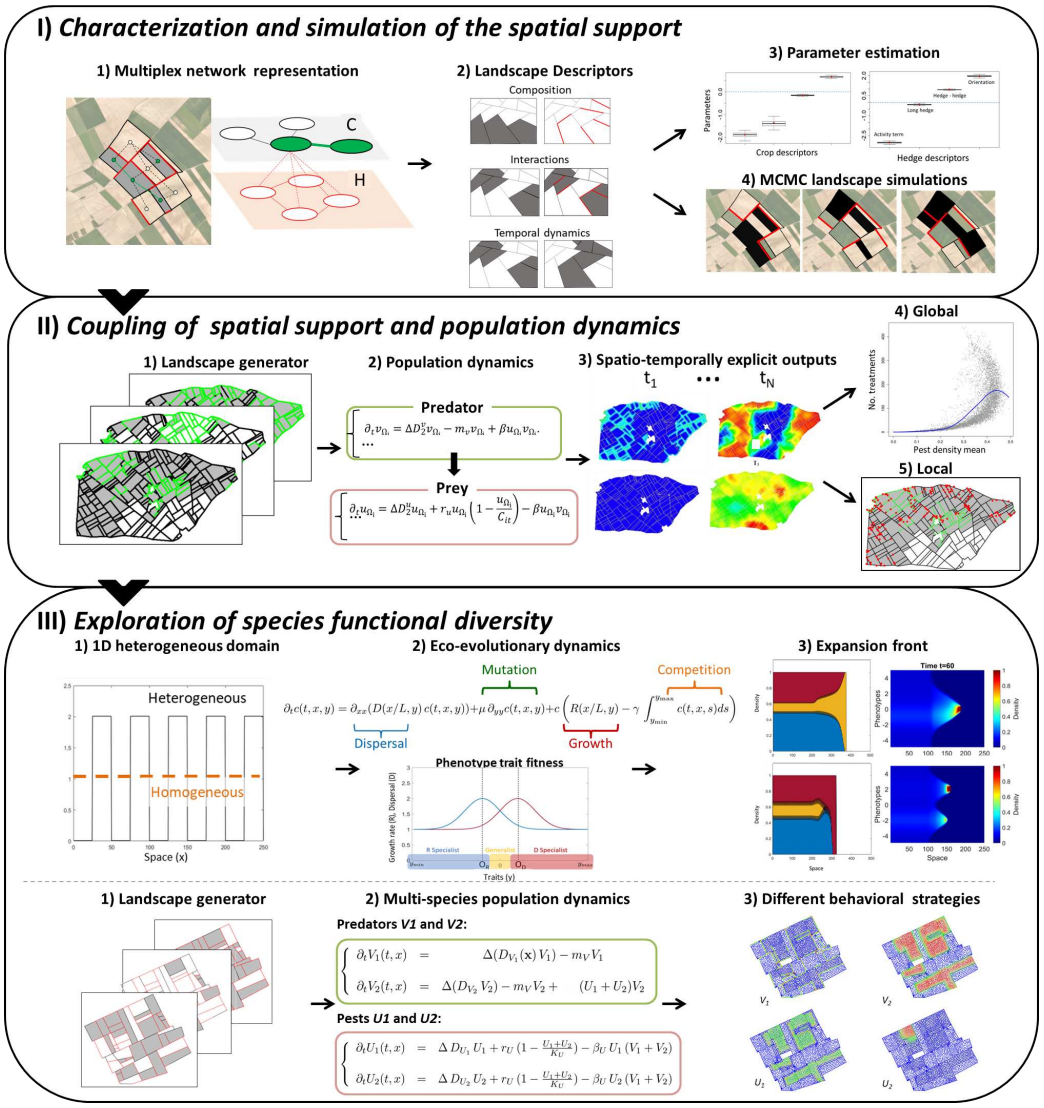

Figure 1 – Thesis structure

Part I
Modelling the spatio-temporal heterogeneity of agricultural landscapes

Figure 2 – A landscape in central France with pastures, fields, and forestland mix, creating a "bocage" landscape. Image taken on April 10, 2016. PlanetScope image © 2016 Planet Labs, Inc. cc-by-sa 4.0.

Chapter 1

Complexity in agricultural landscapes: definitions, functions and representations

1.1 Agricultural landscape structure

A landscape is a spatially heterogeneous area defined by the land surface and its associated habitats at different spatial scales (Turner, 1989). Fundamental landscape characteristics are structure, function, and change (Forman et al., 1986). *Structure* refers to the spatial relationships between distinctive ecosystems, which depend on the size, shape, number, kind and configuration of components. *Function* refers to the interactions between the spatial elements, such as the flow of energy, materials, and organisms among the component ecosystems. *Change* refers to alteration in time of structure and function (Turner, 1989). Indeed, structural landscape heterogeneity involves different cover types identified by their physical characteristics, without reference to species; functional landscape heterogeneity involves different cover types depending on differences in resource utilisation and includes species or species groups (Fahrig et al., 2011). Then, spatial heterogeneity could be quantified by landscape configuration (*i.e.*, size, shape and spatial arrangement of land-use patches) and landscape composition (*i.e.*, proportion of land-use types), see Figure 1.1 (Fahrig et al., 2011; Fahrig, 2013; Martin et al., 2019). As landscapes are spatially heterogeneous mosaics, their structure, function, and change are scale-dependent: spatio-temporal patterns and heterogeneity are dependent on the considered scale (Turner, 1989). Landscape functions, such as the flow of organisms, depend on scale and on species dispersal abilities and perception of the surrounding environment (Whittaker et al., 1970). Changes in landscape structure or function are scale-dependent as a dynamic landscape may exhibit a stable mosaic at one

spatial scale but not at another (Turner, 1989).

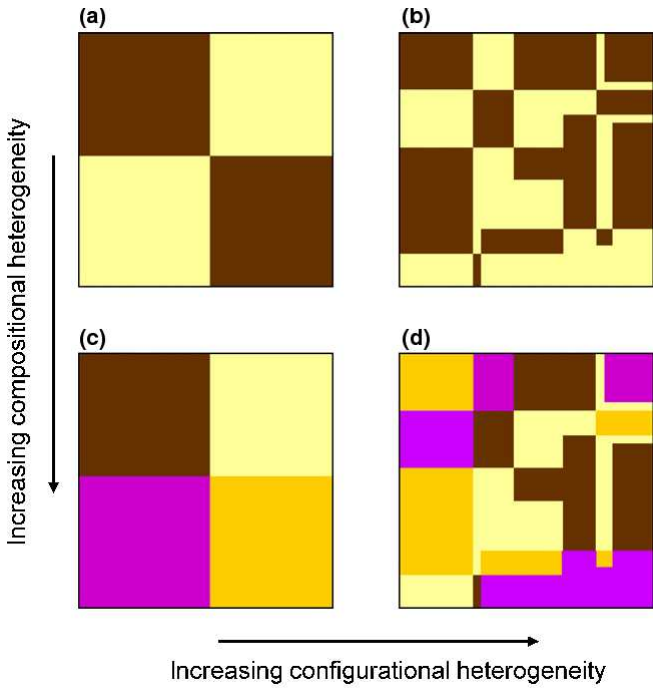

Figure 1.1 – Landscape heterogeneity with two major axes: compositional and configurational heterogeneity. Each large square represents a landscape, and different colours represent different cover types within landscapes. From Fahrig et al. (2011).

Agricultural landscapes are strongly human-driven landscapes, and they cover about $40-50\%$ of continental areas with an increasing trend to meet the growing demand of food production (FAO, 2006; Gaucherel et al., 2014). Around the world, agricultural ecosystems show variation in structure and function, due to diverse crops, different socioeconomic conditions and diverse climatic regions (Power, 2010). However, in general, an agricultural landscape can be viewed as a spatially heterogeneous area composed by a collection of cultivated fields and semi-natural areas. Agroecosystems are key habitats not only for food production purpose, but also for other ecosystem services, such as biodiversity, pollination and pest control (Power, 2010; Foresight, 2011). Agricultural area could be represented as a matrix or mosaic of patches defining the dominant land cover, while the interconnections are constituted by linear elements (Van Der Zanden et al., 2013). During the last decades, the agricultural intensification has resulted in strong changes in agricultural landscapes, mostly in Western Europe and North America (Robinson and Sutherland, 2002). Specifically, we are observing a simplification of agricultural landscapes characterised by the expansion and upscaling of arable field sizes, simplified crop patterns with fewer crop types and the reduction of natural habitats to leave only small fragments (Baillod, 2016). Thus, arable fields become

the dominant landscape element. A key point is that cropping systems are ephemeral habitats that are often subject to frequent and intensive disturbances (Landis, 1999). On the other hand, non-crop habitats, such as field margins, ditches, grassland, hedgerows and wood lots, are relatively undisturbed and temporally permanent areas and, thus, are capable of holding a substantial biodiversity richness acting as biodiversity reservoirs for plants, insects, birds and mammals (Bianchi et al., 2006; Schmidt et al., 2005).

1.2 The role of semi-natural habitats (SNH) within agricultural landscapes

The structure of semi-natural habitats (SNH) embedded in agricultural landscapes is highly variable, ranging from wild and cultivated elements being almost indistinguishable and intermeshed, such as in tropical agroforestry landscapes (Tscharntke et al., 2011), to being strongly separated as in intensive monoculture landscapes, see Figure 1.2 (Poggi et al., 2021). SNHs, such as hedgerows, ditches, ponds, grass strips, are of great importance since they provide ecosystem services, such as erosion limitation, water supply and flood regulation, pesticide and nutrient mitigation, weed and pest spreading regulation (Power, 2010). These ecosystem services, if fostered and supported, could be an advantage and an opportunity to limit the dependence on agricultural inputs (*e.g.*, fertilisers, pesticides, irrigation water). Consequently, the spatial arrangement of non-crop habitats and cultures strongly influences the ecological system responses (Fahrig et al., 2011; Maalouly et al., 2013; Ricci et al., 2013; Martin et al., 2019). The variability of habitats in ecosystems, and their functional diversity, may also represent conditions for the development of biodiversity-based agricultural landscapes, as well as resilience of ecosystems (Chapin I et al., 2000; Poggi et al., 2021). In fact, the juxtaposition of different land cover types, considering different crops and SNHs, both with different shapes and sizes, results in higher levels of complexity, both in terms of landscape composition and configuration, which influence species dispersal and colonisation of neighbouring patches (Perović et al., 2015). The presence of different land cover types can guarantee complementary resources during the life cycles of each species, thereby increasing species diversity and favouring complex trophic network relationships (Dunning et al., 1992; Perović et al., 2015; Tscharntke et al., 2012; Poggi et al., 2021).

1.3 Landscape models

The structure of a given landscape results from accumulated past changes, and it is continuously reshaped by natural and human drivers (Poggi et al., 2018). In order to describe the spatio-temporal dynamics of landscapes represented by field mosaics and their shapes and properties, models can provide a key contribution and can also support the design of sus-

Figure 1.2 – Spatial structure of cultivated fields and SNHs across different farming systems. Source: © IGN from Poggi et al. (2021).

tainable landscapes (Poggi et al., 2018). Given the complexity of the landscape system, the broad range of spatial scales, the temporal dynamics and the multiple objectives that must be satisfied, empirical experiments alone cannot provide exhaustive answers since they are based on few case studies and relatively specific systems and scientific questions.

In general, a model is defined as an abstract mathematical representation of a system or process (Turner et al., 2001). Therefore, most models are used to explore assumptions and hypotheses rather than to represent system structure and dynamics exhaustively. As Box (1979) stated: *"All models are wrong, but some are useful"*. They allow for problem definition, the identification of the relevant concepts, data analysis and result communication (Turner et al., 2001). Models should always be considered as scientific tools which enable us understand how a system works and, then, explore the suite of varying conditions in time and space (Turner et al., 2001). Scientists model landscapes for mainly two reasons: to better understand landscape dynamics themselves (*intrinsic needs*), and/or to offer realistic frames to host other ecological, biological, sociological and/or physical processes (*extrinsic needs*) (Rounsevell et al., 2012; Gaucherel et al., 2014). In this sense, the wide variety of available or possible models could be used to provide insights and to guide the transformation and transition towards future landscapes, for example by performing scenario simulation under different conditions or multi-objective optimisations (Nendel and Zander, 2019; Poggi et al., 2021). Moreover, landscape models could be coupled with outputs from global climate models (Hayhoe et al., 2017) and species distribution models (Franklin, 2010) to predict the effects of environmental changes on species and ecosystems. Different lines of research are possible: i) Landscape representation, to further conceptualisation as technological developments and precision agriculture bring increasing information; ii) Landscape conception,

to build bridges between disciplines underpinning agricultural landscape modelling (*e.g.*, agronomy, geography, ecology, economy and computer science); iii) Landscape manipulation, to identify future scenarios for shifting from current agricultural landscapes to novel and more sustainable ones, but, here, research remains rare (Poggi et al., 2021).

Agricultural landscapes are highly complex systems for which modelling offers a fundamental tool to provide guidance on their future conception and manipulation (Poggi et al., 2021). Agricultural landscape models describe landscapes as mosaics of fields having shapes and properties that vary in space and time (Turner et al., 2001; Gaucherel et al., 2014; Poggi et al., 2018). Different approaches exist for generating landscapes with various structures (*i.e.*, the spatial arrangement of land covers), and for studying biotic or abiotic processes (Langhammer et al., 2019). Landscape models aim to generate virtual landscapes by using algorithms that systematically and automatically vary landscape features, such as percentage of land-cover, habitat fragmentation, or spatial auto-correlation. This allows simulating different virtual, but structurally realistic, maps of land cover by trying to combine both realism and the possibility of varying landscape features (Gardner, 1999; Saura and Martinez-Millan, 2000; Gardner and Urban, 2007; Sciaini et al., 2018; Langhammer et al., 2019). Landscape mosaics can be represented by two complementary approaches, raster and vector representations, depending on the goal of the study and how their constitutive parts are handled, see Figure 1.3 (Bonhomme et al., 2017; Gaucherel et al., 2006b). Differences between raster and vector landscapes arise from their spatial composition. A raster is a matrix data structure that represents a regular grid of cells that are the smallest units and that are defined by two pieces of information (i.e the spatial coordinates and the cell value). A vector is a spatial object (i.e. points, lines, and polygons) defined by the exact coordinates of its bounding vertices and could have different attribute values (Langhammer et al., 2019).

Most of the existing models work with the raster mode and simulate cell mosaics (Gardner, 1999; Saura and Martinez-Millan, 2000; Pe'er et al., 2013; Engel et al., 2012; van Strien et al., 2016). In agricultural landscapes, for example, Begg and Dye (2014) develop a modelling framework that couples a landscape mosaic generator and a population module. The generator module is a stochastic algorithm that works by continually subdividing a two-dimensional space to produce a mosaic of rectangular fields. Engel et al. (2012) design a simple landscape structure composed of 15 crop types by varying crop proportion and the mean field size. van Strien et al. (2016) generate landscapes integrating different landscape metrics at field or class level, and their approach allows varying the configuration and the composition. The model of van Strien et al. (2016) is based on an optimisation algorithm that tries to optimise the configuration and the composition that correspond to the target set for the landscape metrics. Raster-based approaches are commonly used for modelling processes operating between contiguous cells and result in gradual landscape dynamics (Langhammer et al., 2019).

However, agricultural mosaics display a patchy structure consisting of a moderately

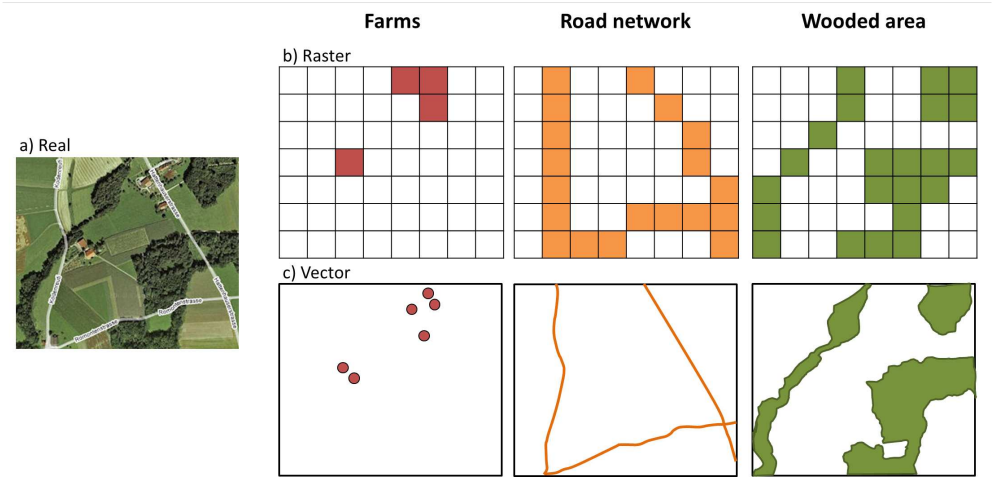

Figure 1.3 – Comparison of the raster (panel b) and vector (panel c) approaches to the representation of real agricultural landscape (panel a). In raster representation, the information is contained in cells as elementary units. In vector representation, the information is described using different geometrical features *i.e.*, farms as points, roads as linear elements, wooded area as polygons.

large number of contiguous polygons with rectilinear boundaries, and there can also be fringe structure on their borders, such as hedgerows (Gaucherel, 2008). Indeed, for agricultural landscapes strongly characterized by patches and corridors, the vector approach is very well suited (Gaucherel et al., 2006a,b; Le Ber et al., 2009; Papaïx et al., 2014a; Inkoom et al., 2017; Langhammer et al., 2019). For example, Gaucherel et al. (2006a,b) develop a model that simulates the patches and fringe structures. In their work, a pixel definition of the polygon is kept in order to simulate continuous processes. In follow-up work, Gaucherel (2008) proposes models for polygonal landscapes mosaics, based on the comparison of different tessellation approaches. Le Ber et al. (2009) simulate agricultural landscape defined by two different tessellation methods (*i.e.*, Voronoi and rectangular) and two types of stochastic cropping pattern distribution. Papaïx et al. (2014a) develops a landscape generator that generates the landscape mosaic based on a T-tessellation algorithm developed by Kiêu et al. (2013). Many tessellation models have the advantage of being parametric, where a set of parameters controls the main features of the simulated landscapes. Moreover, these models are stochastic and can be used to produce essentially infinite collections of replicated virtual landscapes with similar landscape metrics (Papaïx et al., 2014a). This allows checking the robustness of the results to changes in residual landscape variability. However, using such approaches it can be difficult to reproduce fine grain spatial structures, as they do not capture the full complexity of landscapes nor do they provide realistic landscape structures. The combination of parametric with nonparametric approaches may enable this gap to be bridged (Straubhaar et al., 2011). The majority of the above-mentioned models are validated by testing whether generated landscapes are able to reproduce realistic landscape features.

The validation is performed by comparing certain landscape metrics (see Section 1.4) with real landscapes (Adamczyk-Chauvat et al., 2020; Gaucherel et al., 2006a,b; Le Ber et al., 2009; Pe'er et al., 2013; van Strien et al., 2016; Inkoom et al., 2017; Zamberletti et al., 2020). Some of them use also these metrics as input for the simulation algorithm to approximate the generated landscape to the target one (Langhammer et al., 2019).

1.4 How to assess and analyse landscape patterns

Before the relationship among landscape structure and the processes of interest can be understood, landscape patterns must be identified and quantified in meaningful ways (Turner, 1990). The quantification through mathematical functions, using indicators or metrics, is a useful tool for the analysis of landscape patterns, which may be patch-based and expressed through discrete land-cover classes. A wide variety of methods, indices and metrics exist and enable measuring landscape patterns across a multitude of applications (Turner, 1990; McGarigal and Marks, 1995; Cushman et al., 2008; Kupfer, 2012; Frazier and Kedron, 2017). As for the terminology, the common usage of the term *"landscape metrics"* mostly refers to indices developed for categorical map patterns (McGarigal et al., 2002), but it is also used for topographic measures (Iampietro et al., 2005) that characterize landscape. Landscape metrics may also just refer to some combination of several characteristics that are important to a particular species (Fernández et al., 2007). In order to make metrics relatively easy to calculate (Calabrese and Fagan, 2004), software packages are widely used, and many metrics have also been integrated into existing geographic information system (GIS) software *e.g.,* Patch Analyst in ArcView; and module Pattern in IDRISI (Uuemaa et al., 2009). An example are the metrics proposed by McGarigal and Marks (1995) who developed the dedicated software FRAGSTAT, also available through the open-source R package *landscapemetrics* (Hesselbarth et al., 2019). However, the proliferation of various metrics, many of them strongly correlated among each other, poses a serious challenge to determine how many components of landscape structure are relevant and which metrics should be used (Cushman et al., 2008). The desirable idea is to rely on the smallest number of independent metrics which sufficiently quantify landscape structure (Cushman et al., 2008). Cushman et al. (2008) use principal component analysis (PCA) and cluster analysis to identify independent components of landscape structure, which results in a moderate number of universal and consistent combinations of FRAGSTAT metrics describing major attributes of landscape structure at the landscape level. Leitao and Ahern (2002) propose a core ensemble of metrics relevant for landscape planning. However, some of the landscape metrics are difficult to interpret because their behaviour has not yet been evaluated in depth (Uuemaa et al., 2009; McGarigal et al., 2002). A solution to this problems can be obtained through neutral landscape models, which may be employed to systematically generate maps with varying map properties and to compare the generated patterns with those of real landscapes. This

allows for testing and better understanding the behaviour of various metrics (Li et al., 2005). Another common group of metrics are graph-theoretic measures, where graph-theoretic approaches are used to represent the landscape as a network of habitat patches through the mathematical "graph" definition (Urban and Keitt, 2001; Minor and Urban, 2008; Saura and Martinez-Millan, 2000; Lü et al., 2016). Metrics are then defined relative to nodes, edges or the entire habitat network (Urban and Keitt, 2001; Lü et al., 2016). Once evaluated, a combination of relevant metrics could be used for better characterising landscape structure or investigating the processes, spatial dynamics or patterns and the relationships of interest.

1.5 Open issues and future challenges

The representation of agricultural landscapes remains challenging due to the complexity of the system, the elevated number of properties and features to be addressed, different spatio-temporal scales and the elevated number of processes involved within it (Poggi et al., 2021). In general, large-scale patterns are now commonly integrated in landscape metrics and models; fine-scale elements, instead, are generally not considered as they require a higher spatial resolution (Poggi et al., 2021). However, such elements are fundamental as they may influence the local landscape heterogeneity and may explain local dynamics.

In the raster representation for the landscape structure, as proposed by McGarigal and Cushman (2005), there is a very realistic representation of landscape heterogeneity describing the landscape by continuous surface characteristics without arbitrary land-use classification (Lausch et al., 2015). This approach seems well suited to landscapes with a relatively high degree of naturalness and with strong temporal dynamics in vegetation patterns, and to landscapes characterised by gradual and continuous processes (Lausch et al., 2015; Langhammer et al., 2019). Traditional geostatistical analysis allows for metrics that can appropriately characterize spatial variation in continuous surfaces; however, the definition of linkages between landscape representation and ecological processes should be better addressed (Poggi et al., 2021). Moreover, there is the need to develop novel techniques to efficiently reduce the model complexity in order to fully take advantage of all the available data and maintain a high level of precision.

On the other hand, the patch mosaic paradigm (Forman et al., 1986) depicts the landscape as a mosaic of discrete, homogeneous areas, and we can quantitatively assess their spatial arrangement (landscape configuration) and their constituent diversity (composition). For this approach, numerous landscape indicators have been developed to quantify different spatial and compositional aspects of landscape patterns and to link them with the process of interest, such as ecological processes (Lausch et al., 2015). Its main weakness that calls for further research is the lack of the description of the within-patch heterogeneity, which leads to information loss that may be important to explain certain dynamical processes. Nevertheless, this approach appears well suited in many human-dominated environments,

such as urban areas or agricultural landscapes where discrete and homogeneous areas are separated by sharp and discrete boundaries.

These two modeling paradigms have different data requirements and allow for different quantification methods, and the choice should be driven by the scope of the work. For this reason, the models presented in the existing literature focus on different aspects, levels of detail and methodology, which makes direct comparisons of the two approaches performance on a specific task difficult (Langhammer et al., 2019). Moreover, the alignment of computer generated landscapes with real landscapes still has much potential for improvement. Further development of specific algorithms for calibration and validation of models with respect to real landscapes, using high resolution data and integrating relevant abiotic factors, should be addressed (Langhammer et al., 2019).

Chapter 2

Stochastic modelling of allocation in vector-based representations of agricultural landscapes

In this PhD thesis, we pave the way to the parameter-controlled generation of virtual but realistic agricultural landscapes featuring different spatial patterns (*e.g.*, geometry, connectivity) and temporal patterns (*e.g.*, crop rotation), thus providing a useful tool and a new methodology to explore the relationships between landscape structures and processes at stake within it. Our main goals are to develop an intuitive and flexible framework to easily represent landscape elements and their interactions, to infer model parameters from landscape datasets, and to simulate different landscape structures. Specifically, we point out the importance of taking into account the interplay among linear elements and patches, which is often not clearly defined but has been highlighted as a key aspect for many ecosystem services and ecological processes. We aim to present modelling approaches which are not constrained by high computational load and memory requirements, and which can be easily adapted to different spatio-temporal scales.

Here, we discuss two modelling approaches for the allocation of land-use categories over a fixed geometrical landscape structure. The first approach is developed over the spatial support of the so-called Selommes region, where we only have the spatial support (a tessellation) but no observed data for the allocation. The model performs stochastic land-use category allocation by simulating Gaussian Random Fields (GRFs) and thresholding the simulated values with the aim of easily performing the 2D and 1D element category allocation based on few parameters that determine the Gaussian correlation structure and threshold values. This approach was previously developed in Sabir et al. (2018). In the work conducted during my thesis, this stochastic landscape generator is used in Section 4

of Chapter 4. In Section 2.1, we give a rapid overview of its definition and its main concepts. The second landscape modelling approach uses discrete Markov random fields to simulate land-use category allocation; it allows for a more precise and detailed characterization of landscape features for surface and linear elements at relatively small scales by considering "mechanistic" interactions between such elements. This second model is calibrated and simulated for the study region of the Lower Durance Valley, where land-use data are available for parameter inference and model validation. As the Markov random field model has been completely developed in the context of my thesis, we provide a detailed exposition of its implementation and results in Section 2.2. In both approaches, the landscape is represented through a vectorial approach defined on a tessellation of 2D space with polygon-shaped cells. Linear segments correspond to polygon edges. To achieve a partition of space through polygon-shaped patches without "empty" areas, and to align hedgerows with polygon edges, we preprocess the real landscape towards a polygon tessellation of 2D space (Boots et al., 1999), based on a heuristic loss criterion measuring the distance between original and transformed landscape (Adamczyk-Chauvat et al., 2020). Landscape elements are characterized by their geometry (*e.g.*, vertex coordinates, size and shape), and by categorical information defining the land-cover (*e.g.*, crop or alternative crop). Here, we suppose that the underlying structure defining patch and edge geometry is fixed; our aim is to model the categorical information for the given geometrical structure. Specifically, we can allocate each polygon and linear element with its own land-use category.

2.1 Simulating agricultural structures through Gaussian Random Fields (GRFs)

For this study, the geometrical landscape structure is fixed and based on the real landscape of the study region of Selommes with an extent of 5.55 km, but the model is generic and can be adapted straightforwardly to other landscapes. The landscape is transformed into a T-tessellation (Kiêu et al., 2013; Adamczyk-Chauvat et al., 2020) composed of 188 polygons with a total of 577 edges. The aim of this model is to easily generate a high number of agricultural landscapes featuring different compositions and configurations of land-use categories. The underlying purpose is to use these generated landscapes as spatial support for the population dynamic model presented in Chapter 4 to explore the relationships among landscape structure and population model outputs. Thus, we vary few, but representative model parameters (*i.e.*, crop proportion, hedge proportion and hedge and crop aggregation) to generate a high number of different landscape structures.

In order to allocate a certain proportion of polygons and edges with a category, we use Gaussian Random Fields (GRFs). The GRF is not an observed part of the landscape, i.e., it is latent, and a threshold on the GRF values is set to attribute specific landscape elements depending on the value being below or above the threshold. The strength of spatial depen-

dence in the GRF (*i.e.*, the spatial auto-correlation) governs the strength of clustering when allocating categories to landscape elements. For example, strong dependence means that relatively large contiguous areas fall either below or above the threshold, which generates spatially clustered structures of landscape elements with the same allocation category. A GRF denoted by W is a random surface over continuous 2D space, for which the multivariate distribution of the values $(W(x_1), W(x_2), \ldots, W(x_n))$ observed at a finite number of locations $x_1, x_2, \ldots, x_n$ in the landscape corresponds to a multivariate normal distribution. This distribution is characterised by its mean vector, which we set to 0 for identifiability reasons, and its covariance matrix Σ, here defined using an exponential correlation function depending on the Euclidean distance between any two points x_j and x_i. The range parameter of the correlation function governs the strength of clustering of category allocation to landscape elements. To handle the interactions between the allocation of hedge and crop, we simulated two correlated GRFs for crop and hedge (See Box1). The GRFs are simulated on specific locations x_i representing the elements under consideration (*e.g.*, midpoints for linear elements, barycenter points for convex surface elements). When working with only two categories, the categories are then selected by fixing a threshold for the values of the GRF and by attributing category 1 if the value is above the threshold, and the alternative category 0 otherwise. Given a simulation of a GRF, the proportion of each category can then be simply controlled by varying the threshold value until the desired proportion is obtained. Thus, this landscape model is defined by the parameters of hedge proportion, crop proportion, spatial aggregation and GRF correlation, thus allowing the simulation different landscape structures. More specific details about the allocation methods are explained in the Box 1, while parameter settings are presented in the Table 1 of the paper (Zamberletti et al., 2021b). An example of different landscape structures generated by different parametrisations is shown in Figure 2.1, where we set different proportions and aggregation levels of hedges and crop fields.

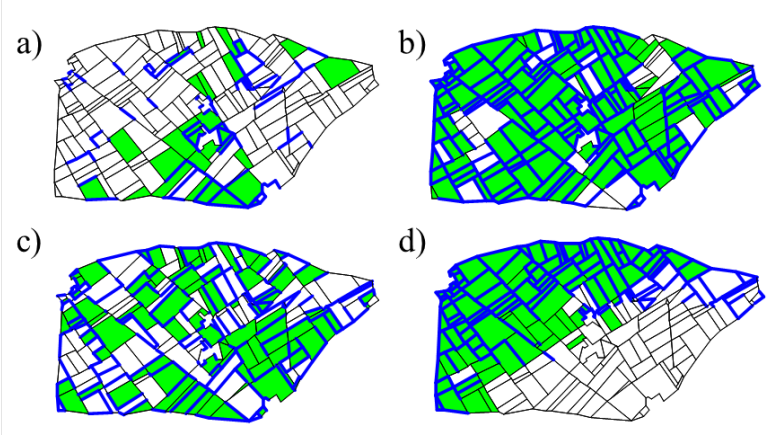

Figure 2.1 – Examples of simulated landscape structures with interacting elements. Two allocation categories for fields: (i) crop (green) and (ii) alternative crop (white), and for edges: (i) hedges (blue) (ii) no-hedges (black). a) increasing proportion of crop and hedges from low (left) to high (right) with fixed aggregation and fixed crop and hedge correlation; b) increasing crop and hedges aggregation level from low (left) to high (right) with fixed proportion of crop and hedges and fixed crop and hedge correlation.

Box 1: A stochastic landscape model based on GRFs

A GRF, denoted by W, is a random surface defined over continuous 2D space. The multivariate distribution of the values $(W(x_1), W(x_2), \ldots, W(x_n))$, observed at any finite number of locations $x_1, x_2, \ldots, x_n$ in the landscape, corresponds to a multivariate normal distribution, characterised by its mean vector (here set to 0), and its covariance matrix Σ (here defined by an exponential correlation function depending on the Euclidean distance between any two points x_j and x_i).
Formally, the GRF distribution at any collection of n locations $x_1, x_2, \ldots, x_n$ can be written follows:

$$(W(x_1), W(x_2), \ldots, W(x_n)) \sim N((0, 0, \ldots, 0), \Sigma) \text{ with } \Sigma_{ij} = \exp(-(|x_i - x_j|/\phi)),$$

with $\phi > 0$ the *spatial range* parameter, which acts as an aggregation parameter.
To assign an allocation category, we initially define a separate GRF for each type of element of the landscape geometry (*i.e.*, linear and surface elements), with independence among these GRFs (in the stochastic sense). Therefore, we generate two independent GRFs $W_1(s), W_2(s)$ with exponential correlation functions depending on range parameters $\phi_1 > 0$ and $\phi_2 > 0$, respectively, in order to obtain simulations from two GRFs with independent aggregation structures. Then, if we aim to handle the interactions between the category allocation of hedge and crop, we can correlate the two independent GRFs through correlation parameters (ρ_h and ρ_c) governing the strength of interaction among the GRFs (*linear coregionalization model*). The resulting two correlated GRFs for crop $(W_c(s))$ and hedge $(W_h(s))$ are defined as follows:

$$W_h(s) = \rho_h W_1(s) + \sqrt{(1 - \rho_h^2)} W_2(s),$$

$$W_c(s) = \rho_c W_1(s) + \sqrt{(1-\rho_c^2)} W_2(s).$$

To obtain a more parsimonious structure with a single cross-correlation parameter, we fix $\rho_h = 1$ such that W_1 defines the GRF used for hedges, and we use $\rho = \rho_c \in [-1, 1]$ to control the correlation between W_h and W_c.

2.2 Simulating agricultural structures through Markov Random Fields

Introduction

In this second modelling approach, we start from the same geometrical landscape representation defined through the T-tessellation of polygons and linear elements, but, here, we develop an approach based on graph-theory concepts. Habitat elements (*i.e.*, polygons, linear elements) are represented by nodes, and their functional connections are represented by links (Urban and Keitt, 2001). Then, the vector landscape can be summarised by a multiplex network defined through the graph for patches and for linear elements with links (edges) in the graph based on spatial adjacency among them. For example, Figure 2.2 shows an illustration of a multiplex network to represent how real landscape structures and landscape element interactions could be transformed into interconnected graphs. Here, two objects interact if they have a link connecting them, meaning they are adjacent. Interactions are possible among all the objects of the same type, such as in the layers of crop (C) (Panel a) and in the layer of hedges (H) (Panel b), and among elements of different types such as the inter-layer among C and H (Panel c). For landscape modelling, we consider two types of such networks. A *potential network* represents all possible pairwise interactions (i.e., all the interactions between adjacent patches (a), adjacent linear elements (b) and adjacent linear elements and patches (c)). Next, given an allocation of this landscape support, the second network type (also called *active network*) is used to represent the adjacency of objects allocated with the same category (e.g., *crop* category for patches, *hedge* for linear elements), or of objects allocated with specific types of categories. We use the active network to encode structures that we consider as ecologically relevant, such as spatial aggregation (or inhibition) among crop fields or among hedges. By construction, the edges of the active network are a subset of the edges of the potential network.

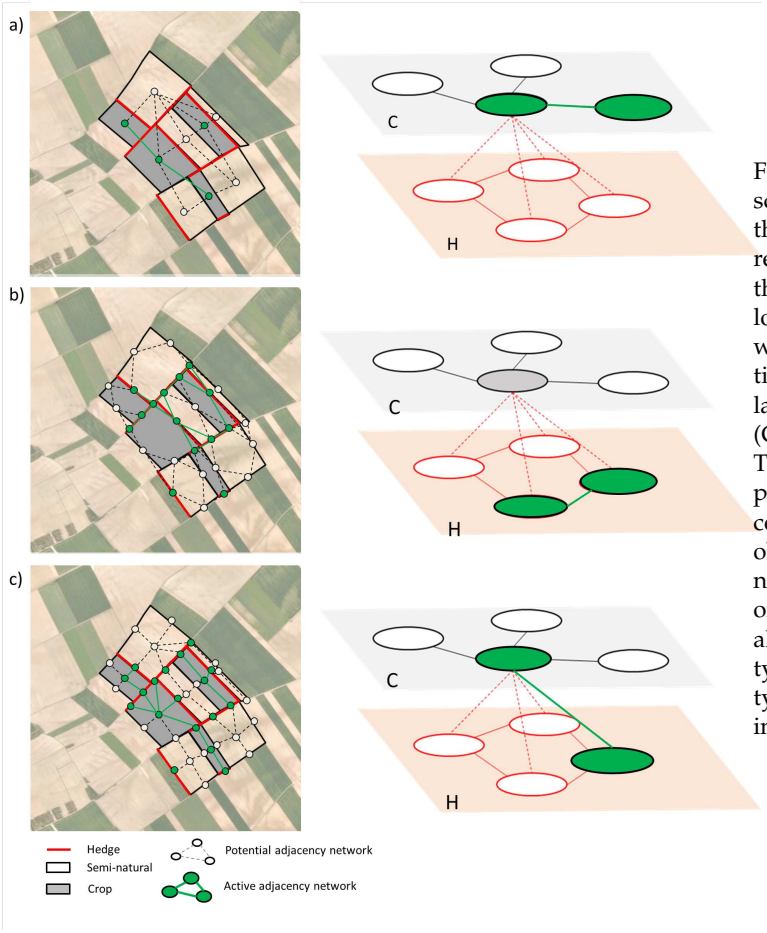

Figure 2.2 – Example of landscape representation through the multiplex network for a real landscape composed of the network layer of crop allocation (C) (Panel a), the network layer of hedge allocation (H) (Panel b), the multilayer network connecting layer (C) and layer (H) (Panel c). The landscape is simplified in potential networks, where all connections among adjacent objects are possible, and active networks (in green), where only the connections among allocated objects of the same type or of specific different types are maintained depending on their categories.

Thanks to this kind of representation of a given landscape, it is possible to evaluate landscape metrics characterising landscape properties at local scale or at global scale, see some examples of landscape metrics in Figure 2.3. In the following, the metrics we use for the model calibration are called landscape descriptors, and we distinguish them from the ensemble of available metrics. Moreover, parameters can be estimated to assess the importance and effect of each descriptor for each specific landscape considered. This allows for landscape characterisation by selecting proper and suitable descriptor combinations specific to each spatial study domain. Our approach permits to assess the adequacy and suitability of different descriptor combinations and to take into account the most relevant and interesting properties for each specific landscape.

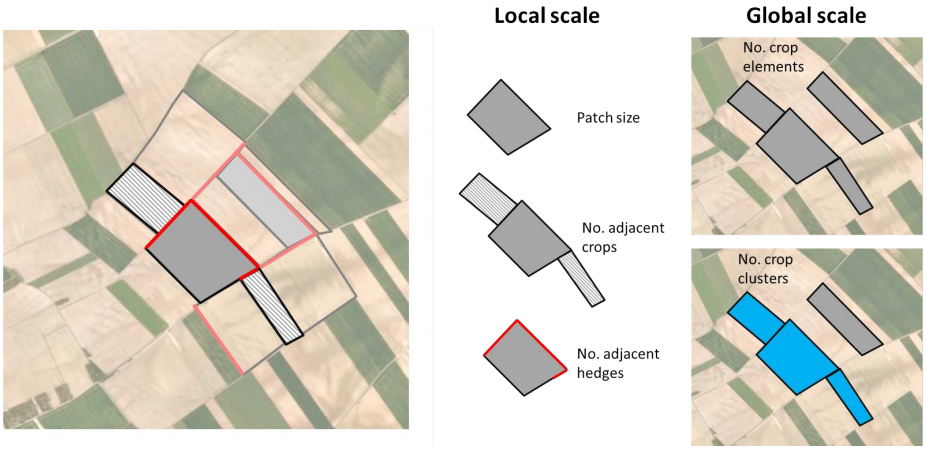

Figure 2.3 – Landscape metrics examples at local scale (middle) and global scale (right).

Landscape properties can be controlled through model parameters. Our main goal is to develop a tool able to generate visually realistic landscapes: starting from an observed landscape composition and configuration, or using various parameter settings in our parametric model, we wish to virtually generate a high number of statistically similar landscapes showing the same observed or selected properties. For example, in Figure 2.4, we show several simulations to visually explore the influence of parameters (β_k) related to the *landscape descriptors* k. In the example, we focus on parameters controlling three types of interactions: *crop-crop adjacency* (β_{adj}^{CC}), *hedge-hedge adjacency* (β_{adj}^{HH}), and *crop-hedge adjacency* (β_{adj}^{CH}). In each simulation run, we set only one of the coefficients to a non-zero value among $\{-1, 1\}$; other descriptors are set to 0. Negative coefficients produce fragmented allocation structures of the two corresponding categories, while a positive coefficient results in clustered configurations of categories.

In order to capture a real landscape composition and configuration, we construct different models of Markov random field type, and we discuss model selection and validation (Hammersley and Clifford, 1971; Besag, 1972). We develop the estimation of coefficients of landscape descriptors on real landscapes through a maximum pseudo-likelihood approach. Given the parametrisation estimated for the real landscape, we simulate a high number of virtually generated landscapes to test significance of coefficients (*e.g.*, to answer the question if there is significant spatial aggregation of crop fields) and to validate the models. Model validation is performed by quantitatively comparing observed and simulated summaries: 1) the descriptors used in the model estimation; 2) the variograms; 3) landscape metrics for vector and raster based representation. Specifically, we highlight that type 2 and 3 are not explicitly encoded into the model structure and calibration. Type 1 concerns statistical validation: the theoretical distribution of a landscape descriptor should be in line with its observed value; we check this through Monte–Carlo samples of the fitted model. Regarding type 2, variograms (Cressie, 2015; van Lieshout, 2019), we adopt a geostatistical perspective

(Saura and Martinez-Millan, 2000) that focuses on the variability and geographic scales of the landscape, which has already proven useful to characterise land use properties (Garrigues et al., 2006, 2008). Regarding type 3 of summaries, various metrics have been used to assess if simulated landscape structures appropriately represent landscape functionality and ecological relevancy (Kupfer, 2012; Frazier and Kedron, 2017). Some commonly used metrics require landscapes to be represented as a mosaic of discrete habitat patches. Many other metrics have been developed for landscapes conceptualised as environmental rasters (i.e., for raster representations, see McGarigal and Marks, 1995; Cushman et al., 2010). Here, we assess how data patterns are reproduced by models through metrics based on graph theory (Urban and Keitt, 2001; Minor and Urban, 2008; Urban et al., 2009; Lü et al., 2016, *network metrics*, see), or *raster metrics* (McGarigal and Marks, 1995).

In the Box 2, there is a close-up on some methodological details, which are fully discussed in (Zamberletti et al., 2020).

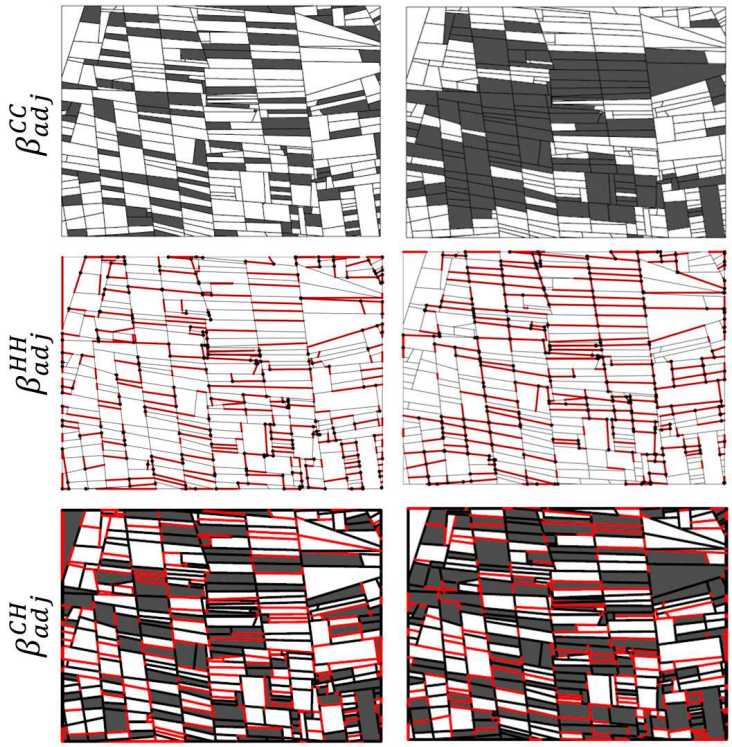

Figure 2.4 – Landscape simulation examples. First line: varying *crop-crop adjacency* (β_{adj}^{CC}); Second line: varying *hedge-hedge adjacency* (β_{adj}^{HH}); Third line: varying *crop-hedge adjacency* (β_{adj}^{CH}). Columns from left to right: coefficient values $-1, 1$. Patches are allocated with two categories shown in grey (*i.e.*, crop) and white (*i.e.*, alternative crop), linear elements are allocated with two categories shown in black (*i.e.*, no-hedge) and red (*i.e.*, hedge).

Box 2: Representation and Markov Random field models for landscapes

Landscape representation

We propose to represent a landscape as a collection $\mathcal{O} = \{o_1, \ldots, o_n\}$ of n geometric objects $o_i = (x_i, z_i)$, $i = 1, \ldots, n$, where each element is composed of two sets of data x_i and z_i. The information in $\boldsymbol{z} = (z_1, \ldots, z_n)$ represents the geometrical structure; the vector $\boldsymbol{x} = (x_1, \ldots, x_n)$ represents categories (with $\ell_i \geq 1$ possible categories for the ith element) that we allocate to the geometric elements in the landscape, like land-use types, and that we aim to model.

We use a graphical representation of landscape to capture spatial or functional adjacency of landscape elements, such as patches or linear segments. Here, we define a collection of objects with two types, $\mathbf{o} = (\mathbf{o}^C, \mathbf{o}^H)$ (see Figure 2.5a), where $o_i^C = (x_i^C, z_i^C)$, $i = 1, \ldots, n^C$, represent patches (layer C), and $o_i^H = (x_i^H, z_i^H)$, $i = 1, \ldots, n^H$, represent linear segments (layer H); see Figure 2.5b. Thus, patches and linear elements are represented as graph nodes within their layer, and their inter-layer and intra-layer relationships are represented by edges. To define graph connections in mathematical notation, we express that two distinct objects o_1 and o_2 are directly connected through an edge in the graph (i.e., they are adjacent) by using the following notation: $o_1 \sim o_2$, $o_1, o_2 \in \mathcal{O}$. We assume that two patches o_i^C, o_j^C are connected, $o_i^C \sim o_j^C$, if they are adjacent, i.e., if they share part of their physical boundary. Two linear elements are connected if they intersect or have a vertex in common. Finally, inter-layer connections $o_i^C \sim o_j^H$ arise if the linear element o_j^H is located on the boundary of patch o_i^C. Based on this landscape representation, we develop parametric probability distributions over the set of possible allocations $\boldsymbol{x} \in \mathcal{X}$, conditional on the (fixed) information in $\boldsymbol{z} = (z_1, \ldots, z_n)$ and on their structural adjacency.

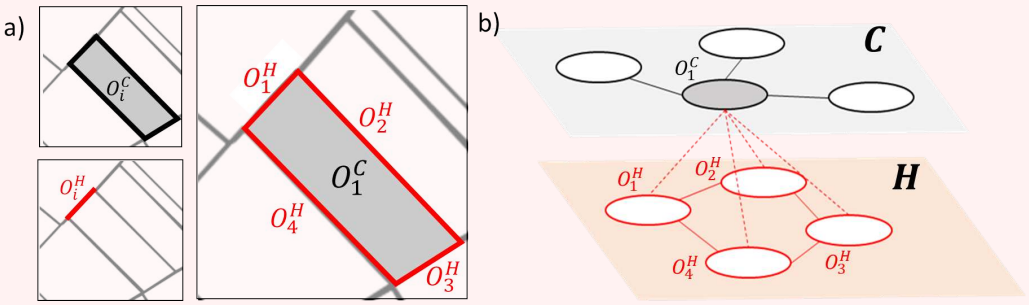

Figure 2.5 – Landscape representation. a) Polygon objects (patches, in grey) and linear segment objects (in red). b) Multi-layer network of connections. Layer C: single network layer of connections between patches; layer H: single network layer of connections between linear elements; links between C and H represent connections of patches and linear elements.

Probabilistic mechanistic models for landscape descriptors

Given the multiplex network structure, we utilize Gibbs energies to define probabilistic models of mechanistic nature, including Markov processes; see, e.g., Cressie (1991); van Lieshout (2019). We construct a model using m functions $T_k : \mathcal{X} \to (-\infty, \infty)$, $k = 1, \ldots, m$, that each measures the value $T_k(\boldsymbol{x} \mid \boldsymbol{z})$ of a summary statistic for the allocations in $\boldsymbol{x}$ given the fixed information in $\boldsymbol{z}$. The functions T_k take the role of *landscape descriptors* (see Figure 2.3 for some examples) and are used

as sufficient statistics of the Gibbs model by defining the probability of observing an allocation $\boldsymbol{x}$ as follows, with coefficient vector $\boldsymbol{\beta} \in \mathbb{R}^m$:

$$p(\boldsymbol{x}) = \frac{1}{c(\boldsymbol{\beta})} \exp\left(- \sum_{k=1}^{m} \beta_k T_k(\boldsymbol{x}) \right), \quad \boldsymbol{x} \in \mathcal{X}, \quad \boldsymbol{\beta} \in \mathbb{R}^m. \tag{2.1}$$

The theoretical notion of sufficient statistics means that the functions T_k encapsulate all the information that the model uses to assign a probability of occurrence to the landscape structures $\boldsymbol{x}$. In particular, if we want to estimate the parameters $\boldsymbol{\beta}$, all the information that can help with their estimation is contained in the values $T_k(\boldsymbol{x})$. The normalizing constant $c(\boldsymbol{\beta}) > 0$, also known as the partition function, ensures that probabilities in (2.1) sum up to 1, but it is often very difficult (*i.e.*, computationally prohibitive) to evaluate. However, by considering the following conditional probability of allocation of one landscape element given the allocations of all the other landscape elements, the normalizing constant $c(\boldsymbol{\beta})$ cancels out:

$$p(x_i \mid \boldsymbol{x}_{-i}) = \frac{p(\boldsymbol{x})}{\sum_{y \in \mathcal{X}_i} p(\boldsymbol{x}_{-i}, x)} = \frac{\exp\left(-\sum_{k=1}^{m} \beta_k T_k(\boldsymbol{x})\right)}{\sum_{x \in \mathcal{X}_i} \exp\left(-\sum_{k=1}^{m} \beta_k T_k(\boldsymbol{x}_{-i}, x)\right)}, \tag{2.2}$$

where the denominator adds up the probabilities over all landscape structures obtained when varying the category of o_i but keeping the rest of the landscape fixed. In the two-level case with $x_i \in \{0, 1\}$, in the following we show how parameters β_k can be estimated through classical logistic regression.

Statistical inference

For estimation, we use a pseudo-likelihood based on conditional distributions; see Besag (1972, 1974); Møller and Waagepetersen (1998); van Lieshout (2000); Stoehr (2017), and particularly Section 3.5 of van Lieshout (2019). Given n objects $\boldsymbol{x} = (x_1, \ldots, x_n)$ with their allocation categories, we define the pseudo-likelihood as the product of the conditional probabilities of the category x_i given all the other variables $\boldsymbol{x}_{-i}$; i.e., it is the composite likelihood (Varin et al., 2011) of conditional distributions given as

$$\mathcal{L} = \prod_{i=1}^{n} p(x_i \mid \boldsymbol{x}_{-i}, \boldsymbol{z}) \tag{2.3}$$

where the conditional probability $p(x_i \mid \boldsymbol{x}_{-i}, \boldsymbol{z})$ is defined in Equation (2.1) and does not depend on the unknown normalizing constant $c(\boldsymbol{\beta})$.

We propose approaches to statistically compare models with different landscape descriptor configurations and to assess their goodness-of-fit, for instance by comparing maximum pseudo-loglikelihood values or the Mean Squared Errors (MSE) based on k-fold cross-validation. To rank models, we could also use formal information criteria that take the model complexity (*i.e.*, the number of parameters) into account to avoid overfitting, which allows identifying parameter configurations that are both parsimonious and informative. Standard likelihood-based information criteria (AIC, BIC) are not easily adaptable to our pseudo-likelihood approach if we want to

compare models that have a different number of parameters, but it is possible to rank models with the same number of parameters (and therefore with the same penalty for model complexity) based on their maximum pseudo-log-likelihood value. To compare models with different numbers of parameters, we focus on predictive criteria such as MSE, calculated using cross-validation techniques.

Application to the Lower Durance Valley

Spatial domain definition and characterisation

We implement our framework on the Lower Durance Valley as case study using three different domains, see Figure 2.6a. We select three subdomains D1, D2 and D3 with contrasting properties and dimensions, shown in Figure 2.6b and numerically summarized in Table 2.1: D1 is relatively small and with low crop proportion; D2 has the same surface area but equal proportions of crop; D3 delimits a much larger domain including D1 and D2. We allow for two allocation categories of both patches and linear elements: *crop* or *alternative crop* (network C) ; presence or absence of a hedgerow (network H).

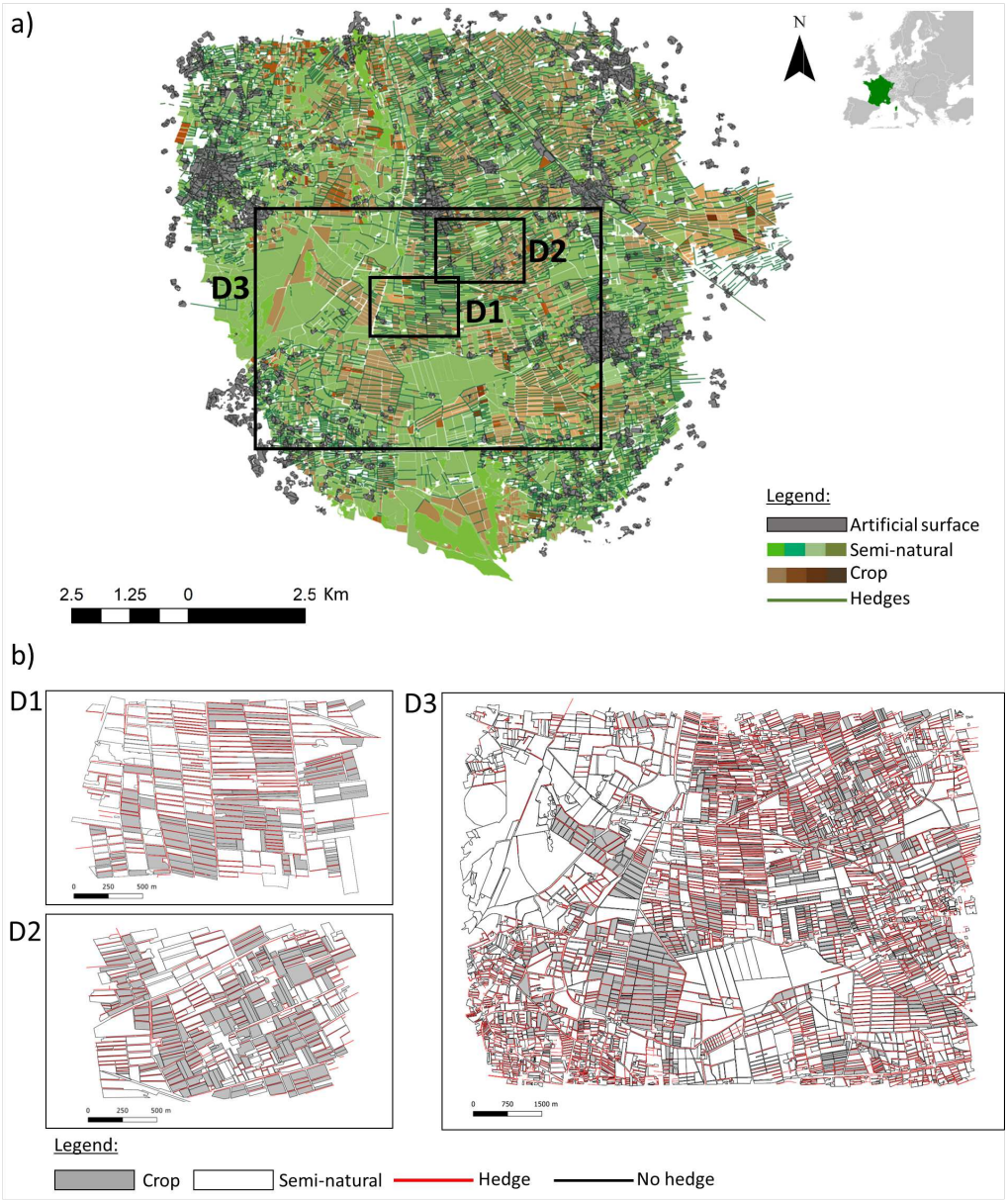

Figure 2.6 – Lower Durance Valley study area. a) Full area with three subdomains. b) Subdomains D1, D2, D3. The Lower Durance Valley is characterised mainly by agricultural land cover: green-shaded patches represent SNHs (i.e., woods, open area, grassland); brown-shaded patches represent 34 different cultures (e.g., apple, pear, vineyards). Artificial surface (dark gray) consists of built structures and urbanized area. The area is rich in linear elements (*i.e.*, segments), including small water courses, roads and hedges (Panel a). In the selected domains (Panel b), we selected as "crop" the category of “apple/pear orchard", as it is the most abundant culture (gray patches), and we simplify the rest of the landscape surface using the level alternative crop (white patches) in order to establish a continuous cover with two categories. Patch boundaries are presented as linear elements, which are marked in red when hedges are present.

	D1	D2	D3
Area (km^2)	3.3	2.3	41.1
% of Alternative crop	73	50	76
% of Crop	27	50	24
Hedgerows (km)	44.6	33.6	386.4
No. of patches	368	468	4379
No. of linear segments	1105	1405	12517

Table 2.1 – Summary of selected subregions of the Lower Durance Valley study area; see Figure 2.6.

We consider four models, denoted M1–M4, to test different combinations of landscape descriptors, see Box Eq. (2.1). Table 2.2 (top) illustrates relevant choices of landscape descriptors at local level (*i.e.*, evaluated for each object), such as geometrical properties and adjacency. We also consider landscape descriptors providing a more global perspective, such as a descriptor for *connected components* of landscape elements of the same category (see also Møller and Waagepetersen, 1998, which highlight Markov-like properties in this case). Table 2.2 (bottom) shows models and descriptor combinations, where descriptors are selected checking the correlation among them. In the Supplement of the manuscript Zamberletti et al. (2020) (Supplement 1.2), the temporal dynamic is also discussed to simulate crop rotation. In our application, we do not show an example of temporal dynamics since we do not have dynamic land cover data. However, we have formulated and detailed the specification and implementation also for this type of *landscape descriptor*.

Examples of landscape descriptors		
Composition	Activity term	T^{C}_{act}, T^{H}_{act}
	Patch area	$T^{C}_{\text{area,p}}$
	Long segments	T^{H}_{length}
	Horizontal segments	T^{H}_{orient}
Interaction (Adjacency)	Patch-patch	T^{CC}_{adj}
	Segment-segment	T^{HH}_{adj}
	Patch-segment	T^{CH}_{adj}

Landscape models		
	C	H
M1	T^{C}_{act}, $T^{C}_{\text{area,0.25}}$, $T^{C}_{\text{area,0.75}}$, T^{CH}_{adj}, T^{CC}_{adj}	T^{H}_{act}, T^{H}_{length}, T^{H}_{orient}, T^{HH}_{adj}
M2	cf. M1	T^{H}_{act}, T^{H}_{orient}, T^{HH}_{adj}
M3	T^{C}_{act}, $T^{H}_{\text{area,0.25}}$, T^{CH}_{adj}, T^{CC}_{adj}	cf. M1
M4	T^{C}_{act}, $T^{H}_{\text{area,0.25}}$, $T^{C}_{\text{area,0.75}}$, T^{CH}_{adj}, T^{cluster}_{C}	cf. M1

Table 2.2 – Examples of landscape descriptors (top) and model configurations (bottom). Notations: C and H refer to patches, and linear elements, respectively. Landscape models show descriptors related to crop patches in network C, and to hedges in linear element network H.

Parameter estimation

We performed parameter estimation for all possible combinations of spatial domains and models. Here, we discuss an example showing a comparison among estimated parameters for different spatial domains (*i.e.*, D1, D2 and D3) with the same model (Figure 2.7). Boxplots of estimations are obtained by the parametric bootstrap using 100 simulations. The parametric bootstrap consists of generating simulations from the estimated model and of re-estimating the parameters for the simulated models. We detect no bias in the estimators since the parameters estimated for the real landscape always lie in the central region of the values obtained of bootstrap estimations. Moreover, we find that all estimated parameters are significant for the Markov interaction in the networks C and H (positive coefficient of C-C, H-H), for the area descriptor (negative coefficient of *Small area* and of *Large area*), for

the hedge orientation descriptor (positive coefficient of *Horizontal H*), and for the activity terms. No strong signal is found for a dominance of long hedge segments (*Long H*) in D1 and of Markov interaction between C and H. All descriptors are significant for the large domain D3. The signs of estimates are the same across D1–D3 for all significant effects, implying structurally similar behavior. Overall, estimated parameters tend to have comparable magnitudes across D1–D3. Given the parameter estimates of our model, the crop category is usually less allocated on relatively small and relatively large fields. Crop fields and hedges tend to cluster in space, *i.e.*, they tend to be allocated on adjacent patches and linear elements, respectively, such that they provide relatively large and contiguous habitats, and relatively long continuous movement corridors. There is a dominating horizontal orientation of hedges for protecting against strong North-South winds in the study region. Crop-hedge adjacency has negative coefficients and is significant only for the large domain M1-D3, suggesting a slight tendency of hedges to not being directly adjacent to crop fields. In M1-D2, we discern a particularly strong signal of *Long H* indicating many short, strongly horizontally oriented hedges.

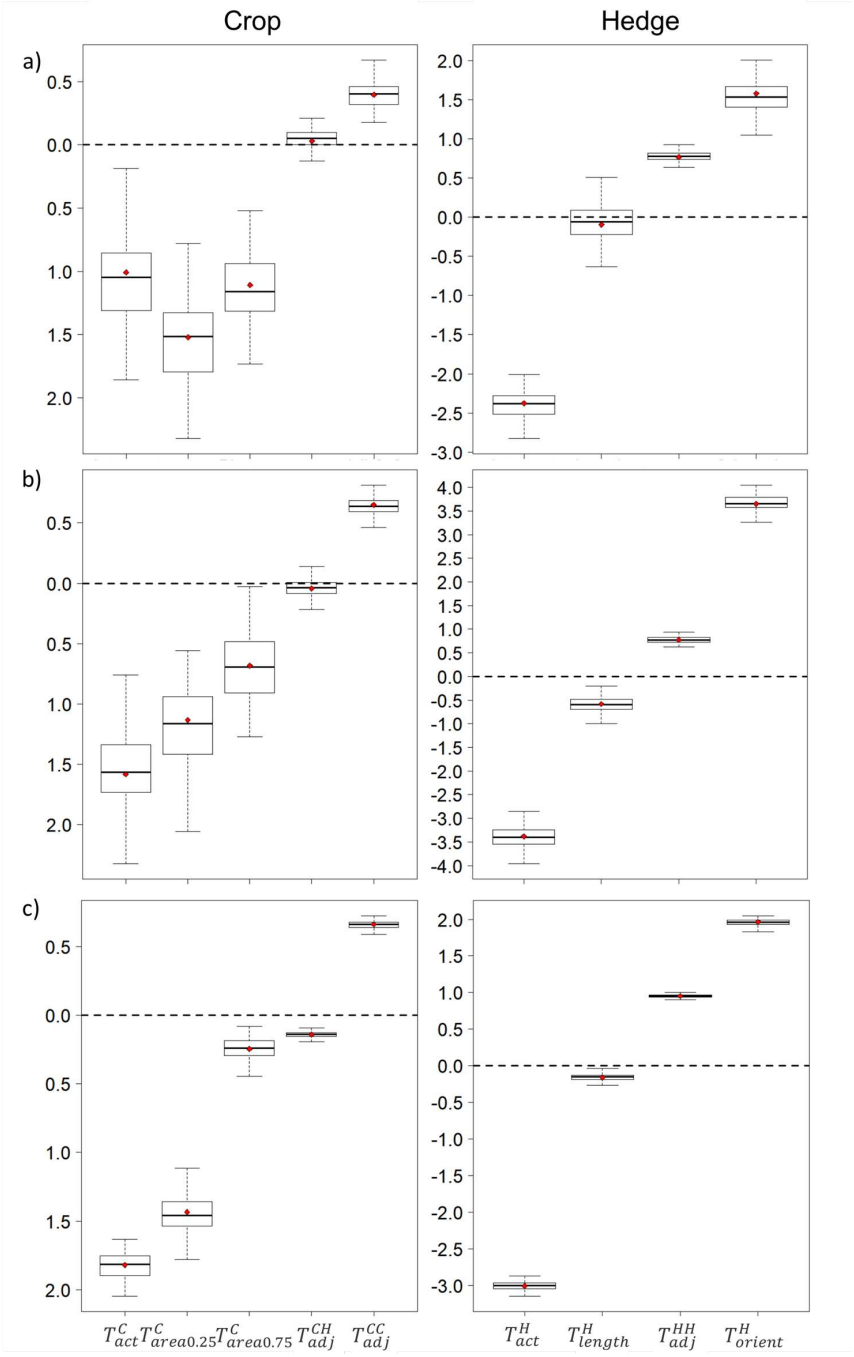

Figure 2.7 – Boxplots obtained through a parametric bootstrap of estimated parameters from model M1 over spatial domains D1 (Panel a) D2 (Panel b), D3 (Panel c) for crop (left) and hedges (right), see Figure 2.6. Descriptors are defined in Table 2.2

Model validation

We check if landscape descriptors, as well as the variograms and the graph- and raster-based metrics we introduced, are appropriately reproduced by the models. Here, we focus on the performance results in D1 for crop allocation by showing the comparison among different models M1-M3-M4. Figure 2.8 shows observed and simulated landscape descriptors, i.e., sufficient statistics for the estimated coefficients. Models M1, M3, M4 tend to produce realistic values, especially M1.

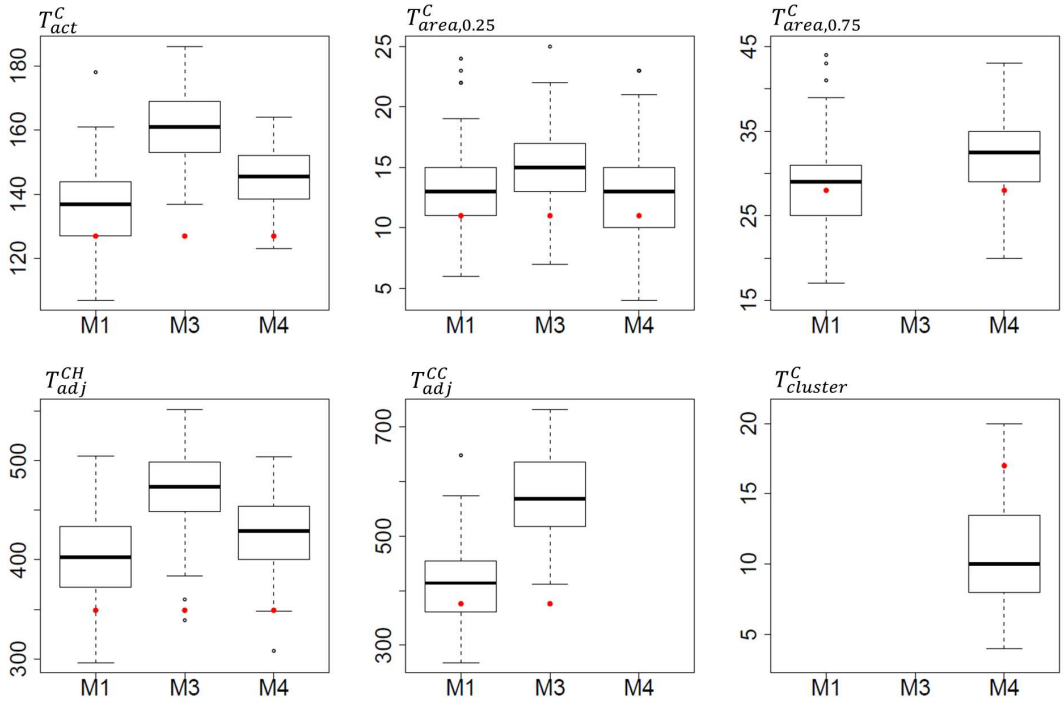

Figure 2.8 – Landscape descriptors for domain D1 and network C (Crop) in M1, M3, M4. Boxplots summarise 100 simulations of fitted models. Red dots are observed values.

Figure 2.9 shows empirical one-category (Crop) and two-category (Crop-Hedge) variograms with pointwise simulation envelopes. All variograms show a relatively steep slope at the origin and tend to flatten for larger distances, such that the general shape of the empirical data variogram is well reproduced by the models. In several cases, especially with M3, empirical variograms of the dataset clearly fall outside the envelope, such that the observed variability of landscape features with distance is not appropriately captured. In general, the structure of M1 (with the large patch area descriptor, and Markov interaction for crops) improves the match between data and model variograms, in contrast to M4 using the global interaction descriptor based on the number of connected components.

For network-scale metrics (last row of Figure 2.10) we show the real landscape value

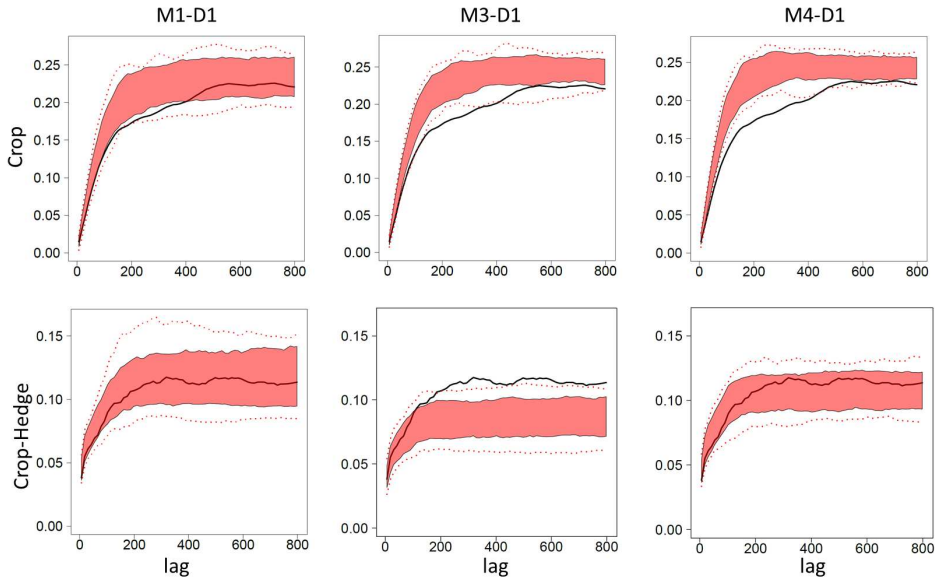

Figure 2.9 – Variogram analysis of models M1, M3, M4 for domain D1. One-category variogram for crop (top row); two-category variogram for crop and hedges (bottom row). Empirical variogram of observed landscape (black line); pointwise simulation envelopes (red-shaded area: 5%-95%; dotted red lines: minimum/maximum).

within the boxplot of simulated values. Observed metrics fall within or close to the interquartile range of the simulated ones for the crop network, while they lie outside the boxplot whiskers for the hedge network but are still of the same order of magnitude. Model M1 does not directly control the number or dimension of clusters, only local interactions through the Markov model. This explains better performance for *neighborhood-based centralities* in comparison to *path-based centralities* and metrics. However, in the Supplement 1.5 and 1.7, we show that using a global descriptor instead of a local descriptor in M4 does not substantially improve performance for path-based centralities; see Section 7. Raster-based landscape metrics of FRAGSTAT (McGarigal and Marks, 1995) are shown in Figure 2.11. In most cases, the observed metrics fall within the whiskers of the boxplots, and in the other cases the order of magnitude is still relatively well captured by the fitted model.

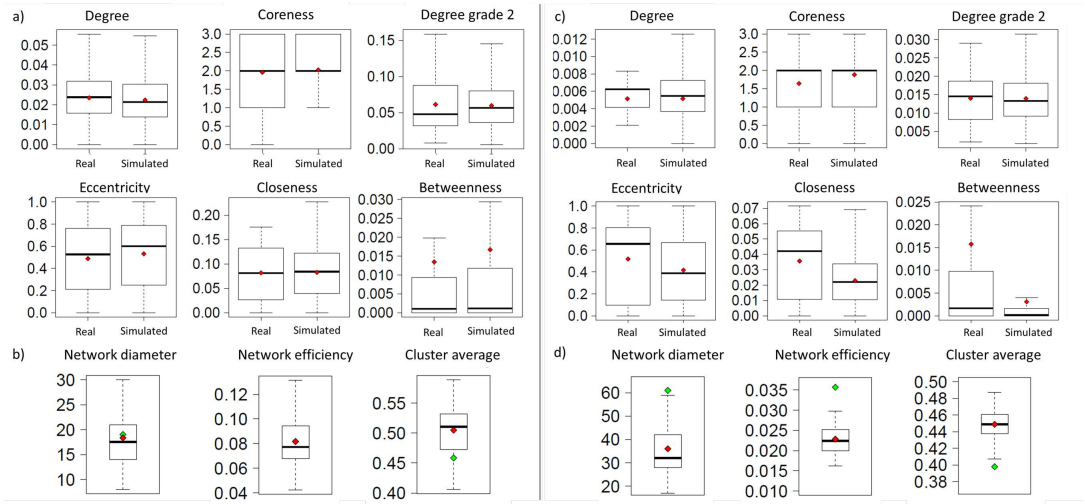

Figure 2.10 – Validation metrics M1-D1 for crop network *C* (left) and hedge network *H* (right). Panels a,c: metrics at node scale (red dots: mean values). Panels b,d: metrics at network scale (boxplots: simulations; red dots: mean values of simulations; green dots: observed values.

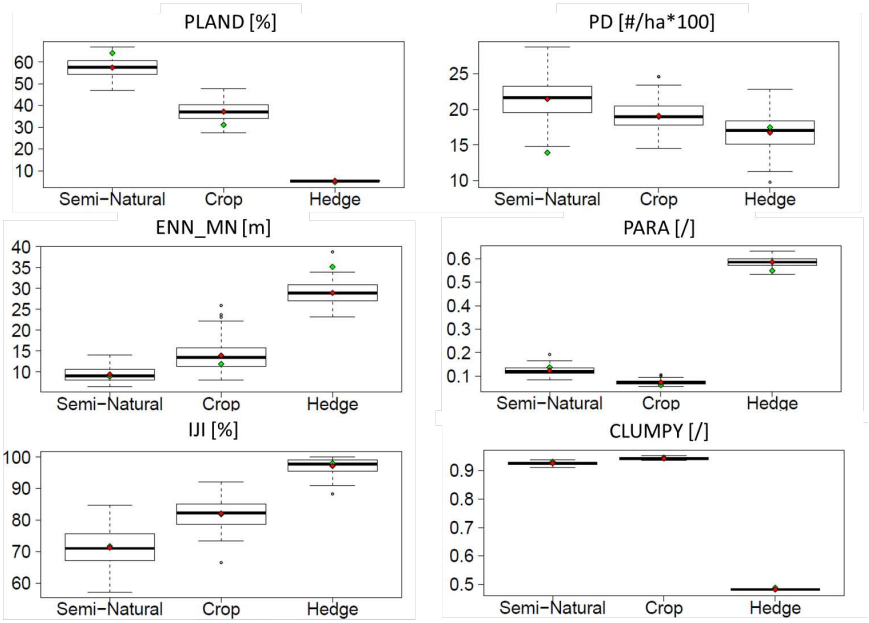

Figure 2.11 – Raster-based metrics for M1-D1. Simulated values (boxplots); mean of simulated values (red dots); observed value (green dots).

2.3 Discussion

We have developed stochastic agricultural landscape models and statistical inference with a focus on the land-use allocation of patches and linear elements. Both GRF and Markov models turn out to be intuitive and flexible tools for simulation and offer direct control and interpretation with respect to local behaviour. These approaches allow handling relatively large landscapes by capitalising on low computational requirements due to vector-based representations and to adjacency-based networks numerically represented through sparse matrix structures for encoding interactions. Specifically, we have introduced the following methodological novelties:

i) Mathematical representation of landscape compositions and configurations through multiplex networks. Specifically, we focus on the integration of different landscape elements interacting among each other (*i.e.*, patch and linear elements).

ii) Generative stochastic parametric models coupling land-use allocation of patches and linear elements, relying on Markov interactions based on the network established in (i);

iii) Model simulations through Markov Chain Monte Carlo (MCMC) using a Gibbs sampler that is fast, and simple to implement;

iv) Statistical inference of model parameters using real landscapes;

v) Validation of relevant landscape characteristics based on statistical model selection tools and on a comparison of summaries for vector and raster representations between real and simulated landscapes.

We point out that vectors do not require to fix a specific grid resolution and, therefore, give better control over small-surface elements, and provide a sparser and more functional representation of patchy geometric structures. Moreover, a strength of our approaches is that they are geared towards flexible and realistic parametric stochastic modeling of fringe structures, such as hedgerows.

The first modeling approach is relatively simple since its construction is based on GRFs. By contrast, it allows easily dealing with large landscapes while maintaining a relatively high degree of flexibility to control surface and linear element interactions. Thus, it appears to be well suited for generating diverse landscape structures while balancing computational complexity, parameter number and flexibility. We here have not developed statistical inference for the model parameters in this approach (*i.e.*, covariance parameters and thresholds for the GRFs), but it could be achieved using standard geostatistical estimation approaches. In the Markov model, using a network-based representation of interactions among landscape elements, we construct Gibbs energies based on network structure (see, e.g., the recent collection of papers introduced by Fienberg, 2010), and more specifically models pertaining

to the class of discrete Markov random fields, see Hammersley and Clifford (1971); Besag (1972); van Lieshout (2000); Green et al. (2003); Gaetan and Guyon (2010); van Lieshout (2019). The advantage of using Gibbs energies and Markov structures is that this setting provides a natural distributional framework for controlling various landscape descriptors. This allows for higher flexibility with the possibility to select the most suitable descriptors for each landscape. By contrast, this may result in a higher level of complexity depending on the number of descriptors considered and on their definition. Here, we have focused on descriptors based on single objects or on pairwise Markov interactions, which leads to robust modeling, estimation and simulation procedures. We found it generally difficult to improve models by the use of more globally specified interaction descriptors. We highlighted the flexibility of the approach by comparing outcomes of different models over the same domain. We also tested models over domains having different characteristics and size.

A motivation for our approach was that previously existing modeling frameworks lack statistical tools for parameter inference and model validation. Validation procedures are usually solely based on visually checking whether simulated landscapes are able to reproduce realistic landscape features by comparing observed and simulated landscape metrics (e.g., from the FRAGSTAT library, McGarigal and Marks, 1995). Such metrics are often directly used within simulation algorithms to enforce convergence towards target values (Langhammer et al., 2019). Besides introducing formal statistical tools for selecting descriptors and models, we here check more systematically if the fitted model is able to appropriately reproduce three types of summaries of the real landscape. Overall, the descriptors of the model and other landscape metrics are satisfactorily reproduced by simulations from models fitted to Lower Durance Valley data. From our detailed model comparison, we identify that some models have a better performance than others in reproducing real landscapes. This essentially depends on the combination of landscape descriptors considered and their correlation. However, not all relevant metrics can be reproduced through our model without bias. For example, the grid discretization of space in the raster approach may produce instabilities in treating small-scale small-area patterns, especially those related to linear segments. Linear element allocation also showed some discrepancy between model and data for large-scale clustering properties. To remedy the issue of appropriately simulating an important landscape summary that is not directly controlled by the model, we can add additional constraints during simulation, using techniques such as Simulated Annealing (e.g., Papaïx et al., 2014a).

To conclude, vector-based models such as ours are more parsimonious and meaningful from an ecological point of view (Gaucherel et al., 2012; Bonhomme et al., 2017), and they enable explicit handling of different spatial and temporal scales. In raster-based approaches, an appropriate representation of small-surface elements such as hedges would require a very high and computationally unwieldy resolution, where a homogeneous large-surface patch would be made up of a very large number of pixels, instead of a single geometric

object in our model. Our multiplex network structure assures low computational cost and memory requirements. The parameter estimation and validation assure the possibility of reproducing properties similar to real landscapes in the simulation; and the generative stochastic parametric model simulation through MCMC allows the generation of a high number of statistically similar landscapes.

Perspectives and open questions

- Coupling the Markov model with the GRF model to improve the consideration of large scale properties as long as small scale properties. Indeed, the GRF model performs very well in simulating large-scale properties; instead, Markov models allow for better taking into account local properties in an accurate way. Coupling would be possible by extending the Markov model to have a GRF in its activity term. This will introduce a spatial random effect that controls large-scale differences in the local proportions of different category levels, such as crop and alternative crop. This extension would unite the benefits of the two models and allow for higher flexibility.

- Extending the presented Markov model to n possible categories for estimation and pattern analysis. It is possible to implement the Markov model with more than two possible categories for landscape elements in order to estimate and simulate more complex landscapes and land-use types. For this purpose, the logistic likelihood estimation approach must be replaced by a more generic maximum pseudo-likelihood technique. MCMC-based simulation remains straightforward.

- Extending the use of Gibbs to a more general and flexible modelling framework. Gibbs energies could be used to model and simulate more general numeric labels (e.g., continuous variables) associated with landscape elements, for instance the crop yield in a field, or the proportions of a crop field used for specific crop types when several crops are planted in the same field in some small-scale-alternating way. Then, the proposed approach could be extended to more general models of the so-called exponential family type (e.g., Brown, 1986).

- Applying our approach over different landscape to allow for comparison among landscape structures and specific features. It would be interesting to develop a fully automated variable selection method in order to effortlessly identify the most suitable landscape descriptors for each landscape type, yielding models where we retain a moderate number of representative parameters.

- Developing and estimating time dynamics on real landscapes. The integration of temporal descriptors, as illustrated through the simulations in Supplement 1.2, would be an interesting perspective for future development of such classes of models. This

extension would allow us to consider processes such as crop rotation, which we cannot estimate for the case study dataset due to lack of dynamic land-cover allocation data.

- Establishing statistical modeling and simulation for the landscape including its geometrical support. We intend to integrate the allocation model with (existing) generative tessellation model for the geometrical support. This would establish a more holistic modelling of the configuration and composition of the landscape (Kiêu et al., 2013; Adamczyk-Chauvat et al., 2020).

- Integrating the stochastic landscape model for land-use allocation with human decisions. To provide operationally relevant management tools, we could couple our stochastic allocation model with decision tools for agricultural optimisation where an appropriate land-use allocation strategy for the desired management objectives is identified. In fact, currently we cannot directly model human action in the temporal dynamics of agricultural environments (Bonhomme et al., 2017; Poggi et al., 2018), for which we would have to couple our model with a decision tool.

Part II
Predator-pest dynamics in agricultural landscapes for biological control outcomes

Figure 2.12 – Ladybird (*Coccinellidae*) preying on aphids. © BBC

Chapter 3

Predator-pest dynamics in agricultural landscapes for biological control outcomes

In Part 1, we have put the focus on the characterisation of agricultural landscapes in order to be able to depict their proper structures and to define a consistent spatial domain where to simulate the ecological processes of interest. We have specifically modeled various landscape elements, such as linear elements or patches, to take into account their properties and to separately and jointly consider their effects. Moreover, we have taken into consideration various landscape properties and features to perform land-use category allocation, which determines habitat composition and configuration. The indicators and validation metrics we proposed may also give guidance to gain new insights on ecological processes. The stochasticity of models with its inner structure of Markov random field type allows us to virtually generate statistically similar landscapes using representative model parameters, which could support the analysis of robustness and sensitivity for both landscape and population models.
In Part 2, we use the landscape model presented in Part 1 to simulate population dynamics of predator-pest type, which allows us to investigate how the spatial heterogeneity of complex landscapes influences ecological dynamics and the resulting biological control (BC) outcomes.

3.1 Landscape ecology

The relationships between spatial pattern and ecological processes go under the definition of landscape ecology. As stated by Risser (1987), *landscape ecology* focuses explicitly upon

spatial patterns, considering the development and dynamics of spatial heterogeneity, spatial and temporal interactions and exchanges across heterogeneous landscape, influences of spatial heterogeneity on biotic and abiotic processes, and management of spatial heterogeneity. Specifically, landscape ecology recognises and addresses the importance of the spatial composition (*i.e.*, number of habitats) and configuration (*i.e.*, habitat arrangements) in influencing ecological processes (Turner et al., 2015). Moreover, the focus is not restricted to a specific spatio-temporal scale, rather the emphasis is on identifying the scales that best explain the relationships between spatial heterogeneity and the processes or response variables of interest (Turner et al., 2015). The main aim is to understand the interactions of organisms with their environment and how they deal with spatial heterogeneity. This is of fundamental importance since most landscape patterns are continually altered by natural disturbances and human activities, affecting the relative abundance and spatial arrangement of different habitats and/or habitat quality (Turner et al., 2015). Thus, in order to meet sustainability goals and preserve ecosystem functioning, there is strong interest in investigating the influences of such changes on the distribution, abundance and persistence of species across landscapes and their consequence on ecosystem functioning. Specifically, there are some key landscape elements that have been reported to influence species dynamics:

- *Patch size*: Patch size is an important characteristic of landscape structure: larger and more heterogeneous patches contain more species and often a greater number of individuals than smaller and more homogeneous patches of the same habitat (Kappes et al., 2009). In fact, an increase in within-patch heterogeneity (*e.g.*, vertical complexity, micro-site variety) will generally increase species richness. However, despite many observations of species richness increasing with patch size, the effect of patch size alone cannot easily be determined as it is influenced also by the conditions of the surrounding landscape (Wiens, 2002).
- *Edge*: Also habitat boundary abundance is capable of influencing species diversity within a patch, specifically Fagan et al. (1999) listed major effects: i) boundaries may be barriers or filters to movement, ii) agents which alter mortality rates, iii) areas providing energetic subsidies or refuge, and iv) regions where novel inter-species interactions may occur.
- *Corridors*: Corridor creation can promote movement to connect habitat patches and facilitate the flow or movement of individuals, genes, and ecological processes, and thus can increase population persistence by providing an exchange of individuals among a population. Since corridors are strongly influenced by edge effects, their interior habitat is often minimal and may even be absent (Wiens, 2002).
- *Surrounding landscape*: Characteristics of the surrounding landscape (*i.e.*, matrix) affects local populations within a patch as species presence, abundance and diversity at a given location or within a particular patch is often explained by characteristics of the focal patch, by landscape context and by its connectivity (Roschewitz et al., 2005).

3.2 Why the predator-pest landscape relationship is not an easy matter

In spatially complex landscapes, predator–prey dynamics result from the interaction among landscape structure and species dynamics as spatial patterns can influence organism movements and distribution, thus influencing the probability of prey encounters and kills (Hebblewhite et al., 2005) and the effectiveness of predator strategies (Andruskiw et al., 2008). In agricultural landscapes, the relationship among heterogeneous landscape structure and population dynamics has been mostly considered for insect species, particularly for cases where natural enemies may be predators that help to keep crop pests at low density (Tscharntke et al., 2007). Landscape composition and configuration affect the diversity and abundance of the natural enemy community since different habitats could enhance the presence of different natural enemy species, how they move within and among the habitats and how they use the different resources. Thus, a diversified agricultural landscape mosaic is expected to sustain a broad diversity of predators. Specifically, non-crop habitat may play an important role as it provides often favourable habitats for predators and acts as source habitat from which the less favourable agricultural fields are invaded (Bianchi et al., 2006). However, Bianchi et al. (2006) review different studies that investigate if herbivores biological control (BC) is enhanced in complex landscapes with a high proportion of semi-natural habitats (SNHs). They found that there is considerable variability in species responses to landscape structure, indicating that there is no trivial relationship among landscape complexity and pest suppression (Bianchi et al., 2006; Rusch et al., 2010). Another example is reported by Martin et al. (2013), who evaluate the role of landscape context on pest densities and crop yield and find that herbivore (pest) pressure is greater rather than less in landscapes with more SNHs. There are different explanations behind this relationship: i) SNHs are prerequisite for many organisms, but effects are often taxon-specific (Martin et al., 2019); ii) SNHs may host also different pest species (Chaplin-Kramer et al., 2011a; Tscharntke et al., 2016b); iii) pest and natural enemy species traits and behaviours influence species responses to landscape heterogeneity (Hanski and Mononen, 2011; Legrand et al., 2017; Bonte and Bafort, 2018); iv) negative interactions may arise among different natural enemy species, such as intra-guild predating (Tscharntke et al., 2016b; Letourneau et al., 2009). This suggests that landscape composition and configuration are key in determining biodiversity (Fahrig, 2013), but this is not the only criterion that should be considered when assessing the effect of landscape structure on biological control. Therefore, it is demonstrated that no clear general trends arise, and all the empirical studies present outcomes that are strongly site-specific and valid under distinct conditions.

3.3 Modelling the predator-pest system in the agroecological context

Different experimental approaches can be useful to elucidate biodiversity effects in ecosystems. They show inherent strengths and weaknesses regarding precision, realism, and the possibility of hidden pesticide applications among empirical and experimental comparisons (Letourneau et al., 2009). Aside from these empirical studies, modeling approaches are likely to prove an interesting strategy for assessing the relationships among natural enemy-pest dynamics, landscape structure and BC, but they are based on simplifying assumptions and can not capture all the details of reality (Rusch et al., 2010). Here, our goal is to focus on how different scenarios among landscape structure and different population traits and behaviours may influence pest regulation. In this complex system, it would be difficult to sample every possible combination of conditions or to conduct experiments at the ideal spatial and temporal scales. An empirical approach would not be exhaustive and it would result in a case-study-specific approach. Hence, our choice of coupling a model considering both 2D elements (*i.e.*, patches) and 1D elements (*i.e.*, linear elements) with a population dynamics model is developed to theoretically study a wider range of scenarios and to present a general approach, which could subsequently be adapted for more specific case studies. In our case, the population dynamics model aims to represent the predator-pest relationships among predators and pests.

Understanding and explaining pattern and scale through models is a central problem in landscape ecology (Levin, 1992). Models in ecology could treat the space in an implicit or explicit way. Many theoretical concepts of spatial ecology are treated by spatially implicit models (SIMs), which account for the effects of space with assumptions or parameters without specifying spatial positions (Cantrell and Cosner, 2004). SIMs have the advantage of being simple and broadly applicable, allowing modelers to develop relatively general theoretical outcomes (DeAngelis and Yurek, 2017). The major example of treating both space and population dynamics implicitly is given by the MacArthur and Levins (1967) models for island biogeography and by the classical metapopulation model of Levins (1969a). These models describe populations strictly in terms of their presence or absence and account for patterns of occupancy by balancing stochastic colonisations and extinctions. However, addressing also questions concerning populations or communities in specific positions is needed, since local conditions and organism behaviours may produce dynamics and patterns that cannot fully incorporated into SIMs (DeAngelis and Yurek, 2017). Spatially explicit models (SEMs), instead, are able to describe mechanisms at different spatio-temporal scale. There are many types of SEMs, such as patch models (Hanski, 1994), reaction-diffusion partial differential equations (Cantrell and Cosner, 2004), cellular automata (CA) neighbourhood models (Hogeweg, 1988), and individual-based models (IBM) (Pacala and Silander Jr, 1985).

An advantage of metapopulation and source-sink approaches is that such model's are based on a discrete network of patches and allow for the assessment of the effect of habitat heterogeneity in a straightforward way (Pitt, 2008). For example, Bascompte and Solé (1998) develop a metapopulation model to study the effect of habitat destruction and fragmentation on a predator-pest system. They confirm that the response to habitat fragmentation depends not only on the critical behaviour of the landscape structural properties, but also on the biological properties of the metapopulation as the trophic level, colonisation and extinction probabilities. In general, the higher trophic-level species goes extinct sooner than the lower trophic-level species (Bascompte and Solé, 1998). They discuss that this is a key results in the context of BC since pest enemies belong to higher trophic levels (Hawkins et al., 1993). When differences between patches are considered, it may be relevant to consider source–sink models as patches with excess reproduction are source patches, and sink patches occur when local mortality exceeds reproductive success (Turner et al., 2015). However, the discrete vision of the metapopulation does not correspond to the real environment, a 2D spatial domain, and there is the need to consider patterns in ecological modelling to depict more robust relationships among species spread, their establishment and environmental conditions at different spatial scales (Lonsdale, 1999). Pest and enemy species invasion and dynamics have been often addressed by reaction-diffusion models in homogeneous and heterogeneous environments (Roques et al., 2008; Parisey et al., 2016; Ciss et al., 2014). This is a wide class of spatial models, which treat the space as a continuum and describe the distribution of populations in terms of densities (Skellam, 1951; Shigesada and Kawasaki, 1997; Okubo and Levin, 2013). These models aim to translate local assumptions or data about the movement, mortality, and reproduction of individuals into global outcomes about the persistence or extinction of populations and the coexistence of interacting species (Cantrell and Cosner, 2004). An example is offered by Roques et al. (2008), who propose a two-dimensional reaction-diffusion model to predict the expansion and impacts of an exotic, specialist seed chalcid, *Megastigmus schimitscheki*, which has been introduced into southeastern France from Turkey. The comparison among these models considering different dispersion operators shows that taking account of spatial heterogeneity effects on the individuals' mobility could have an important impact on the predicted attack rates, as it results in lower or higher estimations depending on the diffusion operator selected. Two other types of spatially explicit models which treat space as a discrete grid are IBM (Durrett and Levin, 1994) and CA (Hogeweg, 1988) where each point of the spatial grid has its own event history (Cantrell and Cosner, 2004). Differently, for IBM, the focus is no more on the space, but on the single individual. These models allow exploring variability among individuals, local interactions, complete life cycles, and in particular individual behaviour adapting to the individual's changing internal and external environment (Grimm et al., 2006). However, this great potential of IBMs also is a drawback due to the complexity of the model structure as compared to analytical models. Their outputs are also more difficult

to analyse, understand and communicate than traditional analytical models (Grimm et al., 2006). An example of pest regulation through IBM is presented by (Le Gal et al., 2020), who present an IBM to focus on the role of SNHs for conservation BC. They highlight the important influence of the interplay between the landscape structure and the timing of BC measures on the delivery of pest control services. In their study, increasing SNH proportion at the landscape level enhances the visitation rate of pest-colonised crop, but it also reduces the delay between pest colonisation and predator arrival at the crop fields (Le Gal et al., 2020).

In our work, we have decided to firstly focus on the landscape characterisation to better take into account the main elements that may be key for modelling population dynamics where we pay attention to the composition of habitat patches and linear corridors. This results in a complex landscape composed by a 2D matrix characterising a heterogeneous surface and 1D linear elements characterising edges and corridors. Moreover, since our interest is to answer questions about how different landscape configurations and compositions influence population dynamics in an agro-ecological context, we couple the landscape model with the population dynamic model. This allowed us to explore different combinations of landscape structure and species traits. We describe the predator-pest population dynamics of a pest and its natural predator through a reaction-diffusion model on a 2D-1D spatial domain. We choose a reaction-diffusion model as it can explain three types of spatial phenomena that are important when studying pest and predator dynamics: waves of invasion by exotic species, the formation of patterns in homogeneous space, and the effects of the size, shape, and heterogeneity of the spatial environment on the persistence of species and the structure of communities (Cantrell and Cosner, 2004). We could have used other types of models, such as IBM or CA or interacting particle systems if highly detailed specific predictions were required. However, as said before, major limitations would have arisen with respect to the analysis, the extraction of general properties (Cantrell and Cosner, 2004) and the matching with the landscape model composed by 1D and 2D elements (*i.e.*, 2D1D landscape model). This 2^{nd} Part analyses population dynamics outcomes for BC from a global perspective in the Chapter 4, and the spatio-temporal population dynamics outcomes at local scale in the Chapter 5.

Chapter 4

More pests but less pesticide applications: ambivalent effect of landscape complexity on Conservation Biological Control

In this Chapter, we face the challenge of investigating a more general approach with a model characterising the joint influence of landscape structure and species traits on Conservation Biological Control (CBC) service.

Specifically, we aim to investigate the following research questions: 1) Can landscape composition and configuration reduce the number of pesticide applications by enhancing CBC? 2) How do species traits related to dispersal, predation and population demography modify the effect of landscape heterogeneity?

To answer to these questions, we develop the following main novelties:

i) The simulation of predator-pest dynamics within a 2D-1D landscape representation, allowing for taking into account and investigating the key role of semi-natural corridors within an heterogeneous landscape matrix;

ii) the assessment of the joint effect of species traits and landscape features on the population dynamics and pesticide applications, which allows distinguishing among different effects and their importance on BC outcomes;

iii) the consideration of different spatio-temporal scales, allowing for a global-scale and field-scale characterisation of the population dynamics and BC outcomes.

Our study corroborates that spatial heterogeneity, landscape structure (i.e., the size and physical arrangement of patches), species traits and their interactions play a key role for CBC. Moreover, we also reveal how the relationship of pests and pesticide applications (in case of pest density exceedance above an economic threshold) is shaped by landscape structure. We highlight seemingly unexpected outcomes where hedge presence is not sufficient to ensure a decrease in pest density but still results in a decrease in pesticide applications.

Predator-pest models within agricultural landscapes

The predator-pest dynamics represent the dynamics of the codling moth (*Cydia pomonella*) pest and of one of its main predators, the family of ground beetles (*Carabidae*), in apple orchards. Codling moths respond strongly to the spatial distribution of orchards over landscapes (Ricci et al., 2009). Franck et al. (2011) have found low genetic differentiation among codling moth populations over large distances, but mild genetic differentiation among populations collected on different host plants. In addition, pesticide applications have strong effects on genetic differentiation resulting from spatial and temporal population size variations (Franck et al., 2011). This indicates that codling moths can disperse over large distances in agricultural landscapes, which supports the conjecture that hedges do not substantially impact their dispersal, such that pesticide applications to break the local pest dynamics are important. Thus, in the model, we assume that the pest can be encountered only in fields and that it has positive growth only in fields allocated with crop. In addition, field boundaries do not affect the pest population dynamics; *i.e.*, the life cycle of *Cydia pomonella* is mostly based in apple orchards, and it perceives the landscape as a heterogeneous 2D environment. Finally, we impose the triggering of local pesticide applications when the pest density exceeds a fixed threshold on average in a crop patch.

The presence of semi-natural areas, such as hedges, promotes the presence of pest predators (Maalouly et al., 2013; Thies and Tscharntke, 1999) by offering shelters and by providing complementary resources when pests are not present in fields (Lefebvre et al., 2017). Lefebvre et al. (2017) present a field study investigating the routine movement of arthropods among apple orchards and adjacent hedgerows. They found that there are frequent movements for foraging (to orchards) and for escaping pesticide applications (to hedges), demonstrating the important influence of hedgerows on the presence of numerous predators in apple orchards. Thus, we consider that hedges form the main habitat of the predator. The predator can spill over from hedges to fields and there feed on pest in fields as an alternative resource. However, it is generally attracted to hedges, which are its preferred habitat, so that migration from fields to hedges is relatively high. The predator is known to be averse to moving outside its natural habitat; therefore, migration from hedges to fields is always lower than migration from fields to hedges (Lefebvre et al., 2017).

Coupling the landscape model with the population dynamics model

We use the stochastic landscape model developed in Section 2.1 of Part 1 to generate different agricultural landscapes where we simulate the spatially explicit population dynamics model of a predator-pest system integrating dispersal both on agricultural fields and on the hedge network. Landscape structures are characterised by fields, which can be allocated by crop or an alternative crop that is pest resistant, and by linear elements defining field boundaries, which can be allocated by hedges or no-hedges. Different landscape structures are generated by varying parameters controlling crop proportion, hedge proportion and hedge and crop aggregation (see Table 4.1).

Parameters	Description	Range	Units	Reference
For landscape model				
ϕ	Spatial aggregation of hedges and crops	$[5.55 * 10^{-2} - 5.55]$	km	-
P_c	Proportion of crop	$[0 - 1]$	-	-
P_h	Proportion of hedges	$[0 - 1]$	-	-
ρ	Correlation between crops and hedges GRFs	0.5	-	-
Parameters for population dynamic model				
D_2^v	2D predator diffusion rate	$[0.000625 - 0.012]$	$km^2 d^{-1}$	1,2
$1/m_v$	Predator life-span	$[20 - 66]$	d	1,2
β	Predating rate	$[0.01 - 0.010]$	$pest^{-1} d^{-1}$	2
ρ_{21}	Predator migration rate from field to hedge	0.05	$km^{-1} d^{-1}$	-
D_1^1	1D predator diffusion rate	0.012	$km^2 d^{-1}$	1,2
r_v	Predator intrinsic growth rate	$[0.010 - 0.020]$	d^{-1}	3
K_{h_i}	Predator carrying capacity in hedge	1	$predatorskm^{-2}$	-
ρ_{12}	Predator migration rate from hedge to field	$[0 - 0.05]$	d^{-1}	-
D_2^u	2D pest diffusion rate	$[0.000625 - 0.012]$	$km^2 d^{-1}$	1,2
r_u	Pest intrinsic growth rate	$[0.010 - 0.020]$	d^{-1}	3
C_{it}	Pest carrying capacity in crop field	$C_{it} = \begin{cases} 20 & \text{no pesticide application} \\ 0.1 & \text{after pesticide application} \end{cases}$	$pestskm^{-2}$	-
$1/m_u$	Pest life-span	$[20 - 66]$	d	2

Table 4.1 – Population dynamics model parameters. References: 1) Corbett and Rosenheim (1996), 2) Pearce et al. (2006), 3) Xia et al. (1999).

The population model is defined by a system of partial differential equations and considers both 2D diffusion on patches and 1D diffusion on linear elements (Roques and Bonnefon, 2016). Simulations are performed over a $[0, 100]$-time interval representing a cropping season with a time step of 1 day. The model parameters and their range of simulated values are reported in Table 4.1. The predator-pest dynamics is illustrated in the Supplement 2.2 by plots of the temporal dynamics (Figure 4). Here, in Figure 4.1, we present snapshots of the dynamics over the whole landscape. The equations defining the models are reported in the Box 3.

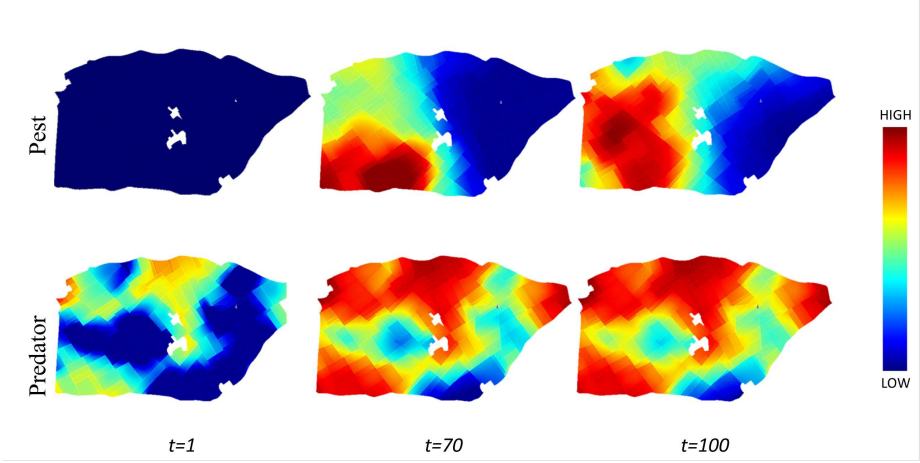

Figure 4.1 – Snapshots of pest and predator spatial dynamics. Simulations of predator-pest population dynamics at different time intervals $t = 1, 70, 100$. At the initial stage, the pest density (first line) is very low, followed by random introduction of pest. As time proceeds, pest density increases (from left to right). As time proceeds, predator density (second line) increases and diffuses to surrounding fields. At the final time step, there is a high pest density where predators are absent.

Initially, predators are present in all hedges at carrying capacity, since hedges are their natural habitat. The pest is introduced randomly in space and time in crop fields. The average number of pest introductions in a single simulation is proportional to the crop field area in the landscape, and a Poisson distribution is used to simulate the number of pest introductions. Inoculated crop fields are picked at random with probability depending on their relative surface. During the simulation, a pesticide application is applied to a crop field when the pest density in that field reaches a given threshold. The effect of the pesticide application remains active for a short period of time by drastically reducing pests based on modifying the carrying capacity. We have made a strong assumption about pesticide applications in our model, as they are only effective for pest and do not influence predator dynamics.

In order to match the biology of the pest (*Codling moth*) and predator (family of ground beetles) dynamics detailed in Section 4, predator-pest dynamics are coupled over the 2D1D landscape model using the following assumptions: (i) pests do not perceive linear elements as a barrier, (ii) linear elements without a hedge do not represent a barrier for the predator, (iii) the predator is attracted by hedges, thus migration from fields to hedges is relatively high, (iv) the predator shows aversion to move outside its natural habitat, thus migration from hedges to fields is lower than migration from fields to hedges. We define 11500 distinct parameter combinations according to a Sobol experimental design (see the range of parameters in Table 4.1) among population and landscape parameters. For each parameter combination, we consider 15 landscape replicates, leading to a total of 172500 simu-

lations. Numerical simulations of the spatio-temporal partial differential equation system of predator-pest dynamics are performed using the Freefem++ finite-element framework (Hecht, 2012a). Results are analysed through sensitivity analyses and Generalised Linear Models. Details are provided in the Box 3.

Box 3: Coupling landscape models with predator-pest dynamics

Agricultural landscapes as the spatial support

The landscape is represented through a vectorial approach and it is composed of 2D polygons representing patches, separated by 1D segments representing linear elements. Landscape elements are characterised by their geometry (e.g., vertex coordinates, size and shape), and by categorical information defining the land-cover (e.g., crop or SNH). We use the landscape generator model presented in Section 2.1 to allocate a proportion of polygons and edges as crops, representing the principal culture, and hedges, representing SNHs, respectively.

Predator-pest model

We model a generalist predator not showing strong attraction towards pests. Hedges are the main predator habitat, and the predator feeds on pests when moving into the fields. The predator dynamics are characterised as follows:

- In 1D landscape elements:
  Linear 1D elements of the landscape matrix are denoted by h_i. A 1-dimensional reaction-diffusion model on linear elements is defined for the predator v_{h_i}:

$$\begin{cases} \partial_t v_{h_i} = \partial_{xx} D_1^v v_{h_i} + r_v v_{h_i}(1 - \frac{v_{h_i}}{K_{h_i}}) & \text{if the edge } h_i \text{ has a hedge,} \\ v_{h_i} = 0 & \text{otherwise,} \end{cases} \tag{4.1}$$

  where: D_1^v is the diffusion parameter of the predator along the hedges, r_v is the intrinsic growth rate of the predator, and K_{h_i} is the carrying capacity of the hedge i.

- In 2D landscape elements:
  Polygon-shaped 2D fields are denoted by Ω_i. The population density of predators v_{Ω_i} in each field is modelled by a reaction-diffusion equation with mobility parameter within field D_2, predating rate β, and life-span $1/m$:

$$\partial_t v_{\Omega_i} = \Delta D_2^v v_{\Omega_i} - m v_{\Omega_i} + \beta u_{\Omega_i} v_{\Omega_i} \tag{4.2}$$

The pest dynamics are characterised as follows:

- In 1D landscape elements:
  We make the assumption that edges do not host the pest u_{h_i}, and that they do not modify directly their population dynamics: $u_{h_i} = 0$ for all i.
- In 2D landscape elements:
  The pest u_{Ω_i} is assumed to live only in fields. In addition, the crop fields represent a source

of pest, whereas the non-crop fields are a sink for the pest. In the absence of dispersal from fields hosting the crop, the pest population vanishes in fields hosting the non-crop type. The bidimensional reaction-diffusion model is defined as follows:

$$\begin{cases} \partial_t u_{\Omega_i} = \Delta D_2^u u_{\Omega_i} + r_{u_{\Omega_i}}(1 - \frac{u_{\Omega_i}}{C_{it}}) - \beta u_{\Omega_i} v_{\Omega_i} & \text{for crop,} \\ \partial_t u_{\Omega_i} = \Delta D_2^u u_{\Omega_i} - m_{u_{\Omega_i}} - \beta u_{\Omega_i} v_{\Omega_i} & \text{for alternative resistant crop,} \end{cases} \tag{4.3}$$

where $D_{u_2}^u$ is the diffusion parameter of the pest in fields, r_u is its intrinsic growth rate on the crop category, β is the predating rate, and $1/m_u$ is the life-span rate of the pest on alternative pest resistant crop fields. In a crop field, a pesticide application is applied when the average pest population density in that field exceeds a given threshold, which we here fix to 0.2 $pests km^{-2}$. Pesticide applications reduce the carrying capacity C_{it} of the field i. We set $C_{it} = K_{\Omega_i}$ if no chemical pesticide is applied, and $C_{it} = \frac{200}{K_{\Omega_i}}$ if the chemical pesticide is applied.

This results in a pesticide application efficacy providing a 99.5% pest reduction, which can be considered as an ideal-optimal case. More realistic values of pesticide application efficacy could be around 70%; this scenario is analysed in the Supplement 2.4, where the sensitivity of results to the pesticide application threshold is also tested. We point out that we identify the carrying capacity as a general saturation level for pest and predator density that does not correspond necessarily to the number of individuals per km^2. Similarly, mortality other than for predation or pesticide applications could have occurred in crop fields, but we have opted against this option for the sake of parsimony.

Analysis

- We assess the Sobol sensitivity indices on the mean and standard deviation of predator density, pest density and number of pesticide applications by averaging the outputs over landscape replicates and crop fields. First-order indices are estimated with Sobol–Saltelli's method (Sobol' et al., 2007; Saltelli et al., 2010), whereas total indices are estimated with Sobol–Jansen's method (Jansen, 1999). These analysis are performed within the R software v. 3.0.3 (R Team, 2003), using the packages fOptions (v. 3010.83) and sensitivity (v. 1.11).
- We applied Generalized linear models (GLMs) to further explore direction and magnitude of variations in response variables with respect to landscape parameters. Pest and predator densities and the number of pesticide applications are analysed with the Gamma distribution for the response variable and a log link function. The presence/absence of pesticide applications is analysed with a GLM with binomial distribution. We develop GLM formulas containing interactions among covariates (see Table 1) up to 2nd order, and we implement a step-wise variable selection algorithm using the Bayesian information criterion (BIC) in order to select the "best subset' of variables for each model.
- We use Generalized Linear Mixed-Effect models (GLMMs) to analyse pesticide application occurrences at field scale by taking into account their spatial position in the landscape. These analyses are performed using the R package lme4 with R version 3.2.3 (31).

Main results

Sensitivity analysis

The sensitivity analysis of the mean of model outputs across landscape replicates allows ranking the importance of different covariates for explaining variations in the response variable. Predator population density is mainly explained by predator spillover from hedge to field (ρ_{12}) and by the total proportion of hedges (P_h), whereas interactions among parameters have little impact on the outputs (Figure 4.2a right). For the pest population density and the average number of pesticide applications, crop proportion (P_c) and pest growth rate (r_u) are the most important parameters to explain model output variability, again with only little interaction between model parameters (Figure 4.2b right). The sensitivity analysis of standard deviation of model outputs across landscape replicates gives different importance to the input variables as compared to the mean values. For the predator, crop proportion (P_c), predator migration (ρ_{12}), hedge proportion (P_h) and crop and hedge spatial aggregation (ϕ) explain respectively 55%, 19%, 9% and 9% of the variability of model outputs (Figure 4.2a left). For the pest and pesticide applications, results are consistent with the analysis on the mean (Figure 4.2b left). Complete results are found in the Supplement 2.3.

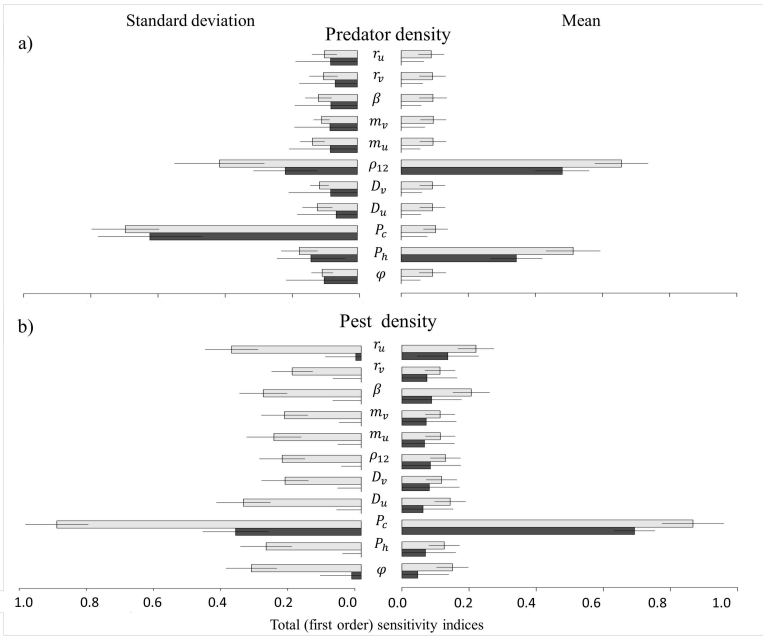

Figure 4.2 – Sobol sensitivity analysis. Total sensitivity indices (light grey bar) and first-order sensitivity indices (black bar) of space-time averaged values for predator density (a) and pest density (b), based on the mean (right) or on the standard deviation (left) over replicated simulations (with 15 replicates). The length of the bar indicates the mean of the sensitivity index, and the solid line indicates its 95% confidence interval.

Landscape structure effects on the predator-pest dynamics

Estimated coefficients of landscape variables (denoted $E_{variable}$ in the following) on predator density highlight a positive effect of hedge proportion ($E_{P_h} = 0.40 \pm 0.05$), a negative effect of crop proportion ($E_{P_c} = -0.20 \pm 0.04$) and a positive interaction among both variables ($E_{P_h:P_c} = 0.08 \pm 0.02$), which implies that hedges can buffer the negative effect of increased crop proportion. Migration from hedges to fields ($E_{\rho_{12}} = 0.56 \pm 0.01$) has the highest positive effect on predator density with again a positive interaction with crop proportion. As expected, crop proportion ($E_{P_c} = 1.50 \pm 0.16$), as well as crop and hedge spatial aggregation ($E_{\phi} = 0.55 \pm 0.02$), have a strong positive effect on pest density. Both variables interact negatively ($E_{\phi:P_c}$) $= -0.11 \pm 0.01$), as high aggregation results in an increase of the size of contiguous crop fields, which lowers the effect of increased crop proportion. The positive effect of crop proportion is lowered by its interaction with hedge proportion ($E_{P_h:P_c} = 0.03 \pm 0.06$) and also with predator migration from hedges to fields ($E_{P_c:\rho_12} = 0.06 \pm 0.06$). Interestingly, an increase in hedge proportion ($E_{P_h} = 0.09 \pm 0.11$) has a positive effect on pest density. Indeed, predator presence over all the landscape helps to stabilize the pest population by keeping it under the thresholds triggering a pesticide application. Among species traits, predator migration from hedges to fields ($E_{\rho_{12}} = -0.13 \pm 0.12$) has the highest negative impact on pest density. Pest diffusion ($E_{D_u} = -1.03 \pm 0.01$), due to a dilution effect, and the predation rate ($E_{\beta} = -0.24 \pm 0.01$), have also a negative impact on the pest, while the growth rate ($E_{r_u} = 0.4 \pm 0.01$) contributes positively to pest density. When testing the sensitivity of our results depending on the pesticide application variables (i.e., pesticide application efficacy [optimal vs realistic] and pesticide thresholds [low vs high], see the Supplement 4.4), we find that there is no variation in the direction of the estimated effects, but the magnitude of the effect may increase or decrease depending on the scenario considered. However, when pest reduction is lower due to low pesticide efficacy, or, when pest reduction is slower due to an elevated pesticide threshold, hedges show a more important role in slowing down pest dynamics thanks to predator presence providing a more efficient CBC.

Effect of local landscape features on pesticide application at local scale

Presence of pesticide applications is negatively influenced by field area and perimeter ($E_{Area} = -0.32 \pm 0.01$, $E_{Perimeter} = -0.10 \pm 0.03$). These effects reflect both a slower pest diffusion in large fields and higher incoming fluxes of predators in fields with long perimeter. Conversely, when applications occurred in a field, their total number increases with field perimeter due to spillover from the neighbourhoods. An increase in the number of adjacent crop fields produces a positive effect on the presence ($E_{Adj_C} = 0.74 \pm 0.01$) and number ($E_{Adj_C} = 0.20 \pm 0.002$) of pesticide applications, while an increase in the number of adjacent hedges leads to a negative effect on the presence ($E_{Adj_H} = -0.07 \pm 0.01$) and number ($E_{Adj_H} = -0.05 \pm 0.001$) of pesticide applications. Whereas in the global model the

	Density				Pesticide applications		
	Coefficient	**Predator**	**Pest**		**Coefficient**	**P/A**	**No.**
L	E_{P_h}	+	+	**L**	E_{P_h}	+	-
	E_{P_c}	-	+		$E_{\rho_{12}}$	+	-
	$E_{P_h:P_c}$	+	+		$E_{\phi:P_c}$	+	-
	$E_{\rho_{12}}$	+	-	**P**	E_{area}	-	-
	$E_{\phi:P_c}$	ns	-		E_{perim}	-	+
	$E_{P_c:\rho_{12}}$	+	+		E_{Adj_C}	+	+
	E_{D_u}	+	-		E_{Adj_H}	-	-
	E_{β}	+	-		$E_{Adj_{Tr}}$	+	+
	E_{r_u}	+	+				

Table 4.2 – Estimated coefficients (as far as discussed in the text) for effects on predator and pest density (left) and on the presence/absence (P/A) and number (No.) of pesticide applications (right) at landscape (L) and patch level (P). + means a positive effect, − means a negative effect, NS means a non significative effect.

increase of hedge proportion is associated with a positive effect on the presence of pesticide applications, we attribute the negative effect at local level to the fact that the predator tends to locally maintain the pest density under the application threshold, especially after a first pesticide application. The number of pesticide applications in adjacent fields is positively correlated to the local presence ($E_{Adj_{Tr}} = 2.99 \pm 0.01$) and number ($E_{Adj_{Tr}} = 0.13 \pm 0.001$) of pesticide applications, indicating local infestation of the pest. See also Table 4.2 for a summary of the effects at landscape and field scale.

Discussion

In this chapter, we characterise the joint influence of landscape structure and species traits on CBC service. We point out that spatial heterogeneity, landscape structure (i.e., the size and physical arrangement of patches and hedges), species traits and their interactions play a key role for CBC outcomes and may trigger unexpected dynamics.

Crop proportion is the major determinant of increasing pest population and resulting in an increased number of pesticide applications over the whole landscape. Indeed, increasing crop proportion in fragmented landscapes ensures food availability to the pest all over the landscape (Zhao et al., 2013, 2015; Tscharntke et al., 2016a). In highly aggregated landscapes, the size of contiguous crop patches is already large enough to sustain a relatively large pest population, thus lowering the effect of an increase in crop proportion (Veres et al., 2013). The effects of crop proportion and spatial aggregation are intimately linked to pest growth rate and dispersal capability. Indeed, unfavourable landscape properties for the pest (*i.e.*, low proportion and high fragmentation) can be compensated by a higher growth rate. However, the effect of dispersal is a double-edged sword since high dispersal helps spreading on fragmented landscapes, but comes with a larger amount of propagules lost in unsuitable

habitats, potentially leading to a dilution effect (Tscharntke et al., 2005; Baggio et al., 2011; Rand et al., 2006).

As expected, hedge proportion (*i.e.*, SNHs) positively affects predator presence in agricultural landscapes. In addition, the predator's ability to move between SNHs and crop habitats is the parameter that increases most strongly the predator density, since it enables predators to reach complementary resources in crop fields more easily. Predator fluxes from adjacent habitat is reported to have a major impact on pest populations in crop fields (Tscharntke et al., 2016a, 2005; Rand et al., 2006). Spillover from hedges to patches not only depends on predator propensity to forage outside their natural habitat, but also on semi-natural patch connectivity and on crops and predator reservoir interface (Coppolillo et al., 2004). Thus, different combinations of SNH proportion and aggregation influence landscape structural connectivity and are also important determinants of predator efficiency in regulating crop pests (Coppolillo et al., 2004).

Hedges are modeled as source of predators where they have a logistic growth. This is a simplification for predator dynamics in their natural habitat, as we do not consider potential prey presence in hedges and predator foraging behaviour in crop fields. For example, the growth rate, instead of being constant, could depend on the time spent in the fields and on the number of consumed preys (see Chapter 8). In addition, predating rate and consumption rate are crucial in determining the efficiency of CBC (Pettorelli et al., 2015). Finally, another strong assumption may be that pesticide applications do not affect predator mortality, and we do not explore a broad-spectrum pesticide scenario. In general, broad-spectrum pesticides are more commonly applied (Koss et al., 2004), but there are pest management programs where selective insecticides have been proved to be particularly effective along with a CBC strategy, such as combining direct targeted reduction in pest numbers with predator conservation (Koss et al., 2004; Hilbeck et al., 1998). Moreover, accounting for broad-spectrum pesticide application effects may result in a secondary pest breakout (Dutcher, 2007; Gross and Rosenheim, 2011; Steinmann et al., 2011)), where pests benefits from the predator reduction. Additional pesticide loads would be necessary to decrease pest density, while continuously breaking down predator density (Steinmann et al., 2011). Thus, finally, the effect of SNH and predators and their relationships for CBC outcomes would be confounded and masked. However, in our work, an indirect effect could be observed, as in crop fields a positive predator growth rate relies only on pest, such that a strong pest reduction due to pesticide applications is automatically translated into a strong impact on predator density when such pesticide applications occur. Thus, adding extra-mortality in crop fields should not modify the results that much. To account for major pesticide application effects, an impact on predator mortality in its natural habitat should be considered.

Predator migration from hedges to crop fields has a major influence on pest density and related pesticide applications. High crop proportion enhances pest density, but this effect is counter-balanced by the joint effect of hedge proportion and predator spillover, which

favours predator pressure and reduces pesticide application. Indeed, hedges ensure an increased landscape functional connectivity, which enables predators to successfully disperse and feed on complementary resources in the fields. Interestingly, we found that if SNHs can sustain a high population of predators (Fabian et al., 2013), this is not sufficient to achieve a decrease in pest density. Indeed, by keeping the pest population density under the pesticide application threshold, the predator population can favour its spread across the landscape, thus increasing pest density at the landscape scale, even if fewer pesticide applications are applied. Most of the studies consider the amount of SNH as a proxy for predator presence and focus on how landscape structure directly influences CBC. However, as highlighted by our results (see also Fabian et al. (2013)), the extent to which species are influenced by landscape heterogeneity depends on their traits. For example, Le Gal et al. (2020) argue that predators with an oriented movement are better able to deliver pest control services. They discuss the interplay among predator mobility, proportion of crop and SNHs. More generally, SNH predator spillover is expected to be particularly strong when (i) predator attack rates on prey are high, (ii) predator movement abilities are substantial, and (iii) predator mortality rates in the recipient habitat are low (Holt et al., 2001). However, we point out that the predator we model is a generalist predator not showing strong aggregation behaviour to pests. Pests represent a predator resource in fields, while predators can persist in the landscape also without pests as they have a positive growth in hedges. Different outcomes would be probably observed considering a specialist predator showing an aggregating behaviour around local pest outbreaks (Bianchi et al., 2010). As for example in Bianchi et al. (2010), specialist predators are found to be more effective agents in suppressing local outbreaks than generalist ones.

The flux of predator migration from hedge to field, and the distance over which pest and predator can spread, both depend on local configurational variables such as field size, shape, amount of shared edge, and connectivity (Haan et al., 2020). Large fields can support high pest volumes, but it has been demonstrated that the relationship between field size and pest density can take several forms depending on assumptions, conditions and species considered (Segoli and Rosenheim, 2012). Our results show a negative effect of large field area on the need to use pesticides and on the number of required applications, which, accordingly to Segoli and Rosenheim (2012), may come from the elevated growth rate of the prey combined with its good dispersal ability. An increasing pesticide application number is favoured by long field perimeter as it facilitates high fluxes of pest incoming from surrounding fields. However, when a hedge is present on field boundary, we observe a reduction in pesticide number as there is an increase of predator spillover from hedges into fields (Bianchi et al., 2006). Interestingly, we show a contrasted effect of hedge depending on the scale considered. At global scale, the proportion of hedges shows a positive effect on pest density and has a negative effect only on pesticide application presence. At local scale, an elevated number of hedges on crop boundary shows an even more important impact on

CBC by negatively affecting both the local presence and number of pesticide applications (Fabian et al., 2013) (see Chapter 5).

We find that natural habitat enhances predator population, but it does not systematically translate into a strong correlation with pest density decrease. However, a relatively high predator density often helps maintaining pest density below the economic threshold level above which pesticides are applied, thus preventing highly localized pest densities. By contrast, predator migration from hedges to fields is fundamental for CBC; it reduces pest density and guarantees high predator fluxes and different habitat connectivity. At field scale, landscape geometrical features, hedge presence and habitat connectivity are able to influence predator-pest dynamics, and therefore they affect the number of pesticide applications in a different way from a global perspective. This highlights the importance of conducting a multi-scale analysis to consider the differences in outcomes at landscape and patch scale for pest CBC (Veres et al., 2013). Up to now, we have considered global outputs by averaging pest and predator densities over crop fields. However, populations are obviously structured in space and time. Thus, in the next Chapter 5 we focus on how landscape structure impacts predator-pest spatio-temporal dynamics, which brings further insights on pest outbreak determinants in relation to predator–prey dynamics and interactions. For example, in Figure 4.3, two landscapes characterised by the same crop proportion but different hedge network structures are showed. Pesticide application events occur in the same number, but with completely different patterns. Thus, up to this point of our analysis, we can not detect any effect of the hedge network structure, as we aggregate the output in space and time for a global analysis. By contrast, in the next Chapter 5, we wonder if landscape features and population dynamics can explain local patterns by taking into account spatio-temporal information at both local and global scale.

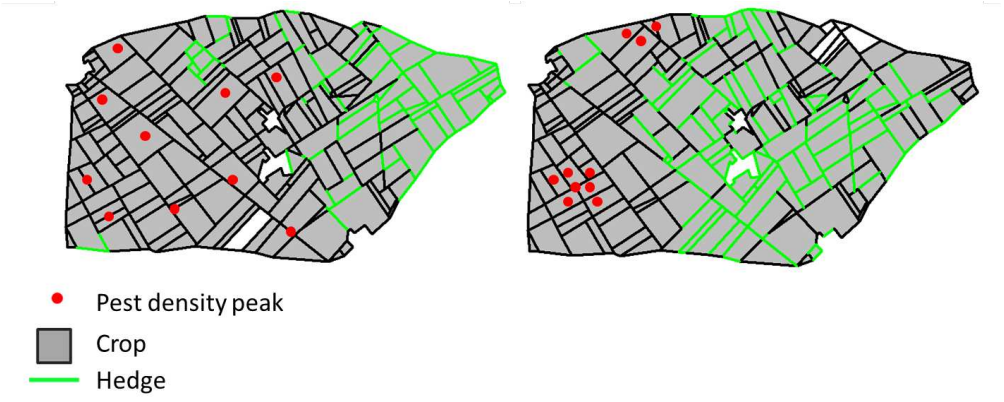

Figure 4.3 – Landscapes with the same number of pest density peak (10) but with a different spatial distribution

Chapter 5

Spatio-temporal point processes as meta-models for population dynamics in heterogeneous agricultural landscapes

Dealing with ecological processes involves studying different spatial and temporal scales, since ecosystem patterns and processes cover various spatio-temporal ranges and may have multiple drivers acting across different extents (Fritsch et al., 2020). The characterisation of the spatial distribution of landscape features and individuals in response to a complex interplay of processes across scales can be very well accounted for by Spatially Explicit Model (SEM). Different SEM types have been proposed, such as continuous-space reaction-diffusion partial differential equations (Roques, 2013), patch models (Hanski, 1994), cellular automata neighbourhood models (Hogeweg, 1988), or individual-based models (IBM, Grimm and Railsback, 2005).

The development of advanced numerical models has greatly improved our ability to accurately describe complex dynamics incorporating fine-grain interactions over a large extent. However, as models aim to provide a realistic but simplified representation of reality, the spatio-temporal extent is often properly adapted by scaling decisions (Fritsch et al., 2020). In-model scaling methods give control over simplifications when building the model or allow us to incorporate and transfer relevant information across different scales. Scaling techniques may also be used before or after building the model, to define model parameters or analyse model outputs. In this work, The predator-pest model is defined through a system of partial differential equations over a large spatio-temporal domain, and its solution returns large output sets. Thus, we focus on post-model scaling and propose a parsimonious

approach to deal with the complexity of SEM outputs while keeping fine-scale information on the ecological dynamics.

A solution to deal with this complexity could be the application of non-spatial analysis methods via spatial and temporal output aggregation (Gotelli, 2000; Webb, 2000; Fritsch et al., 2020). This is the solution we first applied and presented in Chapter 4. An alternative solution is given by meta-models and meta-analysis, which offer the possibility of reducing model output complexity by establishing a simplified mathematical relationship between the input and output of the system (Simpson et al., 2001). Their main aim is to replace complex numerical models by more parsimonious representations that provide a better understanding and faster analysis tools for optimisation and exploration, specifically when performing uncertainty or sensibility analysis (Simpson et al., 2001; Jia and Taflanidis, 2013; Saint-Geours, 2012; Ratto et al., 2012). Where possible, an elegant way to build meta-models is the approximation through an analytical model, which is fitted to the large-scale output and allows for simplification (Grimm and Railsback, 2005). Analytical solutions can provide insight from different aggregation levels, but their construction and use are not always unequivocal (see Johst et al., 2013). Spatial statistics techniques are potential candidates of great interest and should be further explored (Fritsch et al., 2020).

Here, we show how spatio-temporally explicit outputs of population dynamics model in landscape ecology could be analysed through a meta-modelling approach to get a more parsimonious representation. Due to the high-dimensional spatial mesh and temporal resolution, we do not work directly with the spatially resolved pest and predator density output. Thus, outputs are simplified to point patterns by considering individual positions, key events or significant hotspots determining local dynamics. The resulting patterns can be modelled as spatio-temporal point processes (STPP), and the pattern itself, or rather its structure, is the response variable that one seeks to explain through the structure of the spatial support, and its temporal changes, described through predictor variables (Diggle, 2003; Illian et al., 2012; Renshaw, 2015; Illian and Burslem, 2017). Point processes can be defined over continuous space and time, such that there is no need to work with fixed spatial and temporal units; they can be used for descriptive analyses and stochastic modelling of patterns. For example, Law et al. (2009) apply STPP tools by computing first- and second-order statistics, *i.e.*, expected numbers of points and point pairs, for characterising observed plant patterns; Gabriel et al. (2017); Opitz et al. (2020); Pimont et al. (2020) develop models for wildfire occurrences through STPP to overcome challenges given by the multi-scale structure of data and by strong non-stationarities in space and time driven by weather, land-cover and land-use.

This approach allows us to investigate the role of landscape structure in influencing the point process intensity summarising the predator-pest dynamics, and we address two general questions: (I) How can landscape effects and population dynamics traits be coupled

at different spatio-temporal scales?; (II) What are the spatio-temporal relationships between pest introductions, pest density peaks and landscape heterogeneity?

To answer these questions, the main novelty of our work resides in the characterisation of spatio-temporal population dynamics through STPPs. A hierarchical framework is developed (Figure 5.1), where (i) the stochastic landscape model to generate the spatial support (Section 2.1), and (ii) the predator-pest simulation are the steps addressed in Chapter 4. This is the starting point of this Chapter, where we propose to represent spatio-temporally explicit outputs as point patterns identifying space-time-indexed key events of pest dynamics, that we subsequently model by constructing and estimating regression equations for marked STPPs where points are marked by magnitude of the event they represent. The response variables we aim to model are the occurrences and the magnitude of the pest density peaks. Response variables are explained by taking into account both global and local landscape features, species life-history traits, and the occurrences of pest introduction, pest peaks and pesticide applications in appropriately chosen spatio-temporal neighborhoods around the location and time where the response variable is observed.

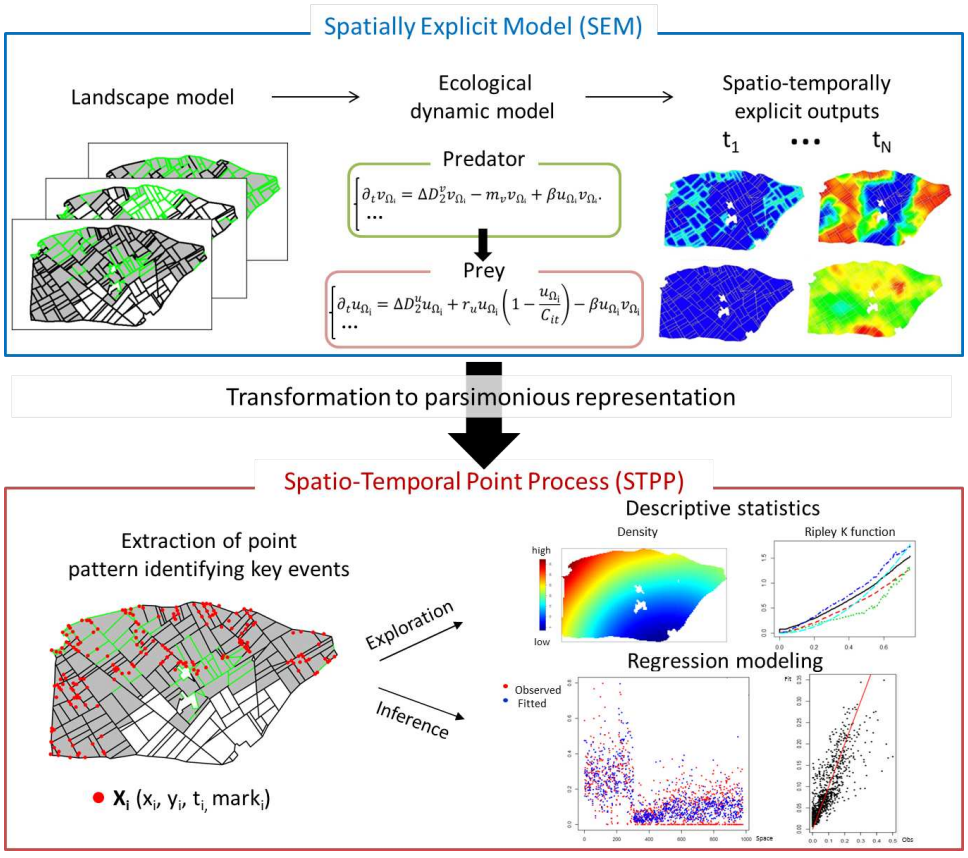

Figure 5.1 – Overview of meta-modeling workflow.

Pest-predator dynamic patterns

Predator-pest simulations of the spatially-explicit population model presented in Section 4 provide the spatio-temporal pest and predator densities, from which we extract and store the spatial positions, the times and the value of pest density maxima. Following our modelling framework, we identify as events (i) the spatio-temporal pesticide application occurrences (*i.e.*, pest threshold exceedance or pest peak) and (ii) the spatio-temporal pest introductions. For example, when pest threshold exceedance occurs in a patch, we apply a pesticide application in this patch and, to define the event episode as a point, we extract the time t of threshold exceedance, the pest density maximum in the patch with its Euclidean coordinates (x, y), and the average pest density over the patch. In Figure 5.2, two simulations are shown for different time steps, where the spatio-temporal occurrences of pest introductions and pesticide peaks within different landscape allocations are highlighted. This example also illustrates the conjecture that the spatial hedge structure plays a role for pest dynamic by influencing its evolution jointly in space and time. Deeper exploratory quantitative analyses of spatio-temporal relationships between different types of points are proposed in the Supplement 3.1, while we focus on statistical model-based analyses in what follows.

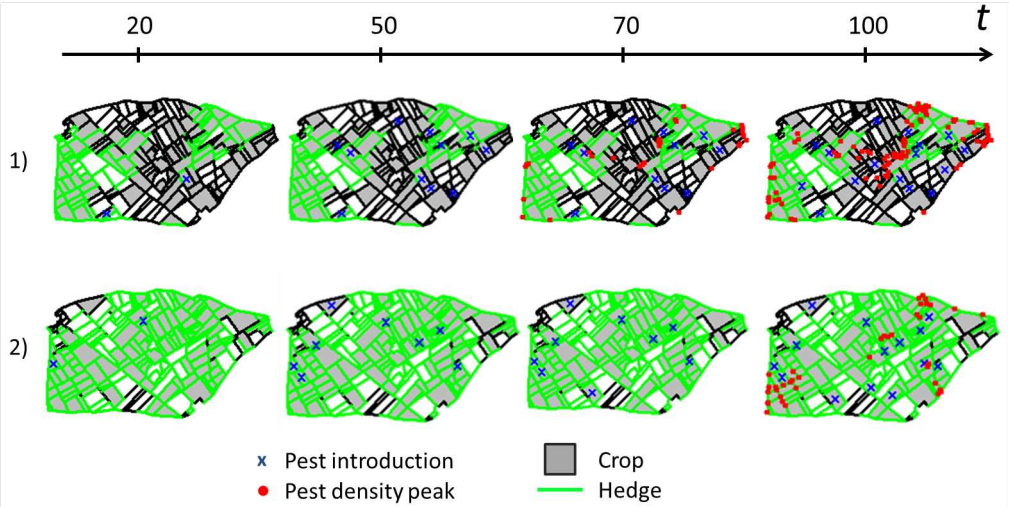

Figure 5.2 – Two simulation examples (by row) illustrating the spatio-temporal pest dynamics depending on landscape structure through pest introductions, and through pest density peaks after threshold exceedances.

Pest density peaks as a Spatio-Temporal Point Process (STPP)

Point patterns representing individual or event distributions in space and time can be modelled as STPPs (see Diggle (2003); Illian et al. (2008); Baddeley et al. (2015) for formal defi-

nitions). Each point can be endowed with additional qualitative or quantitative information defined as a “point mark". In our application, the pattern of events is defined by the coordinates in space and time of pest peaks with both qualitative (pest introduction) and quantitative marks (pest maximum density). Thanks to the theory of STPPs it is possible to analyse the point distribution properties locally in space and time, and to estimate models for predictive purposes (*e.g.*, number of events, point-to-point correlations, and distribution of their numerical or categorical marks). We focus on modelling the point process intensity function (local point density) (Illian et al., 2013), see Box 4. Our modelling goal is to predict the intensity of pest density peaks and the associated values of maximum pest density, and explain their variability in space, through time and across different simulations. We divided the spatial domain in a relatively large number of small cells, and we assume a homogeneous point process intensity within each cell during each interval of time. The spatial discretisation we use is shown in Figure 5.3, and background on its structure and construction is provided in the paper Zamberletti et al. (2021a) and in the Supplement 3.4.

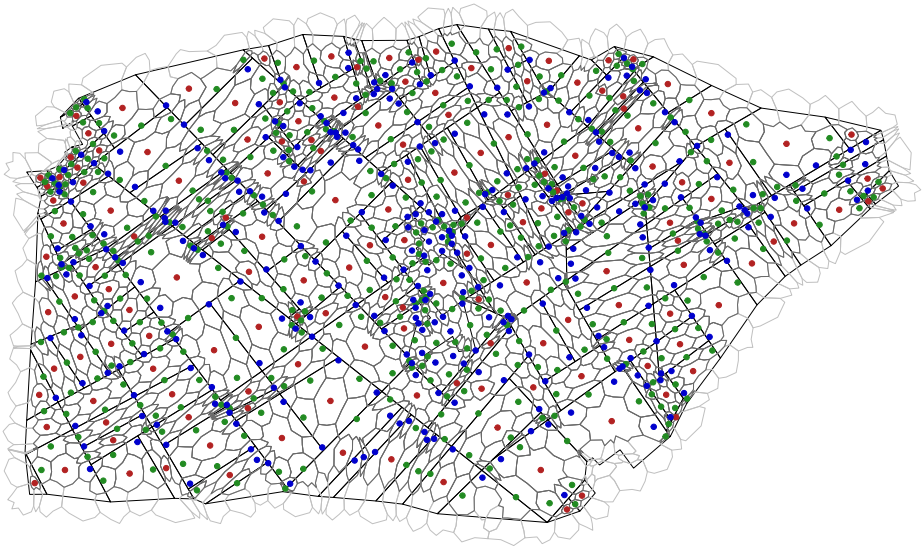

Figure 5.3 – Spatial discretisation of the regression models. Complete mesh discretisation (light grey), mesh cells used in the analysis (dark grey), landscape patches (black). Cell centroids of different colour refer to different cell types: cell in patch center (red), cell connecting exactly two patches (green), cell connecting more than two patches (blue).

Box 4: Spatio-temporal point process (STPP)

A point process is a random collection of points X that is defined on a space-time observation window $\mathcal{W}$ of $\mathbb{R}^d$, where we here use $d = 3$ to represent two spatial dimensions and time, and $X(\mathcal{W})$ is the random number of points in $\mathcal{W}$. For details, we refer the reader to Diggle (2003); Moller and Waagepetersen (2003); Illian et al. (2008); Baddeley et al. (2015).
Realisations of X are called point patterns. We can then work with arbitrary subsets (or mapping units) A of $\mathcal{W}$ (*e.g.*, space-time cylinders defined as patch or triangulation cell times time-step), for which we can locally analyse the events' distribution (*e.g.*, number of event points, and distribution of numerical attributes associated to events), see Figure 5.4. In addition to the spatial locations of the objects represented by the points, qualitative or quantitative attributes on the objects may be available. These additional variables are commonly referred to as marks, and they can be considered alongside the pattern and included as part of a marked point process model. Given a random mark $m_x \in M$ associated with each point $x \in X$, where M is the mark space, the marked point process is defined as $X_m = \{(x, m_x) : x \in X\}$. The mark space M may be subset of $\mathbb{R}^{g_M}$ (with $g_M \geq 1$) for continuous marks; if $M = \{1, \ldots, k\}$ then X_m is a multi-type point process with k different point types.

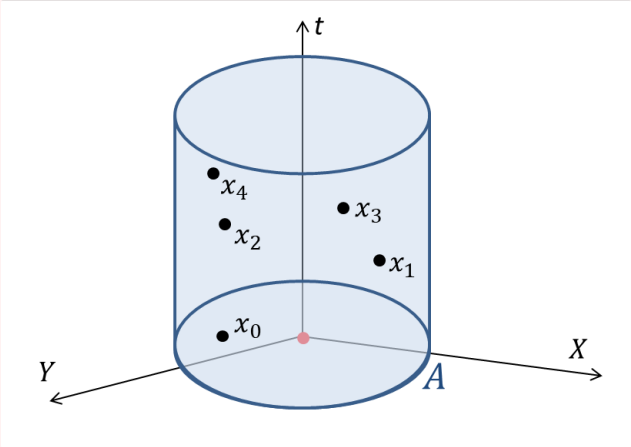

Figure 5.4 – Spatio-temporal point process representation on the subset A. X and Y represent the spatial dimension, t represents the temporal dimension, $X = \{x_0, x_1, \ldots, x_4\}$ is the point pattern realised within the subset A.

The most important characteristic of a point process is its intensity function λ, which can be locally interpreted as the average number of events per space-time unit; this density allows calculating the expected number of points in a set A by considering the cumulated intensity in A, *i.e.*, by calculating the integral $\mathbb{E}(X(A)) = \int_A \lambda(x)\,\mathrm{d}x$ where $x \in \mathbb{R}^d$.

Index	Covariate	Spatial reference	Range	Unit
Spatio-temporal (*STC*)				
1	No. of pesticide applications in the patch at $t-1$	patch	0-40	-
2	N. of pesticide applications in the patch cumulated up to $t-2$	patch	0-97	-
3	No. of pesticide applications in neighbor patches at $t-1$	patch	0-337	-
4	No. of pesticide applications in neighbor patches cumulated up to $t-2$	patch	0-861	-
5	No. of pest density peaks at $t-1$	cell	0-15	-
6	No. of pest density peaks cumulated up to $t-2$	cell	0-36	-
7	No. of pest density peaks in neighbor cells at $t-1$	cell	0-45	-
8	No. of pest density peaks in neighbor cells cumulated up to $t-2$	cell	0-97	-
9	No. of pest introduction in cell at $t-1$	cell	0-30	-
10	No. of pest introduction in cell cumulated up to $t-2$	cell	0-30	-
11	No. of pest introduction in neighbor cells at $t-1$	cell	0-30	-
12	No. of pest introduction in neighbor cells cumulated up $t-2$	cell	0-39	-
Spatial (*SC*)				
13	Cell dimension	cell	0-0.069	km^2
14	Binary indicator if the cell is among 2 patches	cell	0-1	-
15	Binary indicator (1/0) if the cell is among 3 or more patches	cell	0-1	-
16	Proportion of hedges within the buffer centered in the cell	buffer	0-1	%
17	Proportion of crops within the buffer centered in the cell	buffer	0-1	%
18	Landscape crop and hedge aggregation	landscape	0-5.54	-
19	Landscape crop proportion	landscape	0-1	%
20	Landscape hedge proportion	landscape	0-1	%
Population dynamics (*PDC*)				
21	Pest diffusion in crop patch	landscape	0.06-12	km^2d^{-1}
22	Predator diffusion in crop patch	landscape	0.07-12	km^2d^{-1}
23	Predator migration from hedge to crop	landscape	0.1-1	

Table 5.1 – Covariate list for the space-time regression model of pest density peak patterns. The temporal unit d stands for *day*.

Pest density peak meta-modelling

For predicting pest density peak intensities and maximum pest density peak values, we develop and estimate regression equations for marked STPPs. Both global and local landscape features, species life-history traits, and the occurrences of pest introductions, pest peaks and pesticide applications are used as covariate information. We construct two separate generalised linear model (GLM) formulas as meta-models that incorporate the available covariate information. Response variables and covariates are evaluated over each spatial cell (Figure 5.3) and time step (see Box 5 and the paper (Zamberletti et al., 2021a) for model equation specification).

Box 5: Regression equations for marked STPP to model pest density peaks

Model covariates

We evaluate spatio-temporal (STC), spatial (SC) and population dynamics (PDC) covariates to put the spatio-temporal event patterns, landscape structure and population dynamics into relation.

$$STC(s,t) = \sum_{k=1}^{12} \beta_k z_k(s,t), \quad SC(s) = \sum_{k=13}^{20} \beta_k z_k(s), \quad PDC = \sum_{k=21}^{23} \beta_k z_k, \quad \boldsymbol{\beta} \in \mathbb{R}^{23}, \tag{5.1}$$

The $\boldsymbol{\beta}$ vector gathers the covariate coefficients to be estimated separately for each model, and the values z_k are covariates summarised in Table 5.1 and provided for each space-time cell; more information on their selection and computation is given in the Supplement 3.5. We applied a coarser temporal discretisation (*i.e.*, time step of 10 over the temporal interval $[0, 100]$) as compared to the population dynamics model in order to reduce the computational complexity. A residual analysis is performed to evaluate if the predicted values obtained by the GLMs are uncorrelated and homogeneously distributed in space and time for the intensity peak occurrences and for the peak values of pest density (See the Supplement 3.7).

Meta-model for the occurrence intensity of pest density peaks

To model the maximum pest density value associated with each pest peak point, we consider a log-Gaussian GLM, *i.e.*, we combine a log-link function with a Gaussian distribution of regression errors:

$$\lambda(s,t) = \exp\left(\beta_0^{\lambda} + STC(s,t) + SC(s) + PDC\right) \tag{5.2}$$

with global intercept β_0^{λ} and coefficients of the other variables to be estimated.
The value $\lambda(s,t)$ represents the average number of pest peaks occurring in a unit of space and time around the point (s,t), and is assumed to be constant within each cell of the mesh during each time interval of 10.

Meta-model for magnitudes of pest density peaks

To model the maximum pest density value associated with each pest peak point, we consider a log-Gaussian GLM, *i.e.*, we combine a log-link function with a Gaussian distribution for the regression errors:

$$P_{max}(s,t) = \exp\left(\beta_0^{P_{max}} + STC(s,t) + SC(s) + PDC + \varepsilon(s,t)\right) \tag{5.3}$$

with global intercept $\beta_0^{P_{max}}$ and coefficients of the other variables to be estimated, where $P_{max}(s,t)$ is the maximum pest density value associated to the point where the pesticide application is applied, conditional to the occurrence of such a point. The term $\varepsilon(s,t) \sim \mathcal{N}(0,\sigma^2)$ corresponds to the spatially and temporally independent and identically distributed Gaussian error terms.

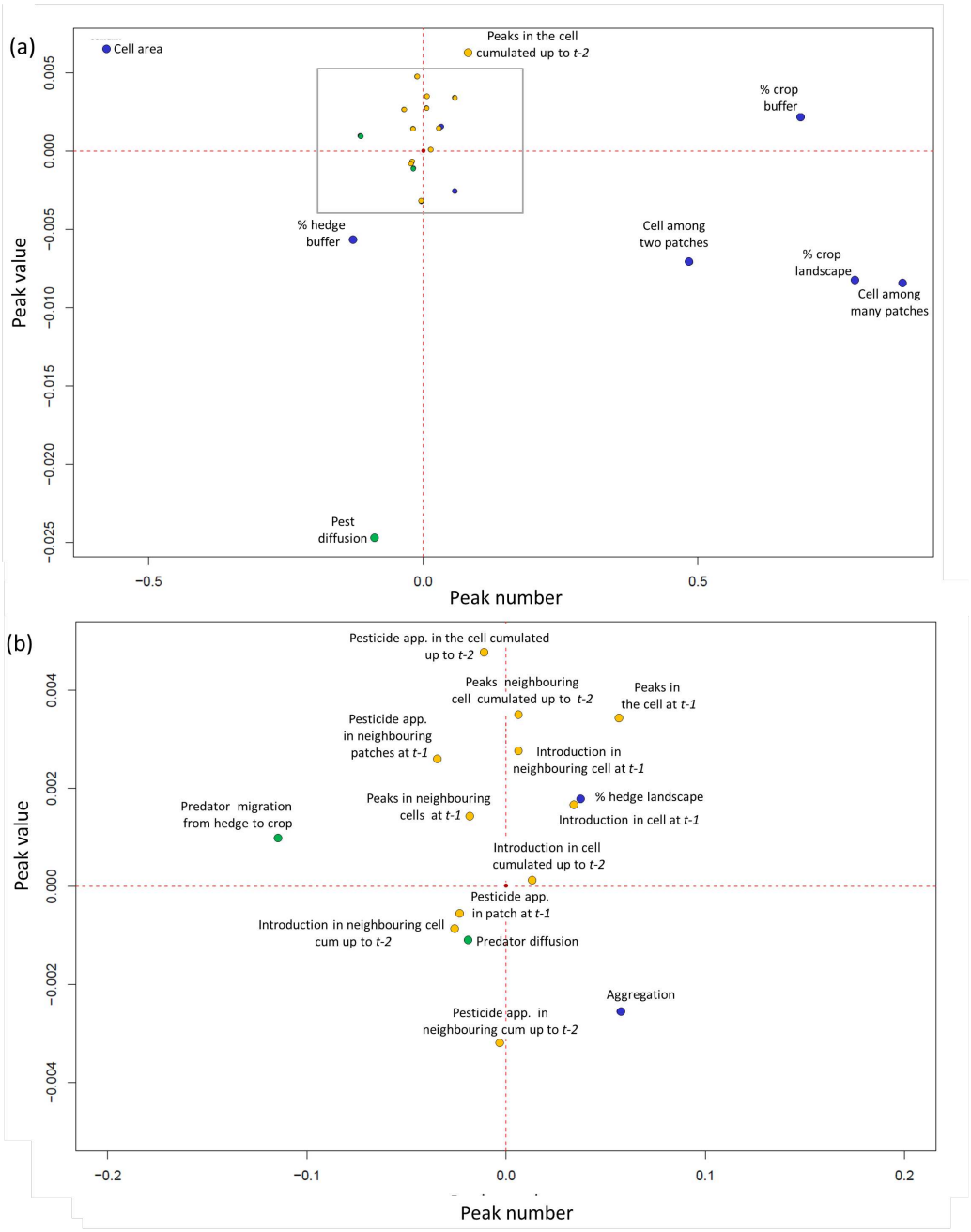

Figure 5.5 – Estimated regression coefficients for the models of peak occurrence intensity (x-axis) and the model of the peak value (y-axis). Colours of dots indicate covariate types: *STC* (orange), *SC* (blue), *PDC* (green).

Main results

To assess the effect of different local and global drivers (*i.e.*, STC, SC, PDC), we analyse the estimated GLM coefficients for the models in Equations 5.2 and 5.3 in Box 5 (Figure 5.5).

Before estimation, covariates have been normalised to empirical mean 0 and variance 1 to compare more easily the magnitudes of estimated effects.

In Figure 5.5a, we identify the drivers leading to the strongest effect on the peak number and value. For example, as expected, crop coverage at local scale (*i.e.*, in the buffer) and at global scale (*i.e.*, in the whole landscape) strongly favours the abundance of suitable habitat for pests, which can easily spread and find resources. By contrast, the strongest negative effect on pest peak values is pest diffusion and may be due to a dilution effect: high pest diffusion allows the pest to easily move, so the pest population tends to spread homogeneously over the whole landscape. Therefore, few local hotspots arise, and the pesticide threshold for average pest density over a field is less often exceeded. Both response variables related to pest peaks are also strongly reduced by local predator presence, which in turn is mainly driven by a high local presence of hedges.

Figure 5.5b shows a zoom of covariate effects with a lower magnitude. High numbers of pest peaks along with high peak concentration values (top-right quadrant in Figure 5.5b) are relatively strongly favoured by the presence of previous peaks in the same cell or in the surrounding ones (both at $t-1$, and cumulated up to $t-2$). Similarly, an elevated number of pest introductions in neighbouring cells leads to high pest concentration due to pest spillover. On the other hand, the application of pesticide applications locally in the patch or in neighbouring patches at previous time steps leads in general to a decrease of both the number and the concentration value of peaks. Results show a negative effect of hedge proportion in the buffer on pest activity. However, there also arises a weaker but positive effect of the hedge proportion over the whole landscape, which may appear counter-intuitive at first glance. Since response variables are evaluated at cell scale, having a large hedge proportion in the whole landscape but a low proportion of hedges in the buffer clearly results in a concentration of pest where hedges are missing. In addition, hedges help to keep the pest below the pesticide application threshold and therefore favour its propagation through the landscape (see Chapter 4 and Zamberletti et al. (2021b)); therefore, the pest may reach areas of lower predation pressure more easily and pull out. Predator spillover (*i.e.*, movement from hedge to field) results in a decrease of the number of threshold exceedances, but it may increase pest peak values since the predators are not homogeneously present in the patches and over the whole landscape. Predators have stronger influence near hedges (*e.g.*, in cells overlapping different patches) but less in the center of the patch (central cells).

Discussion

In this Chapter, we propose post-model scaling using regression meta-models based on marked STPPs. This approach enabled us to assess and compare the contribution of different spatio-temporal covariates and life-history traits to the direction and strength of variation in crucial events of population dynamics issued from spatially explicit models. The use of statistical regression meta-models makes our approach flexible and easy to implement, while numerous and diverse covariates describing local and global characteristics can be incorporated. We applied our methodology to the outputs of a SEM describing the biological control in agricultural landscapes of a crop pest by its natural predator. We found significantly different effects of landscape structures at various spatial scales on the population dynamics patterns.

The adaptation of our approach of defining a marked STPP meta-model may be relevant and insightful in various other contexts. Examples where STPP modeling is useful are occurrence locations and times of earthquake epicentres (Lombardo et al., 2019), wildfires (Opitz et al., 2020), epidemiological outbreaks (White et al., 2018a), biodiversity hotspots and species distribution (Soriano-Redondo et al., 2019), pollutant concentrations (Lindström et al., 2014) or local maxima or minima in meteorological events (Heaton et al., 2011). In most ecological processes, space and time are closely intertwined and not separable, where pest introductions and subsequent peaks depend on local temporal dynamics driven by local spatial structure. Thus, here, we design our approach to allow for joint analysis of spatial and temporal scales. For ecological processes related to those we study, White et al. (2018a) address how landscape structure impacts simulated disease dynamics in an individual-based susceptible–infected–recovered model. They quantify disease dynamics by outbreak maximum prevalence and duration, coupled with landscape heterogeneity defined by patchiness and proportion of available habitat. They find that fragmentation promotes pathogen persistence, except for simulation with high conspecific density, slower recovery rates and larger perceptual ranges, where more complex disease dynamics emerged; the most fragmented landscapes were not necessarily the most conducive to outbreaks or pathogen persistence. Our work has similar thrust by exploring the effect of landscape heterogeneity on pest density peaks. However, by taking advantage of the STPP modelling, we focus on spatio-temporal positions of peaks, and we investigate which factors locally influence occurrence intensity and magnitude of these events. The meta-model allows us to depict complex spatial dynamics and patterns even if multiple processes occur at competing scales (White et al., 2018b). To assess fine-scale biodiversity, Azaele et al. (2015) capture species patterns through correlations among different species' abundances across sample plots. Therefore, they use counts over spatial units (*i.e.*, plots), determined by the sampling design and leading to relatively large counts, and they contrasted their results with common species–area curves (Fritsch et al., 2020). They conclude that this mathematical framework

provides a common language to link different spatial scales. Our approach goes beyond a purely descriptive "geostatistical" analysis since we take into account the space-time position of each of the points as well as their relationships with nearby key elements. This representation parsimoniously summarises spatially continuous dynamics into discrete occurrences of spatio-temporal key events and allows modeling them for explanatory and predictive purposes. Our regression model for occurrence intensities also aggregates individual events, but we work with relatively small counts by choosing appropriate, problem-specific space-time units.

Ecosystem patterns and processes can cover a wide range of space and time, and they depend on multiple drivers acting over different scales (Fritsch et al., 2020). Problematic loss of information may arise in procedures of scaling-up or scaling-down when coupled with the complexity of the involved systems. Our work strikes a pragmatic balance with respect to the inevitable trade-off between model simplicity, to obtain clear insights into important factors, and model complexity, to achieve a more complete and realistic representation of the system (Lacy et al., 2013). Spatio-temporal meta-models present a flexible solution by capturing the functional linkages between model components. They show great potential to reveal properties in ecological systems that are difficult to identify when considering only the complex model output with large data volumes as a whole (Lacy et al., 2013). Our STPP model allows for a relatively complex spatio-temporal local analysis of system dynamics. It therefore provides insights into the role of different effects and takes process-specific scales into account by using categorical or numerical marks. Through statistical inferences, it becomes possible to identify significant relationships of key events with their drivers focusing on biotic interactions, habitat heterogeneity and spatio-temporal stochastic effects, and to provide predictions (Baddeley et al., 2015). A large body of literature on meta-models (or surrogate models, or emulators) in various disciplines focuses on Gaussian processes or machine-learning techniques (*e.g.*, Forrester et al., 2008; Kleijnen, 2015), whereas our work highlights the potential of point-process-based approaches for dynamical systems. This novel way of conducting meta-analyses is applicable to various collections of relevant events arising in dynamical processes available at high spatio-temporal resolution. We emphasise that our methods leverage spatio-temporal and multivariate point pattern techniques, while the state-of-the-art in point pattern analyses deals mostly with purely spatial patterns or does not well represent the temporal dimension (Wiegand et al., 2017). Our extensions are well-suited for spatio-temporal mechanisms and population dynamics parameters, where the assessment of their relative and joint role is crucial for characterising emerging diversity patterns.

In the application to the predator-pest dynamics, we benefit of this kind of approach to distinguish the roles of different covariates types and the effects of different scales. Spatio-temporal covariates (STC) contribute spatio-temporally structured information, such as the number or magnitudes of previous or concomitant events around a given location and

time, which conveys additional information to understand the evolution of pest dynamics. Le Gal et al. (2020) highlight the important influence of the interplay between the landscape structure and the timing of CBC measures on the delivery of pest control services. They show that increasing the SNH proportion at the landscape level enhances the visitation rate of pest-colonised crop cells, but it also reduces the delay between pest colonisation and predator arrival at the crop fields (Le Gal et al., 2020). In our model, we have opted for simulating the time and position of pest arrival according to a Poisson process with intensity proportional to crop area. We find that locations showing frequent and high density peaks in previous time steps are likely to incur new peaks. On the other hand, local previous pesticide applications in a patch negatively influence the dynamics since they efficiently reduce the pest density in this patch. Introductions of pest act as an accelerator of local pest dynamics, and after a short period we often assist to both high frequency and high magnitudes of peaks in the surrounding fields.

Spatial covariates (SC) are time-invariant landscape characteristics that may influence pest peaks. Crop proportion is the main driver for pest in our models, and leads to a clear positive response of pest insects to increasing cover of a suitable crop (Ricci et al., 2019; Rand et al., 2014; Zhao et al., 2015; Avelino et al., 2012; Tscharntke et al., 2007). Our results show that considering it at local scale or at global scale leads to different peak patterns. When crop aggregation and percentage coverage are high in the whole landscape, exceedance events of pest density are relatively homogeneously spread over the area with generally relatively low pest density values throughout. Instead, when high crop coverage is only local (*i.e.*, in the buffer), the resulting pattern shows a locally higher number of exceedance events with high peaks; pests find their preferred habitat in a more limited space and tend to concentrate there. In Chapter 4, we show that in landscapes with strong aggregation of crop fields the area of contiguous crop may cause a dilution effect with a positive effect on pest population, a negative effect on pesticide application occurrence, and a positive effect on the pesticide application numbers in the whole landscape. Therefore, if pesticide applications are necessary in a patch, they tend to arise in relatively high numbers over the full observation period. Hedge distribution and proportion can be viewed as a proxy for predator presence and reveal when predators may play a role in reducing pest density (Bianchi et al., 2006; Tscharntke et al., 2007). The effects attributed to SNHs (*e.g.*, hedges) are ambiguous with both positive, negative or neutral impacts on CBC (Chaplin-Kramer et al., 2011b; Karp et al., 2018). In our models, total hedge proportion has a small but positive effect on both the number and the magnitude of peaks. A reason could be that the global proportion of hedges does not inform about hedge connectivity and distribution (*e.g.*, homogeneously or in clusters). If there is a high hedge coverage, predators are expected to be homogeneously distributed in the landscape, thus stabilising the pest population and potentially reaching an equilibrium in the whole landscape for pest and predator density. However, this does not imply that pest density remains under the pesticide application threshold; it could happen

that other parameters influence its dynamics by favouring pest population (*e.g.*, crop coverage or pest growth rate) or decreasing predator presence in field (*e.g.*, mortality, spillover from hedge). This results in a homogeneous predator presence that is not sufficient to prevent pest density from exceeding the threshold. In our model, another reason could stem from statistical confusion in the regression models between the effects of global hedge proportion and global crop proportion since the simulated landscape model tends to position hedges more often in crop areas than in the rest of the landscape. However, when focusing on local buffers around a cell, local hedge structure and the resulting predator concentration play a bigger role by reducing both number of pest peaks and their magnitude.

Population dynamics covariates (PDC) are related to species traits. Here we consider the effect of varying population parameters related to species mobility in the environment. We find that predator diffusion ability over the landscape is fundamental to reduce the presence of pest. Interestingly, we do not notice the same effect for predator migration speed from hedge to field. This predator trait acts most strongly at locations close to hedges, *i.e.*, around patch borders, with a strong decrease in the number of peaks, while the peak value is not affected but is high mostly in the patch core areas.

Our analysis provides explanations of spatio-temporal event occurrence and magnitude with respect to local and global drivers, which could be of importance for prediction and management decisions. For example, within the context of our application, improved understanding of local spatio-temporal relationships and dynamics helps to schedule specific local control strategies by targeting the locations that more frequently suffer from pest peaks, and by identifying the moments when local control strategies can be expected to be most efficient to control pest dynamics.

Perspectives and open questions

- Modelling the effects of pesticide on predators. As discussed in Chapter 4, the pesticide only influences indirectly predator dynamics through increased pest mortality. Even if selective insecticides exist and allow focusing only on the target pest species, a more complete analysis would be to consider also broad-spectrum insecticides, which kill pests and predators indiscriminately (Bianchi et al., 2013).

- Exploring the sensibility of CBC outcomes depending on the economic threshold of pesticide application in more details. This threshold is a variable that could be controlled by farmers depending on the economic value of crops and the pest damages (Bianchi et al., 2013; Ragsdale et al., 2007).

- Considering a more complex predator-pest system, taking species traits and strategies into account (see Part III), or developing a model that considers different life stages.

For example, *Codling moth*, in common with other lepidopteran hosts, supports a rich assemblage of parasitoid species that attack the host at successive stages in the life cycle and differ in mode of development (Mills, 2005). This would allow identifying the most vulnerable life stages where the pest regulation by pesticide applications or predators would be likely more effective. In addition, life cycles of pests and predators may be of quite different lengths, and population stages could be present at the same or different time (May and Hassell, 1988).

- Applying the developed theoretical model on real biological system. This would allow us to contrast the general outcomes of our modelling framework with real system observations. Moreover, it would give the opportunity of estimating population dynamics parameter on real data in a study-site specific application. Finally, as the approach would be applied on a specific system, different simulation scenarios could be tested to offer the possibility of studying biological management strategies and of providing concrete suggestions instead of general guidelines.

Part III
Trophic networks, species traits and behaviours within complex agricultural landscapes

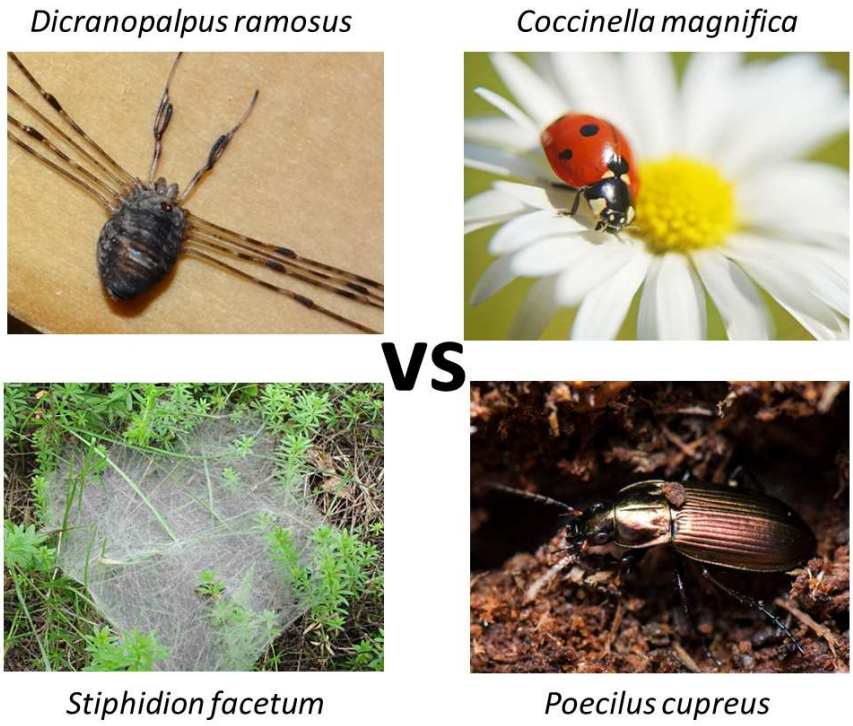

Figure 5.6 – Different predating strategies. First line (from left to right): nocturnal vs diurnal; Second line (from left to right): sit-and-wait vs actively foraging

Chapter 6

Multi-species interactions within complex agricultural landscapes

In Part 2, we have analysed the joint role of the landscape structure and population dynamics for biological control outcomes at global and local scale. In general, we highlight the key role of landscape linear elements (*i.e.*, hedges) as semi-natural habitats (SNH) for pest regulation. SNHs are considered as proxy of natural enemy abundance, but we have demonstrated that the presence of SNHs is not enough to drastically reduce the pest density. SNHs are able to sustain a high population of natural enemies, which act by keeping the pest population density under the treatment threshold. The predator population can favour pest spread across the landscape, thus increasing pest density at the landscape scale, even if fewer treatments are applied. In addition, we show that the influence of species depends also on their traits. The major influence on pest density and related treatments is represented by the predators' ability to disperse from hedges to crop fields. Thus, a large hedge proportion and high predator spillover jointly favour predator pressure and reduce pesticide treatment applications. In this situation, hedges ensure an increased landscape functional connectivity that enables predators to successfully disperse and feed on complementary resources in the fields. In this first analysis in Chapter 4, we have aggregated outputs over time and space, but we recognise that interesting information may be masked, such as local spatio-temporal relationships or patterns. Since we have used spatially-explicit models (SEMs) to achieve a high level of detail and precision, we presented in Chapter 5 an approach to overcome the computational complexity, the high amount of data and memory requirements and the problem of outputs that are difficult to analyse. We have developed a meta-model based on a spatio-temporal point process (STPP) to analyse SEM output with the aim to characterise spatio-temporal population dynamics and landscape heterogeneity relationships in an agricultural context. We provide local insights on spatio-temporal dynamics of the pest-predator system. In this 3rd Part, we now go further with the aim

of exploring the role of landscape heterogeneity in shaping the strategy and the trophic interactions of different species depending on their traits.

Species richness, functional and genetic diversity

The influence of species richness on arthropod BC has been largely discussed and reviewed in Schmitz (2007) and Letourneau et al. (2009). Species richness has been commonly used to assess species diversity within ecosystems. However, predators cannot be treated collectively as a single trophic level, since this would assume that predator species have identical effects and functions in ecosystems and would therefore be functionally substitutable (Schmitz, 2007). Predators can interact synergistically or antagonistically, and, consequently, an elevated number of natural enemy species does not directly correspond to a positive effect on pest regulation (Crowder and Jabbour, 2014). Indeed, they may show a negative impact when natural enemies are in competition and disturb each other, which limits the predator density or the predator pressure efficacy (Northfield et al., 2010; Finke and Snyder, 2010). Functional diversity may be relevant for assessing the effect of species diversity on biological control relationships (Crowder and Jabbour, 2014). Species can be lumped into functional groups based on ecological traits, similar behaviours and resource utilisation. Species in the same group are considered as ecologically redundant, whereas species in different groups are considered as complementary (Hillebrand and Matthiessen, 2009; Northfield et al., 2012). Species richness is beneficial for BC when species act complementary in term of pest suppression (Northfield et al., 2010; Finke and Snyder, 2010). Natural enemy species may complement each other in predation time (*e.g.*, day vs night, different seasons), space (*e.g.*, different habitat domains) (Snyder, 2019; Schmitz et al., 2017) and attack strategy (*e.g.*, actively searching vs sit-and-wait) (Northfield et al., 2012). For example, Northfield et al. (2017) distinguish different outcomes for a simple trophic network composed of two predators and a prey depending on the space used by each species. One can identify the cases where the predators have a substituting effect, where they have a negative interaction among them, or where the system evolves towards intra-guild predation; see Figure 6.1.

The functional role of each species in the ecosystem may be determined by any morphological, behavioural, or physiological trait that is associated with a biotic interaction or ecological function of interest. By contrast, a unique and unequivocal measure of functional diversity is not so straightforward to define due to the large number of traits, the diverse influence of traitas, and the difficulty of measuring trait diversity (Tilman, 1996). Petchey and Gaston (2006) deeply review how functional diversity could be crucial in assessing and predicting the impact of organisms on ecosystems, but also discuss the critical points in developing consistent predictive measures. When species are categorised in functional groups, there can be certain levels of functional redundancy (*i.e.*, a high number of

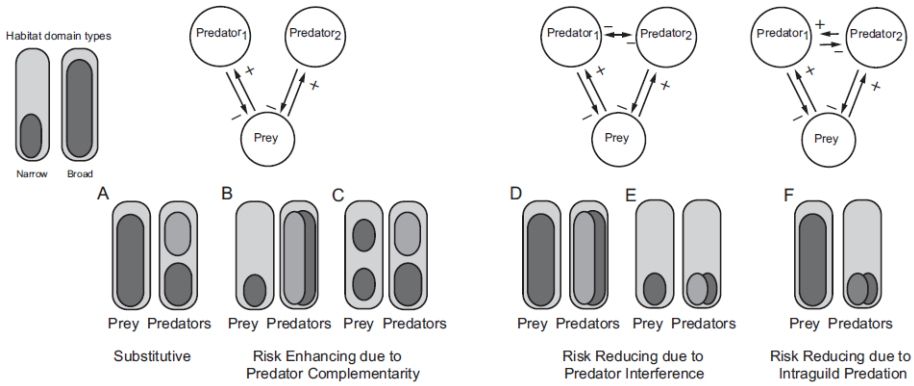

Figure 6.1 – Different relationships of multiple predator influence on a prey depending on the spatial interactions determined by the predator and prey habitat occupations from Northfield et al. (2017).

species within the same functional group) (Balvanera et al., 2006), which however should not be considered in negative terms. In fact, the number of different enemy species within a functional group can predict the durability of this function for herbivore suppression. For example, Schweiger et al. (2007) find that agricultural intensification caused extirpation of species unevenly across functional groups of syrphid fly predators: specialists get lost due to habitat degradation, instead Generalist species are able to persist. However, characterising enemy diversity or defining their assemblages may require attention to factors beyond the number of species that share prey and the number of predators within the same functional group (Letourneau et al., 2009). Letourneau et al. (2009) discuss the difficulty of generalising and predicting BC outcomes by using species richness and functional diversity. In fact, species losses and introductions in natural enemy communities have unpredictable effects on herbivore suppression due to the wide range of enemy-enemy interactions that can occur. Moreover, this enemy species interference may change and evolve not only depending on the interactions among them, but also depending on host density, for example through intensified within-host competition and host-feeding attacks (Kato, 1994), or via increased bird predation of parasitised hosts (Tscharntke, 1992). In addition, species having the same function in the present environmental context may respond differently in the future as they may adapt their traits and behaviours in different ways in response to changing drivers. Species in the same functional group may operate at different scales, thus, providing mutual reinforcement and contributing to the resilience of a function (Peterson et al., 1998). In general, since species richness and species functional diversity are naturally linked (Tilman, 1996; Cadotte et al., 2011), it is always important to consider both of them and their correlation within each environmental context (Tilman et al., 2001).

The adaptive foraging game

As predator–prey interactions are often represented as consumptive acts between two species (Gotelli et al., 2008), this may entail that all predators are viewed as being functionally equivalent for capturing and consuming prey, and that all preys are passive victims (Schmitz et al., 2017). Consequently, in such frameworks it is assumed that the interaction type and strength are invariant among species and environmental contexts (Peckarsky et al., 2008). However, predator–prey interaction can vary in space and time depending on variation in the predators' hunting and feeding mode and the preys' mobility and escape ability, and the surrounding environment (Schmitz et al., 2017). The predators' feeding mode may determine the size range and the prey species consumed: sit-and-wait predators are more keen on capturing actively moving prey, whereas actively moving predators are more keen on capturing sedentary prey. When predators and preys face an environmental change, they may undergo changes in their hunting mode and escaping mode, respectively, which leads to morphological or behavioural changes (Schmitz et al., 2017). In this setting, prey-predator systems can be defined as *adaptive foraging games* (Kotler, 2016; Brown et al., 2001; Schmitz et al., 2017): the predators' objective is to capture and subdue the prey, whereas the preys' objective is to be able to evade or fend off their predators. For example, preys may become more vigilant, shift their foraging time budget, or shift between foraging habitats and refuge habitats, or increase their mobility. The way in which predators can affect prey species' behaviour, that in turn can influence other elements of the food web, constitutes the *ecology of fear* (Brown et al., 1999). In fact, the interplay between adaptation and species interactions not only explains the community assembly dynamics but also the functioning of complex food webs (Urban et al., 2008). These reciprocal interactions between ecological and evolutionary processes are called *eco-evolutionary processes* or *feedback* (eco-evo) (Becks et al., 2012; Legrand et al., 2017; Bonte and Bafort, 2018). A rapid evolution in response to such selection mechanisms can affect the ecological dynamics, which in turn produce feedback on the evolutionary processes (Burton et al., 2010; Bonte and Bafort, 2018).

6.1 The distribution of species traits

The degree of trait variation between interacting species can explain considerable variation in the nature and strength of trophic interactions (McGill et al., 2006; Schmitz et al., 2015). Usually, in functional trait approaches, mean trait values are assumed to adequately represent species interactions and their effects on community structure (Schmitz et al., 2015). However, using mean trait values or simply species identity ignores considerable intraspecific trait variation (Start and Gilbert, 2017; Sommer and Schmitz, 2020; Schmitz et al., 2015). In Figure 6.2 taken from Sommer and Schmitz (2020), we see different frequency distributions representing variation among individuals for any given trait. In Panel a), all

individuals show an identical trait response: all individuals in the population undergo the same direction and magnitude of trait response. In this case, as all individuals have an identical trait response, the mean is an accurate characterisation of the population's heterospecific interactions. In Panels b) and c), individuals do not show an identical trait response but converge towards a similar mean (b), or show opposing directional responses (c). In these cases, considering only the mean value is not enough to appropriately capture differences among individuals (Sommer and Schmitz, 2020). Consistent differences among individuals in their suites of behaviours are defined as animal personality, which may play an important role for trophic dynamics. For example, predator personality can determine activity rates and patterns of attack. Start and Gilbert (2017) study how predator personality and density interactively structure prey abundance, community composition and the strength of trophic cascades. Sommer and Schmitz (2020) study how personality differences in a species of herbivore prey mediated tri-trophic interactions involving its predator and its plant resources.

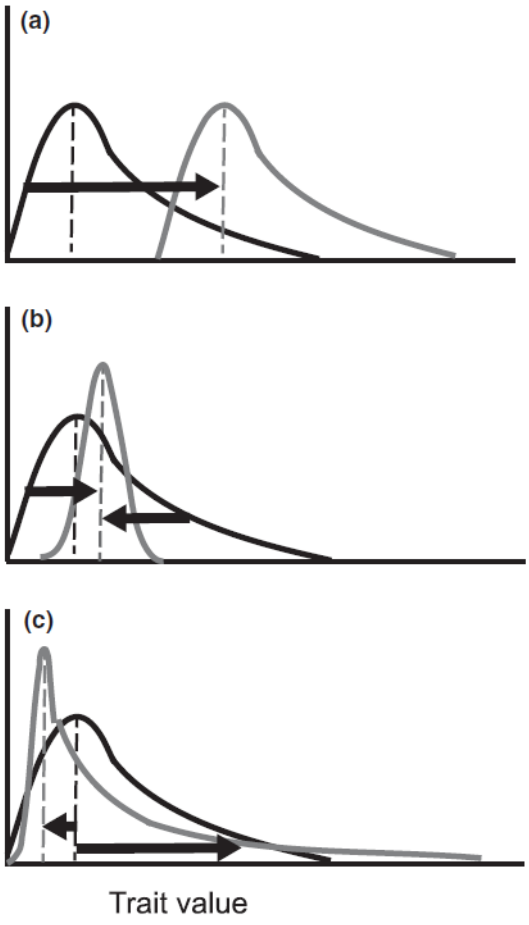

Figure 6.2 – Different frequency distributions of an individual trait within a population. The initial trait distribution is represented by black curves; the changed trait distribution is represented by light gray curves. (Panel a) all individuals show an identical trait response, (Panel b) individual traits converge towards a similar mean, with the resulting trait distribution showing smaller variance and a shifted mean value within the population. (Panel c) individual traits undergo opposing directional responses, with the resulting trait distribution showing higher variance and a shifted mean within the population (Sommer and Schmitz, 2020).

Systems involving pests and their natural enemies are characterised by a multitude of species and behavioural diversity and are influenced by environmental conditions. Our goal is to provide a deeper investigation of the species functional diversity and the key elements which influence the dynamic of pests and natural enemies in complex landscapes. In the following Chapter 7, we specifically focus on how the traits related to dispersal and growth rate may evolve during a species invasion. The aim is to assess how species are able to adapt to a heterogeneous environment and the subsequent eco-evo dynamics. Here, we concentrate on evolutionary aspects by looking at trait selection and mutation in an eco-evolutionary trade-off between growth and dispersal on a propagation front in a heterogeneous 1D environment. Then, in Chapter 8 coupling the take-home messages from Part II and Chapter 7, we enlarge the predator-pest system with more complex dynamics to investigate the role of heterogeneity in shaping the selected behavioural strategies. This idea is developed by considering complex landscapes simulated through the model presented in the Section 2.2, where we enlarge the population dynamics system of Chapter 4 by considering two predators and two pests with opposite behaviours.

Chapter 7

On the evolutionary trade-off between growth and dispersal during a range expansion

Even if individual variability may cover a very large range of trait values, functional trait approaches have mostly been studied by considering only the mean trait value over the population, as we have done in Chapters 4 and 5. By contrast, trait variation is central to understand how individuals interact along them, how they are influenced by the surrounding environment (Start and Gilbert, 2017), and which evolutionary dynamics result from these mechanisms. For example, the mean value will not capture differences among individuals if trait responses are not identical; see Sommer and Schmitz (2020). Some theoretical studies have investigated how intra-specific trait variation affects population dynamics (Vindenes et al., 2008; Doebeli, 1996), interspecific competition (Lankau, 2009; Lichstein et al., 2007), and predator-pest or host-parasitoid or host-pathogen systems (Okuyama, 2008; Saloniemi, 1993). These studies consider variation in diverse traits, such as traditional phenotypes (*e.g.*, size or morphology) or emergent traits (*e.g.*, competitive ability, prey attack rate, or vulnerability to enemies) or fitness-related traits (*e.g.*, fecundity or survival) (Bolnick et al., 2011). Their results are very dissimilar (and sometimes conflicting) and depend strongly on the specific modelling approach and underlying assumptions.

A better characterisation of functional trait variation is of key importance since it has consequences for evolutionary processes describing how species respond to new pressures, changes of trophic dynamics or of the environmental context (Sommer and Schmitz, 2020). Intraspecific variation underpins evolution that can alter ecological processes and lead to feedbacks (Bolnick et al., 2011). Reciprocal interactions between ecological and evolutionary processes, which enable the organisms to both shape their environment and adapt to it, are

called Eco-evolutionary processes or feedback (eco-evo) (Becks et al., 2012; Legrand et al., 2017; Bonte and Bafort, 2018).

When considering eco-evo processes, the spatial structure of the landscape has a fundamental role, especially in rapidly changing systems like natural environments. Such environments are currently cut into fragments by human activities, in particular by agricultural practices and urbanisation in terrestrial ecosystems (Legrand et al., 2017). The fragmented landscape structure may influence genetic variation (DiBattista, 2008) and may induce a 'meta-functioning' at the levels of populations, communities and ecosystems, which affects evolutionary forces and the related ecological processes (Legrand et al., 2017). Especially, the fragmented landscape structure can deeply impact the evolution of dispersal traits and the covariation between dispersal and other traits (Cote et al., 2017). These changes act on balancing eco-evo processes, since dispersal in itself and through its covariation with multiple phenotypic traits has important effects on both ecological and evolutionary processes (Legrand et al., 2017). Dispersal affects capabilities to exchange individuals and genes among different habitats and influences trophic network dynamics across ecosystems (Legrand et al., 2017). Movement traits have been proved to be related to body dimension and condition (Duthie et al., 2015; Helms and Kaspari, 2015; Steenman et al., 2015), thus affecting competitive abilities, food web interactions (Bonte and de la Pena, 2009) or metabolic processes (Hirt et al., 2017). Variation in dispersal traits may also lead to the 'spatial sorting' of high-dispersal individuals at the expansion front that accelerate invasion (Shine et al., 2011; Bouin et al., 2012). Therefore, these traits are fundamental during invasion, colonisation and expansion processes: when species shift their range, they face a new selection pressure, and a rapid evolution can affect their ecological dynamics, which in turn lead to feedback on the evolutionary potential (Burton et al., 2010; Bonte and Bafort, 2018). However, there are many examples where individuals who invest more in the development of their traits related to the dispersal strategy reduce the effort in foraging and reproduction at the same time (e.g. by reducing their mating period or by using lower egg mass) (Baguette and Schtickzelle, 2006; Hanski et al., 2006; Bonte and Bafort, 2018). In such cases, two favourable evolutionary strategies are possible: dispersing faster, or growing stronger (Deforet et al., 2019). This results in a species' trait trade-off that shapes the eco-evo population dynamics and species spread in the environment.

Species introductions for biological control or pest invasions are likely subject to eco-evolutionary processes due to rapid human-induced environmental change within the complex landscape mosaic. Thus, it is relevant to study ecological processes and related properties, for example by evaluating the speed of pest species propagating in the agricultural crop and SNH intermixing and their population development capabilities (Szűcs et al., 2019). In fact, since agricultural landscapes are complex heterogeneous mosaics, pest or biocontrol agents experience novel abiotic and biotic conditions in unknown environments, which may impose strong natural selection leading to evolutionary changes (Szűcs et al., 2019).

Classical biological control is based on the idea that once a biocontrol agent is successfully settled, it can expand its range by following pest distribution and persist in the landscape (Eilenberg et al., 2001). However, biocontrol agents have species-specific dispersal-related traits that can mediate their rates of dispersal. During expansion, evolutionary processes can impact the fitness, reproductive rates, and dispersal ability of individuals on the front. Such a rapid evolution, in turn, can feed back to alter ecological characteristics (*e.g.*, growth rates or competitive traits) of individuals on the population expansion front that are likely to affect the dynamics of introduced populations (Pelletier et al., 2009; Szűcs et al., 2019).

The relationship between species life-history traits and environmental properties in a spatio-temporal context is often addressed by a mathematical formalism through the framework of reaction-diffusion models. Speed properties of biological invasions have been firstly assessed by Fisher (1937); Shigesada and Kawasaki (1997); Turchin (1998); Murray (2002) in a homogeneous environment with a normally distributed kernel of dispersal without mutation. Relaxing the hypothesis that the space is homogeneous and adding spatial and/or temporal heterogeneity may speed up or slow down the invasion, depending on which trait is affected by the environment (Shigesada and Kawasaki, 1997). Most theoretical studies based on the reaction-diffusion framework focus on the spreading properties, and, especially, on the existence of travelling wave solutions and their generalizations to spatially-heterogeneous environments (Berestycki and Hamel, 2002, 2005; Berestycki et al., 2005). The particular type of propagating solutions is the so-called pulsating front (Xin, 2000). Some recent works by Benichou et al. (2012); Bouin et al. (2012); Bouin and Calvez (2014); Berestycki et al. (2015) focus on demonstrating the travelling wave existence, and they study the spreading properties by developing an eco-evolutionary model to take into account species adaptation. Berestycki et al. (2015) propose a model where the acceleration dynamics is due to a continual selection of individuals with enhanced dispersion abilities. Thus, their model assumes a continuous and infinite space for the dispersal trait, which can take arbitrarily large values. Their work is based on a homogeneous space, and trade-off with other traits is not considered. They find theoretical and numerical results of expansion front properties (*e.g.*, front position and spreading speed solution) and compare local and nonlocal dynamics. Bouin and Calvez (2014) construct travelling wave solutions and evaluate the spreading speed of travelling waves for Australian cane toad (*Rhinella marina*) dynamics characterised by a unique continuous bounded phenotype trait, the toad motility. Their work addresses the issue of front expansion in ecology, where the studied trait is related to dispersal ability Bouin and Calvez (2014). However, in this case too, the space is homogeneous and there is no trade-off among traits.

In the present Chapter, we develop a reaction-diffusion model to describe the phenotype-space-time dynamics of a consumer species in a heterogeneous space during a range expansion. In contrast to the other Chapters, we follow a mathematical and numerical approach in order to better understand theoretical dynamics. We simplify the population model by con-

sidering only one species and a uni-dimensional space where heterogeneity is defined by a periodic function of favourable and unfavourable habitats. Our choice is driven by the aim of exploring in depth the species dynamics with an eco-evolutionay model that describes trait variation by a phenotype continuum, with the goal to assess the effect of trait trade-off on trait selection during a population expansion. Specifically, we focus on the trade-off between the growth rate R and dispersal rate D. In a spatially homogeneous environment and in the absence of mutations and Allee effects, the standard formula $v = 2\sqrt{R(y)\,D(y)}$ (Kolmogorov et al., 1937) clearly shows that growth and dispersal play a similar role on the spreading speed. We analyse here how this symmetry in the effects of R and D may be broken when facing spatial heterogeneities and/or in the presence of competition between phenotypic traits and of mutations. Specifically, we consider spatially-periodic environments and we modulate the level of spatial fragmentation with the goal of investigating the following questions: i) What is the spreading speed of the population range and the corresponding fastest phenotype trait? ii) What is the role of the competition among phenotypic traits? iii) What is the population composition along the expansion front?

7.1 Eco-evolutionary dynamics

A reaction-diffusion model, fully described in the Box 7, examines a consumer species dynamics where this species exploits a resource and disperses in a one-dimensional space. At time t and location x, the density of the consumer phenotype $y \in (y_{\min}, y_{\max})$ is defined by $c(t,x,y)$ (Equation 7.1). The spatial dispersion ($D(x,y)$) occurs in a one-dimensional environment, corresponding to random walk movements of the individuals (Turchin, 1998; Shigesada and Kawasaki, 1997). The mutation coefficient ($\mu \geq 0$) is proportional to the mutation rate (per individual per generation) and to the average effect of mutations on the phenotype (Hamel et al., 2020). The population grows logistically with heterogeneous growth rate $R(x,y)$. Competition occurs locally on the geographical space but globally over phenotypes through a non-local term, and it is modulated by a parameter γ.

$$\begin{aligned}\partial_t c(t,x,y) =& \partial_{xx}(D(x,y)\,c(t,x,y)) + \mu\,\partial_{yy}c(t,x,y) + \\ &+ c(t,x,y)\left(R(x,y) - \gamma\int_{y_{\min}}^{y_{\max}} c(t,x,s)ds\right).\end{aligned} \tag{7.1}$$

Simulation scenarios

We define three scenarios, depending on the presence of spatial heterogeneity, and on the trait which is impacted (see Box 7 for more details):

Scenario A: spatially homogeneous coefficients (i.e, $R(y)$ and $D(y)$).

Scenario B: heterogeneous growth and homogeneous dispersal (i.e, $R(x, y)$ and $D(y)$).

Scenario C: homogeneous growth and heterogeneous dispersal (i.e, $R(y)$ and $D(x, y)$).

7.2 Methods

We explore the consumer species *R-D* trade-off by analysing the population expansion dynamics depending on space heterogeneity. We focus on the spreading properties (See Box 7, Eq. 7.7), *i.e.*, we assess the range expansion behaviour in space, we identify the fastest phenotypic trait and we characterise the population composition on the expansion front and in the bulk of the population. We derive analytical approximations of the spreading speeds, using approximated models and limiting cases of rapidly and slowly varying environments, and we compare these approximations with numerical results. We further explore the phenotypic trait composition in the population by performing numerical simulations with different parameter value combinations. Specifically, the parameters we focus on are: i) the period of heterogeneity L, considering rapidly (small period $L = 2$) and slowly (large period $L = 10$) varying environments; ii) the distance d between the two optima, where we consider a short distance for weak trade-off ($d = 2$) and a large distance for strong trade-off ($d = 4$); iii) the amplitude of the heterogeneity $a \in (0, 1)$; iv) and, the mutation $\mu = 0$ (no mutations) or $\mu = 0.001$. We computed numerically the phenotype spreading speeds $v_{sim}(y)$ as:

$$v_{sim}(y) = \frac{x_{sim}(y)}{T_{sim}},$$

where $x_{sim}(y)$ is the furthest forward position of the phenotype y at time T_{sim} (T_{sim} is selected large enough such that $v_{sim}(y)$ does not vary much at larger times). Once the spreading speed for each trait is evaluated, either numerically or analytically, the phenotype y^*, which leads to the fastest spreading speed, can be evaluated and classified according to the phenotype classification of the Figure 7.1 as a D specialist, an R specialist and or a Generalist. Then, we use the same classification in order to categorise the whole population composition behind the front. When the environment is heterogeneous, we also take into account the role of the amplitude a in Equations (7.3) and (7.4). The amplitude is represented by the vertical distance among the $R(y)$ and $D(y)$ fitness functions in Scenarios B and C. It is possible to identify an amplitude threshold value influencing the class leading the colonisation front to distinguish when the front is led by the R specialist or by the D specialist. The equations are solved numerically by transforming them into lattice dynamical systems (continuous time, discrete space with small space step), and using a Runge-Kutta method over a fixed spatial domain and a time horizon large enough to ensure a stable dynamic and propagation front. The implementation is performed by using the software Matlab®.

Box 7: Modelling eco-evolutionary dynamics

Consumer eco-evolutionary dynamics

At time t and location $x \in \mathbb{R}$, the density of the consumer phenotype y is defined by $c(t,x,y)$. Spatial dispersion in a one-dimensional environment is described through a Laplace diffusion operator with diffusion parameter $D(x,y)$. Mutations between phenotypes are also described with a Laplace diffusion approximation (Tsimring et al., 1996; Hamel et al., 2020) with constant mutation coefficient $\mu \geq 0$. The function $R(x,y)$ is the (possibly) heterogeneous growth rate. The competition is modulated by the parameter γ. We assume a one-dimensional phenotype $y \in (y_{\min}, y_{\max})$. The reaction-diffusion model for the phenotype-space-time dynamics of the consumer population is defined as follows:

$$\begin{aligned} \partial_t c(t,x,y) = \partial_{xx}(D(x,y)\, c(t,x,y)) + \mu\, \partial_{yy} c(t,x,y) + \\ + c(t,x,y) \left(R(x,y) - \gamma \int_{y_{\min}}^{y_{\max}} c(t,x,s) ds \right). \end{aligned} \tag{7.2}$$

In addition, we assume no-flux boundary conditions at the boundaries $y = y_{\min}$, $y_{\max}$:

$$\partial_y c(t,x,y_{\min}) = \partial_y c(t,x,y_{\max}) = 0,$$

so that in the absence of demography (i.e., if $R = \gamma = 0$), the global population size $\mathbf{C}(t) = \int_{\mathbb{R}\times(y_{\min},y_{\max})} c(t,x,y) dx dy$ remains constant.

Genetic and spatial heterogeneity in dispersal and growth

Spatial heterogeneity in environmental conditions is assumed to impact the consumer growth rate R and its mobility D. Genetic and spatial effects on R and D are assumed to be additive:

$$R(x,y) = R_0 + R_g(y) + a\, R_s(x/L), \tag{7.3}$$

$$D(x,y) = D_0 + D_g(y) + a\, D_s(x/L), \tag{7.4}$$

where R_0 and D_0 are the basal values for growth and diffusion. These basal values are modified according to a genetic effects R_g and D_g, respectively, and spatial effects R_s and D_s, respectively. L controls the heterogeneity for R and D, and it is modeled as piecewise constant function with a period L over x. The coefficient a scales up the amplitude of the spatial heterogeneity, and it can vary from 0 to 1.

Genetic effect

Given the trait value y, the genetic effect on the growth rate R and the diffusion coefficient D is assumed to be Gaussian (Figure 7.1):

$$R_g(y) = \exp(-(y + d/2)^2/(2\sigma^2)), \tag{7.5}$$

$$D_g(y) = \exp(-(y - d/2)^2/(2\sigma^2)), \tag{7.6}$$

where $d = \mid O_D - O_R \mid$ corresponds to the distance between the two optima O_D and O_R. The optimum trait for diffusion is $O_D \in (y_{\min}, y_{\max})$, which represents the consumer optimal dispersal strategy, and the optimum trait for the growth rate is $O_R \in (y_{\min}, y_{\max})$, which represents the consumer optimal resource exploitation strategy. Here, we assume that O_D and O_R are symmetric with respect to 0, thus the two optima correspond to $\pm d/2$ (i.e $O_D = +d/2$ and $O_R = -d/2$, respectively). Specifically, in the Supplement 4B, we calculate a threshold d_{cr} that differentiates cases by selecting the Generalist or the specialists depending on the distance d between the optima. The coefficient σ is the standard deviation of the Gaussian function and indicates the intensity of selection around the optimal trait value. The phenotypic traits are classified into three classes (Figure 7.1): the D specialists (the phenotypic traits with narrow preference range on diffusion strategy), the R specialists (the phenotypic traits with narrow preference range on foraging strategy) and the Generalists (the phenotypic traits with broad preference range on diffusion and foraging strategy). More specifically, as $d = \mid O_D - O_R \mid$, the D specialists have the phenotypic traits belonging to the trait set $[+d/4, y_{max})$, the R specialists have the phenotypic traits belonging to the trait ensemble $(y_{min}, -d/4]$, while the Generalists correspond to the phenotypic traits belonging to the trait ensemble $(-d/4, +d/4)$.

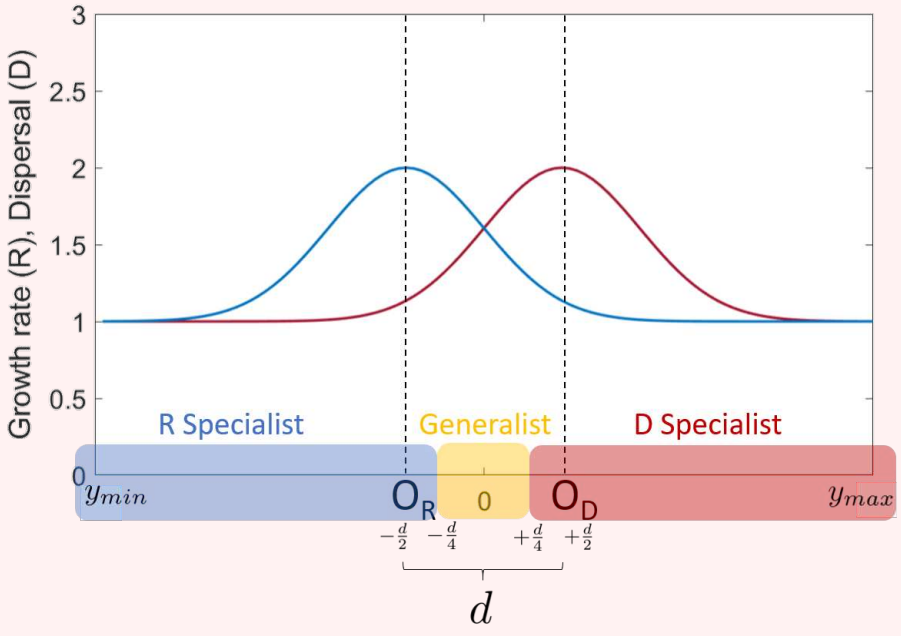

Figure 7.1 – Phenotype classification. The curves represent the dispersal rate $D(x, y)$ (red) and growth rate $R(x, y)$ (blue) as functions of phenotypic traits $y \in (y_{min}, y_{max})$ in the homogeneous case. The coefficient d is the distance among O_D and O_R, which are the optimum for dispersal and growth rate, respectively. The colored boxes highlight the classification of *D Specialist*, *R Specialist* and *Generalist*.

Environmental effect

In Equations (7.3) and (7.4), the terms $R_s(x/L)$ and $D_s(x/L)$ describe the periodic heterogeneity over the space x through periodic functions with period $L > 0$. Varying the period L allows describing different grains of spatial heterogeneity for the resource distribution and dispersal capability. Thus, we choose R_s as a 1-periodic piecewise constant function of mean 0, with $R_s(x) = R_0$ on $[0, 1/2)$ and $R_s(x) = -R_0$ on $[1/2, 1)$. The function D_s is a smooth 1-periodic function, with mean value 0, and bounded from below by $-D_0$ (so that D is always positive). More precisely, we define the 1-periodic function $\delta_1(x)$ such that $\delta_1(x) = D_0$ in $[0, 1/2)$ and $\delta_1(x) = -D_0$ in $[1/2, 1)$. Then, D_s is obtained by regularizing δ_1 with a convolution by a smooth function:

$$D_s(x) = \int_{\mathbb{R}} \delta_1(x - y)\, \phi(y)\, dy,$$

with ϕ a Gaussian function with small variance.

Simulation scenarios

- Scenario A:
  $R(x, y) = R_h(y) := R_0 + R_g(y)$ and $D(x, y) = D_h(y) := D_0 + D_g(y)$.
- Scenario B:
  $R(x, y) = R_0 + R_g(y) + R_s(x/L)$ and $D(x, y) = D_h(y) = D_0 + D_g(y)$.
- Scenario C:
  $R(x, y) = R_h(y) = R_0 + R_g(y)$ and $D(x, y) = D_0 + D_g(y) + D_s(x/L)$.

Methods for assessing the spreading property

The spreading speed V is the asymptotic rate at which a species, initially concentrated in a finite spatial region, expands its spatial range. It can be defined here as the smallest speed v such that, if an observer travels to the right (i.e., towards increasing x values) with speed v, he will observe that the population density converges to 0 (Figure 7.2). In mathematical terms, V is the uniquely defined speed such that the following two properties hold:

$$\begin{aligned} &C(t, x + v\,t) \to 0, \quad \text{as } t \to +\infty, \text{ for all } v > V, \\ &C(t, x + v\,t) \not\to 0, \quad \text{as } t \to +\infty, \text{ for all } v < V, \end{aligned} \tag{7.7}$$

with $C(t, x)$ the population density at spatial position x:

$$C(t, x) = \int_{y_{\min}}^{y_{\max}} c(t, x, y)\, dy.$$

For each phenotype y, the spreading speed $v(y)$ of the phenotype y can be defined as well by replacing $C(t, x)$ with $c(t, x, y)$ in the above expressions (e.g., $c(t, x + v\,t, y) \to 0$ as $t \to +\infty$, for all $v > v(y)$).

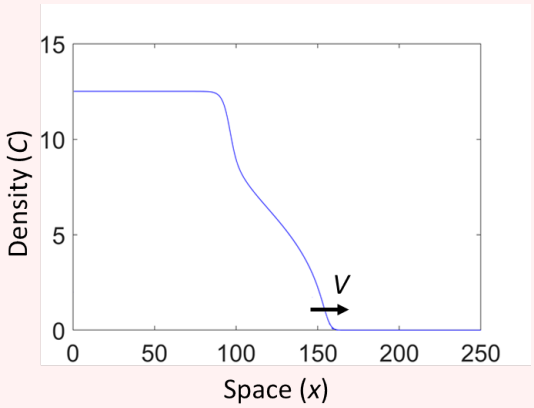

Figure 7.2 – Spreading speed (V) of the propagation front.

The existence of a spreading speed as well as analytical characterisations have been obtained by Kolmogorov et al. (1937); Aronson and Weinberger (1975, 1978); Fife and McLeod (1977) for standard equations with spatially homogeneous coefficients and local competition terms. Comparable results have been obtained in the early 2000s (Berestycki and Hamel, 2002, 2005) with a periodically varying coefficient as in Equation (7.2) and a local competition term, namely for equations of the following form:

$$\partial_t c(t,x,y) = \partial_{xx}(D(x,y)\,c(t,x,y)) + \mu\,\partial_{yy}c(t,x,y) + c(t,x,y)\,(R(x,y) - \gamma\,c(t,x,y))\,. \tag{7.8}$$

Here, the difference with Equation (7.2) is that the individuals with phenotype y only interact with individuals of the same phenotype. We conjecture that the spreading speeds V of the solutions of Equations (7.2) and (7.8) are equal, which is supported by the results of Alfaro et al. (2014). This would imply that the fastest phenotype,

$$y^* = \underset{y\in(y_{\min},y_{\max})}{\operatorname{argmax}}\ v(y),$$

has the same speed with and without non-local interactions. As the fastest phenotype, y^* does not compete with other phenotypes, and its speed should indeed not be influenced by the competition term, and therefore be the same for the two equations. For Equation (7.8), under our three scenarios (A,B,C), more or less explicit formulas for the spreading speed can be obtained available; under more specific conditions (see the Manuscript *On the evolutionary trade-off between growth and dispersal during a range expansion*), they can be simplified to more tractable formulas (see Table 1 of the above manuscript).

7.3 Results

We first compare the phenotype spreading speeds evaluated with the theoretical formulas against the numerical simulations to assess the fastest phenotype (Figure 7.3). Then, we analyse the phenotypic trait composition on the expansion front (Figure 7.4) and over the whole spatial domain (Figure 7.5).

7.3.1 Spreading speed

The spreading speed evaluated by analytical formulations is compared with numerical simulations with both local and non-local equations for different heterogeneity scenarios where we let vary the period L and the distance between optima d (Figure 7.3). In all cases, numerical simulations and analytical formulas are consistent with each other for the fastest phenotype identification. Generally, non-local competition shrinks the phenotypic trait distribution around the optimum value of the spreading speed, which leads to important differences between the theoretical spreading speeds and the observed ones for phenotypes y other than the fastest one. In the case of $d < d_{cr}$ (left column of Figure 7.3, d_{cr} is defined in the Supplement 4B), the Generalist has the fastest trait value on the expansion front in all the scenarios and for all periods L . However, we can notice that the spreading speed curve for the Scenario C is slightly shifted to the right, leading to an imbalance in favour of D. In the case $d > d_{cr}$ (right column of Figure 7.3), the standard behaviour described by Equation 7.8 (local competition) predicts that, on the expansion front, both phenotypes at growth rate and dispersal optima (*i.e.*, O_D and O_R) have similar speed in the Scenario A. Instead, when considering the Equation 7.2, the effect of the competition leads to the selection of the R specialist. This is also the case for the scenario B when the environment is changing quickly. However, in that scenario, a greater value of L leads to comparable spreading speed of both R and D specialists. In the scenario C the spreading speed is lower than in scenario A, and the trade off is completely shifted in favour of the D specialist.

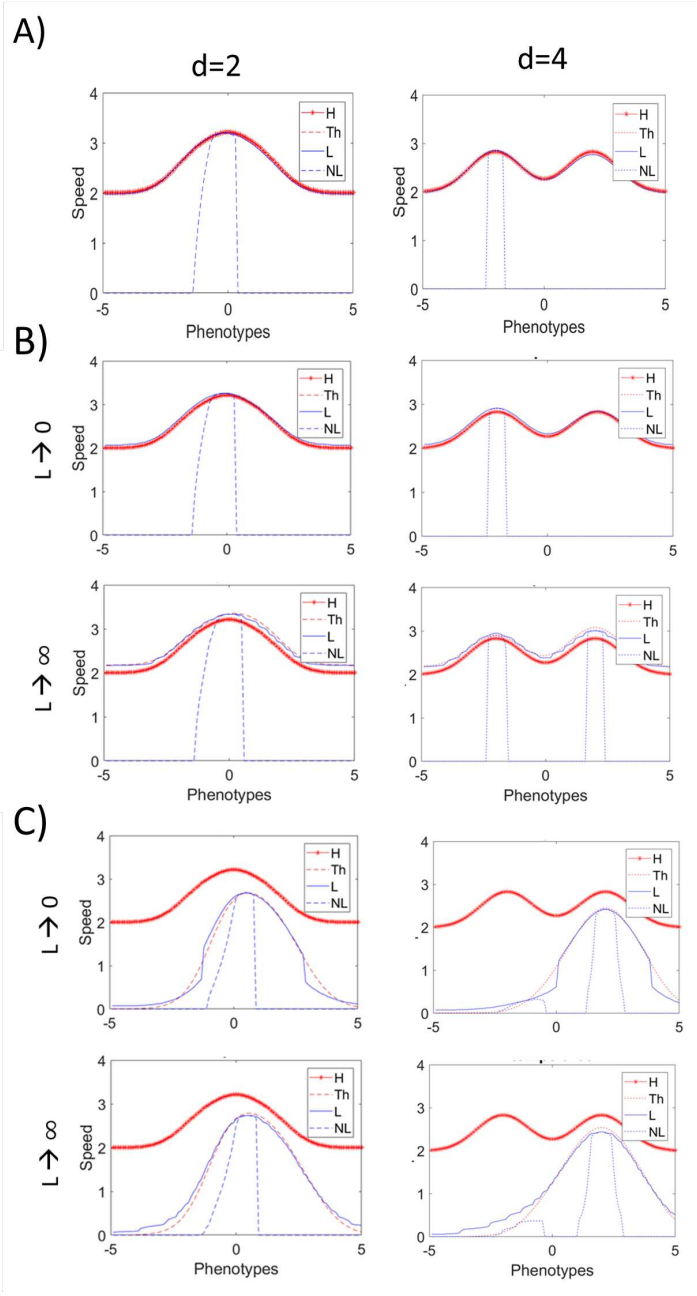

Figure 7.3 – Spreading speed in scenarios (A); (B); (C) for $\mu = 0$ and $a = 1$. The red line with stars stands for the homogeneous case formula (H), the dashed red line stands for the theoretical formula (Th), the continuous blue line stands for the local numerical solution (L), the dashed blue line stands for the non-local numerical solution (NL). Columns show different distance between optima. In panel (b) and (c) different lines show different period values ($L \to 0$ and $L \to \infty$).

7.3.2 Population composition on the front

Here, we assess the composition of the expanding front when varying the period L, the distance among the optima d and the amplitude a of the heterogeneity (Figure 7.4).

In the scenario B (Figure 7.4a), for $L \to 0$, the heterogeneity amplitude a does not produce any effect on the dynamics: when $d < d_{cr}$, the R-D trade-off is always in favor of the Generalist; when $d > d_{cr}$ the R specialist has the fastest phenotype. Instead, for $L \to \infty$ when $d > d_{cr}$, the fastest phenotype could be either the R or the D specialist. When $a < a_{cr}$, the behavior is in favour of the R specialist; when $a > a_{cr}$, the trade-off is shifted in favour of the D specialist.

In the scenario C (Figure 7.4b), both for $L \to 0$ and $L \to \infty$, a alters the trade-off among R and D. For $d < d_{cr}$, the fastest phenotype is always the Generalist. For $d > d_{cr}$, as before, the fastest phenotype could be either R or the D specialist depending on the value of a. Amplitudes below a_{cr} select for the R specialist whereas amplitudes behind a_{cr} select for the D specialist (see also Figure 7.3C for which $a = 1$).

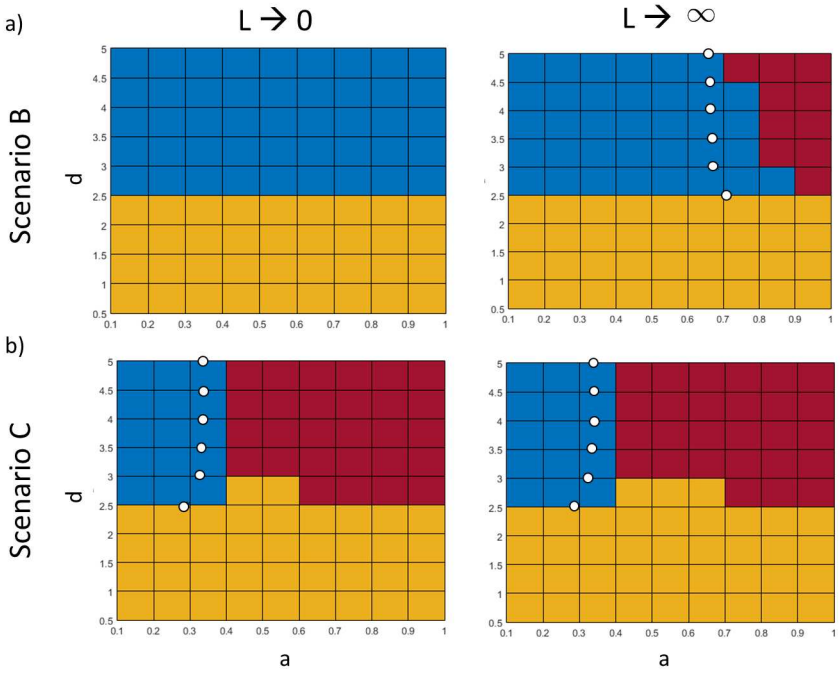

Figure 7.4 – Results of the numerical simulations for assessing the role of the amplitude of scenario B (Panel a) and C (Panel b) for non-local model in case of $L \to 0$ and $L \to \infty$. Parameter ranges are $a = [0.1 - 1]$ by 0.1 steps (x axis) and $d = [0.5 - 5]$ by 0.5 steps (y axis). The colours stand for the fastest phenotypic traits: yellow stands for Generalists, red stands for D specialists and blue for R specialists. The white points represent the value a_{cr} given for each d.

7.3.3 Total population composition

We analyse the composition of the total population behind the front under the different scenarios for the non-local case (Figure 7.5). Under the scenario B with a fast varying environment, the density of phenotype classes is invariant with respect to the amplitude of the heterogeneity and only varies with d. When $d > d_{cr}$, the population is composed by half of Generalists and by half of R specialists. As d increases, the R specialist proportion increases until being the only class present. For a slowly varying environment and for high amplitude value of heterogeneity, the population composition is not completely dominated by the R specialist, but there is a proportion of D specialist coming out. And specifically, this proportion is localised on the expansion front as demonstrated in Figure 7.4. Under the scenario C, when $d < d_{cr}$, there is an increase of the Generalist instead of the R Specialist as the amplitude a increases. When $d > d_{cr}$, there is a clear shift from a proportion in favour of the R specialist to the D specialist as the amplitude a increases. This shows that the D specialist takes the lead on the expansion front but also dominates a great part of the total population behind the front.

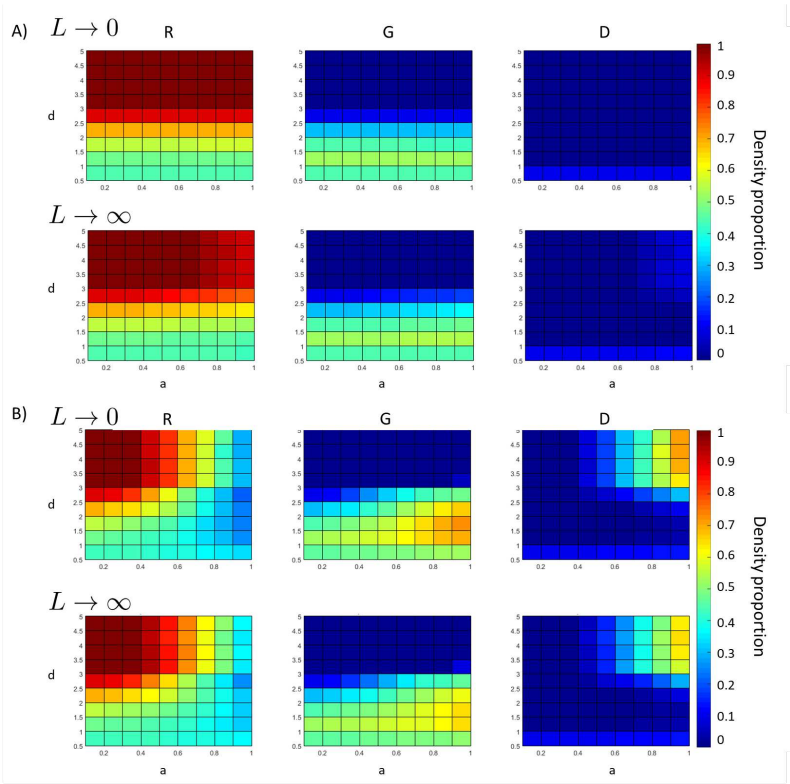

Figure 7.5 – Results of the numerical simulations for assessing the population composition in scenario B (Panel A) and scenario C (Panel B) for the non-local equation and in the case of $L \to 0$ and $L \to \infty$. The amplitude of heterogeneity varies as $a = [0.1 - 1]$ with step size 0.1 (x axis) and the distance between optima varies as $d = [0.5 - 5]$ with step size 0.5 (y axis).The colours represent the density proportion for each phenotype class: R for the R specialist, G for the Generalist and D for the D specialist.

7.3.4 The effect of mutation

In all of the scenarios and parameter combinations, we also evaluate the effect of the mutation. We observe that it only leads to a homogenisation of the phenotypic distribution and therefore to a wider phenotype ensemble that leads the propagation front. However, the mutation does not affect the R-D trade-off outcome: the fastest phenotypic trait is the same without and with mutations.

By contrast, when the system is composed of only the two phenotypes $y = O_R$ and $y = O_D$ instead of a continuum $y \in (y_{\min}, y_{\max})$, and assuming a low mutation rate among them, we numerically find an overall spreading speed (v_f) which is higher than the maximum of the spreading speeds of each phenotype independently, i.e., strictly larger than

$$\max\left(2\sqrt{R_h(O_R)\times D_h(O_R)}, 2\sqrt{R_h(O_D)\times D_h(O_D)}\right)$$

in Scenario A, that corresponds to the faster speed reported by Elliott and Cornell (2012) (see Supplement 4A). Interestingly, in the scenario B, we find that both in a slow and fast varying environment for the heterogeneity in R, the spreading speed still corresponds to v_f as in the homogeneous case. That was not the case in the scenario C, where the fastest speed results to be lower than v_f.

7.4 Discussion

Dispersing faster or growing stronger? Which strategy is selected in populations invading a heterogeneous environment? Range expansion and colonisation of new habitats are primarily driven by reproduction and dispersal (Lewis et al., 2016). However, both traits are generally correlated as organisms can pay a reproductive cost to disperse faster (Baguette and Schtickzelle, 2006; Hanski et al., 2006; Bonte and Bafort, 2018). In addition, spatial heterogeneity in environmental conditions that impacts growth or dispersal can influence such processes by modifying demography and dispersal (Hanski et al., 2006; Ramanantoanina and Hui, 2016). In this work we addressed these questions by gathering analytical solutions from the literature and performing numerical simulations of a reaction-diffusion model describing the demo-genetic dynamics of a population invading a one-dimensional heterogeneous environment. We find that the spatial heterogeneity plays a role in shaping the trait trade-off determining the preferred strategy on the expansion front and in the rest of the population behind. The trade-off strength, the fragmentation of the environment and the amplitude between low and high quality habitat are the key elements that contribute to the strategy shift with respect to the homogeneous case.

When the trade-off is weak, *i.e.*, when the distance between the optimal phenotypes d is below the threshold d_{cr}, evolution leads to the selection of a phenotype with Generalist

features. When heterogeneity impacts the growth rate, the Generalist is the same as in homogeneous environments. This is due to the fact that heterogeneity impacts the average growth rate only through its arithmetic mean. Interestingly, when heterogeneity impacts the diffusion coefficient, the phenotype of the Generalist is shifted toward a greater dispersal ability. Indeed, in that case it is the harmonic mean that appears in the expression of the velocity.

As the trade-off becomes stronger, in a homogeneous environment the phenotypes optimising growth (R specialists) and the phenotypes optimising dispersal (D specialists) have the same speed. This holds true when environmental heterogeneity impacts the growth rate while only the D-specialist confers the maximal speed when dispersal is heterogeneous. However, competition among phenotypes can give advantage to growth. Recently, Deforet et al. (2019) explore the $R - D$ trade-off and determine the conditions favoring evolution of fastest dispersal against the growth rate in a homogeneous space for a population composed of two-morphs. Given two species having r_1, D_1 and r_2, D_2, for species 1 and 2 respectively, they assess the evolutionary outcome depending on the simple condition $r2/r1 > D1/D2$. Basically they find that a lower trait value for either growth or dispersal can be compensated by the other trait in order for a species to dominate the other one. This was not the case in our approach as we are in the particular case where the two morphs at the optimum of the two strategies are such that $r2/r1 = D1/D2$, due to the symmetry assumption.

Habitat fragmentation plays also a crucial role in determining the evolutionary output. Fast varying environments ($L \to 0$) tend to favour stronger growth rate upon faster dispersal, at least when heterogeneity impacts the growth rate. Indeed, resources are heterogeneously distributed, but the distance among favourable habitats is not large, thus the trade-off is more favourable to the selection of the R-strategy on the front as high resource availability and fecundity facilitate expansion by increasing population growth (Burton et al., 2010). By contrast, in slower varying environments ($L \to \infty$), the faster dispersers take advantage of their mobility to reach the most favourable habitats and lead the colonisation front. Evolution leads thus to the selection of a higher dispersal capacity. When environmental heterogeneity impacts dispersal, phenotypes optimising dispersal are selected at the front regardless of habitat fragmentation. This result is in line with the "Spatial sorting theory", where, in an expanding front, dispersal may be strongly favoured and the best dispersers tend to be disproportionately represented on the population front (see Travis and Dytham (2002); Phillips et al. (2008); Shine et al. (2011)). Many examples suggest that population expansion may select for better dispersal Zera and Denno (1997); Chuang and Peterson (2016), even at the cost of slower growth (Chuang and Peterson, 2016; Andrade-Restrepo et al., 2019) as in the case of the cane toads *Rhinella marina* invasion in Australia, where on the margin individuals have longer legs with lower birth rates (Phillips et al., 2006). Similarly, this has been observed for the speckled wood butterfly *Pararge aegeria* among two habitats which differ for their availability of breeding sites. The most

fragmented habitats are associated with an increased dispersal ability, but females at range margins laid significantly fewer eggs than those from populations nearer the centre of the range (Hughes et al., 2003). The picture is different behind the front where we found that the R-strategy is always selected.

In pulled waves, when competition is relaxed on the front, the genetic diversity is consistently low on the front (Roques et al., 2012) due to the filtering of spatial sorting, homogenizing the phenotypic traits selected for dispersal (Cobben et al., 2015; Andrade-Restrepo et al., 2019). The effect of mutation on the spreading speed of an expanding population is addressed numerically by Elliott and Cornell (2012). They investigated the effect of varying R and D on the spreading speed of the system, and they find that the system would spread faster in the presence of both phenotypes than just one phenotype would spread, in the absence of mutations and for certain combinations of R and D values (Elliott and Cornell, 2012; Morris et al., 2019). Morris et al. (2019) derive predictions about the spreading of species characterised by travelling waves and find analytical conditions given by R and D parameter combinations. In Supplement 4A, we consider only the two phenotypes O_D and O_R, and we verify that our case corresponds to the one expressed by Eq. 40 of Morris et al. (2019). Here, we are in the case of Elliott and Cornell (2012) where the spreading speed of the fastest morphs is equal to v_f with low mutation rate and considering a population of two-morphs. However, we find here that a low step-wise mutation in a non-local system composed by a continuous phenotype space is able to slow down the spreading speed that the system would have with only two phenotypes due to the mutation among the nearest neighbors and competition.

Finally, it is important to recall that our results depend on the assumptions about the form of the dispersal and growth rate functions and the heterogeneity definition (i.e. piecewise function of period L on the uni-dimensional domain x). In our model, we do not take into account the Allee effect, which can have consequences for the dynamics of invasion since there are low densities on the invasion front (Chuang and Peterson, 2016; Roques et al., 2012; Andrade-Restrepo et al., 2019). Moreover, integrating such theoretical models and results with empirical data would be beneficial. Future works could develop a more complex dynamic model than the presented one taking into account important effects or introducing another species. This research and results are key for describing different kinds of invasion and colonisation phenomena, such as the expansion of invasive species (Phillips et al., 2006). In an agro-ecological context for biological control, the evaluation the speed of pest species could be relevant to assess the species propagation in the intermixing of habitat of an agricultural landscape (Shigesada, 1986). In addition, the consideration of a more complex landscape structure could allow for the evaluation of the effects of the crop and SNH intermixing, which affects species richness, functional diversity and species interactions. In Chapters 4 and 5, we have already highlighted that predator–pest interactions are strongly determined by the spatial structure and the specific traits of pests and predators,

but we pointed out that species trait diversity is not considered. In the present Chapter, we highlight the importance of considering spatial heterogeneity in determining the trade-off among dispersal and growth rate considering a continuous phenotype space, but we recognised that the studied system is relatively simple and the assumption over the spatial domain are not representative for a real agricultural landscape. In the next Chapter, we start from these perspectives and couple the outcomes of Chapter 2 about landscape structure, the results from predator-pest dynamic model of Chapters 4 and 5 and the outcomes about the trade-off among species traits and behaviours due to spatial heterogeneity in the current Chapter. Then, we implement a predator-pest system where we consider two pest and predator species to take into account different species behaviours and traits in a complex agricultural landscape.

Chapter 8

Should I stay or should I go? Effects of predating strategies in shaping pest dispersal behaviours within heterogeneous landscapes

A fundamental species trait which is highly dependent on spatial context is the dispersal strategy: it allows the exploitation of spatially variable resources, it enables the recolonisation of patches after local extinction, and it assures gene flow between ecological interfaces (Clobert et al., 2009; Barraquand and Murrell, 2012). However, dispersal has been recognised as a complex process, since it is strongly dependent on inner factors (*i.e.*, species life-history traits, morphology, behaviour) but also on external factors (*i.e.*, environments, kin competition, intraspecific competition, predation risk) (Clobert et al., 2009; Cote et al., 2017). In addition, as the energetic investment required for dispersal is substantial, it may have to be traded off with energetic allocation to other traits (See Chapter 7).

Usually, species greatly differ in their dispersal strategies, and different species may use different cues to disperse, leading to different demographic responses to habitat fragmentation (Fahrig, 2003; Clobert et al., 2009). In addition, habitat fragmentation decreases connectivity, and, since the heterogeneity degree and habitat traversability is perceived differently by each individual, the evolution of dispersal is species-specific and may vary over multiple spatio-temporal scales (Cote et al., 2017). Most studies focus on how the mean dispersal behaviour of one species evolves due to fragmentation change (Cote et al., 2017), where various modeling approaches are used, such as metapopulation frameworks (Hanski and Simberloff, 1997), reaction-diffusion models (Kawasaki and Shigesada, 2007; Ramanantoanina, 2015) or Individual Based Model (IBM) (North et al., 2011). Kawasaki and Shige-

sada (2007) firstly propose a patchy environment alternating favourable and unfavourable patches. They assume that the spatial heterogeneity affects only the growth processes and not the dispersal ability. Their main outcome is that the presence of unfavourable fields can decrease the rate of spread dramatically. Dewhirst and Lutscher (2009) used the same environment structure as Kawasaki and Shigesada (2007), but they considered that individual dispersal behaviours are also affected by the environment. They derived the minimal proportion of favourable habitats to ensure a successful invasion as well as the asymptotic rate of spread.

Considering the effects of spatial variability of resources and habitat fragmentation has greatly improved the understanding of the best dispersal strategy or the dispersal evolution in single-resource landscapes (Heino and Hanski, 2001; Bonte et al., 2010; North et al., 2011). Cenzer and M'Gonigle (2019) make a step forward by investigating the role of a more complex landscape composed by two types of resources for assessing the selection of a single-species dispersal strategy. In fact, the presence of multiple resources presents the opportunity for specialisation to the type of resource and to the arrangement of resources in space. The authors highlight that increasing the proportion of habitats promotes a long distance dispersal strategy, as there is a higher probability that individuals encounter suitable habitats. By contrast, an increase in the spatial auto-correlation of resources could lead to a divergence in the dispersal strategy selection.

However, the habitat spatio-temporal variability is not the only force behind the selection for dispersal, but other factors pertaining to the genetic structure of the population should also be considered (Hamilton and May, 1977). For example, studies have confirmed that spatial variation in habitat quality generally leads to selection against dispersal, while kin competition, inbreeding, and temporal variation in habitat quality tent to select for dispersal (Johnson and Gaines, 1990; Bowler and Benton, 2005; Ronce, 2007). A less studied but logical driver of dispersal is predation (Barraquand and Murrell, 2012). Predator–prey interactions vary in space and time depending on the surrounding environment and on their specific behaviours and traits, which characterise predator hunting, feeding strategies and survival ability (Schmitz et al., 2017). Some predators sit and wait for their prey at hidden places (*e.g.*, the sheetweb weaver species *Stiphidion facetum*, see Janetos (1982)), others actively search for preys and adapt their hunting ground according to prey density (*e.g.*, Carabidae *Agonum dorsal*, see Griffiths et al. (1985)) (Ramanantoanina, 2015). In contrast, prey can also improve its survival strategy by developing abilities and behaviours to escape from predators. Consequently, different dispersal behaviours naturally arise from the optimisation of species fitness (Ramanantoanina, 2015). Theoretical and empirical studies highlight different dispersal behaviours in predator-prey systems by assessing the effect of prey-induced dispersal in predators (El Abdllaoui et al., 2007; Ainseba et al., 2008; Tao, 2010) or by assessing the effects of prey refuge and density-dependent mortality on species persistence (Forrester and Steele, 2004). Ramanantoanina et al. (2011) suggest that the rate

of range expansion of the predators is closely tied with that of the prey; in the case of a specialist predator, the predator's range is limited by that of the prey (Kubisch et al., 2014).

From one hand, complex landscapes and resource distribution across space and time would lead to divergent organism responses and dispersal evolution (Papaïx et al., 2014b; Cenzer and M'Gonigle, 2019) and, from the other, predation can be variable in both space and time and it is not always evident how it will promote dispersal within prey (Barraquand and Murrell, 2012). However, the joint effect of environmental heterogeneity and the predating strategy on pests' dispersal behaviour has not been explored yet. Here, we aim to fill this research gap by focusing on the role of dispersal strategy in heterogeneous complex habitats for a multi-prey and multi-predator system. For this purpose, we simulate the dynamics of pests and their natural predators in an agricultural context. The dynamics and presence of predators and pests depend on habitat composition and configuration, and predators and pests differ in their strategical behaviours. Specifically, we investigate the following two questions: (i) What is the role of predating strategies in shaping pest dispersal behaviours depending on landscape heterogeneity? (ii) How is the predators' composition and coexistence influenced by the pest type and landscape heterogeneity? In our simulated model, we first generate complex landscapes composed by linear elements allocated with hedges and by fields allocated with crop or an alternative resistant crop. Then, we simulate population dynamics with two predators and two pests on the generated landscapes. The dynamics of the species are chosen to depend on the spatial structure: predators differ in their dynamics as one species has preferred habitat in hedges and the other one on fields; on the other hand, pests differ in their dispersal traits (*i.e.*, slow or fast dispersal).

8.1 Models

Figure 8.1 highlights the modelling framework: the landscape stochastic generator developed in Section 2.2 is used to stochastically generate the culture and hedge allocations which define the spatial support (1) over which the population dynamics of the model for the two-predators and two-pests dynamics is simulated under different scenarios of predation (2 and 3).

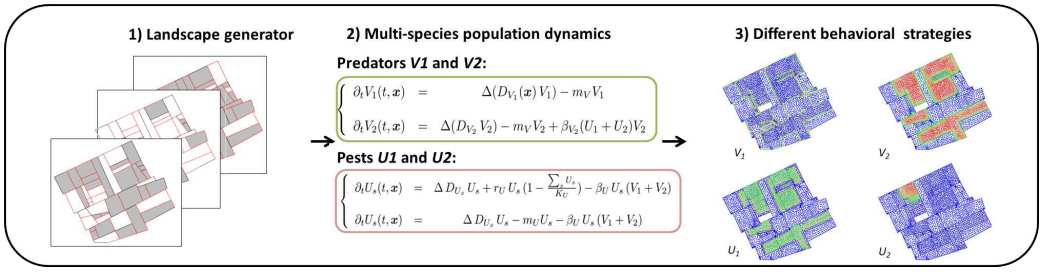

Figure 8.1 – Modelling framework: 1) Landscape stochastic generator model (Zamberletti et al., 2020); 2) two-predators and two-pests dynamics; 3) Spatially explicit outputs obtained at the last time step. All the equation variables in 2) are explained further in the text. We write $\boldsymbol{x}$ to refer to the coordinates for the 2D domain.

8.1.1 Landscape generator

We use the stochastic landscape model presented in Section 2.2 of Part 1 to simulate different agricultural landscapes. The study domain is a portion of the real landscape of the Lower Durance Valley that we have already presented. It contains 42 fields surrounded by 114 linear elements. The allocation classes are as follows: 1) fields can be allocated with crops (C) or with alternative pest-resistant crops (PRC); 2) linear elements can be allocated with hedges (H) or not. We study the system's response to landscape parameters which refer to habitat type proportion and habitat aggregation, as these parameters determine the most influential landscape characteristics for the pest-predator dynamics. Their ranges are detailed in the Table 8.1, and the parameter variable names are the same as those used for defining the model in Section 2.2. The choice of range for the adjacency parameters comes from estimated parameters, which are presented in the undergraduate internship report provided in the Supplement 6. Different parameter configurations are generated by random extractions from a uniform distribution given fixed ranges for the parameters of crops and hedge allocation to define the landscape structures.

Parameters	Description	Range
P_c	Proportion of crop	$[0,1]$
P_h	Proportion of hedges	$[0,1]$
β_{adj}^{CC}	Crop-crop adjacency	$[-5,5]$
β_{adj}^{HH}	hedge-hedge adjacency	$[-5,5]$
β_{adj}^{CH}	Crop-hedge adjacency	$[-5,5]$

Table 8.1 – Parameters of the stochastic landscape generator.

8.1.2 Two-predators and two-pests population dynamics

We expand the population model based on the system of partial differential equations described in Chapter 4. The new model is composed by two predators and two pests, and it takes into account opposite strategies for the behaviours of pests and predators, respectively.

The two predators have opposite behaviour related to habitat preference: one shows a life cycle reliant on hedges, while the other one relies on fields. The hedge predator 1 (V_1) prefers staying in the hedges or or very close, and it goes into fields only for foraging. It has a positive growth only in the hedges, and the growth depends on its pest consummation in the field area surrounding hedges. In this way, it is possible to take into account the interaction among pests and predators in the fields close to hedges. Moreover, as hedges are its preferred habitat, its diffusion on fields is a function of the distance from the hedge network: the more the predator is found far from hedges, the more rapidly it diffuses in order to quickly come back to its preferred habitat. Indeed, this predator spends most of its time in hedges or in their immediate surrounding. By contrast, the field predator (V_2) can be found in the fields, and it is not attracted by hedges since it does not perceive them at all. It shows a homogeneous dispersal, which does not depend on field allocation. It forages on the pests available in the fields.

Pests, instead, have the same dynamics, but different dispersal trait values: there is a slow pest (U_1) and a fast pest (U_2). Pests perceive the habitat as heterogeneous since they have positive growth only in crop fields, identified as their preferred habitat. They are not influenced by hedge presence. In the fields allocated with the PRC they can only disperse and be predated but cannot grow. The systems' parameters are shown in Table 8.2. Note that we do not vary the species parameters to explore only landscape variability jointly with species strategy selection due to predation pressure. Adding species parameter variability would have introduced higher uncertainty and complexity in the system and in the analyses of its simulation outputs. In Figure 8.2, the two-predators and two-pests dynamic system is summarised, and in Box 6 the system is explained in more detail, including its mathematical equations.

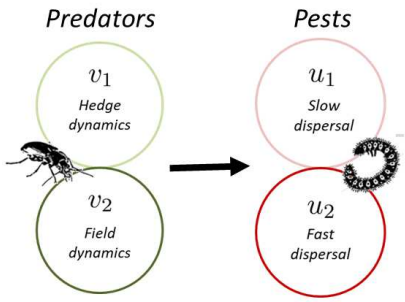

Figure 8.2 – Multi-pest and multi-predator system.

Parameters	Description	Value	Units
Predators			
d_v	1D diffusion	*check*	$m^2 d^{-1}$
β_1*	Predating rate	0.00825	$pest^{-1} d^{-1}$
β_2*	Predating rate	0.05	$pest^{-1} d^{-1}$
m_V	Mortality	0.01	d^{-1}
$\rho_{V_1,1D2D}$	Migration between hedges and fields	0.05	$m^{-1} d^{-1}$
$D_{V_1}(s) = a + b(s)$**	2D dispersal	$a = 0.05; b = 0.5$	$m^2 d^{-1}$
D_{V_2}	2D dispersal	$(D_{U_1} + D_{U_2})/2$	$m^2 d^{-1}$
Pests			
D_{U_1}	2D dispersal	0.08	$m^2 d^{-1}$
D_{U_2}	2D dispersal	3.2	$m^2 d^{-1}$
β_U	Consumption rate	0.05	$predator^{-1} d^{-1}$
r_U	Growth rate	0.01	d^{-1}
K_U	Carrying capacity	1	$pest\, d^{-2}$
m_u	Mortality	0.01	d^{-1}

Table 8.2 – Parameters describing the two-predators and two-preys dynamics. The parameter names correspond to the variables used in the Box 6 where the system of equations is presented.
* The relationship among the value β_1 and β_2 is shown in the Supplement 5.1.
** s is the smallest distance between hedge and field.

8.1.3 Simulation scenarios

To analyse the possible effects of predating strategy on pest dispersal behaviour, we explore 4 scenarios considering different species combination:

- *Scenario 1*: Only pests (U_1 and U_2)
- *Scenario 2*: Hedge predator and pests (V_1, U_1 and U_2)
- *Scenario 3*: Field predator and pests (V_2, U_1 and U_2)
- *Scenario 4*: All predators and pests (V_1, V_2, U_1 and U_2)

At the first time step, pests are punctually introduced using the same density for each introduction, where for each pest we select an introduction field of crop type, which is randomly chosen from a uniform distribution over fields. Hedge predators (V_1) are homogeneously distributed in fields and in hedges ($\int_\Omega V_1 \, d\Omega = \int_H V_1 \, dH$). Field predators ($V_2$) are homogeneously distributed over all fields. Predators are introduced in same abundance at landscape scale ($\int_\Omega V_1 \, d\Omega + \int_H V_1 \, dH = \int_\Omega V_2 \, d\Omega$).
Simulations are performed with a time step equal to 1 day. The final time step (T_f) varies

since it depends on the species dynamics, and we fix it as follows: we simulate Scenario 1 and we identify the time step (T), for which the total prey density reaches 90% of the pest carrying capacity in crop fields. Then, we set T_f to $T_f = 2 \times T$, and we use this value in the simulations of all the scenarios. Numerical simulations of the multi-pest-predator system are performed using the Freefem++ finite-element framework (Hecht, 2012b).

8.1.4 Statistical methods for analysing simulation outputs

We define an experimental design where we randomly draw from a uniform distribution the parameter setting using the ranges presented in Table 8.1. For each parameter setting, we consider 10 replicates, leading to a total of 11000 simulations for each scenario. To explore the direction and magnitude of variations in response variables, we apply Generalized Linear Models (GLMs), where we consider the scenarios along with the landscape variables as covariates. Pest and predator densities, as well as population composition of predators and pests (*i.e.*, the proportions of V_1 and U_2 among the total populations), are analysed as response variables by using the Gaussian distribution with log-link function. The species density is evaluated only on crop fields at the last time step T_f. The hedge predator proportion is evaluated as the V_1-density divided by the total predator density V_1+V_2. The proportion for pests is evaluated in the same way in order to separately assess the composition of predator and pest population. We develop GLM formulas containing covariate interactions up to second order, and we use a stepwise variable selection algorithm based on the Bayesian Information Criterion (BIC) in order to iteratively select the "best subset" of variables for each model. Prior to estimation, covariates have been normalised to have empirical mean 0 and variance 1, which simplifies the comparison of the magnitudes of estimated effects.

Box 6: Modelling with multiple predators and multiple pests

We denote by Ω the whole spatial domain. It is split into two non overlapping sub-domains: crop (C) and alternative pest resistant crop PRC, such that $\Omega = \{\Omega_C, \Omega_{PRC}\}$. A hedge network H is defined by the ensemble of linear 1D elements $H = \{h_1, h_2, ... h_i, ... h_{N_H}\}$, where N_H is the total number of linear elements within the landscape matrix, see Figure 8.3.

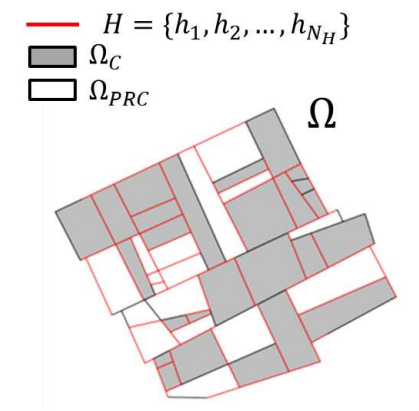

Figure 8.3 – Illustration of a complex heterogeneous landscape.

Predator dynamics

We denote by v_1^i and V_1 the densities of the hedge predators on the 1D element i and on the 2D spatial domain, respectively. Similarly, we define v_2^i and V_2 as the population densities corresponding to the field predators on the 1D element i and on the 2D spatial domain, respectively.

- Hedge predator: The dynamics of the densities v_1^i on the 1D elements are governed by a 1-dimensional reaction-diffusion model:

$$\partial_t v(t,x) = d_v\, \partial_{xx} v + \beta_1\, s(t,x) - m_V\, v + [1\text{D} \leftrightarrow 2\text{D}] + [1\text{D} \leftrightarrow 1\text{D}], \tag{8.1}$$

  with $s(t,x)$ the contribution on the reproduction at the position x of foraging activities in Ω, see the explanations below. The parameter β_1 is the predating rate that takes into account the conversion efficiency; the parameter m_V corresponds to the mortality in the hedges. The first term $d_v \partial_{xx} v$ describes a random walk movement of the individuals in the hedge. The coefficient d_v is the 1D diffusion parameter along the hedges.

  To describe the effect of foraging in the 2D domain on the reproduction, we first point out that the overall instantaneous pest consumption by predator 1 is proportional to

$$\int_\Omega V_1(t,\mathbf{y})\, (U_1 + U_2)(t,\mathbf{y})\, d\mathbf{y}.$$

  Then, we define the relative contribution of a position x in a hedge to the pest consumption

at any given position $\mathbf{y}$ in Ω using the following kernel k:

$$k(x, \mathbf{y}) = \frac{e^{-d(x,\mathbf{y})^2}}{\int_H e^{-d(z,\mathbf{y})^2}\, dz}.$$

Here, H corresponds to the set of all the hedges, and $d(x, \mathbf{y})$ is the Euclidian distance between x and $\mathbf{y}$, where x denotes the position in the hedge and $\mathbf{y}$ a position in the 2D domain. This formula assumes a Gaussian decay of the probability of visiting a given location x with the distance to the source, typical of a diffusion process. Thus, the contribution of the position x in the hedge on the global foraging is:

$$s(t, x) = \int_\Omega k(x, \mathbf{y})\, V_1(t, \mathbf{y})\, (U_1 + U_2)(t, \mathbf{y})\, d\mathbf{y},$$

with $U_1 + U_2$ the density of pests (see below).
Lastly, the terms 1D $\leftrightarrow$ 2D and 1D $\leftrightarrow$ 1D respectively describe the exchanges between the 1D element h_i and 2D spatial domain Ω, and the exchanges between the two sides of the element h_i (i.e., the exchanges between h_i and $h_{i'}$, see Figure 1 in the Supplement 2.1).
On the 2D domain, the dynamics of V_1 are described by a reaction-diffusion equation with a spatially heterogeneous diffusion term:

$$\partial_t V_1(t, \mathbf{x}) = \Delta(D_{V_1}(\mathbf{x})\, V_1) - m_V V_1. \tag{8.2}$$

Here, Δ is the 2D Laplace operator and $\Delta(D_{V_1}(\mathbf{x})\, V_1^i)$ describes a 2D random walk movement of the individuals. In the absence of mortality and interactions, the solution of $\partial_t V_1(t, \mathbf{x}) = \Delta(D_{V_1}(\mathbf{x})\, V_1)$ would tend to become proportional to $1/D_{V_1}(\mathbf{x})$. Thus, to describe a hedge tropism of the predator of type 1 we choose the heterogeneous diffusion coefficient $D_{V_1}(\mathbf{x})$ such that it becomes large when the predator is far from the surrounding hedges. More precisely, we set: $D_{V_1}(\mathbf{x}) = f(s) = a + b(s)$ with $a,\ b > 0$, where s is the distance between the point $\mathbf{x}$ and the closest hedge element h_i, and the choice of a, b depends on the unit of space.

- Field predator: The field predator does not consider the hedge network and perceives the landscape as a heterogeneous 2D space. Its dynamics in h_i is simply expressed by $v_2^i = 0$ for all h_i.
  On the 2D domain, the dynamics of V_2 is described by a reaction-diffusion equation with a spatially heterogeneous diffusion term:

$$\partial_t V_2(t, \mathbf{x}) = \Delta(D_{V_2}\, V_2) - m_V V_2 + \beta_2 (U_1 + U_2) V_2 \tag{8.3}$$

  where m_V is the mortality and β_2 is the predating rate for V_2. The parameter D_{V_2} is the 2D diffusion in the 2D domain which is constant for the predator species V_2, as it is not attracted by hedges. The relationship between β_1 and β_2, and the parameter calibration, are explored in the Supplement 5.1.

Pest dynamics

The dynamics of the density of pest j ($j = \{1, 2\}$), U_j, is described by the following reaction-diffusion equations:

$$\begin{cases} \partial_t U_j(t,\mathbf{x}) &= \Delta\, D_{U_j}\, U_j + r_U\, U_j \left(1 - \frac{\sum_j U_j}{K_U}\right) - \beta_U\, U_j\, (U_1 + U_2) \qquad \text{for } \Omega_C, \\ \partial_t U_j(t,\mathbf{x}) &= \Delta\, D_{U_j}\, U_j - m_U U_j - \beta_U\, U_j\, (U_1 + U_2) \qquad \text{for } \Omega_{PRC}. \end{cases} \tag{8.4}$$

Here, D_{U_k}, with $D_{U_1} << D_{U_2}$, can correspond to slow or fast diffusion rate in the field. The parameter K_U is the pest carrying capacity in crop field, r_U is the intrinsic growth rate, m_U is the mortality, and β_U is the predating rate. For simplicity and parsimony, we assume that the two pest species have the same parameter values except for the diffusion parameter.

8.2 Results

Here, we present the analyses of the results and illustrate them through Figures 8.4, 8.5 and 8.6. Key GLM results are discussed in the text, and full results are given in the Supplement 5.2. The notation $E^{S_n}_{variable}$ stands for the estimated coefficient of the covariate with name *variable* for the Scenario n. Boxplots showing variance among repetitions of the selected variables are shown in the Supplement 5.3.

8.2.1 Predating strategies and landscape structure effects on pest dynamics

In Figure 8.4a the pest density $(U_1 + U_2)$ is analysed by contrasting it with the crop proportion in the simulated landscape. As expected, when predators are not present (Scenario 1), crop proportion has a positive effect on pest density ($E^{S_1}_{P_c} = 0.020 \pm 3.827 \times 10^{-4}$). However, different predating strategies show divergent impacts in reducing pest density depending on crop proportion. In Scenario 3, the pest density is drastically reduced in general, but there is only a relatively weak negative effect when crop and hedge proportions increase ($E^{S_3}_{P_c} = -0.007 \pm 3.827 * 10^{-4}$). In Scenario 4, we find a slightly more marked effect when the crop proportion is high ($E^{S_4}_{P_c} = -0.018 \pm 3.827 * 10^{-4}$). Instead, when only the hedge predator V_1 is present (Scenario 2), pest density is reduced more strongly with increasing crop proportion, and with even more pronounced effects when there is also a high hedge proportion ($E^{S_2}_{P_c} = -0.121 \pm 3.827 \times 10^{-4}$; $E^{S_2}_{P_h} = -0.073 \pm 3.835 \times 10^{-4}$). This is due to the fact that V_1 depends on hedge presence, thus pest density is negatively impacted when hedges are preferentially located on crop field boundaries ($E^{S_2}_{\beta^{CH}_{adj}} = -0.033 \pm 3.838 \times 10^{-4}$). Hedge proportion has a slight effect also under Scenario 4 ($E^{S_4}_{P_h} = -0.003 \pm 3.835 \times 10^{-4}$) as both predators jointly act on prey. From comparing Scenarios 2 and 3, we notice that V_1 is able to reduce the pest density almost as strongly as V_2 only in the case of high crop

coverage. When considering the composition of the pest population (*i.e.*, the proportion of U_2 among $U_1 + U_2$), in general, crop proportion and crop aggregation favour the selection of the fast dispersal strategy ($E^{S_1}_{P_c} = 0.291 \pm 0.002$, $E^{S_2}_{P_c} = 0.218 \pm 0.002$, $E^{S_3}_{P_c} = 0.305 \pm 0.002$, $E^{S_4}_{P_c} = 0.260 \pm 0.002$; and $E^{S_1}_{\beta^{CC}_{adj}} = 0.104 \pm 0.002$, $E^{S_2}_{\beta^{CC}_{adj}} = 0.093 \pm 0.002$, $E^{S_3}_{\beta^{CC}_{adj}} = 0.111 \pm 0.002$, $E^{S_4}_{\beta^{CC}_{adj}} = 0.114 \pm 0.002$, respectively). However, predating strategies also shape differently the pest composition, see Figure 8.4b. Scenario 3 does not produce any changes in pest composition. By contrast, in Scenario 2, there is a clear reduction of the fast pest (U_2) with respect to the benchmark Scenario 1. When U_2 is most favoured by crop presence, the predating strategy led by the hedge predator can reduce the pests' density and shift the pest composition in favour of U_1. In Scenario 4, we notice a combined effect of Scenario 2 and Scenario 3 with more pronounced effects when there is high crop proportion.

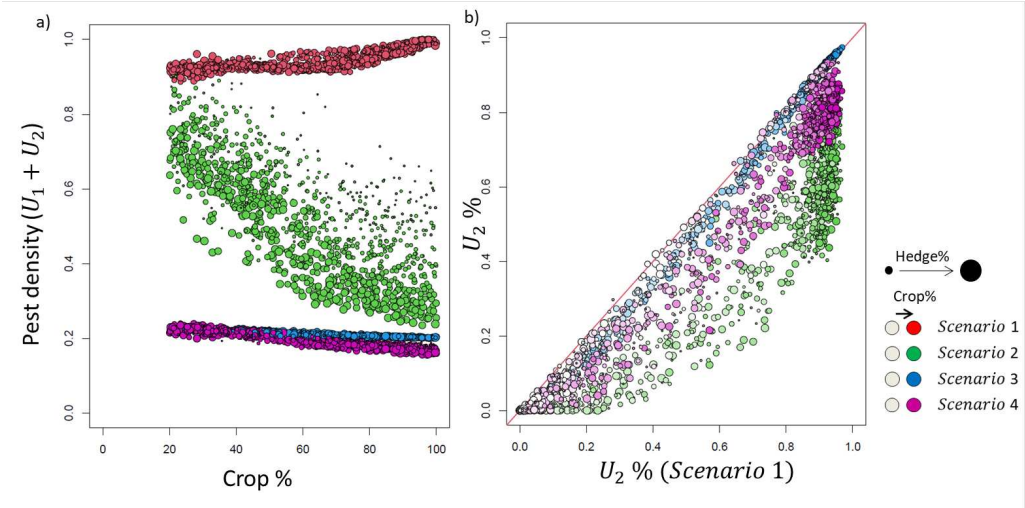

Figure 8.4 – Pest density and composition averaged over 10 replicates. a) Pest density as a function of the crop proportion; b) Proportion of the fast pest (U_2) of the benchmark Scenario 1 contrasted with the proportion of the fast pest (U_2) of Scenarios 2, 3 and 4. Different scenarios are represented by different colors, and point size changes with hedge proportion. The colour gradient in b) represents crop proportion, while the diagonal bisecting line represents the a pest composition equal to the one in Scenario 1.

8.2.2 Landscape structure effects on predator dynamics

The density and composition of predators are shown in Figure 8.5. Landscape characteristics favouring pest abundance also favour predator density, such as crop proportion ($E^{S_2}_{P_c} = 0.083 \pm 2.32 \times 10^{-4}$, $E^{S_3}_{P_c} = 0.004 \pm 2.32 \times 10^{-4}$, $E^{S_4}_{P_c} = 0.028 \pm 2.32 \times 10^{-4}$) and crop aggregation ($E^{S_2}_{\beta^{CC}_{adj}} = 0.005 \pm 2.32 \times 10^{-4}$, $E^{S_3}_{\beta^{CC}_{adj}} = 0.002 \pm 2.32 \times 10^{-4}$, $E^{S_4}_{\beta^{CC}_{adj}} = 0.003 \pm 2.32 \times 10^{-4}$). A favourable landscape structure increases the predator density but also varies the predator composition (Figure 8.5a). In Figure 2a of the Supplement 5.4, we also highlight that

the density increase with crop proportion is driven by the increasing presence of V_1 (in proportion to V_2). Thus, when the crop proportion is high, the hedge predator becomes a stronger competitor that decreases the presence of V_2. A higher crop proportion positively affects predator density and increases the proportion of V_1 ($E^{S_2}_{P_c} = 0.249 \pm 0.001$). Instead, hedge proportion has a role in shaping the population composition (See also Figure 2b of the Supplement 5.4): landscapes characterised by high hedge proportion allow for a high proportion of V_1 ($E^{S_2}_{P_h} = 0.053 \pm 0.001$). By contrast, when the crop coverage is low, the hedge predator V_1 lacks easy access to pests and is not able to persist in the habitat due to the presence of the competing predator V_2 in the fields; this follows from the fact that V_1 always persists in Scenario 2 when it is the only predator (Figure 8.5b). In this case, even if the landscape is characterised by an elevated hedge presence (Figure 8.5a), V_1 is not able to persist as it is disadvantaged with respect to V_2, which has strong dynamics in crop fields and therefore has more direct access to the pest resource.

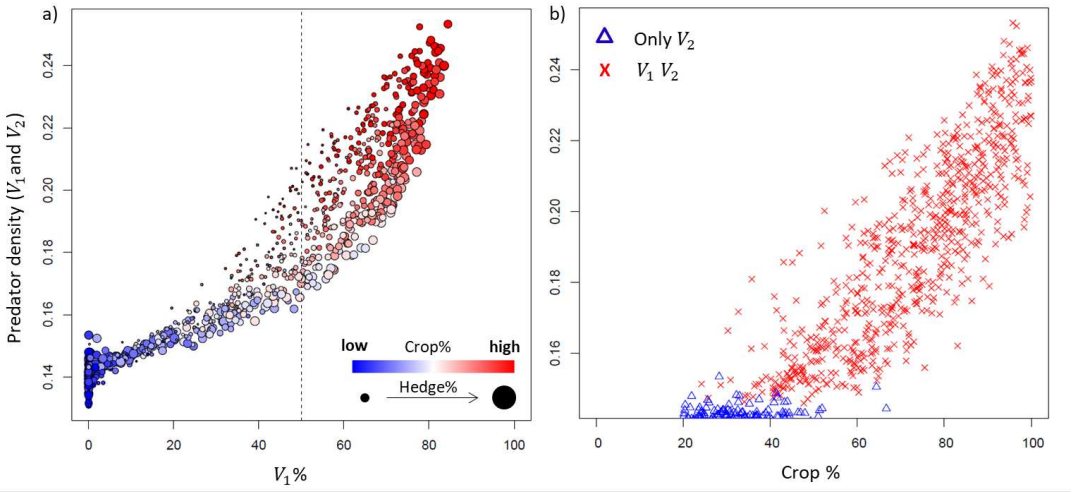

Figure 8.5 – Predator density and composition in Scenario 4 averaged over 10 replicates. a) Predator density as a function predator of hedges (V_1). The colour gradient represents crop proportion, and the point size changes with hedge proportion; b) Predator density as a function of crop proportion. Triangles are used to indicate that only V_2 survives, and red crosses are used when both predators survive.

8.2.3 Predator and pest population composition

Results on the densities of pests and predators can be further explained by jointly looking at the predator and prey composition in Scenario 4. This allows identifying the preferred strategy applied by pests and predators depending on landscape characteristics. In Figure 8.6, the hedge predator proportion (V_1) is contrasted with the proportion of the fast pest (U_2). Predator-pest associated strategies arise mostly in the first and third quadrants.

In the first quadrant (a), the landscape is characterised by high crop and hedge proportion; consequently, there is a prevalence of the hedge predator over the field predator, and of the fast pest over the slow pest. This can be identified as the predating strategy known as sit-and-wait, as predators have limited dispersal ability and are located in the surrounding area of hedges, and highly dispersing pests move rapidly by crossing the whole landscape. For this reason, V_1 mainly predates the pest U_2, thus reducing pest density and shifting the pest composition. This strategy results from landscapes composed of a high crop proportion, favouring the fast pests, and a high proportion of hedges, the principal habitat for V_1. In the third quadrant (b), the landscape is characterised by a low crop proportion, which leads to selection towards a complementary strategy: the actively-researching predating strategy. Due to the high level of landscape fragmentation, the slow dispersing pest, U_1, is favoured together with the field predator V_2, which shows higher dispersal ability. In this case, hedge proportion does not show an important role, as both the pest and the field predator do not rely on this habitat.

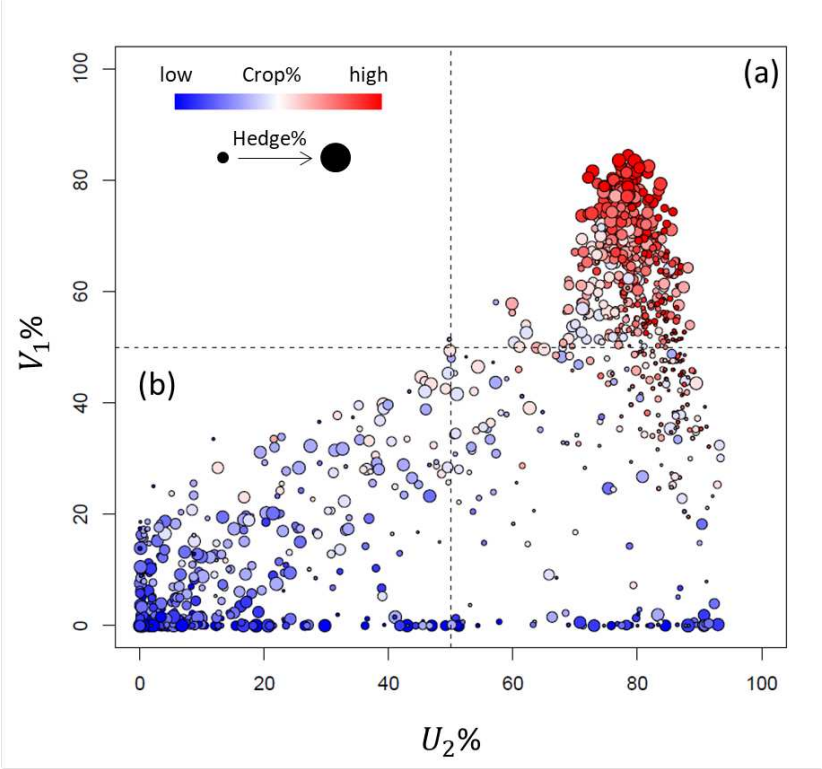

Figure 8.6 – Pest and predator composition averaged over 10 replicates. Proportion of hedge predator V_1 as a function of proportion of the fast pest U_2. The colour gradient represents crop proportion, and point size changes with hedge proportion. Letters indicate the first-quadrant (a), and the third quadrant (b).

8.3 Discussion

Species dispersal behaviours are determined by biotic and abiotic factors (Ramanantoanina, 2015). Predating is one of the most significant biotic interactions affecting individual behaviours. On the other hand, habitat heterogeneity and the distribution of resources in space can influence demographic as well as dispersal processes determining the persistence and the spread of the population (Cenzer and M'Gonigle, 2019). However, theoretical or empirical studies often focus separately and not jointly on the role of habitat heterogeneity (Hanski and Simberloff, 1997; Shigesada, 1986; Kawasaki and Shigesada, 2007; Dewhirst and Lutscher, 2009) or on the role of predators (El Abdllaoui et al., 2007; Ainseba et al., 2008; Chakraborty et al., 2007) in influencing pest dispersal. The joint influence of complex landscape heterogeneity and multiple predators on preys dynamics and dispersal behaviours has not been sufficiently explored. Here, we simulate different landscape structures composed of crops and hedges, and the dynamics of two pest and two predator species having opposite behaviours and dynamics. The present research aims at studying the role of landscape characteristics in shaping behaviours of multiple predators and multiple preys.

One key outcome is that different predating strategies act differently on pest density, and in some cases they also alter the composition of the pest population (Figure 8.4). When there are no predators (Scenario 1), our results are consistent with the literature: high crop proportion favours fast dispersal, while high fragmentation favours slow dispersal. Similarly, North et al. (2011) focus on the evolution of dispersal ability for one species through a spatially explicit IBM taking into account the role of patch size, patch quality, patch turnover rate, and the impact of habitat loss. They show that in a strongly heterogeneous landscape, the long-dispersal strategy is disadvantaged because it is more risky and costly. By contrast, increasing patch size can select for longer dispersal distances, as individual patches support large populations and kin competition is relaxed. In addition, here, we use a more complex landscape, taking into account crop aggregation and hedge proximity.

Then, we test how this situation may evolve when introducing one predator at a time, and with both of the two predators. The introduction of the field predator V_2 reduces the pest density without any influence with respect to landscape characteristics (Scenario 3). By contrast, the effects due to the introduction of the hedge predator V_1 depend on both crop and hedge proportion (Scenario 2). The strongest pest reduction is observed when there is a high proportion of crops, as the increase in the crop proportion makes crop-hedge proximity more likely, which favours control by V1. A hedge proportion increase acts in the same way as favourable habitat increases, thus affecting the proximity of hedge predator to pest.

Under Scenario 2, the pest composition is also altered since the proportion of the pest U_2 is highly reduced with respect to the its proportion in Scenario 1: when environmental conditions favour high abundance of hedge predator, the composition is switched in favour

of slow pests. From the pest point of view, the dispersal ability could be an efficient strategy to avoid predators by rapidly moving away or remaining hidden. From the predator point of view, the dispersal ability could determine the attack strategy by either waiting for the pests or directly searching them (*i.e.*, sit-and-wait vs actively searching predators). Individuals located in habitats at low predation risk should tend to not disperse at all, as moving prey also takes the risk of landing closer to a predator (Barraquand and Murrell, 2012). Here, we observe a co-evolution of the system towards a domination of V_1 and U_2 as soon as the landscape allows V_1 to be maintained, whereas when V_1 is not maintained or in a very low proportion, the system co-evolves towards domination of V_2 and U_1. When we introduce both predating strategies, different outcomes are observed depending on pests species composition and crop proportion. When the crop resource is scarce and the pest population is mainly composed of the slow pest, there is no cumulative effect of V_1 and V_2, but the field predator $V2$ seems to be alone to contribute towards reducing pests. When the crop resource is abundant and the pest population is mainly composed of the fast pest, the two predators are able to reduce pests in a complementary way. Interestingly, based on analysing the predator composition (Figure 8.5), we can highlight that the hedge predator is present and plays a key role when the crop proportion is not too low. This means that predators are able to compensate each other by balancing dispersal and competition among them. This also means that, even if there is some mild variability in the pest density in Scenario 4, predation is not provided by the same predators. In addition, a stronger effect of complementarity may be expected in the case where the field predator V_2 shows a lower predating efficacy with respect V_1. Moreover, we could expect that the hedge predator V_1 may coexist even when the landscape structure is less favourable for it.

Predator density and composition is influenced by both crop and hedge proportion. Specifically, in landscape structures with limited crops and hedges, the coexistence of the two predators is hampered. Indeed, pests depend on habitat availability, and when the proportion of crop is low, the pest density is low and predators compete for a limited resource. If only few hedges are in the neighbourhood of crop fields, the resource is even more limited for the hedge predator and it cannot persist in the landscape. As suggested by Northfield et al. (2017), negative interactions arise among predators when both predator species and pests share the same small or large spatial domain (Schmitz, 2007). In our model, we assume that the hedge predator's intake depends on the numbers of pests encountered in the crop fields close to hedges. Thus, the hedge predator is clearly disadvantaged as it has a more limited foraging space with respect to the predator that lives in the fields. This is clearly shown in Figure 8.5b, where in some cases V_1 is not able to persist. However, we also find that in other cases the predator population is mostly composed of V_1. This is the case when there is a sufficiently high crop proportion that pushes towards selecting the fast dispersal behaviour in the pest population. In this case, the pest can more easily escape the field predators, which have a slower dispersal ability, but pests more often fall

nearby hedges, thus favouring the hedge predator. For this reason, given high crop and hedge resources, the hedge predator is able to persist and over-compete the field predator. More sophisticated predator behaviours could have been taken into account in the model, such as directed searching dependent on pest density. (Mitchell and Lima, 2002) find that in response to a randomly searching predator, the best strategy for prey is to not move, *i.e.*, selection against dispersal would arise; while in response to a directed searcher exploiting prey aggregations, prey should diffuse by spreading on a relatively large spatial scale in the landscape in order to avoid aggregation, *i.e.*, selection in favour of dispersal would arise.

Through the joint analysis of the population composition of predators and pests, we identify the matching strategies: sit-and-wait predators are advantaged when the majority of pests adopt fast dispersal, while actively-searching predators are advantaged when the majority of pests adopt slow dispersal. Our findings are in agreement with Barraquand and Murrell (2012), who study the effect of predation on the evolution of dispersal strategies within a homogeneous environment through an IBM corresponding to a Lotka-Volterra system. They find that increasing the predation intensity and the spatial auto-correlation among predation locations ultimately leads to selection against dispersal for preys. In fact, high prey dispersal leads to a lower spatial segregation between predator and prey, and this leads to lowering the landscape-level density (per spatial unit) of the prey. In their study, the heterogeneity is generated by the predator locations, but in natural systems the habitat types and their structure contribute strongly to landscape heterogeneity and population movements. We found here that the most severe effect is produced by crop and hedge proportions, but we highlight also the role of the landscape configuration. Spatial aggregation of crops favours the fast dispersal strategy as it enhances the presence of available resources and lowers the risk for the fast dispersal strategy to disperse into low-quality habitat (North et al., 2011). By contrast, the adjacency among crop and hedges favours hedge predators and pests encounters.

We have shown how pest dispersal behaviours are influenced by different predation strategies and landscape structures. We also discussed about predator interference and coexistence. A number of extensions could be relevant with respect to the current formulation of our model. Even if behavioural adaptation is considered, the presented model does not consider mutation or behavioural changes. This could be an interesting extension that could lead to even stronger variations in population composition. In addition, we consider only opposite behaviours, but the system could be enlarged to take into account intermediary behaviours or a more continuous gradient with a higher number of species between the very pronounced Generalist or specialist strategies of predators. At the community level, an increasing number of diverse species interactions, coupled with environmental heterogeneity, is expected to increase the stability and resilience of communities (Modlmeier et al., 2015). However, environmental conditions should also be taken into account as they may contribute to selecting a behavioural strategy with respect to another, as in our case. For

example, Poisot et al. (2012) developed a tri-trophic resource–plant–herbivore system, focusing on how different patterns of resource dynamics could impact the structure of an exploitative community. They found that specialisation depends on habitat quality: specialised enemies are selected in high-quality environments, while Generalist enemies are selected in poor-quality environments.

In the agricultural context, functional foraging complementation in natural predator assemblages is expected to augment biocontrol efforts (Modlmeier et al., 2015). For example, Finke and Snyder (2008) showed that greater intraspecific variation in parasitoid specialists fostered greater mortality in aphid communities when compared to species diversity per se. Royauté and Pruitt (2015) empirically tested the effects of a Generalist predator showing behavioural differences (active vs. sedentary) and found that different predator behaviours can generate contrasting prey communities in an agro-ecosystem. These studies allow for the investigation of how natural enemies can be used to fight pests in complex landscapes, and they clearly demonstrated that predator type variation affects biocontrol success. Here, we introduce the landscape heterogeneity as an additional key element that could be used to better understand the relationships between natural predators and pest regulations. Specifically, we argue that landscape structure influences predator behaviours, thus affecting their efficacy as biocontrol agents. From our results, we conclude that key landscape elements determining predator strategy efficacy are given by crop abundance and aggregation jointly with hedge proximity. Interestingly, hedge proportion alone is not strongly influential in determining a variation in the predator density and composition, while an increasing crop proportion assures a higher hedge proximity and, thus, enhances predator-pest encounters. Therefore, we emphasise that landscape structure is an additional parameter to account for implementing efficient biological control strategy along with the species traits and functional diversity.

Perspectives and open questions

- Developing an eco-evolutionary model to study the trade-off among species traits for a prey-predator systems. This is an interesting perspective to move further the results of Chapter 7. It would allow for theoretical insights that could be compared with the numerical results obtained with the complex simulated landscapes. In addition, as in predator-pest systems the dynamics of one species influence the landscape heterogeneity of the other, coevolution between organisms could also be considered.

- Extending of the analysis to the local scale. In Chapter 8, we have presented only results obtained by averaging model outputs over the landscape at the end of the simulation period. More analysis at both global and local scales would allow for a better comprehension of the system and could further validate and improve our key

messages. In particular, an interesting question would be to study how the different strategies coexist in space and time.

- Applying the theoretical approach presented in a biological control context and testing it on a real system. For example, the results of Chapter 7 could be used to assess pest invasions, while Chapter 8 could be useful to better understand the positive/negative/neutral effects of natural predator pest reduction resulting from species interactions.

Part IV
Discussion

What is the motivation for modeling the interaction between agricultural landscapes and ecological dynamics?

In order to meet the agricultural production demand, modern agriculture has simplified traditional agroecosystems and substituted biological functions, generally provided by diverse communities of organisms, with a diffused input of energy and agrochemicals (Bommarco et al., 2013). For example, modern agricultural strategies rely on the addition of organic nutrients, the mechanical loosening of the soil structure that allows for better root penetration and growth, and control of pests and epidemics through pesticides (Tilman et al., 2001). This agricultural upgrade may be successful in meeting the goal of production demand at short term, but agroecosystem simplification affects important ecosystem services (ES) via the loss of biodiversity, such as pest control, pollination, decomposition processes and also crop production (Altieri, 1999; Daily, 1997; Bommarco et al., 2013). Over the last decades, the scientific community and society strongly claimed to better preserve agroecosystems in order to meet future climatic, economic, and social challenges by balancing productivity, stability, and resiliency in a sustainable way that minimizes environmental impacts (Foley et al., 2005; Bianchi et al., 2013). For example, from the 1 January 2014, the European Union member states applied a legislation to achieve the sustainable use of pesticides with the requirement to take all necessary measures to promote low pesticide-input pest management and give priority to nonchemical methods (Bianchi et al., 2013).

One of the prime pest control mechanisms is the ecological intensification based on the idea to match or increase yield levels while minimizing the negative impacts on the environment and avoiding the negative impact on agricultural productivity by integrating the management of ES into crop production (Doré et al., 2011). It is based on the combination of pest control techniques discouraging the development of pest populations and keeping pesticide levels that are economically justified (Bianchi et al., 2013). For example, given the context of this work, the amount and the organisation of cultivated, natural and semi-natural habitats have the potential to promote a bundle of desired ES due to their

influence on the community ecology at multiple spatial and temporal scale (Bianchi et al., 2006; Chaplin-Kramer et al., 2011b; Tscharntke et al., 2016a). In particular, non-crop habitats often includes woody (*e.g.*, forest and hedgerow) and herbacious habitats (*e.g.*, field margins, road verges and meadows),which are relatively undisturbed and permanent areas offering shelters and resources, so that they are a biodiversity pool.

A key issue of ecological intensification is to devise management interventions that aid in limiting possible trade-offs between services. In fact, it can happen that the enhancement of one service negatively affects other services (Bommarco et al., 2013). For example, effective biological weed control reduces cover of weeds, on which many pollinators and natural enemies rely for food; this can lead to reduced pollination and pest control service (Bommarco et al., 2013). Multiple criteria assessment considers potential trade-offs by combining indicators related to productivity, stability and resilience (Doré et al., 2011). In general, this kind of approach is particularly appreciated by policymakers as it allows for an objective cost and benefit comparison of ecological intensification practices in order to meet economic goals in environmentally-friendly way (Batáry et al., 2015).

The ES concept highlights the importance of ecosystems and their ecological processes for human society (Daily, 1997), but its application in management is both welcome and worrying. Welcome because it takes into account the important benefits derived from ecosystems for society and incorporates them into planning and decision-making (Bengtsson, 2015). Worrying because the usefulness of the concept is restricted by a largely insufficient understanding of many underlying dynamical ecological processes (Bommarco et al., 2013; Firbank et al., 2013; Bengtsson, 2015).

Usually these evaluation approaches provide a static picture of the ecosystem without taking into account the system's spatio-temporal dynamics. Only few studies consider the spatio-temporal dimensions that are most relevant to farmers, such as the influence of crop rotations on pollination, biodiversity and pest control (Kleijn et al., 2019). Additionally, information is lacking on benefits from ecological intensification at multiple scales (*i.e.*, from farm to landscape scale) and on the approach to evaluate the effects over different spatial scales. However, this information is important when considering that different species have different dispersal abilities and can be differently influenced by semi-natural habitats or crops up to several kilometres away from the target location (Steffan-Dewenter et al., 2002; Lonsdorf et al., 2009; Shackelford et al., 2013; Jonsson et al., 2014).
Even though this thesis does not directly deal with the ES assessment, we have largely discussed the importance of considering the pest regulation at different spatio-temporal scales. In Chapter 5, we show that foregoing pesticide applications, pest peaks or introductions show effects that determine the pest outbreaks in the immediate future and in surround-

ing areas. For example, the presence of previous local pesticide applications in a field and its neighbouring fields negatively influences the dynamics since pesticide applications efficiently reduce the pest density in the field. Pest arrival acts as an accelerator of local pest dynamics, as was shown by a high frequency and high magnitudes of pest density peaks in the surrounding areas. In addition, the same landscape features may act in a different way depending on the considered scale, as crop proportion at local scale or at landscape scale leads to different pest breakout events. Similarly, global hedge proportion has a small but positive effect on both pest dynamics as at that scale it does not inform about hedge connectivity and distribution, while hedge proportion at local scale characterises local hedge structure, and the resulting predator concentration that plays a bigger role by reducing pest outbreaks.

Even if a cost-benefit analysis approach offers a simple and effective solution to complex and intractable resource management problems (Vira and Adams, 2009), there could arise questions of ethical significance (Jax et al., 2013). The ES evaluation through cost-benefit analysis or indicators has an implicit utilitarian perspective, which obscures the ethical positions in nature conservation promoting the protection of biodiversity regardless of its instrumental value to humans (Jax et al., 2013). In fact, natural capital does not capture the full complexity relations between genes, species, and ecosystems that is associated with the term biodiversity (Wilson, 1997). In addition, the processes by which stocks of natural capital and key processes are transformed into flows of ecosystem services are themselves not straightforward and not clearly determined, and there is high variability (Vira and Adams, 2009). For example, as discussed, even if some studies have found a positive relationship between the diversity and abundance of species and landscape complexity, there could be also notable exceptions with negative or neutral effects (Chaplin-Kramer et al., 2011b; Karp et al., 2018; Kleijn et al., 2019). Furthermore, using the ES economic evaluation and market-based mechanisms has raised concerns about the commodification of nature (Kosoy and Corbera, 2010; Peterson et al., 2010; Robertson, 2004), meaning that ES components or processes are transformed into products or services that can be privately appropriated. A practical example is offered by Carrasco et al. (2014), who discuss how the economic valuation of ES fails to capture biodiversity and food security value of tropical forests, especially for isolated sites. Their main outcomes call for multi-criteria approaches where biodiversity is considered at the same level as ecosystem service values. Moreover, their advise is to avoid using ES values as the only criterion, or rather to use it as bundled objectives together with biodiversity. Recently, other studies go beyond the ES monetary evaluation focusing on ES social-cultural value (Díaz et al., 2011; Milcu et al., 2013; Martín-López et al., 2014; Cáceres et al., 2015). Their idea to provide an alternative rigorous quantitative-qualitative way to compare the perspective of different social actors is thus useful for social-ecological assessment and action.

However, we should recognise that there are no generally agreed upon meanings and boundaries of "ecosystem services" and "biodiversity". It seems reasonable to ask whether biodiversity is an ES in itself, or should be taken into account separately. The answer depends on whether ES are defined as ecosystem components and processes that lead to benefits, or as goods and benefits themselves (as in the MEA (2005) definition) (Jax and Heink, 2015). Moreover, similar to ES, the assessment of biodiversity – e.g., if it is high or low – must rely on numerical criteria and indices. The main point is that ES are always conceptualised in relation to human well-being. By contrast, biodiversity studies and biodiversity conservation do not necessarily focus only on ecological entities according to their potential utility for people.

How should agroecosystems be represented to take the landscape complexity into account?

The representation of agroecosystems is not straightforward: it relies on the available types of data, on the goals of the study and on the process integration. In Chapter 2.2, a special attention is dedicated to the representation of landscape complexity by considering linear elements along with patch elements. We propose a novel methodological approach based on a vector representation, which is particularly suited to this purpose as linear elements could be simply represented by segments. Then, both qualitative and quantitative information can be specified for each element. We discuss and compare our method with the most commonly used raster approach, through which is not possible to identify individual linear elements as they are made up by a sequence of consecutive individual cells. Moreover, in order to define a linear element with a high precision, a high raster resolution is required. This, in turn, will lead to an elevated computational complexity and/or limited area extent. Instead, in the vector approach, multiple attributes related to each landscape element can be considered without strong impact on the computational demand. Defining patch and linear elements as landscape objects offers the possibility of studying their interactions through graph theory. We demonstrated that the ensemble of these features is particularly suitable to reach our modelling aim of focusing on patch and linear element allocation and interaction for describing, inferring and simulating different agricultural landscapes. Lastly, the conceptualisation through graph theory allows us to model habitat interactions and to generate virtual but realistic agricultural landscapes featuring different spatial patterns (geometry, connectivity) and temporal patterns (e.g. crop rotation), thus providing a useful tool to explore the relationships between landscape structure and the processes at stake within it (Poggi et al., 2021).
Concerning the hedge representation, even if the raster format may not be appealing for linear element modelling, there are applications where this kind of representation provides

relevant results and is informative. Betbeder et al. (2017) show methods for estimating resistance map for hedgerows from radar images (*i.e.*, Synthetic Aperture Radar, SAR) and areal photography (AP) to explore hedgerow network connectivity using landscape and local metrics describing hedgerow internal structure and landscape properties. From the AP, hedgerows are digitalised and represented by vector lines then rasterised; from the SAR image, hedgerows are represented by the projection of tree canopy cover. Whereas hedges are usually mapped as lines by considering only their locations, the authors introduce tree density and canopy cover thanks to remote sensing imagery data. They demonstrate that including the internal structure of hedgerows improves connectivity measures and highlight the importance of data source choice when mapping and characterising landscapes to assess landscape connectivity (Wade et al., 2015).

Modern techniques for acquiring aerial and satellite data can provide raw optical and radar multimodal time series of landscape images. These datasets provide a large amount of information that could be used to explore, represent and simulate landscapes with higher precision. For example, the THEIA Land Data Centre is a French inter-agency initiative which promotes the use of satellite data, primarily for environmental research on land surfaces, for public policy monitoring and for management of environmental resources. For agricultural purposes, the main research projects and applications are related to crop mapping and monitoring, crop yield estimation, estimation of environmental variables and estimation of farming practices. In addition, both vector and raster products are available with high resolution (*e.g.*, land cover data with 10 m for raster and 20 m for vector with annual update frequency). Future challenges could also deal with the use of this new valuable data source for a hybrid approach combining raster and vector representation in order to take advantage of the most informative satellite source and the simplest and parsimonious spatial representation. In the model we presented here, it would be possible to assign information such as canopy cover and tree density to each element constituting the hedge network as an attribute and, then, to estimate and model the hedge allocation also with respect to this information. Finally, future research should enhance multilevel and integrated approaches of landscape functioning (Poggi et al., 2021).

How to jointly model landscape complexity and species dynamics?

The integration of agricultural landscape heterogeneity and biophysical processes is fundamental, but remains challenging due to the complexity of both landscape and living systems. For example, landscape structure impacts agricultural pest suppression at global (Haan et al., 2020; Zamberletti et al., 2021b) and local scale (Haan et al., 2020; Zamberletti et al., 2021a) and, thus, biological control in agroecosystems (Thies and Tscharntke, 1999; Zamberletti et al., 2021b,a). There are only relatively few studies that have assessed the

effect of landscape context and species trophic interactions jointly (Turner et al., 2015), and the outcomes of these studies easily lead to conflicting or similar results, and also results of difficult interpretation (Tscharntke et al., 2005; Karp et al., 2018). In fact, the direction of different factors affecting the dynamics is not determined *a priori* in a straightforward way, but it depends on the combination of the specific systems, the species, the spatial domain and the assumptions. Specifically, the high variability in the effects found in such studies could depend on two key points: the species community composition and the environmental context. When modelling, difficulties may arise from the data and information availability, the selection of an approach, the integration of different components without losing key information or using excessive assumptions (Poggi et al., 2018). Usually, the resulting trade-offs lead to studying the relationship among simple species systems and a complex landscape or the relationship among species with a strong simplification on the landscape. The originality of our work presented in Part II is to study jointly the relationships of complex landscapes and a quite detailed and realistic model of population dynamics, which may open up new research questions and approaches.

Field studies, models, and experiments are all useful approaches to understand and predict the effects of the landscape on population dynamics (Turner et al., 2015). Field studies and empirical modelling based on real observations are fundamental and rely mainly on correlative statistical models for analysis and synthesis (Cabral et al., 2017), but drawbacks have been discussed (Guisan and Thuiller, 2005). The main idea of correlative methods is to statistically relate environmental variables directly to species occurrence or abundance, while causal mechanisms are not identified (Dormann et al., 2012). Thus, explanatory power is limited and, consequently, it is difficult to transfer the outcomes across geographic space, time, and environmental space (Dormann et al., 2012). Experimental studies are site- and species-specific, providing results that are difficult to generalise, but they may support and confirm theoretical and numerical results. In contrast, process-based models formulate the ecology of a species defining causality by mathematical functions. Thus, the species abundance and presence come out as a consequence of causal links between spatial structure and population dynamics (Cabral et al., 2017). Theoretical models may appear strongly based on assumptions and more far from reality and may result of difficult comprehension due to some technicality. An important difference is that in the correlative model data cannot be used to test hypothesis because they have been used to define the model, while the process-based model is independent from data, and hence, it can be tested by checking if model results and observations match. A way to bridge the gap between empirical and process-based approaches is the mechanistic-statistical framework (Soubeyrand and Roques, 2014; Hefley et al., 2017). In such a framework, a mechanistic model, deterministic (e.g. PDEs – Partial Differential Equations) (Louvrier et al., 2020; Roques et al., 2021)) or stochastic (Soubeyrand et al., 2009; Papaïx et al., 2021), is used to describe the ecological process un-

der study, while a probabilistic model is used to link the mechanistic model to the data and to provide data-driven estimation of model parameters. Here, we have developed a process-based mechanistic modelling approach, but the only real data we used are the landscape data to perform the inference for a specific agricultural domain. However, the method we developed is general and flexible, and we use the data to show an application example over different study sites using real land-cover data. However, we do not have data for the population dynamics. We are aware that this is a weak point of this work, as it would be interesting to compare modeling outputs with data, or using the data for parameter inference. Our choices of parameters are based on the literature, and certain simplifications and assumptions have been introduced with the help of sensitivity analysis. Nevertheless, our approach allows us to develop a technique that can be generalised and applied to different systems and species. Thus, paring and comparing models with data would be certainly possible by adding the necessary adjustments, and it would be an interesting further development to discuss and validate what we have done.

Landscape heterogeneity mediates predator–prey interactions (Abrams et al., 1996; Schmitz, 1998), since landscape structure and patterns influence the probability of prey encounters (Hebblewhite et al., 2005) and the strategies to avoid predators (Andruskiw et al., 2008). For example, habitat type and its connectivity, patch size, and topographic setting could lead prey to be more or less susceptible to predation pressure (Hebblewhite et al., 2005). Existing approaches have been widely developed following theoretical population ecology, where predator–prey interactions take the form of a dynamic game played in spatially complex landscapes. This body of theory is crucial as it constitutes the basis for understanding how natural ecosystems can maintain critical functions depending on the environmental context (Schmitz, 1998). In the agroecological context of biocontrol, a fundamental aspect is the landscape complexity, as agricultural landscapes could be highly heterogeneous with respect to the culture intermixing or with respect to the different habitat types (*i.e.*, culture, grassland, wooded area, ditches, hedgerows). Natural enemies are more diverse and numerous in complex agricultural landscapes with abundant natural or seminatural habitat as compared to more homogeneous, intensively cultivated landscapes (Chaplin-Kramer et al., 2011b). To study population dynamics in heterogeneous landscapes, one of the simplest frameworks balancing local extinction events and recolonisation is represented by the metapopulation approach (Levins, 1969b; Wiegand et al., 1999). Its success comes from the appealing way through which the complexity of real landscape is reduced to a simpler framework for characterising population dynamics. However, only a limited range of dynamics and landscapes features can be encompassed (Wiens et al., 1993). For example, the consideration of spatial heterogeneity in terms of simple, internally homogeneous, shapeless patches embedded in an adverse matrix leaves out all the key elements which we have widely addressed in this thesis, and which play a key role for specific ecological processes,

such as biological control and pollination (Wiens et al., 1993). Under these circumstances, a more detailed modeling framework is needed to better understand and characterise the processes of interest by explicitly relating demographic processes, as well as dispersal and habitat selection, to the landscape in which these processes occur (Wiegand et al., 1999). A spatially explicit representation of landscape structure coupled with species dynamics seems to be an approach that better allows linking individual's use of space, exploring fine-scale details of landscapes, and investigating how such landscape elements influence species dynamics and interactions (DeAngelis and Yurek, 2017). For example, natural enemy movement from crop and non-crop interfaces is influenced both by habitat composition and configuration of different landscape elements and both by diverse habitat use and dispersal ability, thus affecting species communities and pest regulation (Bianchi et al., 2006). The landscape model we used is particularly suited to this purpose by distinguishing linear elements and field elements, where these two element types have different properties and can be allocated with different habitat types. Then, spatially explicit population dynamics of predators and preys are modeled. Coupling two models allows us to separately focus on the landscape system in a detailed way, and, then, on the definition of the appropriate population dynamics system. In order to match the spatial support with the population dynamics, different dynamics and behaviours are taken into account depending on the specific habitat and species characteristics. This approach is flexible and can represent realistic behaviours by directly reflecting species traits and the mechanisms of how landscape structure affects population dynamics.

In Chapter 4, we mainly focus on the integration of the landscape characteristics in the pest-predator dynamics. Especially, we propose to couple landscape properties and species traits to identify the main effects on CBC. However, as we worked at a global landscape scale and we lose some information in the spatial structure, we developed a novel methodological approach to parsimoniously use all the information provided by the spatially explicit model. In Chapter 5, we depict the pest-predator dynamics through key events, and we proposed to model them by a marked spatio-temporal point process (STPP). The use of STPP is quite common to model real events, biodiversity hotspots and animal positions, but it is rarely used as a surrogate model to capture the information of spatially explicit models with the goal to assess outcomes at global and local scales. Individual-based spatially explicit population models (IBM) could go even further as they are able to integrate life-history information and behavioural rules for each organism and to monitor all the locations it visited. In fact, an organism-centered view of landscape structure specifically links the individuals' use of space (e.g., dispersal and habitat selection) with the landscape structure (Wiegand et al., 1999). For example, Le Gal et al. (2020) highlight the important influence of the interplay between the landscape structure and the timing of CBC measures on the delivery of pest control services, through an IBM. This kind of model allowed them to evaluate variables such as natural enemy visitation rate in crop and the pest colonisation

event. Thus, they provide a very specific and point-centered analysis, and they found that a high proportion of SNH enhances the visitation rate of pest-colonised crop cells, but it also reduces the delay between pest colonisation and predator arrival in the crop fields. Indeed, using an organism-centered model could also allow for focusing more on organism dispersal and specifically on dispersal strategies, movement trajectories and habitat selection of each individual. For example, Barraquand and Murrell (2012) analyse a spatially explicit, individual-based predator-prey model to investigate the effect of predation on the evolution of prey dispersal. In this way, they detect that the balance between the level of competition and predation pressure, which an individual is expected to experience, determines whether prey should disperse. They find that more predation selects for less prey dispersal. Specifically, predators with smaller home ranges also select for less prey dispersal; on the other hand, more prey dispersal is favoured if predators have large home ranges, as species are very mobile, and/or are evenly distributed across the landscape (Barraquand and Murrell, 2012).

How to deal with multiple species showing different behavioural strategies?

Behavioural landscape ecology aims to explore how the behaviour of a particular species responds to landscape heterogeneity and changing landscape patterns (Knowlton and Graham, 2010). This field has been only recently developed, but it gains increasing attention especially in the context of global change (Turner et al., 2015). In order to take into account the landscape influence on species behaviour, we develop our multi-preys multi-predators model by considering a limited number of species defined in a system of PDEs. We integrated within this framework the habitat complexity to investigate the role of landscape heterogeneity for the selection of dispersal strategies of the prey and predator. In our approach, we identify two specific opposite behaviours for prey species and for predator species, without considering all the possible phenotype traits and the broad range of behaviours among individual organisms and their local environment. By using IBMs, it would also be possible to take into account individual members of a population, to easily model complex behaviours and to include many attributes for each individual. IBMs can reproduce accurately the way real individuals act and interact, but a high number of parameters is required, and the issue arises that such information is not always available from data and bibliography. Instead, the choice of the use of a PDE system in this thesis relies in the good balance of complexity, number of parameters and understanding.

When considering classical biological control, direct and indirect interactions among multiple species are likely to be involved when appropriately determining the efficacy of natural reduction of pests. However, there multiple ways in which species can be tied together in complex food web (Holt et al., 2001). So far, the most popular strategies have been

to model species distributions one at a time (Ferrier and Guisan, 2006), and small community modules to focus on strong direct and indirect interactions among a relative small number of species by defining specific community modules (Holt et al., 2001). To contrast two opposite strategies for preys and predators, we could not take into account all the intermediary behaviours, but it is enough to provide the general tendency and the resulting dynamics. Specifically, in our case, working with such a system allowed us to maintain and balance a certain level of detail in the population dynamics and a complex spatial domain to answer to our research questions. Holt et al. (2001) present typical modules defining the most common direct and indirect interactions among preys and predators. They argue that this kind of generalisation can be of importance as empirical systems may closely match the structure modules, and these modules can be considered as building blocks to achieve communities with full complexity. However, community-level modelling may confer significant benefits for applications involving very large numbers of species. Landscape ecology studies have started evaluating the landscape influences on biotic community structure using patch-based analyses of species richness (Turner et al., 2015). Thus, the main research questions are targeted at understanding how community composition varies with landscape, for example, by relating richness (or its components) to environmental conditions. Schindler et al. (2015) specifically discuss about the selection of landscape metrics as predictors for biodiversity, which is a very involved task. They found that an *a priori* determination of the appropriate indicators can be problematic, and even expert opinions seem to be inappropriate in certain circumstances and should be supported by pre-scans and statistical approaches to identify a satisfying set of metrics. Different strategies for modelling biodiversity at the community level are possible, and (Ferrier and Guisan, 2006) provide a comprehensive review of available approaches within each strategy, and they discuss strengths and weaknesses. They conclude that no single approach is likely to be optimal for all purposes and across all data sets. The choice of modelling biodiversity either at the community level or at the species level can be influenced by the study motivation and data type, quality and quantity (Ferrier and Guisan, 2006). Here, we benefit from the simplicity of the community modules to describe a more complex dynamics considering specific traits, different strategies and enabling the assessment of landscape-dynamics relationships.

What's next?

The key point of whole work in this thesis is that it is not restricted to considering only a unique dimension, but we try to explore and integrate different spatio-temporal ranges (*i.e.*, linear and areal landscape elements, global and local scales, temporal pest and predator evolution) and different biodiversity levels (multi-species, behavioural diversity and genetic diversity). Therefore, we have introduced key novelties to the existent literature that could be the starting points from where one could develop the following extensions: (1) efficient

and effective conservation strategies; (2) the assessment of eco-evo complementarity for conservation; (3) more accurate developments of spatio-temporal dimensions.

By coupling the conclusions on landscape complexity properties, as addressed in Part I, with species dynamics, their interactions and their traits, we have demonstrated that landscape heterogeneity has a key importance in determining species dynamics and CBC outcomes at different spatial scales (Part II and III). In addition, as there is a pressing need for more integrated approaches to management and conservation that capture the multifaceted nature of biodiversity, we suggest that spatial conservation planning should go hand-in-hand with landscape planning. This holds especially in the agroecological context, where the organisation and management of culture and SNH influence biodiversity and, thus, the relationships among pests and their natural enemies.

The conclusions provided in Part III highlight that environmental complexity also influences species composition and persistence. This comes from the fact that functional and genetic diversity leads to the development of different behavioural strategies to adapt to the environmental context and to the other species. Considering species richness or genetic diversity would be not the same from the conservation point of view: Forest et al. (2007) show that phylogenetic diversity or species richness would result in a different selection of conservation sites, leading to a trade-off among the different criteria. However, both criteria are key to conserve ecosystems providing insurance against the consequences of short-term and long-term environmental change. Even if the integration of different aspects of biodiversity into conservation assessments can be discussed, a major question could be the definition of the metrics and methodological approach to increase the conservation benefit compared with other conservation measures. In particular, there are cases for which there are not yet commonly defined metrics or approaches. For example, the selection of the right metric of genetic diversity is not trivial, and different metrics could lead to sensibly different results Winter et al. (2013). Only few works are now trying to incorporate functional and genetic diversity measures to quantitatively assess their effects on conservation (*e.g.*, see Robertson et al. (2020)).

In Chapter 5, the identification of events characterising pest-predator dynamics allows for a parsimonious representation of spatially explicit model outputs at different spatio-temporal scales. Taking into account spatial and temporal dimensions becomes relevant when explanations for variations in spatio-temporal are observed with respect to drivers at multiple scales. For example, wheat is the most widely grown crop in the world and it is subject to various pest attacks, such as yellow rust, fusarium head blight, sharp eyespot, powdery mildew, aphid etc. causing important losses to farmers. Conventional calendar-scheduled pesticide application for disease control generally does not consider disease development and its spatial distribution, often resulting in excessive use of pesticides and the associated high costs and negative effects (Su et al., 2019). By contrast, spatio-temporal crop or disease monitoring could be a prerequisite to enable the early and precise disease

control as real-time identification of the occurrence of dangerous pathogens for rapid countermeasures (Su et al., 2019; Hamer et al., 2020). For example, Hamer et al. (2020) focus on the generation of temporal and spatial prediction of the epidemic spread of infestations by combining phytopathological and geographical methods and knowledge. They find that coupling geostatistical regionalisation, machine learning methods, and long-term phytopathological data series prove to be efficient and appropriate, as the improved prediction of actual cases outweigh the increased false positive rate. We acknowledge that spatio-temporal influences are complex and intertwined and, therefore, it is hard to completely understand and implement them into a general monitoring and conservation program. In addition, the larger the spatial and temporal scale the model and analysis have to cover, the more observations are needed with additional efforts (Van den Eynde et al., 2020). Thus, we also stress the importance of using parsimonious and flexible methods to take into account the temporal dimension and various landscape scales in a smart and efficient way.

The conclusion of this work is a call for more integrated methods and efforts that account for the many different dimensions of biodiversity jointly with landscape complexity and heterogeneity by coupling theoretical approaches with real data.

Part V
Bibliography

Abrams, P. A., Menge, B. A., Mittelbach, G. G., Spiller, D. A., and Yodzis, P. (1996). The role of indirect effects in food webs. In *Food webs*, pages 371–395. Springer.

Adamczyk-Chauvat, K., Kassa, M., Kiêu, K., Papaïx, J., and Stoica, R. S. (2020). Gibbsian t-tessellation model for agricultural landscape characterization. *arXiv preprint arXiv:2007.16094*.

Ainseba, B., Bendahmane, M., and Noussair, A. (2008). A reaction–diffusion system modeling predator–prey with prey-taxis. *Nonlinear Analysis: Real World Applications*, 9(5):2086–2105.

Alfaro, M., Coville, J., and Raoul, G. (2014). Bistable travelling waves for nonlocal reaction diffusion equations. *Disc Cont Dyn Systems A*, 34:1775–1791.

Altieri, M. A. (1999). The ecological role of biodiversity in agroecosystems. In *Invertebrate Biodiversity as Bioindicators of Sustainable Landscapes*, pages 19–31. Elsevier.

Andrade-Restrepo, M., Champagnat, N., and Ferrière, R. (2019). Local adaptation, dispersal evolution, and the spatial eco-evolutionary dynamics of invasion. *Ecology letters*, 22(5):767–777.

Andruskiw, M., Fryxell, J. M., Thompson, I. D., and Baker, J. A. (2008). Habitat-mediated variation in predation risk by the american marten. *Ecology*, 89(8):2273–2280.

Aronson, D. G. and Weinberger, H. G. (1975). Nonlinear diffusion in population genetics, combustion and nerve propagation. In *Partial Differential Equations and Related Topics*, volume 446 of *Lectures Notes Math*, pages 5–49. Springer, New York.

Aronson, D. G. and Weinberger, H. G. (1978). Multidimensional nonlinear diffusion arising in population genetics. *Adv Math*, 30(1):33–76.

Avelino, J., Romero-Gurdián, A., Cruz-Cuellar, H. F., and Declerck, F. A. (2012). Landscape context and scale differentially impact coffee leaf rust, coffee berry borer, and coffee root-knot nematodes. *Ecological applications*, 22(2):584–596.

Azaele, S., Maritan, A., Cornell, S. J., Suweis, S., Banavar, J. R., Gabriel, D., and Kunin, W. E. (2015). Towards a unified descriptive theory for spatial ecology: predicting biodiversity patterns across spatial scales. *Methods in Ecology and Evolution*, 6(3):324–332.

Baddeley, A., Rubak, E., and Turner, R. (2015). *Spatial point patterns: methodology and applications with R*. CRC press.

Baggio, J. A., Salau, K., Janssen, M. A., Schoon, M. L., and Bodin, Ö. (2011). Landscape connectivity and predator-prey population dynamics. *Landscape Ecology*, 26(1):33–45.

Baguette, M. and Schtickzelle, N. (2006). Negative relationship between dispersal distance and demography in butterfly metapopulations. *Ecology*, 87(3):648–654.

Baillod, A. B. (2016). Landscape heterogeneity affects arthropod functional diversity and biological pest control. *PhD Dissertation*, (December).

Balvanera, P., Pfisterer, A. B., Buchmann, N., He, J.-S., Nakashizuka, T., Raffaelli, D., and Schmid, B. (2006). Quantifying the evidence for biodiversity effects on ecosystem functioning and services. *Ecology letters*, 9(10):1146–1156.

Bareille, F., Boussard, H., and Thenail, C. (2020). Productive ecosystem services and collective management: Lessons from a realistic landscape model. *Ecological Economics*, 169:106482.

Barraquand, F. and Murrell, D. J. (2012). Intense or spatially heterogeneous predation can select against prey dispersal. *PloS one*, 7(1):e28924.

Bascompte, J. and Solé, R. V. (1998). Effects of habitat destruction in a prey–predator metapopulation model. *Journal of theoretical biology*, 195(3):383–393.

Batáry, P., Dicks, L. V., Kleijn, D., and Sutherland, W. J. (2015). The role of agri-environment schemes in conservation and environmental management. *Conservation Biology*, 29(4):1006–1016.

Becks, L., Ellner, S. P., Jones, L. E., and Hairston Jr, N. G. (2012). The functional genomics of an eco-evolutionary feedback loop: linking gene expression, trait evolution, and community dynamics. *Ecology letters*, 15(5):492–501.

Begg, G. S. and Dye, R. (2014). *Exploring trade-offs and synergies between biological pest control and species conservation*. Scottish Natural Heritage.

Bengtsson, J. (2015). Biological control as an ecosystem service: partitioning contributions of nature and human inputs to yield. *Ecological Entomology*, 40:45–55.

Benichou, O., Calvez, V., Meunier, N., and Voituriez, R. (2012). Front acceleration by dynamic selection in fisher population waves. *Physical Review E*, 86(4):041908.

Benton, T. G., Vickery, J. A., and Wilson, J. D. (2003). Farmland biodiversity: Is habitat heterogeneity the key?

Berestycki, H. and Hamel, F. (2002). Front propagation in periodic excitable media. *Comm Pure Appl Math*, 55(8):949–1032.

Berestycki, H. and Hamel, F. (2005). Gradient Estimates For Elliptic Regularizations of Semilinear Parabolic And Degenerate Elliptic Equations. *Communications in Partial Differential Equations*, 30(1-3):139–156.

Berestycki, H., Hamel, F., and Roques, L. (2005). Analysis of the periodically fragmented environment model: II - Biological invasions and pulsating travelling fronts. *J Math Pures Appl*, 84(8):1101–1146.

Berestycki, N., Mouhot, C., and Raoul, G. (2015). Existence of self-accelerating fronts for a non-local reaction-diffusion equations. *arXiv preprint arXiv:1512.00903*.

Besag, J. (1974). Spatial interaction and the statistical analysis of lattice systems. *Journal of the Royal Statistical Society: Series B (Methodological)*, 36(2):192–225.

Besag, J. E. (1972). Nearest-neighbour systems and the auto-logistic model for binary data. *Journal of the Royal Statistical Society: Series B (Methodological)*, 34(1):75–83.

Betbeder, J., Laslier, M., Hubert-Moy, L., Burel, F., and Baudry, J. (2017). Synthetic aperture radar (sar) images improve habitat suitability models. *Landscape Ecology*, 32(9):1867–1879.

Bianchi, F., Schellhorn, N., Buckley, Y., and Possingham, H. (2010). Spatial variability in ecosystem services: simple rules for predator-mediated pest suppression. *Ecological Applications*, 20(8):2322–2333.

Bianchi, F. A., Ives, A., and Schellhorn, N. (2013). Interactions between conventional and organic farming for biocontrol services across the landscape. *Ecological Applications*, 23(7):1531–1543.

Bianchi, F. J., Booij, C., and Tscharntke, T. (2006). Sustainable pest regulation in agricultural landscapes: a review on landscape composition, biodiversity and natural pest control. *Proceedings of the Royal Society B: Biological Sciences*, 273(1595):1715–1727.

Blitzer, E. J., Dormann, C. F., Holzschuh, A., Klein, A. M., Rand, T. A., and Tscharntke, T. (2012). Spillover of functionally important organisms between managed and natural habitats.

Bolnick, D. I., Amarasekare, P., Araújo, M. S., Bürger, R., Levine, J. M., Novak, M., Rudolf, V. H., Schreiber, S. J., Urban, M. C., and Vasseur, D. A. (2011). Why intraspecific trait variation matters in community ecology. *Trends in ecology & evolution*, 26(4):183–192.

Bommarco, R., Kleijn, D., and Potts, S. G. (2013). Ecological intensification: harnessing ecosystem services for food security. *Trends in ecology & evolution*, 28(4):230–238.

Bonhomme, V., Castets, M., Ibanez, T., Géraux, H., Hély, C., and Gaucherel, C. (2017). Configurational changes of patchy landscapes dynamics. *Ecological Modelling*, 363:1–7.

Bonte, D. and Bafort, Q. (2018). The importance and adaptive value of life history evolution for metapopulation dynamics. *bioRxiv*, page 179234.

Bonte, D. and de la Pena, E. (2009). Evolution of body condition-dependent dispersal in metapopulations. *Journal of Evolutionary Biology*, 22(6):1242–1251.

Bonte, D., Hovestadt, T., and Poethke, H.-J. (2010). Evolution of dispersal polymorphism and local adaptation of dispersal distance in spatially structured landscapes. *Oikos*, 119(3):560–566.

Boots, B., Okabe, A., and Sugihara, K. (1999). Spatial tessellations. *Geographical information systems*, 1:503–526.

Bouin, E. and Calvez, V. (2014). Travelling waves for the cane toads equation with bounded traits. *Nonlinearity*, 27(9):2233.

Bouin, E., Calvez, V., Meunier, N., Mirrahimi, S., Perthame, B., Raoul, G., and Voituriez, R. (2012). Invasion fronts with variable motility: phenotype selection, spatial sorting and wave acceleration. *Comptes Rendus Mathematique*, 350(15-16):761–766.

Bowler, D. E. and Benton, T. G. (2005). Causes and consequences of animal dispersal strategies: relating individual behaviour to spatial dynamics. *Biological reviews*, 80(2):205–225.

Box, G. E. (1979). Robustness in the strategy of scientific model building. In *Robustness in statistics*, pages 201–236. Elsevier.

Brown, J. S., Kotler, B. P., and Bouskila, A. (2001). Ecology of fear: foraging games between predators and prey with pulsed resources. In *Annales Zoologici Fennici*, pages 71–87. JSTOR.

Brown, J. S., Laundré, J. W., and Gurung, M. (1999). The ecology of fear: optimal foraging, game theory, and trophic interactions. *Journal of mammalogy*, 80(2):385–399.

Brown, L. D. (1986). *Fundamentals of statistical exponential families: with applications in statistical decision theory*. Institute of Mathematical Statistics.

Burak, M. K., Monk, J. D., and Schmitz, O. J. (2018). Focus: Ecology and evolution: Eco-evolutionary dynamics: The predator-prey adaptive play and the ecological theater. *The Yale journal of biology and medicine*, 91(4):481.

Burton, O. J., Phillips, B. L., and Travis, J. M. (2010). Trade-offs and the evolution of life-histories during range expansion. *Ecology letters*, 13(10):1210–1220.

Cabral, J. S., Valente, L., and Hartig, F. (2017). Mechanistic simulation models in macroecology and biogeography: state-of-art and prospects. *Ecography*, 40(2):267–280.

Cáceres, D. M., Tapella, E., Quétier, F., and Díaz, S. (2015). The social value of biodiversity and ecosystem services from the perspectives of different social actors. *Ecology and Society*, 20(1).

Cadotte, M. W., Carscadden, K., and Mirotchnick, N. (2011). Beyond species: functional diversity and the maintenance of ecological processes and services. *Journal of applied ecology*, 48(5):1079–1087.

Calabrese, J. M. and Fagan, W. F. (2004). A comparison-shopper's guide to connectivity metrics. *Frontiers in Ecology and the Environment*, 2(10):529–536.

Cantrell, R. S. and Cosner, C. (2004). *Spatial ecology via reaction-diffusion equations*. John Wiley & Sons.

Carrasco, L. R., Nghiem, T., Sunderland, T., and Koh, L. (2014). Economic valuation of ecosystem services fails to capture biodiversity value of tropical forests. *Biological Conservation*, 178:163–170.

Cenzer, M. and M'Gonigle, L. K. (2019). Local adaptation in dispersal in multi-resource landscapes. *Evolution*, 73(4):648–660.

Chakraborty, A., Singh, M., Lucy, D., and Ridland, P. (2007). Predator–prey model with prey-taxis and diffusion. *Mathematical and computer modelling*, 46(3-4):482–498.

Chapin I, F. S., Zavaleta, E. S., Eviner, V. T., Naylor, R. L., Vitousek, P. M., Reynolds, H. L., Hooper, D. U., Lavorel, S., Sala, O. E., Hobbie, S. E., et al. (2000). Consequences of changing biodiversity. *Nature*, 405(6783):234–242.

Chaplin-Kramer, R., O'Rourke, M. E., Blitzer, E. J., and Kremen, C. (2011a). A meta-analysis of crop pest and natural enemy response to landscape complexity.

Chaplin-Kramer, R., O'Rourke, M. E., Blitzer, E. J., and Kremen, C. (2011b). A meta-analysis of crop pest and natural enemy response to landscape complexity. *Ecology letters*, 14(9):922–932.

Chuang, A. and Peterson, C. R. (2016). Expanding population edges: theories, traits, and trade-offs. *Global change biology*, 22(2):494–512.

Ciss, M., Parisey, N., Moreau, F., Dedryver, C.-A., and Pierre, J.-S. (2014). A spatiotemporal model for predicting grain aphid population dynamics and optimizing insecticide sprays at the scale of continental france. *Environmental Science and Pollution Research*, 21(7):4819–4827.

Clobert, J., Le Galliard, J.-F., Cote, J., Meylan, S., and Massot, M. (2009). Informed dispersal, heterogeneity in animal dispersal syndromes and the dynamics of spatially structured populations. *Ecology letters*, 12(3):197–209.

Cobben, M., Verboom, J., Opdam, P., Hoekstra, R., Jochem, R., and Smulders, M. (2015). Spatial sorting and range shifts: consequences for evolutionary potential and genetic signature of a dispersal trait. *Journal of Theoretical Biology*, 373:92–99.

Coppolillo, P., Gomez, H., Maisels, F., and Wallace, R. (2004). Selection criteria for suites of landscape species as a basis for site-based conservation. *Biological conservation*, 115:419–430.

Corbett, A. and Rosenheim, J. A. (1996). Quantifying movement of a minute parasitoid, anagrus epos (hymenoptera: Mymaridae), using fluorescent dust marking and recapture. *Biological control*, 6(1):35–44.

Cote, J., Bestion, E., Jacob, S., Travis, J., Legrand, D., and Baguette, M. (2017). Evolution of dispersal strategies and dispersal syndromes in fragmented landscapes. *Ecography*, 40(1):56–73.

Cressie, N. (1991). Ac (1991). statistics for spatial data. *Wiley, New York.*

Cressie, N. (2015). *Statistics for spatial data*. John Wiley & Sons.

Crowder, D. W. and Jabbour, R. (2014). Relationships between biodiversity and biological control in agroecosystems: current status and future challenges. *Biological control*, 75:8–17.

Cushman, S. A., Gutzweiler, K., Evans, J. S., and McGarigal, K. (2010). The gradient paradigm: a conceptual and analytical framework for landscape ecology. In *Spatial complexity, informatics, and wildlife conservation*, pages 83–108. Springer (New York).

Cushman, S. A., McGarigal, K., and Neel, M. C. (2008). Parsimony in landscape metrics: strength, universality, and consistency. *Ecological indicators*, 8(5):691–703.

Daily, G. C. (1997). *Nature's services: societal dependence on natural ecosystems*. Washington, DC: Island Press.

DeAngelis, D. L. and Yurek, S. (2017). Spatially explicit modeling in ecology: a review. *Ecosystems*, 20(2):284–300.

Deforet, M., Carmona-Fontaine, C., Korolev, K. S., and Xavier, J. B. (2019). Evolution at the edge of expanding populations. *The American Naturalist*, 194(3):291–305.

Dewhirst, S. and Lutscher, F. (2009). Dispersal in heterogeneous habitats: thresholds, spatial scales, and approximate rates of spread. *Ecology*, 90(5):1338–1345.

Díaz, S., Quétier, F., Cáceres, D. M., Trainor, S. F., Pérez-Harguindeguy, N., Bret-Harte, M. S., Finegan, B., Peña-Claros, M., and Poorter, L. (2011). Linking functional diversity and social actor strategies in a framework for interdisciplinary analysis of nature's benefits to society. *Proceedings of the National Academy of Sciences*, 108(3):895–902.

DiBattista, J. D. (2008). Patterns of genetic variation in anthropogenically impacted populations. *Conservation Genetics*, 9(1):141–156.

Diggle, P. (2003). *Statistical Analysis of Spatial Point Patterns, 2nd edn Arnold*. Hodder Education, London, UK.

Doebeli, M. (1996). Quantitative genetics and population dynamics. *Evolution*, 50(2):532–546.

Doré, T., Makowski, D., Malézieux, E., Munier-Jolain, N., Tchamitchian, M., and Tittonell, P. (2011). Facing up to the paradigm of ecological intensification in agronomy: revisiting methods, concepts and knowledge. *European Journal of Agronomy*, 34(4):197–210.

Dormann, C. F., Schymanski, S. J., Cabral, J., Chuine, I., Graham, C., Hartig, F., Kearney, M., Morin, X., Römermann, C., Schröder, B., et al. (2012). Correlation and process in species distribution models: bridging a dichotomy. *Journal of Biogeography*, 39(12):2119–2131.

Dunning, J. B., Danielson, B. J., and Pulliam, H. R. (1992). Ecological processes that affect populations in complex landscapes. *Oikos*, pages 169–175.

Durrett, R. and Levin, S. (1994). The importance of being discrete (and spatial). *Theor Popul Biol*, 46(3):363–394.

Dutcher, J. D. (2007). A review of resurgence and replacement causing pest outbreaks in ipm. *General concepts in integrated pest and disease management*, pages 27–43.

Duthie, A. B., Abbott, K. C., and Nason, J. D. (2015). Trade-offs and coexistence in fluctuating environments: evidence for a key dispersal-fecundity trade-off in five nonpollinating fig wasps. *The American Naturalist*, 186(1):151–158.

Eilenberg, J., Hajek, A., and Lomer, C. (2001). Suggestions for unifying the terminology in biological control. *BioControl*, 46(4):387–400.

El Abdllaoui, A., Auger, P., Kooi, B. W., De la Parra, R. B., and Mchich, R. (2007). Effects of density-dependent migrations on stability of a two-patch predator–prey model. *Mathematical Biosciences*, 210(1):335–354.

El Smaily, M., Hamel, F., and Roques, L. (2009). Homogenization and influence of fragmentation in a biological invasion model. *Disc Cont Dyn Systems A*.

Elliott, E. C. and Cornell, S. J. (2012). Dispersal polymorphism and the speed of biological invasions. *PloS one*, 7(7).

Engel, J., Huth, A., and Frank, K. (2012). Bioenergy production and skylark (alauda arvensis) population abundance–a modelling approach for the analysis of land-use change impacts and conservation options. *Gcb Bioenergy*, 4(6):713–727.

Fabian, Y., Sandau, N., Bruggisser, O. T., Aebi, A., Kehrli, P., Rohr, R. P., Naisbit, R. E., and Bersier, L.-F. (2013). The importance of landscape and spatial structure for hymenopteran-based food webs in an agro-ecosystem. *Journal of Animal Ecology*, 82(6):1203–1214.

Fagan, W. F., Cantrell, R. S., and Cosner, C. (1999). How habitat edges change species interactions. *The American Naturalist*, 153(2):165–182.

Fahrig, L. (2003). Effects of habitat fragmentation on biodiversity. *Annual Review of Ecology, Evolution, and Systematics*, 34:487–515.

Fahrig, L. (2007). Non-optimal animal movement in human-altered landscapes. *Functional ecology*, 21(6):1003–1015.

Fahrig, L. (2013). Rethinking patch size and isolation effects: the habitat amount hypothesis. *Journal of Biogeography*, 40(9):1649–1663.

Fahrig, L., Baudry, J., Brotons, L., Burel, F. G., Crist, T. O., Fuller, R. J., Sirami, C., Siriwardena, G. M., and Martin, J.-L. (2011). Functional landscape heterogeneity and animal biodiversity in agricultural landscapes. *Ecology letters*, 14(2):101–112.

FAO, R. (2006). Prospects for food, nutrition, agriculture and major commodity groups. *World agriculture: towards 2030-2050*.

Fernández, N., Delibes, M., and Palomares, F. (2007). Habitat-related heterogeneity in breeding in a metapopulation of the iberian lynx. *Ecography*, 30(3):431–439.

Ferrier, S. and Guisan, A. (2006). Spatial modelling of biodiversity at the community level. *Journal of applied ecology*, 43(3):393–404.

Fienberg, S. E. (2010). Introduction to papers on the modeling and analysis of network data. *The Annals of Applied Statistics*, pages 1–4.

Fife, P. C. and McLeod, J. (1977). The approach of solutions of nonlinear diffusion equations to traveling front solutions. *Arch Ration Mech Anal*, 65(1):335–361.

Finke, D. L. and Snyder, W. E. (2008). Niche partitioning increases resource exploitation by diverse communities. *Science*, 321(5895):1488–1490.

Finke, D. L. and Snyder, W. E. (2010). Conserving the benefits of predator biodiversity. *Biological Conservation*, 143(10):2260–2269.

Firbank, L., Bradbury, R. B., McCracken, D. I., and Stoate, C. (2013). Delivering multiple ecosystem services from enclosed farmland in the uk. *Agriculture, ecosystems & environment*, 166:65–75.

Fisher, R. A. (1937). The wave of advance of advantageous genes. *Ann Eugen*, 7:335–369.

Foley, J. A., DeFries, R., Asner, G. P., Barford, C., Bonan, G., Carpenter, S. R., Chapin, F. S., Coe, M. T., Daily, G. C., Gibbs, H. K., et al. (2005). Global consequences of land use. *science*, 309(5734):570–574.

Foresight, U. (2011). The future of food and farming. *Final Project Report, London, The Government Office for Science*.

Forest, F., Grenyer, R., Rouget, M., Davies, T. J., Cowling, R. M., Faith, D. P., Balmford, A., Manning, J. C., Procheş, Ş., van der Bank, M., et al. (2007). Preserving the evolutionary potential of floras in biodiversity hotspots. *Nature*, 445(7129):757–760.

Forman, R., Foreman, R., and Godron, M. (1986). *Landscape Ecology*. Wiley.

Forrester, A., Sobester, A., and Keane, A. (2008). *Engineering design via surrogate modelling: a practical guide*. John Wiley & Sons.

Forrester, G. E. and Steele, M. A. (2004). Predators, prey refuges, and the spatial scaling of density-dependent prey mortality. *Ecology*, 85(5):1332–1342.

Franck, P., Ricci, B., Klein, E. K., Olivares, J., Simon, S., Cornuet, J.-M., and Lavigne, C. (2011). Genetic inferences about the population dynamics of codling moth females at a local scale. *Genetica*, 139(7):949.

Franklin, J. (2010). *Mapping Species Distributions: Spatial Inference and Prediction*. Ecology, Biodiversity and Conservation. Cambridge University Press.

Fraterrigo, J. M., Pearson, S. M., and Turner, M. G. (2009). Joint effects of habitat configuration and temporal stochasticity on population dynamics. *Landscape ecology*, 24(7):863–877.

Frazier, A. E. and Kedron, P. (2017). Landscape metrics: Past progress and future directions. *Current Landscape Ecology Reports*, 2(3):63–72.

Fritsch, M., Lischke, H., and Meyer, K. M. (2020). Scaling methods in ecological modelling. *Methods in Ecology and Evolution*, 11(11):1368–1378.

Gabriel, E., Opitz, T., and Bonneu, F. (2017). Detecting and modeling multi-scale space-time structures: the case of wildfire occurrences. *Journal de la Société Française de Statistique*, 158(3):86–105.

Gaetan, C. and Guyon, X. (2010). *Spatial statistics and modeling*, volume 90. Springer.

Garcia, A. F., GRIFFITHS, G. J., and Thomas, C. G. (2000). Density, distribution and dispersal of the carabid beetle nebria brevicollis in two adjacent cereal fields. *Annals of Applied Biology*, 137(2):89–97.

Gardner, R. H. (1999). RULE: map generation and a spatial analysis program. In *Landscape ecological analysis*, pages 280–303. Springer (New York).

Gardner, R. H. and Urban, D. L. (2007). Neutral models for testing landscape hypotheses. *Landscape Ecology*, 22(1):15–29.

Garrigues, S., Allard, D., Baret, F., and Morisette, J. (2008). Multivariate quantification of landscape spatial heterogeneity using variogram models. *Remote Sensing of Environment*, 112(1):216–230.

Garrigues, S., Allard, D., Baret, F., and Weiss, M. (2006). Quantifying spatial heterogeneity at the landscape scale using variogram models. *Remote sensing of environment*, 103(1):81–96.

Gaucherel, C. (2008). Neutral models for polygonal landscapes with linear networks. *Ecological Modelling*, 219(1-2):39–48.

Gaucherel, C., Boudon, F., Houet, T., Castets, M., and Godin, C. (2012). Understanding patchy landscape dynamics: towards a landscape language. *PLoS One*, 7(9):e46064.

Gaucherel, C., Fleury, D., Auclair, D., and Dreyfus, P. (2006a). Neutral models for patchy landscapes. *Ecological Modelling*, 197(1-2):159–170.

Gaucherel, C., Giboire, N., Viaud, V., Houet, T., Baudry, J., and Burel, F. (2006b). A domain-specific language for patchy landscape modelling: The Brittany agricultural mosaic as a case study. *Ecological Modelling*, 194(1-3):233–243.

Gaucherel, C., Houllier, F., Auclair, D., and Houet, T. (2014). Dynamic landscape modelling: the quest for a unifying theory. *Living reviews in landscape Research*, 8(2):5–31.

Gotelli, N. J. (2000). Null model analysis of species co-occurrence patterns. *Ecology*, 81(9):2606–2621.

Gotelli, N. J. et al. (2008). *A primer of ecology*. Number 577.88 G6. Sinauer Associates Sunderland, MA.

Green, P. J., Richardson, S., and Hjort, N. L. (2003). *Highly structured stochastic systems*, volume 27. Oxford University Press.

Griffiths, E., Wratten, S., and Vickerman, G. (1985). Foraging by the carabid agonum dorsale in the field. *Ecological Entomology*, 10(2):181–189.

Grimm, V., Berger, U., Bastiansen, F., Eliassen, S., Ginot, V., Giske, J., Goss-Custard, J., Grand, T., Heinz, S. K., Huse, G., et al. (2006). A standard protocol for describing individual-based and agent-based models. *Ecological modelling*, 198(1-2):115–126.

Grimm, V. and Railsback, S. F. (2005). *Individual-based modeling and ecology*, volume 8. Princeton university press.

Gross, K. and Rosenheim, J. A. (2011). Quantifying secondary pest outbreaks in cotton and their monetary cost with causal-inference statistics. *Ecological Applications*, 21(7):2770–2780.

Guisan, A. and Thuiller, W. (2005). Predicting species distribution: offering more than simple habitat models. *Ecology letters*, 8(9):993–1009.

Haan, N. L., Zhang, Y., and Landis, D. A. (2020). Predicting Landscape Configuration Effects on Agricultural Pest Suppression.

Hamel, F., Fayard, J., and Roques, L. (2010). Spreading speeds in slowly oscillating environments. *Bull Math Biol*, 72(5):1166–1191.

Hamel, F., Lavigne, F., Martin, G., and Roques, L. (2020). Dynamics of adaptation in an anisotropic phenotype-fitness landscape. *Nonlinear Analysis: Real World Applications*, 54:103107.

Hamel, F., Nadin, G., and Roques, L. (2011). A viscosity solution method for the spreading speed formula in slowly varying media. *Indiana Univ Math J*, 60:1229–1247.

Hamer, W. B., Birr, T., Verreet, J.-A., Duttmann, R., and Klink, H. (2020). Spatio-temporal prediction of the epidemic spread of dangerous pathogens using machine learning methods. *ISPRS International Journal of Geo-Information*, 9(1):44.

Hamilton, W. D. and May, R. M. (1977). Dispersal in stable habitats. *Nature*, 269(5629):578–581.

Hammersley, J. M. and Clifford, P. (1971). Markov fields on finite graphs and lattices. *Unpublished manuscript*, 46.

Hanski, I. (1994). A practical model of metapopulation dynamics. *Journal of animal ecology*, pages 151–162.

Hanski, I. and Mononen, T. (2011). Eco-evolutionary dynamics of dispersal in spatially heterogeneous environments. *Ecology letters*, 14(10):1025–1034.

Hanski, I., Saastamoinen, M., and Ovaskainen, O. (2006). Dispersal-related life-history trade-offs in a butterfly metapopulation. *Journal of animal Ecology*, 75(1):91–100.

Hanski, I. and Simberloff, D. (1997). The metapopulation approach, its history, conceptual domain, and application to conservation. *Metapopulation biology*, pages 5–26.

Hawkins, B. A., Thomas, M. B., and Hochberg, M. E. (1993). Refuge theory and biological control. *Science*, 262(5138):1429–1432.

Hayhoe, K., Edmonds, J., Kopp, R., LeGrande, A., Sanderson, B., Wehner, M., and Wuebbles, D. (2017). Climate models, scenarios, and projections.

Heaton, M. J., Katzfuss, M., Ramachandar, S., Pedings, K., Gilleland, E., Mannshardt-Shamseldin, E., and Smith, R. L. (2011). Spatio-temporal models for large-scale indicators of extreme weather. *Environmetrics*, 22(3):294–303.

Hebblewhite, M., Merrill, E., and McDonald, T. (2005). Spatial decomposition of predation risk using resource selection functions: an example in a wolf–elk predator–prey system. *Oikos*, 111(1):101–111.

Hecht, F. (2012a). New development in freefem+. *Journal of Numerical Mathematics*, 20(3-4):251–265.

Hecht, F. (2012b). New development in Freefem++. *J Numer Math*, 20(3-4):251–265.

Hefley, T. J., Hooten, M. B., Hanks, E. M., Russell, R. E., and Walsh, D. P. (2017). Dynamic spatio-temporal models for spatial data. *Spatial statistics*, 20:206–220.

Heino, M. and Hanski, I. (2001). Evolution of migration rate in a spatially realistic metapopulation model. *The American Naturalist*, 157(5):495–511.

Helms, J. and Kaspari, M. (2015). Reproduction-dispersal tradeoffs in ant queens. *Insectes sociaux*, 62(2):171–181.

Hesselbarth, M. H., Sciaini, M., With, K. A., Wiegand, K., and Nowosad, J. (2019). landscapemetrics: an open-source r tool to calculate landscape metrics. *Ecography*, 42(10):1648–1657.

Hilbeck, A., Eckel, C., and Kennedy, G. G. (1998). Impact of bacillus thuringiensis–insecticides on population dynamics and egg predation of the colorado potato beetle in north carolina potato plantings. *BioControl*, 43(1):65–75.

Hillebrand, H. and Matthiessen, B. (2009). Biodiversity in a complex world: consolidation and progress in functional biodiversity research. *Ecology letters*, 12(12):1405–1419.

Hirt, M. R., Lauermann, T., Brose, U., Noldus, L. P., and Dell, A. I. (2017). The little things that run: a general scaling of invertebrate exploratory speed with body mass. *Ecology*, 98(11):2751–2757.

Hogeweg, P. (1988). Cellular automata as a paradigm for ecological modeling. *Applied mathematics and computation*, 27(1):81–100.

Holt, R., Hochberg, M., et al. (2001). Indirect interactions, community modules and biological control: a theoretical perspective. *Evaluating indirect ecological effects of biological control*, 125:13–37.

Hughes, C. L., Hill, J. K., and Dytham, C. (2003). Evolutionary trade-offs between reproduction and dispersal in populations at expanding range boundaries. *Proceedings of the Royal Society of London. Series B: Biological Sciences*, 270(suppl_2):S147–S150.

Iampietro, P. J., Kvitek, R. G., and Morris, E. (2005). Recent advances in automated genus-specific marine habitat mapping enabled by high-resolution multibeam bathymetry. *Marine Technology Society Journal*, 39(3):83–93.

Illian, J., Penttinen, A., Stoyan, D., and Stoyan, H. (2008). *Analysis and Modelling of Spatial Point Patterns, from Spatial Data to Knowledge*. Wiley, Chichester, UK.

Illian, J. B. and Burslem, D. F. (2017). Improving the usability of spatial point process methodology: an interdisciplinary dialogue between statistics and ecology. *AStA Advances in Statistical Analysis*, 101(4):495–520.

Illian, J. B., Martino, S., Sørbye, S. H., Gallego-Fernández, J. B., Zunzunegui, M., Esquivias, M. P., and Travis, J. M. (2013). Fitting complex ecological point process models with integrated nested laplace approximation. *Methods in Ecology and Evolution*, 4(4):305–315.

Illian, J. B., Sørbye, S. H., Rue, H., and Hendrichsen, D. K. (2012). Using inla to fit a complex point process model with temporally varying effects-a case study. *Journal of Environmental Statistics*, 3(7).

Inkoom, J. N., Frank, S., Greve, K., and Fürst, C. (2017). Designing neutral landscapes for data scarce regions in West Africa. *Ecological informatics*, 42:1–13.

Janetos, A. C. (1982). Active foragers vs. sit-and-wait predators: a simple model. *Journal of Theoretical Biology*, 95(2):381–385.

Jansen, M. J. (1999). Analysis of variance designs for model output. *Computer Physics Communications*, 117(1):35–43.

Jax, K., Barton, D. N., Chan, K. M., De Groot, R., Doyle, U., Eser, U., Görg, C., Gómez-Baggethun, E., Griewald, Y., Haber, W., et al. (2013). Ecosystem services and ethics. *Ecological Economics*, 93:260–268.

Jax, K. and Heink, U. (2015). Searching for the place of biodiversity in the ecosystem services discourse. *Biological Conservation*, 191:198–205.

Jia, G. and Taflanidis, A. A. (2013). Kriging metamodeling for approximation of high-dimensional wave and surge responses in real-time storm/hurricane risk assessment. *Computer Methods in Applied Mechanics and Engineering*, 261:24–38.

Johnson, M. L. and Gaines, M. S. (1990). Evolution of dispersal: theoretical models and empirical tests using birds and mammals. *Annual review of ecology and systematics*, 21(1):449–480.

Johst, K., Lima, M., and Berryman, A. A. (2013). Scaling up: how do exogenous fluctuations in individual-based resource competition models re-emerge in aggregated stochastic population models? *Population ecology*, 55(1):173–182.

Jonsson, M., Bommarco, R., Ekbom, B., Smith, H. G., Bengtsson, J., Caballero-Lopez, B., Winqvist, C., and Olsson, O. (2014). Ecological production functions for biological control services in agricultural landscapes. *Methods in Ecology and Evolution*, 5(3):243–252.

Joyce, K., Holland, J., and Doncaster, C. (1999). Influences of hedgerow intersections and gaps on the movement of carabid beetles. *Bulletin of Entomological Research*, 89(6):523–531.

Kappes, H., Jordaens, K., Hendrickx, F., Maelfait, J.-P., Lens, L., and Backeljau, T. (2009). Response of snails and slugs to fragmentation of lowland forests in nw germany. *Landscape Ecology*, 24(5):685–697.

Karp, D. S., Chaplin-Kramer, R., Meehan, T. D., Martin, E. A., DeClerck, F., Grab, H., Gratton, C., Hunt, L., Larsen, A. E., Martínez-Salinas, A., O'Rourke, M. E., Rusch, A., Poveda, K., Jonsson, M., Rosenheim, J. A., Schellhorn, N. A., Tscharntke, T., Wratten, S. D., Zhang, W., Iverson, A. L., Adler, L. S., Albrecht, M., Alignier, A., Angelella, G. M., Anjum, M. Z., Avelino, J., Batáry, P., Baveco, J. M., Bianchi, F. J., Birkhofer, K., Bohnenblust, E. W., Bommarco, R., Brewer, M. J., Caballero-López, B., Carrière, Y., Carvalheiro, L. G., Cayuela, L., Centrella, M., Ćetković, A., Henri, D. C., Chabert, A., Costamagna, A. C., De la Mora, A., de Kraker, J., Desneux, N., Diehl, E., Diekötter, T., Dormann, C. F., Eckberg, J. O., Entling, M. H., Fiedler, D., Franck, P., van Veen, F. J., Frank, T., Gagic, V., Garratt, M. P., Getachew, A., Gonthier, D. J., Goodell, P. B., Graziosi, I., Groves, R. L., Gurr, G. M., Hajian-Forooshani, Z., Heimpel, G. E., Herrmann, J. D., Huseth, A. S., Inclán, D. J., Ingrao, A. J., Iv, P., Jacot, K., Johnson, G. A., Jones, L., Kaiser, M., Kaser, J. M., Keasar, T., Kim, T. N., Kishinevsky, M., Landis, D. A., Lavandero, B., Lavigne, C., Le Ralec, A., Lemessa, D., Letourneau, D. K., Liere, H., Lu, Y., Lubin, Y., Luttermoser, T., Maas, B., Mace, K., Madeira, F., Mader, V., Cortesero, A. M., Marini, L., Martinez, E., Martinson, H. M., Menozzi, P., Mitchell, M. G., Miyashita, T., Molina, G. A., Molina-Montenegro, M. A., O'Neal, M. E., Opatovsky, I., Ortiz-Martinez, S., Nash, M., Östman, Ö., Ouin, A., Pak, D., Paredes, D., Parsa, S., Parry, H., Perez-Alvarez, R., Perović, D. J., Peterson, J. A., Petit, S., Philpott, S. M., Plantegenest, M., Plećas, M., Pluess, T., Pons, X., Potts, S. G., Pywell, R. F., Ragsdale, D. W., Rand, T. A., Raymond, L., Ricci, B., Sargent, C., Sarthou, J. P., Saulais, J., Schäckermann, J., Schmidt, N. P., Schneider, G., Schüepp, C., Sivakoff, F. S., Smith, H. G., Whitney, K. S., Stutz, S., Szendrei, Z., Takada, M. B., Taki, H., Tamburini, G., Thomson, L. J., Tricault, Y., Tsafack, N., Tschumi, M., Valantin-Morison, M., van Trinh, M., van der

Werf, W., Vierling, K. T., Werling, B. P., Wickens, J. B., Wickens, V. J., Woodcock, B. A., Wyckhuys, K., Xiao, H., Yasuda, M., Yoshioka, A., and Zou, Y. (2018). Crop pests and predators exhibit inconsistent responses to surrounding landscape composition. *Proceedings of the National Academy of Sciences of the United States of America*, 115(33):E7863–E7870.

Kato, M. (1994). Structure, organization, and response of a species-rich parasitoid community to host leafminer population dynamics. *Oecologia*, 97(1):17–25.

Kawasaki, K. and Shigesada, N. (2007). An integrodifference model for biological invasions in a periodically fragmented environment. *Jpn J Ind Appl Math*, 24(1):3–15.

Kiêu, K., Adamczyk-Chauvat, K., Monod, H., and Stoica, R. S. (2013). A completely random T-tessellation model and Gibbsian extensions. *Spatial Statistics*, 6:118–138.

Kleijn, D., Bommarco, R., Fijen, T. P., Garibaldi, L. A., Potts, S. G., and van der Putten, W. H. (2019). Ecological intensification: bridging the gap between science and practice. *Trends in ecology & evolution*, 34(2):154–166.

Kleijnen, J. P. (2015). Design and analysis of simulation experiments. In *International Workshop on Simulation*, pages 3–22. Springer.

Knowlton, J. L. and Graham, C. H. (2010). Using behavioral landscape ecology to predict species' responses to land-use and climate change. *Biological Conservation*, 143(6):1342–1354.

Kolmogorov, A. N., Petrovsky, I. G., and Piskunov, N. S. (1937). Étude de l'équation de la diffusion avec croissance de la quantité de matière et son application à un problème biologique. *Bull Univ État Moscou, Sér. Int. A*, 1:1–26.

Kosoy, N. and Corbera, E. (2010). Payments for ecosystem services as commodity fetishism. *Ecological economics*, 69(6):1228–1236.

Koss, A. M., Chang, G. C., and Snyder, W. E. (2004). Predation of green peach aphids by generalist predators in the presence of alternative, Colorado potato beetle egg prey. *Biological Control*, 31(2):237–244.

Kotler, B. (2016). Fun and games: Predator–prey foraging games and related interactions.

Kromp, B. (1999). Carabid beetles in sustainable agriculture: a review on pest control efficacy, cultivation impacts and enhancement. *Agriculture, Ecosystems & Environment*, 74(1-3):187–228.

Kubisch, A., Holt, R. D., Poethke, H.-J., and Fronhofer, E. A. (2014). Where am i and why? synthesizing range biology and the eco-evolutionary dynamics of dispersal. *Oikos*, 123(1):5–22.

Kupfer, J. A. (2012). Landscape ecology and biogeography: Rethinking landscape metrics in a post-FRAGSTATS landscape. *Progress in Physical Geography*, 36(3):400–420.

Lacy, R. C., Miller, P. S., Nyhus, P. J., Pollak, J., Raboy, B. E., and Zeigler, S. L. (2013). Metamodels for transdisciplinary analysis of wildlife population dynamics. *PLoS One*, 8(12):e84211.

Landis, D. A. (1999). Landscape structure and extra-field processes: Impact on management. *Handbook of pest management*, page 79.

Langer, V. (2001). The potential of leys and short rotation coppice hedges as reservoirs for parasitoids of cereal aphids in organic agriculture. *Agriculture, ecosystems & environment*, 87(1):81–92.

Langhammer, M., Thober, J., Lange, M., Frank, K., and Grimm, V. (2019). Agricultural landscape generators for simulation models: A review of existing solutions and an outline of future directions.

Lankau, R. A. (2009). Genetic variation promotes long-term coexistence of brassica nigra and its competitors. *The American Naturalist*, 174(2):E40–E53.

Lausch, A., Blaschke, T., Haase, D., Herzog, F., Syrbe, R.-U., Tischendorf, L., and Walz, U. (2015). Understanding and quantifying landscape structure–a review on relevant process characteristics, data models and landscape metrics. *Ecological Modelling*, 295:31–41.

Lavigne, F., Martin, G., Anciaux, Y., Papaix, J., and Roques, L. (2020). When sinks become sources: adaptive colonization in asexuals. *Evolution*, 74(1):29–42.

Lavorel, S. and Garnier, É. (2002). Predicting changes in community composition and ecosystem functioning from plant traits: revisiting the holy grail. *Functional ecology*, 16(5):545–556.

Law, R., Illian, J., Burslem, D. F., Gratzer, G., Gunatilleke, C., and Gunatilleke, I. (2009). Ecological information from spatial patterns of plants: insights from point process theory. *Journal of Ecology*, 97(4):616–628.

Le Ber, F., Lavigne, C., Adamczyk, K., Angevin, F., Colbach, N., Mari, J.-F., and Monod, H. (2009). Neutral modelling of agricultural landscapes by tessellation methods—application for gene flow simulation. *Ecological Modelling*, 220(24):3536–3545.

Le Gal, A., Robert, C., Accatino, F., Claessen, D., and Lecomte, J. (2020). Modelling the interactions between landscape structure and spatio-temporal dynamics of pest natural enemies: Implications for conservation biological control. *Ecological Modelling*, 420(November 2019):108912.

Le Gal, A., Robert, C., Accatino, F., Claessen, D., and Lecomte, J. (2020). Modelling the interactions between landscape structure and spatio-temporal dynamics of pest natural enemies: Implications for conservation biological control. *Ecological Modelling*, 420:108912.

Lefebvre, M., Papaïx, J., Mollot, G., Deschodt, P., Lavigne, C., Ricard, J.-M., Mandrin, J.-F., and Franck, P. (2017). Bayesian inferences of arthropod movements between hedgerows and orchards. *Basic and Applied Ecology*, 21:76–84.

Legrand, D., Cote, J., Fronhofer, E. A., Holt, R. D., Ronce, O., Schtickzelle, N., Travis, J. M., and Clobert, J. (2017). Eco-evolutionary dynamics in fragmented landscapes. *Ecography*, 40(1):9–25.

Leitao, A. B. and Ahern, J. (2002). Applying landscape ecological concepts and metrics in sustainable landscape planning. *Landscape and urban planning*, 59(2):65–93.

Letourneau, D. K., Jedlicka, J. A., Bothwell, S. G., and Moreno, C. R. (2009). Effects of natural enemy biodiversity on the suppression of arthropod herbivores in terrestrial ecosystems. *Annual Review of Ecology, Evolution, and Systematics*, 40:573–592.

Levin, S. A. (1992). The problem of pattern and scale in ecology: the robert h. macarthur award lecture. *Ecology*, 73(6):1943–1967.

Levins, R. (1969a). Some demographic and genetic consequences of environmental heterogeneity for biological control. *Bull Entomol Soc Am*, 15:237–240.

Levins, R. (1969b). Some demographic and genetic consequences of environmental heterogeneity for biological control. *American Entomologist*, 15(3):237–240.

Lewis, M. A., Petrovskii, S. V., and Potts, J. R. (2016). Reaction–diffusion models: single species. In *The Mathematics Behind Biological Invasions*, pages 69–105. Springer.

Li, X., He, H. S., Bu, R., Wen, Q., Chang, Y., Hu, Y., and Li, Y. (2005). The adequacy of different landscape metrics for various landscape patterns. *Pattern recognition*, 38(12):2626–2638.

Lichstein, J. W., Dushoff, J., Levin, S. A., and Pacala, S. W. (2007). Intraspecific variation and species coexistence. *The American Naturalist*, 170(6):807–818.

Lindström, J., Szpiro, A. A., Sampson, P. D., Oron, A. P., Richards, M., Larson, T. V., and Sheppard, L. (2014). A flexible spatio-temporal model for air pollution with spatial and spatio-temporal covariates. *Environmental and ecological statistics*, 21(3):411–433.

Lombardo, L., Opitz, T., and Huser, R. (2019). Numerical recipes for landslide spatial prediction using r-inla: a step-by-step tutorial. In *Spatial modeling in GIS and R for earth and environmental sciences*, pages 55–83. Elsevier.

Lonsdale, W. M. (1999). Global patterns of plant invasions and the concept of invasibility. *Ecology*, 80(5):1522–1536.

Lonsdorf, E., Kremen, C., Ricketts, T., Winfree, R., Williams, N., and Greenleaf, S. (2009). Modelling pollination services across agricultural landscapes. *Annals of botany*, 103(9):1589–1600.

Louvrier, J., Papaïx, J., Duchamp, C., and Gimenez, O. (2020). A mechanistic–statistical species distribution model to explain and forecast wolf (canis lupus) colonization in south-eastern france. *Spatial Statistics*, 36:100428.

Lovett, G. M., Jones, C. G., Turner, M. G., and Weathers, K. C. (2005). Ecosystem function in heterogeneous landscapes. In *Ecosystem function in heterogeneous landscapes*, pages 1–4. Springer.

Lü, L., Chen, D., Ren, X.-L., Zhang, Q.-M., Zhang, Y.-C., and Zhou, T. (2016). Vital nodes identification in complex networks. *Physics Reports*, 650:1–63.

Maalouly, M., Franck, P., Bouvier, J.-C., Toubon, J.-F., and Lavigne, C. (2013). Codling moth parasitism is affected by semi-natural habitats and agricultural practices at orchard and landscape levels. *Agriculture, ecosystems & environment*, 169:33–42.

MacArthur, R. and Levins, R. (1967). The limiting similarity, convergence, and divergence of coexisting species. *Am Nat*, 101(921):377–385.

Martin, E. A., Dainese, M., Clough, Y., Báldi, A., Bommarco, R., Gagic, V., Garratt, M. P., Holzschuh, A., Kleijn, D., Kovács-Hostyánszki, A., et al. (2019). The interplay of landscape composition and configuration: new pathways to manage functional biodiversity and agroecosystem services across europe. *Ecology letters*.

Martin, E. A., Reineking, B., Seo, B., and Steffan-Dewenter, I. (2013). Natural enemy interactions constrain pest control in complex agricultural landscapes. *Proceedings of the National Academy of Sciences*, 110(14):5534–5539.

Martín-López, B., Gómez-Baggethun, E., García-Llorente, M., and Montes, C. (2014). Trade-offs across value-domains in ecosystem services assessment. *Ecological indicators*, 37:220–228.

May, R. M. and Hassell, M. P. (1988). Population dynamics and biological control. *Philosophical Transactions of the Royal Society of London. B, Biological Sciences*, 318(1189):129–169.

McGarigal, K. and Cushman, S. (2005). The gradient concept of landscape structure [chapter 12]. *In: Wiens, John A.; Moss, Michael R., eds. Issues and Perspectives in Landscape Ecology. Cambridge University Press. p. 112-119.*, pages 112–119.

McGarigal, K., Cushman, S. A., Neel, M. C., Ene, E., et al. (2002). Fragstats: spatial pattern analysis program for categorical maps. *Computer software program produced by the authors at the University of Massachusetts, Amherst. Available at the following web site: www. umass. edu/landeco/research/fragstats/fragstats. html*, 6.

McGarigal, K. and Marks, B. J. (1995). FRAGSTATS: spatial pattern analysis program for quantifying landscape structure. *Gen. Tech. Rep. PNW-GTR-351. Portland, OR: US Department of Agriculture, Forest Service, Pacific Northwest Research Station. 122 p*, 351.

McGill, B. J., Enquist, B. J., Weiher, E., and Westoby, M. (2006). Rebuilding community ecology from functional traits. *Trends in ecology & evolution*, 21(4):178–185.

MEA, M. E. A. (2005). Current state and trends. *Washington, DC*.

Milcu, A. I., Hanspach, J., Abson, D., and Fischer, J. (2013). Cultural ecosystem services: a literature review and prospects for future research. *Ecology and society*, 18(3).

Mills, N. (2005). Selecting effective parasitoids for biological control introductions: Codling moth as a case study. *Biological Control*, 34(3):274–282.

Minor, E. S. and Urban, D. L. (2008). A graph-theory framework for evaluating landscape connectivity and conservation planning. *Conservation biology*, 22(2):297–307.

Mitchell, M. G., Bennett, E. M., and Gonzalez, A. (2014). Agricultural landscape structure affects arthropod diversity and arthropod-derived ecosystem services. *Agriculture, Ecosystems and Environment*, 192:144–151.

Mitchell, W. A. and Lima, S. L. (2002). Predator-prey shell games: large-scale movement and its implications for decision-making by prey. *Oikos*, 99(2):249–259.

Modlmeier, A. P., Keiser, C. N., Wright, C. M., Lichtenstein, J. L., and Pruitt, J. N. (2015). Integrating animal personality into insect population and community ecology. *Current Opinion in Insect Science*, 9:77–85.

Møller, J. and Waagepetersen, R. P. (1998). Markov connected component fields. *Advances in Applied Probability*, pages 1–35.

Moller, J. and Waagepetersen, R. P. (2003). *Statistical inference and simulation for spatial point processes*. CRC Press.

Morris, A., Börger, L., and Crooks, E. (2019). Individual variability in dispersal and invasion speed. *Mathematics*, 7(9):795.

Murray, J. D. (2002). *Mathematical Biology*. Third edition, Interdisciplinary Applied Mathematics 17, Springer-Verlag, New York.

Nendel, C. and Zander, P. (2019). Landscape models to support sustainable intensification of agroecological systems. *Burleigh Dodds Series in Agricultural Science. Burleigh Dodds Science Publishing*, pages 321–354.

North, A., Cornell, S., and Ovaskainen, O. (2011). Evolutionary responses of dispersal distance to landscape structure and habitat loss. *Evolution: International Journal of Organic Evolution*, 65(6):1739–1751.

Northfield, T. D., Barton, B. T., and Schmitz, O. J. (2017). A spatial theory for emergent multiple predator–prey interactions in food webs. *Ecology and evolution*, 7(17):6935–6948.

Northfield, T. D., Crowder, D. W., Jabbour, R., and Snyder, W. E. (2012). Natural enemy functional identity, trait-mediated interactions and biological control. *Trait-mediated indirect interactions: ecological and evolutionary perspectives. Cambridge University Press, New York*, pages 450–465.

Northfield, T. D., Snyder, G. B., Ives, A. R., and Snyder, W. E. (2010). Niche saturation reveals resource partitioning among consumers. *Ecology Letters*, 13(3):338–348.

Okubo, A. and Levin, S. A. (2013). *Diffusion and ecological problems: modern perspectives*, volume 14. Springer Science & Business Media.

Okuyama, T. (2008). Individual behavioral variation in predator–prey models. *Ecological Research*, 23(4):665–671.

Opitz, T., Bonneu, F., and Gabriel, E. (2020). Point-process based Bayesian modeling of space–time structures of forest fire occurrences in Mediterranean France. *Spatial Statistics*, page 100429.

Pacala, S. W. and Silander Jr, J. (1985). Neighborhood models of plant population dynamics. i. single-species models of annuals. *The American Naturalist*, 125(3):385–411.

Papaïx, J., Adamczyk-Chauvat, K., Bouvier, A., Kiêu, K., Touzeau, S., Lannou, C., and Monod, H. (2014a). Pathogen population dynamics in agricultural landscapes: The ddal modelling framework. *Infection, Genetics and Evolution*, 27:509–520.

Papaïx, J., Burdon, J. J., Lannou, C., and Thrall, P. H. (2014b). Evolution of pathogen specialisation in a host metapopulation: joint effects of host and pathogen dispersal. *PLoS Computational Biology*, 10(5):e1003633.

Papaïx, J., Burdon, J. J., Walker, E., Barrett, L. G., and Thrall, P. H. (2021). Metapopulation structure predicts population dynamics in the cakile maritima–alternaria brassicicola host-pathogen interaction. *The American Naturalist*, 197(2):E55–E71.

Parisey, N., Bourhis, Y., Roques, L., Soubeyrand, S., Ricci, B., and Poggi, S. (2016). Rearranging agricultural landscapes towards habitat quality optimisation: In silico application to pest regulation. *Ecological Complexity*, 28:113–122.

Pearce, I. G., Chaplain, M. A., Schofield, P. G., Anderson, A. R., and Hubbard, S. F. (2006). Modelling the spatio-temporal dynamics of multi-species host–parasitoid interactions: heterogeneous patterns and ecological implications. *Journal of Theoretical Biology*, 241(4):876–886.

Peckarsky, B. L., Abrams, P. A., Bolnick, D. I., Dill, L. M., Grabowski, J. H., Luttbeg, B., Orrock, J. L., Peacor, S. D., Preisser, E. L., Schmitz, O. J., et al. (2008). Revisiting the classics: considering nonconsumptive effects in textbook examples of predator–prey interactions. *Ecology*, 89(9):2416–2425.

Pe'er, G., Zurita, G. A., Schober, L., Bellocq, M. I., Strer, M., Müller, M., and Pütz, S. (2013). Simple Process-Based Simulators for Generating Spatial Patterns of Habitat Loss and Fragmentation: A Review and Introduction to the G-RaFFe Model. *PLoS ONE*, 8(5):1–14.

Pelletier, F., Garant, D., and Hendry, A. (2009). Eco-evolutionary dynamics.

Perović, D., Gámez-Virués, S., Börschig, C., Klein, A.-M., Krauss, J., Steckel, J., Rothenwöhrer, C., Erasmi, S., Tscharntke, T., and Westphal, C. (2015). Configurational landscape heterogeneity shapes functional community composition of grassland butterflies. *Journal of Applied Ecology*, 52(2):505–513.

Petchey, O. L. and Gaston, K. J. (2006). Functional diversity: back to basics and looking forward. *Ecology letters*, 9(6):741–758.

Peterson, G., Allen, C. R., and Holling, C. S. (1998). Ecological resilience, biodiversity, and scale. *Ecosystems*, 1(1):6–18.

Peterson, M. J., Hall, D. M., FELDPAUSCH-PARKER, A. M., and Peterson, T. R. (2010). Obscuring ecosystem function with application of the ecosystem services concept. *Conservation Biology*, 24(1):113–119.

Pettorelli, N., Hilborn, A., Duncan, C., and Durant, S. M. (2015). Individual Variability. In *Advances in Ecological Research*, volume 52, pages 19–44. Academic Press Inc.

Phillips, B. L., Brown, G. P., Travis, J. M., and Shine, R. (2008). Reid's paradox revisited: the evolution of dispersal kernels during range expansion. *the american naturalist*, 172(S1):S34–S48.

Phillips, B. L., Brown, G. P., Webb, J. K., and Shine, R. (2006). Invasion and the evolution of speed in toads. *Nature*, 439:803–803.

Pimont, F., Fargeon, H., Opitz, T., Ruffault, J., Barbero, R., Martin-StPaul, N., Rigolot, E., Riviere, M., and Dupuy, J.-L. (2020). Prediction of regional wildfire activity with a probabilistic Bayesian framework. *Ecological Applications (accepted)*.

Pitt, J. P. (2008). *Modelling the spread of invasive species across heterogeneous landscapes*. PhD thesis, Lincoln University.

Poggi, S., Papaïx, J., Lavigne, C., Angevin, F., Le Ber, F., Parisey, N., Ricci, B., Vinatier, F., and Wohlfahrt, J. (2018). Issues and challenges in landscape models for agriculture: from the representation of agroecosystems to the design of management strategies. *Landscape Ecology*, 33(10):1679–1690.

Poggi, S., Vinatier, F., Hannachi, M., Sanz, E. S., Rudi, G., Zamberletti, P., Tixier, P., and Papaïx, J. (2021). How can models foster the transition towards future agricultural landscapes? *Advances in Ecological Research*.

Poisot, T., Thrall, P. H., and Hochberg, M. E. (2012). Trophic network structure emerges through antagonistic coevolution in temporally varying environments. *Proceedings of the Royal Society B: Biological Sciences*, 279(1727):299–308.

Polis, G. A., Power, M. E., and Huxel, G. R. (2004). *Food webs at the landscape level*. University of Chicago Press.

Power, A. G. (2010). Ecosystem services and agriculture: tradeoffs and synergies. *Philosophical transactions of the royal society B: biological sciences*, 365(1554):2959–2971.

Pruitt, J. N., Stachowicz, J. J., and Sih, A. (2012). Behavioral types of predator and prey jointly determine prey survival: potential implications for the maintenance of within-species behavioral variation. *The American Naturalist*, 179(2):217–227.

Ragsdale, D. W., McCornack, B., Venette, R., Potter, B. D., MacRae, I. V., Hodgson, E. W., O'Neal, M. E., Johnson, K. D., O'neil, R., DiFonzo, C., et al. (2007). Economic threshold for soybean aphid (hemiptera: Aphididae). *Journal of Economic Entomology*, 100(4):1258–1267.

Ramanantoanina, A. (2015). Modelling spread with context-based dispersal strategies. *Computational Ecology and Software*, 5(4):354.

Ramanantoanina, A. and Hui, C. (2016). Formulating spread of species with habitat dependent growth and dispersal in heterogeneous landscapes. *Mathematical biosciences*, 275:51–56.

Ramanantoanina, A., Hui, C., and Ouhinou, A. (2011). Effects of density-dependent dispersal behaviours on the speed and spatial patterns of range expansion in predator–prey metapopulations. *Ecological Modelling*, 222(19):3524–3530.

Rand, T. A., Tylianakis, J. M., and Tscharntke, T. (2006). Spillover edge effects: The dispersal of agriculturally subsidized insect natural enemies into adjacent natural habitats.

Rand, T. A., Waters, D. K., Blodgett, S. L., Knodel, J. J., and Harris, M. O. (2014). Increased area of a highly suitable host crop increases herbivore pressure in intensified agricultural landscapes. *Agriculture, Ecosystems & Environment*, 186:135–143.

Ratto, M., Castelletti, A., and Pagano, A. (2012). Emulation techniques for the reduction and sensitivity analysis of complex environmental models.

Renshaw, E. (2015). *Stochastic population processes: analysis, approximations, simulations*. OUP Oxford.

Ricci, B., Franck, P., Toubon, J. F., Bouvier, J. C., Sauphanor, B., and Lavigne, C. (2009). The influence of landscape on insect pest dynamics: A case study in southeastern France. *Landscape Ecology*, 24(3):337–349.

Ricci, B., Franck, P., Valantin-Morison, M., Bohan, D. A., and Lavigne, C. (2013). Do species population parameters and landscape characteristics affect the relationship between local population abundance and surrounding habitat amount? *Ecological Complexity*, 15:62–70.

Ricci, B., Lavigne, C., Alignier, A., Aviron, S., Biju-Duval, L., Bouvier, J., Choisis, J.-P., Franck, P., Joannon, A., Ladet, S., et al. (2019). Local pesticide use intensity conditions landscape effects on biological pest control. *Proceedings of the Royal Society B*, 286(1904):20182898.

Risser, P. G. (1987). Landscape ecology: state of the art. *Landscape heterogeneity and disturbance*, pages 3–14.

Robertson, M. M. (2004). The neoliberalization of ecosystem services: wetland mitigation banking and problems in environmental governance. *Geoforum*, 35(3):361–373.

Robertson, S. et al. (2020). *Advancing the use of evolutionary considerations in spatial conservation planning*. PhD thesis, University of Salford.

Robinson, R. A. and Sutherland, W. J. (2002). Post-war changes in arable farming and biodiversity in great britain. *Journal of applied Ecology*, 39(1):157–176.

Ronce, O. (2007). How does it feel to be like a rolling stone? ten questions about dispersal evolution. *Annu. Rev. Ecol. Evol. Syst.*, 38:231–253.

Ronce, O. and Kirkpatrick, M. (2001). When sources become sinks: migrational meltdown in heterogeneous habitats. *Evolution*, 55(8):1520–1531.

Roques, L. (2013). *Modèles de réaction-diffusion pour l'écologie spatiale*. Editions Quae.

Roques, L., Auger-Rozenberg, M.-A., and Roques, A. (2008). Modelling the impact of an invasive insect via reaction-diffusion. *Math Biosci*, 216(1):47–55.

Roques, L. and Bonnefon, O. (2016). Modelling population dynamics in realistic landscapes with linear elements: A mechanistic-statistical reaction-diffusion approach. *PloS one*, 11(3):e0151217.

Roques, L., Desbiez, C., Berthier, K., Soubeyrand, S., Walker, E., Klein, E. K., Garnier, J., Moury, B., and Papaïx, J. (2021). Emerging strains of watermelon mosaic virus in south-eastern france: model-based estimation of the dates and places of introduction. *Scientific reports*, 11(1):1–11.

Roques, L., Garnier, J., Hamel, F., and Klein, E. K. (2012). Allee effect promotes diversity in traveling waves of colonization. *Proceedings of the National Academy of Sciences*, 109(23):8828–8833.

Roschewitz, I., Gabriel, D., Tscharntke, T., and Thies, C. (2005). The effects of landscape complexity on arable weed species diversity in organic and conventional farming. *Journal of applied ecology*, 42(5):873–882.

Rounsevell, M. D., Pedroli, B., Erb, K.-H., Gramberger, M., Busck, A. G., Haberl, H., Kristensen, S., Kuemmerle, T., Lavorel, S., Lindner, M., et al. (2012). Challenges for land system science. *Land use policy*, 29(4):899–910.

Royauté, R. and Pruitt, J. N. (2015). Varying predator personalities generates contrasting prey communities in an agroecosystem. *Ecology*, 96(11):2902–2911.

Rudolf, V. H. (2007). Consequences of stage-structured predators: Cannibalism, behavioral effects, and trophic cascades. *Ecology*, 88(12):2991–3003.

Rusch, A. ., Chaplin-Kramer, R. ., Gardiner, M. M. ., Hawro, V. ., and Holland, J. (2016). Agricultural landscape simplification reduces natural pest control: a quantitative synthesis. *Agriculture, Ecosystems & Environment*, 221:198–204.

Rusch, A., Valantin-Morison, M., Sarthou, J.-P., and Roger-Estrade, J. (2010). Biological control of insect pests in agroecosystems: effects of crop management, farming systems, and seminatural habitats at the landscape scale: a review. In *Advances in agronomy*, volume 109, pages 219–259. Elsevier.

Sabir, K., Opitz, T., Bonnefon, O., and Papaïx, J. (2018). Simulation of agricultural landscapes to study population dynamics of pest and auxiliary. Technical report, Biostatistique et Processus Spatiaux (UR 546, BioSP) INRA PACA, Avignon, France.

Saint-Geours, N. (2012). *Sensitivity analysis of spatial models: application to cost-benefit analysis of flood risk management plans*. PhD thesis.

Saloniemi, I. (1993). A coevolutionary predator-prey model with quantitative characters. *The American Naturalist*, 141(6):880–896.

Saltelli, A., Annoni, P., Azzini, I., Campolongo, F., Ratto, M., and Tarantola, S. (2010). Variance based sensitivity analysis of model output. Design and estimator for the total sensitivity index. *Computer Physics Communications*, 181:259–270.

Sánchez-Bayo, F. and Wyckhuys, K. A. (2019). Worldwide decline of the entomofauna: A review of its drivers. *Biological conservation*, 232:8–27.

Saura, S. and Martinez-Millan, J. (2000). Landscape patterns simulation with a modified random clusters method. *Landscape Ecology*, 15:661–678.

Schindler, S., von Wehrden, H., Poirazidis, K., Hochachka, W. M., Wrbka, T., and Kati, V. (2015). Performance of methods to select landscape metrics for modelling species richness. *Ecological Modelling*, 295:107–112.

Schmidt, M. H., Roschewitz, I., Thies, C., and Tscharntke, T. (2005). Differential effects of landscape and management on diversity and density of ground-dwelling farmland spiders. *Journal of Applied Ecology*, 42(2):281–287.

Schmitz, O. J. (1998). Direct and indirect effects of predation and predation risk in old-field interaction webs. *The American Naturalist*, 151(4):327–342.

Schmitz, O. J. (2007). Predator diversity and trophic interactions. *Ecology*, 88(10):2415–2426.

Schmitz, O. J., Buchkowski, R. W., Burghardt, K. T., and Donihue, C. M. (2015). Functional traits and trait-mediated interactions: connecting community-level interactions with ecosystem functioning. *Advances in Ecological Research*, 52:319–343.

Schmitz, O. J., Miller, J. R., Trainor, A. M., and Abrahms, B. (2017). Toward a community ecology of landscapes: predicting multiple predator–prey interactions across geographic space. *Ecology*, 98(9):2281–2292.

Schweiger, O., Musche, M., Bailey, D., Billeter, R., Diekötter, T., Hendrickx, F., Herzog, F., Liira, J., Maelfait, J.-P., Speelmans, M., et al. (2007). Functional richness of local hoverfly communities (diptera, syrphidae) in response to land use across temperate europe. *Oikos*, 116(3):461–472.

Sciaini, M., Fritsch, M., Scherer, C., and Simpkins, C. E. (2018). NLMR and landscapetools: An integrated environment for simulating and modifying neutral landscape models in R. *Methods in Ecology and Evolution*, 9(11):2240–2248.

Segoli, M. and Rosenheim, J. A. (2012). Should increasing the field size of monocultural crops be expected to exacerbate pest damage? *"Agriculture, Ecosystems and Environment"*, 150:38–44.

Shackelford, G., Steward, P. R., Benton, T. G., Kunin, W. E., Potts, S. G., Biesmeijer, J. C., and Sait, S. M. (2013). Comparison of pollinators and natural enemies: a meta-analysis of landscape and local effects on abundance and richness in crops. *Biological Reviews*, 88(4):1002–1021.

Shigesada, N. (1986). Traveling periodic waves in heterogeneous environments. *Theor. Popul. Biol.*, 30:143–160.

Shigesada, N. and Kawasaki, K. (1997). *Biological Invasions: Theory and Practice*. Oxford Series in Ecology and Evolution, Oxford: Oxford University Press.

Shine, R., Brown, G. P., and Phillips, B. L. (2011). An evolutionary process that assembles phenotypes through space rather than through time. *Proceedings of the National Academy of Sciences*, 108(14):5708–5711.

Simpson, T. W., Poplinski, J., Koch, P. N., and Allen, J. K. (2001). Metamodels for computer-based engineering design: survey and recommendations. *Engineering with computers*, 17(2):129–150.

Skellam, J. G. (1951). Random dispersal in theoretical populations. *Biometrika*, 38:196–218.

Snyder, W. E. (2019). Give predators a complement: conserving natural enemy biodiversity to improve biocontrol. *Biological control*, 135:73–82.

Sobol', I. M., Tarantola, S., Gatelli, D., Kucherenko, S. S., and Mauntz, W. (2007). Estimating the approximation error when fixing unessential factors in global sensitivity analysis. *Reliability Engineering and System Safety*, 92(7):957–960.

Sommer, N. R. and Schmitz, O. J. (2020). Differences in prey personality mediate trophic cascades. *Ecology and evolution*, 10(17):9538–9551.

Soriano-Redondo, A., Jones-Todd, C. M., Bearhop, S., Hilton, G. M., Lock, L., Stanbury, A., Votier, S. C., and Illian, J. B. (2019). Understanding species distribution in dynamic populations: A new approach using spatio-temporal point process models. *Ecography*, 42(6):1092–1102.

Soubeyrand, S., Laine, A.-L., Hanski, I., and Penttinen, A. (2009). Spatiotemporal structure of host-pathogen interactions in a metapopulation. *The American Naturalist*, 174(3):308–320.

Soubeyrand, S. and Roques, L. (2014). Parameter estimation for reaction-diffusion models of biological invasions. *Population ecology*, 56(2):427–434.

Start, D. and Gilbert, B. (2017). Predator personality structures prey communities and trophic cascades. *Ecology letters*, 20(3):366–374.

Steenman, A., Lehmann, A., and Lehmann, G. (2015). Life-history trade-off between macroptery and reproduction in the wing-dimorphic pygmy grasshopper tetrix subulata (orthoptera tetrigidae). *Ethology Ecology & Evolution*, 27(1):93–100.

Steffan-Dewenter, I., Münzenberg, U., Bürger, C., Thies, C., and Tscharntke, T. (2002). Scale-dependent effects of landscape context on three pollinator guilds. *Ecology*, 83(5):1421–1432.

Steinmann, K. P., Zhang, M., and Grant, J. A. (2011). Does use of pesticides known to harm natural enemies of spider mites (acari: Tetranychidae) result in increased number of miticide applications? an examination of california walnut orchards. *Journal of economic entomology*, 104(5):1496–1501.

Stoehr, J. (2017). A review on statistical inference methods for discrete Markov random fields. *arXiv preprint arXiv:1704.03331*.

Straubhaar, J., Renard, P., Mariethoz, G., Froidevaux, R., and Besson, O. (2011). An improved parallel multiple-point algorithm using a list approach. *Mathematical Geosciences*, 43(3):305–328.

Su, J., Liu, C., Hu, X., Xu, X., Guo, L., and Chen, W.-H. (2019). Spatio-temporal monitoring of wheat yellow rust using uav multispectral imagery. *Computers and electronics in agriculture*, 167:105035.

Szűcs, M., Vercken, E., Bitume, E. V., and Hufbauer, R. A. (2019). The implications of rapid eco-evolutionary processes for biological control-a review. *Entomologia Experimentalis et Applicata*, 167(7):598–615.

Tao, Y. (2010). Global existence of classical solutions to a predator–prey model with nonlinear prey-taxis. *Nonlinear Analysis: Real World Applications*, 11(3):2056–2064.

Thies, C. and Tscharntke, T. (1999). Landscape structure and biological control in agroecosystems. *Science*, 285(5429):893–895.

Tilman, D. (1996). Biodiversity: population versus ecosystem stability. *Ecology*, 77(2):350–363.

Tilman, D., Fargione, J., Wolff, B., D'antonio, C., Dobson, A., Howarth, R., Schindler, D., Schlesinger, W. H., Simberloff, D., and Swackhamer, D. (2001). Forecasting agriculturally driven global environmental change. *science*, 292(5515):281–284.

Travis, J. M. and Dytham, C. (2002). Dispersal evolution during invasions. *Evolutionary Ecology Research*, 4(8):1119–1129.

Tscharntke, T. (1992). Cascade effects among four trophic levels: bird predation on galls affects density-dependent parasitism. *Ecology*, 73(5):1689–1698.

Tscharntke, T., Bommarco, R., Clough, Y., Crist, T., Kleijn, D., Rand, T., Tylianakis, J., Van Nouhuys, S., and Vidal, S. (2007). Conservation biological control and enemy diversity on a landscape scale [erratum: 2008 may, v. 45, issue 2, p. 238-253.]. *Biological control: theory and application in pest management*.

Tscharntke, T., Clough, Y., Bhagwat, S. A., Buchori, D., Faust, H., Hertel, D., Hölscher, D., Juhrbandt, J., Kessler, M., Perfecto, I., et al. (2011). Multifunctional shade-tree management in tropical agroforestry landscapes–a review. *Journal of Applied Ecology*, 48(3):619–629.

Tscharntke, T., Clough, Y., Wanger, T. C., Jackson, L., Motzke, I., Perfecto, I., Vandermeer, J., and Whitbread, A. (2012). Global food security, biodiversity conservation and the future of agricultural intensification. *Biological Conservation*, 151:53–59.

Tscharntke, T., Karp, D. S., Chaplin-Kramer, R., Batáry, P., DeClerck, F., Gratton, C., Hunt, L., Ives, A., Jonsson, M., Larsen, A., et al. (2016a). When natural habitat fails to enhance biological pest control–five hypotheses. *Biological Conservation*, 204:449–458.

Tscharntke, T., Karp, D. S., Chaplin-Kramer, R., Batáry, P., Declerck, F., Gratton, C., Hunt, L., Ives, A., Jonsson, M., Larsen, A., Martin, E. A., Martínez-Salinas, A., Meehan, T. D., O'rourke, M., Poveda, K., Rosenheim, J. A., Rusch, A., Schellhorn, N., Wanger, T. C., Wratten, S., and Zhang, W. (2016b). When natural habitat fails to enhance biological pest control - Five hypotheses. *BIOC*.

Tscharntke, T., Klein, A. M., Kruess, A., Steffan-Dewenter, I., and Thies, C. (2005). Landscape perspectives on agricultural intensification and biodiversity - Ecosystem service management.

Tsimring, L. S., Levine, H., and Kessler, D. A. (1996). RNA virus evolution via a fitness-space model. *Physical review letters*, 76(23):4440–4443.

Turchin, P. (1998). *Quantitative Analysis of Movement: Measuring and Modeling Population Redistribution in Animals and Plants*. Sinauer, Sunderland, MA.

Turner, M. G. (1989). Landscape Ecology : The Effect of Pattern on Process Author (s): Monica Goigel Turner Published by : Annual Reviews Stable URL : http://www.jstor.org/stable/2097089 Linked references are available on JSTOR for this article : LANDSCAPE ECOLOGY : The Effe. *Annual Review of Ecology and Systematics*, 20:171–197.

Turner, M. G. (1990). Spatial and temporal analysis of landscape patterns. *Landscape ecology*, 4(1):21–30.

Turner, M. G., Gardner, R. H., O'neill, R. V., and O'Neill, R. V. (2001). *Landscape ecology in theory and practice*, volume 401. Springer.

Turner, M. G., Gardner, R. H., O'neill, R. V., and O'Neill, R. V. (2015). *Landscape ecology in theory and practice*, volume 401. Springer, 2 edition.

Urban, D. and Keitt, T. (2001). Landscape connectivity: a graph-theoretic perspective. *Ecology*, 82(5):1205–1218.

Urban, D. L., Minor, E. S., Treml, E. A., and Schick, R. S. (2009). Graph models of habitat mosaics. *Ecology letters*, 12(3):260–273.

Urban, M. C., Leibold, M. A., Amarasekare, P., De Meester, L., Gomulkiewicz, R., Hochberg, M. E., Klausmeier, C. A., Loeuille, N., De Mazancourt, C., Norberg, J., et al. (2008). The evolutionary ecology of metacommunities. *Trends in ecology & evolution*, 23(6):311–317.

Uuemaa, E., Antrop, M., Roosaare, J., Marja, R., and Mander, Ü. (2009). Landscape metrics and indices: an overview of their use in landscape research. *Living reviews in landscape research*, 3(1):1–28.

Van den Eynde, R., Van Leeuwen, T., and Haesaert, G. (2020). Identifying drivers of spatio-temporal dynamics in barley yellow dwarf virus epidemiology as a critical factor in disease control. *Pest management science*, 76(8):2548–2556.

Van Der Zanden, E. H., Verburg, P. H., and Mücher, C. A. (2013). Modelling the spatial distribution of linear landscape elements in europe. *Ecological Indicators*, 27:125–136.

van Lieshout, M. (2000). *Markov point processes and their applications*. World Scientific.

van Lieshout, M. N. M. (2019). *Theory of Spatial Statistics: A Concise Introduction*. CRC Press.

van Strien, M. J., Slager, C. T., de Vries, B., and Grêt-Regamey, A. (2016). An improved neutral landscape model for recreating real landscapes and generating landscape series for spatial ecological simulations. *Ecology and evolution*, 6(11):3808–3821.

Varin, C., Reid, N., and Firth, D. (2011). An overview of composite likelihood methods. *Statistica Sinica*, 21:5–42.

Veres, A., to biblio/Biocontrol/Veres2013.pdf Petit, S., Conord, C., and Lavigne, C. (2013). Does landscape composition affect pest abundance and their control by natural enemies? A review.

Vindenes, Y., Engen, S., and Sæther, B.-E. (2008). Individual heterogeneity in vital parameters and demographic stochasticity. *The American Naturalist*, 171(4):455–467.

Vira, B. and Adams, W. M. (2009). Ecosystem services and conservation strategy: beware the silver bullet. *Conservation Letters*, 2(4):158–162.

Wade, A. A., McKelvey, K. S., and Schwartz, M. K. (2015). Resistance-surface-based wildlife conservation connectivity modeling: Summary of efforts in the united states and guide for practitioners. *Gen. Tech. Rep. RMRS-GTR-333. Fort Collins, CO: US Department of Agriculture, Forest Service, Rocky Mountain Research Station. 93 p.*, 333.

Webb, C. O. (2000). Exploring the phylogenetic structure of ecological communities: an example for rain forest trees. *The American Naturalist*, 156(2):145–155.

White, L. A., Forester, J. D., and Craft, M. E. (2018a). Disease outbreak thresholds emerge from interactions between movement behavior, landscape structure, and epidemiology. *Proceedings of the National Academy of Sciences*, 115(28):7374–7379.

White, L. A., Forester, J. D., and Craft, M. E. (2018b). Dynamic, spatial models of parasite transmission in wildlife: Their structure, applications and remaining challenges. *Journal of Animal Ecology*, 87(3):559–580.

Whittaker, R. H. et al. (1970). *Communities and ecosystems.* Macmillan USA.

Wiegand, T., Moloney, K. A., Naves, J., and Knauer, F. (1999). Finding the missing link between landscape structure and population dynamics: a spatially explicit perspective. *The american naturalist*, 154(6):605–627.

Wiegand, T., Uriarte, M., Kraft, N. J., Shen, G., Wang, X., and He, F. (2017). Spatially explicit metrics of species diversity, functional diversity, and phylogenetic diversity: Insights into plant community assembly processes. *Annual Review of Ecology, Evolution, and Systematics*, 48:329–351.

Wiens, J. A. (2002). Central concepts and issues of landscape ecology. In *Applying landscape ecology in biological conservation*, pages 3–21. Springer.

Wiens, J. A., Chr, N., Van Horne, B., and Ims, R. A. (1993). Ecological mechanisms and landscape ecology. *Oikos*, pages 369–380.

Wilson, E. O. (1997). The diversity of life. *Journal of Leisure Research*, 29(4):476.

Winter, M., Devictor, V., and Schweiger, O. (2013). Phylogenetic diversity and nature conservation: where are we? *Trends in ecology & evolution*, 28(4):199–204.

Xia, J., van, der Werf, W., and Rabbinge, R. (1999). Influence of temperature on bionomics of cotton aphid, aphis gossypii, on cotton. *Entomologia Experimentalis et Applicata*, 90(1):25–35.

Xin, J. (2000). Front propagation in heterogeneous media. *SIAM Rev*, 42:161–230.

Zamberletti, P., Papaïx, J., Gabriel, E., and Opitz, T. (2020). Landscape allocation: stochastic generators and statistical inference. *arXiv preprint arXiv:2003.02155*.

Zamberletti, P., Papaïx, J., Gabriel, E., and Opitz, T. (2021a). Spatio-temporal point processes as meta-models for population dynamics in heterogeneous landscapes. *bioRxiv*.

Zamberletti, P., Sabir, K., Opitz, T., Bonnefon, O., Gabriel, E., and Papaïx, J. (2021b). More pests but less treatments: ambivalent effect of landscape complexity on conservation biological control. *bioRxiv, 10.1101/2021.03.19.436155*.

Zera, A. J. and Denno, R. F. (1997). Physiology and ecology of dispersal polymorphism in insects. *Annual review of entomology*, 42(1):207–230.

Zhang, W., Ricketts, T. H., Kremen, C., Carney, K., and Swinton, S. M. (2007). Ecosystem services and dis-services to agriculture. *Ecological economics*, 64(2):253–260.

Zhao, R., Wang, L., Zhang, H., Letters, J. S. S., and undefined 2013 (2013). Analysis on Temporal-Spatial Characteristics of Landscape Pattern of Land-Cover. *Sensor Letters*, 11:1337–1341.

Zhao, Z. H., Hui, C., He, D. H., and Li, B. L. (2015). Effects of agricultural intensification on ability of natural enemies to control aphids. *Scientific Reports*, 5(1):8024.

AVIGNON UNIVERSITÉ

THÈSE DE DOCTORAT D'AVIGNON UNIVERSITÉ

École Doctorale 536
Agrosciences et sciences

Mention de doctorat :
Biologie des populations et écologie

Unité Biostatistique et Processus Spatiaux (BioSP)- INRAE

Présentée par
Patrizia Zamberletti

ANNEX DE LA THÈSE :
STRUCTURE DU PAYSAGE AGRICOLE ET REGULATION DES RAVAGEURS

EFFET DE L'HÉTÉROGÉNÉITÉ SPATIALE DU PAYSAGE SUR LA DYNAMIQUE ÉCO-ÉVOLUTIVE D'UN SYSTÈME PRÉDATEUR-PROIE.

Biostatistique BIOSP & Processus Spatiaux INRAE

RÉGION SUD PROVENCE ALPES CÔTE D'AZUR

Manuscripts

- Poggi, S., Vinatier, F., Hannachi, M., Sanz Sanz, E., Rudi, G., Zamberletti, P., Philippe Tixier, P., & Julien Papaïx J. (2021). How can models foster the transition towards future agricultural landscapes. The Future of Agricultural Landscapes, Part II, 305. Pages: 2-65.
- Zamberletti, P., Papaïx, J., Gabriel, E., & Opitz, T. (2021). Markov random field models for vector-based representations of landscapes. Accepted by *Annals of Applied Statistics*. Pages: 66-89.
- Zamberletti, P., Sabir, K., Opitz, T., Bonnefon, O., Gabriel, E., & Papaïx, J. (2021). More pests but less treatments: ambivalent effect of landscape complexity on Conservation Biological Control. Submitted to *PLOS-Computational biology*. Pages 90-113.
- Zamberletti, P., Papaïx, J., Gabriel, E., & Opitz, T. (2021). Spatio-temporal point processes as meta-models for population dynamics in heterogeneous landscapes. Submitted to *Ecography*. Pages 114-136.
- Zamberletti, P., Roques, L., Lavigne, F., & Papaïx, J. (2021). On the evolutionary trade-off between growth and dispersal during a range expansion. To be submitted to *The American Naturalist*. Pages 137-169.

The supplementary information related to the articles can be found starting from page 170.

How can models foster the transition towards future agricultural landscapes?

Sylvain Poggi[a,*], Fabrice Vinatier[b], Mourad Hannachi[c], Esther Sanz Sanz[d,e], Gabrielle Rudi[b], Patrizia Zamberletti[f], Philippe Tixier[g], and Julien Papaïx[f]

[a]INRAE, Agrocampus Ouest, Université de Rennes, IGEPP, Le Rheu, France
[b]LISAH, Université de Montpellier, INRAE, IRD, Montpellier SupAgro, Montpellier, France
[c]INRAE, UMR SADAPT, AgroParisTech, Université Paris Saclay, Paris, France
[d]ZALF Leibniz Centre for Agricultural Landscape Research, Müncheberg, Germany
[e]INRAE, UR Ecodéveloppement, Avignon, France
[f]INRAE, UR BioSP, Avignon, France
[g]CIRAD, UR GECO, Université de Montpellier, Montpellier, France
[*]Corresponding author: e-mail address: sylvain.poggi@inrae.fr

Contents

Advances in Ecological Research
ISSN 0065-2504
https://doi.org/10.1016/bs.aecr.2020.11.004

Abstract

Modern agriculture faces the dual challenges of feeding a growing human population, while preserving natural resources and slowing current trends in climate change and its impacts. A deep understanding of the functioning of agricultural landscapes appears crucial if we are to move towards sustainable, complex and resilient agroecosystems. Modelling is a powerful tool to address these issues since it can inform these transformations by simulating the multiscale ecological flows and myriad interactions agroecosystems host, and the multilevel stakeholder actions and their feedbacks in landscapes. This chapter shows that models can provide guidance on the transition towards future multifunctional agricultural landscapes. We have focused on process-based models, which allow for a more thorough understanding of the underlying mechanisms and how these may be manipulated. We first examine how models can simulate the structure and the dynamics of agricultural landscapes, emphasizing the complex mosaic of urban, peri-urban, rural and seminatural habitats. Then, we consider the simulation of biotic and abiotic flows and their complex interactions in the mosaic habitats. Using formalisms from the social sciences, we integrate human decision-making and actions into the landscape models, thereby encompassing a major component in the landscape transformation process. Finally, we outline some avenues for future research. We have focused on improvements to landscape representation, and have suggested ways to bridge the gap between future landscape conception and manipulation, thus providing operational guidance for the transition towards future agricultural landscapes that achieve our objectives.

1. Introduction

1.1 Earth faces changes at an unprecedented pace

Our planet has undergone unparalleled change over the past three centuries. The impact of humans now competes with natural forces as a driver of planetary change, justifying the term 'Anthropocene' for the present, human-dominated, geological epoch (Crutzen, 2002). Very few places on Earth have not been affected by humans, either directly or indirectly (Vitousek, 1997). Supported by considerable mechanical and technological developments that rely on fossil–fuel-derived energy, humans have transformed landscapes worldwide and altered, potentially irrevocably, the ecological flows and myriad ecological interactions they host (With, 2019). In this context, landscape-scale models are useful tools to improve our knowledge and guide decision-making at spatial scales (typically 1–1000 km^2) on which

many ecological processes and linkages are manifest (Keane et al., 2015). Ongoing population growth—from 690 million in 1750 to 7.8 billion in 2020—and urbanization have resulted in the expansion of cities into the surrounding rural areas and the homogenisation of agricultural landscapes. Concomitant, intensification of farming practices (land consolidation, shortening of crop rotations, and selection of the most productive cultivars relying on agrichemicals to protect fields from pathogens and pests) has contributed to landscape simplification. Such changes were adopted in answer to the challenge of feeding the increasing world population, but at the expense of the environment as well as animal and human health (Foley, 2005; Rayfuse and Weisfelt, 2012; Tilman, 1999).

Some recent studies spotlight dramatic declines in biodiversity, species richness and abundance, e.g. birds and mammals (Hallmann et al., 2014; Spooner et al., 2018) and entomofauna (Hallmann et al., 2017; Seibold et al., 2019; Vogel, 2017). Sánchez-Bayo and Wyckhuys (2019) assessed and ordered the main drivers of species declines: habitat loss and land use change to intensive agriculture and urbanization; pollution, mainly by synthetic pesticides and fertilizers; biological factors, including pathogens and introduced species; and climate change. By 2050, agriculture will need to produce an additional 50% of food than in 2012 to meet the need of around 9.73 billion people (Armanda et al., 2019; FAO, 2018).

All these signs signal a need to transform the systems responsible for this situation, including farming systems that are responsible for 14.5% of all anthropogenic greenhouse gas emissions (Gerber et al., 2013), pollution of soils (Rodríguez Eugenio et al., 2018) and waters (Carpenter et al., 1998; Mateo-Sagasta et al., 2017), and biodiversity decline (Tilman, 2001; Tsiafouli et al., 2015). Such transformation will have to be multifaceted, since it will modify production systems, socioeconomic organization of labour, crop selection and agricultural practices, but also global diets and food waste.

1.2 Reorganizing farming areas towards a sustainable agriculture

Today, some 55% of the world's population lives in urban areas, and this percentage is rising. By 2050, with the urban population more than doubling its current size, nearly 7 in 10 people in the world will live in cities (World Bank, 2020). The rural agricultural land abandonment that this causes is the most frequent driver of landscape change in many regions of the world (Plieninger et al., 2016). Cities and their surrounding regions will be

challenged to plan and design their development in order to deliver green, inclusive, competitive and resilient services including food supply. In Europe, much of the distinction between rural and urban landscapes has lost because areas classified as peri-urban and characterized by complex landscapes are growing four times faster than urban areas. At this rate, the peri-urban area would double in around 40 years (Piorr et al., 2011). In exhibiting higher structural complexity, future peri-urban landscapes could lead to the formation of mosaics where agricultural, urban and seminatural habitats intermingle. Maintaining agriculture within these peri-urban mosaics will be an essential strategy for ensuring food security and mitigating climate change. This calls for a rethinking of food systems in a farm-to-fork approach linking farming systems to our modes of consumption. Models can foster this transition towards future sustainable complex landscapes by highlighting food production capacities that depend on the context of biotic/abiotic/anthropogenic interactions due to local heterogeneities and landscape structure, and support the design of new farming systems adapted to local conditions (Duru et al., 2015).

Seminatural habitats (composed by hedgerows, ditches and irrigation channels, ponds, grass strips, natural or artificial wetlands, etc.) are of great importance in rural and peri-urban landscapes because they are implicated in ecosystem services such as erosion limitation, water supply and flood regulation, pesticide and nutrient mitigation, weed and pest spreading regulation (Biggs et al., 2017; Burel, 1996; Dollinger et al., 2015; Le Cœur et al., 2002; Power, 2010). These ecosystem services, if supported, presents an opportunity to reduce our dependence on agricultural inputs (fertilizers, pesticides, irrigation water, etc.). Diversity and functional complementarities between species (Caron et al., 2014) is also a condition for the development of biodiversity-based agricultural landscapes, as well as resilience of ecosystems (Chapin et al., 2000).

For this sustainable future of farming, much research points to the importance of considering ecological scales in farming systems (Altieri and Nicholls, 2012). This implies an upscaling of decision and organization of management practices from the plot or farm levels to the landscape level (Elzen et al., 2012). Whereas the plot and the farm levels are driven by individual farmer decision making, managing the landscape is a challenge since it involves a collective decision-making process that includes interdependent stakeholders, including nonfarmers. The landscape can therefore be considered as a system whose properties emerge from its components (e.g. farms). Organizational, regulatory and technical innovations are needed to make agricultural landscapes more manageable (Hannachi and Martinet, 2019).

1.3 Modelling as a central tool to help design future agricultural landscapes

Designing future landscapes with higher complexity, resilience and manageability, requires a modified scientific approach. Transformations across scales cannot be informed by experiments alone, given the complexity of the system, the broad range of spatial scales and the multiple objectives that must be satisfied. Indeed, examples of projects of agricultural landscape redesign are rare (Geertsema et al., 2016; Kremen and Merenlender, 2018; Schulte et al., 2017).

Conversely, the wide variety of models that are available could be used to provide invaluable insight to guide the transformation of farming systems (Nendel and Zander, 2019) and the transition towards future agricultural landscapes. For instance, combining output from global climate models (Hayhoe et al., 2017) and species distribution models (Franklin (2010) and references therein) can predict the effects of environmental changes on species and ecosystems. Combining models that capture feedbacks between biophysical and socioeconomic drivers of land-use change, yet include at the small scale interactions with biodiversity, and at the large scale a model of the world economy, would make it possible to investigate the consequences of reaching equal global production gains by 2030, either by cropland expansion or intensification, and analyse their impacts on agricultural markets and biodiversity (Zabel et al., 2019). More generally, agricultural landscapes provide many ecosystem services (e.g. food production, regulation of water, regulation of greenhouse gases), thereby making it challenging to commit to transformative changes that improve one service without unintended consequences for the others. In that, multiobjective optimisation algorithms (Memmah et al., 2015; Todman et al., 2019) can be helpful, for instance in identifying trade-off frontiers.

Complexity and uncertainty are two cornerstones of modelling. Models allows the exploration of a set of scenarios as a way of exploring uncertainty. By incorporating knowledge from various disciplines (physics, chemistry, biology, ecology, economy, sociology, etc.), coupling components and considering interactions and feedbacks, models contribute to our comprehension of complexity. Here we use agricultural landscape models to tackle these issues of future agricultural landscape design. These tools, in simulating the landscape functioning, can help to inform decision-makers on possible trajectories towards objectives and search options set by "society". Building reliable tools requires a better coupling of landscape patterns and process models to account for feedbacks, integrate the decisions of multiple stakeholders, consider the spatial and temporal heterogeneity of data and processes,

explore alternative landscape organizations and assess multiobjective performance (Poggi et al., 2018). A myriad of technical issues arises when doing this coupling. These include uncertainties of evaluation, model parameter inference, data assimilation, etc. In this paper, we give insights on the added value, current development and limitations of such models to provide guidance on the transition towards future desirable landscapes. Where possible, we focus on process-based models that allow for a more thorough comprehension of the underlying processes at stake and provide our perspective of their beneficial use.

1.4 Chapter structure

In Section 2, we present some major drivers of the modifications of agricultural landscapes, notably urban expansion and sprawl, and highlight the relevance of modelling for forecasting this ongoing evolution. We assume that demographic pressure, demand for food, reduction of fossil energy dependence and environmental requirements will give rise to more complex agricultural landscapes, forming mosaics where contrasted habitat intermingle. In Section 3, we focus on the simulation of biotic and abiotic flows across agricultural landscapes, and the impacts of adding complexity in process-based models of these flows. In Section 4, we show how models can generate transformative knowledge for the design of future agricultural landscapes. We address this issue via insights from the social sciences (e.g. economy, geography), interdisciplinary modelling (notably between social and natural sciences), and transdisciplinary modelling (i.e. participatory modelling involving scientists and practitioners). In Section 5, we suggest some avenues for future research, identifying the need for multiscale and multilevel representations of agricultural landscapes, as well as their conception and their manipulation. Finally, in Section 6 we conclude this chapter with a key set of take-home messages for landscape modelling.

2. Are current models relevant to simulate the complexity of future agricultural landscapes?

The structure of a given landscape results from the accumulation of past changes (legacy effect) driven by multiscale forces (Houet et al., 2010). Given current trends, we assume that future landscapes will be more complex, with a strong intermingling between agricultural, seminatural and urban habitats. Thus, methods and tools that enable the simulation of these three types of land cover, and their interaction, are of major importance.

In this section, we first introduce a way to model the structure and dynamics of agricultural landscapes. We briefly review how urban expansion may be modelled and then focus on peri-urban areas which are likely to become ever more important with the increasing intermingling between agricultural and urban land uses, and discuss the inclusion of agriculture in cities. Finally, we introduce seminatural habitats into the landscape mix, and by recalling their impact on many ecological and physical processes, emphasize the caution that should be exercised when modelling these important habitats.

2.1 Current approaches to represent the agricultural landscape structure

Agricultural landscape models describe landscapes as mosaics of fields having shapes and properties that vary in space and time (Poggi et al., 2018). Different approaches have been proposed for generating landscapes with various structures (i.e. the spatial arrangement of land covers), and for studying biotic or abiotic processes (Langhammer et al., 2019). There are two complementary approaches, raster and vector representations, for modelling such mosaics, depending on the goal of the study and how their constitutive parts are handled (Bonhomme et al., 2017; Gaucherel et al., 2006b).

Most existing models use rasters to simulate cell mosaics (Engel et al., 2012; Gardner, 1999; Pe'er et al., 2013; Saura and Martínez-Millán, 2000; van Strien et al., 2016). The landscape is discrete and played out across a grid, where each grid cell is the smallest elementary spatial unit of the landscape and contains information about that unit of the landscape. Begg and Dye (2015) developed a modelling framework that couples a landscape mosaic generator and a population module to study the interactions between the population dynamics of several crop pests and the cropping system. Engel et al. (2012) designed simple landscape patterns composed by 15 crop types with varying crop proportions and mean field sizes. A more complex approach was developed by van Strien et al. (2016) who generated landscapes integrating different landscape metrics (e.g. number of patches, patch size, patch edge contrast), calculated at the field or class levels, which allowed for variation in the landscape configuration and composition. The raster-based (or grid-based) approach is particularly suited to the modelling of gradual landscape dynamics and continuous processes, due to the regular grid structure facilitating processes operating between contiguous cells.

Real agricultural landscapes display a patchy structure made of contiguous, irregular polygons delineated by rectilinear boundaries, some polygons having border structures such as hedgerows (Gaucherel, 2008), making the

vector-based approach appealing (Gaucherel et al., 2006a,b; Inkoom et al., 2017; Langhammer et al., 2019; Le Ber et al., 2009; Papaïx et al., 2014). For example, Gaucherel et al. (2006a,b) developed a model that simulates tessellated patches and borders structures. Le Ber et al. (2009) simulated agricultural landscapes defined by two different tessellations (Voronoi and rectangular), i.e., the cover of the Euclidian plan by a countable number of geometric shapes, and two types of cropping pattern distributions (random or stochastic). Papaïx et al. (2014) developed a simple landscape generator that generates the polygon landscape mosaic based on a T-tessellation algorithm developed by Kiêu et al. (2013). Tessellation models have the advantage of being parametric, meaning that a set of parameters control the main features of the simulated landscapes. In addition, these models are stochastic, producing collections of replicated virtual landscapes with similar landscape metrics (Papaïx et al., 2014). This allows testing of the robustness of the results to changes in residual landscape variability, as landscape ecological metrics are not sufficient statistically. However, it can prove difficult to reproduce fine grain spatial structures with such approaches as they do not capture the full complexity of landscapes nor do they provide realistic landscape patterns. Combining parametric with nonparametric approaches may enable this gap to be bridged (Straubhaar et al., 2011).

2.2 Spread of land uses mixing agricultural and urban covers

Urban expansion is an increasing global trend (World Bank, 2020). In Europe, peri-urban areas characterized by complex landscapes mixing agricultural and urban covers are growing rapidly. These new contexts call for the constraints and opportunities offered by urban and peri-urban settings to be explored for the purpose of developing future agricultural landscapes.

2.2.1 Simulating urban expansion

The simulation of urban land use within agricultural landscapes relies on an understanding and integration of biophysical and social perspectives (Verburg et al., 2010). The biophysical perspective sets the environmental conditions (e.g. climate, altitude) determining the global change processes. The social perspective encompasses at least the demographic development and rural–urban flows that depend on the territorial context.

The development of cities was initially simulated using a cellular automaton (CA), coupled to a geographical information system (GIS) to define the neighbourhood effects of various land uses (Couclelis, 1997). Subsequently, temporal dynamism was integrated into the CA model using stochastic

process models that describe how one state is likely to change to another state (Markovian models), given the transition probabilities between actual and future land use maps (Sang et al., 2011). Guan et al. (2011) stated that such Markov-CA modelling provides the most suitable approach to study the temporal and spatial dynamics of land use change. Various models have been proposed over the last 20 years: CA models (Barredo et al., 2003), Markov-CA models (Jokar Arsanjani et al., 2013), the Dyna-Clue model (Verburg and Overmars, 2009), the Spacelle (Dubos-Paillard et al., 2003) and Foresight models (Houet et al., 2016) with spatial resolutions spanning from 1 ha to 1 km^2. The main challenges for this modelling have been to take into account spatially explicit, environmental variables that constrain urban expansion in space (Fig. 1), and irregularities in temporal trends that affect transitions from current to future landscapes. In particular, model calibration requires comprehensive and accurate spatial and temporal datasets. Importantly, these modelling approaches do not consider the large number of current land uses or potential new uses, or the specifics of the peri-urban zone in the transition between dense urban and rural areas.

2.2.2 Modelling agriculture in complex peri-urban landscapes

Beyond the ongoing scientific debate about the use of the term peri-urban, its precise location, spatial extent and the definition of boundaries (Friedmann, 2016), peri-urban agriculture can be defined empirically as the farming performed in the space close to towns (FAO, 1999). A growing literature characterizes the dynamics of rural–urban areas using process-based models but these rarely focus on farming in peri-urban landscapes (Silveira et al., 2006). Statistical approaches have been applied at the patch scale to assess the transition probabilities of grid patches from one land-use category to another and notably the impact of urbanization in the land-use patch structure of peri-urban areas. These models are used to assess the loss of cultivated land, and the deterioration of the site conditions of unconverted peri-urban cultivated land due to the fragmentation induced by urban sprawl (Li et al., 2017; Pribadi and Pauleit, 2015). Agriculture in peri-urban landscapes is usually considered in terms of a distance from city-centres, as a distance-gradient inspired by the classical Von Thünen's conceptual model (Sinclair, 1967; Von Thünen, 1826). For Von Thünen, a theoretical agricultural society would be one in which agents live in a single settlement and use the surrounding area to produce essential and nonessential goods. The distance between urban settlements and the areas of agricultural production are therefore extremely important for the placement of these products. This approach has been used

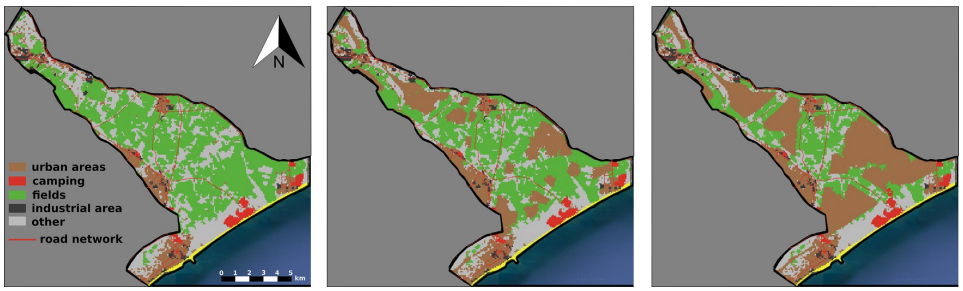

Fig. 1 Illustration of urban expansion (from left to right) in a river delta flowing into the Mediterranean Sea, as modelled with a cellular automaton using the NetLogo® platform. The urban areas (brown areas) are constrained by the distance to the road network (red lines) and the distance to the sea. Land uses derive from a study on the Lower Orb river fluvial plain by Saint-Geours et al. (2015).

in an agent-based simulation model to generate a wide range of agricultural landscapes (Macmillan and Huang, 2008). But, distance to a main urban settlement is, on its own, not sufficient to characterize agriculture in complex and multipolarized peri-urban landscapes, which are diverse, plural and dynamic (Sanz Sanz et al., 2017, 2016). Farming systems connected to cities are indeed characterized by a high degree of complexity related to anthropic developments as well as to the strategies of the different stakeholders (Zasada et al., 2013). This complexity is not integrated in the existing process-based agricultural landscapes generators (Langhammer et al., 2019). Furthermore, landscape change models operating at an aggregated level (including dynamic process-based simulation models) have not been used to predict changes in peri-urban agricultural land use such as intensification, because intensification is a function of the management of physical resources within the context of the prevailing social and economic drivers (Lambin et al., 2000).

Most attempts to evaluate spatial suitability of agriculture in peri-urban landscapes are partly based on qualitative approaches requiring thorough fieldwork associated with statistical and spatial analysis based on GIS (Thapa and Murayama, 2008). Farming systems shape agricultural landscapes, as observed by Rizzo et al. (2013), and thus every type of peri-urban agriculture has its "spatial signature". These are particular spatial structures whose arrangement is identifiable in space resulting in a set of common characteristics, such as crop plot shape, location of farmstead, border relation between farming and urban zones, etc. Complex peri-urban agriculture has recently been modelled by social scientists for the purpose of landscape planning and policy-making by using simple, predictive probabilistic models based on free available data. Sanz Sanz et al. (2018) classed peri-urban farming into spatial units of peri-urban agriculture (USAPU) and proposed a multivariate statistical modelling approach at the NUTS-3 level, that is a small region defined by the European Union for specific diagnoses and statistics (Box 1).

An alternative approach proposed by urban economists for small study areas has been to use peri-urban farm econometric location models based on exhaustive databases at the plot scale and often complex mathematical tools. Geniaux et al. (2011) developed a spatialized hedonic model to estimate land-use change using mixed geographically weighted regression (MGWR) techniques with a two-stage model that links agricultural and developable land markets.

2.2.3 Inclusion of agriculture in cities

Urban agriculture, which can be defined as the cultivation of crops and rearing of animals for food and other uses within cities (Mougeot, 2000), may

BOX 1

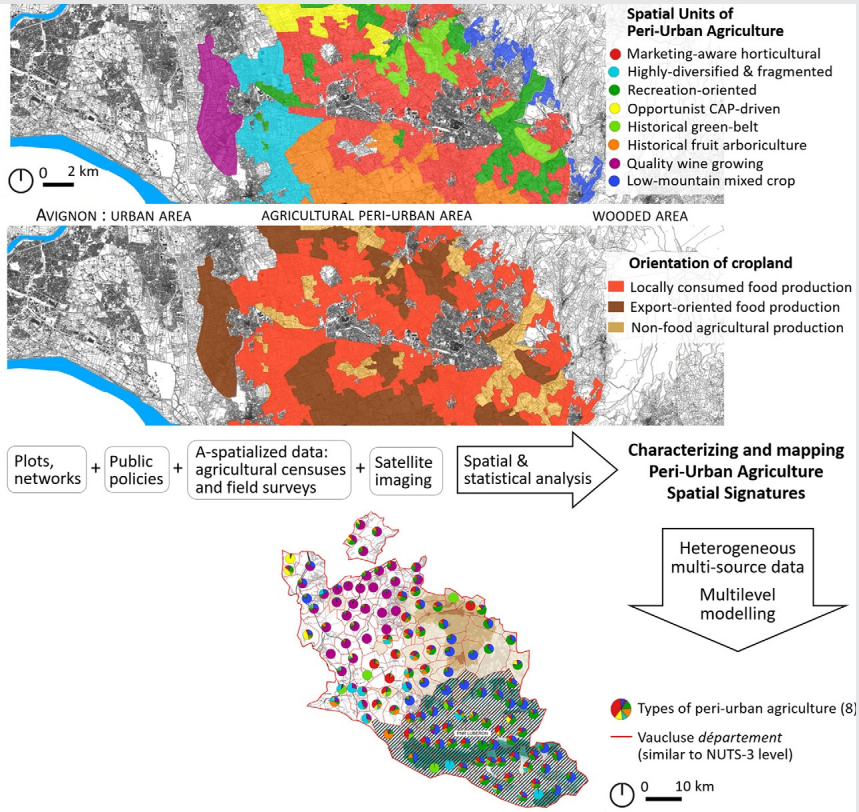

Operational modelling of peri-urban farmland in a Mediterranean context. Sanz Sanz et al. (2018) classified peri-urban farming into spatial signatures, referred to as spatial units of peri-urban agriculture, using a multivariate statistical approach. This was done using an in-depth analysis of a local case study in the Avignon, France, peri-urban area, involving surveys, on-site landscape reading, remote sensing analyses and interviews. The classification obtained from seven municipalities was subsequently used to train a fractional regression model, which was then tested on the rest of this French department (similar to NUTS-3 level; EC European Commission, 2018) to predict the presence and actual proportion of each spatial signature in the total agricultural land of each municipality (151 municipalities). They defined categories of municipality according to the distribution of spatial signatures that open perspectives for public action on peri-urban farming. While providing reliable predictions regarding peri-urban developments, this model proved to be simple and operational for collective decision-making on peri-urban planning. Incorporating this concept of spatial signatures in Markov-CA models (Guan et al., 2011) simulating urban expansion offers promising developments for the study of farming dynamics in the complex peri-urban areas of future landscapes.

lead to a second green revolution (Armanda et al., 2019). Despite being studied in many developing countries (Armanda et al., 2019; Dossa et al., 2011; Mawois et al., 2012), intraurban agriculture suffers from the lack of a modelling framework for elaborating spatiotemporal dynamics. This may be due to the divergence of spatial scales in land use change models (LUCC) between intraurban agriculture and traditional agriculture. In contrast to the relatively large-scale and long-term dynamics of traditional agriculture, intraurban agriculture acts at a local scale in space-confined cities, sometimes on vertically inclined surfaces such as building walls (Specht et al., 2014). Intraurban crops are also based on short cycles and with wide crop diversity (Mawois et al., 2012).

Nevertheless, it is necessary to simulate the spatial allocation of urban agriculture and its temporal dynamics. A potential avenue to explore is to create a specific LUCC model by combining the factors affecting spatial suitability of urban agriculture (Thapa and Murayama, 2008) and the leafy vegetables land use model (LYLU) developed by Mawois et al. (2012). The LUCC model estimates the surface area of each leafy vegetable that depends on plant specificities, amount of resources in the farm, and the sales channel for these products. In the future, such an approach combining LUCC and agronomic models should be able to guide decisions for the estimation of agricultural food supply in urban or peri-urban areas.

2.3 Considering the structure of seminatural habitats

Seminatural habitats have the potential to deliver bundles of desired ecosystem services because of their influence on the community ecology of crop pests and beneficial organisms (Bianchi et al., 2006; Burdon and Thrall, 2008; Chaplin-Kramer et al., 2011), on water flow regulation, soil loss mitigation or pollutant retention and degradation (Dollinger et al., 2015). The structure of seminatural habitats embedded in landscapes dominated by agricultural land can be highly variable. These can range from wild and cultivated elements being almost undistinguishable and intermeshed, such as in tropical agroforestry landscapes (Tscharntke et al., 2011), to being strongly separated such as in intensive monoculture landscapes, with the area and spatial distribution of remnant wildlands varying greatly (Fig. 2).

An enhanced diversity of land cover types, stemming from the inclusion of noncrop and nonmanaged areas of different patch sizes and shapes, can result in higher levels of complexity, both in terms of landscape composition and configuration (Perović et al., 2015). The boundary types (ecotones) and

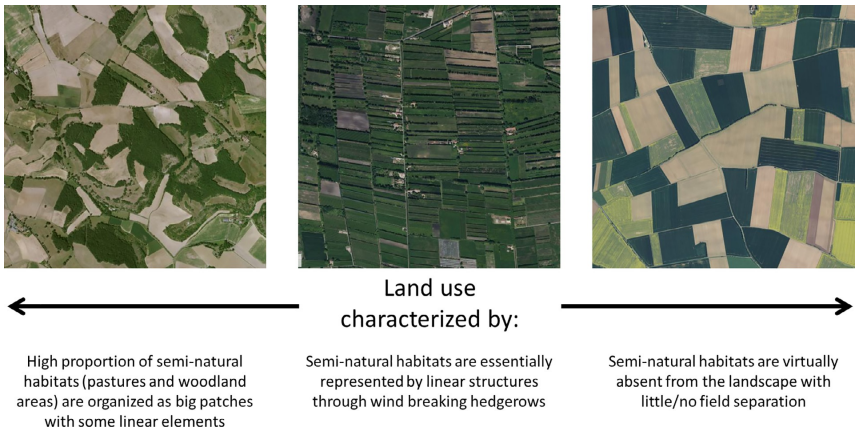

Fig. 2 Spatial structure of the agroecological interface across different farming systems. *Source: ©IGN.*

contrasts between patches affect the dispersal of species and the frequency and probability of colonization of neighbouring patches (Perović et al., 2015; Sattler et al., 2010). These different land cover types can contribute complementary resources during the life cycles of each species, thereby increasing species diversity and favouring complex trophic network relationships (Dunning et al., 1992; Massol et al., 2017; Perović et al., 2015; Philpott et al., 2020; Tscharntke et al., 2012). Seminatural habitat cover on farms is generally assessed by national maps to support the planning and implementation of agri-environmental policies meant for an accurate spatial targeting of biodiversity restoration and preservation (Sullivan et al., 2011). This approach relies on the integration of available datasets, GIS and remote sensing. Remote sensing techniques are very effective when there is a high contrast between neighbouring habitats, for instance to map scrub on seminatural grassland habitats in Ireland (Parr et al., 2006; Sullivan et al., 2011). Based on farm agronomic and economic data and farm practice surveys, broad scale land use classifications have been used to build indicators and identify areas of High Nature Value farmland in France (Pointereau et al., 2007), Belgium (Samoy et al., 2007) and Hungary (Belényesi et al., 2008). Sullivan et al. (2011) developed a model to investigate the relationships between the percent seminatural area and a number of variables that reflect surrounding landscape features and farm management practices. They estimated the likely distribution of hotspots or areas with high cover of seminatural habitats at a regional scale. The main drawbacks of these techniques is that they are site specific and depend on the availability and reliability of landscape data (Pointereau et al., 2007; Sullivan et al., 2011). We show in Section 2.3 that landscape models are appropriate tools to simulate the landscape mosaic composed of cultivated and seminatural patches and their interactions, thereby providing ways to study the relationships between landscape patterns and the landscape processes of interest.

Linear corridor, seminatural habitats, such as field boundaries (hedgerows or ditches), play a major role in the landscape because of their important impact on many agroecological processes. Such border structures should be modelled with care, though, due to their low-ground coverage and the spatiotemporal constraints that they can impose at the landscape scale. For example, Gaucherel et al. (2006a,b) used models based on Gibbs energy terms to control pairwise interactions between landscape elements and to simulate patches and certain border structures. Alternatively, multilayer network frameworks can be used to model the interactions between the different geometrical elements of the landscape (Box 2). In previous examples, the

BOX 2

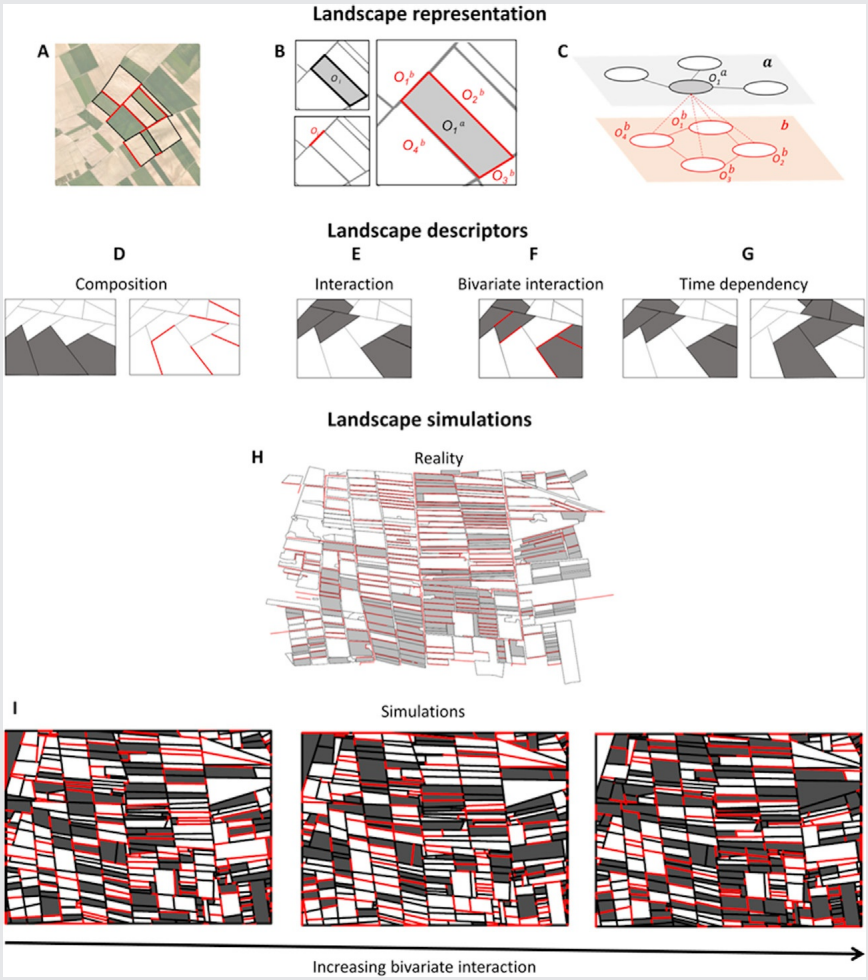

Illustration of a landscape stochastic generator and its parameter statistical inference. The landscape is represented as a collection of *n* geometric objects which can be of different types, such as polygons (i.e. habitat patches such as fields) or linear segments (i.e. linear landscape elements such as rivers or hedges), depicted in (A) and (B). Polygons can be of different categories such as crops, natural habitat, etc. Linear segments can be allocated with categories as single-species hedgerows, mixed-species hedgerows or no hedgerows. Spatial or functional relationships among landscape objects are captured by a graphical representation of the landscape. Interactions between objects are modelled through a

BOX 2—CONT'D

multilayer network (Boccaletti et al., 2014; Kivela et al., 2014), as shown in (C). Each layer corresponds to an object type, and each single-network layer represents the interactions among objects of the same type. Interactions between different network layers represent interactions between objects of the different types. Landscape descriptors (D-G) capture important landscape characteristics and features of both patches and linear elements. Typically, three groups of landscape descriptors are defined (Zamberletti et al., 2020): (i) composition metrics (D) correspond to the contributions of individual objects; (ii) spatial interaction metrics measure the interaction between two adjacent objects of the same type (E) or of different types (F); and, (iii) temporal metrics (G) assess the difference between configurations over two consecutive time steps. These descriptors can be incorporated in a probability measure describing the energy of the current configuration, i.e. a Gibbs energy function (Cressie, 2015; Van Lieshout, 2019), to infer parameters governing the real allocation and perform landscape simulations starting from a given parameter setting. Starting from a real landscape (H), simulations of landscape configurations can be performed using an iterative algorithm (Metropolis-Hastings algorithm) converging towards the stationary distribution of the target model (e.g. Descombes (2013)). The model generates virtual but realistic agricultural scenarios (I) featuring different spatial patterns (e.g. geometry, connectivity) and temporal patterns (e.g. crop rotation).

border structures are constrained by the polygonal meshing of the agricultural fields. However, seminatural habitats (e.g. watercourses) are more perennial imposing their location on agricultural elements. Vinatier and Chauvet (2017) therefore developed an interesting framework that they applied to the simulation of road networks. They proposed a hierarchical model based on successive interleavings of deformed networks, with the deformation being realized on the basis of a reverse Douglas–Peucker algorithm (Douglas and Peucker, 1973). This model could be adapted to account for external variables influencing the network of linear elements such as topography, wind direction, connectivity of habitat patches, etc.

Spatial-point seminatural habitats, such as trees, also deserve inclusion in models due to their potential role in the spread of organisms. For instance, Rossi et al. (2016) simulated the distribution of isolated trees in a landscape using an inhomogeneous Poisson point process model. Remarkably, they discovered that trees outside forests constituted the main source of landscape connectivity for the pine processionary moth, suggesting a potentially huge role in forest insect pest dispersal and invasive species expansion.

In the future, the debate regarding the notion of aggregation or fragmentation of the seminatural habitats within territories, i.e., the land-sparing vs land-sharing strategies (Fischer et al., 2008; Grass et al. , 2021; Mitchell et al., 2015), will continue. Neutral models as those presented above and those discussed in the Section 2.1 may inform this debate. Building such models to consider different landscape constraints may shed light on efficient designs of configurations of seminatural habitats for increasing the multifunctionality of agricultural landscapes.

3. Spatial flows and interactions across agricultural landscapes: Simulation of biotic–abiotic interrelations and trophic networks

For the representation of future agricultural landscapes, complex biotic and abiotic interactions deserve specific attention as many ecosystem services (e.g. erosion limitation, pest regulation) derive from these interactions (de Groot et al., 2010; Fisher et al., 2009). Processes underpinning these interactions can take place in fields or noncultivated areas (e.g. hedgerows, ditches, ponds, wetlands) and at the local or landscape scale (Power, 2010). Interestingly, a better understanding of these interactions may open ways of deploying nature-based solutions (Nesshöver et al., 2017; Rey et al., 2015), which could enhance the resilience of agricultural landscapes against extreme weather events, pest and disease outbreaks, and other anthropogenic stressors, and decrease their dependence on the use of agricultural inputs such as fertilizers and pesticides (Duru et al., 2015).

Here, we first address the modelling of spatial flows in complex landscapes. Then we present how interacting biotic and abiotic flows are currently modelled in agricultural landscapes, and we discuss concepts and models underpinning the simulation of multitrophic interactions in complex landscapes, notably useful to unravel the processes at stake in natural regulation of pests which is pivotal in an agroecosystem favouring biodiversity. Finally, we highlight current trends in measuring and calibrating models of spatial processes based on large spatiotemporal datasets.

3.1 Modelling spatial flows in complex landscapes

In landscapes characterized by a strong intermingling between seminatural habitats, crops and built areas (see Sections 2.2 and 2.3), modelling of spatial flows, such as the movements of individuals, particles, chemicals and fluids (wind, water), between those landscape elements is of primary importance

for a better understanding of landscape resilience. A variety of mathematical tools are available in ecology, such as in random walk models or stochastic differential equations at the scale of an individual for instance or reaction–diffusion models at the scale of a population, but their use in the context of complex environments may require further methodological developments (see Vinatier et al. (2013) for a review). Fluids, such as water and air, are generally considered as three-dimensional continua, characterized by density and velocity fields that vary in space and time. Modelling these fields and their related compartments (atmosphere, vegetation, soil surface, subsurface) at the landscape scale involves uniting approaches from several scientific disciplines, including ecology, and the earth and physical sciences. Except for very simple circumstances, these modelling approaches are not continuous and no general analytical solutions exist to solve the equations representing 3D flow processes (Singh and Woolhiser, 2002). Equations are derived from physical laws (e.g. Darcy laws) and involve parameters that could be measured in the field (e.g. hydraulic conductivity). Here, we present examples of spatial flow representation and modelling in agricultural landscapes in the cases of (i) physical processes and (ii) biological processes.

In landscapes in which increased complexity of geometrical structures stems from the introduction of numerous linear or point elements of significant height, such as hedgerows in bocage landscapes or trees in agroforestry systems, dispersal of airborne propagules may be profoundly affected by different airflows and turbulences between crops cultivated in open lands and crops surrounded by hedgerows or cultivated under shade trees. As an example, tree architecture and its interactions with microclimates may drive the dynamics of fungal diseases in crop fields (Motisi et al., 2019). Spatially explicit models for the simulation of turbulent flows within and above vegetation exist (Dupont and Brunet, 2008), and have already been applied to pollen dispersal (Dupont et al., 2006) and wind gust inside forests during windstorms (Dupont and Brunet, 2006), but their application to highly structured environments covering a large extent with varying height of linear elements remains challenging. The inclusion of hydrological infrastructures forming a high-density network within spatially explicit models also requires the development of specific models to handle the distribution of water within these infrastructures. The hydrological model MHYDAS (Moussa et al., 2002) and its application to a hydrological network on a hilly landscape opens interesting future avenues to explore. In flatter areas through which linear elements with higher flow rates circulate, e.g., streams or channels, hydraulic models are most suited (Baume et al., 2005; Brunner and Bonner, 1994).

Modelling dispersal of organisms and matter in landscapes comprising agroecological elements with specific geometrical properties (e.g. hedgerows, field borders) needs to be treated cautiously to avoid artefactual effects, such as might result from the incorrect estimation of population densities at the interface between elements. Hedgerow networks may act both as ecological corridors along which animal species disperse and as barriers to dispersal, in other circumstances. These source and sink structures for various organisms are classically modelled using spatially explicit models that consider position-dependent mobility and reproduction parameters, at individual and population scales. Depending on various factors such as the size of the population under study or the complexity in individual behaviour that it is necessary to consider, a wide range of mechanistic approaches can be used, from differential equation models to individual-based models (Bourhis et al., 2015; Preisler et al., 2013; Soubeyrand and Roques, 2014; Vinatier et al., 2011). In these models, space is either treated as continuous or as a discrete, regular grid (lattice). Grid-based population models can offer an efficient way to model dispersal because dispersal kernels are easily discretized on a regular lattice (Ricci et al., 2018; Slone, 2011). At the landscape scale (i.e. a large spatial extent), however, the limitations in the grid spatial resolution makes it difficult to consider elements with low grid coverage, such as linear or point elements. In contrast, Roques and Bonnefon (2016) developed a promising approach based on a system coupling two-dimensional (2D) and one-dimensional (1D) reaction-diffusion equations describing the population dynamics of surface and linear elements of the landscape. This approach proved particularly relevant when the presence of a corridor or a barrier (e.g. roads, rivers, hedgerows) significantly alters the model outcomes. Using the example of the range expansion of the tiger mosquito, *Aedes albopictus*, in metropolitan France, the 2D/1D approach provided a better fit and a higher predictive power than a classical 2D reaction-diffusion approach, outlining the importance of considering explicitly corridors such as the road network.

3.2 Simulation of biotic and abiotic interactions in complex landscapes

Simulating biotic-abiotic interrelations requires interdisciplinary approaches. Each discipline may have developed, independently, its own landscape modelling approaches, resulting in an unbalanced representation of biotic, abiotic processes depending on the core discipline of the modellers (Vinatier et al., 2016).

Despite some attempts to unify the biotic and abiotic processes in the same modelling framework (Vinatier et al., 2016), there remain a number

of model design, space-time and computational challenges to be met. We highlight these challenges using the functioning of a hydrological man-made network (noncoated ditches) in an agricultural watershed as a case study (Box 3). Ditches are both hot-spots of plant biodiversity and vectors of water flow transport in agricultural watersheds, thus giving rise to interactions

BOX 3

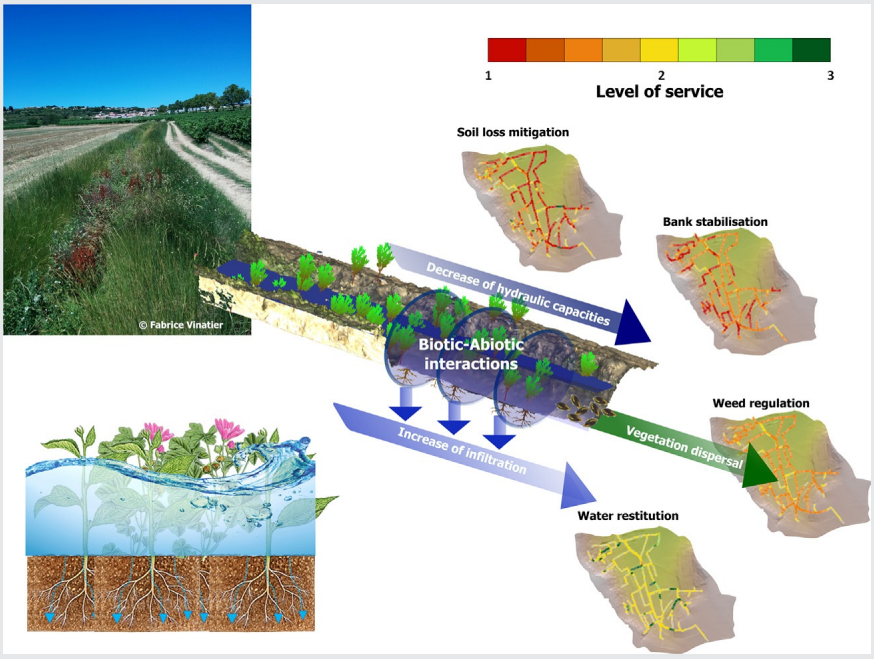

Example of a biotic-abiotic coupling using spatially explicit models. Rudi (2019) aimed to understand to which extent ditch management regimes influences ecohydraulic services provided by vegetation. An explicit representation of the hydraulic network provided by ditches in a Mediterranean watershed was proposed, with a focussed on the interactions between vegetation and water, sediments and plant propagules transport through hydrochory. Following continuum observation-experimentation-modelling, a spatially explicit model was developed at the grain of a ditch section and the extent of a small watershed, then applied to simulate indicators of service linked to water, weeds and soil regulation. The model, built on concepts from two contrasting disciplines, ecology and hydraulics, is expected to help design nature-based solutions on the basis of plant biodiversity for the regulation of water and soil resources.

whose comprehension relies on the multidisciplinary science of ecohydrology (Porporato and Rodriguez-Iturbe, 2002). In terms of model design, the simulation of the abiotic, water component, which drives the functioning of the hydrographical network, is carried out by assuming an Eulerian representation of the flows. In the Eulerian representation, water is modelled as a continuous quantity following mass conservation laws. In the case of vegetated ditches, the biotic components in direct interaction with the water flow, i.e., the plants and their propagules, are generally modelled as discrete elements by adopting an object-oriented Lagrangian representation. Integrating the biotic component (vegetation) in hydrological infrastructures used a trait-based approach (Merritt et al., 2010) that considers the whole plant community response to the flows as an aggregated property of the system, instead of considering the aggregation of individual plant-flow interactions. However, such trait-based approaches, although widely adopted in plant community ecology (Violle et al., 2007), has rarely been considered in terms of the specific traits of interacting with water flows and this will require a large sampling effort to establish the appropriate traits and their value for the wild plant species found in landscapes.

For the space–time challenge, the complex dynamics of biotic and abiotic components acting at different time scales require a coupled modelling of short, intense events (e.g. rainfall events and runoff) and more continuous processes (e.g. plant community selection and growth). In ecology and hydrology, there are a wide range of models for simulating rainfall and runoff events (see Moradkhani and Sorooshian (2008) for a review), and a diversity of models simulating weed community dynamics in agricultural landscapes (see, for example, Duru et al. (2009); Gardarin et al. (2012)) and riparian communities (García-Arias and Francés, 2016). These two types of models are not readily coupled because the response of vegetation to a series of disturbances is poorly understood, due to the lack of long-term monitoring (Blomqvist et al., 2009), a paucity of vegetation community response parameters and the difficulty of disentangling the underlying effects of hydrology and agricultural practices. This limited capacity to model vegetation response to disturbance impairs the inclusion of the effect of vegetation on pulsed fluxes of water due to uncertainties in our understanding of vegetation succession and development. Fine-scale ecohydraulic models simulating the interaction between a plant and a Eulerian flow do exist (Nepf, 2012), but their complexity entails high computational costs that hinder their use at the landscape scale.

The computational challenge would suggest that it is infeasible to model individual plant-flow interactions at the landscape level. We might,

however, use upscaling methods to scale-up from local observations/modelling/simulations to landscape simulations. High-frequency monitoring procedures could be used to define a phenomenological model of the structure–function relationship of the biotic system and its effect on abiotic processes at a local scale. To this end, several landscape elements (plots, hedgerows, ponds, etc.) were recently equipped with different sensors to measure all parameters characterizing the system. In vegetated ditches, biotic parameters have been monitored using drones to measure the spatial variability and evolution of plant cover porosity (Rudi et al., 2018; Vinatier et al., 2018). Abiotic parameters might also be assessed in controlled conditions in hydraulic flumes with different organizations of vegetation patches to measure the friction exerted by vegetation as a function of flow rates and water height (Vinatier et al., 2017). These parameters and metrics observed at a local scale could then be scaled-up for exploitation at the landscape scale (Box 3). Another way to meet the computational challenge would be to run several simulations of a fine-scale ecohydraulic model to produce a set of relations between biotic/abiotic parameters. The use of machine learning/artificial intelligence to detect, model and predict the structure–function response of the vegetation to flows opens promising perspectives to face the current numerical issues that slow and limit the exploration of these relationships.

3.3 Simulation of multitrophic interactions in complex landscapes

The simulation of interaction/trophic networks among living communities at the landscape scale remains a hard task (Tixier et al., 2013). Most recent advances were made using Bayesian network approaches (Häussler et al., 2020) or path analysis (Beduschi et al., 2015; Jacquot et al., 2019). It is particularly difficult because it encompasses both the interactions between species (or trophic groups) and their dispersal at multiple scales (from within the plot to the landscape scale or even the region). Unravelling these interactions is crucial because identifying the processes that lead to the natural regulation of pests and diseases are sorely needed in low-input agriculture (Macfadyen et al., 2009). In the diversified landscapes of the future, richer plant diversity will be deployed, from basic intercropping that mixes two cultivated species, via highly biodiversified patches inside or near the cultivated fields to large patches of natural or seminatural areas maintained in the landscapes (e.g. forest patches). We hypothesise that in areas with higher plant richness, trophic networks will become more complex. To date there are no multiscale and

multitrophic model able to address comprehensively the issue of optimizing the integration of plant biodiversity at all these scales in order to maximize the services supported by associated communities, and primarily the natural control of pests and diseases or the conservation of biodiversity.

Simulating trophic interactions across heterogeneous landscapes can be done with models based on the metacommunity concept (Leibold et al., 2004; Massol and Petit, 2013) that simulates interactions within and between the communities in distinct patches, e.g., cultivated fields or seminatural areas. If flows of individuals (e.g. beneficial predators spreading from diversified patches to cultivated fields) are well described, the metacommunity framework (Fig. 3A) is powerful to simulate the overall dynamic in patches and within the landscape. To date, metacommunity models have not yet been implemented on concrete cases to answer applied issues. The challenge for simulating innovative landscapes which include new patterns of plant

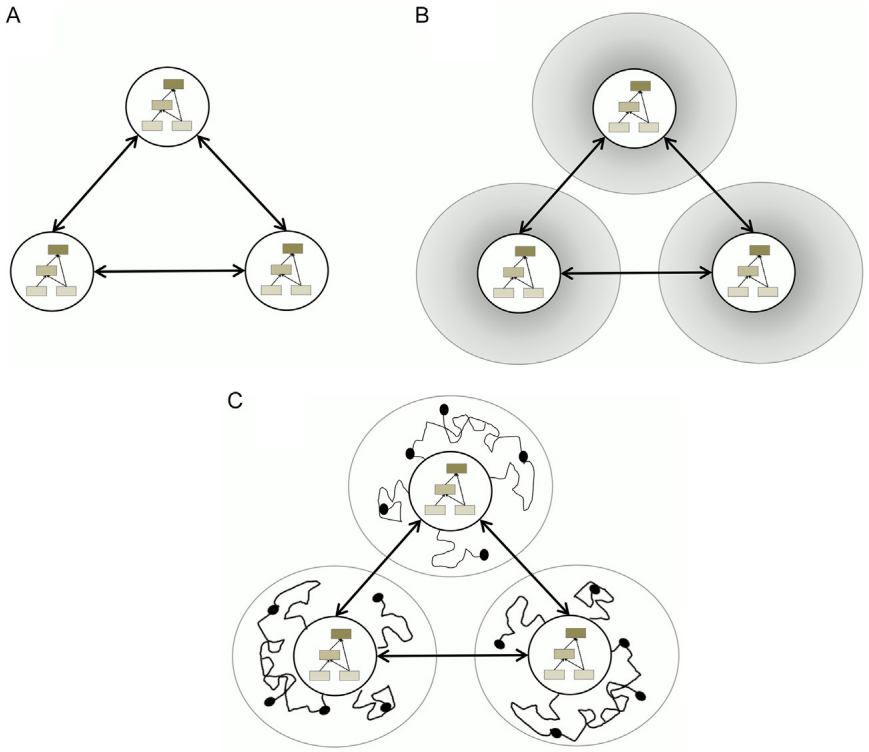

Fig. 3 (A) Classical metacommunity model (meta-food web: each community includes a food web model) as emphasized by Massol et al. (2011); (B) metacommunity model with foraging zones; and (C) metacommunity model with Individual Based Model in the foraging zone.

diversification around and inside cultivated fields is to tackle the issue of the zone of influence of these habitats and their potential as a sink for beneficial organisms. This could be achieved using spatially explicit models where each plant diversified patch has a surrounding "foraging zone" (Fig. 3B). The concept of foraging zone has more often been used in marine or mammal ecology to represent the area where animals can forage (Bailleul et al., 2007; Weimerskirch et al., 2009). In the case of natural enemies, this concept might be helpful for the prediction of the effect of each plant diversified patch on the regulation of pests in the surrounding cultivated fields. Foraging zones may be described using differential equation models or, alternatively, simulated using individual based models (Fig. 3C) which are particularly suitable to simulate species dispersal in heterogeneous environments (Collard et al., 2018). Another concept that could be used to rethink interactions between communities at the landscape scale are "island ecology" theories. This framework is particularly useful for considering the effect of the size of patches and their distance on immigration and extinction rates and finally on species composition of patches (Warren et al., 2015). Macarthur and Wilson (1967) stated that the diversity of islands could be formalized by a diversity-dependent dynamic balance between immigration and extinction. They assumed that the immigration rate for an island falls as the number of species on the island increases and that the rate of extinction of species increases as the number of species increases. Such island ecological concepts may prove useful for the study of plant-diversified patch-islands in a sea of homogeneous cropped land (landscape or field).

Whatever the approach, the parameterisation of metacommunity models is a crucial step towards designing of resilient agroecosystems. While metacommunity models have been extensively studied from the theoretical perspective, they have rarely been parameterized with real data. The difficulties of this are twofold. The first challenge consists in characterizing the dispersal of the most important species (pests, natural enemies, alternative preys), as data remain scarce. The knowledge of dispersal capacities as well as effect of landscape elements, especially barrier or corridors, are pivotal for optimizing the trade-off between the dispersal of beneficial communities and pests. The ongoing developments of monitoring tools, such as video tracking systems, and increases in the performance of signal or image processing using artificial intelligence, our knowledge regarding the dispersal of pests and other trophic groups will undoubtedly improve.

The parameterization of the interaction between trophic groups is the other challenge to take up in order to get realistic and useful food web

models. Recent technological advances of DNA metabarcoding approaches make possible unravelling trophic links between preys and predators (Mollot et al., 2014). These approaches are powerful as they uncover predator-prey consumption links that may be difficult to observe in the field, especially in arthropod communities. However, such methods are difficult to apply in a dynamic way. Another promising approach that could be particularly valuable for understanding community dynamics and identifying interactions is the combination of automated imagery in-field and artificial intelligence detection algorithms. The CORIGAN pipeline (Tresson et al., 2019) provides hierarchical classification of the detected species on pictures taken in the field, for example. Such approaches have the advantage of: (i) making in-field identifications of taxa at play in communities with a minimal disturbance; and, (ii) observing the dynamics of interactions between taxa. They may also enable the measurement of nontrophic interactions (avoidance, cooperation) that are believed to be important but are often not considered in the interpretation of food webs (Loreau and de Mazancourt, 2013; Ohgushi, 2008). Such nontrophic interactions could be particularly important at the edges between cultivated habitats and noncultivated habitats.

Although models will be key tools for designing the landscapes of the future, their relevance will depend on the quality of their parametrization. New methodological approaches for characterizing communities and their interactions represent a real opportunity to parameterize multiscale multitrophic models.

3.4 Measuring and calibrating spatial processes from large spatiotemporal datasets

Investing greater confidence in the spatiotemporal models discussed so far in this paper, will require that we collect data at multiple spatial and temporal scales, test the model simulations against this data and validate the model behaviours regarding variations in their inputs. In this subsection, we focus on the dispersal of organisms as an illustration of the variety of datasets that might be analysed.

Estimation of the dispersal capabilities of organisms is crucial for a consistent model of spatiotemporal dynamics. For organisms that disperse passively, an observed colonization event results from both a dispersal process and the subsequent survival, and it is often difficult to disentangle these processes. For organisms that disperse actively, the behaviour of individuals has to be considered in addition to dispersal and survival. In heterogeneous environments and in complex community structures, heterogeneity in survival

and modification of behavioural strategies can blur the estimation of actual dispersal. To cope with these difficulties, collecting high-resolution spatio-temporal data are essential, either by sampling populations at given locations or by tracking individuals. Citizen scientists have contributed millions of observations of species to databases over the past decade (e.g. Ries and Oberhauser (2015) or Tulloch et al. (2013)) and these provide invaluable sources of information for studies on genetics, trophic ecology, etc. These databases suffer, however, from a number of shortcomings and biases, as they often result from heterogeneous sampling protocols with unknown sampling efforts. Data from digital sensors are also now being collected at wide spatial scales, and these might in the future provide estimates of species dispersal as part of the era of Big Data. These digital data offer the advantage that they are documented, and they can be preserved for later species identity verification (Kays et al., 2020). Recent imagery and tracking systems (Dell et al., 2014; Hodgson et al., 2018; Kays et al., 2015; Steenweg et al., 2017), combined with new developments in machine learning (LeCun et al., 2015; Olsen et al., 2019; Wäldchen and Mäder, 2018), could provide data in real-time and at unprecedented resolution, that will prove invaluable for the study of habitat suitability, ecological interactions, impact of climate change, response to anthropogenic disturbance, effect of conservation policies, etc.

Inference of dispersal parameters from landscape models has to accommodate a diversity of data types (pest occurrence or abundance, crop phenology, agricultural practices, etc.), potentially collected at multiple temporal and spatial scales, some of them massive (Big Data from remote imagery or next-generation sequencing in the case of genetic studies), others possibly sporadic (e.g. field measurements, survey on technical operations), and generally giving access to a partial and indirect observation of the mechanisms under study. In this context, hierarchical modelling approaches offer a framework for parameter inference as it decomposes the model into multiple layers encompassing the set of parameters, the process at stake and the observation process (Cressie et al., 2009). It can cope with multiple, simultaneous observation processes, operating at different scales, and their related uncertainties and errors. The complexity of hierarchical models, however, can lead to models whose likelihood functions are analytically intractable and cannot be solved without the use of simulation or numerical approximation techniques. Hierarchical Bayesian frameworks are particularly convenient when dealing with heterogeneous data (Clark, 2004). These rely on specific estimation algorithms to infer parameters using Monte Carlo methods. We would note, however, that Monte Carlo methods generally require a large number of

iterations, making them difficult to use when the process model takes time to simulate. In that case, classical optimization tools could be more appropriate to find the parameters maximizing the likelihood function even if they render the computation of uncertainty around the estimated values difficult. In the particular case of Gaussian latent variables, the integrated nested Laplace approximation (INLA) approach is recommended (Illian et al., 2013). When compared with mathematical models, simulation models (e.g. individual-based models) offer the possibility of incorporating fine-scale and complex processes but can lead to intractable likelihood functions. Where this is the case, approximate Bayesian computation (ABC; Beaumont (2010)) and pattern-oriented modelling (POM; Grimm et al. (2005)) may be used to infer parameter values. These methods are based on intensive simulations of the model and the comparison of model outputs to data through summary statistics and a measure of quality of fit. Although these different methodologies provide interesting and powerful tools that help us to move from pure correlative data analysis to an integrative analysis explicitly introducing the underlying processes of interest, model complexity and parameter identifiability remain key issues.

Model exploration is classically performed through global sensitivity analysis. In the case of spatial models, however, this is challenging because of the complexity of integrating the landscape as an input factor and the consideration of spatial outputs. Spatial sensitivity analysis evaluates how models respond to landscape descriptors. These descriptors do not define a unique landscape but rather decompose landscape variability into a measurable and controllable component through quantitative variables and a residual variability. It is important therefore to build landscape replicates for each set of descriptors to perform a robust sensitivity analysis (Papaïx et al., 2014). In the literature, three strategies are described to deal with spatial outputs: mapping local sensitivity indices to study correlations with landscape characteristics (Saint-Geours et al., 2014); performing the sensitivity analysis on the components of a multivariate analysis (Lamboni et al., 2011); and, summarizing the spatial output as nonspatial output to use classical sensitivity analysis methods. Other methods to explore model outcomes use scenarios, i.e. a set of contrasting initial conditions and parameters. Landscape scenarios can encompass alternative landscape structures and land-use organizations to explore ways to increase sustainability. They can also help assess the effects of various political decisions, social or environmental contexts, and evolutions of landscape systems. Simulating scenarios provides a viable approach to anticipate the impact of changes on agricultural landscapes and to pinpoint potential pathways to be explored (Tieskens et al., 2017; Verburg et al., 2016).

A major challenge lies in the adoption of such results for policy applications, which essentially demands the correspondence of model output to real world data (Topping et al., 2013).

4. Learnings from social sciences on how landscape models can "transform" reality

"This is just a model!" is sometimes heard when landscape modelling is discussed with practitioners or policymakers. This sentence expresses a scepticism towards the social utility of modelling and a perception of models as rather hypothetical than proper knowledge. But is modelling really a vain thing for action and decision? Can we foster the capacity of models to generate usable and transformative knowledge for future agricultural landscapes? These questions can be addressed via a focus on social sciences insights. We first examine how landscape modelling is used in social sciences to generate knowledge and/or action (Section 4.1). We then use the performativity concept (a concept from social sciences that aims to understand how theory and knowledge can create or shape a new reality in the field) to analyse how modelling in general can foster the capacity to change the reality of landscapes (Section 4.2).

4.1 Landscape modelling in social sciences

Much research has been done in the social sciences and in interdisciplinary science incorporating the social sciences on the subject of landscape modelling. This research is often used by policymakers, practitioners and academics to identify and shape strategies and objectives for public action or to evaluate the state of progress and the incomes of measure implemented. While not claiming to be exhaustive, we identify three main types of landscape modelling involving social sciences according to their approaches and the ultimate aim of the model.

4.1.1 Comprehensive ex-post research on in situ drivers of landscape changes

A great deal of landscape modelling studies focuses on deciphering the trajectory of real landscapes (Benoît et al., 2012; Bieling et al., 2013; Hersperger and Bürgi, 2009; Mignolet et al., 2004; Mottet et al., 2006; Serra et al., 2008; Xiao et al., 2014). The approach is generally based on an analysis of the real landscape historical evolution in terms of land cover (Fuchs et al., 2015) and/or farming practices (Medley et al., 1995) with the aim of understanding

the socioecological drivers of landscape change. The drivers are commonly political (e.g. agricultural policy, subsides or regulations), economic (e.g. markets and commercialization opportunities), cultural (e.g. public attitudes, values and beliefs), technological (appearance and spread of new technologies for the use of natural resources or for cropping), and natural/spatial factors (e.g. soil characteristics, climate change, the spatial configuration of landscape patches).

The main added value of this type of landscape research is that it enables an improved understanding of the human and social mechanisms behind landscape change. It also enlightens us about the barriers to landscape change. These types of landscape research have shown that, except in the case of non-anthropogenic (i.e. wild ecosystems) and abandoned landscapes, there is never a single driver that operates alone to determine landscape change, but rather a combination of many different drivers that come into play (Bürgi et al., 2005; Plieninger et al., 2016). This characterizes the inevitable complexity of the landscape as an object of socioeconomic research and action.

4.1.2 Ex-ante research for in silico evaluation of scenarios or policy measures

Computational, in silico, research has been used to evaluate and simulate public policies or behavioural strategies in spatially explicit or simplified landscapes (Overmars et al., 2007). The approach is based on simulation models (Box 4) and typically evaluates the design of new instruments and strategies of landscape change (Martinet, 2013). It is important to note that increasingly research focusses on the combination of multiple and interconnected functions, measures and human practices within the landscapes (Groot et al., 2009). Such multifunctional landscape modelling research enables the visualization and comprehension of trade-offs between services (Box 4; see also for example co-viability theory (Béné and Doyen, 2008; Doyen and Martinet, 2012)), or ecosystem services (Rossing et al., 2007; Zander et al., 2008). These model-based policy evaluations also reveal possible barriers and impact inequalities of policies. For instance, Bareille et al. (2020) examined farmers' benefits from the coordinated landscape-scale management of biological control in a realistic, heterogeneous farmland landscape. Using an agronomic-ecologic-economic model, Bareille et al. (2020) simulated various strategies from no management to collective landscape-scale management, including situations of individual management. Their results show that if the coordinated management of biological

BOX 4

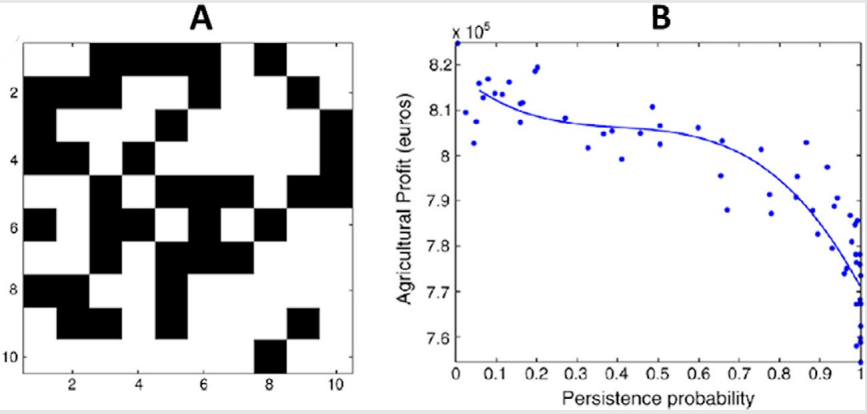

Effectiveness of public policies for biological conservation in dynamic agricultural landscapes. National or supranational entities (e.g. the European Union with the Common Agricultural Policy) invest significant funding to mitigate the environmental effects of intensive agriculture, calling in turn for an economic evaluation of such expenditure. In their theoretical study, Barraquand and Martinet (2011) developed a framework to examine the effect of monetary incentives on the probability of persistence of a metapopulation used as a proxy for biological conservation. They considered a dynamic mosaic landscape (A) composed of two land uses: grassland (white cells), assumed to favour the local population dynamics, and cropland (black cells), which has a negative effect on population growth. Their ecological-economic model links simulated farmers' behaviour (private land-use decisions in a context of agricultural output price volatility) to the biological population through the resulting dynamic landscape. A set of policy instruments were explored: incentives for implementing habitat favourable to biological conservation, in the form of subsidies to grassland, tax for practices unfavourable to biodiversity such as agricultural input, and their joint effect. Beyond cost-benefit analyses, the authors determined the production possibility frontier of the dynamic landscape in terms of agricultural profit and biological conservation (B), thus the expected trade-off between agricultural and ecological outcomes.

Figures from Barraquand, F., Martinet, V., 2011. Biological conservation in dynamic agricultural landscapes: effectiveness of public policies and trade-offs with agricultural production. Ecol. Econ. 70, 910–920. https://doi.org/10.1016/j.ecolecon.2010.12.019.

control at the landscape scale improves collective benefits, the heterogeneity of farms entails strong inequalities in terms of farmers benefit from the coordination process. In turn, farmers may reject the coordination policy unless specific measures support vulnerable farms.

The main added value of *ex ante* research is that it highlights conflicts, choices and trade-offs, thereby fosters a public decision for targetable strategies for the future. They are often used as an applied modelling exercise to help form decision-making and action. The limit of these modelling approaches, however, is that they generally focus on the state regulator as a key actor and on the subsidies or taxes as the levers for landscape change (Pascual and Perrings, 2007); they are top-down. Excluding many stakeholders in this way may limit the full understanding the drivers of landscape change. Indeed, studies have shown that local cooperatives and agri-production buyers, local agricultural input suppliers (Hannachi and Coléno, 2015), local extension services (Labarthe, 2009), and nonagricultural actors (Cardona, 2012) all have some power to change landscapes. Moreover, this diversity of stakeholders operates at different scales (Poggi et al., 2018). Thus, there is a need to consider, integrate and connect decisions and drivers from multiple stakeholders to make landscapes more "manageable", i.e., to enable the emergence of a multistakeholder's action that allows to collectively plan and control landscapes.

4.1.3 Collective transdisciplinary learning as a tool for the evaluation of future landscapes

Since the impact of the landscape socioecological phenomenon in question is in the hands of many independent land-holders, considering actions and management strategies under direct centralized control (top-down process) will be tricky without parallel changes in political systems. In such context, the focus should be on communication and education to increase the awareness of stakeholders' to their interdependence and their vision of the social costs and benefits of their actions. In this perspective, approaches for decision-making using multiagent systems, like Agent-Based Models (ABM), have flourished (Huber et al., 2018), as they offer an appropriate tool to study the interactions among agents and/or their environment. Agent-based models simulate the actions and interactions of acting agents (be they individuals or collective entities such as organizations or firms) with a view to assessing their effects on the system as a whole. They combine elements of game theory, complex systems, computational sociology and evolutionary programming. ABM can cope with numerous agents, each with an individual behaviour

or personality, that may interact via cooperation, coordination, competition and negotiation mechanisms. Such models enable the exploration of the effects of individual and collective actions on the environment, and can be seen as "bottom-up" models since they simulate emergent phenomena without any a priori assumptions regarding the local agents' cooperation and the aggregate system properties (Brown et al., 2016; Magliocca et al., 2015). The impact on the agents and the environment of management strategies can then be simulated and evaluated. This type of modelling is recognized as a methodology that facilitates collective learning. Therefore, many scientists call for a strong integration of stakeholders in the simulation process, e.g., via role-playing games (e.g. Becu et al. (2017)), and even in model conception through participative modelling (Farias et al., 2019; Le Page and Perrotton, 2017). This last option of incorporating various stakeholders at the conception and simulation steps, appears one of the better options for inducing socially optimal behaviour in the landscape, as it relies on a common understanding of the environmental issue between stakeholders, and not only on the responsiveness of farmers, consumers or any other stakeholder to the policy measures and actions.

It is generally accepted that the best decisions are made by those who will bear the consequences. It is axiomatic, therefore, that the more the agent-based modelling is participative, the more it may formalize and improve the knowledge of a system. Participatory models are particularly recognized for the production of shared and innovative solutions for a problem solving (Voinov and Bousquet, 2010), and thus they have a strong transformative potential for landscape change. Among the different participatory modelling approaches, companion modelling appears particularly suited to engender landscape reality changes (Etienne, 2014). Companion modelling is an approach combining ABM and role-playing games, advocating three major principles: construction of the model with stakeholders, transparency of the process and adaptiveness, with the model evolving as the problems change during the research. Companion modelling aims to support collective decision-making process in terms of sustainable landscape management (Box 5). It has been implemented in a diversity of landscape issues over the world, including management of the erosive runoff in Seine Maritime in France (Souchère et al., 2010), adaptation of extensive grazing strategies to climate change in Uruguay (Dieguez Cameroni et al., 2014), water resource management in Burkina Faso (Daré and Venot, 2018), forest and livestock management in the Larzac in France (Simon and Etienne, 2010). This approach relies on the formalization of a conceptual model based on iterative interactions between landscape stakeholders' representatives,

BOX 5

Application of companion modelling to conflict resolution and organizational innovations. Renewable natural resources at the landscape scale are often the subject of conflicts due to the lack of coordination between stakeholders and insufficient awareness of collective interdependency. It was the case in Lingmuteychu (Bhutan) where conflicts among villages and among farmers had arisen because of the stress for use of water in a rice terraces landscape, particularly during the highland rice transplanting period. The traditional way of working was upset by the adoption of new commercial crops that improved farmer income, but gave rise locally to disputes on the use of water as well as farmers food security issues. The Lingmuteychu watershed was chosen as an experimental site by the local Ministry of Agriculture to explore solutions to the conflict over water management (Gurung et al., 2006). The local deciders chose to use the companion modelling approach as a mediation tool between the nine villages involved. The initiative comprised two rounds. The first round (2003–2004) consisted of the design of a preliminary role-playing game on water sharing between two villages. To this end, surveys, focus groups and literature reviews were done to shape the social, hydrogeological and agricultural outline. This first game was used in many sessions to collectively understand and validate the way of decision making of various types of farmers and the collective consequences in each village and at the whole landscape level. The second round (2005–2006) consisted of the design of a new role-playing game that was more abstract and concerned seven stepped villages sharing water. This second role-playing game was used for many sessions involving differing village representatives according to various play modes in terms of communication (with and

BOX 5—CONT'D

without inter-village communication). This approach raised awareness of the importance of coordination among stakeholders. Along the game session collective debriefs, the players identified the information to share, and when and how to do it. Beyond the conflict resolution locally in Lingmuteychu, the companion modelling method induced the creation of an organizational innovation: a sub-catchment resource management committee where common action plan among villages are set and carried out. Moreover, this case study was used to draw up by-laws of the watershed committee and inspired other regions in Bhutan.

Photographs: ©Guy Trébuil (CIRAD).

scientific experts (notably on the natural or biophysical process) and modellers. This conceptual model combines shared representations among practitioners and researchers. Then, it is used to produce a serious game that is subsequently played with local stakeholders in game sessions. Here the model serves as an intermediary object, in the sense that it helps clarify and formalize the points of view and provide a discussion space. The collective discussion of the simulation that results enables support for a positive confrontation of the different points of view and the reality of the situations. As Skrimizea et al. (2020) argue, such collective learnings are key for the transformative changes required to ensure sustainability in agriculture.

4.2 How to foster the capacity of models to perform reality and change landscapes

But, how can these landscape modelling research impact the reality and drive future landscape change?

One response is that more the modelling research is participative and include stakeholders, the more it has the potential to change stakeholder behaviour, and thus to shape a change within the landscape (Voinov and Bousquet, 2010). Interactions between modellers and stakeholders and practitioners enable a better mutual understanding that can foster the interest of practitioners in the model outcomes. Moreover, a modelling design that includes stakeholders' perceptions, room for manoeuvre and information needs, is a design that is more likely to produce usable knowledge for practitioners and decision-makers.

But is nonparticipatory research and modelling able to change landscapes? The concept of performativity provides a potential response to this question. The concept of performativity stems from the works of Austin on language (Austin, 1962). Austin identified two kinds of utterances: the "constative" utterances, which can be predictive or descriptive and which can be true or false, and "performative" utterances, which have the intrinsic power to change social reality under certain circumstances, as for example, when a judge or a clergyman officiates at a marriage (Austin, 1962). Many researchers in social sciences extended the Austin conception to scientific theories to explore and understand how researchers can change the world via their utterances. According to this perspective, a theory is said to be performative when it contributes to a change in the reality it describes (Callon, 1998; Latour, 2005). Such thoughts and analyses have been applied to economic and financial markets theories (Callon, 1998; MacKenzie et al., 2007) and management theories (Cabantous and Gond, 2011; Muniesa, 2014). These researches have shown that social science theories have the potential to be performative, in that they can create the social reality they are supposed to describe and analyse. This concept of performativity offers a novel and interesting perspective to understand interactions between science and practice development. If we extend the concept of performativity to landscape modelling (which involves social sciences), the question is whether and how it can be performative even if it has been developed in academic contexts (i.e. without being a participative research).

According to Austin (1962), an utterance performs if some conditions, called "felicity conditions", are reached. Felicity conditions refer to the conditions that must be in place and the criteria that must be satisfied to induce and achieve the change in social reality. Many of these felicity conditions strongly relate to the speakers of the utterance and their status, and this makes it difficult to transpose all of them to theories or models. Some can be applied to theories and models, however, and here we attempt to extend them to landscape modelling researches. If we extend the concept of performativity and its felicity conditions to landscape modelling, a first felicity condition, inspired by Latour (1987), can be named as a tripod "generic-explicit-combinable". This condition means that, to perform, landscape modelling should be generic-enough so that it can be applied to management practices and fit in different landscape management or social contexts. In other words, if the model is too specific or linked to a very explicit landscape, this will limit the capacity of the model to influence or drive the reality.

But, the modelling needs also to be sufficiently explicit, otherwise it becomes too intangible and uninspiring for practitioners. Finally, the landscape modelling needs to be combinable so that its statements can be cumulated, aggregated or shuffled with other models and insights, and this can let the practitioners and/or policymakers to adapt and to test it in their contexts, even as it becomes complex.

The second felicity condition relates to theories' performativity. These researches show that a necessary condition of the performativity of a given theory is the existence of sociomaterial devices that embody the theory's assumptions (Callon, 1998; MacKenzie et al., 2007). Sociomaterial devices stands for dashboards, control panels or indicators, etc., i.e., operational devices that can be used in everyday life by practitioners and decision-makers and which may thus shape their routines. This means that to become performative, it is pivotal for landscape modelling research to be incorporated into devices used by landscapes' stakeholders. For example, to cope with the issue of controlling cross pollination between GMO and non-GMO corn crops, French farmers' cooperatives used GMO pollen dispersion models to create geographic information systems and decision systems allowing the management of farmers' production plans at the landscape scale (Hannachi and Coléno, 2015). These systems shaped the cooperatives marketing supply for farmers and allowed cooperatives to play a strategic role, ensuring a relevant spatial distribution of crops and appropriate harvest dates. This step of connecting researchers' models into practitioners' devices is a transdisciplinary issue that builds on the knowledge of multiple scientific disciplines (such as computer sciences, ergonomics, etc.) as well as practitioners' knowledge. This will be crucial for the performativity of landscape modelling. The third felicity condition for the performativity of landscapes modelling research is that the practitioners' devices that incorporate the landscape modelling research must be efficient (Muniesa, 2014). It means that they must provide relevant information on the relevant timeline to generate pertinent and efficient decisions enabling the practitioners to reach their objectives.

The extension of the performativity concept to landscape modelling provides some interesting insights. It leads to the identification of three felicity conditions under which we can increase the capacity of the landscape models to change the reality of landscapes. All these insights are hypotheses that need to be explored and tested but it addresses where landscape modelling research can be performative and drive landscape effective changes even where it has not produced intentional actionable knowledge.

5. Avenues for future research

In previous sections we have outlined the wide range of models available to represent and simulate the complex structure of landscapes (Section 2), to model the interacting biotic and abiotic flows within landscapes (Section 3), and to encompass social sciences to foster the use of models to generate knowledge and transformative actions (Section 4). In this section we suggest some avenues for future research.

5.1 Agricultural landscape representation and simulation

5.1.1 Enhancing a multilevel and integrated approach of landscape functioning

The understanding and management of landscapes should rely on a more systemic approach by considering multiscale biotic and abiotic processes and their interactions, multilevel stakeholder's decision-making and actions, feedbacks between processes and actions. Interestingly, the systemic approach considers explicitly properties that emerge from the interactions (competition, cooperation) between the system's components, which would not normally occur under the assumption that these components evolve independently.

At the same time, promoting a systemic approach should not distract us from the importance of the individual level since individual independence also provides key information regarding the functioning of agricultural landscapes. Dedeurwaerdere and Hannachi (2019), as an example, demonstrated that in a social organization characterized by an anarchy and nondialogue among farmers about rice seed choices in the Yuanyuang region of China. The independence of farmers fostered a strong autonomy of decision-making and nonconformism to pressure on the choice of rice seed. As a consequence, the local cultivated rice diversity was sufficiently large to achieve a sustainable control of rice diseases at the landscape level. Bareille et al. (2020) examined individual farmer and collective benefits from a landscape-scale management of biological control. Using an agronomic-ecologic-economic model of farm system constraints (e.g. allocation of land uses), the authors demonstrated that a landscape-scale management of biological control generates strong inequalities in terms of farmer benefits. These inequalities between individuals are a major cause of concern and conflict in landscape collective management that calls for a redistribution of subsidies or specific payment for the vulnerable farmers.

Thus, future research should enhance multilevel and integrated approaches of landscape functioning. The consideration of all possible processes and their interactions is not possible, however, because the complexity of the resulting model impedes a rigorous analysis of the outcomes. Therefore, despite previous research efforts, these approaches remain a challenge that will require a concerted research effort.

5.1.2 Refining the representation of the agricultural landscape structure

The representation of agricultural landscapes remains challenging, and deserves attention as there is plethora of evidence arguing for the effect of the landscape structure on key processes or phenomena at the core of agriculture sustainability. Among many examples, increasing the heterogeneity of the crop mosaic (crop diversity and mean field size) enhances multitrophic diversity (Sirami et al., 2019), landscape structure impacts agricultural pest suppression (Haan et al., 2020) and biological control in agroecosystems (Thies and Tscharntke, 1999). If large-scale patterns are now commonly integrated in landscape metrics and in models simulating virtual landscapes, fine-scale elements are generally not considered as they require a higher spatial resolution. However, such elements are important as they directly influence the local heterogeneity of the landscape.

The classic but still commonly used patch mosaic paradigm (Forman, 1995; Forman and Godron, 1986; Wiens et al., 1993) essentially adopts a human-centric view of landscapes, which are depicted as a mosaic of discrete, homogeneous cover types characterized by their composition and configuration. Such categorical conceptualisation fails to represent the continuous spatial heterogeneity and may result in the loss of information as most ecological attributes are inherently continuous in their spatial variation (e.g. soil properties, climate, and vegetation index). The gradient concept of landscape structure, as proposed by McGarigal and Cushman (2005), offers a more realistic representation of landscape heterogeneity where landscape structure is described by continuous surface characteristics without arbitrary land-use classification thus avoiding delineation of discrete areas with sharp boundaries (Lausch et al., 2015). Increasingly aerial and satellite data provide raw optical and radar multimodal time series of landscape images that can efficiently feed such continuous representations. A challenge consists in interpreting these images to quantify the properties of landscape elements. For instance, Betbeder et al. (2017) showed that synthetic aperture radar images enabled to estimate the resistance values associated with hedgerows

according to their suitability in terms of canopy cover and landscape grain for forest carabid beetles. Future research should produce metrics that characterize continuous surfaces, which could characterize interesting linkages between landscape representation (i.e. composition, configuration, connectivity) and ecological processes.

Landscapes may also be conceptualized using a graph-theoretical approach where habitat patches are represented by nodes and their functional connections are represented by edges (Urban and Keitt, 2001). Some developments in progress (Box 2) open promising avenues to generate virtual but realistic agricultural landscapes featuring different spatial patterns (geometry, connectivity) and temporal patterns (e.g. crop rotation), thus providing a useful tool to explore the relationships between landscape structure and processes at stake within it.

It is particularly complicated to access to the diversity, sequence and location of crop practices of agricultural landscapes (Leenhardt et al., 2010). Most studies aim at classifying subregions as homogeneous clusters based on datasets of crop practice sequences considering cropping systems as static (Dury et al., 2012). For example, Xiao et al. (2014) described the spatial distribution of crop sequences at a large regional scale mining crop sequences in land survey dataset with hidden Markov models and clustering based on the similarity of occurrence of crop sequences. Such approaches can help identify homogeneous zones in agricultural landscapes and study their characteristics. Conversely, Murgue et al. (2016) proposed an approach that consists in progressively hybridizing databases and local actors' and experts' knowledge to finely model the spatiotemporal distribution of cropping systems. All this, when combined, highlights the importance of defining a typology of crop practices and the need for databases describing fine scale crop practices.

Future research could consider a combination of the patch mosaic, gradient concept, and graph-theoretical paradigms to describe landscapes, as advocated by Frazier and Kedron (2017). Overall, the ultimate goal still consists of the development of an integrated representation of landscapes, accounting for the multiscale representation of system organization and control, and in which changes in the landscape pattern interrelate with the dynamics of the biophysical processes under study.

5.2 Landscape conception and manipulation

Across the different sections of this chapter, we have highlighted the wide range of landscape models that integrate biophysical processes and

stakeholders' views with different levels of complexity. In Fig. 4, we propose a classification of studies reported in the literature of landscape planning (*lato* sensu) according to two axes, without any claim for exhaustiveness but rather seeking to shed light on contrasted modelling approaches. The horizontal axis separates conceptual and theoretical studies from studies in which stakeholders are actively involved in the modelling process. The vertical axis separates studies oriented towards landscape conception (answering the question "which landscape is optimal or suboptimal with respect to given criteria?") from those focusing on landscape manipulation (answering the question "how to operate changes leading to a target landscape?"). From this simple typology we identify two main research perspectives that we present below: (i) moving towards a conceptualisation of landscape manipulation; and, (ii) reconciling theoretical approaches and stakeholders' involvement.

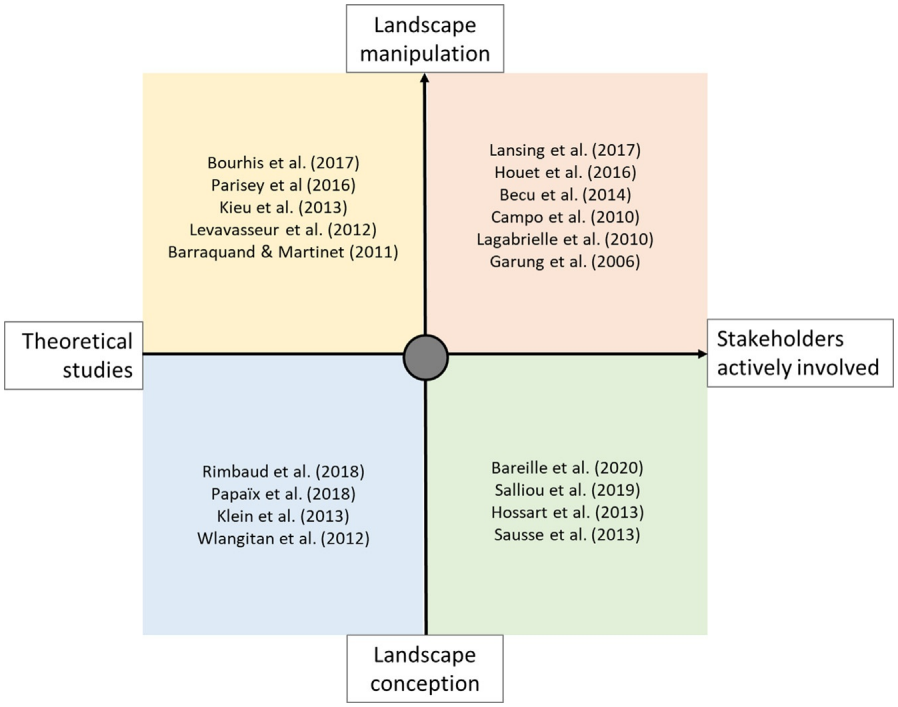

Fig. 4 Conceptual classification of landscape planning studies (*lato* sensu). Cited references provide examples of studies falling in different categories, without any claim for exhaustiveness.

5.2.1 Moving towards a conceptualisation of landscape manipulation

The conception of new landscape configurations relates to the definition of a spatial or spatiotemporal configuration of some landscape characteristics (e.g. crop diversity, structure of seminatural patches) that is considered as optimal or suboptimal with respect to a given, potentially multidimensional, criterion. The conception of new landscape configurations from theoretical approaches is generally based on two different approaches (landscape conception involving the participation of stakeholders is discussed later). The first approach consists in understanding how some landscape characteristics impact a given biophysical process. For example, Papaïx et al. (2018) and Rimbaud et al. (2018) developed a spatially explicit epidemiological model that described the demography and evolution of a pathogen population across a landscape composed of a mosaic of fields where different crop cultivars were grown. The goal of these studies was to understand how the spatiotemporal structure of cultivar deployment at the landscape scale modified the disease spread and the level of adaptation of the pathogen population on each crop cultivar, these measures having direct economic and ecological impacts through yield loss, resistance durability, and the use of pesticides. The key point here is that the analysis is performed globally over the parameter space leading to a general picture of how epidemics proceed in agricultural landscapes. The second approach relies on the optimisation of model outcomes over the landscape characteristics. Optimisation heuristics search for the best combinations of input landscape descriptors to meet multiple output criteria (Memmah et al., 2015). Klein et al. (2013) performed multiobjective regional optimisation for identifying optimum land management adaptations to climate change. Integrating a generic crop model and different climate scenarios they designed a multiobjective optimisation routine and identified conflicts between productivity and environmental goals. In a similar approach, Walangitan et al. (2012) analysed socioeconomic and ecological conflicts in the use of land resources of Lake Tondano (Indonesia).

Modelling approaches allowing the conception of new landscape configurations generally integrate complex outputs and detailed biophysical models. However, such approaches do not generate possible trajectories of a shift from a given landscape towards a more sustainable one. This dynamical aspect describing which trajectory could lead to the desired configuration is what we refer to as landscape manipulation (Fig. 4). Further theoretical and methodological developments are needed to better capture landscape dynamics (Houet et al., 2010) and identify relevant and feasible trajectories with their related costs. Some theoretical studies explicitly focus

on the dynamics describing which modifications have to be done to improve landscape performances regarding some specified outcome. Bourhis et al. (2017), see also Box 6, specifically addressed this issue based on a mechanistic model that fitted the traits of a theoretical flying insect pest. They investigated which modifications impacting the feeding and laying sites of the insect were relevant depending on the characteristics of the initial landscape. In the same way, Parisey et al. (2016) compared different landscape configurations built under agronomic constraints allowing them to propose rearrangements of landscapes that achieved a better biological regulation of weeds. Interestingly, in the specific context where landscapes are defined as a set of polygons forming a T-tessellation, Kiêu et al. (2013) demonstrated that it is theoretically possible to explore all landscape structures using only three geometrical operations modifying the shape of the fields. Another promising perspective to account for the landscape trajectory could be the use of models developed in evolutionary biology to describe the evolutionary trajectory of populations (e.g. Tenaillon (2014)). In these models, an individual is described by a set of phenotypic traits that determines its selective advantage (i.e. its fitness) in a given environment. Individuals can produce offspring that inherit their traits, but some modifications of these traits can occur through mutations. Thus, the population evolves through the mutation-selection balance. When applied to the context of landscape modification, different landscapes with different configurations represent individuals whose selective advantage can be evaluated through a set of criteria. The representation of the fitness landscape could help identify changes associated with elevated costs.

5.2.2 Reconciling theoretical approaches and stakeholders' implication

Fig. 4's horizontal axis shows that purely theoretical landscape studies, which might investigate the effects of spatiotemporal heterogeneities of landscape features on biophysical processes or socioeconomic outcomes, exist towards the extreme left of the abscissa. An example of this category is the work by Bourhis et al. (2017) who examined relevant landscape alterations in terms of minimizing the fitness of a crop pest. At the opposite end of the x-axis lie studies in which stakeholders play a central role in the landscape conception or transformation, including for example works from Hossard et al. (2013), Lagabrielle et al. (2010), Salliou et al. (2019) and Sausse et al. (2013). Lansing et al. (2017) provided a remarkable example showing that a self-organized cooperative management of rice terraces in Bali achieved a resilient system that both increased and equalized harvests. Naturally, there are studies along

BOX 6

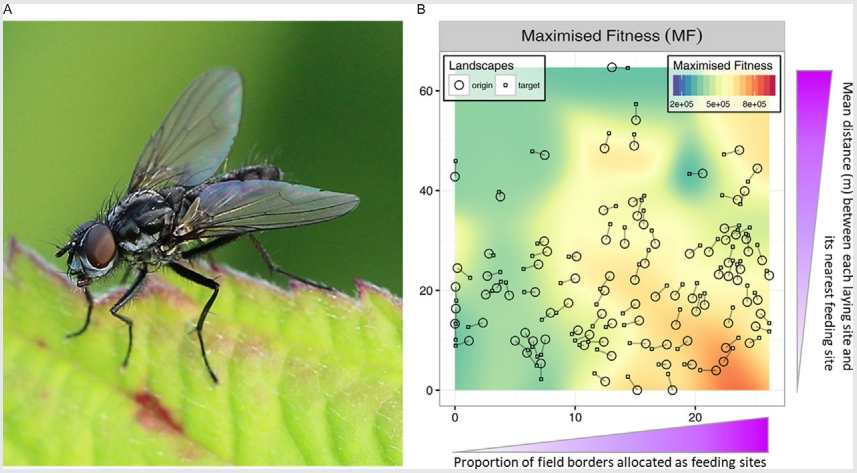

Illustration of a theoretical landscape planning problem. Bourhis et al. (2017) developed a model that made the strong and mechanistic link between the landscape structure and the population dynamics of flying insect pests (e.g. the cabbage root fly, Panel A) with an ability for high dispersal and directed flight. Foraging strategies hinged on the distribution of two competing resources (feeding and laying sites) affecting the pest's energy supply. Two landscape metrics described the competing resources spatial co-occurrence: the interface length (IL) which described the proportion of field borders allocated as feeding sites, and the Euclidean nearest neighbour (ENN) which measured the mean distance between each laying site and its nearest feeding site. A wide variety of landscapes was generated to explore the metric space (IL, ENN). The maximized fitness (MF) of the pest population measured the favourability of each landscape in terms of reproduction success. (Panel B) displays 94 original landscapes (circles) with the corresponding optimized values of fitness (MF) and their interpolated surface (background colormap). The interpolated surface allows an informed navigation in the metric space, in which the landscapes can be relocated to become more suppressive regarding pests. Assuming restrictive constraints, such as a constant landscape composition and using the field crop (laying sites) rotation as a single mechanism for change in the landscape, target selection for landscape modification are displayed (squares). This approach demonstrates the potential of landscape pest modelling for solving theoretical landscape planning problems.

Photo from https://commons.wikimedia.org/wiki/File:Delia_radicum_01.JPG (retrieved on 30-18-2020) licensed under the Creative Commons Attribution-Share Alike 4.0 International licence. *Panel B adapted from Bourhis, Y., Poggi, S., Mammeri, Y., Le Cointe, R., Cortesero, A.-M., Parisey, N., 2017. Foraging as the landscape grip for population dynamics—a mechanistic model applied to crop protection. Ecol. Model. 354, 26–36. https://doi.org/10.1016/j.ecolmodel.2017.03.005.*

the gradient of this axis. Theoretical studies can account implicitly for stakeholders, for example by formalizing policies such as incentives and taxation at the national or supranational (e.g. European) scale (Barraquand and Martinet, 2011). At a finer scale, in their study on farmers' benefits from the coordinated landscape-scale management of biological control in a realistic landscape with heterogeneous farms, Bareille et al. (2020) considered two realistic farm systems ("swine" and "cattle") with specific crop-allocation rules that were calibrated based on interviews with farmers. However, additionally to ongoing research, we advocate for a better mix between theoretical studies and those involving stakeholders.

Pure conceptual or theoretical approaches are essential to explore the relevance of landscape structures regardless of social and economic constraints, as they can potentially bring innovations that were not accessible without isolation from the specific context. But farmers and other landscape stakeholders (e.g. cooperatives, local extension services, local environmental associations, water catchment managers) demand increasingly to play an active role in planning and decision-making that affect them, their communities and the agricultural landscapes they inhabit. They are also increasingly aware of their own capabilities to provide inputs to planning processes, including models (Voinov et al., 2016). Moreover, it is generally agreed that better decisions are implemented with less conflict and more success when they are driven by stakeholders. Consideration of stakeholders can be done at various levels of integration. Stakeholders can either be involved in the conception of the systems' dynamics, or in the assessment of a set of empirical rules describing agent behaviour (Becu et al., 2014). Elsewhere, they can be involved in participatory modelling, contributing to the model design, the construction of scenarios to be simulated and the analysis and discussion of model outcomes. Participatory Companion Modelling (see Section 4.1.3 and Box 5), has successfully been applied to natural resource management issues in spatial entities ranging from the village to the small watershed involving multilevel stakeholders (Campo et al., 2010; Etienne, 2014).

Another challenge in reconciling theoretical approaches and stakeholder involvement stems from the complexity of models. Excessive computation time may limit the exploration of scenarios or impede any direct interaction with stakeholders who are themselves involved in process with a different time frame. This issue opens up possible uses for meta-modelling to convert overly complex models into simpler ones, while preserving the functional link between model inputs and outcomes but markedly improving simulation times and costs; facilitating a wider exploration of the variable space and greater stakeholder involvement.

6. Conclusion

Factors including human population growth, urban sprawl, dependency on modern agriculture and on chemical inputs, and its subsequent impacts on the health and the environment, make it challenging to feed humankind while preserving natural resources and slowing current trends in climate change and its effects. In this context, the understanding and management of landscapes is of utmost importance, as it has become vital to shift towards sustainable agricultural landscapes. Transformative changes are necessary to meet these challenges, and providing solutions to the trade-offs in the many functions provided by agricultural landscapes (e.g. food production, biodiversity conservation, soil loss mitigation) and that underpin ecosystem services.

In this chapter, we have shown that a wide range of modelling approaches can be used to anticipate and simulate the complexity of future agricultural landscapes. Where possible, we have outlined how spatially explicit and mechanistic models address future landscape construction, shedding light on agriculture in expanding cities as well as in rural-urban areas (Box 1). Assuming an increasing complexity of landscapes, characterized by a highly intricate structure, we have illustrated (Box 2) how models can capture aspects of agricultural landscapes and generate virtual but realistic simulations featuring different spatial (e.g. geometry, connectivity) and temporal patterns (e.g. crop rotation).

However, the design of agricultural landscapes faces a daunting prospect: a myriad of processes and their interactions are in play. Inevitably, modelling spatial flows across complex landscapes is challenging, but it is also an essential step towards the design of resilient landscapes. We have attempted to give an overview of the main issues when modelling and simulating biotic and abiotic flows, as well as multitrophic interactions, in complex landscapes. We used the functioning of ditch networks in agricultural watershed as a case study (Box 3) to advocate for the reinforcement of multidisciplinary sciences.

The transition towards future agricultural landscapes puts landscape stakeholders centre stage. However, the multiplicity of stakeholder actors (individual farmers, agricultural cooperatives, local and national regulators, estate owners, etc.) that shape the landscape and whose decision-making are influenced by the landscape patterns, and also who operates at which spatial and temporal scale, presents considerable problems of model formulation.

We presented some contrasted examples of formalisms to integrate human actions and decisions in landscape models. Theoretical models and their simulations consider stakeholders implicitly and address questions such as the evaluation of policies (Box 4), other models actively involve landscape stakeholders to solve natural resource management conflicts and promote institutional innovations (Box 5). The level of model genericity or territory-specificity should be adjusted to the research and action objectives. Independently, we question to which extent the concept of performativity might provide interesting insights on how the research in landscape modelling could drive effective changes in the reality of landscapes even if it has not produced intentional actionable knowledge.

Agricultural landscapes are highly complex systems for which modelling appears an inescapable tool in the toolkit required to provide guidance on their future conception and manipulation. Models open up many possible lines of research. Landscape representation, in models, may lead to further conceptualisation as technological developments (e.g. high throughput data from satellites or drones) and precision agriculture bring increasing information. In terms of landscape conception, building bridges between disciplines underpinning agricultural landscape modelling (e.g. agronomy, geography, ecology, economy and computer science) becomes pivotal. Regarding landscape manipulation, research remains rare, and while we identified some studies showing potential for solving theoretical landscape planning issues (Fig. 4, Box 6), we also pinpointed gaps in the identification of future trajectories—or sequences of landscape modifications—enabling a shift from current agricultural landscapes to novel and more sustainable ones.

While we only briefly addressed landscape resilience, it is an issue that will increasingly become important for future research. Over the past decades, and notably in the last few years, major disturbances (bushfire, drought, flooding, pest outbreak, pandemics) have occurred and caused dramatic damage. Landscapes, more than ever, need be resilient to such disturbance. But, this also calls into question the capacity of models to accommodate perturbations and disruptions, because it exacerbates problems of model complexity and tractability.

The transition towards future agricultural landscapes represents a formidable challenge for scientists of many disciplines and for practitioners. It will require a sharing of the overarching goal to design landscapes that serve both nature and people, and we would argue that landscape modelling has a central role in this goal.

Acknowledgements

S.P., F.V., and J.P. thank the PAYOTE scientific network funded by the French National Research Institute for Agriculture, Food and Environment (INRAE) for fruitful discussions. F.V. and G.R. thank Marc Voltz for his assistance in the redaction of Section 3.1 of this manuscript.

References

Altieri, M.A., Nicholls, C.I., 2012. Agroecology scaling up for food sovereignty and resiliency. In: Lichtfouse, E. (Ed.), Sustainable Agriculture Reviews. Springer Netherlands, Dordrecht, pp. 1–29. https://doi.org/10.1007/978-94-007-5449-2_1.

Armanda, D.T., Guinée, J.B., Tukker, A., 2019. The second green revolution: innovative urban agriculture's contribution to food security and sustainability—a review. Glob. Food Secur. 22, 13–24. https://doi.org/10.1016/j.gfs.2019.08.002.

Austin, J.L., 1962. How to Do Things with Words. Harvard University Press. ed, Cambridge (MA).

Bailleul, F., Charrassin, J.-B., Monestiez, P., Roquet, F., Biuw, M., Guinet, C., 2007. Successful foraging zones of southern elephant seals from the Kerguelen Islands in relation to oceanographic conditions. Philos. Trans. R. Soc. B Biol. Sci. 362, 2169–2181. https://doi.org/10.1098/rstb.2007.2109.

Bareille, F., Boussard, H., Thenail, C., 2020. Productive ecosystem services and collective management: lessons from a realistic landscape model. Ecol. Econ. 169, 106482. https://doi.org/10.1016/j.ecolecon.2019.106482.

Barraquand, F., Martinet, V., 2011. Biological conservation in dynamic agricultural landscapes: effectiveness of public policies and trade-offs with agricultural production. Ecol. Econ. 70, 910–920. https://doi.org/10.1016/j.ecolecon.2010.12.019.

Barredo, J.I., Kasanko, M., McCormick, N., Lavalle, C., 2003. Modelling dynamic spatial processes: simulation of urban future scenarios through cellular automata. Landsc. Urban Plan. 64, 145–160. https://doi.org/10.1016/S0169-2046(02)00218-9.

Baume, J.P., Malaterre, P.O., Belaud, G., Le Guennec, B., 2005. SIC: a 1D hydrodynamic model for river and Irrigation canal modeling and regulation. Métod. Numér. Em Recur. Hidr. 7.

Beaumont, M.A., 2010. Approximate Bayesian computation in evolution and ecology. Annu. Rev. Ecol. Evol. Syst. 41, 379–406. https://doi.org/10.1146/annurev-ecolsys-102209-144621.

Becu, N., Raimond, C., Garine, E., Deconchat, M., Kokou, K., 2014. Coupling environmental and social processes to simulate the emergence of a Savannah landscape mosaic under shifting cultivation and assess its sustainability. J. Artif. Soc. Soc. Simul. 17, 1. https://doi.org/10.18564/jasss.2397.

Becu, N., Amalric, M., Anselme, B., Beck, E., Bertin, X., Delay, E., Long, N., Marilleau, N., Pignon-Mussaud, C., Rousseaux, F., 2017. Participatory simulation to foster social learning on coastal flooding prevention. Environ. Model. Software 98, 1–11. https://doi.org/10.1016/j.envsoft.2017.09.003.

Beduschi, T., Tscharntke, T., Scherber, C., 2015. Using multi-level generalized path analysis to understand herbivore and parasitoid dynamics in changing landscapes. Landsc. Ecol. 30, 1975–1986. https://doi.org/10.1007/s10980-015-0224-2.

Begg, G.S., Dye, R., 2015. Exploring trade-offs and synergies between biological pest control and species conservation (Commissioned Report No. 692). Scottish Natural Heritage.

Belényesi, M.B., Podmaniczky, L., Balczo, B., 2008. Delineation of high nature value areas in Hungary. Hung J. Landsc. Ecol., 5.

Béné, C., Doyen, L., 2008. Contribution values of biodiversity to ecosystem performances: a viability perspective. Ecol. Econ. 68, 14–23. https://doi.org/10.1016/j.ecolecon.2008.08.015.

Benoît, M., Rizzo, D., Marraccini, E., Moonen, A.C., Galli, M., Lardon, S., Rapey, H., Thenail, C., Bonari, E., 2012. Landscape agronomy: a new field for addressing agricultural landscape dynamics. Landsc. Ecol. 27, 1385–1394. https://doi.org/10.1007/s10980-012-9802-8.

Betbeder, J., Laslier, M., Hubert-Moy, L., Burel, F., Baudry, J., 2017. Synthetic aperture radar (SAR) images improve habitat suitability models. Landsc. Ecol. 32, 1867–1879. https://doi.org/10.1007/s10980-017-0546-3.

Bianchi, F.J.J.A., Booij, C.J.H., Tscharntke, T., 2006. Sustainable pest regulation in agricultural landscapes: a review on landscape composition, biodiversity and natural pest control. Proc. R. Soc. Lond. B Biol. Sci. 273, 1715–1727.

Bieling, C., Plieninger, T., Schaich, H., 2013. Patterns and causes of land change: empirical results and conceptual considerations derived from a case study in the Swabian Alb, Germany. Land Use Policy 35, 192–203. https://doi.org/10.1016/j.landusepol.2013.05.012.

Biggs, J., von Fumetti, S., Kelly-Quinn, M., 2017. The importance of small waterbodies for biodiversity and ecosystem services: implications for policy makers. Hydrobiologia 793, 3–39. https://doi.org/10.1007/s10750-016-3007-0.

Blomqvist, M.M., Tamis, W.L.M., de Snoo, G.R., 2009. No improvement of plant biodiversity in ditch banks after a decade of agri-environment schemes. Basic Appl. Ecol. 10, 368–378. https://doi.org/10.1016/j.baae.2008.08.007.

Boccaletti, S., Bianconi, G., Criado, R., del Genio, C.I., Gómez-Gardeñes, J., Romance, M., Sendiña-Nadal, I., Wang, Z., Zanin, M., 2014. The structure and dynamics of multilayer networks. Phys. Rep. 544, 1–122. https://doi.org/10.1016/j.physrep.2014.07.001.

Bonhomme, V., Castets, M., Ibanez, T., Géraux, H., Hély, C., Gaucherel, C., 2017. Configurational changes of patchy landscapes dynamics. Ecol. Model. 363, 1–7. https://doi.org/10.1016/j.ecolmodel.2017.08.007.

Bourhis, Y., Poggi, S., Mammeri, Y., Cortesero, A.-M., Le Ralec, A., Parisey, N., 2015. Perception-based foraging for competing resources: assessing pest population dynamics at the landscape scale from heterogeneous resource distribution. Ecol. Model. 312, 211–221. https://doi.org/10.1016/j.ecolmodel.2015.05.029.

Bourhis, Y., Poggi, S., Mammeri, Y., Le Cointe, R., Cortesero, A.-M., Parisey, N., 2017. Foraging as the landscape grip for population dynamics—a mechanistic model applied to crop protection. Ecol. Model. 354, 26–36. https://doi.org/10.1016/j.ecolmodel.2017.03.005.

Brown, C., Brown, K., Rounsevell, M., 2016. A philosophical case for process-based modelling of land use change. Model. Earth Syst. Environ. 2, 50. https://doi.org/10.1007/s40808-016-0102-1.

Brunner, G.W., Bonner, V., 1994. HEC River Analysis System (HEC-RAS) (No. Technical Paper No. 147). US Army Corps of Enginners. Hydrologic Engineer Center.

Burdon, J.J., Thrall, P.H., 2008. Pathogen evolution across the agro-ecological interface: implications for disease management: pathogen evolution in agro-ecosystems. Evol. Appl. 1, 57–65. https://doi.org/10.1111/j.1752-4571.2007.00005.x.

Burel, F., 1996. Hedgerows and their role in agricultural landscapes. Crit. Rev. Plant Sci. 15, 169–190. https://doi.org/10.1080/07352689.1996.10393185.

Bürgi, M., Hersperger, A.M., Schneeberger, N., 2005. Driving forces of landscape change—current and new directions. Landsc. Ecol. 19, 857–868. https://doi.org/10.1007/s10980-005-0245-3.

Cabantous, L., Gond, J.-P., 2011. Rational decision making as performative praxis: explaining rationality's *Éternel Retour*. Organ. Sci. 22, 573–586. https://doi.org/10.1287/orsc.1100.0534.

Callon, M., 1998. The Laws of the Markets. The Sociological Revew/Basil Blackwell. ed, Oxford.

Campo, P.C., Bousquet, F., Villanueva, T.R., 2010. Modelling with stakeholders within a development project. Environ. Model. Software 25, 1302–1321. https://doi.org/10.1016/j.envsoft.2010.01.005.

Cardona, A., 2012. Territorial agri-food systems: relinking farming to local and environmental stakes to change farming systems. In: Producing and Reproducing Farming Systems. New Modes of Organisation for Sustainable Food Systems of Tomorrow. Presented at the Proceedings of the 10th European IFSA Symposium.

Caron, P., Biénabe, E., Hainzelin, E., 2014. Making transition towards ecological intensification of agriculture a reality: the gaps in and the role of scientific knowledge. Curr. Opin. Environ. Sustain. 8, 44–52. https://doi.org/10.1016/j.cosust.2014.08.004.

Carpenter, S.R., Caraco, N.F., Correll, D.L., Howarth, R.W., Sharpley, A.N., Smith, V.H., 1998. Nonpoint pollution of surface waters with phosphorus and nitrogen. Ecol. Appl. 8, 559–568. https://doi.org/10.1890/1051-0761(1998)008[0559:NPOSWW]2.0.CO;2.

Chapin III, F.S., Zavaleta, E.S., Eviner, V.T., Naylor, R.L., Vitousek, P.M., Reynolds, H.L., Hooper, D.U., Lavorel, S., Sala, O.E., Hobbie, S.E., Mack, M.C., Díaz, S., 2000. Consequences of changing biodiversity. Nature 405, 234–242. https://doi.org/10.1038/35012241.

Chaplin-Kramer, R., O'Rourke, M.E., Blitzer, E.J., Kremen, C., 2011. A meta-analysis of crop pest and natural enemy response to landscape complexity. Ecol. Lett. 14, 922–932.

Clark, J.S., 2004. Why environmental scientists are becoming Bayesians: modelling with Bayes. Ecol. Lett. 8, 2–14. https://doi.org/10.1111/j.1461-0248.2004.00702.x.

Collard, B., Tixier, P., Carval, D., Lavigne, C., Delattre, T., 2018. Spatial organisation of habitats in agricultural plots affects per-capita predator effect on conservation biological control: an individual based modelling study. Ecol. Model. 388, 124–135. https://doi.org/10.1016/j.ecolmodel.2018.09.026.

Couclelis, H., 1997. From cellular automata to urban models: new principles for model development and implementation. Environ. Plan. B Plan. Des. 24, 165–174. https://doi.org/10.1068/b240165.

Cressie, N.A.C., 2015. Statistics for Spatial Data, Revised edition. John Wiley & Sons, Inc, Hoboken, NJ.

Cressie, N., Calder, C.A., Clark, J.S., Hoef, J.M.V., Wikle, C.K., 2009. Accounting for uncertainty in ecological analysis: the strengths and limitations of hierarchical statistical modeling. Ecol. Appl. 19, 553–570. https://doi.org/10.1890/07-0744.1.

Crutzen, P.J., 2002. Geology of mankind. Nature 415, 23. https://doi.org/10.1038/415023a.

Daré, W., Venot, J.-P., 2018. Room for manoeuvre: user participation in water resources management in Burkina Faso. Dev. Policy Rev. 36, 175–189. https://doi.org/10.1111/dpr.12278.

de Groot, R.S., Alkemade, R., Braat, L., Hein, L., Willemen, L., 2010. Challenges in integrating the concept of ecosystem services and values in landscape planning, management and decision making. Ecol. Complex. 7, 260–272. https://doi.org/10.1016/j.ecocom.2009.10.006.

Dedeurwaerdere, T., Hannachi, M., 2019. Socio-economic drivers of coexistence of landraces and modern crop varieties in agro-biodiversity rich Yunnan rice fields. Ecol. Econ. 159, 177–188. https://doi.org/10.1016/j.ecolecon.2019.01.026.

Dell, A.I., Bender, J.A., Branson, K., Couzin, I.D., de Polavieja, G.G., Noldus, L.P.J.J., Pérez-Escudero, A., Perona, P., Straw, A.D., Wikelski, M., Brose, U., 2014. Automated image-based tracking and its application in ecology. Trends Ecol. Evol. 29, 417–428. https://doi.org/10.1016/j.tree.2014.05.004.

Descombes, X. (Ed.), 2013. Stochastic Geometry for Image Analysis. John Wiley & Sons, Inc., Hoboken, NJ, USA. https://doi.org/10.1002/9781118601235.

Dieguez Cameroni, F.J., Terra, R., Tabarez, S., Bommel, P., Corral, J., Bartaburu, D., Pereira, M., Montes, E., Duarte, E., Morales Grosskopf, H., 2014. Virtual experiments using a participatory model to explore interactions between climatic variability and management decisions in extensive grazing systems in the basaltic region of Uruguay. Agr. Syst. 130, 89–104. https://doi.org/10.1016/j.agsy.2014.07.002.

Dollinger, J., Dagès, C., Bailly, J.-S., Lagacherie, P., Voltz, M., 2015. Managing ditches for agroecological engineering of landscape. A review. Agron. Sustain. Dev. 35, 999–1020. https://doi.org/10.1007/s13593-015-0301-6.

Dossa, L.H., Abdulkadir, A., Amadou, H., Sangare, S., Schlecht, E., 2011. Exploring the diversity of urban and peri-urban agricultural systems in Sudano-Sahelian West Africa: an attempt towards a regional typology. Landsc. Urban Plan. 102, 197–206. https://doi.org/10.1016/j.landurbplan.2011.04.005.

Douglas, D.H., Peucker, T.K., 1973. Algorithms for the reduction of the number of points required to represent a digitized line or its caricature. Cartogr. Int. J. Geogr. Inf. Geovisualization 10, 112–122. https://doi.org/10.3138/FM57-6770-U75U-7727.

Doyen, L., Martinet, V., 2012. Maximin, viability and sustainability. J. Econ. Dyn. Control 36, 1414–1430. https://doi.org/10.1016/j.jedc.2012.03.004.

Dubos-Paillard, E., Guermond, Y., Langlois, P., 2003. Analyse de l'évolution urbaine par automate cellulaire. Le modèle SpaCelle. In: Espace Géographique Fr. 32, p. 357. https://doi.org/10.3917/eg.324.0357.

Dunning, J.B., Danielson, B.J., Pulliam, H.R., 1992. Ecological processes that affect populations in complex landscapes. Oikos 65, 169. https://doi.org/10.2307/3544901.

Dupont, S., Brunet, Y., 2006. Simulation of turbulent flow in an Urban Forested Park damaged by a windstorm. Bound.-Lay. Meteorol. 120, 133–161. https://doi.org/10.1007/s10546-006-9049-5.

Dupont, S., Brunet, Y., 2008. Influence of foliar density profile on canopy flow: a large-eddy simulation study. Agric. For. Meteorol. 148, 976–990. https://doi.org/10.1016/j.agrformet.2008.01.014.

Dupont, S., Brunet, Y., Jarosz, N., 2006. Eulerian modelling of pollen dispersal over heterogeneous vegetation canopies. Agric. For. Meteorol. 141, 82–104. https://doi.org/10.1016/j.agrformet.2006.09.004.

Duru, M., Adam, M., Cruz, P., Martin, G., Ansquer, P., Ducourtieux, C., Jouany, C., Theau, J.P., Viegas, J., 2009. Modelling above-ground herbage mass for a wide range of grassland community types. Ecol. Model. 220, 209–225. https://doi.org/10.1016/j.ecolmodel.2008.09.015.

Duru, M., Therond, O., Martin, G., Martin-Clouaire, R., Magne, M.-A., Justes, E., Journet, E.-P., Aubertot, J.-N., Savary, S., Bergez, J.-E., Sarthou, J.P., 2015. How to implement biodiversity-based agriculture to enhance ecosystem services: a review. Agron. Sustain. Dev. 35, 1259–1281. https://doi.org/10.1007/s13593-015-0306-1.

Dury, J., Schaller, N., Garcia, F., Reynaud, A., Bergez, J.E., 2012. Models to support cropping plan and crop rotation decisions. A review. Agron. Sustain. Dev. 32, 567–580. https://doi.org/10.1007/s13593-011-0037-x.

EC European Commission, 2018. Regions in the European Union: Nomenclature of Territorial Units for Statistics, NUTS 2016/EU 28: Edition 2018. Publications Office of the European Union, Luxembourg.

Elzen, B., Barbier, M., Cerf, M., Grin, J., 2012. Stimulating transitions towards sustainable farming systems. In: Darnhofer, I., Gibbon, D., Dedieu, B. (Eds.), Farming Systems Research into the 21st Century: The New Dynamic. Springer Netherlands, Dordrecht, pp. 431–455. https://doi.org/10.1007/978-94-007-4503-2_19.

Engel, J., Huth, A., Frank, K., 2012. Bioenergy production and skylark (*Alauda arvensis*) population abundance—a modelling approach for the analysis of land-use change

impacts and conservation options. GCB Bioenergy 4, 713–727. https://doi.org/10.1111/j.1757-1707.2012.01170.x.
Etienne, M., 2014. Companion Modelling: A Participatory Approach to Support Sustainable Development. Springer, Dordrecht.
FAO, 1999. Urban and peri-urban agriculture. In: Committee on Agriculture, 15th Session Urban and Peri-Urban Agriculture.
FAO, 2018. The State of Food and Agriculture. Migration, agriculture and rural development. Food and Agriculture Organization of the United Nations, Rome, p. 2018.
Farias, G., Leitzke, B., Born, M., Aguiar, M., Adamatti, D.F., 2019. Systematic review of natural resource management using multiagent systems and role-playing games. Res. Comput. Sci. 148, 91–102. https://doi.org/10.13053/rcs-148-11-7.
Fischer, J., Brosi, B., Daily, G.C., Ehrlich, P.R., Goldman, R., Goldstein, J., Lindenmayer, D.B., Manning, A.D., Mooney, H.A., Pejchar, L., Ranganathan, J., Tallis, H., 2008. Should agricultural policies encourage land sparing or wildlife-friendly farming? Front. Ecol. Environ. 6, 380–385. https://doi.org/10.1890/070019.
Fisher, B., Turner, R.K., Morling, P., 2009. Defining and classifying ecosystem services for decision making. Ecol. Econ. 68, 643–653. https://doi.org/10.1016/j.ecolecon.2008.09.014.
Foley, J.A., 2005. Global consequences of land use. Science 309, 570–574. https://doi.org/10.1126/science.1111772.
Forman, R.T.T., 1995. Some general principles of landscape and regional ecology. Landsc. Ecol. 10, 133–142.
Forman, R.T.T., Godron, M., 1986. Landscape Ecology. Cambridge University Press, Cambridge.
Franklin, J., 2010. Mapping Species Distributions: Spatial Inference and Prediction. Cambridge University Press, Cambridge. https://doi.org/10.1017/CBO9780511810602.
Frazier, A.E., Kedron, P., 2017. Landscape metrics: past progress and future directions. Curr. Landsc. Ecol. Rep. 2, 63–72. https://doi.org/10.1007/s40823-017-0026-0.
Friedmann, J., 2016. The future of periurban research. Cities 53, 163–165. https://doi.org/10.1016/j.cities.2016.01.009.
Fuchs, R., Verburg, P.H., Clevers, J.G.P.W., Herold, M., 2015. The potential of old maps and encyclopaedias for reconstructing historic European land cover/use change. Appl. Geogr. 59, 43–55. https://doi.org/10.1016/j.apgeog.2015.02.013.
García-Arias, A., Francés, F., 2016. The RVDM: modelling impacts, evolution and competition processes to determine riparian vegetation dynamics: the RVDM: modelling riparian vegetation dynamics. Ecohydrology 9, 438–459. https://doi.org/10.1002/eco.1648.
Gardarin, A., Dürr, C., Colbach, N., 2012. Modeling the dynamics and emergence of a multispecies weed seed bank with species traits. Ecol. Model. 240, 123–138. https://doi.org/10.1016/j.ecolmodel.2012.05.004.
Gardner, R.H., 1999. RULE: map generation and a spatial analysis program. In: Klopatek, J.M., Gardner, R.H. (Eds.), Landscape Ecological Analysis. Springer New York, New York, NY, pp. 280–303. https://doi.org/10.1007/978-1-4612-0529-6_13.
Gaucherel, C., 2008. Neutral models for polygonal landscapes with linear networks. Ecol. Model. 219, 39–48.
Gaucherel, C., Fleury, D., Auclair, D., Dreyfus, P., 2006a. Neutral models for patchy landscapes. Ecol. Model. 197, 159–170. https://doi.org/10.1016/j.ecolmodel.2006.02.044.
Gaucherel, C., Giboire, N., Viaud, V., Houet, T., Baudry, J., Burel, F., 2006b. A domain-specific language for patchy landscape modelling: the Brittany agricultural mosaic as a case study. Ecol. Model. 194, 233–243. https://doi.org/10.1016/j.ecolmodel.2005.10.026.

Geertsema, W., Rossing, W.A., Landis, D.A., Bianchi, F.J., van Rijn, P.C., Schaminée, J.H., Tscharntke, T., van der Werf, W., 2016. Actionable knowledge for ecological intensification of agriculture. Front. Ecol. Environ. 14, 209–216. https://doi.org/10.1002/fee.1258.

Geniaux, G., Ay, J.-S., Napoléone, C., 2011. A spatial hedonic approach on land use change anticipations. J. Reg. Sci. 51, 967–986. https://doi.org/10.1111/j.1467-9787.2011.00721.x.

Gerber, P.J., Steinfeld, H., Henderson, B., Mottet, A., Opio, C., Dijkman, J., Falcucci, A., Tempio, G., 2013. Tackling Climate Change through Livestock: A Global Assessment of Emissions and Mitigation Opportunities. Food and Agriculture Organization of the United Nations (FAO), Rome.

Grass, et al., 2021. The future of European land-sharing/−sparing connectivity landscapes. In: Bohan, D., Vanbergen, A (Eds.), Advances in Ecological Research. Elsevier, p. 64 (this issue).

Grimm, V., Revilla, E., Berger, U., Jeltsch, F., Mooij, W.M., Railsback, S.F., Thulke, H.H., Weiner, J., Wiegand, T., DeAngelis, D.L., 2005. Pattern-oriented modeling of agent-based complex systems: lessons from ecology. Science 310, 987–991.

Groot, J.C.J., Rossing, W.A.H., Tichit, M., Turpin, N., Jellema, A., Baudry, J., Verburg, P.H., Doyen, L., van de Ven, G.W.J., 2009. On the contribution of modelling to multifunctional agriculture: learning from comparisons. J. Environ. Manage. 90, S147–S160. https://doi.org/10.1016/j.jenvman.2008.11.030.

Guan, D., Li, H., Inohae, T., Su, W., Nagaie, T., Hokao, K., 2011. Modeling urban land use change by the integration of cellular automaton and Markov model. Ecol. Model. 222, 3761–3772. https://doi.org/10.1016/j.ecolmodel.2011.09.009.

Gurung, T.R., Bousquet, F., Trébuil, G., 2006. Companion modeling, conflict resolution, and institution building: sharing irrigation water in the Lingmuteychu Watershed. Bhutan. Ecol. Soc. 11 (2), 36 (online) http://www.ecologyandsociety.org/vol11/iss2/art36/.

Haan, N.L., Zhang, Y., Landis, D.A., 2020. Predicting landscape configuration effects on agricultural pest suppression. Trends Ecol. Evol. 35 (2), 175–186. https://doi.org/10.1016/j.tree.2019.10.003.

Hallmann, C.A., Foppen, R.P.B., van Turnhout, C.A.M., de Kroon, H., Jongejans, E., 2014. Declines in insectivorous birds are associated with high neonicotinoid concentrations. Nature 511, 341–343. https://doi.org/10.1038/nature13531.

Hallmann, C.A., Sorg, M., Jongejans, E., Siepel, H., Hofland, N., Schwan, H., Stenmans, W., Müller, A., Sumser, H., Hörren, T., Goulson, D., de Kroon, H., 2017. More than 75 percent decline over 27 years in total flying insect biomass in protected areas. PLoS One 12, e0185809. https://doi.org/10.1371/journal.pone.0185809.

Hannachi, M., Coléno, F.-C., 2015. Towards a managerial engineering of coopetition the findings of the study of the management of GMOs in the French grain merchant industry. Manag. Organ. Stud. 3, p1. https://doi.org/10.5430/mos.v3n1p1.

Hannachi, M., Martinet, V., 2019. In: Petit, S., Lavigne, C. (Eds.), Vers une co-conception de paysages pour la santé des plantes et avec des acteurs du territoire, in: Paysage, biodiversité fonctionnelle et santé des cultures (in French), pp. 185–205.

Häussler, J., Barabás, G., Eklöf, A., 2020. A Bayesian network approach to trophic metacommunities shows that habitat loss accelerates top species extinctions. Ecol. Lett. 23 (12), 1849–1861. https://doi.org/10.1111/ele.13607. ele. 13607.

Hayhoe, K., Edmonds, J., Kopp, R.E., LeGrande, A.N., Sanderson, B.M., Wehner, M.F., Wuebbles, D.J., 2017. Ch. 4: Climate Models, Scenarios, and Projections. Climate Science Special Report: Fourth National Climate Assessment. vol. I U.S. Global Change Research Program. https://doi.org/10.7930/J0WH2N54.

Hersperger, A.M., Bürgi, M., 2009. Going beyond landscape change description: quantifying the importance of driving forces of landscape change in a Central Europe case study. Land Use Policy 26, 640–648. https://doi.org/10.1016/j.landusepol.2008.08.015.

Hodgson, J.C., Mott, R., Baylis, S.M., Pham, T.T., Wotherspoon, S., Kilpatrick, A.D., Raja Segaran, R., Reid, I., Terauds, A., Koh, L.P., 2018. Drones count wildlife more accurately and precisely than humans. Methods Ecol. Evol. 9, 1160–1167. https://doi.org/10.1111/2041-210X.12974.

Hossard, L., Jeuffroy, M.H., Pelzer, E., Pinochet, X., Souchere, V., 2013. A participatory approach to design spatial scenarios of cropping systems and assess their effects on phoma stem canker management at a regional scale. Environ. Model. Software 48, 17–26. https://doi.org/10.1016/j.envsoft.2013.05.014.

Houet, T., Verburg, P.H., Loveland, T.R., 2010. Monitoring and modelling landscape dynamics. Landsc. Ecol. 25, 163–167. https://doi.org/10.1007/s10980-009-9417-x.

Houet, T., Aguejdad, R., Doukari, O., Battaia, G., Clarke, K., 2016. Description and validation of a "non path-dependent" model for projecting contrasting urban growth futures. Cybergeo Eur. J. Geogr. https://doi.org/hal-01326063.

Huber, R., Bakker, M., Balmann, A., Berger, T., Bithell, M., Brown, C., Grêt-Regamey, A., Xiong, H., Le, Q.B., Mack, G., Meyfroidt, P., Millington, J., Müller, B., Polhill, J.G., Sun, Z., Seidl, R., Troost, C., Finger, R., 2018. Representation of decision-making in European agricultural agent-based models. Agr. Syst. 167, 143–160. https://doi.org/10.1016/j.agsy.2018.09.007.

Illian, J.B., Martino, S., Sørbye, S.H., Gallego-Fernández, J.B., Zunzunegui, M., Esquivias, M.P., Travis, J.M.J., 2013. Fitting complex ecological point process models with integrated nested Laplace approximation. Methods Ecol. Evol. 4, 305–315. https://doi.org/10.1111/2041-210x.12017.

Inkoom, J.N., Frank, S., Greve, K., Fürst, C., 2017. Designing neutral landscapes for data scarce regions in West Africa. Eco. Inform. 42, 1–13. https://doi.org/10.1016/j.ecoinf.2017.08.003.

Jacquot, M., Massol, F., Muru, D., Derepas, B., Tixier, P., Deguine, J.-P., 2019. Arthropod diversity is governed by bottom-up and top-down forces in a tropical agroecosystem. Agric. Ecosyst. Environ. 285, 106623. https://doi.org/10.1016/j.agee.2019.106623.

Jokar Arsanjani, J., Helbich, M., Kainz, W., Darvishi Boloorani, A., 2013. Integration of logistic regression, Markov chain and cellular automata models to simulate urban expansion. Int. J. Appl. Earth Obs. Geoinf. 21, 265–275. https://doi.org/10.1016/j.jag.2011.12.014.

Kays, R., Crofoot, M.C., Jetz, W., Wikelski, M., 2015. Terrestrial animal tracking as an eye on life and planet. Science 348, aaa2478. https://doi.org/10.1126/science.aaa2478.

Kays, R., McShea, W.J., Wikelski, M., 2020. Born-digital biodiversity data: millions and billions. Divers. Distrib. 26 (5), 644–648. ddi.12993 https://doi.org/10.1111/ddi.12993.

Keane, R.E., McKenzie, D., Falk, D.A., Smithwick, E.A.H., Miller, C., Kellogg, L.-K.B., 2015. Representing climate, disturbance, and vegetation interactions in landscape models. Ecol. Model. 309, 33–47.

Kiêu, K., Adamczyk-Chauvat, K., Monod, H., Stoica, R.S., 2013. A completely random T-tessellation model and Gibbsian extensions. Spat. Stat. 6, 118–138. https://doi.org/10.1016/j.spasta.2013.09.003.

Kivela, M., Arenas, A., Barthelemy, M., Gleeson, J.P., Moreno, Y., Porter, M.A., 2014. Multilayer networks. J. Complex Netw. 2 (3), 203–271. SSRN Electron. J. https://doi.org/10.2139/ssrn.2341334.

Klein, T., Holzkämper, A., Calanca, P., Seppelt, R., Fuhrer, J., 2013. Adapting agricultural land management to climate change: a regional multi-objective optimization approach. Landsc. Ecol. 28, 2029–2047. https://doi.org/10.1007/s10980-013-9939-0.

Kremen, C., Merenlender, A.M., 2018. Landscapes that work for biodiversity and people. Science 362, eaau6020. https://doi.org/10.1126/science.aau6020.

Labarthe, P., 2009. Extension services and multifunctional agriculture. Lessons learnt from the French and Dutch contexts and approaches. J. Environ. Manage. 90, S193–S202. https://doi.org/10.1016/j.jenvman.2008.11.021.

Lagabrielle, E., Botta, A., Daré, W., David, D., Aubert, S., Fabricius, C., 2010. Modelling with stakeholders to integrate biodiversity into land-use planning—lessons learned in Réunion Island (Western Indian Ocean). Environ. Model. Software 25, 1413–1427. https://doi.org/10.1016/j.envsoft.2010.01.011.

Lambin, E., Rounsevell, M.D., Geist, H., 2000. Are agricultural land-use models able to predict changes in land-use intensity? Agric. Ecosyst. Environ. 82, 321–331. https://doi.org/10.1016/S0167-8809(00)00235-8.

Lamboni, M., Monod, H., Makowski, D., 2011. Multivariate sensitivity analysis to measure global contribution of input factors in dynamic models. Reliab. Eng. Syst. Saf. 96, 450–459. https://doi.org/10.1016/j.ress.2010.12.002.

Langhammer, M., Thober, J., Lange, M., Frank, K., Grimm, V., 2019. Agricultural landscape generators for simulation models: a review of existing solutions and an outline of future directions. Ecol. Model. 393, 135–151. https://doi.org/10.1016/j.ecolmodel.2018.12.010.

Lansing, J.S., Thurner, S., Chung, N.N., Coudurier-Curveur, A., Karakaş, Ç., Fesenmyer, K.A., Chew, L.Y., 2017. Adaptive self-organization of Bali's ancient rice terraces. Proc. Natl. Acad. Sci. U. S. A. 114, 6504–6509. https://doi.org/10.1073/pnas.1605369114.

Latour, B., 1987. Science in Action: How to Follow Scientists and Engineers through Society. Harvard University Press. ed.

Latour, B., 2005. Reassembling the Social-an Introduction to Actor-Network-Theory. Oxford University Press. ed, Oxford.

Lausch, A., Blaschke, T., Haase, D., Herzog, F., Syrbe, R.-U., Tischendorf, L., Walz, U., 2015. Understanding and quantifying landscape structure—a review on relevant process characteristics, data models and landscape metrics. Ecol. Model. 295, 31–41. https://doi.org/10.1016/j.ecolmodel.2014.08.018.

Le Ber, F., Lavigne, C., Adamczyk, K., Angevin, F., Colbach, N., Mari, J.F., Monod, H., 2009. Neutral modelling of agricultural landscapes by tessellation methods-application for gene flow simulation. Ecol. Model. 220, 3536–3545.

Le Cœur, D., Baudry, J., Burel, F., Thenail, C., 2002. Why and how we should study field boundary biodiversity in an agrarian landscape context. Agric. Ecosyst. Environ. 89, 23–40. https://doi.org/10.1016/S0167-8809(01)00316-4.

Le Page, C., Perrotton, A., 2017. KILT: a modelling approach based on participatory agent-based simulation of stylized socio-ecosystems to stimulate social learning with local stakeholders. In: Sukthankar, G., Rodriguez-Aguilar, J.A. (Eds.), Autonomous Agents and Multiagent Systems. Springer International Publishing, Cham, pp. 31–44. https://doi.org/10.1007/978-3-319-71679-4_3.

LeCun, Y., Bengio, Y., Hinton, G., 2015. Deep learning. Nature 521, 436–444. https://doi.org/10.1038/nature14539.

Leenhardt, D., Angevin, F., Biarnès, A., Colbach, N., Mignolet, C., 2010. Describing and locating cropping systems on a regional scale. A review. Agron. Sustain. Dev. 30, 131–138. https://doi.org/10.1051/agro/2009002.

Leibold, M.A., Holyoak, M., Mouquet, N., Amarasekare, P., Chase, J.M., Hoopes, M.F., Holt, R.D., Shurin, J.B., Law, R., Tilman, D., Loreau, M., Gonzalez, A., 2004. The metacommunity concept: a framework for multi-scale community ecology: the metacommunity concept. Ecol. Lett. 7, 601–613. https://doi.org/10.1111/j.1461-0248.2004.00608.x.

Li, W., Wang, D., Li, H., Liu, S., 2017. Urbanization-induced site condition changes of peri-urban cultivated land in the black soil region of Northeast China. Ecol. Indic. 80, 215–223. https://doi.org/10.1016/j.ecolind.2017.05.038.

Loreau, M., de Mazancourt, C., 2013. Biodiversity and ecosystem stability: a synthesis of underlying mechanisms. Ecol. Lett. 16, 106–115. https://doi.org/10.1111/ele.12073.

Macarthur, R.H., Wilson, E.O., 1967. The Theory of Island Biogeography. Princeton University Press. https://doi.org/10.2307/j.ctt19cc1t2.

Macfadyen, S., Gibson, R., Polaszek, A., Morris, R.J., Craze, P.G., Planqué, R., Symondson, W.O.C., Memmott, J., 2009. Do differences in food web structure between organic and conventional farms affect the ecosystem service of pest control? Ecol. Lett. 12, 229–238. https://doi.org/10.1111/j.1461-0248.2008.01279.x.

MacKenzie, D., Muniesa, F., Siu, L., 2007. Do Economists Make Markets? On the Performativity of Economics. Princeton University Press, New Jersey.

Macmillan, W., Huang, H.Q., 2008. An agent-based simulation model of a primitive agricultural society. Geoforum 39, 643–658. https://doi.org/10.1016/j.geoforum.2007.07.011.

Magliocca, N.R., van Vliet, J., Brown, C., Evans, T.P., Houet, T., Messerli, P., Messina, J.P., Nicholas, K.A., Ornetsmüller, C., Sagebiel, J., Schweizer, V., Verburg, P.H., Yu, Q., 2015. From meta-studies to modeling: using synthesis knowledge to build broadly applicable process-based land change models. Environ. Model. Software 72, 10–20. https://doi.org/10.1016/j.envsoft.2015.06.009.

Martinet, V., 2013. Effect of soil heterogeneity on the welfare economics of biofuel policies. Land Use Policy 32, 218–229. https://doi.org/10.1016/j.landusepol.2012.10.013.

Massol, F., Petit, S., 2013. Interaction networks in agricultural landscape mosaics. In: Advances in Ecological Research. Elsevier, pp. 291–338. https://doi.org/10.1016/B978-0-12-420002-9.00005-6.

Massol, F., Gravel, D., Mouquet, N., Cadotte, M.W., Fukami, T., Leibold, M.A., 2011. Linking community and ecosystem dynamics through spatial ecology: an integrative approach to spatial food webs. Ecol. Lett. 14, 313–323. https://doi.org/10.1111/j.1461-0248.2011.01588.x.

Massol, F., Dubart, M., Calcagno, V., Cazelles, K., Jacquet, C., Kéfi, S., Gravel, D., 2017. Island biogeography of food webs. In: Advances in Ecological Research. Elsevier, pp. 183–262. https://doi.org/10.1016/bs.aecr.2016.10.004.

Mateo-Sagasta, J., Zadeh, S.M., Turral, H., Burke, J., 2017. Water pollution from agriculture: a global review. In: Executive Summary (CGIAR Research Program on Water, Land and Ecosystems). International Water Management Institute, FAO, Rome, p. 35.

Mawois, M., Le Bail, M., Navarrete, M., Aubry, C., 2012. Modelling spatial extension of vegetable land use in urban farms. Agron. Sustain. Dev. 32, 911–924. https://doi.org/10.1007/s13593-012-0093-x.

McGarigal, K., Cushman, S., 2005. The gradient concept of landscape structure. In: Issues and Perspectives in Landscape Ecology. Cambridge University Press, pp. 112–119.

Medley, K.E., Okey, B.W., Barrett, G.W., Lucas, M.F., Renwick, W.H., 1995. Landscape change with agricultural intensification in a rural watershed, southwestern Ohio, U.S.A. Landsc. Ecol. 10, 161–176. https://doi.org/10.1007/BF00133029.

Memmah, M.-M., Lescourret, F., Yao, X., Lavigne, C., 2015. Metaheuristics for agricultural land use optimization. A review. Agron. Sustain. Dev. 35, 975–998. https://doi.org/10.1007/s13593-015-0303-4.

Merritt, D.M., Scott, M.L., LeRoy Poff, N., Auble, G.T., Lytle, D.A., 2010. Theory, methods and tools for determining environmental flows for riparian vegetation: riparian vegetation-flow response guilds: Riparian vegetation-hydrologic models. Freshw. Biol. 55, 206–225. https://doi.org/10.1111/j.1365-2427.2009.02206.x.

Mignolet, C., Schott, C., Benoît, M., 2004. Spatial dynamics of agricultural practices on a basin territory: a retrospective study to implement models simulating nitrate flow. The case of the seine basin. Agronomie 24, 219–236. https://doi.org/10.1051/agro:2004015.

Mitchell, M.G.E., Suarez-Castro, A.F., Martinez-Harms, M., Maron, M., McAlpine, C., Gaston, K.J., Johansen, K., Rhodes, J.R., 2015. Reframing landscape fragmentation's effects on ecosystem services. Trends Ecol. Evol. 30, 190–198. https://doi.org/10.1016/j.tree.2015.01.011.

Mollot, G., Duyck, P.-F., Lefeuvre, P., Lescourret, F., Martin, J.-F., Piry, S., Canard, E., Tixier, P., 2014. Cover cropping alters the diet of arthropods in a Banana plantation: a Metabarcoding approach. PLoS One 9, e93740. https://doi.org/10.1371/journal.pone.0093740.

Moradkhani, H., Sorooshian, S., 2008. General review of rainfall-runoff modeling: model calibration, data assimilation, and uncertainty analysis. In: Sorooshian, S., Hsu, K.-L., Coppola, E., Tomassetti, B., Verdecchia, M., Visconti, G. (Eds.), Hydrological Modelling and the Water Cycle. Springer Berlin Heidelberg, Berlin, Heidelberg, pp. 1–24. https://doi.org/10.1007/978-3-540-77843-1_1.

Motisi, N., Ribeyre, F., Poggi, S., 2019. Coffee tree architecture and its interactions with microclimates drive the dynamics of coffee berry disease in coffee trees. Sci. Rep. 9, 1–12. https://doi.org/10.1038/s41598-019-38775-5.

Mottet, A., Ladet, S., Coqué, N., Gibon, A., 2006. Agricultural land-use change and its drivers in mountain landscapes: a case study in the Pyrenees. Agric. Ecosyst. Environ. 114, 296–310. https://doi.org/10.1016/j.agee.2005.11.017.

Mougeot, L., 2000. Urban Agriculture: Definition, Presence, Potentials and Risks. In: Growing Cities, Growing Food: Urban Agriculture on the Policy Agenda. ZEL, Feldafing (GER).

Moussa, R., Voltz, M., Andrieux, P., 2002. Effects of the spatial organization of agricultural management on the hydrological behaviour of a farmed catchment during flood events. Hydrol. Process. 16, 393–412. https://doi.org/10.1002/hyp.333.

Muniesa, F., 2014. The Provoked Economy: Economic Reality and the Performative Turn, first ed. Routledge. https://doi.org/10.4324/9780203798959.

Murgue, C., Therond, O., Leenhardt, D., 2016. Hybridizing local and generic information to model cropping system spatial distribution in an agricultural landscape. Land Use Policy 54, 339–354. https://doi.org/10.1016/j.landusepol.2016.02.020.

Nendel, C., Zander, P., 2019. Landscape models to support sustainable intensification of agroecological systems. In: Burleigh Dodds Series in Agricultural Science. Burleigh Dodds Science Publishing, pp. 321–354. https://doi.org/10.19103/AS.2019.0061.17.

Nepf, H.M., 2012. Hydrodynamics of vegetated channels. J. Hydraul. Res. 50, 262–279. https://doi.org/10.1080/00221686.2012.696559.

Nesshöver, C., Assmuth, T., Irvine, K.N., Rusch, G.M., Waylen, K.A., Delbaere, B., Haase, D., Jones-Walters, L., Keune, H., Kovacs, E., Krauze, K., Külvik, M., Rey, F., van Dijk, J., Vistad, O.I., Wilkinson, M.E., Wittmer, H., 2017. The science, policy and practice of nature-based solutions: an interdisciplinary perspective. Sci. Total Environ. 579, 1215–1227. https://doi.org/10.1016/j.scitotenv.2016.11.106.

Ohgushi, T., 2008. Herbivore-induced indirect interaction webs on terrestrial plants: the importance of non-trophic, indirect, and facilitative interactions. Entomol. Exp. Appl. 128, 217–229. https://doi.org/10.1111/j.1570-7458.2008.00705.x.

Olsen, A., Konovalov, D.A., Philippa, B., Ridd, P., Wood, J.C., Johns, J., Banks, W., Girgenti, B., Kenny, O., Whinney, J., Calvert, B., Azghadi, M.R., White, R.D., 2019. DeepWeeds: a multiclass weed species image dataset for deep learning. Sci. Rep. 9, 2058. https://doi.org/10.1038/s41598-018-38343-3.

Overmars, K.P., Verburg, P.H., Veldkamp, T.A., 2007. Comparison of a deductive and an inductive approach to specify land suitability in a spatially explicit land use model. Land Use Policy 24, 584–599. https://doi.org/10.1016/j.landusepol.2005.09.008.

Papaïx, J., Adamczyk-Chauvat, K., Bouvier, A., Kiêu, K., Touzeau, S., Lannou, C., Monod, H., 2014. Pathogen population dynamics in agricultural landscapes: the Ddal modelling framework. Infect. Genet. Evol. 27, 509–520. https://doi.org/10.1016/j.meegid.2014.01.022.

Papaïx, J., Rimbaud, L., Burdon, J.J., Zhan, J., Thrall, P.H., 2018. Differential impact of landscape-scale strategies for crop cultivar deployment on disease dynamics, resistance durability and long-term evolutionary control. Evol. Appl. 11, 705–717. https://doi.org/10.1111/eva.12570.

Parisey, N., Bourhis, Y., Roques, L., Soubeyrand, S., Ricci, B., Poggi, S., 2016. Rearranging agricultural landscapes towards habitat quality optimisation: in silico application to pest regulation. Ecol. Complex. 28, 113–122. https://doi.org/10.1016/j.ecocom.2016.07.003.

Parr, S., O'Donovan, G., Finn, J., 2006. Mapping the broad habitats of the burren using satellite imagery. End of Project Report, Teagasc.

Pascual, U., Perrings, C., 2007. Developing incentives and economic mechanisms for in situ biodiversity conservation in agricultural landscapes. Agric. Ecosyst. Environ. 121, 256–268. https://doi.org/10.1016/j.agee.2006.12.025.

Pe'er, G., Zurita, G.A., Schober, L., Bellocq, M.I., Strer, M., Müller, M., Pütz, S., 2013. Simple process-based simulators for generating spatial patterns of habitat loss and fragmentation: a review and introduction to the G-RaFFe model. PLoS One 8, e64968. https://doi.org/10.1371/journal.pone.0064968.

Perović, D., Gámez-Virués, S., Börschig, C., Klein, A.-M., Krauss, J., Steckel, J., Rothenwöhrer, C., Erasmi, S., Tscharntke, T., Westphal, C., 2015. Configurational landscape heterogeneity shapes functional community composition of grassland butterflies. J. Appl. Ecol. 52, 505–513. https://doi.org/10.1111/1365-2664.12394.

Philpott, S.M., Lucatero, A., Bichier, P., Egerer, M.H., Jha, S., Lin, B., Liere, H., 2020. Natural enemy–herbivore networks along local management and landscape gradients in urban agroecosystems. Ecol. Appl. 30 (8). https://doi.org/10.1002/eap.2201.

Piorr, A., Ravetz, J., Tosics, I., 2011. Peri-Urbanisation in Europe: Towards European Policies to Sustain Urban-Rural Futures. University of Copenhagen/Academic Books Life Sciences.

Plieninger, T., Draux, H., Fagerholm, N., Bieling, C., Bürgi, M., Kizos, T., Kuemmerle, T., Primdahl, J., Verburg, P.H., 2016. The driving forces of landscape change in Europe: a systematic review of the evidence. Land Use Policy 57, 204–214. https://doi.org/10.1016/j.landusepol.2016.04.040.

Poggi, S., Papaïx, J., Lavigne, C., Angevin, F., Le Ber, F., Parisey, N., Ricci, B., Vinatier, F., Wohlfahrt, J., 2018. Issues and challenges in landscape models for agriculture: from the representation of agroecosystems to the design of management strategies. Landsc. Ecol. 33, 1679–1690. https://doi.org/10.1007/s10980-018-0699-8.

Pointereau, P., Paracchini, M.-L., Terres, J., Jiguet, F., Le Bas, Y., Katarzyna, B., 2007. Identification of high nature value farmland in France through statistical information and farm practice surveys. EUR- scientific and technical research reports.

Porporato, A., Rodriguez-Iturbe, I., 2002. Ecohydrology-a challenging multidisciplinary research perspective/Ecohydrologie: Une perspective stimulante de recherche multidisciplinaire. Hydrol. Sci. J. 47, 811–821. https://doi.org/10.1080/02626660209492985.

Power, A.G., 2010. Ecosystem services and agriculture: tradeoffs and synergies. Philos. Trans. R. Soc. B Biol. Sci. 365, 2959–2971. https://doi.org/10.1098/rstb.2010.0143.

Preisler, H.K., Ager, A.A., Wisdom, M.J., 2013. Analyzing animal movement patterns using potential functions. Ecosphere 4, art32. https://doi.org/10.1890/ES12-00286.1.

Pribadi, D.O., Pauleit, S., 2015. The dynamics of peri-urban agriculture during rapid urbanization of Jabodetabek metropolitan area. Land Use Policy 48, 13–24. https://doi.org/10.1016/j.landusepol.2015.05.009.

Rayfuse, R., Weisfelt, N., 2012. The Challenge of Food Security. Edward Elgar Publishing. https://doi.org/10.4337/9780857939388.

Rey, F., Cécillon, L., Cordonnier, T., Jaunatre, R., Loucougaray, G., 2015. Integrating ecological engineering and ecological intensification from management practices to ecosystem services into a generic framework: a review. Agron. Sustain. Dev. 35, 1335–1345. https://doi.org/10.1007/s13593-015-0320-3.

Ricci, B., Petit, S., Allanic, C., Langot, M., Parisey, N., Poggi, S., 2018. How effective is large landscape-scale planning for reducing local weed infestations? A landscape-scale modelling approach. Ecol. Model. 384, 221–232. https://doi.org/10.1016/j.ecolmodel.2018.06.029.

Ries, L., Oberhauser, K., 2015. A citizen Army for science: quantifying the contributions of citizen scientists to our understanding of monarch butterfly biology. Bioscience 65, 419–430. https://doi.org/10.1093/biosci/biv011.

Rimbaud, L., Papaïx, J., Barrett, L.G., Burdon, J.J., Thrall, P.H., 2018. Mosaics, mixtures, rotations or pyramiding: what is the optimal strategy to deploy major gene resistance? Evol. Appl. 11, 1791–1810. https://doi.org/10.1111/eva.12681.

Rizzo, D., Marraccini, E., Lardon, S., Rapey, H., Debolini, M., Benoît, M., Thenail, C., 2013. Farming systems designing landscapes: land management units at the interface between agronomy and geography. Geogr. Tidsskr.-Dan. J. Geogr. 113, 71–86. https://doi.org/10.1080/00167223.2013.849391.

Rodríguez Eugenio, N., McLaughlin, M.J., Pennock, D.J., 2018. Soil Pollution: A Hidden Reality. FAO, Rome, p. 142.

Roques, L., Bonnefon, O., 2016. Modelling population dynamics in realistic landscapes with linear elements: a mechanistic-statistical reaction-diffusion approach. PLoS One 11, e0151217. https://doi.org/10.1371/journal.pone.0151217.

Rossi, J.-P., Garcia, J., Roques, A., Rousselet, J., 2016. Trees outside forests in agricultural landscapes: spatial distribution and impact on habitat connectivity for forest organisms. Landsc. Ecol. 31, 243–254. https://doi.org/10.1007/s10980-015-0239-8.

Rossing, W.A.H., Zander, P., Josien, E., Groot, J.C.J., Meyer, B.C., Knierim, A., 2007. Integrative modelling approaches for analysis of impact of multifunctional agriculture: a review for France, Germany and the Netherlands. Agric. Ecosyst. Environ. 120, 41–57. https://doi.org/10.1016/j.agee.2006.05.031.

Rudi, G., 2019. Modelling and Analysis of Eco-Hydraulic Services of Ditch and Channel Networks in Mediterranean Agrosystems (in French). Montpellier SupAgro.

Rudi, G., Bailly, J.-S., Belaud, G., Vinatier, F., 2018. Characterization of the long-distance dispersal of Johnsongrass (*Sorghum halepense*) in a vegetated irrigation channel: hydrochorous dispersal of Johnsongrass in a vegetated channel. River Res. Appl. 34, 1219–1228. https://doi.org/10.1002/rra.3356.

Saint-Geours, N., Bailly, J.-S., Grelot, F., Lavergne, C., 2014. Multi-scale spatial sensitivity analysis of a model for economic appraisal of flood risk management policies. Environ. Model. Software 60, 153–166. https://doi.org/10.1016/j.envsoft.2014.06.012.

Saint-Geours, N., Grelot, F., Bailly, J.-S., Lavergne, C., 2015. Ranking sources of uncertainty in flood damage modelling: a case study on the cost-benefit analysis of a flood mitigation project in the Orb Delta, France: ranking sources of uncertainty in flood damage modelling. J. Flood Risk Manage. 8, 161–176. https://doi.org/10.1111/jfr3.12068.

Salliou, N., Vialatte, A., Monteil, C., Barnaud, C., 2019. First use of participatory Bayesian modeling to study habitat management at multiple scales for biological pest control. Agron. Sustain. Dev. 39, 7. https://doi.org/10.1007/s13593-018-0553-z.

Samoy, D., Lambotte, M., Biala, K., Terres, J.M., Paracchini, M.L., 2007. Validation and Improvement of High Nature Value Identification: National Approach in the Walloon Region in Belgium and the Czech Republic (JRC Scientific and Technical Reports). Institute for Environment and Sustainability, Luxembourg.

Sánchez-Bayo, F., Wyckhuys, K.A.G., 2019. Worldwide decline of the entomofauna: a review of its drivers. Biol. Conserv. 232, 8–27. https://doi.org/10.1016/j.biocon.2019.01.020.

Sang, L., Zhang, C., Yang, J., Zhu, D., Yun, W., 2011. Simulation of land use spatial pattern of towns and villages based on CA–Markov model. Math. Comput. Model. 54, 938–943. https://doi.org/10.1016/j.mcm.2010.11.019.

Sanz Sanz, E., Napoleone, C., Hubert, B., 2016. Peri-urban farmland characterisation. A methodological proposal for urban planning. In: Sustainable Urban Agriculture and Food Planning. Taylor and Francis Group, London, pp. 73–90.

Sanz Sanz, E., Napoléone, C., Hubert, B., 2017. A systemic methodology to characterize peri-urban agriculture for a better integrationn of agricultural stakes in urban planning. Espace Géogr. 46, 174. https://doi.org/10.3917/eg.462.0174.

Sanz Sanz, E., Martinetti, D., Napoléone, C., 2018. Operational modelling of peri-urban farmland for public action in Mediterranean context. Land Use Policy 75, 757–771. https://doi.org/10.1016/j.landusepol.2018.04.003.

Sattler, T., Duelli, P., Obrist, M.K., Arlettaz, R., Moretti, M., 2010. Response of arthropod species richness and functional groups to urban habitat structure and management. Landsc. Ecol. 25, 941–954. https://doi.org/10.1007/s10980-010-9473-2.

Saura, S., Martínez-Millán, J., 2000. Landscape patterns simulation with a modified random cluster method. Landsc. Ecol. 15, 661–678. https://doi.org/10.1023/A:1008107902848.

Sausse, C., Le Bail, M., Lecroart, B., Remy, B., Messéan, A., 2013. How to manage the coexistence between genetically modified and conventional crops in grain and oilseed collection areas? Elaboration of scenarios using role playing games. Land Use Policy 30, 719–729. https://doi.org/10.1016/j.landusepol.2012.05.018.

Schulte, L.A., Niemi, J., Helmers, M.J., Liebman, M., Arbuckle, J.G., James, D.E., Kolka, R.K., O'Neal, M.E., Tomer, M.D., Tyndall, J.C., Asbjornsen, H., Drobney, P., Neal, J., Van Ryswyk, G., Witte, C., 2017. Prairie strips improve biodiversity and the delivery of multiple ecosystem services from corn–soybean croplands. Proc. Natl. Acad. Sci. U. S. A. 114, 11247–11252. https://doi.org/10.1073/pnas.1620229114.

Seibold, S., Gossner, M.M., Simons, N.K., Blüthgen, N., Müller, J., Ambarlı, D., Ammer, C., Bauhus, J., Fischer, M., Habel, J.C., Linsenmair, K.E., Nauss, T., Penone, C., Prati, D., Schall, P., Schulze, E.-D., Vogt, J., Wöllauer, S., Weisser, W.W., 2019. Arthropod decline in grasslands and forests is associated with landscape-level drivers. Nature 574, 671–674. https://doi.org/10.1038/s41586-019-1684-3.

Serra, P., Pons, X., Saurí, D., 2008. Land-cover and land-use change in a Mediterranean landscape: a spatial analysis of driving forces integrating biophysical and human factors. Appl. Geogr. 28, 189–209. https://doi.org/10.1016/j.apgeog.2008.02.001.

Silveira, J.J., Espíndola, A.L., Penna, T.J.P., 2006. Agent-based model to rural–urban migration analysis. Phys. Stat. Mech. Appl. 364, 445–456. https://doi.org/10.1016/j.physa.2005.08.055.

Simon, C., Etienne, M., 2010. A companion modelling approach applied to forest management planning. Environ. Model. Software 25, 1371–1384. https://doi.org/10.1016/j.envsoft.2009.09.004.

Sinclair, R., 1967. Von Thünen and urban sprawl. Ann. Assoc. Am. Geogr. 57, 72–87. https://doi.org/10.1111/j.1467-8306.1967.tb00591.x.

Singh, V.P., Woolhiser, D.A., 2002. Mathematical modeling of watershed hydrology. J. Hydrol. Eng. 7, 270–292. https://doi.org/10.1061/(ASCE)1084-0699(2002)7:4(270).

Sirami, C., Gross, N., Baillod, A.B., Bertrand, C., Carrié, R., Hass, A., Henckel, L., Miguet, P., Vuillot, C., Alignier, A., Girard, J., Batáry, P., Clough, Y., Violle, C., Giralt, D., Bota, G., Badenhausser, I., Lefebvre, G., Gauffre, B., Vialatte, A., Calatayud, F., Gil-Tena, A., Tischendorf, L., Mitchell, S., Lindsay, K., Georges, R., Hilaire, S., Recasens, J., Solé-Senan, X.O., Robleño, I., Bosch, J., Barrientos, J.A., Ricarte, A., Marcos-Garcia, M.Á., Miñano, J., Mathevet, R., Gibon, A., Baudry, J., Balent, G., Poulin, B., Burel, F., Tscharntke, T., Bretagnolle, V., Siriwardena, G., Ouin, A., Brotons, L., Martin, J.-L., Fahrig, L., 2019. Increasing crop heterogeneity enhances multitrophic diversity across agricultural regions. Proc. Natl. Acad. Sci. U. S. A. 116, 16442–16447. https://doi.org/10.1073/pnas.1906419116.

Skrimizea, E., Lecuyer, L., Bunnefeld, N., Butler, J.R.A., Fickel, T., Hodgson, I., Holtkamp, C., Marzano, M., Parra, C., Pereira, L., Petit, S., Pound, D., Rodríguez, I., Ryan, P., Staffler, J., Vanbergen, A.J., Van den Broeck, P., Wittmer, H., Young, J.C., 2020. Sustainable agriculture: recognizing the potential of conflict as a positive driver for transformative change. In: Advances in Ecological Research. Elsevier, pp. 255–311. https://doi.org/10.1016/bs.aecr.2020.08.003.

Slone, D.H., 2011. Increasing accuracy of dispersal kernels in grid-based population models. Ecol. Model. 222, 573–579. https://doi.org/10.1016/j.ecolmodel.2010.11.023.

Soubeyrand, S., Roques, L., 2014. Parameter estimation for reaction-diffusion models of biological invasions. Popul. Ecol. 56, 427–434. https://doi.org/10.1007/s10144-013-0415-0.

Souchère, V., Millair, L., Echeverria, J., Bousquet, F., Le Page, C., Etienne, M., 2010. Co-constructing with stakeholders a role-playing game to initiate collective management of erosive runoff risks at the watershed scale. Environ. Model. Software 25, 1359–1370. https://doi.org/10.1016/j.envsoft.2009.03.002.

Specht, K., Siebert, R., Hartmann, I., Freisinger, U.B., Sawicka, M., Werner, A., Thomaier, S., Henckel, D., Walk, H., Dierich, A., 2014. Urban agriculture of the future: an overview of sustainability aspects of food production in and on buildings. Agric. Hum. Values 31, 33–51. https://doi.org/10.1007/s10460-013-9448-4.

Spooner, F.E.B., Pearson, R.G., Freeman, R., 2018. Rapid warming is associated with population decline among terrestrial birds and mammals globally. Glob. Chang. Biol. 24, 4521–4531. https://doi.org/10.1111/gcb.14361.

Steenweg, R., Hebblewhite, M., Kays, R., Ahumada, J., Fisher, J.T., Burton, C., Townsend, S.E., Carbone, C., Rowcliffe, J.M., Whittington, J., Brodie, J., Royle, J.A., Switalski, A., Clevenger, A.P., Heim, N., Rich, L.N., 2017. Scaling-up camera traps: monitoring the planet's biodiversity with networks of remote sensors. Front. Ecol. Environ. 15, 26–34. https://doi.org/10.1002/fee.1448.

Straubhaar, J., Renard, P., Mariethoz, G., Froidevaux, R., Besson, O., 2011. An improved parallel multiple-point algorithm using a list approach. Math. Geosci. 43, 305–328. https://doi.org/10.1007/s11004-011-9328-7.

Sullivan, C.A., Bourke, D., Skeffington, M.S., Finn, J.A., Green, S., Kelly, S., Gormally, M.J., 2011. Modelling semi-natural habitat area on lowland farms in western Ireland. Biol. Conserv. 144, 1089–1099. https://doi.org/10.1016/j.biocon.2010.12.028.

Tenaillon, O., 2014. The utility of Fisher's geometric model in evolutionary genetics. Annu. Rev. Ecol. Evol. Syst. 45, 179–201. https://doi.org/10.1146/annurev-ecolsys-120213-091846.

Thapa, R.B., Murayama, Y., 2008. Land evaluation for peri-urban agriculture using analytical hierarchical process and geographic information system techniques: a case study of Hanoi. Land Use Policy 25, 225–239. https://doi.org/10.1016/j.landusepol.2007.06.004.

Thies, C., Tscharntke, T., 1999. Landscape structure and biological control in agroecosystems. Science 285, 893–895.

Tieskens, K.F., Shaw, B.J., Haer, T., Schulp, C.J.E., Verburg, P.H., 2017. Cultural landscapes of the future: using agent-based modeling to discuss and develop the use and management of the cultural landscape of south West Devon. Landsc. Ecol. 32, 2113–2132. https://doi.org/10.1007/s10980-017-0502-2.

Tilman, D., 1999. Global environmental impacts of agricultural expansion: the need for sustainable and efficient practices. Proc. Natl. Acad. Sci. U. S. A. 96, 5995–6000. https://doi.org/10.1073/pnas.96.11.5995.

Tilman, D., 2001. Forecasting agriculturally driven global environmental change. Science 292, 281–284. https://doi.org/10.1126/science.1057544.

Tixier, P., Peyrard, N., Aubertot, J.-N., Gaba, S., Radoszycki, J., Caron-Lormier, G., Vinatier, F., Mollot, G., Sabbadin, R., 2013. Modelling interaction networks for enhanced ecosystem Services in Agroecosystems. In: Advances in Ecological Research. Elsevier, pp. 437–480. https://doi.org/10.1016/B978-0-12-420002-9.00007-X.

Todman, L.C., Coleman, K., Milne, A.E., Gil, J.D.B., Reidsma, P., Schwoob, M.-H., Treyer, S., Whitmore, A.P., 2019. Multi-objective optimization as a tool to identify possibilities for future agricultural landscapes. Sci. Total Environ. 687, 535–545. https://doi.org/10.1016/j.scitotenv.2019.06.070.

Topping, C.J., Odderskær, P., Kahlert, J., 2013. Modelling skylarks (Alauda arvensis) to predict impacts of changes in land management and policy: development and testing of an agent-based model. PLoS One 8, e65803. https://doi.org/10.1371/journal.pone.0065803.

Tresson, P., Tixier, P., Puech, W., Bagny Beilhe, L., Roudine, S., Pagès, C., Carval, D., 2019. CORIGAN: assessing multiple species and interactions within images. Methods Ecol. Evol. 10, 1888–1893. https://doi.org/10.1111/2041-210X.13281.

Tscharntke, T., Clough, Y., Bhagwat, S.A., Buchori, D., Faust, H., Hertel, D., Hölscher, D., Juhrbandt, J., Kessler, M., Perfecto, I., Scherber, C., Schroth, G., Veldkamp, E., Wanger, T.C., 2011. Multifunctional shade-tree management in tropical agroforestry landscapes—a review: multifunctional shade-tree management. J. Appl. Ecol. 48, 619–629. https://doi.org/10.1111/j.1365-2664.2010.01939.x.

Tscharntke, T., Tylianakis, J.M., Rand, T.A., Didham, R.K., Fahrig, L., Batáry, P., Bengtsson, J., Clough, Y., Crist, T.O., Dormann, C.F., Ewers, R.M., Fründ, J., Holt, R.D., Holzschuh, A., Klein, A.M., Kleijn, D., Kremen, C., Landis, D.A., Laurance, W., Lindenmayer, D., Scherber, C., Sodhi, N., Steffan-Dewenter, I., Thies, C., van der Putten, W.H., Westphal, C., 2012. Landscape moderation of biodiversity patterns and processes—eight hypotheses. Biol. Rev. 87, 661–685. https://doi.org/10.1111/j.1469-185X.2011.00216.x.

Tsiafouli, M.A., Thébault, E., Sgardelis, S.P., de Ruiter, P.C., van der Putten, W.H., Birkhofer, K., Hemerik, L., de Vries, F.T., Bardgett, R.D., Brady, M.V., Bjornlund, L., Jørgensen, H.B., Christensen, S., Hertefeldt, T.D., Hotes, S., Gera Hol, W.H., Frouz, J., Liiri, M., Mortimer, S.R., Setälä, H., Tzanopoulos, J., Uteseny, K., Pižl, V., Stary, J., Wolters, V., Hedlund, K., 2015. Intensive agriculture reduces soil biodiversity across Europe. Glob. Chang. Biol. 21, 973–985. https://doi.org/10.1111/gcb.12752.

Tulloch, A.I.T., Possingham, H.P., Joseph, L.N., Szabo, J., Martin, T.G., 2013. Realising the full potential of citizen science monitoring programs. Biol. Conserv. 165, 128–138. https://doi.org/10.1016/j.biocon.2013.05.025.

Urban, D., Keitt, T., 2001. Landscape connectivity: a graph-theoretic perspective. Ecology 82, 1205–1218. https://doi.org/10.1890/0012-9658(2001)082[1205:LCAGTP]2.0.CO;2.

Van Lieshout, M.N.M., 2019. Theory of Spatial Statistics: A Concise Introduction. CRC Press, Boca Raton, Florida.

van Strien, M.J., Slager, C.T.J., de Vries, B., Grêt-Regamey, A., 2016. An improved neutral landscape model for recreating real landscapes and generating landscape series for spatial ecological simulations. Ecol. Evol. 6, 3808–3821. https://doi.org/10.1002/ece3.2145.

Verburg, P.H., Overmars, K.P., 2009. Combining top-down and bottom-up dynamics in land use modeling: exploring the future of abandoned farmlands in Europe with the dyna-CLUE model. Landsc. Ecol. 24, 1167–1181. https://doi.org/10.1007/s10980-009-9355-7.

Verburg, P.H., van Berkel, D.B., van Doorn, A.M., van Eupen, M., van den Heiligenberg, H.A.R.M., 2010. Trajectories of land use change in Europe: a model-based exploration of rural futures. Landsc. Ecol. 25, 217–232. https://doi.org/10.1007/s10980-009-9347-7.

Verburg, P.H., Dearing, J.A., Dyke, J.G., van der Leeuw, S., Seitzinger, S., Steffen, W., Syvitski, J., 2016. Methods and approaches to modelling the Anthropocene. Glob. Environ. Chang. 39, 328–340. https://doi.org/10.1016/j.gloenvcha.2015.08.007.

Vinatier, F., Chauvet, M., 2017. A neutral model for the simulation of linear networks in territories. Ecol. Model. 363, 8–16. https://doi.org/10.1016/j.ecolmodel.2017.08.022.

Vinatier, F., Tixier, P., Duyck, P.F., Lescourret, F., 2011. Factors and mechanisms explaining spatial heterogeneity: a review of methods for insect populations. Methods Ecol. Evol. 2, 11–22.

Vinatier, F., Gosme, M., Valantin-Morison, M., 2013. Explaining host–parasitoid interactions at the landscape scale: a new approach for calibration and sensitivity analysis of complex spatio-temporal models. Landsc. Ecol. 28, 217–231. https://doi.org/10.1007/s10980-012-9822-4.

Vinatier, F., Lagacherie, P., Voltz, M., Petit, S., Lavigne, C., Brunet, Y., Lescourret, F., 2016. An unified framework to integrate biotic, abiotic processes and human activities in spatially explicit models of agricultural landscapes. Front. Environ. Sci. 4. https://doi.org/10.3389/fenvs.2016.00006.

Vinatier, F., Bailly, J.-S., Belaud, G., 2017. From 3*D* grassy vegetation point cloud to hydraulic resistance: application to close-range estimation of Manning coefficients for intermittent open channels. Ecohydrology 10, e1885. https://doi.org/10.1002/eco.1885.

Vinatier, F., Dollinger, J., Rudi, G., Feurer, D., Belaud, G., Bailly, J.-S., 2018. The use of photogrammetry to construct time series of vegetation permeability to water and seed transport in agricultural waterways. Remote Sens. (Basel) 10, 2050. https://doi.org/10.3390/rs10122050.

Violle, C., Navas, M.-L., Vile, D., Kazakou, E., Fortunel, C., Hummel, I., Garnier, E., 2007. Let the concept of trait be functional! Oikos 116, 882–892. https://doi.org/10.1111/j.0030-1299.2007.15559.x.

Vitousek, P.M., 1997. Human domination of Earth's ecosystems. Science 277, 494–499. https://doi.org/10.1126/science.277.5325.494.

Vogel, G., 2017. Where have all the insects gone? Science 356, 576–579. https://doi.org/10.1126/science.356.6338.576.

Voinov, A., Bousquet, F., 2010. Modelling with stakeholders. Environ. Model. Software 25, 1268–1281. https://doi.org/10.1016/j.envsoft.2010.03.007.

Voinov, A., Kolagani, N., McCall, M.K., Glynn, P.D., Kragt, M.E., Ostermann, F.O., Pierce, S.A., Ramu, P., 2016. Modelling with stakeholders—next generation. Environ. Model. Software 77, 196–220. https://doi.org/10.1016/j.envsoft.2015.11.016.

Von Thünen, J.H., 1826. Von Thünen's Isolated State. Pergamon Press, Glasgow.

Walangitan, H.D., Setiawan, B., Tri Raharjo, B., Polii, B., 2012. Optimization of land use and allocation to ensure sustainable agriculture in the catchment area of Lake Tondano, Minahasa, North Sulawesi, Indonesia. Int. J. Civ. Env. Eng. 12, 68–75. IJCEE-IJENS.

Wäldchen, J., Mäder, P., 2018. Machine learning for image based species identification. Methods Ecol. Evol. 9, 2216–2225. https://doi.org/10.1111/2041-210X.13075.

Warren, B.H., Simberloff, D., Ricklefs, R.E., Aguilée, R., Condamine, F.L., Gravel, D., Morlon, H., Mouquet, N., Rosindell, J., Casquet, J., Conti, E., Cornuault, J., Fernández-Palacios, J.M., Hengl, T., Norder, S.J., Rijsdijk, K.F., Sanmartín, I., Strasberg, D., Triantis, K.A., Valente, L.M., Whittaker, R.J., Gillespie, R.G., Emerson, B.C., Thébaud, C., 2015. Islands as model systems in ecology and evolution: prospects fifty years after MacArthur-Wilson. Ecol. Lett. 18, 200–217. https://doi.org/10.1111/ele.12398.

Weimerskirch, H., Shaffer, S., Tremblay, Y., Costa, D., Gadenne, H., Kato, A., Ropert-Coudert, Y., Sato, K., Aurioles, D., 2009. Species- and sex-specific differences in foraging behaviour and foraging zones in blue-footed and brown boobies in the Gulf of California. Mar. Ecol. Prog. Ser. 391, 267–278. https://doi.org/10.3354/meps07981.

Wiens, J.A., Stenseth, N.C., Horne, B.V., Ims, R.A., 1993. Ecological mechanisms and landscape ecology. Oikos 66, 369. https://doi.org/10.2307/3544931.

With, K.A., 2019. Essentials of Landscape Ecology, first ed. Oxford University Press. https://doi.org/10.1093/oso/9780198838388.001.0001.

World Bank, 2020. Urban development. [WWW Document]. URL https://www.worldbank.org/en/topic/urbandevelopment/overview. (accessed 9.1.20).

Xiao, Y., Mignolet, C., Mari, J.-F., Benoît, M., 2014. Modeling the spatial distribution of crop sequences at a large regional scale using land-cover survey data: a case from France. Comput. Electron. Agric. 102, 51–63. https://doi.org/10.1016/j.compag.2014.01.010.

Zabel, F., Delzeit, R., Schneider, J.M., Seppelt, R., Mauser, W., Václavík, T., 2019. Global impacts of future cropland expansion and intensification on agricultural markets and biodiversity. Nat. Commun. 10, 2844. https://doi.org/10.1038/s41467-019-10775-z.

Zamberletti, P., Papaïx, J., Gabriel, E., Opitz, T., 2020. Landscape Allocation: Stochastic Generators and Statistical Inference. arXiv:2003.02155 Q-Bio Stat.

Zander, P., Groot, J.C.J., Josien, E., Karpinski, I., Knierim, A., Meyer, B.C., Madureira, L., Rambonilaza, M., Rossing, W.A.H., 2008. Farm models and economic valuation in the context of multifunctionality: a review of approaches from France, Germany, the Netherlands and Portugal. Int. J. Agric. Resour. Gov. Ecol. 7, 339. https://doi.org/10.1504/IJARGE.2008.020084.

Zasada, I., Loibl, W., Köstl, M., Piorr, A., 2013. Agriculture under human influence: a spatial analysis of farming systems and land use in European rural-Urban-regions. Eur. Countrys. 5 (1), 71–88. https://doi.org/10.2478/euco-2013-0005.

Submitted to the Annals of Applied Statistics

MARKOV RANDOM FIELD MODELS FOR VECTOR-BASED REPRESENTATIONS OF LANDSCAPES

BY PATRIZIA ZAMBERLETTI*, JULIEN PAPAÏX*, EDITH GABRIEL* AND THOMAS OPITZ*

*Biostatistics and Spatial Processes, INRAE, Avignon, France**
patrizia.zamberletti@inrae.fr; julien.papaix@inrae.fr; edith.gabriel@inrae.fr; thomas.opitz@inrae.fr

In agricultural landscapes, the spatial distribution of cultivated and semi-natural elements strongly impacts habitat connectivity and species dynamics. To allow for landscape structural analysis and scenario generation, we here develop statistical tools for real landscapes composed of geometric elements, including 2D patches but also 1D linear elements (e.g., hedges). Utilizing the framework of discrete Markov random fields, we design generative stochastic models that combine a multiplex network representation based on spatial adjacency with Gibbs energy terms to capture the distribution of landscape descriptors for land-use categories. We implement simulation of agricultural scenarios with parameter-controlled spatial and temporal patterns (e.g., geometry, connectivity, crop-rotation), and we demonstrate through simulation that pseudo-likelihood estimation of parameters works well. To study statistical relevance of model components in real landscapes, we discuss model selection and validation, including cross-validated prediction scores. Model validation with view towards ecologically relevant landscape summaries is achieved by comparing observed and simulated summaries (network metrics, but also metrics and appropriately defined variograms using a raster discretization). Models fitted to subregions of the Lower Durance Valley (France) indicate strong deviation from random allocation and realistically capture landscape patterns. In summary, our approach improves the understanding of agroecosystems and enables simulation-based theoretical analysis of how landscape patterns shape biological and ecological processes.

1. Introduction. Agroecosystems are the basis for food production and other ecosystem services such as biodiversity, pollination and pest control (Power, 2010; Foresight, 2011). Landscape heterogeneity plays an important role for many agroecological processes. It can be expressed through landscape *configuration*, referring to the size, shape, and spatial-temporal arrangement of land-use patches (e.g., clustering, repulsiveness), and through landscape *composition*, referring to the number and proportion of land-use types (Martin et al., 2019). Generative models are widely applied in landscape ecology for simulating virtual landscapes (i.e., a mosaic of fields having shapes and properties that vary in space and time, and provide a support for biotic and abiotic processes) to systematically study the effects and impacts of landscape heterogeneity on ecosystem processes; see the recent reviews of Poggi et al. (2018); Langhammer et al. (2019). The purpose of such models is to generate a high number of virtual but structurally realistic maps of land-cover (Gardner, 1999; Saura and Martinez-Millan, 2000; Gardner and Urban, 2007; Sciaini et al., 2018), and often parameters related to landscape features such as the percentage of land-cover, the habitat fragmentation, or spatial autocorrelation (Langhammer et al., 2019) can be controlled. In this paper, we focus on modeling agricultural landscapes, and we consider neutral landscape models where the model does not directly interact with the biotic or abiotic processes (Gardner et al., 1987; With and King, 1997).

Keywords and phrases: Graphical model, Markov-chain Monte-Carlo simulation, Multiplex-network, Pseudo-likelihood, Statistical landscape modeling, Stochastic geometry

Existing models use either a vector-based or a raster-based representation, with the majority of models being of raster type. The raster approach is particularly useful for modelling gradual landscape dynamics and continuous processes (e.g., Lin et al., 2014). However, agricultural landscapes are strongly characterized by polygon-shaped patches and piecewise linear corridors along polygon boundaries, such that vector approaches seem preferable (Gaucherel et al., 2006a,b; Le Ber et al., 2009; Papaïx et al., 2014; Inkoom et al., 2017; Langhammer et al., 2019). In particular, fringe structures such as hedgerows, roads or ditches aligned along polygon boundaries, have an important impact on many agroecological processes despite their small surface proportion. In a vector-based framework, Gaucherel et al. (2006a,b) use models based on Gibbs energy terms to control certain pairwise interactions between landscape elements with the aim of simulating patches and certain fringe structures. Papaïx et al. (2014) develop a landscape generator without fringe structures that generates the landscape mosaic with two types of fields based on the Gibbsian T-tessellation model of Kiêu et al. (2013). However, existing modeling frameworks lack tools for parameter inference and model validation. Validation procedures are usually solely based on testing whether simulated landscapes are able to reproduce realistic landscape features by comparing observed and simulated landscape metrics (e.g., from the FRAGSTAT library, McGarigal and Marks, 1995). Such metrics are often directly used within simulation algorithms to enforce convergence towards target values (Langhammer et al., 2019).

Vector-based approaches are independent of the grid resolution and give better control over small-surface elements, and they provide a sparser and more functional representation of patchy geometric structures without continuous gradients. The approach that we develop is geared towards flexible and realistic parametric stochastic modeling of fringe structures, such as hedgerow networks. For these reasons, we advocate to turn away from the raster paradigm when modeling agricultural landscapes. Using a network-based representation of interactions among landscape elements, we construct Gibbs energies based on network structure (see, e.g., the recent collection of papers introduced by Fienberg, 2010), and more specifically models pertaining to the widely used class of discrete Markov random fields, see the seminal work of Hammersley and Clifford (1971); Besag (1972). Approaches relevant to our work are the nearest-neighbour Markov structures of Baddeley and Møller (1989) and the representations based on connected components introduced in Møller and Waagepetersen (1998). Recent developments and reviews are exposed in van Lieshout (2000); Green et al. (2003); Gaetan and Guyon (2010); van Lieshout (2019). The use of Gibbs energies, and of Markov structures in particular, provides a natural distributional framework for controlling landscape descriptors. Likelihood-based statistical inference in such classification models, here formulated for categories of landscape elements, is notoriously difficult due to an intractable normalizing constant. We therefore resort to well-established pseudo-likelihood estimation, for which model selection and validation are more intricate and need to be performed carefully, especially in our setting with only a single observed realization of the process.

We suppose that the polygon structure of patches in a bounded subset of planar space $\mathbb{R}^2$ is given, i.e., a tessellation of space serves as fixed support of the model. It can be obtained by preprocessing a real landscape, or we may use simulations of a parametric tessellation model to generate realistic features (e.g., Kiêu et al., 2013). We model the stochastic land-use allocation mechanism of patches and linear elements by assigning categories to the polygons and their edges, where dynamic structures such as crop rotation are possible.

An overarching goal is to generate visually realistic landscapes. We develop the following methodological novelties: i) a mathematical representation of landscape composition and configuration through multilayer networks; ii) generative stochastic parametric models coupling land-use allocation of patches and linear elements, relying strongly on Markov interactions based on the network established in (i); iii) simulation of such models using Markov

Chain Monte Carlo (MCMC) with the Gibbs sampler; iv) statistical inference using real landscape data; v) validation of relevant landscape characteristic based on a comparison of summaries for vector and raster representations between real and simulated landscapes. Our approach can handle relatively large landscapes by capitalizing on low computational requirements thanks to vector-based representations and to sparse-matrix structures for encoding interactions.

The paper is structured as follows. Section 2 presents real landscape data and preprocessing steps for an agricultural region in southeastern France, for which previous studies have highlighted a key role of agricultural practices and hedgerow configuration for biodiversity and pest control (Ricci et al., 2009; Maalouly et al., 2013; Lefebvre et al., 2016). In Section 3, we propose the mathematical representation, modeling and simulation of landscapes. Tools for statistical inference, including model selection and validation, are developed in Section 4. In Section 5, we apply the developed framework to the above data, and we discuss how the goodness-of-fit and the generation of realistic landscape metrics is influenced by the choice of the descriptors in the model. A discussion in Section 6 concludes the paper. Supplementary material contains details on the simulation algorithm and additional estimation and simulation results (Zamberletti et al., 2021).

2. Landscape data. Real data for agricultural landscapes are based on remote sensing images, digital land registers, land-cover data bases such as CORINE (Büttner and Maucha, 2006), and field data. Often, manual annotation steps are necessary to complete and clean data. We study the Lower Durance Valley in southeastern France depicted in Figure 1a, stretching over 163 km^2 and mainly characterized by agricultural activity (87%) and urbanized areas, with main cultures of open area (46%) and apple/pear orchards (24%).

Data are based on manual digitalization (ArcView software) using an official French database of aerial photographs (BD ORTHO, IGN, 2004, 0.5 m resolution, updated with field monitoring in 2009).

The region has a total length of 1146 km of hedgerows, which we will represent as linear segments, whose average length amounts to 105 m. A particularity of the region is a dominance of East-West oriented hedges, whose function is to break the strong Mistral winds blowing from the North.

For the data application in this paper, we select three subdomains D1, D2 and D3 with contrasting properties and dimensions, shown in Figure 1b and numerically summarized in Table 1: D1 is relatively small and dominated by semi-natural surfaces; D2 has the same surface area but equal proportions of semi-natural and crop; D3 delimits a much larger domain including D1 and D2.

	D1	D2	D3
Area (km^2)	3.37	2.3	41.13
% of Semi-natural	73	50	76
% of Crop	27	50	24
Hedgerows (km)	44.64	33.61	386.36
No. of patches	368	468	4379
No. of linear segments	1105	1405	12517

Table 1: Summary of selected subregions of the Lower Durance Valley study area; see Figure 1.

We use a simplified representation of the landscape as a tessellation of 2D space with polygon-shaped cells. Linear segments (e.g., hedgerows) correspond to polygon edges. To achieve a partition of space through polygon-shaped patches, and to align hedgerows with

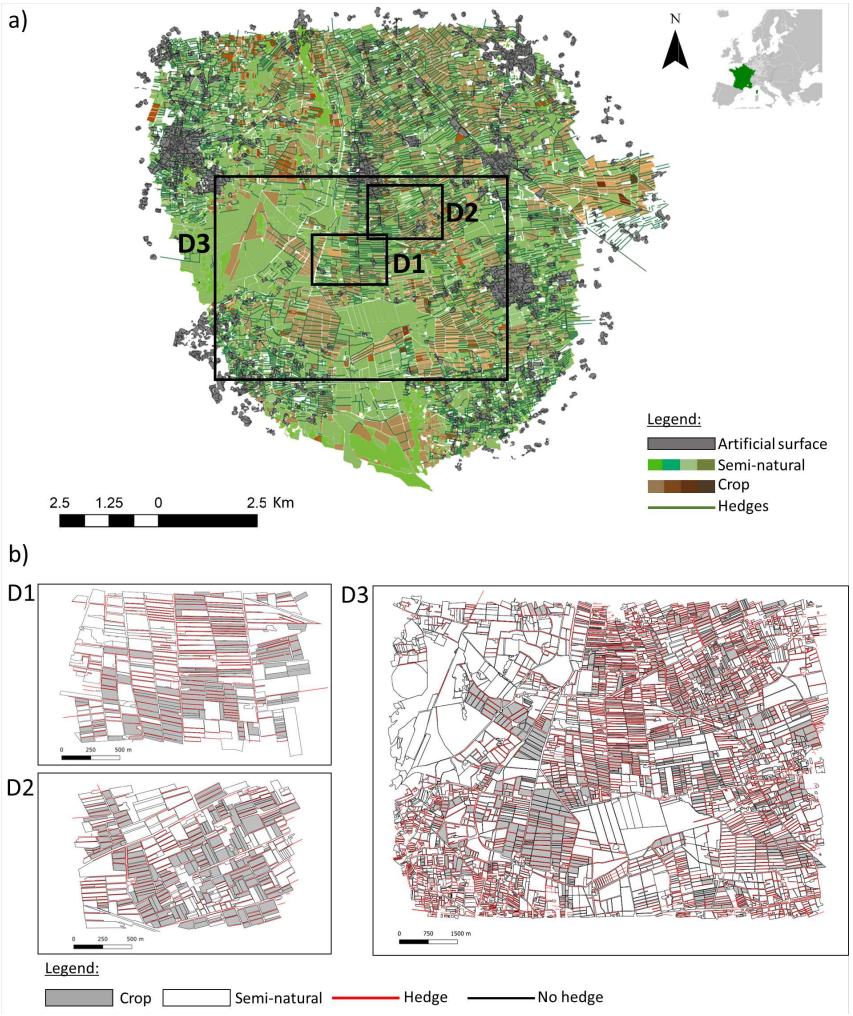

FIG 1. *Lower Durance Valley study area. a) Full area with three subdomains. b) Subdomains D1, D2, D3. The Lower Durance Valley is characterised mainly by agricultural cover: green-shaded patches represent semi-natural area (i.e., woods, open area, grassland); brown-shaded patches represent 34 different cultures (e.g., apple, pear, vineyards). Artificial surface (dark gray) consists of built structures and urbanized area. The area is rich in linear elements (i.e., segments), including small water courses, roads and hedges (Panel a). In the selected domains (Panel b), we selected as "crop" the category of "apple/pear orchard", as it is the most abundant culture (gray patches), and we simplify the rest of the landscape surface as semi-natural area (white patches) in order to establish a continuous cover with two categories. Patch boundaries are presented as linear elements, which are marked in red when hedges are present.*

polygon edges, we preprocess the landscape towards a polygon tessellation of 2D space (Boots et al., 1999), based on a heuristic loss criterion measuring the distance between original and transformed landscape (Adamczyk-Chauvat et al., 2020). Figure 2 illustrates that preprocessing modifications for domain D2 are mostly minor. For simplicity, we here attribute

always one of the two categories of "crop" or "semi-natural" to the patches in the three study domains. Specifically, we gather several types of semi-natural habitat into a single category, including some patches with built structures (farms, greenhouses...). In principle, the subsequent modeling would also allow for parts of the landscape with unspecified category. While we here consider tessellations as a fixed support for linear element attribution and crop rotation, tessellation simulation algorithms for agricultural landscapes (Kiêu et al., 2013; Papaïx et al., 2014; Poggi et al., 2018) would enable the generation of new, synthetic but realistic supports for our models.

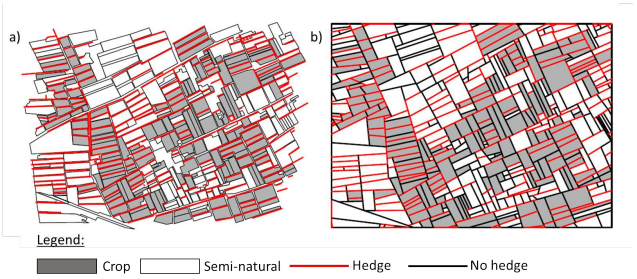

FIG 2. *Preprocessing of domain D2. a) Original digitalized shapefile; b) Preprocessed landscape tessellation defined over a rectangular domain.*

3. Stochastic modeling and simulation of landscape allocation.

3.1. *Mathematical landscape representation.* We propose to represent a landscape as a collection $\mathcal{O} = \{o_1, \ldots, o_n\}$ of n geometric objects as follows,

$$o_i = (x_i, z_i), \quad x_i \in \mathcal{X}_i = \{0, 1, \ldots, \ell_i - 1\}, \quad i = 1, \ldots, n, \tag{1}$$

where each element is composed of two sets of data x_i and z_i. The information in $\boldsymbol{z} = (z_1, \ldots, z_n)$ represents the geometrical structure of the landscape, determining object dimension and their organisation, and it is considered as being fixed. The vector $\boldsymbol{x} = (x_1, \ldots, x_n)$ represents categories that we allocate to the geometric elements in the landscape, such as land-use types among hedges, water courses (for linear elements) or crop, grassland (for patches), and that we aim to model. We suppose that $x_i \in \mathcal{X}_i$ with a finite space $\mathcal{X}_i$ of $\ell_i \geq 1$ possible categories for the ith element, where the index 0 usually represents a baseline category. The objects $o_i = (x_i, z_i)$ could represent different geometric types, such as polygons (i.e., habitat patches) or linear segments (i.e., linear landscape elements), see Figure 3a. For polygon objects, the data component z_i could contain this type information, and in addition the geographical coordinates of its vertices, its surface area, and potentially other exogenous covariates. For instance, we could allocate each polygon with a category among the following three options: *crop* ($x_i = 1$), *(semi-)natural habitat* ($x_i = 2$), *other* ($x_i = 0$). A linear segment could be allocated with a category among *hedgerow* ($x_i = 1$) or *no hedgerow* ($x_i = 0$). In the case $\ell_i = 1$ with only a single category $x_i = 0$ no choice of allocation has to be made. The space of all possible combinations of allocations is $\mathcal{X} = \mathcal{X}_1 \otimes \mathcal{X}_2 \otimes \ldots \otimes \mathcal{X}_n$. This finite collection contains $|\mathcal{X}| = \ell_1 \times \ell_2 \times \ldots \times \ell_n$ possible allocations. If the geometric structure contained in z_i may vary through time, it is possible to describe temporal dynamics (if present) by the sequence $x_{i,\tau}$, $\tau = 1, 2, \ldots$ of categories allocated within patches over discrete time.

3.2. *Network model of landscape.* We use a graphical representation of landscape to capture spatial or functional adjacency of landscape elements such as patches or linear segments in Figure 1b. Adjacency of objects is modeled through a multilayer or multiplex network, i.e., a set of single network layers with some nodes connected between layers (Boccaletti et al., 2014; Kivelä et al., 2014). Each layer in this graphical representation corresponds to an object type; nodes stand for individual objects; edges in single network layers represent adjacency of objects of the same type; edges between different network layers represent adjacency of objects of different type. There are two types of networks that can be considered. First, for the specification of the Markov models we develop, we need a network that represents the fixed landscape support where the layers correspond to patches and to linear segments, respectively, in our setting. The probability of landscape category allocations in *pairwise Markov models* is then constructed from individual contributions of the nodes and edges in this network. Second, given a landscape allocation, we can consider the network where each layer corresponds to a specific allocation category. In the case of categories "crop" and "semi-natural" for patches, and of categories "hedge" and "no hedge" for linear segments, we obtain four layers. This second network type is useful for calculating landscape metrics taking into account allocation.

We illustrate the structure of the first network used for constructing Markov models. We define a collection of objects with two types, $\mathbf{o} = (\mathbf{o}^C, \mathbf{o}^H)$ (see Figure 3a), where $o_i^C = (x_i^C, z_i^C)$, $i = 1, \dots, n^C$ represent patches (layer C), and $o_i^H = (x_i^H, z_i^H)$, $i = 1, \dots, n^H$ represent linear segments (layer H); see Figure 3b. We express that two distinct objects o_1 and o_2 are directly connected through an edge in the graph (i.e., they are adjacent) using the following notation:

$$o_1 \sim o_2, \quad o_1, o_2 \in \mathcal{O}. \tag{2}$$

For the models in this paper, we assume that two patches o_i^C, o_j^C are connected, $o_i^C \sim o_j^C$, if they are adjacent, i.e., if they share part of their physical boundary; two linear elements are connected if they intersect or have a vertex in common; finally, inter-layer connections $o_i^C \sim o_j^H$ arise if the linear element o_j^H is located on the boundary of patch o_i^C. This structure is similar to the nearest-neighbour relations discussed in Section 4 of Baddeley and Møller (1989) with respect to Markov properties.

For mathematical operations based on the network structure, we encode the object interactions in the *network matrix* (or *adjacency matrix*) $\mathcal{A}$:

$$\mathcal{A} = \begin{pmatrix} A^C & A^{CH} \\ A^{HC} & A^H \end{pmatrix}, \quad \mathcal{A}_{i,j} = \begin{cases} 1, & o_i \sim o_j, \\ 0, & o_i \not\sim o_j, \end{cases} \quad i, j \in \{1, \dots, n^C + n^H\}, \tag{3}$$

where $A^C \in \mathbb{R}^{n^C \times n^C}$ and $A^H \in \mathbb{R}^{n^H \times n^H}$ represent the network matrices of intra-layer connections of C and H, respectively, and $A^{CH} \in \mathbb{R}^{n^C \times n^H}$ encodes inter-layer connections among C and H. For simplicity, we here assume symmetric connections with binary weights, such that $\mathcal{A}_{ij} \in \{0, 1\}$ and $\mathcal{A} = \mathcal{A}^T$, but the extension to asymmetric and directed connections with $\mathcal{A}_{ij} \in \mathbb{R} \setminus \{0\}$ if $o_i \sim o_j$ would be straightforward. Non-binary weights could be based on distance or sizes of connected elements.

Based on this landscape representation, we develop parametric probability distributions over the allocations $\boldsymbol{x} \in \mathcal{X}$, conditional on the (fixed) information in $\boldsymbol{z} = (z_1, \dots, z_n)$ and $\mathcal{A}$. We put focus on Markov models where we assume conditional independence of category x_i with respect to $\boldsymbol{z}$ and the categories of objects not directly connected with o_i through the $\sim$-relation of adjacency.

We adopt notations such as $\boldsymbol{o}_{-i}$ to refer to the set $\mathcal{O} \setminus \{o_i\}$. Therefore, we make the following assumption of equality of conditional distributions:

$$x_i \,|\, (z_i,\, o_{-i}) \quad \stackrel{d}{=} \quad x_i \,|\, (\boldsymbol{z},\, \{o_j \in \mathcal{O} \,|\, o_i \sim o_j\}), \quad i = 1, \ldots, n^C + n^H. \tag{4}$$

This framework allows for flexible dependence structures expressed through the adjacency matrix $\mathcal{A}$ with sparse structure, i.e., with a relatively small proportion of non-zero entries.

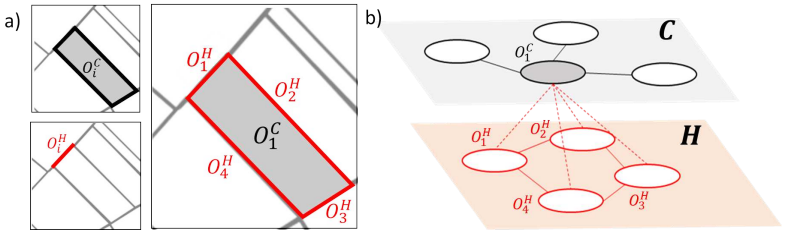

FIG 3. *Landscape representation. a) Polygon objects (patches, in grey) and linear segment objects (in red). b) Multi-layer network of connections. Layer C: single network of connections between patches; layer H: single network of connections between linear elements; links between C and H represent connections of patches and linear elements.*

3.3. *Probabilistic mechanistic models for landscape descriptors.* We utilize Gibbs energies to define probabilistic models of mechanistic nature, including Markov processes; see, e.g., Cressie (1991); van Lieshout (2019). We construct a model using m functions $T_k : \mathcal{X} \to (-\infty, \infty)$, $k = 1, \ldots, m$, that each measure the value $T_k(\boldsymbol{x} \mid \boldsymbol{z})$ of a summary statistic for the allocations in $\boldsymbol{x}$ given the fixed information in $\boldsymbol{z}$. In the following, we often omit $\boldsymbol{z}$ for notational simplicity when no confusion arises; e.g., we simply write $T_k(\boldsymbol{x})$. We refer to the T_k as *landscape descriptors* and use them as sufficient statistics of the model by defining the probability of observing an allocation $\boldsymbol{x}$ as follows, with coefficient vector $\boldsymbol{\beta} \in \mathbb{R}^m$:

$$p(\boldsymbol{x}) = \frac{1}{c(\boldsymbol{\beta})} \exp\left(-\sum_{k=1}^{m} \beta_k T_k(\boldsymbol{x}) \right), \quad \boldsymbol{x} \in \mathcal{X}, \quad \boldsymbol{\beta} \in \mathbb{R}^m. \tag{5}$$

The normalizing constant $c(\boldsymbol{\beta}) > 0$, also known as the *partition function*, ensures that probabilities in (5) sum up to 1.

Since the number of possible configurations $|\mathcal{X}|$ is finite, the normalizing constant is finite and the model is well-defined. In practice, the number of configurations is usually very large, such that numerical computation of the constant $c(\boldsymbol{\beta})$ is not tractable. If all descriptors T_k can be represented as sums of terms for single objects or two objects linked in the network through the $\sim$-relation in (2), the Markov property (4) holds.

We will also explore extensions beyond pairwise interactions but related to connected components where the descriptor is still defined through the graph structure. Instead of the *global specification* in Equation (5), we now consider a *local specification*, i.e., the allocation of x_i conditional to fixed information z_i and the rest of the landscape. Therefore, we determine the probability of observing category x_i given $\boldsymbol{z}$ and the allocations $\boldsymbol{x}_{-i}$ of all the other elements,

where we use the notation $(\boldsymbol{x}_{-i}, x) = (x_1, \ldots, x_{i-1}, x, x_{i+1}, \ldots, x_n)$ to indicate an (arbitrary) category x attributed to the object o_i. Then, the normalizing constant $c(\boldsymbol{\beta})$ cancels out

in the conditional probability

$$p(x_i \mid \boldsymbol{x}_{-i}) = \frac{p(\boldsymbol{x})}{\sum_{y \in \mathcal{X}_i} p(\boldsymbol{x}_{-i}, x)} = \frac{\exp\left(-\sum_{k=1}^{m} \beta_k T_k(\boldsymbol{x})\right)}{\sum_{x \in \mathcal{X}_i} \exp\left(-\sum_{k=1}^{m} \beta_k T_k(\boldsymbol{x}_{-i}, x)\right)}, \tag{6}$$

where the denominator adds up the probabilities over all landscape configurations obtained when varying the category of o_i but keeping the rest of the landscape fixed. In the two-level case with $x_i \in \{0, 1\}$, we show in Section 4.1 how parameters β_k can be estimated through classical logistic regression.

3.4. *Examples of parametric models.* Landscape descriptors are intended to capture important landscape characteristics. In *composition terms*, such functions are the sum of contributions of individual objects; in *configuration terms* (or *interaction terms*), we add up contributions that evaluate the spatial interaction of two or more objects. An example specification is as follows, with three generic spatial landscape descriptors given by

$$T^C_{\text{act}}(\boldsymbol{x}) = \sum_{i=1}^{n^C} t(x_i^C), \;\; T^{CC}_{\text{adj}}(\boldsymbol{x}) = \sum_{o_i^C \sim o_j^C} t(x_i^C, x_j^C), \;\; T^{CH}_{\text{adj}}(\boldsymbol{x}) = \sum_{o_i^C \sim o_j^H} t(x_i^C, x_j^H), \tag{7}$$

Then, T_{act} is a composition term, T^{CC}_{adj} an interaction term for network layer C, T^{CH}_{adj} is an interaction term for inter-layer interactions of C and H. Figure 4 illustrates landscape descriptor evaluation on a subarea of D1 using the network to represent landscape interactions. The adjacency network of landscape elements is fixed for all landscape allocations and is based on the information in $\boldsymbol{z}$. It is defined among all the objects of the same layer C (Figure 4a), layer H (Figure 4b) and the interlayer of C and H (Figure 4c). It represents all pairwise interactions (i.e., all the interactions between adjacent patches (4a), adjacent linear segments (Figure 4b) and adjacent linear elements and patches (Figure 4c)). Next, given an allocation of this landscape support, the second network type (also called *active network*) is used to represent the adjacency of objects allocated with the same category (e.g., *crop* category for patches, *hedge* for linear elements). To calculate the landscape descriptors T_k, we illustrate the additive contribution of a single object provides in Figure 5. The fixed information in $\boldsymbol{z}$ characterises the objects through their geometrical properties and assesses how the category allocation could be influenced by features such as the size of the patch (Figure 5b,c), the length or orientation of the linear elements, and determines the adjacency with respect to other objects (Figure 5d,e).

Table 2 illustrates relevant choices of landscape descriptors involving C and H, i.e., patches and linear elements, with 2 allocation categories (i.e., $x_i \in \{0, 1\}$): *crop* ($x_i^C = 1$) or *natural habitat* ($x_i^C = 0$), and *hedgerow* ($x_i^H = 1$) or *no hedgerow* ($x_i^H = 0$). In the supplementary material (Section 2) (Zamberletti et al., 2021), a temporal descriptor for crop rotation is illustrated.

We employ the label of *activity terms* for composition terms where $T(\boldsymbol{x})$ is the count of the number of objects of a specific category. To ensure identifiability, we fix a reference category (e.g., $x_i^C = 0$ for objects of type C) and specify the activity term and its coefficient $\beta^C_{x_i^C} \in \mathbb{R}$ only for categories $x_i^C \neq 0$, such that it is expressed relative to $x_i^C = 0$, and implicitly we have $\beta^C_{x_i^C = 0} = 0$. A positive coefficient $\beta^C_{x_i^C = 1} > 0$ gives relative preference to category 1 over category 0, such that landscapes tend to have more objects of category 1 than of category 0 for type C, provided that the energy terms of other landscape descriptors do not conversely influence the proportion of categories. Markov models with only two-level categories and terms for activity and pairwise interaction can be viewed as variants of the classical Ising model

(Gallavotti, 2013), and more generally of auto-logistic regression models, see Hammersley and Clifford (1971); Besag (1972) and Section 3 of van Lieshout (2019).

Instead, we could also consider landscape descriptors providing a more global perspective on the graph. As an example, we study a global descriptor related to the notion of *connected components* of landscape elements of the same category (see also Møller and Waagepetersen, 1998, which highlight Markov-like properties in this case). By definition, a connected component is a subgraph in which any two vertices are linked to each other along paths of graph edges defined by the $\sim$-related in (2), while there are no connections to any other vertices in the complementary graph. A connected component could represent a cluster of patches or linear elements allocated with the same category. The number of connected components in a landscape conveys global information about spatial clustering of an allocation category, and it can be evaluated through dedicated algorithms (Hopcroft and Tarjan, 1973). Formally, we define the landscape descriptor $T_{cluster}$ as the minimum possible number of sets in any partition $S_1, S_2, ..., S_K$ of $\boldsymbol{O}$ satisfying the following property: $o_i, o_j \in S_k$ if a path along edges between objects in S_k exists from o_i to o_j.

Examples of landscape descriptors			
Composition	Activity term	T^C_{act}, T^H_{act}	$t(x_i^C) = \mathbb{I}(x_i^C = 1)$
	Patch area	$T^C_{\text{area,p}}$	$t(x_i^C; p) = 1(x_i^C = 1,\ \text{area}(o_i^C) \leq \mathbb{Q}_p(\text{area}(o_i^C)))$
	Long segments	T^H_{length}	$t(x_i^H) = 1(x_i^H = 1,\ \text{length}(o_i^H) \geq \mathbb{E}[\text{length}(o_i^H)])$
	Horizontal segments	T^H_{orient}	$t(x_i^H) = 1\left(x_i^H = 1, \text{angle}(o_i^H) \in [0, \frac{\pi}{6}] \cup \left[\frac{5\pi}{6}, 2\pi\right]\right)$
Interaction (Adjacency)	Patch-patch	T^{CC}_{adj}	$t(x_i^C, x_j^C) = a_{ij}^C$
	Segment-segment	T^{HH}_{adj}	$t(x_i^H, x_j^H) = a_{ij}^H$
	Patch-segment	T^{CH}_{adj}	$t(x_i^C, x_j^H) = a_{ij}^{CH}$

Landscape models

	C	H
M1	$T^C_{\text{act}}, T^C_{\text{area},0.25}, T^C_{\text{area},0.75}, T^{CH}_{\text{adj}}, T^{CC}_{\text{adj}}$	$T^H_{\text{act}}, T^H_{\text{length}}, T^H_{\text{orient}}, T^{HH}_{\text{adj}}$
M2	cf. M1	$T^H_{\text{act}}, T^H_{\text{orient}}, T^{HH}_{\text{adj}}$
M3	$T^C_{\text{act}}, T^H_{\text{area},0.25}, T^{CH}_{\text{adj}}, T^{CC}_{\text{adj}}$	cf. M1
M4	$T^C_{\text{act}}, T^H_{\text{area},0.25}, T^C_{\text{area},0.75}, T^{CH}_{\text{adj}}, T^{\text{cluster}}_C$	cf. M1

Table 2: Examples of landscape descriptors (top) and model configurations (bottom). Notations: C and H refer to patches, and linear elements, respectively; $\mathbb{I}$ is the indicator function; $\mathbb{Q}_p$ is the (empirical) p-percent quantile ($p \in (0, 1)$); $\mathbb{E}$ is the (empirical) expected value. The function angle returns the radians angle of a linear segment in $[-\pi/2, \pi/2)$ with respect to the West-East direction (i.e., the axis $(0, 1)^T$). Landscape models show descriptors related to crop patches in network C, and to hedges in linear element network H.

3.5. *Simulation examples.* Iterative simulation of Gibbs random fields with finite state spaces through Markov Chain Monte Carlo techniques is in general relatively straightforward and stable (see, e.g., Section 3.6 of van Lieshout, 2019). We here implement the Gibbs

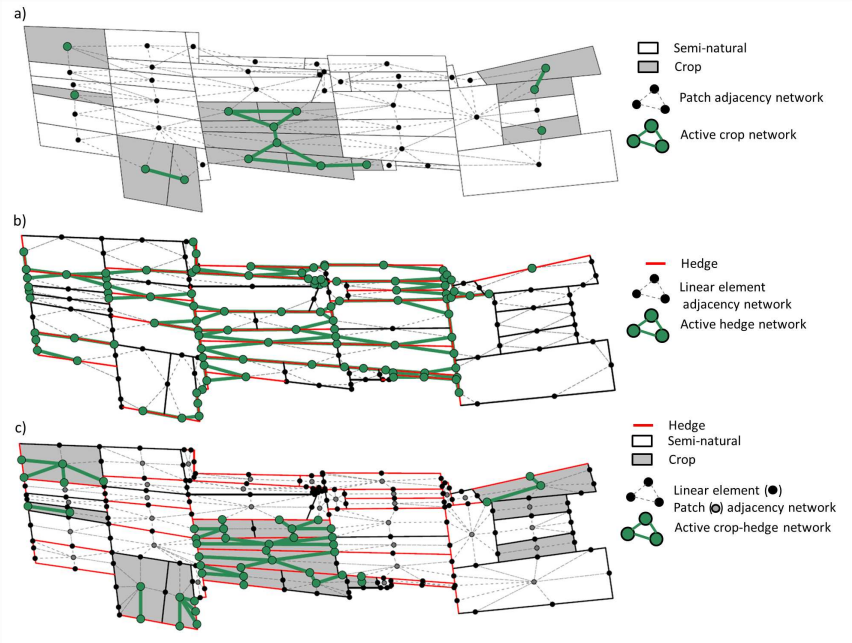

FIG 4. *Example of landscape descriptor evaluation over a small portion of D1 for the network layer C of crop allocation (Panel a) , the network layer H of hedge allocation (Panel b), the multi-layer network connecting layer C and layer H (Panel c). The landscape is simplified in potential networks, where all connections among adjacent objects are possible, and an active networks, where only the connections among allocated objects of the same type or different type are maintained depending on their categories. The landscape descriptors for this landscape small sample for the layer C are evaluated as:* $T^{C}_{act} = 14$, $T^{C}_{area,0.25} = 12$, $T^{CH}_{adj} = 168$, $T^{CC}_{adj} = 58$*; and for the layer H are evaluated as:* $T^{H}_{act} = 101$, $T^{H}_{length} = 49$, $T^{HH}_{adj} = 379$, $T^{H}_{orient} = 74$. *Formulations for computing these landscape descriptors are expressed in Equation 7 and in Table 2.*

sampler; see the supplementary material for details (Zamberletti et al., 2021), where we also check MCMC convergence diagnostics such as trace plots of descriptors.

We show several simulations for the domain D1 to visually explore the influence of parameters β_k in (5); see Figure 6. We focus on three types of Markov interactions: *crop-crop adjacency* (β^{CC}_{adj}), *hedge-hedge adjacency* (β^{HH}_{adj}), and *crop-hedge adjacency* (β^{CH}_{adj}), as defined in Table 2. In each simulation run, we set only one of the coefficients to a non-zero value among $\{-1, -1/3, 1/3, 1\}$; other descriptors are not controlled in the model. The MCMC simulation runs take from several seconds (D1, D2) to several minutes (D3) before approximately reaching the stationary distribution. For all simulations in this paper, we have fixed relatively large numbers of burn-in steps of $N_0 = 10^4$ (D1, D2) and of $N_0 = 10^6$ (D3) to ensure that chains always reach the stationary distribution. Negative coefficients produce fragmented allocation structures of the two corresponding categories, while a positive coefficient results in clustered configurations of categories. In Figure 6c, a negative coefficient of the *crop-hedge adjacency* leads to many hedges being located away from crop-patch boundaries, while they tend to concentrate on such boundaries for positive coefficients.

4. Statistical inference and model validation.

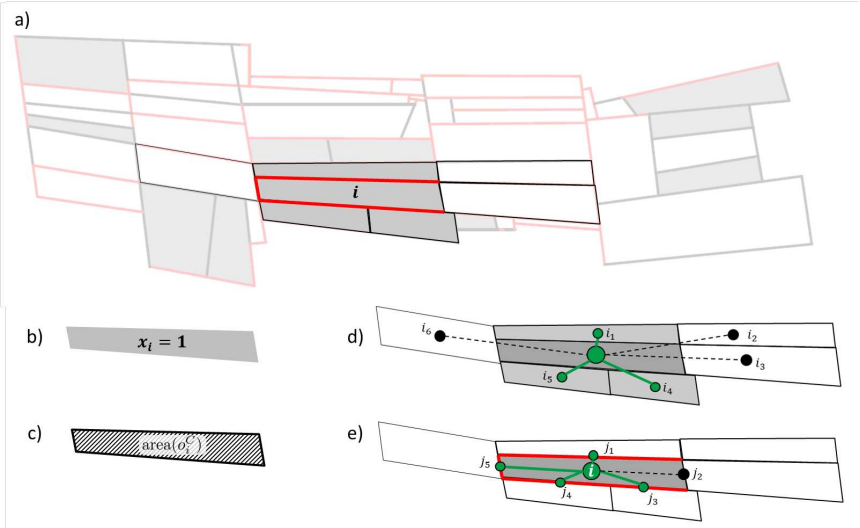

FIG 5. *Given Figure 4, we focus on a single object* $o_i = (z_i, x_i)$*, where* $z_i = \text{coords}(o_i), \text{area}(o_i)$ *and* $x_i = crop, x_i = 1$*) (Panel a), with detailed landscape descriptor specification (Panels b-e). Specification for object* O_i *are evaluated as: (b)* $t^C_{act}(x_i) = 1$*, (c)* $t^C_{area,0.25}(x_i) = 0$*, (d)* $t^{CH}_{adj}(x_i) = 4$*, (e)* $t^{CC}_{adj}(x_i) = 3$*. Formulations for the evaluation specific landscape descriptors are found in Table 2.*

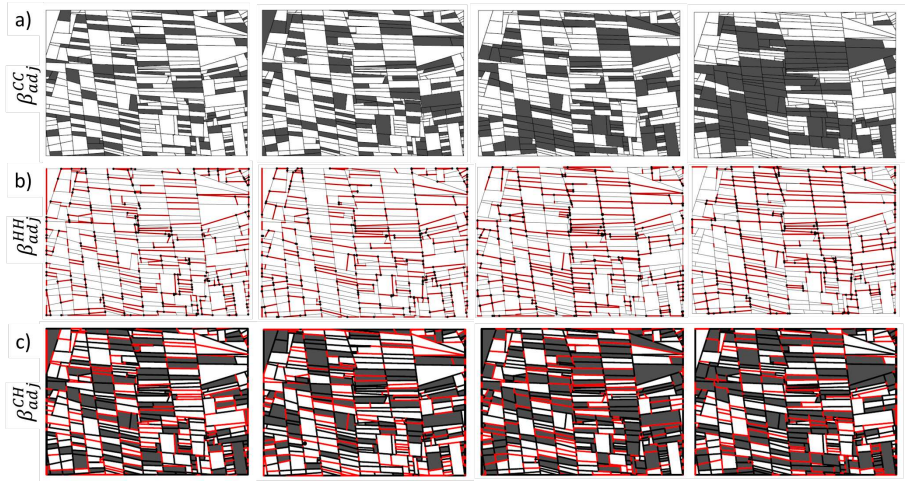

FIG 6. *Landscape simulations on D1. Panel a): varying crop-crop adjacency; Panel b): varying hedge-hedge adjacency; Panel c): varying crop-hedge adjacency. Columns from left to right: coefficient* $-1, -0.33, 0.33, 1$.

4.1. *Parameter inference.* We infer the allocation mechanism of real landscapes by first estimating the parameter vector $\boldsymbol{\beta}$ of candidate models, and then studying significance and other diagnostics. The likelihood function is not tractable in practice due to the normalizing constant $c(\boldsymbol{\beta})$ in the probability mass function (5). Instead, we use a pseudo-likelihood based

on conditional distributions; see Besag (1972, 1974); Møller and Waagepetersen (1998); van Lieshout (2000); Stoehr (2017), and particularly Section 3.5 of van Lieshout (2019). Given n objects $\boldsymbol{x} = (x_1, \dots, x_n)$ with their allocation categories, we define the pseudo-likelihood as the product of the conditional probability of the category x_i given all the other variables $\boldsymbol{x}_{-i}$; i.e., it is the composite likelihood (Varin et al., 2011) of conditional distributions given as

$$\mathcal{L} = \prod_{i=1}^{n} p(x_i \mid \boldsymbol{x}_{-i}, \boldsymbol{z}) \tag{8}$$

where the conditional probability $p(x_i \mid \boldsymbol{x}_{-i}, \boldsymbol{z})$ is defined in Equation (6) and does not depend on the normalizing constant $c(\boldsymbol{\beta})$; in Markov models, it depends only on information from adjacent objects in $\boldsymbol{o}_{-i}$.

For binary $x_i \in \mathcal{X}_i = \{0, 1\}$, we write $\tilde{\boldsymbol{x}}$ for $\boldsymbol{x}$ with x_i replaced by the alternative level; then, (6) is equivalent to the logistic regression equation

$$\log \frac{p(x_i \mid \boldsymbol{x}_{-i})}{1 - p(x_i \mid \boldsymbol{x}_{-i})} = \sum_{k=1}^{m} \beta_k \left(T_k(\boldsymbol{x}) - T_k(\tilde{\boldsymbol{x}}) \right). \tag{9}$$

Parameter estimation of $\boldsymbol{\beta}$ can then be carried out using standard software for logistic regression (if $\ell_i = 2$), or using the more general pseudo-likelihood framework (if $\ell_i > 2$).

The maximum pseudo-likelihood estimator $\widehat{\boldsymbol{\beta}}$ is asymptotically consistent and normal when independent replicates of the spatial process have been observed (Jensen et al., 1991; Varin et al., 2011).

However, in the single-replicate setting it is difficult to obtain standard errors and confidence bounds since standard asymptotic theory for maximum likelihood and maximum pseudo-likelihood estimation is based on replicated data structures. Moreover, one should check if estimation bias arises with finite-sample data. Block-bootstrapping procedures using a spatial partition of the study area (Lahiri, 2013) could provide a solution in cases of very large study areas, especially with Markov models whose spatial dependence strength decays relatively fast for larger distances; however, such bootstrap schemes would be difficult to implement on moderately large domains such as D1, D2 and D3 in Figure 1, and handling the multiplex networks may be awkward. Instead, we propose to resort to a parametric bootstrap, using MCMC simulation of the estimated model to generate pseudo-replicates of the observed data, which then allows us to check if estimation is stable and unbiased, to obtain confidence intervals, and more specifically to check if a descriptor is significant.

We proceed as follows: generate n_{boot} independent simulations (e.g., $n_{\text{boot}} = 99$) of the fitted model using $\boldsymbol{\beta} = \widehat{\boldsymbol{\beta}}$, and reestimate the coefficient vector for each simulation to obtain a sample of the pseudo-likelihood estimator; then, use this sample to check for estimation bias and derive Monte-Carlo confidence intervals. For a test of the null hypothesis of $\beta_k = 0$ for fixed $k \in \{1, \dots, m\}$, i.e., to check if the landscape descriptor T_k is significant, we implement a Monte-Carlo test where we repeatedly simulate the fitted model, but with the modification $\hat{\beta}_k = 0$. Then, we here reject the null if the value $\hat{\beta}_k$ does not lie within the one-sided Monte–Carlo confidence interval of $\hat{\beta}_k$, i.e., if less than $\alpha\%$ (e.g., $\alpha = 5$) of the β_k-values estimated for the simulations have the same sign and higher absolute value than the value estimated for the data (see, e.g., Davison and Hinkley, 1997).

4.2. *Pseudo-likelihood-based model selection.* We propose approaches to statistically compare models with different landscape descriptor configurations and to assess their goodness-of-fit.

As first criterion, we consider the maximum pseudo-loglikelihood value, denoted by mpll. We have to rank models based on information criteria that take the model complexity (i.e.,

the number of parameters) into account to avoid overfitting, and to identify parameter configurations that are both parsimonious and informative. Relevant information criteria such as the composite likelihood information criterion (CLIC) are hard to calculate in a single-replicate setting, such that we only use them to compare models with the same number of parameters; i.e., we directly compare mpll values to rank CLICs in this case.

The second criterion, applicable to compare any types of models, is the Mean Squared Error (MSE) based on k-fold cross-validation. In k-fold cross-validation, we partition the original dataset into k groups (e.g., $k = 5$), and reestimate the model repeatedly by holding out one fold a time. For each hold-out set, we then summarise the skill of the model by a prediction score, here chosen as the MSE between the predicted probability of an allocation category and its actual value. The MSE is also known as the *Brier score* (Brier, 1950), and it is a proper score function as defined by Gneiting and Raftery (2007). We evaluate scores separately on each hold-out set, and then average the k resulting values to obtain the global score. We here propose to generate a random partition into k folds of the same size separately for each layer of the network (e.g., patches, edges).

4.3. *Model diagnostics using landscape summaries.* We propose to check if the fitted model is able to appropriately reproduce three types of summaries of the real landscape: 1) landscape descriptors used in the model (i.e., sufficient statistics); 2) variograms (using a raster representation), as defined in the following, to measure the variability of crop, hedge, and crop-hedge structures with respect to Euclidean distance in space; 3) general landscape metrics commonly used in landscape ecology, based on vector or raster representations.

Type 1 concerns statistical validation: the theoretical distribution of a landscape descriptor should be in line with its observed value; we check this through Monte–Carlo samples of the fitted model.

Regarding type 2, variograms (Cressie, 2015; van Lieshout, 2019), we adopt a geostatistical perspective (Saura and Martinez-Millan, 2000) that focuses on the variability and geographic scales of the landscape, which has already proven useful to characterize land use properties (Garrigues et al., 2006, 2008). We here define two variogram variants. The first variant, called *one-category variogram*, explores the spatial variability of the presence $Z_c(s) \in \{0, 1\}$ (1 for present, 0 for absent) of a category c at any location s in the study domain D. The second variant, called *two-category variogram*, explores the spatial interaction of two distinct categories c_1, c_2 (e.g., crop and hedges). We define $Z_{c_1,c_2}(s) \in \{0, 1\}$ only for locations s where either c_1 or c_2 is present (other locations are considered as not being part of the domain of the process), and we set $Z_{c_1,c_2}(s) = 1$ if c_1 is present at s, otherwise the value is 0. For both variants, denoted by γ_c and γ_{c_1,c_2}, respectively, we calculate experimental variograms, assuming stationarity and isotropy, according to the empirical counterpart of $\gamma(h) = \mathbb{E}(Z(s_1) - Z(s_2))^2$, where $\|s_2 - s_1\| = h$ for distances $h \geq 0$.

Regarding type 3 of summaries, various metrics have been used to assess if simulated landscape patterns appropriately represent landscape functionality and ecological relevancy (Kupfer, 2012; Frazier and Kedron, 2017); some metrics are known to be strongly correlated in practice. We assess if models of type (5), endowed with a small number of landscape descriptors, are able to generate metric values close to the observed one. Simulation of fitted models is used to generate a representative sample of the theoretical model-based distributions of metrics.

Some commonly used metrics require landscapes to be represented as a mosaic of discrete habitat patches, as in our case. Many other metrics have been developed for landscapes conceptualized as environmental gradients (i.e., for raster representations, see McGarigal and Marks, 1995; Cushman et al., 2010). Here, we assess how data patterns are reproduced by models through metrics based on graph theory (Urban and Keitt, 2001; Minor and Urban,

2008; Urban et al., 2009; Lü et al., 2016, *network metrics*, see), or *raster metrics* (McGarigal and Marks, 1995), where we transform our vector-based patch-mosaic representation into a raster; see Table 3 for a summary.

We focus on standard network metrics (Urban and Keitt, 2001; Minor and Urban, 2008), evaluated either at node scale (with one value per node), or at network scale. These active networks associated to a specific allocation have one layer for each allocation category (e.i., crop network C, and hedge for network H), recall Section 3.3, and there are edges if two adjacent objects ($(x_1, z_1) = o_1 \sim o_2 = (x_2, z_2)$) have been allocated the same category, i.e., $x_1 = x_2$. Node scale helps to identify vital nodes associated with structural or functional objectives (Lü et al., 2016), while network scale summarizes the global topology (Urban and Keitt, 2001; Calabrese and Fagan, 2004). For metrics based on gradient theory, we follow Cushman et al. (2008) and choose those metrics identified as "highly universal and consistent class-level landscape structure components". We use the `R` package `raster` (Hijmans et al., 2015) to transform vector objects (i.e., polygons and linear segments) into rasters with categorical values, and the package `landscapemetrics` to evaluate raster metrics (Hesselbarth et al., 2019). In the case of two polygon types (crops/hedges) and two edge types (presence/absence of hedge), we obtain 3 pixel categories in the raster, also called habitats: crop, semi-natural, and hedge; absence of hedges is not a class in itself.

Name	Description	Support	Range	Reference
Degree*	Number of connected nodes	node	[0, 1]	[1],[2]
Coreness	K-shell decomposition for a node's spreading influence	node	[0,∞)	[1],[2]
Degree grade 2*	Number of connected nodes at most 2 nodes away	node	[0, 1]	[1],[2]
Eccentricity*	Maximum shortest path to connected nodes	node	[0, 1]	[1],[2]
Closeness	Reciprocal of total length of shortest paths to connected nodes	node	[0,∞)	[1],[2]
Betweenness*	Potential power to control information flow	node	[0, 1]	[1],[2]
Diameter	Longest path	network	[0,∞)	[1]
Efficiency	Efficiency of information exchange	network	[0,∞)	[2],[3]
Cluster avg.	Proportion of interconnected adjacent nodes of a vertex	network	[0,1]	[2],[3]
PLAND [%]	Percentage of a habitat in the landscape	raster	[0,100]	[4],[5]
PD [# / ha $\times$ 100]	Patch density	raster	[0,∞)	[4],[5]
ENN [m]	Mean Euclidean nearest neighbor distance	raster	[0,∞)	[4],[5]
PARA [/]	Perimeter-area ratio of contiguous habitat	raster	[0,∞)	[4],[5]
IJI [%]	Interspersion/juxtaposition index measuring spatial intermixing of different habitats	raster	[0,100]	[4],[5]
CLUMPY [/]	Clumpiness index measuring deviation from randomness	raster	[-1,1]	[4],[5]

Table 3: Landscape metrics. A star * indicates metrics normalized with the number of nodes. Metric type is either "node" (node-scale network metrics), "network" (global network metrics), or "raster". Listed references are as follows: [1] Urban et al. (2009), [2] Lü et al. (2016), [3] Latora and Marchiori (2001), [4] McGarigal and Marks (1995), [5] Cushman et al. (2008)

5. Application to the Lower Durance Valley in southern France. We fit parametric stochastic models for the category allocation mechanism of crops and hedges in the domains D1, D2 and D3 using the logistic regression equation (9), and we discuss descriptor selection by assessing a moderate number of landscape descriptors.

5.1. *Structure of descriptors and models.* We allow for two allocation categories of both patches and linear elements: *crop* or *semi-natural area* (network C) ; presence or absence of a hedgerow for (network H).

We consider four models for (5), denoted M1–M4, and summarized in Table 2, to test different combinations of landscape descriptors in the general model (5). To avoid collinearity of descriptors, we first check correlations between the covariates arising in the logistic

		Landscape descriptors	D1	D2	D3
C	M1	$T^C_{\text{act}}, T^C_{\text{area},0.25}, T^C_{\text{area},0.75}, T^{CH}_{\text{adj}}, T^{CC}_{\text{adj}}$	**-198.9**, **0.184**	**-236.4**, **0.171**	**-1778.3** , **0.130**
	M3	$T^C_{\text{act}}, T^C_{\text{area},0.25}, T^{CH}_{\text{adj}}, T^{CC}_{\text{adj}}$	-205.6, 0.191	-239.5, 0.173	-1781.5, **0.130**
	M4	$T^C_{\text{act}}, T^C_{\text{area},0.25}, T^C_{\text{area},0.75}, T^{CH}_{\text{adj}}, T^C_{\text{cluster}}$	-202.1, 0.191	-243.5, 0.182	-1970.0, 0.151
H	M1	$T^H_{\text{act}}, T^H_{\text{length}}, T^H_{\text{orient}}, T^{HH}_{\text{adj}}$	**-608.5**, 0.186	**-633.3** , **0.143**	**-6399.6**, **0.169**
	M2	$T^H_{\text{act}}, T^H_{\text{orient}}, T^{HH}_{\text{adj}}$	-608.6, **0.185**	-640.7, 0.144	-6405.4, **0.169**

Table 4: Values of mpll and MSE in 5-fold cross-validation for each combination of model (M1–M4, Crop/Hedge network) and spatial domain (D1–D3). Highest mpll and lowest MSE are highlighted in bold for each domain and Crop/Hedge.

regression (9) for each spatial domain; see Figure 5 in the supplementary material (Zamberletti et al., 2021). Strong negative correlation is observed between T^{CC}_{adj}(crop adjacency) and T^C_{cluster} (number of connected crop components), such that we avoid including both of them in the same model, and we seek to assess which of the two descriptors better captures crop-to-crop interaction (M1/M3 vs. M4).

The patch area distribution shows high variance, and we include descriptors for the effect of patch area in network C. While the behavior of large patches can strongly influence the proportions of crop and semi-natural habitat, small field sizes may benefit biodiversity through easier access to adjacent fields with complementary resources (Sirami et al., 2019). Therefore, we use a patch area condition using $T^C_{\text{area,p}}$ in Table 2 with $p = 0.25$ and $p = 0.75$ (M1), and we check redundancy by removing $T^H_{\text{area},0.75}$ in M3.

For hedges, Figure 5 in the supplementary material shows strong positive correlation between T^H_{length} (long hedges, where we count the number of hedges positioned on edges longer than the average edge length) and T^H_{orient} (horizontal hedges), which is related to the windbreak function of many hedges against strong Mistral winds blowing from the North; to check redundancy of these two descriptors, we include only T^H_{length} in M2, in contrast to M1–M3 (Zamberletti et al., 2021).

We present a detailed analysis of model M1 in D1, denoted as M1-D1, and we point out some salient results of the comparison of $M1$, $M3$ and $M4$, and of other domains D2 and D3. Detailed results can be found in the supplementary material (Zamberletti et al., 2021).

5.2. *Likelihood-based model comparison.* Table 4 reports mpll values, and mean-squared errors (MSE) obtained through 5-fold cross-validation; recall Section 4.2. In the network H, the hedge length descriptor T^H_{length}, included in M1 but not M2, does not provide notable improvements except for the domain D2, where the correlation between the logistic regression covariates related to T^H_{length} and T^H_{orient} is relatively weaker. In the network C, the comparison of the crop models in M1, M3 and M4 reveals that M1 consistently performs best for both criteria; i.e., explicit control over large patches is required, and the Markov interaction model based on adjacency provides better results than direct control over the number of connected crop components.

5.3. *Estimated parameters.* In Table 5, we report coefficient estimates of β_k, as well as standard errors and significance with respect to the null $\beta_k = 0$, based on Monte–Carlo procedures using 100 simulations; see Section 4.1. Figure 7 in the supplementary material shows boxplots of the parametric bootstrap estimations, and we detect no bias in the estimators(Zamberletti et al., 2021). All estimated parameters are significant for the Markov interaction in the networks C and H (positive coefficient of C-C, H-H), for the area descriptor (negative coefficient of *Small area* and of *Large area*), for the hedge orientation descriptor (positive coefficient of *Horizontal H*), and for the activity terms. No strong signal is found for

		Crop					Hedge			
		Activity	Small area	Large area	C-H	C-C	Activity	Long H	H-H	Horizontal H
M1-D1	Estimate	**-1.01**	**-1.52**	**-1.13**	0.03	**0.40**	**-2.38**	-0.10	**0.77**	**1.58**
	SD	0.34	0.35	0.29	0.07	0.10	0.19	0.19	0.07	0.19
M3-D1	Estimate	**-1.08**	**-1.24**	-	-0.05	**0.37**	**-2.38**	-0.10	**0.77**	**1.58**
	SD	0.37	0.34	-	0.09	0.10	0.19	0.19	0.07	0.19
M4-D1	Estimate	-0.16	**-1.80**	**-1.15**	0.06	**-0.99**	**-2.38**	-0.10	**0.77**	**1.58**
	SD	0.25	0.39	0.32	0.08	0.47	0.19	0.19	0.07	0.19
M1-D2	Estimate	**-1.58**	**-1.13**	**-0.68**	-0.04	**0.65**	**-3.38**	**-0.58**	**0.77**	**3.65**
	SD	0.32	0.32	0.28	0.07	0.08	0.23	0.17	0.08	0.2
M1-D3	Estimate	**-1.82**	**-1.44**	**-0.25**	**-0.14**	**0.66**	**-3.01**	**-0.16**	**0.95**	**1.96**
	SD	0.09	0.14	0.07	0.02	0.02	0.06	0.05	0.02	0.05

Table 5: Parameter estimates for crop-related (C) and hedge-related (H) descriptors. Crop-hedge interaction (C-H), Crop-crop interaction (C-C). "SD" values and significance (at the 95% level, indicated through bold face) are based on 100 parametric bootstrap simulations. C-C is of Markov type (using T^{CC}_{adj}) in M1/M3, and is global (using T^{C}_{cluster}) in M4.

a dominance of long hedge segments (*Long H*) in D1, confirming results in Section 5.2, and of Markov interaction between C and H. All descriptors are significant for the large domain D3. The signs of estimates are the same across D1–D3 for all significant effects, implying structurally similar behavior. The different sign in M4 for C-C interaction is due to different specification as a global descriptor using the number of connected components. Overall, estimated parameters tend to have comparable magnitudes across D1–D3.

We interpret these results as follows: given the parameter estimates of our model, the crop category is usually not allocated on relatively small and relatively large fields; later results will confirm the superior performance of M1 over M3/M4, the latter without the large area descriptor. Crop fields and hedges tend to cluster in space, i.e., they tend to be allocated on adjacent patches and linear elements, respectively, such that they provide relatively large and contiguous habitats, and relatively long continuous movement corridors. Moreover, the connected component descriptor in M4 has negative coefficients, i.e., the study domains seem to be characterised by relatively few large crop clusters. There is a dominating horizontal orientation of hedges for protecting against strong winds. Crop-hedge adjacency has negative coefficients and is significant only for the large domain M1-D3, suggesting a slight tendency of hedges to not being directly adjacent to crop fields. In M1-D2, we discern a particularly strong signal of *Long H* indicating many short, strongly horizontally oriented hedges.

5.4. *Summary diagnostics of observed and simulated landscape.* We check if landscape descriptors, as well as one- and two-category variograms and graph- and raster-based metrics introduced in Section 4.3, are appropriately reproduced by the models for crop allocation to patches in D1. We focus on M1, which was found to show good relative performance in the preceding diagnostics. We generate 100 independent simulations of the fitted model. For scalar metrics, and for fixed distances in the variogram analysis, we report results for approximate two-sided Monte-Carlo test procedures at 95% confidence level with respect to the null hypothesis that the observed summary could have been generated by the fitted model. Results for the hedge network and for other domains (M1-D2, M1-D3) are structurally similar; they are reported in the supplementary material (Zamberletti et al., 2021).

5.4.1. *Landscape descriptors.* Figure 7 shows observed and simulated landscape descriptors, i.e., sufficient statistics for the estimated coeffients. Models M1, M3, M4 tend to produce realistic values, especially M1.

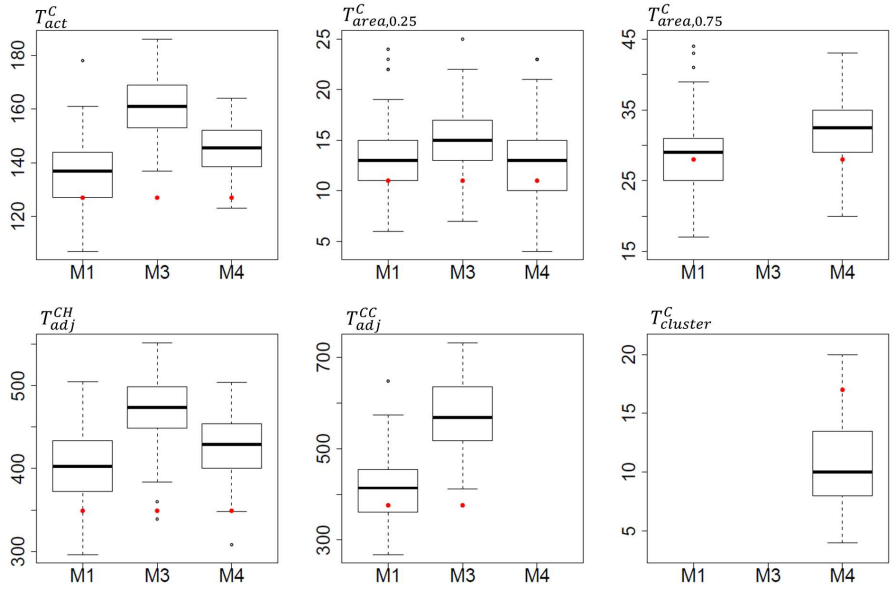

FIG 7. *Landscape descriptors for domain D1 and network C (Crop) in M1, M3, M4. Boxplots summarize* 100 *simulations of fitted models. Red dots are observed values.*

5.4.2. *Variogram analysis.* Figure 8 shows empirical one-category (Crop) and two-category (Crop-Hedge) variograms with pointwise simulation envelopes. All variograms show a relatively steep slope at the origin and tend to flatten for larger distances, such that the general shape of the empirical data variogram is well reproduced by the models. In several cases, especially with M3, empirical variograms of the dataset clearly fall outside the envelope, such that the observed variability of landscape features with distance is not appropriately captured. In general, the structure of M1 (with the large patch area descriptor, and Markov interaction for crops) improves the match between data and model variograms—in contrast to M4 using the global interaction descriptor based on the number of connected components. One-category variograms for hedges are appropriately captured by models (supplementary material (Zamberletti et al., 2021)).

5.4.3. *Network metrics.* Figure 9 shows observed and simulated network metrics. For node-scale metrics (two top rows), we observe good overlap of boxplots of observed and simulated values for the crop and hedgerow network, with the exception of *Betweenness* (number of the shortest paths going through a node when connecting any two other nodes) where we tend to simulate too large values for crop, and too small values for hedges. Some outlying values are not shown since *Betweenness* is very heavy-tailed due to high variability among different networks, which may explain the mismatch between observed and simulated values. Heavy-tailedness highlights that few crop patches serve as bridges connecting different crop clusters, which is fundamental to global connectivity of the landscape (Estrada and Bodin, 2008; Urban et al., 2009; Belgrano et al., 2015); this property is preserved in the fitted model.

For network-scale metrics (last row of Figure 9) we show the real landscape value within the boxplot of simulated values. Observed metrics fall within or close to the interquartile

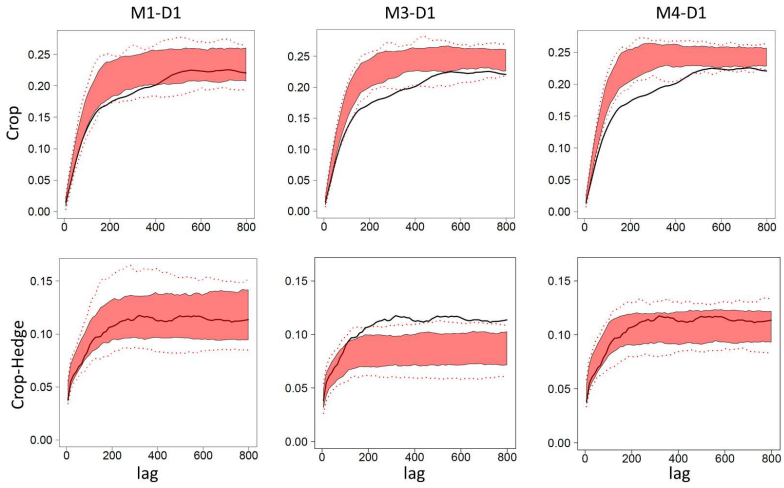

FIG 8. *Variogram analysis of models M1, M3, M4 for domain D1. One-category variogram for crop (top row); two-category variogram for crop and hedges (bottom row). Empirical variogram of observed landscape (black line); pointwise simulation envelopes (red-shaded area: 5%-95%; dotted red lines: minimum/maximum).*

range of the simulated ones for the crop network, while they lie outside the boxplot whiskers for the hedge network but are still of the same order of magnitude. Moreover, we define and report so-called pseudo-p-values in Section 7 of the supplementary material to allow for automatic screening of network and raster metrics (Zamberletti et al., 2021).

Model M1 does not directly control the number or dimension of clusters, only local interactions through the Markov model. This explains better performance for *neighborhood-based centralities* in comparison to *path-based centralities* and metrics. However, using a global descriptor instead of a local descriptor in M4 does not substantially improve performance for path-based centralities; see Section 7 in the supplementary material (Zamberletti et al., 2021).

5.4.4. *Raster metrics.* Figure 10 shows the raster-based landscape metrics of FRAGSTAT; see Section 4.3 and Table 3.

In most cases, observed metric fall within the whiskers of the boxplots, and in the other cases the order of magnitude is still relatively well captured by the fitted model.

5.4.5. *Correlation analysis of landscape summaries.* Different landscape summaries (descriptors, metrics) may comprise similar information, and strong correlation may arise among such variables. If we seek a realistic representation of a specific metric through the model, the landscape descriptors included in the model (or combinations of them) should be strongly correlated with this metric. To assess such relationships, i.e., if the model may allow us to target specific values of metrics of interest, we generate a sample of size 100 of the model through the MCMC approach from Section 3.5. We then use linear regression with the landscape descriptors as predictors and one landscape metric at a time as dependent variable, and then consider the part of the standard deviation of the response not explained by the predictors. For illustration, we analyse differences among the models M1 and M3 (where M1 has an additional descriptor $T^{C}_{\mathrm{area},0.75}$ related to the allocation of large patches with crop)

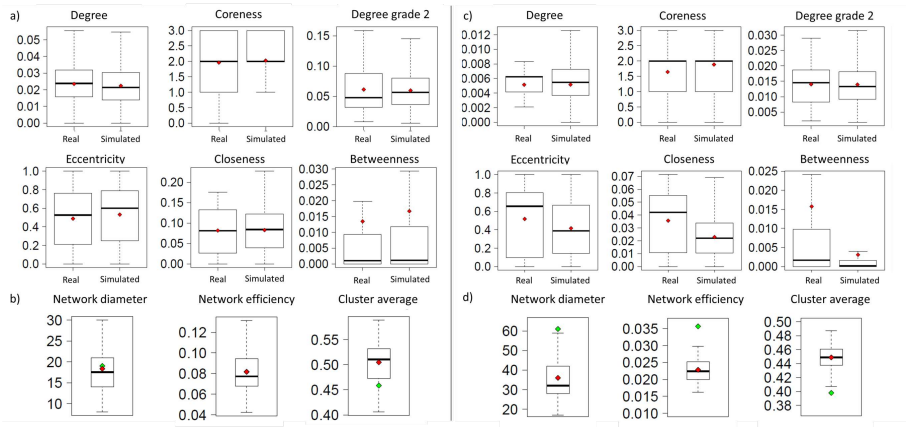

FIG 9. *Validation metrics M1-D1 for crop network C (left) and hedge network H (right). Panels a,c: metrics at node scale (red dots: mean values). Panels b,d: metrics at network scale (boxplots: simulations; red dots: mean values of simulations; green dots: observed values.*

for domain D1 through the correlation analysis in Figure 11a. The descriptor $T^C_{\text{area},0.75}$ is generally more strongly correlated with other metrics for crop patches than $T^C_{\text{area},0.25}$, which tends to substantially reduce residual standard deviation not explained by the descriptors of the model, as shown in Figure 11b.

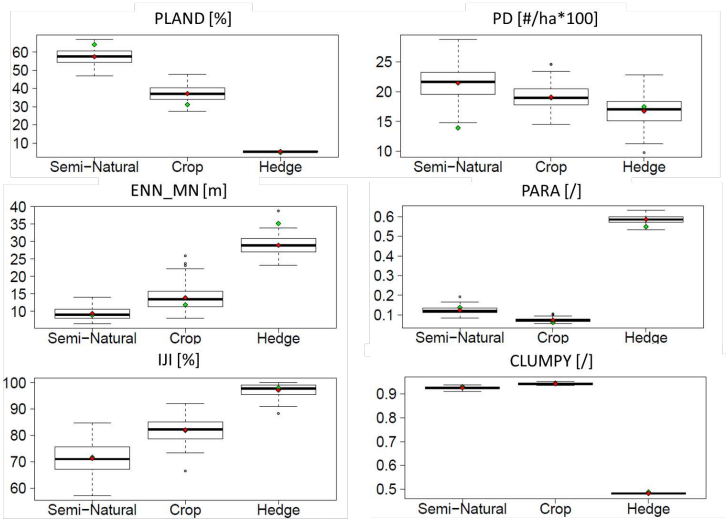

FIG 10. *Raster-based metrics for M1-D1. Simulated values (boxplots); mean of simulated values (red dots); observed value (green dots).*

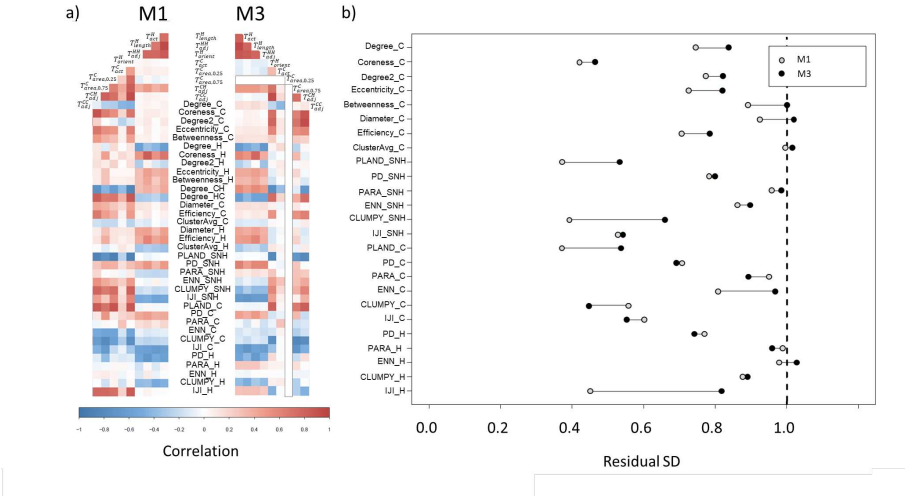

FIG 11. *Correlation analysis for M1-D1, M3-D1. Panel a: Correlations among landscape descriptors and metrics (notation: C – patch network; H – linear element network; CH – patch to linear element connections; SNH – Semi-natural habitat (raster)). Panel b: Comparison of patch-related metrics between M1-D1 and M3-D1 based on residual standard deviation.*

6. Conclusion. We have developed stochastic agricultural landscape models and statistical inference with a focus on the land-use allocation mechanism of patches and linear elements, using network models as an intuitive and flexible tool for direct control and interpretation with respect to local behavior. We have focused on descriptors based on single objects or pairwise Markov interactions, which leads to robust modeling, estimation and simulation procedures, while we found it generally difficult to improve models by the use of more globally specified interaction descriptors. Overall, the descriptors of the model and other landscape metrics were satisfactorily reproduced by simulations from models (especially M1) fitted to Lower Durance Valley data. We highlighted the flexibility of the approach by comparing outcomes of different models over the same domain, and we also tested models over domains having different and relatively large size. The generality of calibrated models was evaluated through variograms and metrics whose values are not explicitly encoded into the model structure. Time dynamics, such as crop rotation, cannot be estimated for the dataset due to lack of dynamic land-cover allocation data. The integration of temporal descriptors, as illustrated through the simulations in the supplementary material, would be an interesting perspective for future development of such classes of models (Zamberletti et al., 2021). The proposed model class succeeds in capturing key patterns of configuration and composition in real landscapes.

The developed approach focuses on the task of classification, i.e., of attributing to each landscape element one class among a finite number of possible classes. The use of Gibbs energies could be extended to more general numeric labels (e.g., continuous variables) associated with landscape elements, for instance the crop yield in a field, or the proportions of a crop field used for specific crop types when several crops are planted in the same field in some small-scale-alternating way. Then, the proposed approach could be extended to more general models of exponential family type (e.g., Brown, 1986).

We have provided a set of diagnostic and inferential tools to assess model performance from different perspectives and select an appropriate candidate. Not all relevant metrics can

be reproduced through our model without bias, especially on raster scale where the grid discretization of space may produce instabilities in treating small-scale small-area patterns, especially those related to linear segments. Linear element allocation also showed some discrepancy between model and data for large-scale clustering properties. To remedy the issue of appropriately simulating an important landscape summary that is not directly controlled by the model, we can add constraints during simulation, using techniques such as Simulated Annealing (e.g., Papaïx et al., 2014).

We outline the potential of Approximate Bayesian Computation (ABC) for parameter estimation and likelihood-free model selection using Bayes factors (e.g., Grelaud et al., 2009). Using landscape descriptors for the ABC target summaries yields asymptotically consistent estimators under mild conditions since descriptors are sufficient statistics. However, rather long computation times may arise with this method.

Vector-based models such as ours are more parsimonious and meaningful from an ecological point of view (Gaucherel et al., 2012; Bonhomme et al., 2017), and they enable explicitly handling different spatial and temporal scales. In raster-based approaches, an appropriate representation of small-surface elements such as hedges would require a very high and unwieldy resolution, where a homogeneous large-surface patch would be made up of a very large number of pixels, instead of a single geometric object in our model. Our multiplex network structure assures low computational cost and memory requirements.

We do not directly model human action in the temporal dynamics of agricultural environments (Bonhomme et al., 2017; Poggi et al., 2018), for which we would have to couple our model with a decision tool. Future developments also comprise the integration of our allocation model with (existing) generative parametric tessellation models for the geometrical support (Kiêu et al., 2013).

Acknowledgements. We are thankful to Claire Lavigne and Katarzyna Adamczyk for their help and wise suggestions for landscape data processing and for the discussion part.

SUPPLEMENTARY MATERIAL

Supplementary Material: Technical report with extended results
doi: COMPLETED BY THE TYPESETTER; .pdfAdditional details for the simulation algorithm and results for the case study in Section 5.

REFERENCES

Adamczyk-Chauvat, K., Kassa, M., Kiêu, K., Papaïx, J., and Stoica, R. S. (2020). Gibbsian t-tessellation model for agricultural landscape characterization. *arXiv preprint arXiv:2007.16094*.

Baddeley, A. and Møller, J. (1989). Nearest-neighbour markov point processes and random sets. *International Statistical Review/Revue Internationale de Statistique*, pages 89–121.

Belgrano, A., Woodward, G., and Jacob, U. (2015). *Aquatic functional biodiversity: an ecological and evolutionary perspective*. Academic Press.

Besag, J. (1974). Spatial interaction and the statistical analysis of lattice systems. *Journal of the Royal Statistical Society: Series B (Methodological)*, 36(2):192–225.

Besag, J. E. (1972). Nearest-neighbour systems and the auto-logistic model for binary data. *Journal of the Royal Statistical Society: Series B (Methodological)*, 34(1):75–83.

Boccaletti, S., Bianconi, G., Criado, R., Del Genio, C. I., Gómez-Gardenes, J., Romance, M., Sendina-Nadal, I., Wang, Z., and Zanin, M. (2014). The structure and dynamics of multilayer networks. *Physics Reports*, 544(1):1–122.

Bonhomme, V., Castets, M., Ibanez, T., Géraux, H., Hély, C., and Gaucherel, C. (2017). Configurational changes of patchy landscapes dynamics. *Ecological Modelling*, 363:1–7.

Boots, B., Okabe, A., and Sugihara, K. (1999). Spatial tessellations. *Geographical information systems*, 1:503–526.

Brier, G. W. (1950). Verification of forecasts expressed in terms of probability. *Monthly weather review*, 78(1):1–3.

Brown, L. D. (1986). *Fundamentals of statistical exponential families: with applications in statistical decision theory*. Institute of Mathematical Statistics.

Büttner, G. and Maucha, G. (2006). The thematic accuracy of CORINE land cover 2000. assessment using LUCAS (land use/cover area frame statistical survey). *European Environment Agency: Copenhagen, Denmark*.

Calabrese, J. M. and Fagan, W. F. (2004). A comparison-shopper's guide to connectivity metrics. *Frontiers in Ecology and the Environment*, 2(10):529–536.

Cressie, N. (1991). Ac (1991). statistics for spatial data. *Wiley, New York*.

Cressie, N. (2015). *Statistics for spatial data*. John Wiley & Sons.

Cushman, S. A., Gutzweiler, K., Evans, J. S., and McGarigal, K. (2010). The gradient paradigm: a conceptual and analytical framework for landscape ecology. In *Spatial complexity, informatics, and wildlife conservation*, pages 83–108. Springer (New York).

Cushman, S. A., McGarigal, K., and Neel, M. C. (2008). Parsimony in landscape metrics: strength, universality, and consistency. *Ecological indicators*, 8(5):691–703.

Davison, A. C. and Hinkley, D. V. (1997). *Bootstrap methods and their application*. Cambridge university press.

Estrada, E. and Bodin, Ö. (2008). Using network centrality measures to manage landscape connectivity. *Ecological Applications*, 18(7):1810–1825.

Fienberg, S. E. (2010). Introduction to papers on the modeling and analysis of network data. *The Annals of Applied Statistics*, pages 1–4.

Foresight, U. (2011). The future of food and farming. *Final Project Report, London, The Government Office for Science*.

Frazier, A. E. and Kedron, P. (2017). Landscape metrics: Past progress and future directions. *Current Landscape Ecology Reports*, 2(3):63–72.

Gaetan, C. and Guyon, X. (2010). *Spatial statistics and modeling*, volume 90. Springer.

Gallavotti, G. (2013). *Statistical mechanics: A short treatise*. Springer Science & Business Media.

Gardner, R. H. (1999). RULE: map generation and a spatial analysis program. In *Landscape ecological analysis*, pages 280–303. Springer (New York).

Gardner, R. H., Milne, B. T., Turnei, M. G., and O'Neill, R. V. (1987). Neutral models for the analysis of broad-scale landscape pattern. *Landscape Ecology*, 1(1):19–28.

Gardner, R. H. and Urban, D. L. (2007). Neutral models for testing landscape hypotheses. *Landscape Ecology*, 22(1):15–29.

Garrigues, S., Allard, D., Baret, F., and Morisette, J. (2008). Multivariate quantification of landscape spatial heterogeneity using variogram models. *Remote Sensing of Environment*, 112(1):216–230.

Garrigues, S., Allard, D., Baret, F., and Weiss, M. (2006). Quantifying spatial heterogeneity at the landscape scale using variogram models. *Remote sensing of environment*, 103(1):81–96.

Gaucherel, C., Boudon, F., Houet, T., Castets, M., and Godin, C. (2012). Understanding patchy landscape dynamics: towards a landscape language. *PLoS One*, 7(9):e46064.

Gaucherel, C., Fleury, D., Auclair, D., and Dreyfus, P. (2006a). Neutral models for patchy landscapes. *Ecological Modelling*, 197(1-2):159–170.

Gaucherel, C., Giboire, N., Viaud, V., Houet, T., Baudry, J., and Burel, F. (2006b). A domain-specific language for patchy landscape modelling: The Brittany agricultural mosaic as a case study. *Ecological Modelling*, 194(1-3):233–243.

Gneiting, T. and Raftery, A. E. (2007). Strictly proper scoring rules, prediction, and estimation. *Journal of the American Statistical Association*, 102(477):359–378.

Green, P. J., Richardson, S., and Hjort, N. L. (2003). *Highly structured stochastic systems*, volume 27. Oxford University Press.

Grelaud, A., Robert, C. P., Marin, J.-M., Rodolphe, F., Taly, J.-F., et al. (2009). ABC likelihood-free methods for model choice in Gibbs random fields. *Bayesian Analysis*, 4(2):317–335.

Hammersley, J. M. and Clifford, P. (1971). Markov fields on finite graphs and lattices. *Unpublished manuscript*, 46.

Hesselbarth, M. H., Sciaini, M., With, K. A., Wiegand, K., and Nowosad, J. (2019). landscapemetrics: an open-source r tool to calculate landscape metrics. *Ecography*, 42(10):1648–1657.

Hijmans, R. J., van Etten, J., Cheng, J., Mattiuzzi, M., Sumner, M., Greenberg, J. A., Lamigueiro, O. P., Bevan, A., Racine, E. B., Shortridge, A., et al. (2015). Package 'raster'. *R package*.

Hopcroft, J. and Tarjan, R. (1973). Algorithm 447: Efficient algorithms for graph manipulation. *Commun. ACM*, 16(6):372–378.

Inkoom, J. N., Frank, S., Greve, K., and Fürst, C. (2017). Designing neutral landscapes for data scarce regions in West Africa. *Ecological informatics*, 42:1–13.

Jensen, J. L., Moller, J., et al. (1991). Pseudolikelihood for exponential family models of spatial point processes. *The Annals of Applied Probability*, 1(3):445–461.

Kiêu, K., Adamczyk-Chauvat, K., Monod, H., and Stoica, R. S. (2013). A completely random T-tessellation model and Gibbsian extensions. *Spatial Statistics*, 6:118–138.

Kivelä, M., Arenas, A., Barthelemy, M., Gleeson, J. P., Moreno, Y., and Porter, M. A. (2014). Multilayer networks. *Journal of complex networks*, 2(3):203–271.

Kupfer, J. A. (2012). Landscape ecology and biogeography: Rethinking landscape metrics in a post-FRAGSTATS landscape. *Progress in Physical Geography*, 36(3):400–420.

Lahiri, S. N. (2013). *Resampling methods for dependent data*. Springer Science & Business Media.

Langhammer, M., Thober, J., Lange, M., Frank, K., and Grimm, V. (2019). Agricultural landscape generators for simulation models: A review of existing solutions and an outline of future directions. *Ecological modelling*, 393:135–151.

Latora, V. and Marchiori, M. (2001). Efficient behavior of small-world networks. *Physical review letters*, 87(19):198701.

Le Ber, F., Lavigne, C., Adamczyk, K., Angevin, F., Colbach, N., Mari, J.-F., and Monod, H. (2009). Neutral modelling of agricultural landscapes by tessellation methods—application for gene flow simulation. *Ecological Modelling*, 220(24):3536–3545.

Lefebvre, M., Franck, P., Toubon, J.-F., Bouvier, J.-C., and Lavigne, C. (2016). The impact of landscape composition on the occurrence of a canopy dwelling spider depends on orchard management. *Agriculture, Ecosystems & Environment*, 215:20–29.

Lin, Y., Deng, X., Li, X., and Ma, E. (2014). Comparison of multinomial logistic regression and logistic regression: which is more efficient in allocating land use? *Frontiers of earth science*, 8(4):512–523.

Lü, L., Chen, D., Ren, X.-L., Zhang, Q.-M., Zhang, Y.-C., and Zhou, T. (2016). Vital nodes identification in complex networks. *Physics Reports*, 650:1–63.

Maalouly, M., Franck, P., Bouvier, J.-C., Toubon, J.-F., and Lavigne, C. (2013). Codling moth parasitism is affected by semi-natural habitats and agricultural practices at orchard and landscape levels. *Agriculture, ecosystems & environment*, 169:33–42.

Martin, E. A., Dainese, M., Clough, Y., Báldi, A., Bommarco, R., Gagic, V., Garratt, M. P., Holzschuh, A., Kleijn, D., Kovács-Hostyánszki, A., Marini, L., Potts, S. G., Smith, H. G., Al Hassan, D., Albrecht, M., Andersson, G. K., Asís, J. D., Aviron, S., Balzan, M. V., Baños-Picón, L., Bartomeus, I., Batáry, P., Burel, F., Caballero-López, B., Concepción, E. D., Coudrain, V., Dänhardt, J., Diaz, M., Diekötter, T., Dormann, C. F., Duflot, R., Entling, M. H., Farwig, N., Fischer, C., Frank, T., Garibaldi, L. A., Hermann, J., Herzog, F., Inclán, D., Jacot, K., Jauker, F., Jeanneret, P., Kaiser, M., Krauss, J., Le Féon, V., Marshall, J., Moonen, A. C., Moreno, G., Riedinger, V., Rundlöf, M., Rusch, A., Scheper, J., Schneider, G., Schüepp, C., Stutz, S., Sutter, L., Tamburini, G., Thies, C., Tormos, J., Tscharntke, T., Tschumi, M., Uzman, D., Wagner, C., Zubair-Anjum, M., and Steffan-Dewenter, I. (2019). The interplay of landscape composition and configuration: new pathways to manage functional biodiversity and agroecosystem services across Europe. *Ecology letters*, 22(7):1083–1094.

McGarigal, K. and Marks, B. J. (1995). FRAGSTATS: spatial pattern analysis program for quantifying landscape structure. *Gen. Tech. Rep. PNW-GTR-351. Portland, OR: US Department of Agriculture, Forest Service, Pacific Northwest Research Station. 122 p*, 351.

Minor, E. S. and Urban, D. L. (2008). A graph-theory framework for evaluating landscape connectivity and conservation planning. *Conservation biology*, 22(2):297–307.

Møller, J. and Waagepetersen, R. P. (1998). Markov connected component fields. *Advances in Applied Probability*, pages 1–35.

Papaïx, J., Adamczyk-Chauvat, K., Bouvier, A., Kiêu, K., Touzeau, S., Lannou, C., and Monod, H. (2014). Pathogen population dynamics in agricultural landscapes: The ddal modelling framework. *Infection, Genetics and Evolution*, 27:509–520.

Poggi, S., Papaïx, J., Lavigne, C., Angevin, F., Le Ber, F., Parisey, N., Ricci, B., Vinatier, F., and Wohlfahrt, J. (2018). Issues and challenges in landscape models for agriculture: from the representation of agroecosystems to the design of management strategies. *Landscape Ecology*, 33(10):1679–1690.

Power, A. G. (2010). Ecosystem services and agriculture: tradeoffs and synergies. *Philosophical transactions of the royal society B: biological sciences*, 365(1554):2959–2971.

Ricci, B., Franck, P., Toubon, J.-F., Bouvier, J.-C., Sauphanor, B., and Lavigne, C. (2009). The influence of landscape on insect pest dynamics: a case study in southeastern france. *Landscape ecology*, 24(3):337–349.

Saura, S. and Martinez-Millan, J. (2000). Landscape patterns simulation with a modified random clusters method. *Landscape Ecology*, 15:661–678.

Sciaini, M., Fritsch, M., Scherer, C., and Simpkins, C. E. (2018). NLMR and landscapetools: An integrated environment for simulating and modifying neutral landscape models in R. *Methods in Ecology and Evolution*, 9(11):2240–2248.

Sirami, C., Gross, N., Baillod, A. B., Bertrand, C., Carrié, R., Hass, A., Henckel, L., Miguet, P., Vuillot, C., Alignier, A., Girard, J., Batáry, P., Clough, Y., Violle, C., Giralt, D., Bota, G., Badenhausser, I., Lefebvre, G., Gauffre, B., Vialatte, A., Calatayud, F., Gil-Tena, A., Tischendorf, L., Mitchell, S., Lindsay, K., Georges, R., Hilaire, S., Recasens, J., Solé-Senan, X. O., Robleño, I., Bosch, J., Barrientos, J. A., Ricarte, A., Marcos-Garcia, M. Á., Miñano, J., Mathevet, R., Gibon, A., Baudry, J., Balent, G., Poulin, B., Burel, F., Tscharntke, T., Bretagnolle, V., Siriwardena, G., Ouin, A., Brotons, L., Martin, J. L., and Fahrig, L. (2019). Increasing crop heterogeneity enhances multitrophic diversity across agricultural regions. *Proceedings of the National Academy of Sciences of the United States of America*, 33(116):16442–16447.

Stoehr, J. (2017). A review on statistical inference methods for discrete Markov random fields. *arXiv preprint arXiv:1704.03331*.

Urban, D. and Keitt, T. (2001). Landscape connectivity: a graph-theoretic perspective. *Ecology*, 82(5):1205–1218.

Urban, D. L., Minor, E. S., Treml, E. A., and Schick, R. S. (2009). Graph models of habitat mosaics. *Ecology letters*, 12(3):260–273.

van Lieshout, M. (2000). *Markov point processes and their applications*. World Scientific.

van Lieshout, M. N. M. (2019). *Theory of Spatial Statistics: A Concise Introduction*. CRC Press.

Varin, C., Reid, N., and Firth, D. (2011). An overview of composite likelihood methods. *Statistica Sinica*, 21:5–42.

With, K. A. and King, A. W. (1997). The use and misuse of neutral landscape models in ecology. *Oikos*, 79(2):219–229.

Zamberletti, P., Papaïx, J., Gabriel, E., and Opitz, T. (2021). Supplement to "markov random field models for vector-based representations of landscapes".

More pests but less pesticide applications: ambivalent effect of landscape complexity on conservation biological control

Patrizia Zamberletti[1]*¶, Khadija Sabir[2¶], Thomas Opitz[1], Olivier Bonnefon[1], Edith Gabriel[1], Julien Papaïx[1]

[1] INRAE Biostatistique et Processus Spatiaux , INRA-PACA, Avignon, France

[2] Institute of Horticultural Production Systems, Leibniz University Hannover, Hannover Germany.

* Corresponding author

E-mail: patrizia.zamberletti@inrae.fr (PZ)

¶ These authors contributed equally to this work

Abstract

In agricultural landscapes, the amount and organization of crops and semi-natural habitats (SNH) have the potential to promote a bundle of ecosystem services due to their influence on ecological community at multiple spatio-temporal scales. SNH are relatively undisturbed and are often source of complementary resources and refuges, therefore supporting more diverse and abundant natural pest enemies. However, the nexus of SNH proportion and organization with pest suppression is not trivial. It is thus crucial to understand how the behavior of pest and natural enemy species, the underlying landscape structure, and their interaction, may influence conservation biological control (CBC). Here, we develop a generative stochastic landscape model to simulate realistic agricultural landscape compositions and configurations of fields and linear elements. Generated landscapes are used as spatial support over which we simulate a spatially explicit predator-prey dynamic model. We find that increased SNH presence boosts predator populations by sustaining high predator density that regulates and keeps pest density below the pesticide application threshold. However, predator presence over all the landscape helps to stabilize the pest population by keeping it under this threshold, which tends to increase pest density at the landscape scale. In addition, the joint effect of SNH presence and predator dispersal ability among hedge and field interface results in a stronger pest regulation, which also limits pest growth. Considering properties of both fields and linear elements, such as local structure and geometric features, provides deeper insights for pest regulation; for example, hedge presence at crop field boundaries clearly strengthens CBC. Our results highlight that the integration of species behaviors and traits with landscape structure at multiple scales is necessary to provide useful insights for CBC.

Author Summary

In the agricultural context, the loss of semi-natural surfaces often results in high pest abundance requiring elevated pesticide loads. Habitat heterogeneity resulting from the agricultural intermixing of arable fields and semi-natural areas is key to allow organism fluxes across agro-ecological interfaces by influencing ecological processes. Semi-natural habitats (SNH) are often restricted to linear structures, such as hedgerows, but they play an important role by hosting a large number of species. However, the effect of hedgerows is controversial, as it

50 could result in a positive, ineffective or negative effect for CBC. Usually, the impacts of landscape structure on
51 pest population dynamics and resulting CBC are assessed through field experiments with a specific focus, which
52 cannot be generalized, lack flexibility and are limited by the need to manipulate relatively large landscapes.
53 Here, we tackle the challenge to investigate the controversial role of semi-natural habitats for CBC by presenting
54 a simulation-based approach, which allows us to characterize the joint influence of landscape structure and
55 species traits on CBC service. Our study corroborates that spatial heterogeneity, species traits and their
56 interactions are fundamental for CBC. We show that hedge presence alone is not sufficient to lead to strong pest
57 reduction, but hedge-based predators help to maintain the pest density under the pesticide threshold. Instead,
58 SNH presence coupled with appropriate predator traits leads to stronger decrease of pest population. Moreover,
59 we highlight an important scaling effect of SNH, which at the local scale has an even more important impact on
60 CBC as local properties are considered.
61

62 ## Introduction

63 Agricultural landscape simplification results in substantial loss of semi-natural mosaics and of non-crop field
64 margins. It is often associated with high pest abundance, which in turn requires a higher pesticide input (1,2).
65 Consequently, a negative relationship emerges between intensity of agriculture and agricultural landscape
66 biodiversity (3) because of a partial replacement and suppression of the ecological services provided by
67 communities of beneficial organisms (4,5). Habitat heterogeneity is key to allow cross-system fluxes of
68 organisms across agro-ecological interfaces by influencing ecological dynamics within those habitats (6,7) and
69 potentially increasing predator abundance and diversity in agricultural systems (8,9). In addition, complex
70 landscape favours habitat and resource diversity for predators thanks to increased availability of alternative
71 preys, higher microclimate heterogeneity, the presence of refuges from their own predators and for
72 overwintering (10). In arable land, semi-natural habitat (SNH) is typically restricted to hedgerows. These linear
73 structures play an important role as relatively perennial line corridors because of their temporal stability with
74 respect to crop fields. Their presence supports predator dispersal and movement to escape from disturbances and
75 to find food resources scattered in time and space (11,12).

While SNH favours the presence or abundance of functional groups of organisms in landscapes, it can also result in ineffective conservation biological control (CBC) (12,13) with no, or even negative effects on pest control (12–14). A meta-analysis revealed that pest pressure in complex landscapes is reduced in 45% of cases, not affected in 40% of cases and increased in 15% of cases (9). The analysis in (15) highlights the difficulty of stating general and systematic pest and predator interactions and responses; it is based on a very large pest control dataset from which a remarkable variability in pest and enemy responses to different landscape metrics is found. For example, the effect of landscape structure on pests remains inconclusive, as many crop pests also benefit from nearby non-crop habitat (12–14). It may occur that SNH offers more complementary resources to pests rather than to predators to complete their life cycle (6). Predator abundance is not always enough to guarantee a consistent reduction of pest species (16) in case of the presence of alternative prey (known as *dilution effect*) (17), or increased intra-guild predation (18). Life history traits, in particular those traits related to mating systems, competitive skills, movement abilities and habitat use, are also of major importance by affecting species' responses to landscape heterogeneity and being readily linked with ecological processes (19). Thus, effect direction and magnitude jointly depend on organisms and landscapes under study (20,21).

In general, the impacts of landscape structure on pest population dynamics are investigated through empirical correlative approaches with global descriptors at landscape level, due to the difficulty of manipulating large landscapes for local analyses and due to the lack of the spatio-temporal dimension. The main drawback of these approaches is the difficulty of linking correlation levels to population dynamic processes, such as local population growth or migration behavior (22). A complementary approach, combining theoretical modeling and computer simulations, consists in coupling generative landscape models with population dynamics models to explore how different landscape configurations, including the hedge network structure, affect CBC (23) .

A major goal of this work is to implement a general simulation-based approach to obtain theoretical insights on CBC by incorporating landscape effects and species traits, which can serve as basis to formulate practical recommendations. In order to assess what are the main factors that influence the predator-pest population densities in complex landscapes, following questions are investigated: (i)Can landscape composition and configuration reduce the number of pesticide applications by enhancing CBC? (ii) How do species traits related

to dispersal, predation and population demography modify the effect of landscape heterogeneity? Specifically, we develop a stochastic landscape model to simulate realistic agricultural landscape compositions and configurations of fields and linear elements for crop and semi-natural allocation. The generated landscapes are used as spatial support over which we simulate spatially explicit predator-pest dynamics. The population model accurately links 2D diffusion on surface, 1D diffusion on linear elements, and the flux interchanges among them to put particular attention on the linear element integration; see the video file provided in the supplement for illustration. Predators use hedges as their natural habitat where their population naturally develops, but they can also move into crop field to feed on pests. Pests consider crop fields as their natural habitats where they show positive growth, while they are not influenced by hedge elements. Our study explores how the joint consideration of spatial heterogeneity, landscape structure, species traits and their interactions helps to achieve effective CBC. We present and discuss results in the following sections; the technical description of our model and statistical methods is given in Section 4.

2 Results

2.1 Sensitivity of predator density, pest density and pesticide applications to model parameters

Fig. 1 shows the results of a Sobol sensitivity analysis, where sensitivity indices are denoted by $I_{variable}$ in the following and are calculated from replicated simulations with the same underlying parameter configuration. The sensitivity analysis of the mean of model outputs across landscape replicates (Fig. 1a right) shows that variations in mean predator population density are mainly explained by predator migration ($I_{\rho_{12}} = 50\%$) and by the proportion of hedges ($I_{P_h} = 41\%$), whereas interactions among parameters have little impact on the outputs. For the mean pest population density and the average number of pesticide applications, crop proportion ($I_{P_c} = 78\%$ and $I_{P_c} = 83\%$, respectively) and pest growth rate ($I_{r_u} = 17\%$ and $I_{r_u} = 15\%$, respectively) are the most important parameters to explain model output variability, again with only little interaction between model parameters (Fig. 1b right). Complete results for pesticide applications are given in the S1.

The sensitivity analysis of standard deviation of model outputs across landscape replicates gives different importance to the input variables as compared to the mean values. For the predator density, crop proportion (P_c), predator migration (ρ_{12}), hedge proportion (P_h) and spatial crops and hedges aggregation (φ) explain

respectively 55%, 19%, 9% and 9% of the variability of model outputs (Fig. 1a left). For the pest and pesticide applications, results are consistent with the results obtained for the mean. However, interactions between model parameters are important to explain variations in the standard deviation of predator and pest density, as well as of pesticide applications among landscape replicates. This implies that particular landscape structures, characterized by a combination of several descriptors, have to be considered to fully understand the drivers of predator-pest dynamics.

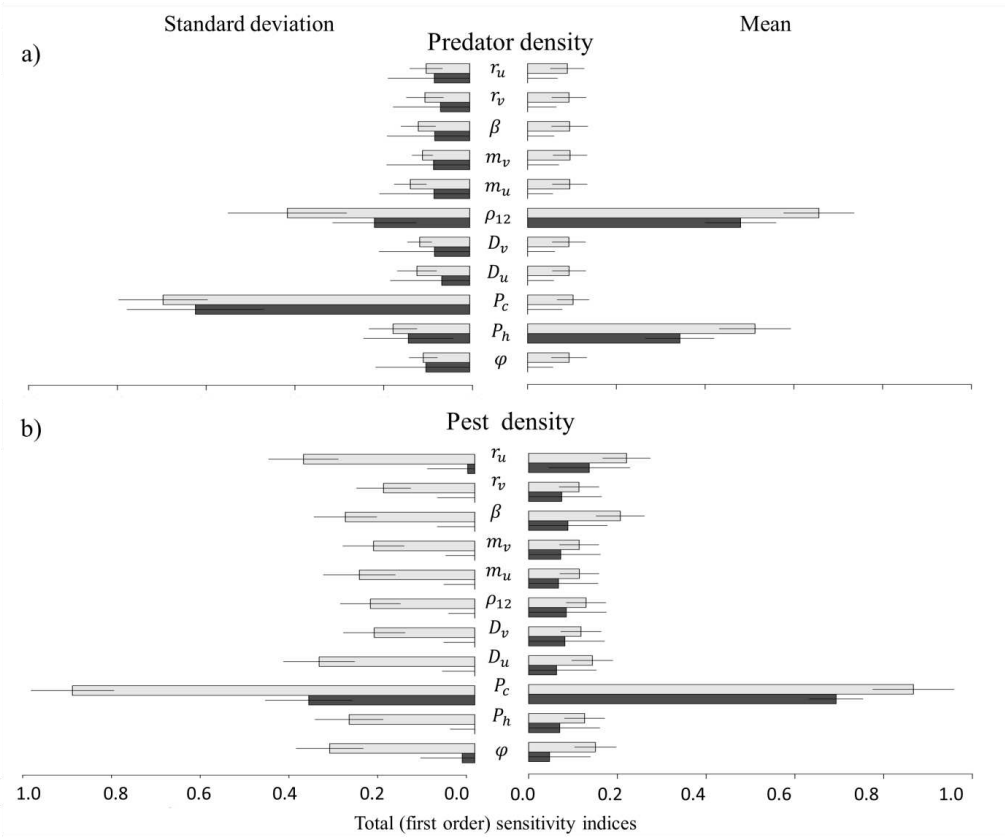

Fig. 1. **Sobol sensitivity analysis.** Total sensitivity indices (light grey bar) and first-order sensitivity indices (black bar) of space-time averaged values for predator density (a) and pest density (b), based on the mean (right) or on the standard deviation (left) calculated over replicated simulations. The length of the bar indicates the mean of the sensitivity index, and the solid line indicates its 95% confidence interval.

3.2 Landscape structure effects on the predator-pest dynamics

Estimated coefficients of landscape variables (denoted $E_{variable}$ in the following) on predator density highlight a positive effect of hedge proportion ($E_{P_h} = 0.40 \pm 0.05$), a negative effect of crop proportion ($E_{P_c} = -0.20 \pm 0.04$) and a positive interaction among both variables ($E_{P_h:P_c} = 0.08 \pm 0.02$), which implies that hedges can buffer the negative effect of increased crop proportion. Migration from hedges to fields ($E_{\rho_{12}} = 0.56 \pm 0.01$) has the highest positive effect on predator density with again a positive interaction with crop proportion.

As expected, crop proportion $\left(E_{P_c} = 1.50 \pm 0.16\right)$, as well as spatial crop and hedge aggregation ($E_{\varphi} = 0.55 \pm 0.02$), have a strong positive effect on pest density. Both variables interact negatively ($E_{\varphi:P_c} = -0.11 \pm 0.01$), as high aggregation results in an increase of the size of contiguous crop fields, which lowers the effect of increased crop proportion. The positive effect of crop proportion is lowered by its interaction with hedge proportion ($E_{P_h:P_c} = 0.03 \pm 0.06$) and also with predator migration from hedge to fields ($E_{P_c:\rho_{12}} = 0.06 \pm 0.06$). Counterintuitively at first sight, an increase in hedge proportion ($E_{P_h} = 0.09 \pm 0.11$) has a positive effect on pest density. Indeed, predator presence over all the landscape helps to stabilize the pest population by keeping it under the thresholds that would trigger a pesticide application. This is further confirmed by the fact that hedge proportion ($E_{P_h} = 0.32 \pm 0.57$), predator spillover from hedges to fields ($E_{\rho_{12}} = 0.61 \pm 0.34$) and concurrence of high crop proportion and aggregation ($E_{\varphi:P_c} = 0.24 \pm 0.09$) have a positive effect on the presence of pesticide applications, but a negative effect on pesticide application numbers ($E_{P_h} = -0.11 \pm 0.07$, $E_{\rho_{12}} = -0.19 \pm 0.08$, $E_{\varphi:P_c} = -0.07 \pm 0.01$).

Among species traits, predator migration from hedges to fields ($E_{\rho_{12}} = -0.13 \pm 0.12$) has the highest negative impact on pest density. Pest diffusion ($E_{D_u} = -1.03 \pm 0.01$), due to a dilution effect, and the predating rate ($E_{\beta} = -0.24 \pm 0.01$), have also a negative impact on the pest, while the growth rate ($E_{r_u} = 0.41 \pm 0.01$) contributes positively to pest density. S1 Fig. 3 shows all estimated effects and their confidence intervals for predator and pest density and pesticide application presence/absence and number, see also Table 1.

By checking the sensitivity of our results with respect to the pesticide application variables (*i.e.,* pesticide application efficacy [optimal vs realistic] and pesticide thresholds [low vs high], see the Supplement), we find that there is no variation of the direction of the estimated effects, but the magnitude of the effect can increase or decrease depending on the scenario considered. Specifically, when pest reduction is lower due to low pesticide efficacy, or, when pest reduction is slower due to an elevated pesticide threshold, hedges show a more important effect in slowing down pest dynamics thanks to predator presence providing a more efficient CBC.

3.4 Effect on pesticide application at local scale

Locally, presence of pesticide applications is negatively influenced by field area and perimeter ($E_{Area} = -0.32 \pm 0.01$, $E_{Perimeter} = -0.10 \pm 0.03$). These effects reflect both a slower pest diffusion in large fields and higher predator incoming fluxes to fields with long perimeter. Conversely, when pesticide applications occurred in a field, the total number of pesticide applications increases with field perimeter due to spillover form the neighborhoods. An increase in the number of adjacent crop fields produces a positive effect on the presence ($E_{Adj_C} = 0.74 \pm 0.01$) and number ($E_{Adj_C} = 0.20 \pm 0.002$) of pesticide applications, while an increase in the number of adjacent hedges leads to a negative effect on the presence ($E_{Adj_H} = -0.07 \pm 0.01$) and number ($E_{Adj_H} = -0.05 \pm 0.001$) of pesticide applications. Whereas in the global model the increase of hedge proportion is associated with a positive effect on the presence of pesticide applications, we attribute the negative effect at local level to the fact that the predator tends to locally maintain the pest density under the pesticide threshold, especially after a first pesticide application. The number of pesticide applications in adjacent fields is positively correlated to their local presence ($E_{Adj_{Tr}} = 2.99 \pm 0.01$) and number ($E_{Adj_{Tr}} = 0.13 \pm 0.001$), indicating local proliferation of the pest. S1 Fig. 4 shows all estimated local effects and confidence intervals for pesticide application presence/absence and number, see also Table 1.

Table 1. Estimated coefficients (only those discussed in the text). Estimated coefficient on predator and pest density (left) and on the presence/absence (P/A) and number (No.) of pesticide applications (right) at landscape and patch level. + indicates a positive effect, – a negative effect, NS a non significant effect.

		Density				Pesticide application	
	Coefficient	Predator	Pest		Coefficient	P/A	No.
Landscape	E_{P_h}	+	+	*Landscape*	E_{P_h}	+	-
	E_{P_c}	-	+		$E_{\rho_{12}}$	+	-
	$E_{P_h:P_c}$	+	+		$E_{\varphi:P_c}$	+	-
	$E_{\rho_{12}}$	+	-	*Patch*	E_{area}	-	-
	$E_{\varphi:P_c}$	NS	-		E_{perim}	-	+
	$E_{P_c:\rho_{12}}$	+	+		E_{Adj_C}	+	+
	E_{D_u}	+	-		E_{Adj_H}	-	-
	E_{β}	+	-		$E_{Adj_{Tr}}$	+	+
	E_{r_u}	+	+				

3 Discussion

Sustainable management of pests and diseases in agro-ecosystems requires a better understanding of how landscape structure drives and alters population dynamics. By simulating different landscape configurations including linear corridors, and the predator-pest dynamics, the present research aims at characterizing the joint influence of landscape structure and species traits on CBC service. Our study corroborates that spatial heterogeneity, landscape structure (i.e., the size and physical arrangement of patches), species traits and their interactions play a key role for CBC.

High crop proportion is the major determinant of increasing pest population and results in an increased number of pesticide applications over the whole landscape. Indeed, increasing crop proportion in fragmented landscapes ensures food availability to the pest all over the landscape (1,2,12). In highly aggregated landscapes, the size of contiguous crop patches is already large enough to sustain a relatively large pest population, thus lowering the effect of an increase in crop proportion (14). The effects of crop proportion and spatial crop and hedge aggregation are intimately linked to pest growth rate and dispersal capability. Indeed, unfavorable landscape properties for the pest (i.e., low proportion and high fragmentation) can be compensated by a higher

growth rate. However, the effect of dispersal is a double-edged sword since high dispersal helps spreading on fragmented landscapes but comes with a larger amount of propagules lost in unsuitable habitats, potentially leading to a dilution effect (3,33,34).

As expected, hedge proportion (i.e., SNHs) positively affects predator presence in agricultural landscapes. In addition, the predator's ability to move between SNHs and crop habitats is the parameter that increases most strongly the predator density, since it enables predators to reach complementary resources in crop fields more easily. Predator fluxes from adjacent habitat is reported to have a major impact on pest populations in crop fields (3,12,26). Spillover from hedges to fields not only depends on predator propensity to forage outside their natural habitat, but also on semi-natural patch connectivity and on crops and predator reservoir interface (27). Thus, different combinations of SNH proportion and aggregation influence landscape structural connectivity and are also important determinants of predator efficiency in regulating crop pests (27).

In our representation, hedges are modeled as a source of predators where these have logistic growth. This is a simplification for predator dynamics in their natural habitat, as we do not consider potential prey presence in hedges and predator foraging behavior in crop fields. For example, the growth rate, instead of being constant, could depend on the time spent in the fields and on the number of consumed preys. In addition, predating rate and consumption rate are crucial in determining the efficiency of CBC (28). Here, these parameters are not identified as influential in the dynamics, maybe because they are assumed identical (parameter β in our model). Finally, another strong assumption of our model is that we refer to a selective pesticide application which does not affect predator mortality, such that we do not explore a broad-spectrum pesticide scenario. In general, broad-spectrum pesticides are more commonly applied (17), but there are pest management programs where selective insecticides have been proved to be particularly effective in combination with a CBC strategy by weaving together direct targeted reduction in pest numbers with predator conservation (17,29). Moreover, introducing broad-spectrum pesticide application effects may result in secondary pest breakouts (30–32), where pests benefit from the predator reduction. Then, additional pesticide loads would be necessary to decrease pest density, which in turn continuously decimates the predator population (33). Therefore, the effect of SNH and predators, and their relationships for CBC outcomes, would be confused and masked. In our work, an indirect effect could be

observed: in crop fields, a positive predator growth rate relies only on pest availability, such that a strong pest reduction due to pesticide applications is automatically translated into a strong impact on predator density when such pesticide applications occur.

In our analysis, we found that the predator's ability to disperse from hedges to crop fields has a major influence on pest density and related pesticide applications. High crop proportion enhances pest density, but this effect is counter-balanced by the joint effect of hedge proportion and predator spillover from hedges to fields, which favors predator pressure and reduces pesticide applications. Indeed, hedges ensure an increased functional landscape connectivity, which enables predators to successfully disperse and feed on complementary resources in the fields. Interestingly, however, we found that if SNHs can sustain a high population of predators (34), this is not sufficient to achieve a decrease in pest density. Indeed, by keeping the pest population density under the pesticide application threshold, the predator population can favor its spread across the landscape, thus increasing pest density at the landscape scale, even if fewer pesticide applications are applied. Most of the studies consider the amount of SNH as a proxy for predator presence and focus on how landscape structure directly influences CBC. However, as highlighted by our results (see also (37)), the extent to which species are influenced by landscape heterogeneity depends on their traits. For example, (36) argue that predators with an oriented movement are better able to deliver pest control services. They discuss the interplay among predator mobility, proportion of crop and SNHs. More generally, predator fluxes from SNH are expected to be particularly strong when (i) predator attack rates on prey are high, (ii) predator movement abilities are substantial, and (iii) predator mortality rates in the recipient habitat are low (37). However, we point out that the predator we model is a generalist predator that does not show strong aggregation behaviour towards pests. Pests represent a predator resource in field, but predators can persist in the landscape also without pests as they have a positive growth in hedges. Different outcomes would be probably observed when considering a specialist predator showing an aggregating behaviour around local pest outbreaks (38). As for example in (38), specialist predators are found to be more effective agents in suppressing local outbreaks than generalist ones.

The amount of predator spillover from hedges to fields, and the distance over which pest and predator can spread, both depend on local configurational variables such as field size, shape, amount of shared edge, and

connectivity (20). Large fields can support high pest volumes, but it has been demonstrated that the relationship between field size and pest density can take several forms depending on assumptions, conditions and species considered (39). Our results show a negative effect of large field area on the need and quantity of pesticide applications, which, according to (39), may come from the elevated growth rate of the prey combined with its good dispersal ability. By contrast, a high number of pesticide applications is favoured by long field perimeters, as these facilitate high fluxes of pest coming in from surrounding fields. However, when a hedge is present on a field boundary, we observe a reduction in numbers of pesticide applications, as there is an increase of predator spillover from hedges into fields (9). Interestingly, we show a contrasted effect of hedges depending on the scale considered. At global scale, the proportion of hedges shows a positive effect on pest density and has a negative effect only on the presence of pesticide application. At local scale, an elevated number of hedges on crop boundaries shows an even more important impact on CBC by negatively affecting both the local presence and number of pesticide applications (34).

Landscape simplification is a major driver of pest abundance and consequently has strong impacts on the necessity of pesticide applications and their frequency. We find that natural habitat enhances predator population, but it does not systematically translate into a strong correlation with pest density decrease. However, a relatively high predator density often helps maintaining pest density below the threshold level above which pesticides are applied, thus preventing highly localized pest densities. However pest population can already have a moderate density level over substantial surfaces and therefore may quickly propagate in every point of the space. Indeed, in our model the hedges are generally expected to play a positive role, but our results at global scale show that the final outcome must be analyzed in a much more nuanced way. By contrast, predator spillover from hedges to fields is fundamental for CBC; it reduces pest density and guarantees high predator fluxes and different habitat connectivity. At field scale, landscape geometric features, hedge presence and habitat connectivity are able to influence predator-pest dynamics, and therefore they affect the number of pesticide applications. This highlights the importance of conducting a multi-scale analysis to consider the differences in outcomes at landscape and patch scale for pest CBC (14). In most of our analyses, we considered global outputs by averaging pest and predator densities over crop fields. However, populations are obviously structured in

space and time. Thus, a complementary analysis studying how landscape structure impacts spatio-temporal predator-pest dynamics would bring deeper insights on pest outbreak determinants. Moreover, a larger number of pest and predator species, inter/intra-species interactions and also different trophic network structures, could be considered in future work to better understand the role of pest and predator diversity on CBC efficacy.

4 Models and methods

4.1 Stochastic landscape model

The landscape is represented through a vectorial approach, which is appropriate for representing the highly regular geometric patterns of agricultural landscapes (40,41). It is composed of polygons representing fields, separated by edges. Landscape elements are characterized by their geometry (e.g., vertex coordinates, size and shape), and by categorical information defining the land-cover (e.g., crop or natural habitat). The landscape geometric structure is fixed and based on a real landscape with an extent of 5.55 km. The landscape is transformed into a T-tessellation (42,43) composed of 188 polygons with a total of 577 edges.

We use Gaussian random fields (GRFs) to allocate a proportion of polygons and edges as crops representing the principal culture and hedges to provide SNHs, respectively. A threshold on the simulated GRF values is set to attribute specific landscape elements depending on the value being below or above the threshold. By definition, a GRF denoted by W is a random surface over continuous 2D space, for which the multivariate distribution of the values $(W(x_1), W(x_2), \dots, W(x_n))$ observed at a finite number of locations $x_1, x_2, \dots, x_n$ in the landscape corresponds to a multivariate normal distribution, characterized by its mean vector and its covariance matrix Σ. The mean is fixed to 0 and the exponential correlation function is used for Σ, such as $\Sigma_{ij} = e^{-\left(\frac{|x_i - x_j|}{\varphi}\right)}$, where $|x_j - x_i|$ is the Euclidean distance between any two points x_j and x_i. The range parameter $\varphi \geq 0$ governs the strength of clustering of category allocation to landscape elements. To handle the interactions between the allocation of hedge and crop, we simulated two correlated GRFs for crop ($W_c(s)$) and hedge ($W_h(s)$):

$$W_c(s) = \rho W_h(s) + \sqrt{1-\rho^2}\widetilde{W}(s), \qquad (1)$$

where $\rho \in [-1,1]$ controls the correlation between W_h and $\widetilde{W}$, which is a GRF independent from W_h. The parameter used for the landscape models with their range of values can be found in Table 2. Fig. 2 shows an example of four landscapes simulated according to different proportions and aggregation levels of hedges and crop fields.

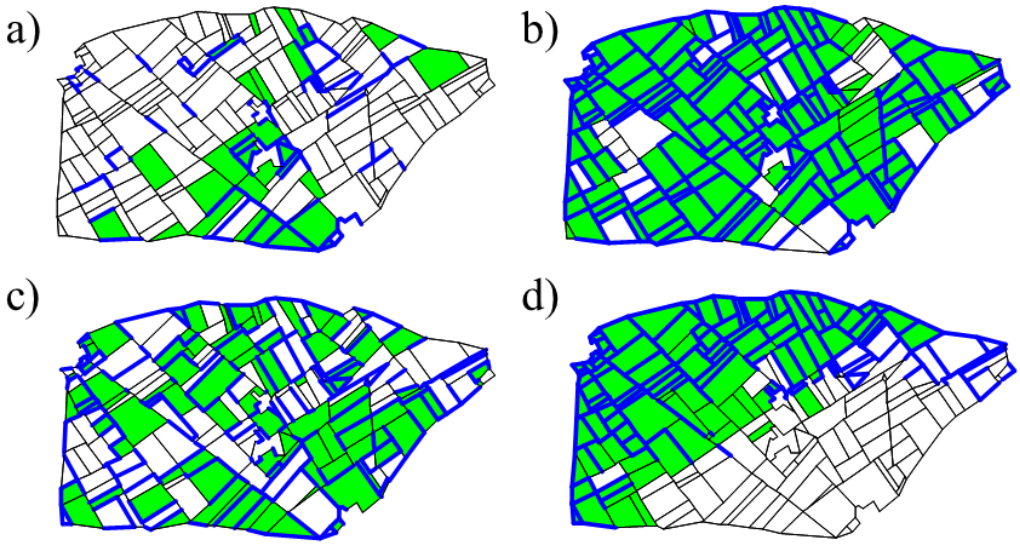

Fig. 2. **Simulation examples.** Examples of simulated landscape structures with interacting elements using the following allocation categories: for fields, (i) crop (green) and (ii) non-crop (white); for edges, (i) hedge (blue) and (ii) no-hedge (black). First row: low (a) and high (b) proportions of crop and hedges (0.2 and 0.8, respectively), with fixed parameter configuration for aggregation and fixed correlation between crop and hedges (0.5). Second row: low (c) and high (d) crop and hedge aggregation level from left to right, with fixed proportion of crop and hedges (0.5) and fixed correlation between crop and hedges (0.5).

4.2 Predator-pest model

We developed a spatially explicit predator-pest model based on a system of partial differential equations. The model is built on a previously developed model that considers both 2D diffusion on polygons and 1D diffusion on edges (11). Simulations are performed over a [0,100]-time interval representing a cropping season with a time

step of 1 day. The model parameters and their range of simulated values are reported in Table 2. Numerical simulations of the spatio-temporal partial differential equation system of predator-pest dynamics are performed using the Freefem++ finite-element framework (44). The predator-pest dynamics is illustrated by snapshots at different time step (Fig. 3) and by plots of the temporal dynamics in the supplement, and by a video for the whole simulation period over the spatial domain.

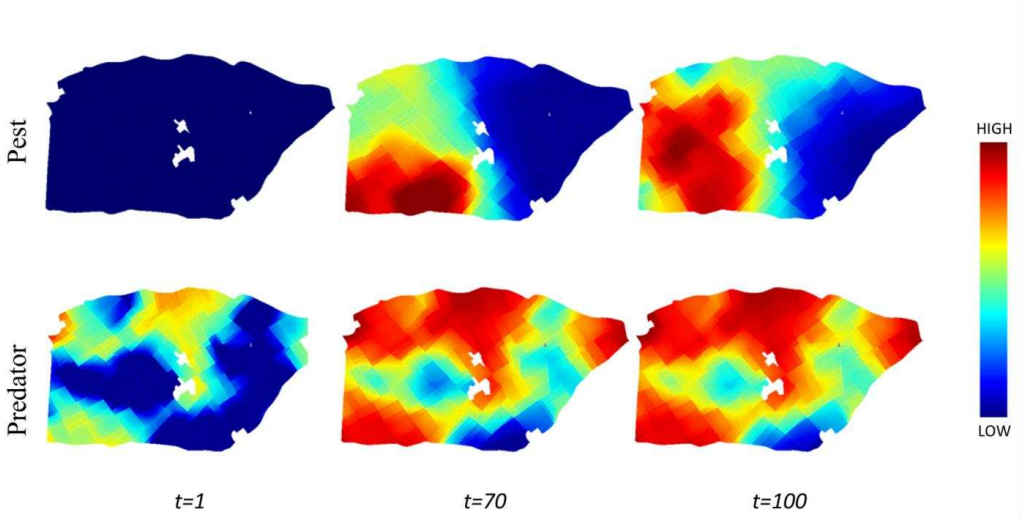

Fig. 3 Snapshots of pest and predator spatial dynamics. Simulation of predator-pest population dynamics at different time intervals *t={1, 70, 100}*. At the initial stage, the pest density (first line) is very low, followed by random introduction of pest. As time proceeds, the pest density increases (from left to right), anad predator density (last line) also increases and diffuses to surrounding fields. At the final time step, high pest density arises where predators are absent.

Table 2. Description of parameter values. *Spatial aggregation is the parameter controlling the adjacency of crop elements among each other and hedge elements among each other.

Parameters	Description	Values		Units	References
		Min	max		
For landscape model					
φ	Spatial aggregation of hedges and crops*	5.55/100	5.55	km	
P_c	Proportion of crop	0	1	-	
P_h	Proportion of hedges	0	1	-	

ϱ	Correlation between crops and hedges GRF_S	0.5	-		
Parameters for population dynamic mode					
D_2^v	2D diffusion rate of the predator	0.000625	0.012	km^2d^{-1}	Corbett et al., 1996; Pearce et al. 2006
$1/m_v$	Lifespan of the predator	20	66	d^1	Pearce et al. 2006
β	Predating rate	0.01	0.010	$pest^{-1}d^{-1}$	Pearce et al. 2006
ρ_{21}	Migration rate of the predator from field to hedge	0.05		$km^{-1}d^{-1}$	
D_1^v	1D diffusion rate of the predator	0.012		km^2d^{-1}	Corbett et al., 1996; Pearce et al. 2006
r_v	Intrinsic growth rate of the predator on hedges	0.010	0.020	d^{-1}	Xia et al., 1999
K_{h_i}	Carrying capacity of hedges for the predator	1		$predators\ km^{-2}$	
ρ_{12}	Migration rate of the predator from hedge to field	0	0.05	d^{-1}	
D^u	2D diffusion rate of the pest	0.000625	0.012	km^2d^{-1}	Corbett et al., 1996; Pearce et al. 2006
r_u	Intrinsic growth rate of the pest	0.010	0.020	d^{-1}	Xia et al., 1999
C_{it}	Carrying capacity of 2D system for the pest	20 (without pesticide) 0.1 (after pesticide)		$pests\ km^{-2}$	
$1/m_u$	Lifespan of the pest	20	66	d	Pearce et al. 2006

4.2.1 Predator dynamics

We model a generalist predator not showing strong aggregation behavior around pests. Hedges are the predator's main habitat, which feeds on pests when moving into the fields. Using notations t for time and x for a spatial location, we thus assume the following 1-dimensional reaction-diffusion model for the predator density v_{h_i} on the edge h_i:

$$\begin{cases} \partial_t v_{h_i} = \partial_{xx} D_1^v v_{h_i} + r_v v_{h_i}\left(1 - \dfrac{v_{h_i}}{K_{h_i}}\right) & \text{if the edge } h_i \text{ carries a hedge,} \\ v_{h_i} = 0 & \text{otherwise,} \end{cases} \quad (2)$$

where D_1^v is the diffusion parameter of the predator along hedges, r_v is the intrinsic growth rate of the predator, and K_{h_i} is the carrying capacity of the hedge i. If two hedges are linked together at one of their endpoints, then the dynamics in Equation (7) apply continuously across the junction.

346 In addition, the predator forages on fields where it feeds on the pest. The population density v_{Ω_i} of predators
347 in a field Ω_i is modelled by a reaction-diffusion equation with mobility parameter within field D_2^v, predating rate
348 β, and life span $1/m_v$:

$$\partial_t v_{\Omega_i} = \Delta D_2^v v_{\Omega_i} - m_v v_{\Omega_i} + \beta u_{\Omega_i} v_{\Omega_i}. \quad (3)$$

349 **4.2.2 Pest dynamics**

350 We suppose that edges do not modify directly pest population dynamics. Writing u_{h_i} for the pest density in
351 an edge h_i, we set

$$u_{h_i} = 0 \quad \text{for all } i. \quad (4)$$

352 The pest is a specialist of the principal crop and, without dispersal, it shows positive growth only in crop
353 fields. The bidimensional reaction-diffusion model for the pest density u_{Ω_i} in field u_{Ω_i} is

$$\begin{cases} \partial_t u_{\Omega_i} = \Delta D_2^u u_{\Omega_i} + r_u u_{\Omega_i}\left(1 - \frac{u_{\Omega_i}}{C_{it}}\right) - \beta u_{\Omega_i} v_{\Omega_i} & \text{for } \Omega_i \text{ with crop,} \\ \partial_t u_{\Omega_i} = \Delta D_2^u u_{\Omega_i} - m_u u_{\Omega_i} - \beta u_{\Omega_i} v_{\Omega_i} & \text{for } \Omega_i \text{ with non-crop,} \end{cases} \quad (5)$$

354 where D_2^u is the diffusion parameter of the pest in fields, r_u is its intrinsic growth rate on crop category, β is the
355 predating rate, and $1/m_u$ is the life span of the pest on non-crop fields.
356 In a crop field, a pesticide application is performed when the average pest population density in that field
357 exceeds a given threshold, which we here fix to 0.2 pests km^{-2}. Pesticide applications strongly reduce the
358 carrying capacity C_{it} of the field i (Eq. (5)):

359 $$\begin{cases} C_{it} = K_{\Omega_i} & \text{if no pesticide application is applied,} \\ C_{it} = \frac{K_{\Omega_i}}{200} & \text{during the period } e_t \text{ for which the pesticide application is efficient.} \end{cases} \quad (6)$$

360 This results in a pesticide application efficacy providing a 99.5% pest reduction, which can be considered an
361 ideal-optimal case in practice. More realistic values of pesticide application efficacy should be around 70%
362 (45,46); this alternative scenario is analyzed in the supplement, where the sensitivity to the pesticide application
363 threshold is also tested.
364 Instead of a applying a reduction of the carrying capacity, we could have used an additional linear mortality
365 term to account for the effects of pesticide applications, but this would have implied the modification of both

366 growth and carrying capacity. For that reason, and to keep the model parsimonious, possible effects of pesticide
367 applications are assumed to change only the carrying capacity (Eq. 6), which is equivalent to using quadratic
368 additional mortality term.
369 We point out that here we set the carrying capacity as a general saturation level for pest and predator densities,
370 but it does not necessarily correspond to the number of individuals per km^2. Similarly, mortality other than for
371 predating or pesticide applications could have occurred in crop fields, but we have opted against this option for
372 the sake of parsimony.

373 **4.2.3 Coupling predator-pest dynamics over the entire landscape**

374 Using the framework described in (11), the dynamics described by equations (2) to (6) are coupled over the
375 full landscape using the following assumptions (see the Supplementary Information (SI) for more details): (i)
376 edges (with or without a hedge) do not represent a barrier for the pest, (ii) edges without a hedge do not represent
377 a barrier for the predator, (iii) the predator is attracted by hedges, thus migration from fields to hedges (ρ_{21}) is
378 relatively high, (iv) the predator shows aversion to move outside its natural habitat, thus migration from hedges
379 to fields (ρ_{12}) is lower than migration from fields to hedges. We consider reflecting conditions on landscape
380 boundaries, meaning that in- and out-fluxes between the landscape and its surrounding environment are equal.
381 Since pest population grows in crop habitat but not in non-crop habitat in our model, an increase in pest
382 density with a higher crop proportion is expected. Similarly, since predators prefer hedges, higher hedge
383 proportion favours predator movement through the landscape, thus, increasing predator density and predating
384 pressure.

385 **4.2. Pest arrival and spatio-temporal design**

386 Initially, the predator is present in all hedges at carrying capacity. The pest is introduced randomly in space
387 and time. The average number of pest inoculations in a single simulation is proportional to the proportion of crop
388 field area in the landscape, and we draw the actual number of inoculations from a Poisson distribution. The
389 maximal average number of pest inoculations is 25 and arises when the crop is grown in all fields. Inoculated
390 crop fields are picked at random with probability depending on their relative surface.

4.3 Statistical methods for analyzing simulation outputs

We define an experimental design based on Sobol's sequences leading to 11,500 distinct parameter configurations (47–49). For each parameter combination, we consider 15 landscape replicates, leading to a total of 172,500 simulations. We first conduct a Sobol sensitivity analysis on the mean and standard deviation of predator density, pest density and number of pesticide applications by averaging the outputs over landscape replicates and crop fields. First-order indices were estimated with Sobol–Saltelli's method (50,51), whereas total indices are estimated with Sobol–Jansen's method (50,52). These analysis are performed within the R software version 3.0.3 (R Team, 2003), using the packages fOptions (v. 3010.83) and sensitivity (v. 1.11).

Then, to further explore direction and magnitude of variations in response variables with respect to landscape parameters, we applied Generalized Linear Models (GLMs). Pest and predator densities, and pesticide application numbers (if different from 0), are analysed as response variable by using the Gamma distribution with log-link function. Additionally, presence/absence of pesticide applications during a simulation is analyzed using a GLM with binomial distribution. We develop GLM formulas containing covariable interactions (see Table 2) up to second order, and we use a step-wise variable selection algorithm based on the Bayesian Information Criterion (BIC) in order to iteratively select the "best subset" of variables for each model.

Finally, we use Generalized Linear Mixed-Effect models to analyze occurrences of pesticide applications by taking into account their spatial position in the landscape. We use the log-transformed area ($Area$) and perimeter ($Perimeter$) to take into account the geometrical properties of the fields, and we use the number of adjacent crop fields (Adj_C), the number of adjacent hedges (Adj_H), and the number of pesticide applications applied in the adjacent crop fields (Adj_{Tr}) to take into account the composition and dynamics in local neighbourhoods. In addition, we include the estimated linear effects from the global models as offsets. The random effect is structured by the landscape simulation to account for its specific dynamics. By analogy with the global GLMs, the presence/absence of pesticide applications is analyzed using the binomial response distribution, and numbers of pesticide applications are analyzed with the Gamma distribution for the response variable with a log-link

function. Again, we consider predictor interactions up to 2nd order. These analyses are performed using the R package lme4 with R version 3.2.3 (53).

Acknowledgments:

We are thankful to Claire Lavigne and Katarzyna Adamczyk for their help and wise suggestions for landscape data processing and for the discussion part. Khadija Sabir has been supported by the Erasmus+ - KA1 Erasmus Mundus Joint Master Degrees Programme of the European Commission within the PLANT HEALTH Project.

Bibliography

1. Zhao R, Wang L, Zhang H, Letters JS-S. Analysis on Temporal-Spatial Characteristics of Landscape Pattern of Land-Cover. Sens Lett. 2013;11:1337–41.
2. Zhao ZH, Hui C, He DH, Li BL. Effects of agricultural intensification on ability of natural enemies to control aphids. Sci Rep. 2015;5(1):8024.
3. Tscharntke T, Rand TA, Bianchi FJA. The landscape context of trophic interactions: insect spillover across the crop-noncrop interface. Ann Zool Fennici. 2005;42(4):421–32.
4. Kremen C, Williams NM, Thorp RW. Crop pollination from native bees at risk from agricultural intensification. Proc Natl Acad Sci U S A. 2002;99(26):16812–6.
5. Thies C, Roschewitz I, Tscharntke T. The landscape context of cereal aphid-parasitoid interactions. Proc R Soc B Biol Sci. 2005;272(1559):203–10.
6. Blitzer EJ, Dormann CF, Holzschuh A, Klein AM, Rand TA, Tscharntke T. Spillover of functionally important organisms between managed and natural habitats. Vol. 146, Agriculture, Ecosystems and Environment. 2012. p. 34–43.
7. Hendrickx F, Maelfait JP, Van Wingerden W, Schweiger O, Speelmans M, Aviron S, et al. How landscape structure, land-use intensity and habitat diversity affect components of total arthropod diversity in agricultural landscapes. J Appl Ecol. 2007;44(2):340–51.
8. Tscharntke T, Klein AM, Kruess A, Steffan-Dewenter I, Thies C. Landscape perspectives on agricultural intensification and biodiversity - Ecosystem service management. Ecology Letters. John Wiley & Sons, Ltd; 2005;8: 857–74.

9. Bianchi, Felix JJA and Booij, CJH and Tscharntke T. Sustainable pest regulation in agricultural landscapes: a review on landscape composition, biodiversity and natural pest control. Proc R Soc London B Biol Sci. 2006;17(2):585–96.

10. Rusch A, Valantin-Morison M, Sarthou JP, Roger-Estrade J. Biological control of insect pests in agroecosystems. Effects of crop management, farming systems, and seminatural habitats at the landscape scale: A review. Vol. 109, Advances in Agronomy. Elsevier Ltd; 2010;109: 219–259.

11. Roques L, Bonnefon O. Modelling Population Dynamics in Realistic Landscapes with Linear Elements: A Mechanistic-Statistical Reaction-Diffusion Approach. PLoS One. 2016;11(3):e0151217.

12. Tscharntke T, Karp DS, Chaplin-Kramer R, Batáry P, Declerck F, Gratton C, et al. When natural habitat fails to enhance biological pest control - Five hypotheses. Biological Conservation. 2016;204:449-58.

13. Chaplin-Kramer R, O'Rourke ME, Blitzer EJ, Kremen C. A meta-analysis of crop pest and natural enemy response to landscape complexity. Ecol Lett. 2011;14(9):922–32.

14. Veres A, Petit S, Conord C, Lavigne C. Does landscape composition affect pest abundance and their control by natural enemies? A review. Agriculture, Ecosystems and Environment. Elsevier B.V. 2013;166:110–7.

15. Karp DS, Chaplin-Kramer R, Meehan TD, Martin EA, DeClerck F, Grab H, et al. Crop pests and predators exhibit inconsistent responses to surrounding landscape composition. Proc Natl Acad Sci U S A. 2018;115(33): 7863–70.

16. Martin EA, Dainese M, Clough Y, Báldi A, Bommarco R, Gagic V, et al. The interplay of landscape composition and configuration: new pathways to manage functional biodiversity and agroecosystem services across Europe. Ecol Lett. 2019;22(7):1083-94.

17. Koss AM, Chang GC, Snyder WE. Predation of green peach aphids by generalist predators in the presence of alternative, Colorado potato beetle egg prey. Biol Control. 2004;31(2):237–44.

18. Halaj J, Wise DH. Impact of a detrital subsidy on trophic cascades in a terrestrial grazing food web. Ecology. 2002;83(11):3141–51.

19. Bonte D, Bafort Q. The importance and adaptive value of life history evolution for metapopulation dynamics. bioRxiv. 2018;179234.

20. Haan NL, Zhang Y, Landis DA. Predicting landscape configuration effects on agricultural pest suppression. Trends in ecology & evolution. 2020;35(2):175-86.

21. Imbert C, Papaïx J, Husson L, Warlop F, Lavigne C. Estimating population dynamics parameters of cabbage pests in temperate mixed apple tree-cabbage plots compared to control vegetable plots. Crop Prot. 2020 Mar 1;129.

473 22. Ricci B, Franck P, Toubon JF, Bouvier JC, Sauphanor B, Lavigne C. The influence of landscape on insect pest
474 dynamics: A case study in southeastern France. Landsc Ecol. 2009;24(3):337–49.
475 23. Poggi S, Vinatier F, Hannachi M, Sanz Sanz E, Rudi G, Zamberletti P. How can models foster the transition
476 towards future agricultural landscapes. The Future of Agricultural Landscapes, Part II. 2021 Mar 18:305.
477 24. Zaller JG, Moser D, Drapela T, Schmöger C, Frank T. Insect pests in winter oilseed rape affected by field and
478 landscape characteristics. Basic Appl Ecol. 2008 Oct 6;9(6):682–90.
479 25. Baggio JA, Salau K, Janssen MA, Schoon ML, Bodin Ö. Landscape connectivity and predator–prey population
480 dynamics. Landscape Ecology. 2011 Jan;26(1):33-45.
481 26. Rand TA, Tylianakis JM, Tscharntke T. Spillover edge effects: The dispersal of agriculturally subsidized insect
482 natural enemies into adjacent natural habitats. Annu Rev Ecol Syst. 2006;9(5):603–14.
483 27. Coppolillo P, Gomez H, Maisels F, Wallace R. Selection criteria for suites of landscape species as a basis for site-
484 based conservation. Biological Conservation. 2004 Feb 1;115(3):419-30.
485 28. Pettorelli N, Hilborn A, Duncan C, Durant SM. Individual variability: the missing component to our understanding
486 of predator–prey interactions. Advances in ecological research. 2015 Jan 1;52:19-44.
487 29. Hilbeck A, Eckel C, Kennedy GG. Impact of Bacillus thuringiensis–insecticides on population dynamics and egg
488 predation of the Colorado potato beetle in North Carolina potato plantings. BioControl. 1998 Mar;43(1):65-75.
489 30. Dutcher JD. A review of resurgence and replacement causing pest outbreaks in IPM. General concepts in integrated
490 pest and disease management. 2007:27-43.
491 31. Gross K, Rosenheim JA. Quantifying secondary pest outbreaks in cotton and their monetary cost with causal-
492 inference statistics. Ecological Applications. 2011 Oct;21(7):2770-80.
493 32. Steinmann KP, Zhang M, Grant JA. Does use of pesticides known to harm natural enemies of spider mites (Acari:
494 Tetranychidae) result in increased number of miticide applications? An examination of California walnut orchards.
495 Journal of economic entomology. 2011 Oct 1;104(5):1496-501.
496 33. Hill MP, Macfadyen S, Nash MA. Broad spectrum pesticide application alters natural enemy communities and may
497 facilitate secondary pest outbreaks. PeerJ. 2017 Dec 19;5:e4179.
498 34. Fabian Y, Sandau N, Bruggisser OT, Aebi A, Kehrli P, Rohr RP, Naisbit RE, Bersier LF. The importance of
499 landscape and spatial structure for hymenopteran-based food webs in an agro-ecosystem. Journal of Animal
500 Ecology. 2013 Nov;82(6):1203-14.
501 35. Tscharntke T, Tylianakis JM, Rand TA, Didham RK, Fahrig L, Batáry P, et al. Landscape moderation of

biodiversity patterns and processes - eight hypotheses. Vol. 87, Biological Reviews. 2012. p. 661–85.

36. Le Gal A, Robert C, Accatino F, Claessen D, Lecomte J. Modelling the interactions between landscape structure and spatio-temporal dynamics of pest natural enemies: Implications for conservation biological control. Ecological Modelling. 2020 Mar 15;420:108912.

37. Holt RD, Hochberg ME. Indirect Interactions, Community Modules and Biological Control: a Theoretical Perspective. Eval Indirect Ecol Eff Biol Control. 2001;3:13–37.

38. Bianchi FJJA, Schellhorn NA, Buckley YM, Possingham HP. Spatial variability in ecosystem services: Simple rules for predator-mediated pest suppression. Ecol Appl. 2010 Dec;20(8):2322–33.

39. Segoli M, Rosenheim JA. Should increasing the field size of monocultural crops be expected to exacerbate pest damage? "Agriculture, Ecosyst Environ. 2012;150:38–44.

40. Papaïx J, Adamczyk-Chauvat K, Bouvier A, Kiêu K, Touzeau S, Lannou C, Monod H. Pathogen population dynamics in agricultural landscapes: The Ddal modelling framework. Infection, Genetics and Evolution. 2014 Oct 1;27:509-20.

41. Langhammer M, Thober J, Lange M, Frank K, Grimm V. Agricultural landscape generators for simulation models: A review of existing solutions and an outline of future directions. Ecological Modelling. 2019 Feb 1;393:135-51.

42. Kiêu K, Adamczyk-Chauvat K, Monod H, Stoica RS. A completely random T-tessellation model and Gibbsian extensions. Spatial Statistics. 2013 Nov 1;6:118-38.

43. Adamczyk-Chauvat K, Kassa M, Kiêu K, Papaïx J, Stoica RS. Gibbsian T-tessellation model for agricultural landscape characterization. arXiv preprint arXiv:2007.16094. 2020 Jul 31.

44. Hecht F. New development in FreeFem++. Journal of numerical mathematics. 2012 Dec 1;20(3-4):251-66.

45. Neil KA, Gaui SO, Mcrae KB. Control of the English grain aphid [Sitobion avenae (F.)] (Homoptera: Aphididae) and the oat-birdcherry aphid [Rhopalosiphum padi (L.)] (Homoptera: Aphididae) on winter cereals. Can Entomol. 1997;129(6):1079–91.

46. Abo El-Ghar GES, Abd AE. Impact of two synthetic pyrethroids and methomyl on management of the cabbage aphid, brevicoryne brassicae (L.) and its associated parasitoid, diaeretiella rapae (M'Intosh). Pestic Sci. 1989;25(1):35–41.

47. Sobol' IM. On the distribution of points in a cube and the approximate evaluation of integrals. USSR Comput Math Math Phys. 1967 Jan 1;7(4):86–112.

48. Antonov IA, Saleev VM. An economic method of computing LPτ-sequences. USSR Comput Math Math Phys. 1979

Jan 1;19(1):252–6.

49. Sobol IM. Uniformly distributed sequences with an additional uniform property. USSR Comput Math Math Phys. 1976 Jan 1;16(5):236–42.

50. Saltelli A, Annoni P, Azzini I, Campolongo F, Ratto M, Tarantola S. Variance based sensitivity analysis of model output. Design and estimator for the total sensitivity index. Computer physics communications. 2010 Feb 1;181(2):259-70.

51. Sobol' IM, Tarantola S, Gatelli D, Kucherenko SS, Mauntz W. Estimating the approximation error when fixing unessential factors in global sensitivity analysis. Reliab Eng Syst Saf. 2007 Jul;92(7):957–60.

52. Jansen MJ. Analysis of variance designs for model output. Computer Physics Communications. 1999 Mar 1;117(1-2):35-43.

53. LME4 Author. Linear Mixed-Effects Models using "Eigen" and S4 [R package lme4 version 1.1-26]. 2020.

Supporting information

S1: Supplementary Information of the paper: "More pests but less pesticide applications: ambivalent effect of landscape complexity on conservation biological control". More details about the model and results, and a video illustrating an example of spatio-temporal pest-predator dynamics.

Spatio-temporal point processes as meta-models for population dynamics in heterogeneous landscapes

Patrizia Zamberletti[1], Julien Papaïx[1], Edith Gabriel[1], and Thomas Opitz[1]

[1]*Biostatistics and Spatial Processes, INRAE, Avignon, France*

Email : patrizia.zamberletti@inrae.fr, julien.papaix@inrae.fr, edith.gabriel@inrae.fr,thomas.opitz@inrae.fr

Adress: INRAE-BioSP, 228 route de l'aérodrome, Domaine St Paul, Site Agroparc, CS 40509, 84914 Avignon, cedex 9

Corresponding author: P. Zamberletti

Spatio-temporal point processes as meta-models for population dynamics in heterogeneous landscapes

Abstract

Landscape heterogeneity affects population dynamics, which determine species persistence, diversity and interactions. These relationships can be accurately represented by advanced spatially-explicit models (SEMs) allowing for high levels of detail and precision. However, such approaches are characterised by high computational complexity, high amount of data and memory requirements, and spatio-temporal outputs may be difficult to analyse. A possibility to deal with this complexity is to aggregate outputs over time or space, but then interesting information may be masked and lost, such as local spatio-temporal relationships or patterns. An alternative solution is given by meta-models and meta-analysis, where simplified mathematical relationships are used to structure and summarise the complex transformations from inputs to outputs. Here, we propose an original approach to analyse SEM outputs. By developing a meta-modelling approach based on spatio-temporal point processes (STPPs), we characterise spatio-temporal population dynamics and landscape heterogeneity relationships in agricultural contexts. A landscape generator and a spatially-explicit population model simulate hierarchically the pest-predator dynamics of codling moth and ground beetles in apple orchards over heterogeneous agricultural landscapes. Spatio-temporally explicit outputs are simplified to marked point patterns of key events, such as local proliferation or introduction events. Then, we construct and estimate regression equations for multi-type STPPs composed of event occurrence intensity and magnitudes. Results provide local insights into spatio-temporal dynamics of pest-predator systems. We are able to differentiate the contributions of different driver categories (*i.e.*, spatio-temporal, spatial, population dynamics). We highlight changes in the effects on occurrence intensity and magnitude when considering drivers at global or local scale. This approach leads to novel findings in agroecology where the organisation of cultivated fields and semi-natural elements are known to play a crucial role for pest regulation. It aids to formulate guidelines for biological control strategies at global and local scale.

Keywords: spatio-temporal pattern, multi-type spatio-temporal point process, meta-model, spatially explicit model, system dynamics, landscape heterogeneity

1 Introduction

Community structure, population dynamics and species interactions within and between trophic levels are not limited within single plot's borders but depend on the spatial context (*e.g.*, patch size, spatial configuration, landscape composition, habitat connectivity; see Delaune et al. (2019)) and on ecological processes at different spatial scales (Pickett and Siriwardena, 2011). The key to understanding and predicting community structure and population distribution lies in the explication of the latent mechanisms and causes underlying observed patterns, which may emerge from the collective behaviour at smaller scale units or may be imposed by larger-scale constraints and the related temporal scale (Levin, 1992). Moreover, the influence of different spatial and temporal scales is closely related with species life-history traits, such as their ability to disperse, body size, competition, habitat specialisation, or trophic position (Rusch et al., 2010; O'Rourke et al., 2011). For example, foraging range and dispersal ability may determine the landscape elements that contribute to population dynamics and trophic interactions (Eber, 2001; Fahrig, 2001; Tscharntke and Brandl, 2004). Changes in spatial arrangement of habitats and composition could induce investment in the adaptation of dispersal-related traits (Tscharntke and Brandl, 2004).

Hence, dealing with ecological processes involves studying different spatial and temporal scales, since ecosystem patterns and processes cover various spatio-temporal ranges and may have multiple drivers acting across different extents (Fritsch et al., 2020). The characterisation of the spatial distribution of landscape features and individuals in response to such complex interplay of processes across scales belongs to the field of *landscape ecology*. To account for this complexity, the development of spatially explicit computer modelling and simulations are central for addressing theoretical questions. Many Spatially Explicit Model (SEM) types have been proposed, such as continuous-space reaction-diffusion partial differential equations (Roques, 2013), patch models (Hanski and Thomas, 1994), cellular automata neighborhood models (Hogeweg, 1988), or individual-based models (IBM, Grimm et al., 2005). DeAngelis and Yurek (2017) show the importance and the benefits of using SEMs compared to Spatially Implicit Models (SIMs) through different examples, including a savanna ecosystem. They find that the details and small-scale processes captured by SEMs are fundamental drivers for the ecosystem and its dynamics. SEMs can simulate the emergence of both small- and large-scale patterns from these processes and reveal deep details of dynamics such as predator–prey interactions and food web chains.

The development of advanced numerical models has greatly improved our ability to accurately describe complex dynamics incorporating fine-grain interactions over a large extent. However, as models aim to provide a realistic but simplified representation of reality, the spatio-temporal extent is often properly adapted by scaling decisions (Fritsch et al., 2020). In-model scaling methods give control over simplifications when

building the model or allow us to incorporate and transfer relevant information across different scales. Scaling techniques may also be used before or after building the model, to define model parameters or analyse model outputs. In this work we focus on post-model scaling and propose a parsimonious approach to deal with the complexity of SEM outputs while keeping fine-scale information on the ecological dynamics. A solution to deal with this complexity could be the application of non-spatial analysis methods via spatial and temporal output aggregation (Gotelli, 2000; Webb, 2000; Fritsch et al., 2020). For example, Nathan et al. (2019) use spatially-explicit IBMs to study the hybridisation dynamics among species by describing their relationships across ecological scales, and then model outputs are integrated over space and time. In this case, however, all fine-scale information is lost, thus impeding any analysis of the drivers acting across different scales. An alternative solution is represented by meta-models and meta-analysis, which offer the possibility of reducing model output complexity by establishing a simplified mathematical relationship between the input and output of the system (Simpson et al., 2001). Their main aim is to replace complex numerical models by more parsimonious representations that provide a better understanding and faster analysis tools for optimisation and exploration, specifically when performing uncertainty or sensibility analysis (Simpson et al., 2001; Jia and Taflanidis, 2013; Saint-Geours, 2012; Ratto et al., 2012). Where possible, an elegant way to build meta-models is the approximation through an analytical model, which is fitted to the large-scale output and allows for simplification (Grimm and Railsback, 2005). Analytical solutions can provide insight from different aggregation levels, but their construction and use are not always unequivocal (see Johst et al., 2013). Spatial statistic techniques are potential candidates of great interest and should be further explored (Fritsch et al., 2020). For example, Jia and Taflanidis (2013) present a systematic implementation and optimisation of kriging meta-models for hurricane wave and surge prediction maps based on high-dimensional outputs to reduce complexity while preserving spatial dimension. In functional Magnetic Resonance Imaging analysis, Kang et al. (2014) show a meta-analysis approach to synthesise brain mapping information from images. Given brain activation maps, they propose a spatial point process approach to model peak activation locations, which were identified as local maxima of brain activation area, explaining the brain task involved.

Here, we show how spatio-temporally explicit outputs of population dynamics models in landscape ecology can be analysed through a meta-modelling approach. Such outputs are simplified to point patterns composed of individual positions, key events or significant hotspots defining local dynamics. The resulting patterns can be modelled as spatio-temporal point processes (STPP), and the pattern itself, or rather its structure, is the response variable that one seeks to explain through the structure of the spatial support, and its temporal changes, described through appropriately defined predictor variables (Diggle, 2003; Illian et al., 2012; Renshaw, 2015; Illian and Burslem, 2017). Point processes can be defined over continuous space and time, such that there is no need to work with fixed spatial and temporal units; they can be used for

descriptive analyses and stochastic modelling of patterns. For example, Law et al. (2009) apply STPP tools by computing first- and second-order statistics, *i.e.*, expected numbers of points, and of point pairs with given point-to-point distance, for characterising observed plant patterns; Gabriel et al. (2017); Opitz et al. (2020); Pimont et al. (2020) develop models for wildfire occurrences through STPPs to overcome challenges given by the multi-scale structure of data and by strong non-stationarities in space and time driven by weather, land-cover and land-use.

The main novelty of our work resides in the characterisation of spatio-temporal population dynamics through STPPs. As a case study application, we focus on the relationships among agricultural landscape structure and the dynamics of a pest and its natural enemy. A hierarchical framework is developed (Figure 1): (i) a stochastic landscape model, characterised by parameters determining the landscape configuration and composition, is constructed and simulated; (ii) a spatially explicit population dynamics model, characterised by parameters determining the pest-predator structure and its spatial heterogeneity, is constructed and simulated. We propose to represent spatio-temporally explicit outputs returned by this modelling chain as point patterns identifying space-time-indexed key events of pest dynamics, that we subsequently model by constructing and estimating statistical regression equations for multi-type STPPs. The response variables we aim to model are the occurrences and the magnitude of the pest density peaks. Response variables are explained by taking into account both global and local landscape features, species life-history traits, and the occurrences of pest inoculation, pest peaks and treatments in appropriately chosen spatio-temporal neighborhoods around the location and time where the response variable was observed. This approach allows us to investigate the role of landscape structure in influencing the point process intensity summarising the pest-predator dynamics, and we address two general questions: (1) How can landscape effects and population dynamics traits at different spatio-temporal scales be coupled? (2) What are the spatio-temporal relationships between pest inoculations, pest density peaks and landscape heterogeneity?

2 Simulation models for landscape-pest-predator dynamics

2.1 Pest-predator models within agricultural landscapes

We model agricultural landscapes composed by crops, semi-natural areas and hedges through a stochastic landscape generator. Landscape simulations are the spatial support for a spatially explicit population model of auxiliaries and pests with opportune chemical treatments on pests. To couple the landscape complex and the spatially explict population model, we allow for dispersal both on agricultural fields and on hedge network (Figure 1). The agricultural landscape is composed of patches (*i.e.*, polygons) and linear elements (*i.e.*,

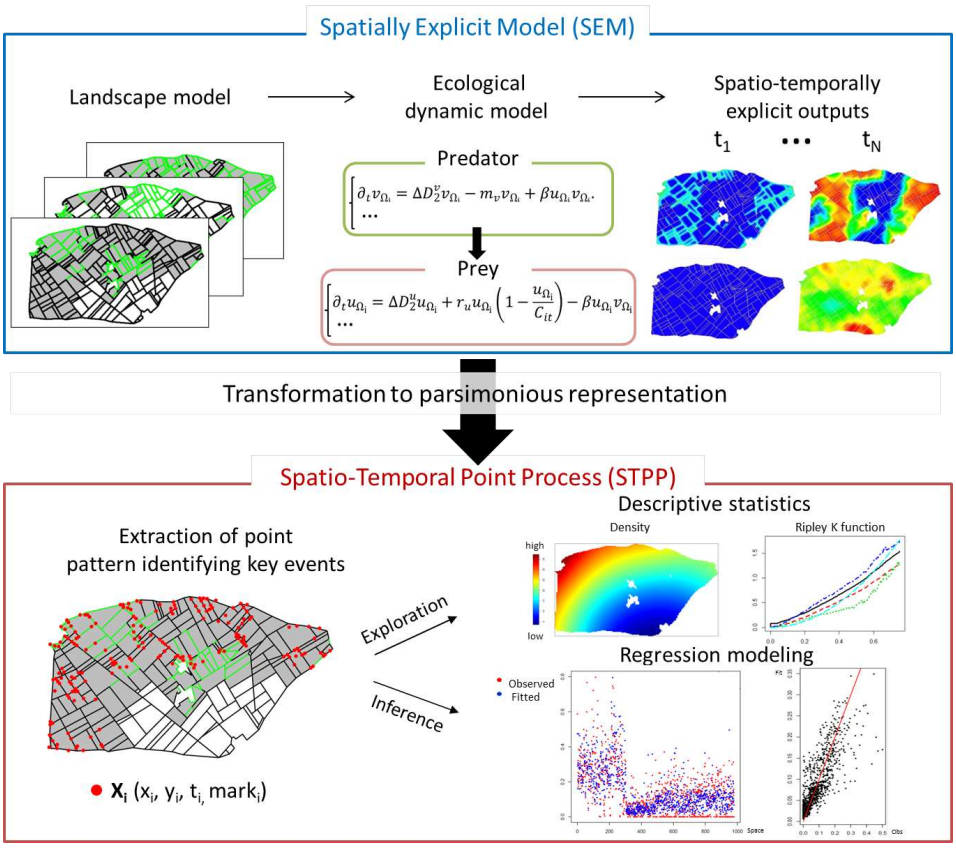

Figure 1: Overview of meta-modeling workflow.

segments) (Zamberletti et al., 2021). We generate a wide variety of structurally different composition and configuration scenarios for the allocation of crop over patches and of hedges over linear elements by varying representative parameters (*i.e.*, crop and hedge proportion and their aggregation); details are provided in the Supplement. Within these generated spatial supports, we then simulate the dynamic of the codling moth (*Cydia pomonella*) pest and of one of its main predators, the family of ground beetles (*Carabidae*), in apple orchards. The pest-predator model is defined by a spatially explicit and density-based model of reaction-diffusion type (Roques and Bonnefon, 2016).

Codling moths respond strongly to the spatial distribution of orchards over landscapes (Tischendorf, 2001; Ricci et al., 2009). Franck et al. (2011) have found low genetic differentiation among codling moth populations over large distances, but mild genetic differentiation among populations collected on different host plants. In addition, insecticide treatments have strong effects on genetic differentiation resulting from

spatial and temporal population size variations (Franck et al., 2011). This indicates that codling moths can disperse over large distances in agricultural landscapes, which supports the conjecture that hedges do not substantially impact their dispersal, such that insecticide treatments to break the pest dynamics are important. Thus, in the model, we assume that the pest can be encountered only in fields and that it has positive growth only in fields allocated with crop. In addition, field boundaries do not affect the pest population dynamics; *i.e.*, the life cycle of *Cydia pomonella* is mostly based in apple orchards, and it perceives the landscape as a heterogeneous 2D environment. Finally, we impose the application of local insecticide treatments when the pest density exceeds a fixed threshold on average in a crop patch.

The presence of semi-natural areas, such as hedges, promotes the presence of pest auxiliaries (Maalouly et al., 2013; Thies and Tscharntke, 1999) by offering shelter and by providing complementary resources when pests are not present in fields (Lefebvre et al., 2017). Lefebvre et al. (2017) present a field study investigating the routine movement of arthropods among apple orchards and adjacent hedgerows. They found that there are frequent movements for foraging (to orchards) and for escaping treatments (to hedges), demonstrating the important influence of hedgerows on the presence of numerous predators in apple orchards. Thus, we consider that hedges form the main habitat of the predator. The predator can spill over from hedges to fields and there feed on pest in fields as an alternative resource. However, it is generally attracted to hedges, which are its preferred habitat, so that migration from fields to hedges is relatively high. The predator is known to be averse to moving outside its natural habitat; therefore, migration from hedges to fields is always lower than migration from fields to hedges (Lefebvre et al., 2017).

Details about the pest-predator dynamics among 1D and 2D elements are fully presented in Roques and Bonnefon (2016). All the parameters are shown in the Supplement. To fix parameter ranges, we had performed a sensitivity analysis in a preliminary step since observation data of pests and predators are not available (Zamberletti et al., 2021). Initially, the predator is present in all hedges at carrying capacity. The pest is introduced randomly in space and time. The time unit can be considered as the day. Overall, $172,500$ simulations were run by varying landscape and population parameter configurations (see parameter ranges in Table 1 of the Supplement), with 15 simulations for each configuration where parameters are fixed but landscape realisations are stochastic.

2.2 Pest-predator spatio-temporal patterns

Simulations provide the spatio-temporal pest and predator densities. We characterise the influence of landscape spatio-temporal structure on the prey-predator dynamics by using point patterns. Following our modelling framework, we identify as events (i) the spatio-temporal treatment occurrence (*i.e.*, pest threshold

exceedance or pest peak) and (ii) the spatio-temporal pest introductions. For example, when pest threshold exceedance occurs in a patch, we apply a treatment in this patch and, to define the event episode as a point, we extract the time t of threshold exceedance, the pest density maximum in the patch with its Euclidean coordinates (x, y), and the average pest density over the patch. In Figure 2, two simulations are shown for different time steps, where the spatio-temporal occurrences of pest inoculations and treatments within different landscape allocations are highlighted. This example also illustrates the conjecture that the spatial hedge structure plays a role for pest dynamic by influencing its evolution jointly in space and time. Deeper exploratory quantitative analyses of spatio-temporal relationships between different types of points are proposed in the Supporting information, while we focus on statistical model-based analyses in what follows.

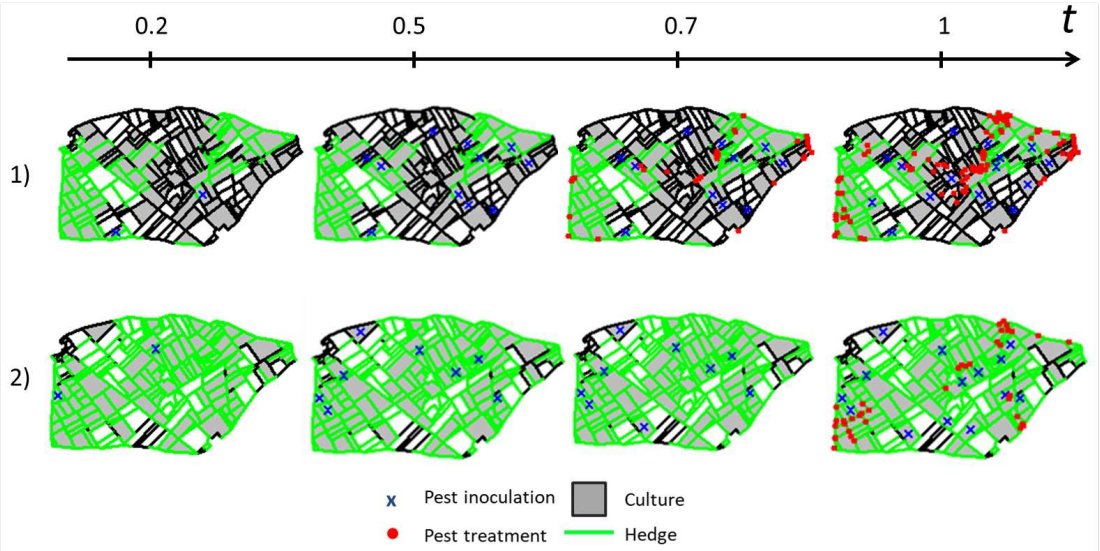

Figure 2: Two simulation examples (by row) illustrating the spatio-temporal pest dynamics depending on landscape structure through pest inoculations, and through pest density peaks after threshold exceedances.

3 Methods: STPP-based analysis of pest-predator dynamics

3.1 Pest density as STPP

Point patterns representing individual or event distributions in space and time can be modelled as STPPs (see Diggle (2003); Illian et al. (2008); Baddeley et al. (2015) for formal definitions). Each point can be endowed with additional qualitative or quantitative information defined as a "point mark". In our application, the

pattern of events is defined by the coordinates in space and time of pest peaks with both qualitative (pest inoculation) and quantitative marks (pest maximum density). Thanks to the theory of STPPs it is possible to analyse the point distribution properties locally in space and time, and to estimate models for predictive purposes (*e.g.*, number of events, point-to-point correlations, and distribution of their numerical or categorical marks). We focus on modelling the point process intensity function (local point density) (Illian et al., 2013). Our modelling goal is to predict the intensity of pest density peaks and the associated values of maximum pest density, and explain their variability in space, through time and across different simulations. We divided the spatial domain in a relatively large number of small cells, and we assume a homogeneous point process intensity within each cell during each interval of time. The spatial discretisation we use is shown in Figure 3, and background on its structure and construction is provided in the Supplement.

3.2 Pest density peak meta-modelling

For predicting the intensity of pest density peaks and associated values of maximum pest density, we develop and estimate regression equations for multi-type STPPs. Both global and local landscape features, species life-history traits, and the occurrences of pest introductions, pest peaks and treatments are used as covariate information. We construct two separate generalized linear model (GLM) formulas as meta-models that incorporate the available covariate information. Response variables and covariates are evaluated over each spatial cell (Figure 3) and time step. The spatio-temporal (STC), spatial (SC) and population dynamics (PDC) covariates put the spatio-temporal event patterns, landscape structure and population dynamics into relation:

$$STC(s,t) = \sum_{k=1}^{12} \beta_k z_k(s,t), \quad SC(s) = \sum_{k=13}^{20} \beta_k z_k(s), \quad PDC = \sum_{k=21}^{23} \beta_k z_k, \quad \boldsymbol{\beta} \in \mathbb{R}^{23}, \tag{1}$$

The $\boldsymbol{\beta}$ vector gathers the covariate coefficients to be estimated separately for each model, and the values z_k are covariates summarised in Table 1 and provided for each space-time cell. More information on their selection and computation is given in the Supporting information, as well as residual analysis to evaluate the predicted values obtained by the GLMs.

3.2.1 Meta-model for the occurrence intensity of pest density peaks

To model the occurrence intensity of pest density of pest peak points, we consider a GLM with Poisson response, *i.e.*, we combine a log-link function with a Poisson response distribution:

Table 1: Covariates used in the space-time regression model of pest density peak patterns. The temporal unit d stands for *day*.

Index	Covariate	Spatial reference	Range	Unit
Spatio-temporal (*STC*)				
1	No. of treatments in the patch at $t-1$	patch	0-40	-
2	No. of treatments in the patch cumulated up to $t-2$	patch	0-97	-
3	No. of treatments in neighbor patches at $t-1$	patch	0-337	-
4	No. of treatments in neighbor patches cumulated up to $t-2$	patch	0-861	-
5	No. of pest density peaks at $t-1$	cell	0-15	-
6	No. of pest density peaks cumulated up to $t-2$	cell	0-36	-
7	No. of pest density peaks in neighbor cells at $t-1$	cell	0-45	-
8	No. of pest density peaks in neighbor cells cumulated up to $t-2$	cell	0-97	-
9	No. of pest introduction in cell at $t-1$	cell	0-30	-
10	No. of pest introduction in cell cumulated up to $t-2$	cell	0-30	-
11	No. of pest introduction in neighbor cells at $t-1$	cell	0-30	-
12	No. of pest introduction in neighbor cells cumulated up $t-2$	cell	0-39	-
Spatial (*SC*)				
13	Cell dimension	cell	0-0.069	km^2
14	Binary indicator if the cell is among 2 patches	cell	0-1	-
15	Binary indicator (1/0) if the cell is among 3 or more patches	cell	0-1	-
16	Proportion of hedges within the buffer centered in the cell	buffer	0-1	%
17	Proportion of crops within the buffer centered in the cell	buffer	0-1	%
18	Landscape crop and hedge aggregation	landscape	0-5.54	-
19	Landscape crop proportion	landscape	0-1	%
20	Landscape hedge proportion	landscape	0-1	%
Population dynamics (*PDC*)				
21	Pest diffusion in crop patch	landscape	0.06-12	km^2d^{-1}
22	Predator diffusion in crop patch	landscape	0.07-12	km^2d^{-1}
23	Predator migration from hedge to crop	landscape	0.1-1	

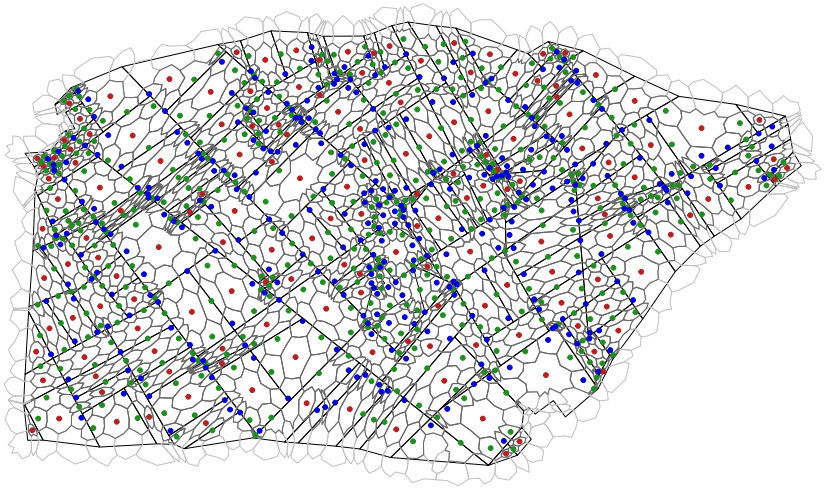

Figure 3: Spatial discretisation of the regression models. Complete mesh discretisation (light grey), mesh cells used in the analysis (dark grey), landscape patches (black). Cell centroids of different colour refer to different cell types: cell in patch center (red), cell connecting exactly two patches (green), cell connecting more than two patches (blue).

$$\lambda(s,t) = \exp\left(\beta_0^{\lambda} + STC(s,t) + SC(s) + PDC\right) \tag{2}$$

with global intercept β_0^{λ} and coefficients of the other variables to be estimated. The value $\lambda(s,t)$ represents the average number of pest peaks occurring in a unit of space and time around the point (s,t), and is assumed to be constant within each cell of the mesh during each time interval of 0.1.

3.2.2 Meta-model for magnitudes of pest density peaks

To model the maximum pest density value associated with each pest peak point, we consider a log-Gaussian GLM, *i.e.*, we combine a log-link function with a Gaussian response distribution:

$$P_{max}(s,t) = \exp\left(\beta_0^{P_{max}} + STC(s,t) + SC(s) + PDC + \varepsilon(s,t)\right) \tag{3}$$

with global intercept $\beta_0^{P_{max}}$ and coefficients of the other variables to be estimated, where $P_{max}(s,t)$ is the maximum pest density value associated to the point where the treatment is applied conditional to the occurrence of such a point. The term $\varepsilon(s,t) \sim \mathcal{N}(0,\sigma^2)$ corresponds to the spatially and temporally independent and identically distributed Gaussian error terms.

4 Results: spatiotemporal drivers of pest hotspots in pest-predator agroecological system

We present main results obtained by estimating the GLMs in Equations 2 and 3. Additional results of a covariate correlation analysis and of residual analysis are reported in the Supporting information; they show that the models defined in Equations 2 and 3 appropriately capture the spatio-temporal variability of the observed data (*i.e.*, population dynamic model outputs).

The estimated GLM coefficients for the models in Equations 2 and 3 are summarized in Figure 4. Prior to estimation, covariates have been normalised to empirical mean 0 and variance 1 to compare more easily the magnitudes of estimated effects.

We first discuss the strongest effects corresponding to points outside the inner rectangle in Figure 4a. The strongest positive effects on the number of pest peaks arise for covariates favouring pest dynamics. Specifically, crop coverage at local scale (*i.e.*, in the buffer) and at global scale (*i.e.*, in the whole landscape) favours the abundance of suitable habitat for pests, which can easily spread and find resources. Regarding the pest peak value, the cell size has the strongest positive contribution. An explanation is that the pest density is likely to be highest where the inoculation takes place, and a large cell is more often inoculated than a smaller cell. By contrast, cell dimension contributes the strongest negative effect on the number of peaks, since peaks tend to concentrate in the periphery of the patches, thus in cells containing borders among different patches.

Pest diffusion has the strongest negative effect on pest peak values, it may be due to a dilution effect. In addition, since high pest diffusion allows the pest to easily move, pest population tends to spread homogeneously over the whole landscape. Therefore, few local hotspots arise, and the pesticide threshold is less often exceeded. Both response variables related to pest peaks are also strongly reduced by local predator presence, which in turn is mainly driven by a high local presence of hedges. The spatio-temporal covariate group (STC) shows generally weaker effects on pest dynamics, except for the local cumulated number of pest

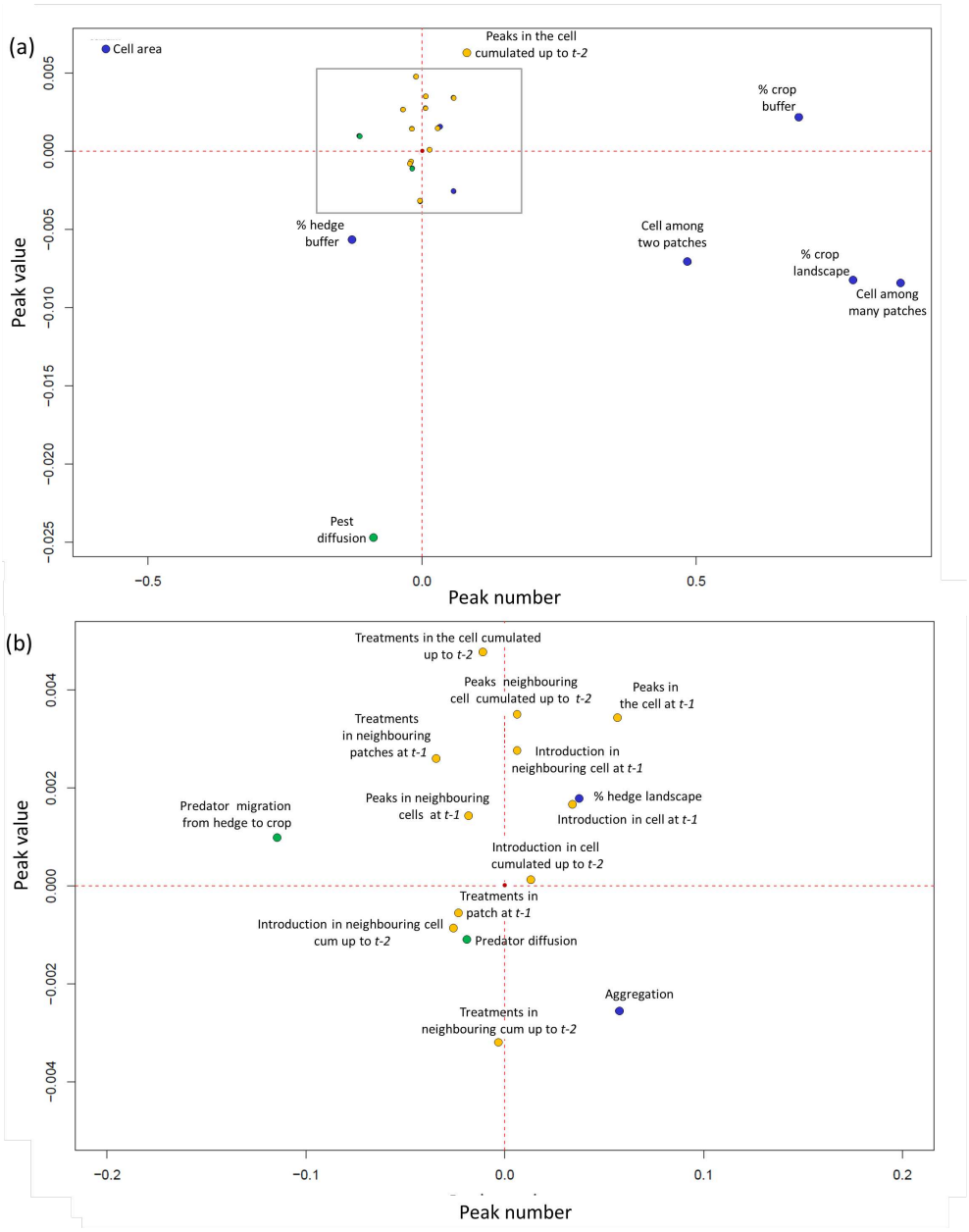

Figure 4: Estimated regression coefficients for the models of peak occurrence intensity (x-axis) and the model of the peak value (y-axis). Dot colours indicate covariate types: STC (orange), SC (blue), PDC (green).

peaks during earlier time intervals. It positively influences the number and the value of pest peaks since pests are already present at high density in the surrounding area if there have been peaks during earlier intervals. Such locations may have characteristics that make them particularly pest-prone and favourable for pest dynamics.

The zoom in Figure 4b shows covariate effects with a lower magnitude. High numbers of pest peaks along with high peak concentration values (top-right quadrant in Figure 4) are relatively strongly favoured by the presence of previous peaks in the same cell or in the surrounding ones (both at $t-1$, and cumulated up to $t-2$). Similarly, an elevated number of introductions in neighbouring cells leads to high pest concentration due to pest spillover. On the other hand, the application of treatments locally in the patch or in neighbouring patches at previous time steps leads in general to a decrease of both the number and the concentration value of peaks.

Results show a negative effect of hedge proportion in the buffer on pest activity. However, there also arises a weaker but positive effect of the hedge proportion over the whole landscape, which may appear counter-intuitive at first glance. Since response variables are evaluated at cell scale, having a large hedge proportion in the whole landscape but a low proportion of hedges in the buffer clearly results in a concentration of pest where hedges are missing. In addition, hedges help to keep the pest below the treatment threshold and therefore favour its propagation through the landscape (see Zamberletti et al. (2021)); therefore, the pest may reach areas of lower predation pressure more easily and pull out. In addition, our model shows that the landscape aggregation has a weak positive effect on peak occurrence numbers at cell level. Pest density threshold exceedances occur homogeneously over large areas of contiguous crop, but these peaks are of relatively small magnitude because hotspots with high pest clusters and concentration do not build up. Predator spillover (*i.e.*, movement from hedge to field) results in a decrease of the number of threshold exceedances, but it may increase pest peak values since the predators are not homogeneously present in the patches and over the whole landscape. Predators have stronger influence near hedges (*e.g.*, in cells overlapping different patches) but less in the center of the patch (central cells).

5 Discussion

In this work we propose post-model scaling using regression meta-models based on marked STPPs. This approach enabled us to assess and compare the contribution of different spatio-temporal covariates and life-history traits to the direction and strength of variation in crucial events of population dynamics issued from spatially explicit models. The use of statistical regression meta-models makes our approach flexible and easy to implement, while numerous and diverse covariates describing local and global characteristics

can be incorporated. We applied our methodology to the outputs of a SEM describing the biological control in agricultural landscapes of a crop pest by its natural predator. We found significantly different effects of landscape structures at various spatial scales on the population dynamics patterns.

The adaptation of our approach of defining a marked STPP meta-model may be relevant and insightful in various contexts. Examples are occurrence locations and times of earthquake epicentres (Lombardo et al., 2019), wildfires (Opitz et al., 2020), epidemiological outbreaks (White et al., 2018a), biodiversity hotspots and species distribution (Soriano-Redondo et al., 2019), pollutant concentrations (Lindström et al., 2014) or local maxima or minima in meteorological events (Heaton et al., 2011). In most ecological process space and time are closely intertwined and not separable as in our case, where pest introductions and subsequent peaks depend on local temporal dynamics driven by local spatial structure. Thus, here, we designed our approach to allow for joint analysis of spatial and temporal scales. For ecological processes related to those we study, White et al. (2018a) addressed how landscape structure impacts simulated disease dynamics in an individual-based susceptible–infected–recovered model. They quantified disease dynamics by outbreak maximum prevalence and duration, coupled with landscape heterogeneity defined by patchiness and proportion of available habitat. They find that fragmentation promotes pathogen persistence, except for simulation with high conspecific density, slower recovery rates and larger perceptual ranges, where more complex disease dynamics emerged; the most fragmented landscapes were not necessarily the most conducive to outbreaks or pathogen persistence. Our work has similar thrust by exploring the effect of landscape heterogeneity on pest density peaks. However, by taking advantage of the STPP modelling, we focus on spatio-temporal positions of peaks, and we investigate which factors locally influence occurrence intensity and magnitude of these events. The meta-model allowed us to depict complex spatial dynamics and patterns even if multiple processes occur at competing scales (White et al., 2018b). To assess fine-scale biodiversity, Azaele et al. (2015) captured species patterns through correlations among different species' abundances across sample plots. Therefore, they used counts over spatial units (*i.e.*, plots), determined by the sampling design and leading to relatively large counts, and they contrasted their results with common species–area curves (Fritsch et al., 2020). They concluded that this mathematical framework provides a common language to link different spatial scales. Our approach goes beyond a purely descriptive "geostatistical" analysis since we take into account the space-time position of each of the points as well as their relationships with nearby key elements. This representation parsimoniously summarises spatially continuous dynamics into discrete occurrences of spatio-temporal key events and allows modeling them for explanatory and predictive purposes. Our regression model for occurrence intensities also aggregates individual events, but we work with relatively small counts by choosing appropriate, problem-specific space-time units.

Ecosystem patterns and processes can cover a wide range of space and time, and they depend on multiple

drivers acting over different scales (Fritsch et al., 2020). Problematic loss and the lack of information may arise in procedures of scaling-up or scaling-down when coupled with the complexity of the involved systems. Our work strikes a pragmatic balance with respect to the inevitable trade-off between model simplicity, to obtain clear insights into important factors, and model complexity, to achieve a more complete and realistic representation of the system (Lacy et al., 2013). Spatio-temporal meta-models present a flexible solution by capturing the functional linkages between model components. They show potential to reveal properties in ecological systems that are difficult to identify when considering only the complex model output with large data volumes as a whole (Lacy et al., 2013). Our STPP model allowed for a relatively complex spatio-temporal local analysis of system dynamics. It therefore provides insights into the role of different effects and takes process-specific scales into account by using categorical or numerical marks. Through statistical inferences it becomes possible to identify significant relationships of key events with their drivers focusing on biotic interactions, habitat heterogeneity and spatio-temporal stochastic effects predictions (Baddeley et al., 2015).

A large body of literature on meta-models (or surrogate models, or emulators) in various disciplines focuses on Gaussian processes or machine-learning techniques (*e.g.*, Forrester et al., 2008; Kleijnen, 2015), whereas our work highlights the potential of point-process-based approaches for dynamical systems. This novel way of conducting meta-analyses is applicable to various collections of relevant events arising in dynamical processes available at high spatio-temporal resolution. We emphasise that our methods leverage spatio-temporal and multivariate point pattern techniques, while the state-of-the-art in point pattern analyses deals mostly with purely spatial patterns or does not well represent the temporal dimension (Wiegand et al., 2017). Our extensions are well-suited for spatio-temporal mechanisms and population dynamic parameters where the assessment of their relative and joint role is crucial for characterising emerging diversity patterns.

We have constructed a collection of predictor variables in which spatio-temporal covariates (STC) contribute spatio-temporally structured information, such as the number or magnitudes of previous or concomitant events around a given location and time, to convey information related to the local evolution of pest dynamics. In a similar context, Le Gal et al. (2020) highlighted the important influence of the interplay between the landscape structure and the timing of CBC measures on the delivery of pest control services. They showed that increased semi-natural habitat proportion at the landscape level enhances the visitation rate of pest-colonised crop cells, but it also reduces the delay between pest colonisation and predator arrival in the crop fields. In our model, we have opted for simulating the time and position of pest arrival according to a Poisson process with intensity proportional to crop area. We found that locations showing frequent and high density peaks in previous time steps are likely to incur new peaks. On the other hand, local previous

treatments in a patch negatively influence the dynamics since they efficiently reduce the pest density in this patch. Introductions of pest act as an accelerator of local pest dynamics, and after a short period we often assist to both high frequency and high magnitudes of peaks in the surrounding fields.

Spatial covariates (SC) in our regression meta-models are time-invariant landscape characteristics that may influence pest peaks. Crop proportion is the main driver for pest in our models, and leads to a clear positive response of pest insects to increasing cover of a suitable crop (Ricci et al., 2019; Rand et al., 2014; Zhao et al., 2015; Avelino et al., 2012; Tscharntke et al., 2007). Our results show that considering it at local scale or at global scale leads to different peak patterns. When crop aggregation and percentage coverage are high in the whole landscape, exceedance events of pest density are relatively homogeneously spread over the area with generally relatively low pest density values throughout. Instead, when high crop coverage is only local (*i.e.*, in the buffer), the resulting pattern shows a locally higher number of exceedance events with high peaks; pests find their preferred habitat in a more limited space and tend to concentrate there. Zamberletti et al. (2021) showed that in landscapes with strong aggregation of crop fields the area of contiguous crop may cause a dilution effect, with a positive effect on pest population, a negative effect on treatment occurrence, and a positive effect on the treatment numbers in the whole landscape. Therefore, if treatments are necessary in a patch, they tend to arise in relatively high numbers over the full observation period. Hedge distribution and proportion can be viewed as a proxy for predator presence and reveal when predators may play a role in reducing pest density (Bianchi et al., 2006; Tscharntke et al., 2007). The effects attributed to semi-natural habitat (*e.g.*, hedges) are ambiguous with both positive, negative or neutral impacts on CBC (Chaplin-Kramer et al., 2011; Karp et al., 2018). In our models, total hedge proportion has a small but positive effect on both the number and the magnitude of peaks. A reason could be that the global proportion of hedges does not inform about hedge connectivity and distribution (*e.g.*, homogeneously or in clusters). If there is a high hedge coverage, predators are expected to be homogeneously distributed in the landscape, thus stabilising the pest population and potentially reaching an equilibrium in the whole landscape for pest and predator density. However, this does not imply that pest density remains under the treatment threshold; it could happen that other parameters influence its dynamics by favouring pest population (*e.g.*, crop coverage or pest growth rate) or decreasing predator presence in field (*e.g.*, mortality, spillover from hedge). This results in a homogeneous predator presence that is not sufficient to prevent pest density from exceeding the threshold. In our model, another reason could stem from statistical confusion in the regression models between the effects of global hedge proportion and global crop proportion since the simulated landscape model tends to position hedges more often in crop areas than in the rest of the landscape. However, when focusing on local buffers around a cell, local hedge structure, and the resulting predator concentration, play a bigger role by reducing both number of pest peaks and their magnitude.

Population dynamics covariates (PDC) in our models are related to species traits. Here we consider the effect of varying population parameters related to species mobility in the environment. We focus on how the structure of landscape elements influences species spread with respect to the studied events. We find that predator diffusion ability over the landscape is fundamental to reduce the presence of pest. Interestingly, we do not notice the same effect for predator migration speed from hedge to field. This predator trait acts strongly at locations close to hedges, *i.e.*, around patch borders, with a strong decrease in the number of peaks, while the peak value is not affected but is high mainly in the patch core areas.

In the agro-ecological context, our analysis aids prediction and management decisions. For example, improved understanding of local spatio-temporal relationships and dynamics helps to schedule specific local control strategies by targeting the locations that frequently suffer from pest peaks and the moments when local control strategies can be expected to be most efficient to control pest dynamics.

References

Avelino, J., Romero-Gurdián, A., Cruz-Cuellar, H. F., and Declerck, F. A. (2012). Landscape context and scale differentially impact coffee leaf rust, coffee berry borer, and coffee root-knot nematodes. Ecological applications, 22(2):584–596.

Azaele, S., Maritan, A., Cornell, S. J., Suweis, S., Banavar, J. R., Gabriel, D., and Kunin, W. E. (2015). Towards a unified descriptive theory for spatial ecology: predicting biodiversity patterns across spatial scales. Methods in Ecology and Evolution, 6(3):324–332.

Baddeley, A., Rubak, E., and Turner, R. (2015). Spatial point patterns: methodology and applications with R. CRC press.

Bianchi, F. J., Booij, C., and Tscharntke, T. (2006). Sustainable pest regulation in agricultural landscapes: a review on landscape composition, biodiversity and natural pest control. Proceedings of the Royal Society B: Biological Sciences, 273(1595):1715–1727.

Chaplin-Kramer, R., O'Rourke, M. E., Blitzer, E. J., and Kremen, C. (2011). A meta-analysis of crop pest and natural enemy response to landscape complexity. Ecology letters, 14(9):922–932.

DeAngelis, D. L. and Yurek, S. (2017). Spatially explicit modeling in ecology: a review. Ecosystems, 20(2):284–300.

Delaune, T., Ballot, R., Gouwie, C., Maupas, F., Sausse, C., Félix, I., Brun, F., and Barbu, C. (2019).

370 Spatiotemporal drivers of crop pests and pathogens abundance at the landscape scale. bioRxiv, page
371 641555.

372 Diggle, P. (2003). Statistical Analysis of Spatial Point Patterns. Hodder Education, London, UK, 2nd
373 edition.

374 Eber, S. (2001). Multitrophic interactions: the population dynamics of spatially structured plant-herbivore-
375 parasitoid systems. Basic and Applied Ecology, 2(1):27–33.

376 Fahrig, L. (2001). How much habitat is enough? Biological conservation, 100(1):65–74.

377 Forrester, A., Sobester, A., and Keane, A. (2008). Engineering design via surrogate modelling: a practical
378 guide. John Wiley & Sons.

379 Franck, P., Ricci, B., Klein, E. K., Olivares, J., Simon, S., Cornuet, J.-M., and Lavigne, C. (2011). Genetic
380 inferences about the population dynamics of codling moth females at a local scale. Genetica, 139(7):949.

381 Fritsch, M., Lischke, H., and Meyer, K. M. (2020). Scaling methods in ecological modelling. Methods in
382 Ecology and Evolution, 11(11):1368–1378.

383 Gabriel, E., Opitz, T., and Bonneu, F. (2017). Detecting and modeling multi-scale space-time structures:
384 the case of wildfire occurrences. Journal de la Société Française de Statistique, 158(3):86–105.

385 Gotelli, N. J. (2000). Null model analysis of species co-occurrence patterns. Ecology, 81(9):2606–2621.

386 Grimm, V. and Railsback, S. F. (2005). Individual-based modeling and ecology, volume 8. Princeton
387 university press.

388 Grimm, V., Revilla, E., Berger, U., Jeltsch, F., Mooij, W. M., Railsback, S. F., Thulke, H.-H., Weiner, J.,
389 Wiegand, T., and DeAngelis, D. L. (2005). Pattern-oriented modeling of agent-based complex systems:
390 lessons from ecology. science, 310(5750):987–991.

391 Hanski, I. and Thomas, C. D. (1994). Metapopulation dynamics and conservation: a spatially explicit model
392 applied to butterflies. Biological Conservation, 68(2):167–180.

393 Heaton, M. J., Katzfuss, M., Ramachandar, S., Pedings, K., Gilleland, E., Mannshardt-Shamseldin, E., and
394 Smith, R. L. (2011). Spatio-temporal models for large-scale indicators of extreme weather. Environmetrics,
395 22(3):294–303.

396 Hogeweg, P. (1988). Cellular automata as a paradigm for ecological modeling. Applied mathematics and
397 computation, 27(1):81–100.

Illian, J., Penttinen, A., Stoyan, D., and Stoyan, H. (2008). Analysis and Modelling of Spatial Point Patterns, from Spatial Data to Knowledge. Wiley, Chichester, UK.

Illian, J. B. and Burslem, D. F. (2017). Improving the usability of spatial point process methodology: an interdisciplinary dialogue between statistics and ecology. AStA Advances in Statistical Analysis, 101(4):495–520.

Illian, J. B., Martino, S., Sørbye, S. H., Gallego-Fernández, J. B., Zunzunegui, M., Esquivias, M. P., and Travis, J. M. (2013). Fitting complex ecological point process models with integrated nested laplace approximation. Methods in Ecology and Evolution, 4(4):305–315.

Illian, J. B., Sørbye, S. H., Rue, H., and Hendrichsen, D. K. (2012). Using inla to fit a complex point process model with temporally varying effects – a case study. Journal of Environmental Statistics, 3(7).

Jia, G. and Taflanidis, A. A. (2013). Kriging metamodeling for approximation of high-dimensional wave and surge responses in real-time storm/hurricane risk assessment. Computer Methods in Applied Mechanics and Engineering, 261:24–38.

Johst, K., Lima, M., and Berryman, A. A. (2013). Scaling up: how do exogenous fluctuations in individual-based resource competition models re-emerge in aggregated stochastic population models? Population ecology, 55(1):173–182.

Kang, J., Nichols, T. E., Wager, T. D., and Johnson, T. D. (2014). A bayesian hierarchical spatial point process model for multi-type neuroimaging meta-analysis. The annals of applied statistics, 8(3):1800.

Karp, D. S., Chaplin-Kramer, R., Meehan, T. D., Martin, E. A., DeClerck, F., Grab, H., Gratton, C., Hunt, L., Larsen, A. E., Martínez-Salinas, A., et al. (2018). Crop pests and predators exhibit inconsistent responses to surrounding landscape composition. Proceedings of the National Academy of Sciences, 115(33):E7863–E7870.

Kleijnen, J. P. (2015). Design and analysis of simulation experiments. In International Workshop on Simulation, pages 3–22. Springer.

Lacy, R. C., Miller, P. S., Nyhus, P. J., Pollak, J., Raboy, B. E., and Zeigler, S. L. (2013). Metamodels for transdisciplinary analysis of wildlife population dynamics. PLoS One, 8(12):e84211.

Law, R., Illian, J., Burslem, D. F., Gratzer, G., Gunatilleke, C., and Gunatilleke, I. (2009). Ecological information from spatial patterns of plants: insights from point process theory. Journal of Ecology, 97(4):616–628.

Le Gal, A., Robert, C., Accatino, F., Claessen, D., and Lecomte, J. (2020). Modelling the interactions between landscape structure and spatio-temporal dynamics of pest natural enemies: Implications for conservation biological control. Ecological Modelling, 420:108912.

Lefebvre, M., Papaïx, J., Mollot, G., Deschodt, P., Lavigne, C., Ricard, J.-M., Mandrin, J.-F., and Franck, P. (2017). Bayesian inferences of arthropod movements between hedgerows and orchards. Basic and Applied Ecology, 21:76–84.

Levin, S. A. (1992). The problem of pattern and scale in ecology: the robert h. macarthur award lecture. Ecology, 73(6):1943–1967.

Lindström, J., Szpiro, A. A., Sampson, P. D., Oron, A. P., Richards, M., Larson, T. V., and Sheppard, L. (2014). A flexible spatio-temporal model for air pollution with spatial and spatio-temporal covariates. Environmental and ecological statistics, 21(3):411–433.

Lombardo, L., Opitz, T., and Huser, R. (2019). Numerical recipes for landslide spatial prediction using r-inla: a step-by-step tutorial. In Spatial modeling in GIS and R for earth and environmental sciences, pages 55–83. Elsevier.

Maalouly, M., Franck, P., Bouvier, J.-C., Toubon, J.-F., and Lavigne, C. (2013). Codling moth parasitism is affected by semi-natural habitats and agricultural practices at orchard and landscape levels. Agriculture, ecosystems & environment, 169:33–42.

Nathan, L. R., Mamoozadeh, N., Tumas, H. R., Gunselman, S., Klass, K., Metcalfe, A., Edge, C., Waits, L. P., Spruell, P., Lowery, E., et al. (2019). A spatially-explicit, individual-based demogenetic simulation framework for evaluating hybridization dynamics. Ecological Modelling, 401:40–51.

Opitz, T., Bonneu, F., and Gabriel, E. (2020). Point-process based Bayesian modeling of space–time structures of forest fire occurrences in Mediterranean France. Spatial Statistics, page 100429.

O'Rourke, M. E., Rienzo-Stack, K., and Power, A. G. (2011). A multi-scale, landscape approach to predicting insect populations in agroecosystems. Ecological Applications, 21(5):1782–1791.

Pickett, S. R. and Siriwardena, G. M. (2011). The relationship between multi-scale habitat heterogeneity and farmland bird abundance. Ecography, 34(6):955–969.

Pimont, F., Fargeon, H., Opitz, T., Ruffault, J., Barbero, R., Martin-StPaul, N., Rigolot, E., Riviere, M., and Dupuy, J.-L. (2020). Prediction of regional wildfire activity with a probabilistic Bayesian framework. Ecological Applications (accepted).

Rand, T. A., Waters, D. K., Blodgett, S. L., Knodel, J. J., and Harris, M. O. (2014). Increased area of a highly suitable host crop increases herbivore pressure in intensified agricultural landscapes. Agriculture, Ecosystems & Environment, 186:135–143.

Ratto, M., Castelletti, A., and Pagano, A. (2012). Emulation techniques for the reduction and sensitivity analysis of complex environmental models. Environmental Modelling and Software, 34:1–4.

Renshaw, E. (2015). Stochastic population processes: analysis, approximations, simulations. OUP Oxford.

Ricci, B., Franck, P., Toubon, J.-F., Bouvier, J.-C., Sauphanor, B., and Lavigne, C. (2009). The influence of landscape on insect pest dynamics: a case study in southeastern france. Landscape ecology, 24(3):337–349.

Ricci, B., Lavigne, C., Alignier, A., Aviron, S., Biju-Duval, L., Bouvier, J., Choisis, J.-P., Franck, P., Joannon, A., Ladet, S., et al. (2019). Local pesticide use intensity conditions landscape effects on biological pest control. Proceedings of the Royal Society B, 286(1904):20182898.

Roques, L. (2013). Modèles de réaction-diffusion pour l'écologie spatiale. Editions Quae.

Roques, L. and Bonnefon, O. (2016). Modelling population dynamics in realistic landscapes with linear elements: a mechanistic-statistical reaction-diffusion approach. PloS one, 11(3).

Rusch, A., Valantin-Morison, M., Sarthou, J.-P., and Roger-Estrade, J. (2010). Biological control of insect pests in agroecosystems: effects of crop management, farming systems, and seminatural habitats at the landscape scale: a review. In Advances in agronomy, volume 109, pages 219–259. Elsevier.

Saint-Geours, N. (2012). Sensitivity analysis of spatial models: application to cost-benefit analysis of flood risk management plans. PhD thesis.

Simpson, T. W., Poplinski, J., Koch, P. N., and Allen, J. K. (2001). Metamodels for computer-based engineering design: survey and recommendations. Engineering with computers, 17(2):129–150.

Soriano-Redondo, A., Jones-Todd, C. M., Bearhop, S., Hilton, G. M., Lock, L., Stanbury, A., Votier, S. C., and Illian, J. B. (2019). Understanding species distribution in dynamic populations: A new approach using spatio-temporal point process models. Ecography, 42(6):1092–1102.

Thies, C. and Tscharntke, T. (1999). Landscape structure and biological control in agroecosystems. Science, 285(5429):893–895.

Tischendorf, L. (2001). Can landscape indices predict ecological processes consistently? Landscape ecology, 16(3):235–254.

Tscharntke, T., Bommarco, R., Clough, Y., Crist, T., Kleijn, D., Rand, T., Tylianakis, J., Van Nouhuys, S., and Vidal, S. (2007). Conservation biological control and enemy diversity on a landscape scale [erratum: 2008 may, v. 45, issue 2, p. 238-253.]. Biological control: theory and application in pest management.

Tscharntke, T. and Brandl, R. (2004). Plant-insect interactions in fragmented landscapes. Annual Reviews in Entomology, 49(1):405–430.

Webb, C. O. (2000). Exploring the phylogenetic structure of ecological communities: an example for rain forest trees. The American Naturalist, 156(2):145–155.

White, L. A., Forester, J. D., and Craft, M. E. (2018a). Disease outbreak thresholds emerge from interactions between movement behavior, landscape structure, and epidemiology. Proceedings of the National Academy of Sciences, 115(28):7374–7379.

White, L. A., Forester, J. D., and Craft, M. E. (2018b). Dynamic, spatial models of parasite transmission in wildlife: Their structure, applications and remaining challenges. Journal of Animal Ecology, 87(3):559–580.

Wiegand, T., Uriarte, M., Kraft, N. J., Shen, G., Wang, X., and He, F. (2017). Spatially explicit metrics of species diversity, functional diversity, and phylogenetic diversity: Insights into plant community assembly processes. Annual Review of Ecology, Evolution, and Systematics, 48:329–351.

Zamberletti, P., Sabir, K., Opitz, T., Bonnefon, O., Gabriel, E., and Papaix, J. (2021). More pests but less treatments: ambivalent effect of landscape complexity on conservation biological control. bioRxiv, 10.1101/2021.03.19.436155.

Zhao, Z.-H., Hui, C., He, D.-H., and Li, B.-L. (2015). Effects of agricultural intensification on ability of natural enemies to control aphids. Scientific reports, 5:8024.

On the evolutionary trade-off between growth and dispersal during a range expansion

Patrizia Zamberletti[1,*]

Lionel Roques[1]

Florian Lavigne[1]

Julien Papaïx[1]

1. Biostatistics and Spatial Processes, INRAE, Avignon, France;

∗ Corresponding author; e-mail:patrizia.zamberletti@inrae.fr.

Manuscript elements: Figure 1, Figure 2, Figure 3, Figure 4, Figure 5, Table 1, Table 2,Table 3, online appendices A (including Figure A1, Table A1).

Keywords: Eco-evo model, Reaction-diffusion system, Evolutionary R-D trade-off, Heterogeneous space, non-local competition.

Manuscript type: Article.

Prepared using the suggested LaTeX template for *Am. Nat.*

Abstract

Eco-evolutionary processes play a key role shaping the invasion dynamics of populations expanding in new habitats. This could be important for assessing colonization phenomena as the expansion of invasive species or for biological control as evaluating the pest propagation in the agricultural habitat intermixing. The expansion process is driven by co-evolving species traits, in particular, those traits related to body dimensions, competitive skills, movement abilities controlling also their responses to landscape heterogeneity gradients. Typically, individuals who invest more in the development of their traits related to the dispersal strategy reduce investment in reproduction. Thus, there are two possible trading-off eco-evolutionary strategies: growing faster or dispersing faster ($R - D$ trade-off). We explore the spreading dynamics of a consumer species exploiting a resource in a heterogeneous environment through a reaction-diffusion model. We focus on the co-evolution of growth-rate and dispersal traits for assessing the phenotype having the highest spreading speed and leading the propagation front. We evaluate spreading properties numerically and analytically, when theoretical formulas are available, using different simulation scenario and parameter combinations. Our main results show that the heterogeneity has a fundamental role in shaping the $R - D$ trade-off determining the phenotype selection and phenotypic trait proportion within the propagating front and beyond the front.

Introduction

Accounting for the interaction between ecological and evolutionary dynamics is crucial to understand many processes in ecology such as evolutionary rescue (Lavigne et al., 2020), migrational meltdown (Ronce and Kirkpatrick, 2001), biological invasion (Szűcs et al., 2019) . Indeed, when species shift their range, they face a new selection pressure, a rapid evolution can affect their ecological dynamics which in turn feedback on the evolutionary potential (Bonte and Bafort, 2018; Burton et al., 2010). Population expansion is an ecological process mainly driven by traits related to reproduction and dispersal (Deforet et al., 2019; Turchin, 1998a). Dispersal affects capabilities to exchange individuals and genes among different habitats (Legrand et al., 2017). Dispersal traits have been proved to be related to body dimension and condition (Duthie et al., 2015; Helms and Kaspari, 2015; Steenman et al., 2015), affecting competitive abilities, food web interactions (Bonte and de la Pena, 2009) or metabolic processes (Hirt et al., 2017). As a consequence, there are many examples where individuals who invest more in the development of their traits related to the dispersal strategy reduce the effort in foraging and reproduction (e.g. reducing their mating period or with lower egg mass) (Baguette and Schtickzelle, 2006; Bonte and Bafort, 2018; Hanski et al., 2006). In such cases, two possible evolutionary strategies exist: dispersing faster or growing stronger (Deforet et al., 2019). This results in a species' trait trade-off that shapes the ecological and evolutionary dynamics of populations.

Usually the attention is given to traits as dispersal and growth affected by environmental heterogeneity (Lewis et al., 2002, 2016; Turchin, 1998b), but adaptation of those traits has been less taken into consideration (Morris et al., 2019) under the assumption

that evolutionary dynamics its a slower processes than demography (Alex Perkins et al., 2013; Griette et al., 2015). By contrast, there is evidence that evolution could be very rapid during invasions. For example, Alex Perkins et al. (2013) focus on how life-history or dispersal traits impact spread rates of the cane toad *Rhinella marina*in Australia by combining a stage-structured population dynamics model and an evolutionary quantitative genetic model. They point out that rapid evolution of life-history and dispersal traits at the invasion front could have led to a more than twofold increase in the distance spread by cane toads *Rhinella marina* across northern Australia. Indeed, spatial sorting of high-dispersal individuals at the expansion front drives dispersal evolution at the invasion front and may result in the accumulation of individuals with extreme dispersal abilities at its edge, accelerating invasion (Alex Perkins et al., 2013; Bouin et al., 2012; Shine et al., 2011). Another example is wing polymorphism, which plays a role in the interaction between dispersal and other key life history traits such as reproduction (Zera and Denno, 1997).The flight capability (defined by developed wings and flight muscles) is negatively correlated with age at first reproduction and fecundity (Denno, 1994). Thus, the energy efforts for flight and reproduction leads a trade-off for internal resources (Zera and Denno, 1997). In epidemic context, since pathogens are likely to exhibit rapid evolution on front expansion, epidemic invasions could be influenced by spatial structure: invasion success of a mutant pathogen depends on the life-history traits of the mutant and the location of the mutant relative to the front of the epidemic (Griette, 2019; Wei and Krone, 2005).

Speed properties of biological invasions have been firstly assessed by Fisher (1937); Murray (2002); Shigesada and Kawasaki (1997); Turchin (1998a) in a homogeneous environment with a normally distributed kernel of dispersal without mutation. The or-

ganisms spread as a traveling wave with a speed equal to $2\sqrt{RD}$, where where R is the exponential growth rate of the population at low density and D is the diffusion coefficient (Shigesada and Kawasaki, 1997). Relaxing the hypothesis that the space is homogeneous and adding spatial and/or temporal heterogeneity may speed up or slow down the invasion depending on which trait is affected by the environment (Shigesada and Kawasaki, 1997). Most theoretical studies based on the reaction-diffusion framework focus on the spreading properties, and, especially, on the existence of travelling wave solutions and their generalizations to spatially-heterogeneous environments (Berestycki and Hamel, 2002, 2005; Berestycki et al., 2005).Some recent works by Benichou et al. (2012); Berestycki et al. (2015); Bouin and Calvez (2014); Bouin et al. (2012) focus on demonstrating the travelling wave existence and studying the spreading properties developing a eco-evolutionary model to take into account species adaptation. Berestycki et al. (2015) propose a model where the acceleration dynamics is due to a continual selection of individual with enhanced dispersion abilities. Thus, it considers a continuum not limited space for the dispersal trait, which can take arbitrarily large values. Their work is based on a homogeneous space and trade-off with other traits is not considered. They find theoretical and numerical results of expansion front properties (*e.g*, front position and spreading speed solution) and compare local and nonlocal dynamics. Bouin and Calvez (2014) construct travelling waves solutions and evaluate the spreading speed of travelling waves for Australian cane toads *Rhinella marina* dynamics defined by a continuum bounded phenotype traits. Their work address the issue of front expansion in ecology, where the studied trait is related to dispersal ability Bouin and Calvez (2014). However, also in this case, the space is homogeneous and there is no trade-off among traits.

In this work, we develop a reaction-diffusion model to describe the phenotype-space-

time dynamics of a consumer species in a heterogeneous space during a range expansion. We focus on the trade-off between the growth rate $R(x,y)$ and dispersal rate $D(x,y)$, which are both defined as functions of the space variable x and the phenotype variable y. Thus, contrarily to several recent reaction-diffusion approaches (Benichou et al., 2012; Bouin and Calvez, 2014; Bouin et al., 2012) where the trait D was also the phenotypic variable of the model, we describe the trade-off between R and D by assuming that they depend on an underlying abstract trait y and reach their respective optimal value for different values of this trait. In a spatially homogeneous environment and in the absence of mutations and Allee effects, the standard formula $v = 2\sqrt{R(y)\,D(y)}$ (Kolmogorov et al., 1937) clearly shows that growth and dispersal play a similar role on the spreading speed. We analyze here how this symmetry in the effects of R and D may be broken when facing spatial heterogeneities, in the presence of competition between phenotypic traits or in the presence of mutations. Specifically, we investigate the following questions: i) What is the spreading speed v of the population range and the corresponding fastest phenotype y^*? ii) What is the role of the competition among phenotypic traits? iii) What is the population composition along the expansion front?

Model

Eco-evolutionary dynamics

At time t and location x, the density of the consumer phenotype y is defined by $c(t,x,y)$. We describe the spatial dispersion in a one-dimensional environment with a Laplace diffusion operator, corresponding to random walk movements of the individuals, with a mobility parameter (also called diffusion coefficient) $D(x,y)$ (Shigesada and Kawasaki, 1997; Turchin, 1998a). We assume a one-dimensional phenotype $y \in (y_{\min}, y_{\max})$. The

mutations between phenotypes are also described with a Laplace diffusion approximation (Hamel et al., 2020; Tsimring et al., 1996) with constant mutation coefficient $\mu \geq 0$. The mutation coefficient μ is proportional to the mutation rate (per individual per generation) and to the average mutation effect on phenotype (Hamel et al., 2020). Finally, the population grows logistically with heterogeneous growth rate $R(x, y)$. Competition occurs locally on the geographical space but globally over phenotypes though a non-local term, and is modulated by a parameter γ. This leads to the following reaction-diffusion model for the phenotype-space-time dynamics of the consumer population:

$$\partial_t c(t,x,y) = \partial_{xx}(D(x,y)\, c(t,x,y)) + \mu\, \partial_{yy} c(t,x,y) + c\left(R(x,y) - \gamma \int_{y_{\min}}^{y_{\max}} c(t,x,s)ds\right). \tag{1}$$

In addition, we assume no-flux boundary conditions at the boundaries $y = y_{\min}, y_{\max}$:

$$\partial_y c(t,x,y_{\min}) = \partial_y c(t,x,y_{\max}) = 0,$$

so that in the absence of demography (i.e., if $R = \gamma_c = 0$), the global population size $\mathbf{C}(t) = \int_{\mathbb{R}\times(y_{\min},y_{\max})} c(t,x,y)dxdy$ remains constant.

Modelling genetic and spatial heterogeneity in dispersal and growth

Spatial heterogeneity in environmental conditions are assumed to impact the consumer growth rate R and its mobility D. Genetic and spatial effects on R and D are assumed to be additive:

$$R(x,y) = R_0 + R_g(y) + a\, R_s(x/L), \tag{2}$$

$$D(x,y) = D_0 + D_g(y) + a\, D_s(x/L), \tag{3}$$

where R_0 and D_0 are the basal values for growth and diffusion. These basal values are modified according to a genetic effect, R_g, respectively D_g, and a spatial effect, R_s, respectively D_s. The coefficient a scales up the amplitude of the spatial heterogeneity, it can vary from 0 to 1.

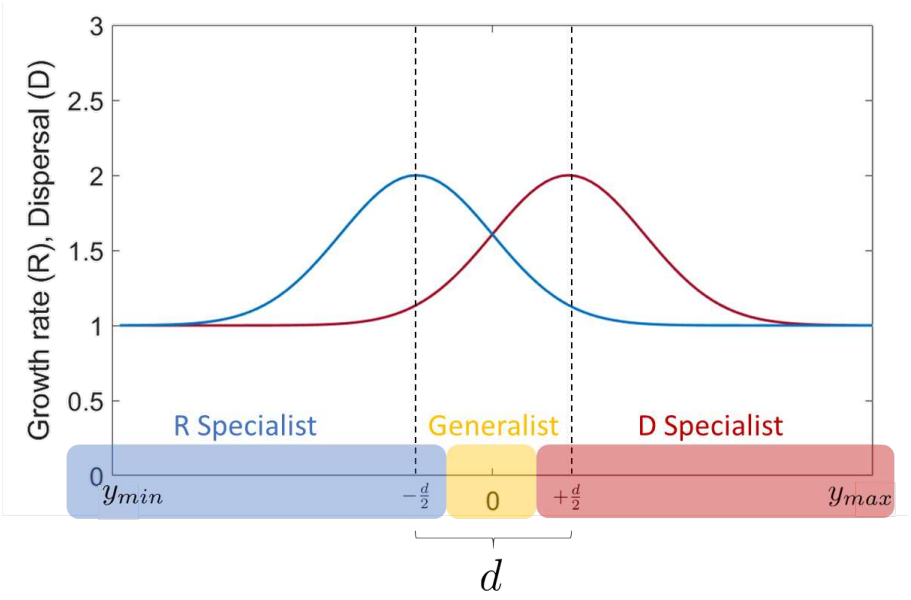

Figure 1: Phenotype classification. The curves represent the dispersal rate $D(x,y)$ (red) and growth rate $R(x,y)$ (blue) in function of phenotypic traits $y \in (y_{min}, y_{max})$ in the homogeneous case. The coefficient d is the distance among the optimum for dispersal and growth rate. The colored boxes highlight the classification of *D Specialist*, *R Specialist* and *Generalist*.

Genetic effect. Given its trait value y the genetic effect on the growth rate R and the diffusion coefficient D is assumed to be Gaussian (Figure 1):

$$R_g(y) = \exp(-(y + d/2)^2/(2\sigma^2)), \tag{4}$$

$$D_g(y) = \exp(-(y - d/2)^2/(2\sigma^2)), \tag{5}$$

where d corresponds to the distance between the two optima. The optimum trait for diffusion represents the consumer optimal dispersal strategy, and the optimum trait for the growth rate represents the consumer optimal resource exploitation strategy. Here, we assume that the optimum values are symmetric with respect to 0, corresponding to the values of $-d/2$ and $+d/2$ for the growth rate and dispersal, respectively . The coefficient σ is the standard deviation of the Gaussian function and indicates the intensity of selection around the optimal trait value. The phenotypic traits are classified in three classes depending on d (Figure 1): the D specialists (the phenotypic traits with narrow preference range on diffusion strategy), the R specialists (the phenotypic traits with narrow preference range on foraging strategy) and the generalists (the phenotypic traits with broad preference range on diffusion and foraging strategy).

Environmental effect. In Equations (2) and (3), the terms $R_s(x/L)$ and $D_s(x/L)$ describe the periodic heterogeneity over the space x through periodic functions with period $L > 0$. Varying the period L allows describing different grain of spatial heterogeneity for the resource distribution and dispersal capability. Thus, R_s is a 1-periodic piecewise constant function of mean 0, with $R_s(x) = R_0$ on $[0, 1/2)$ and $R_s(x) = -R_0$ on $[1/2, 1)$. Equivalently, D_s is a smooth 1-periodic function, with mean value 0, and bounded from below by $-D_0$ (so that D is always positive). More precisely, we define the 1-periodic function $\delta_1(x)$ such that $\delta_1(x) = D_0$ in $[0, 1/2)$ and $\delta_1(x) = -D_0$ in $[1/2, 1)$. Then, D_s is

obtained by regularizing δ_1 with a convolution by a smooth function:

$$D_s(x) = \int_{\mathbb{R}} \delta_1(x-y)\,\phi(y)\,dy,$$

with ϕ a Gaussian function with small variance (Figure 1).

Simulation scenario

We define three scenarios, depending on the presence of spatial heterogeneity, and on if it impacts growth or dispersal:

- Scenario A: spatially homogeneous coefficients. In this case, $R(x,y) = R_h(y) := R_0 + R_g(y)$ and $D(x,y) = D_h(y) := D_0 + D_g(y)$.
- Scenario B: heterogeneous growth and homogeneous dispersal. In this case, $R(x,y) = R_0 + R_g(y) + R_s(x/L)$ and $D(x,y) = D_h(y) = D_0 + D_g(y)$.
- Scenario C: homogeneous growth and heterogeneous dispersal. In this case, $R(x,y) = R_h(y) = R_0 + R_g(y)$ and $D(x,y) = D_0 + D_g(y) + D_s(x/L)$.

Methods

We explore the consumer species $R - D$ trade-off by analyzing the population expansion dynamics depending on space heterogeneity. We focus on the spreading properties, i.e., we assess the range expansion behavior in space, we identify the fastest phenotypic trait and we characterize the population composition on the expansion front and in the bulk of the population. We derive analytical approximations of the spreading speeds, using approached models and limiting cases of rapidly and slowly varying environments and

we compare these approximations with numerical results.

The spreading speed

The spreading speed V is the asymptotic rate at which a species, initially concentrated in a finite spatial region, expands its spatial range. It can be defined here as the smallest speed w, such that, if an observer travels to the right (i.e., towards increasing x values) with the speed w, he will observe the the population density converge to 0. In mathematical terms, V is the only speed such that:

$$\begin{aligned} C(t, x + w\,t) &\to 0, \quad \text{as } t \to +\infty, \text{ for all } w > V, \\ C(t, x + w\,t) &\not\to 0, \quad \text{as } t \to +\infty, \text{ for all } w < V, \end{aligned} \tag{6}$$

with $C(t, x)$ the population density at spatial position x:

$$C(t, x) = \int_{y_{\min}}^{y_{\max}} c(t, x, y)\, dy.$$

For each phenotype y, the spreading speed $v(y)$ of the phenotype y can be defined as well by replacing $C(t, x)$ with $c(t, x, y)$ in the above expressions (e.g., $c(t, x + w\,t, y) \to 0$ as $t \to +\infty$, for all $w > v(y)$).

The existence of a spreading speed as well as analytical characterizations have been obtained by (Aronson and Weinberger, 1975, 1978; Fife and McLeod, 1977; Kolmogorov et al., 1937) for standard equations with spatially homogeneous coefficients and local competition terms. Comparable results have been obtained in the early 2000s (Berestycki and Hamel, 2002, 2005) with a periodically varying coefficient as in Equation (1) and a local competition term, namely for equations of the form:

$$\partial_t c(t, x, y) = \partial_{xx}(D(x, y)\, c(t, x, y)) + \mu\, \partial_{yy} c(t, x, y) + c(t, x, y)\, (R(x, y) - \gamma\, c(t, x, y)). \tag{7}$$

Here, the difference with Equation (1) is that the individuals with phenotype y only interact with individuals with the same phenotype. As we did not assume an Allee effect in Equation (1), the solutions should be pulled by the individuals in the leading edge of the colonization (Roques et al., 2012a; Stokes, 1976). Their speed should therefore only depend on the growth term through its linearization around 0, here $R(x,y)\,c$. We therefore conjecture that the spreading speeds V of the solutions of Equations (1) and (7) are equal. This conjecture is supported by the results of Alfaro et al. (2014), which deal with a non-local equation of the form (1), with a constant diffusion term D and with a growth term of the form $R(x,y) = r(y - B\,x)$, with $r(y) = r_{\max} - b\,y^2$ (to each position x is attached an optimal phenotype $B\,x$). This would imply that the fastest phenotype,

$$y^* = \underset{y\in(y_{\min},y_{\max})}{\operatorname{argmax}}\ v(y)$$

has the same speed for the two Equations (1) and (7) with and without non-local interactions. As the fastest phenotype, y^* does not compete with other phenotypes and its speed should indeed not be influenced by the competition term, and therefore be the same for the two equations.

For Equation (7), under our three scenarios (A,B,C), more or less explicit formulas for the spreading speed are available. First, when the environment is spatially homogeneous (Scenario A) *i.e.* when $R(x,y) = R_h(y)$ and $D(x,y) = D_h(y)$ and in the absence of mutations ($\mu = 0$), the spreading speed associated with a phenotype y is $v(y) = 2\sqrt{R_h(y)\,D_h(y)}$ (Kolmogorov et al., 1937). In that case, and according to the values of d and σ (see Equations (4) and (5)), the fastest phenotypes can be the generalist, $y^* = 0$ or the two specialists, $y^* = -d/2$ and $y^* = d/2$, see Appendix B. The overall spreading speed defined by Equation (6) is $V = 2\sqrt{R_h(y^*)\,D_h(y^*)}$. When the environmental heterogeneity only impacts the growth rate $R(x,y)$ keeping the diffusion

coefficient spatially homogeneous $D(x,y) = D_h(y)$ (Scenario B), a general formula for
165 the spreading speed has been obtained by Berestycki and Hamel (2005). Their results also encompass the case of a heterogeneous diffusion coefficient $D(x,y)$ but spatially homogeneous growth rate $R(x,y) = R_h(y)$ (Scenario C). However, in this case, their result
168 holds true for equations with "Fickian" spatial diffusion term, i.e. $\partial_x(D(x,y)\,\partial_x c)$ instead of Fokker-Planck diffusion $\partial_{xx}(D(x,y)\,c)$ in (7) (Roques, 2013; Turchin, 1998a).

In the spatially heterogeneous cases (Scenarios B, C) the formulas rely on variational
171 characterizations which make them hardly tractable, even numerically (see Appendix B). More tractable formulas for the phenotype spreading speeds can be obtained for rapidly varying (i.e. when the period is small, $L \to 0$) and slowly varying (i.e. when the period
174 is large, $L \to \infty$) environments in the absence of mutations ($\mu = 0$) (El Smaily et al., 2009; Hamel et al., 2010, 2011). These formulas are summarized in Table 1, see also Appendix B for more mathematical details.

Table 1: Theoretical phenotype spreading speeds for Equation (7) with $\mu = 0$ (no mutation) for rapidly varying environments $L \to 0$ and slowly varying environments $L \to \infty$.

	Spatial heterogeneity	$L \to 0$	$L \to \infty$
Scenario A	$R_h(y)$, $D_h(y)$	$v(y) = 2\sqrt{R_h(y)\,D_h(y)}$	$v(y) = 2\sqrt{R_h(y)\,D_h(y)}$.
Scenario B	$R(x,y)$, $D_h(y)$	$v_0(y) = 2\sqrt{R_h(y)\,D_h(y)}^{*}$	$v_\infty(y) = 4\sqrt{D_h(y)} \times \frac{(R^+(y))^2+(R^-(y))^2+(R^+(y)+R^-(y))\sqrt{\triangle(y)}}{(R^+(y)+R^-(y)+2\sqrt{\triangle(y)})^{\frac{3}{2}}}^{**}$
Scenario C (Fickian diffusion)	$R(y)$, $D(x,y)$	$v_0(y) = 2\sqrt{R_h(y)} < D >_H (y)^{***}$	$v_\infty(y) = 2\sqrt{R_h(y)} < \sqrt{D} >_H (y)^{***}$

Where:

* $v_0(y) = 2\sqrt{R_h(y)\,D_h(y)}$ with $\overline{R}_x(y) = \int_0^1 R(x,y)\,dx = R_h(y)$, as $R_s(x)$ has mean value 0

** $R^+(y) = R_h(y) + R_0$, $R^-(y) = R_h(y) - R_0$, $\triangle(y) = (R^+(y))^2 + (R^-(y))^2 - R^+(y)\,R^-(y)$

***$< F >_H (y) = \left(\int_0^1 \frac{1}{F(x,y)}\,dx\right)^{-1}$ is the harmonic mean of $F(x,y)$

Simulation experiment

We check the accuracy of the analytical approximations in Table 1 and we further explore the phenotypic trait composition in the population by performing numerical simulations with different parameter value combinations. Specifically, the parameters we focus on are: i) the period of heterogeneity L, considering a rapidly (small period $L = 2$) and slowly (large period $L = 10$) varying environments; ii) the distance d between the two optima, where we consider a short distance for weak trade-off ($d = 2$) and a large distance for strong trade-off ($d = 4$); iii) the amplitude of the heterogeneity $a \in (0, 1)$; iv) and, the mutation $\mu = 0$ (no mutations) or $\mu = 0.001$. Both Equations (1) and (7) were simulated.

We computed numerically the phenotype spreading speeds $v_{sim}(y)$ as:

$$v_{sim}(y) = \frac{x_{sim}(y)}{T_{sim}},$$

where $x_{sim}(y)$ is the furthest forward position of the phenotype y at time T_{sim} (T_{sim} is selected large enough such that $v_{sim}(y)$ does not vary much at larger times). The location $x_{sim}(y)$ is defined as the furthest forward position such that as $c(t, x, y) \geq c_{lim}$ for all $x(y) < x_{sim}(y)$, with c_{lim} a fixed threshold (small enough such that the results do not depend much on c_{lim}). Here after, $v_{sim}(y)$ is defined as $v(y)$ to simplify the notation. Once the spreading speed for each trait is evaluated, either numerically or analytically, the phenotype y^*, which leads to the fastest spreading speed, can be evaluated. We follow the phenotype classification of the Figure 1 in D specialists, R specialists and Generalist, to determine which phenotype class is leading the front. Then, we use the same classification in order to categorise the whole population composition behind the front.

When the environment is heterogeneous, we also take into account the role of the amplitude a in Equations (2) and (3). The amplitude is represented by the vertical distance among the $R_h(y)$ and $D_h(y)$ fitness functions in Scenario B and C. It is possible to identify an amplitude threshold value influencing the class leading the colonization front to distinguish when the front is led by the R specialist or by by the D specialist. The threshold value results by the intersection among the $R_h(y)$ curve and $D_h(y)$ curve separating the phenotype domain within two intervals. The subtended area of the R_h curve, over the interval where $D_h(y) < R_h(y)$, is the area proportion where there is higher R than D (p_1); instead, the subtended area of the $R_h(y)$ curve, over the interval where $D_h(y) > R_h(y)$, is the area proportion where there is low R with respect to D (p_2). We define the *amplitude critic value* a_{cr} as the amplitude that leads having p_1 equals to p_2 and we evaluate it for different combination of d and a. Thus, when $p_1 > p_2$ the class leading the front is the R specialist, while when $p_2 > p_1$ the class leading the front is the D specialist.

The equations are solved numerically by transforming them into lattice dynamical systems (continuous time, discrete space with small space step), and using a Runge-Kutta method over a fixed spatial domain and a time horizon large enough to ensure a stable dynamic and propagation front. The implementation is performed by using the software Matlab®.

Results

We first compare the phenotype spreading speeds evaluated with the theoretical formulas vs the numerical simulations to assess the fastest phenotype (Figure 2). Then, we analyze the phenotypic trait composition on the expansion front (Figure 3 and **??**) and

over whole spatial domain (Figure 4).

Spreading speed

The spreading speed evaluated by analytical formulations is compared with numerical simulations in both local and non-local equations for different heterogeneity scenario varying the period L and the optimum distance d (Figure 2). In all cases, the fastest phenotype is well-captured by the analytical formulas. Generally, non-local competition shrinks the phenotypic trait distribution around the spreading speed optimum value leading to important differences between the theoretical spreading speeds and the observed ones for phenotypes y other than the fastest one. In the case of $d < d_{cr}$ (left column Figure 2, d_{cr} is defined in the Appendix), the generalist has the fastest trait value on the expansion front in all the scenario and period L . However, we can notice that the spreading speed curve for the Scenario C is slightly shifted to the right, leading to an imbalance in favor of D. In the case $d > d_{cr}$ (right column Figure 2), the standard behavior described by Equation 7 (local competition) predicts that, on the expansion front, both phenotypes at growth rate and dispersal optimum have similar speed in the Scenario A. Instead, when considering the Equation 1, the effect of the competition leads to the selection of the R specialist. This is also the case for the scenario B when the environment is changing quickly. However, in that scenario, a greater value of L leads both R and D specialists having comparable spreading speed. In the scenario C the spreading speed is lower than in scenario A and the trade off is completely shifted in favor of the D specialist.

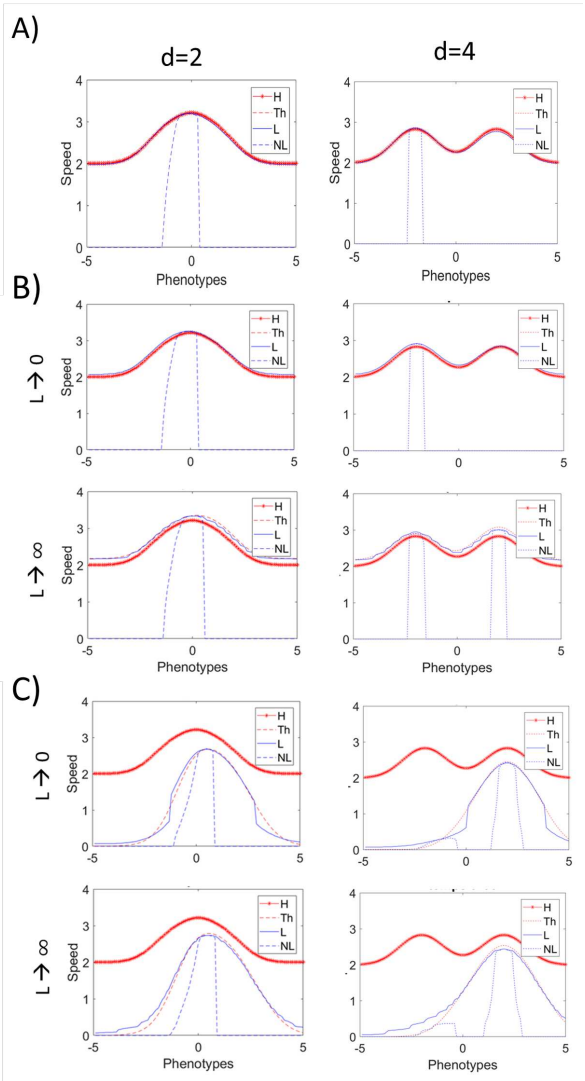

Figure 2: Spreading speed in scenario (A); (B); (C) for $\mu = 0$ and $a = 1$. Red line with stars stands for the homogeneous case formula (H), dashed red line stands for theoretical formula (Th), continuous blue line stands for the local numerical solution (L), dashed blue line stands for the non-local numerical solution (NL). Columns show different optimum distance. In panel (b) and (c) different lines show different period value ($L \to 0$ and $L \to \infty$).

Population composition on the front

Here, we assess the composition of the expanding front varying the period L, the distance among the optimum d and the amplitude a of the heterogeneity. In Figure 3, results of different scenario and parameter combinations are analysed coloring each cell of the plot with the color that correspond to the fastest phenotype (i.e yellow for generalist, blue for the R specialist, red for the D specialist).

In the scenario B, for $L \to 0$, the heterogeneity amplitude a does not produce any effect on the dynamics: when $d < d_{cr}$, the $R - D$ trade-off is always in favor of the Generalist; when $d > d_{cr}$ the R specialist has the fastest phenotype. Instead, for $L \to \infty$ when $d > d_{cr}$, the fastest phenotype could be either the R or the D specialist. When $a < a_{cr}$, the behavior is in favour of the R specialist; when $a > a_{cr}$, the trade-off is shifted in favor of the D specialist (Figure 3A).

In the scenario C, both for $L \to 0$ and $L \to \infty$, a alters the trade-off R and D. For $d < d_{cr}$, the fastest phenotype is always the generalist. For $d > d_{cr}$, as before, the fastest phenotype could be either R or the D specialist depending on the value of a. Amplitudes below a_{cr} select for the R specialist whereas amplitudes behind a_{cr} select for the D specialist (see also Figure 2C for which $a = 1$).

Total population composition

We analyse the composition of the total population behind the front under the different scenario for the non-local case (Figure 4). Under the scenario B with a fast varying environment, the density of phenotype class is invariant with respect to the amplitude of the heterogeneity and only varies depending on d. When $d > d_{cr}$, the population is

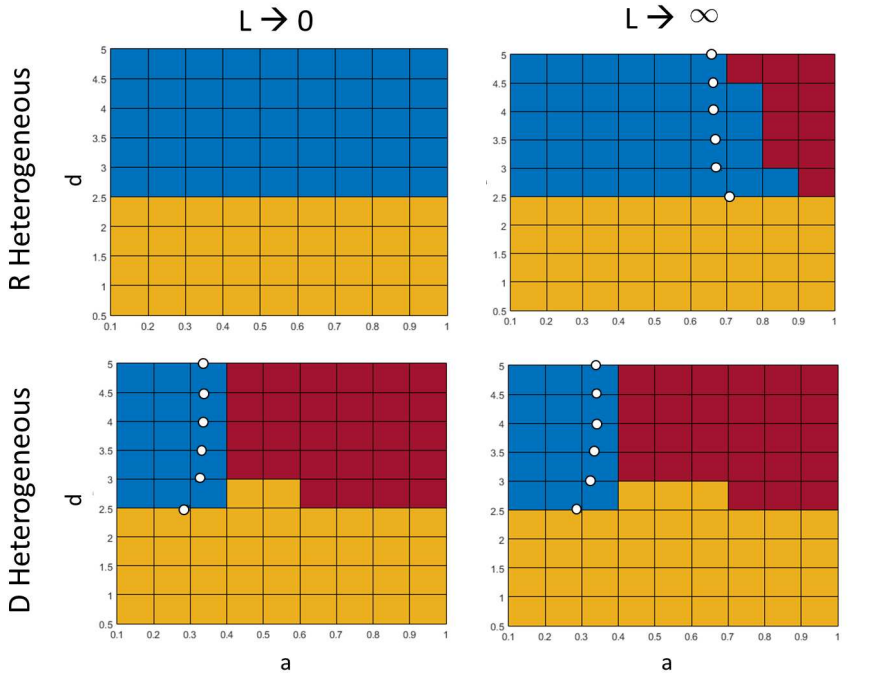

Figure 3: Results of the numerical simulations for assessing the role of the amplitude of scenario B and C for non-local in case of $L \to 0$ and $L \to \infty$. $a = [0.1 - 1]$ by 0.1 (x axis) and $d = [0.5 - 5]$ by 0.5 (y axis). The colors stand for the fastest phenotypic traits: yellow stands for generalists, red stands for D specialists and blue for R specialists. The white points represent the a_{cr} given for each d.

composed by half generalist and half R specialist. As d increases, the R specialist proportion increases up to to be the only class presents. For a slowly varying environment and for high amplitude value of heterogeneity, the population composition is not completely dominated by the R specialist, but there is a proportion of D specialist coming out. And specifically, this proportion is localised on the expansion front as demonstrated in Figure 3. Under the scenario C, when $d < d_{cr}$, there is an increase of the generalist instead of the R Specialist as the amplitude a increases. When $d > d_{cr}$, there is a clear shift from a proportion in favor of the R specialist to the D specialist as the amplitude a increases showing that the D specialist takes the leading of the expansion front but also a great part of the total population behind the front.

The effect of mutation

In all the scenarios and parameter combinations, we also evaluate the effect of the mutation. We observe that it only leads to an homogenization of the phenotypic distribution and therefore to a wider phenotype ensemble that leads the propagation front. However, the mutation does not affect the R-D trade-off outcome: the fastest phenotypic trait is the same without and with mutations.

By contrast, when the system is composed of only the two phenotypes $y = O_R$ and $y = O_D$ instead of a continuum $y \in (y_{\min}, y_{\max})$, with a low mutation rate, we numerically find an overall spreading speed (v_f) which is higher than the maximum of the spreading speeds of each phenotype independently, i.e., strictly larger than

$$\max\left(2\sqrt{R_h(O_R)\,D_h(O_R)}, 2\sqrt{R_h(O_D)\,D_h(O_D)}\right)$$

in Scenario A, that corresponds to the faster speed reported by Elliott and Cornell (2012)

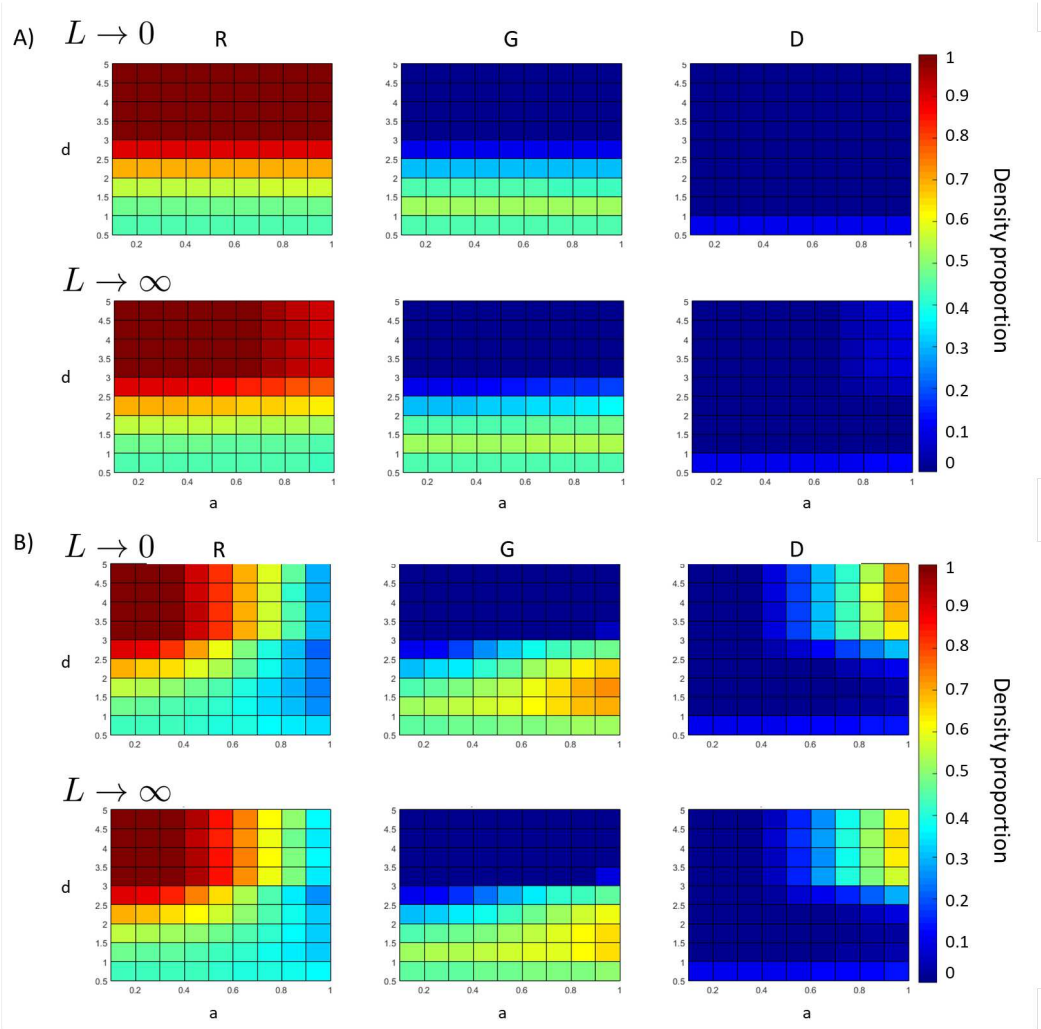

Figure 4: Results of the numerical simulations for assessing the population composition for scenario B (Panel A) and scenario C (Panel B) for non-local equation in case of $L \to 0$ and $L \to \infty$. The amplitude of heterogeneity varies as $a = [0.1 - 1]$ by 0.1 (x axis) and the optimum distance varies as $d = [0.5 - 5]$ by 0.5 (y axis).The colors represent the density proportion for each phenotype class: R for the R specialist, G for the generalist and D for the D specialist.

(see Appendix A). Interestingly, in the scenarios B and C, we find that both in a slow and fast varying environment for the heterogeneity in R, the spreading speed still corresponds to v_f as in the homogeneous case. That was not the case in the scenario C.

Discussion

Dispersing faster or growing stronger? Which strategy is selected in populations invading a heterogeneous environment ? Range expansion and colonization of new habitats are primarily driven by reproduction and dispersal (Lewis et al., 2016). However, both traits are generally correlated as organisms can pay a reproductive cost to disperse faster (Baguette and Schtickzelle, 2006; Bonte and Bafort, 2018; Hanski et al., 2006). In addition, spatial heterogeneity in environmental conditions that impacts growth or dispersal can influence such processes by modifying demography and dispersal (Hanski et al., 2006; Ramanantoanina and Hui, 2016). In this work we addresses these questions gathering analytical solutions from the literature and performing numerical simulations of a reaction-diffusion model describing the demo-genetic dynamics of a population invading a one-dimensional heterogeneous environment. We find that the spatial heterogeneity play a role in shaping the trait trade-off determining the preferred strategy on the expansion front and in the rest of the population behind. The trade-off strength, the fragmentation and the amplitude are the key elements that contribute to the strategy shift with respect to the homogeneous case.

When the trade-off is weak, i.e. when the distance between the optimal phenotypes is below the threshold $d < d_{cr}$, evolution leads to the selection of a phenotype with generalist features. When heterogeneity impacts the growth rate, the generalist is the same as in homogeneous environments. This is due to the fact that heterogeneity impacts the

average growth rate only through its arithmetic mean. Interestingly, when heterogeneity impacts the diffusion coefficient, the phenotype of the generalist is shifted toward a greater dispersal ability. Indeed, in that case it is the harmonic mean that appears in the expression of the velocity.

As the trade-off becomes stronger, in an homogeneous environment the phenotypes optimizing growth (R specialist) and the phenotype optimizing dispersal (D specialist) have the same speed. This holds true when envionmental heterogeneity impacts the growth rate while only the D-specialist confers the maximal speed when dispersal is heterogeneous. However, competition among phenotypes can give advantage to growth. Recently, Deforet et al. (2019) explore the $R - D$ trade-off and determine the conditions favoring evolution of fastest dispersal against the growth rate in a homogeneous space for a population composed of two-morphs. Given two species having r_1, D_1 and r_2, D_2, for species 1 and 2, respectively, they assess the evolutionary outcome depending on the simple condition $r2/r1 > D1/D2$. Basically they find that a lower trait value for either growth or dispersal can be compensated by the other trait in order for a species to take over the other one. This was not the case in our approach as we are in the particular case where the two morphs at the optimum of the two strategy results in the particular case $r2/r1 = D1/D2$, due to the symmetry assumption.

Habitat fragmentation plays also a crucial role in determining the evolutionary output. Fast varying environments ($L \to 0$), tend to favour stronger growth rate upon faster dispersal at least when heterogeneity impacts the growth rate. Indeed, resources are heterogeneously distributed, but the distance among favorable habitats is not large, thus the trade-off is more favorable to the selection of thte R-strategy on the front as high resource availability and fecundity facilitate expansion by increasing population growth

(Burton et al., 2010). By contrast, in slower varying environment ($L \to \infty$), the faster dispersers take advantage of their mobility to reach the most favourable habitats and lead the colonization front. Evolution leads thus to the selection of a higher dispersal capacity. When environmental heterogeneity impacts dispersal, phenotypes optimizing dispersal are selected at the front regardless of habitat fragmentation. This result is in line with the "Spatial sorting theory", where, in an expanding front, dispersal may be strongly favoured because of spatial sorting and selection where the best dispersers tend to be disproportionately represented on the population front (see Phillips et al. (2008); Shine et al. (2011); Travis and Dytham (2002)). Many examples suggest that population expansion may select for better dispersal Chuang and Peterson (2016); Zera and Denno (1997), even at the cost of slower growth (Andrade-Restrepo et al., 2019; Chuang and Peterson, 2016) as the cane toads *lat name* invasion in Australia, where on the margin individuals have longer legs with lower birth rates (Phillips et al., 2006). Similarly, this has been observed for the speckled wood butterfly *Pararge aegeria* among two habitats which differ for their availability breeding sites. The most fragmented habitat are associated with an increased dispersal ability, but females at range margins laid significantly fewer eggs than those from populations nearer the centre of the range (Hughes et al., 2003). The picture is different behind the front where we found that the R-strategy is always selected.

In pulled waves, when competition is relaxed on the front, the genetic diversity is consistently low on the front (Roques et al., 2012b) due to the filtering of spatial sorting, homogenizing the phenotypic traits selected for dispersal (Andrade-Restrepo et al., 2019; Cobben et al., 2015). The effect of mutation on the spreading speed of an expanding population is addressed numerically by Elliott and Cornell (2012). They investigated the

effect of varying R and D on the spreading speed of the system and they find that the system would spread faster in the presence of both phenotype than just one phenotype would spread in the absence of mutation for certain combination of D and R values (Elliott and Cornell, 2012; Morris et al., 2019). Morris et al. (2019) derive predictions about the spreading of species characterised by travelling waves and find analytical conditions given by R and D parameter combinations. In our case, the two fastest phenotypes alone verify the hypothesis for which the speed v_f should appear as $D_h(O_R)/D_h(O_D) = R_h(O_D)/R_h(O_R)$ The phenotypes $y = O_D$ and $y = O_R$, alone, would have the same spreading speed: $2\sqrt{R_h(O_D)D_h(O_D)} = 2\sqrt{R_h(O_R)D_h(O_R)}$, respectively. Thus, our case correspond to the one expressed by Eq. 40 of Morris et al. (2019), see Appendix. We are in the case of Elliott and Cornell (2012) where the spreading speed of the fastest morphs is equal to v_f with low mutation rate and considering a population of two-morphs. However, in our system the fact of having a continuum space of phenotypes with a step-wise mutation does not verify the same conditions since each phenotype mutates with the nearest neighbors and they are not only the two optimum phenotypic traits (see Appendix B). Thus, we find that a low step-wise mutation in a non-local system composed by a continuum phenotype space, is able to slow down the spreading speed that the system would have with only two phenotypic traits due to the mutation among the nearest neighbors and competition.

Finally, it is important to recall that our results depend on the assumptions about the form of the dispersal and growth rate functions and the heterogeneity definition (i.e. piece-wise function of period L on the uni-dimensional domain x). In our model, we do not take into account of the Alee effect, which it is demonstrated to have consequences for the dynamics of invasion since there are low densities on the invasion front

(Andrade-Restrepo et al., 2019; Chuang and Peterson, 2016; Roques et al., 2012a). Future works could develop a more complex dynamic model than the presented one taking into account important effects (e.g Allee effects) or introducing another species (e.g prey-predation). Moreover, integrating such theoretical models and results with empirical data would be beneficial. This research and results are key for describing different kind of invasion and colonization phenomena as the expansion of invasive species (Phillips et al., 2006) or in an agro-ecological context for biological control as evaluating the speed of pest species propagating in the intermixing of habitat of an agricultural landscape (Shigesada, 1986).

Literature Cited

Alex Perkins, T., B. L. Phillips, M. L. Baskett, and A. Hastings (2013). Evolution of
387 dispersal and life history interact to drive accelerating spread of an invasive species. Ecology letters 16(8), 1079–1087.

Alfaro, M., J. Coville, and G. Raoul (2014). Bistable travelling waves for nonlocal reaction
390 diffusion equations. Disc Cont Dyn Systems A 34, 1775–1791.

Andrade-Restrepo, M., N. Champagnat, and R. Ferrière (2019). Local adaptation, dispersal evolution, and the spatial eco-evolutionary dynamics of invasion. Ecology
393 letters 22(5), 767–777.

Aronson, D. G. and H. G. Weinberger (1975). Nonlinear diffusion in population genetics, combustion and nerve propagation. In
396 Partial Differential Equations and Related Topics, Volume 446 of Lectures Notes Math, pp. 5–49. Springer, New York.

Aronson, D. G. and H. G. Weinberger (1978). Multidimensional nonlinear diffusion
399 arising in population genetics. Adv Math 30(1), 33–76.

Baguette, M. and N. Schtickzelle (2006). Negative relationship between dispersal distance and demography in butterfly metapopulations. Ecology 87(3), 648–654.

402 Benichou, O., V. Calvez, N. Meunier, and R. Voituriez (2012). Front acceleration by dynamic selection in fisher population waves. Physical Review E 86(4), 041908.

Berestycki, H. and F. Hamel (2002). Front propagation in periodic excitable media.
405 Comm Pure Appl Math 55(8), 949–1032.

Berestycki, H. and F. Hamel (2005). Gradient Estimates For Elliptic Regularizations of Semilinear Parabolic And Degenerate Elliptic Equations. Communications in Partial Differential Equations 30(1-3), 139–156.

Berestycki, H., F. Hamel, and L. Roques (2005). Analysis of the periodically fragmented environment model: II - Biological invasions and pulsating travelling fronts. J Math Pures Appl 84(8), 1101–1146.

Berestycki, N., C. Mouhot, and G. Raoul (2015). Existence of self-accelerating fronts for a non-local reaction-diffusion equations. arXiv preprint arXiv:1512.00903.

Bonte, D. and Q. Bafort (2018). The importance and adaptive value of life history evolution for metapopulation dynamics. bioRxiv, 179234.

Bonte, D. and E. de la Pena (2009). Evolution of body condition-dependent dispersal in metapopulations. Journal of Evolutionary Biology 22(6), 1242–1251.

Bouin, E. and V. Calvez (2014). Travelling waves for the cane toads equation with bounded traits. Nonlinearity 27(9), 2233.

Bouin, E., V. Calvez, N. Meunier, S. Mirrahimi, B. Perthame, G. Raoul, and R. Voituriez (2012). Invasion fronts with variable motility: phenotype selection, spatial sorting and wave acceleration. Comptes Rendus Mathematique 350(15-16), 761–766.

Burton, O. J., B. L. Phillips, and J. M. Travis (2010). Trade-offs and the evolution of life-histories during range expansion. Ecology letters 13(10), 1210–1220.

Chuang, A. and C. R. Peterson (2016). Expanding population edges: theories, traits, and trade-offs. Global change biology 22(2), 494–512.

Cobben, M., J. Verboom, P. Opdam, R. Hoekstra, R. Jochem, and M. Smulders (2015). Spatial sorting and range shifts: consequences for evolutionary potential and genetic signature of a dispersal trait. Journal of Theoretical Biology 373, 92–99.

Deforet, M., C. Carmona-Fontaine, K. S. Korolev, and J. B. Xavier (2019). Evolution at the edge of expanding populations.

Denno, R. F. (1994). Life history variation in planthoppers. In Planthoppers, pp. 163–215. Springer.

Duthie, A. B., K. C. Abbott, and J. D. Nason (2015). Trade-offs and coexistence in fluctuating environments: evidence for a key dispersal-fecundity trade-off in five nonpollinating fig wasps. The American Naturalist 186(1), 151–158.

El Smaily, M., F. Hamel, and L. Roques (2009). Homogenization and influence of fragmentation in a biological invasion model. Disc Cont Dyn Systems A.

Elliott, E. C. and S. J. Cornell (2012). Dispersal polymorphism and the speed of biological invasions. PloS one 7(7).

Fife, P. C. and J. McLeod (1977). The approach of solutions of nonlinear diffusion equations to traveling front solutions. Arch Ration Mech Anal 65(1), 335–361.

Fisher, R. A. (1937). The wave of advance of advantageous genes. Ann Eugen 7, 335–369.

Griette, Q. (2019). Singular measure traveling waves in an epidemiological model with continuous phenotypes. Transactions of the American Mathematical Society 371(6), 4411–4458.

Griette, Q., G. Raoul, and S. Gandon (2015). Virulence evolution at the front line of spreading epidemics. Evolution 69(11), 2810–2819.

Hamel, F., J. Fayard, and L. Roques (2010). Spreading speeds in slowly oscillating environments. Bull Math Biol 72(5), 1166–1191.

Hamel, F., F. Lavigne, G. Martin, and L. Roques (2020). Dynamics of adaptation in an anisotropic phenotype-fitness landscape. Nonlinear Analysis: Real World Applications 54, 103107.

Hamel, F., G. Nadin, and L. Roques (2011). A viscosity solution method for the spreading speed formula in slowly varying media. Indiana Univ Math J 60, 1229–1247.

Hanski, I., M. Saastamoinen, and O. Ovaskainen (2006). Dispersal-related life-history trade-offs in a butterfly metapopulation. Journal of animal Ecology 75(1), 91–100.

Helms, J. and M. Kaspari (2015). Reproduction-dispersal tradeoffs in ant queens. Insectes sociaux 62(2), 171–181.

Hirt, M. R., T. Lauermann, U. Brose, L. P. Noldus, and A. I. Dell (2017). The little things that run: a general scaling of invertebrate exploratory speed with body mass. Ecology 98(11), 2751–2757.

Hughes, C. L., J. K. Hill, and C. Dytham (2003). Evolutionary trade-offs between reproduction and dispersal in populations at expanding range boundaries. Proceedings of the Royal Society of London. Series B: Biological Sciences 270(suppl_2), S147–S150.

Kolmogorov, A. N., I. G. Petrovsky, and N. S. Piskunov (1937). Étude de l'équation de la diffusion avec croissance de la quantité de matière et son application à un problème biologique. Bull Univ État Moscou, Sér. Int. A 1, 1–26.

Lavigne, F., G. Martin, Y. Anciaux, J. Papaix, and L. Roques (2020). When sinks become sources: adaptive colonization in asexuals. Evolution 74(1), 29–42.

Legrand, D., J. Cote, E. A. Fronhofer, R. D. Holt, O. Ronce, N. Schtickzelle, J. M. Travis, and J. Clobert (2017). Eco-evolutionary dynamics in fragmented landscapes. Ecography 40(1), 9–25.

Lewis, M. A., B. Li, and H. F. Weinberger (2002). Spreading speed and linear determinacy for two-species competition models. Journal of mathematical biology 45(3), 219–233.

Lewis, M. A., S. V. Petrovskii, and J. R. Potts (2016). Reaction–diffusion models: single species. In The Mathematics Behind Biological Invasions, pp. 69–105. Springer.

Morris, A., L. Börger, and E. Crooks (2019). Individual variability in dispersal and invasion speed. Mathematics 7(9), 795.

Murray, J. D. (2002). Mathematical Biology. Third edition, Interdisciplinary Applied Mathematics 17, Springer-Verlag, New York.

Phillips, B. L., G. P. Brown, J. M. Travis, and R. Shine (2008). Reid's paradox revisited: the evolution of dispersal kernels during range expansion. the american naturalist 172(S1), S34–S48.

Phillips, B. L., G. P. Brown, J. K. Webb, and R. Shine (2006). Invasion and the evolution of speed in toads. Nature 439, 803–803.

Ramanantoanina, A. and C. Hui (2016). Formulating spread of species with habitat dependent growth and dispersal in heterogeneous landscapes. Mathematical biosciences 275, 51–56.

Ronce, O. and M. Kirkpatrick (2001). When sources become sinks: migrational meltdown in heterogeneous habitats. Evolution 55(8), 1520–1531.

Roques, L. (2013). Modèles de réaction-diffusion pour l'écologie spatiale. Editions Quae.

Roques, L., J. Garnier, F. Hamel, and E. K. Klein (2012a). Allee effect promotes diversity in traveling waves of colonization. Proc Natl Acad Sci USA 109(23), 8828–8833.

Roques, L., J. Garnier, F. Hamel, and E. K. Klein (2012b). Allee effect promotes diversity in traveling waves of colonization. Proceedings of the National Academy of Sciences 109(23), 8828–8833.

Shigesada, N. (1986). Traveling periodic waves in heterogeneous environments. Theor. Popul. Biol. 30, 143–160.

Shigesada, N. and K. Kawasaki (1997). Biological Invasions: Theory and Practice. Oxford Series in Ecology and Evolution, Oxford: Oxford University Press.

Shine, R., G. P. Brown, and B. L. Phillips (2011). An evolutionary process that assembles phenotypes through space rather than through time. Proceedings of the National Academy of Sciences 108(14), 5708–5711.

Steenman, A., A. Lehmann, and G. Lehmann (2015). Life-history trade-off between macroptery and reproduction in the wing-dimorphic pygmy grasshopper tetrix subulata (orthoptera tetrigidae). Ethology Ecology & Evolution 27(1), 93–100.

Stokes, A. N. (1976). On two types of moving front in quasilinear diffusion. Math Biosci 31, 307–315.

Szűcs, M., E. Vercken, E. V. Bitume, and R. A. Hufbauer (2019). The implications of rapid eco-evolutionary processes for biological control-a review. Entomologia Experimentalis et Applicata 167(7), 598–615.

Travis, J. M. and C. Dytham (2002). Dispersal evolution during invasions. Evolutionary Ecology Research 4(8), 1119–1129.

Tsimring, L. S., H. Levine, and D. A. Kessler (1996). RNA virus evolution via a fitness-space model. Physical review letters 76(23), 4440–4443.

Turchin, P. (1998a). Quantitative Analysis of Movement: Measuring and Modeling Population Redistribution in Animals and Plants. Sinauer, Sunderland, MA.

Turchin, P. (1998b). Quantitative analysis of movement: measuring and modeling population redistribution in animals and plants. Sinauer Associates.

Wei, W. and S. M. Krone (2005). Spatial invasion by a mutant pathogen. Journal of theoretical biology 236(3), 335–348.

Zera, A. J. and R. F. Denno (1997). Physiology and ecology of dispersal polymorphism in insects. Annual review of entomology 42(1), 207–230.

Supplementary information

- Supplement 1: Supplementary information of the paper: *Markov random field models for vector-based representations of landscapes.* Pages: 171-186
- Supplement 2: Supplementary information of the paper: *More pests but less pesticide1applications: ambivalent effect of landscape complexity on conservation biological control.* Pages: 187-196
- Supplement 3: Supplementary information of the paper: *Spatio-temporal point processes as meta-models for population dynamics in heterogeneous landscapes.* Pages: 197-207
- Supplement 4: Supplementary information of the paper: *On the evolutionary trade-off between growth and dispersal during a range expansion.* Pages: 208-213
- Supplement 5: Supplementary information of the chapter: *Should I stay or should I go? Effects of predating strategies in shaping pests dispersal behaviours within heterogeneous landscapes.* Pages: 214-222
- Supplement 6: Undergraduate project report. Lingeshwari Ramlugon. (2021) *Etude sur les relations entre la structure dupaysage et la dynamique multi-proies-predateurs pour la lutte biologique* Pages: 223-252

Supplement 1

Submitted to the Annals of Applied Statistics

,

SUPPLEMENTARY MATERIAL FOR "MARKOV RANDOM FIELD MODELS FOR VECTOR-BASED REPRESENTATIONS OF LANDSCAPES "

BY PATRIZIA ZAMBERLETTI, JULIEN PAPAÏX, EDITH GABRIEL, THOMAS OPITZ

1. Gibbs sampler.

1.1. *General setting.* We implement a Markov Chain Monte Carlo algorithm of Gibbs sampler type (Gibbs–MCMC) to iteratively simulate a discrete Markov chain whose stationary distribution corresponds to the target model (e.g., Casella and George, 1992), where the configuration of the allocated land-use categories $\boldsymbol{x}$ is the state variable of the system.

The main steps of Gibbs–MCMC are as follows:

i) we define an initial state $\boldsymbol{x}^{(0)}$; and then iteratively run through steps ii and iii:
ii) we generate a new state $\tilde{\boldsymbol{x}}$ given the current state $\boldsymbol{x}^{(j)}$, selecting a component of the vector $\boldsymbol{x}^{\tilde{(j)}}$ and sampling its category update from the distribution of that component conditioned on all the other components sampled so far.
iv) finally, after I_0 iterations, return the configuration $\boldsymbol{x}^{(I_0)}$.

If we need more than one realization of the landscape, we can either run several chains in parallel, or we may run a single chain but return a sample given by the states indexed by $I_0 + \ell I$, $\ell = 1, 2, \ldots$, with the burn-in period $I_0 > 0$ and $L - 1$ intermediate states left out to avoid autocorrelation in the final sample. Since the parameter vector $\boldsymbol{\beta}$ of the model is fixed during each MCMC run, the intractable normalizing constant $c(\boldsymbol{\beta})$ in the probability mass function of the model cancels out in the conditional probabilities used for Gibbs sampling. During the iterations we have to update the calculation of the set of landscape descriptors for each new configuration $\tilde{\boldsymbol{x}}$. With respect to the choice of the initial state $\boldsymbol{x}^{(0)}$ of the system, we have to ensure that $p(\boldsymbol{x}^{(0)}) > 0$, and that valid Gibbs sampling paths $\boldsymbol{x}^{(1)}, \ldots, \boldsymbol{x}^{(j)}$ to and from any configuration $\boldsymbol{x}^{(j)}$ with $p(\boldsymbol{x}^{(j)}) > 0$ are proposed with strictly positive probability. All of the models presented in the paper satisfy $p(\boldsymbol{x}) > 0$ for all possible configurations $\boldsymbol{x}$, such that any initial state is valid. In more general cases, hereditary properties when moving between configurations must be checked. We initialize the system state either at random by drawing the category of an object o_i among all ℓ_i available categories, or by attributing a single category to each object type, or by using an observed configuration from real data.

1.2. *Detailed description of the algorithm.* Here, we present in detail the steps of the algorithm for the iterative but simultaneous simulation of patches and linear elements: at each iteration i, we randomly select an element type (i.e. patch, layer a, or linear element, layer b) to be updated, and then we select an object of this type, followed by a category selection conditioned to all the other elements. If there is more than one time step, i.e., if there are temporal dynamics with time steps $\tau = 1, ..., H_\tau$ and time horizon $H_\tau \in \mathbb{N}$, we also choose at random one of the time steps to be updated.

As outlined above, we propose to use an algorithm where at successive steps for the network, we select at random one of the object of this type and the new category of the element are sampled from the distribution of that component conditioned on all other components sampled so far. The new category is sampled among the available categories conditioned to the allocated categories over the other elements. We denote the full configuration of categories during iteration step i of the algorithm by $\boldsymbol{x}^{(i)}$.

Given

- I, the total number of iterations, and ,
- time steps $\tau = 1, ..., H_\tau$, with H_τ the time horizon, where H_τ is fixed to 1 in the case of purely spatial simulation,

the algorithm for landscape configuration works as follows:

1. Initialize patches in network C as $\boldsymbol{x}_\tau^{C,(0)} = \boldsymbol{x}^{C,(0)}$ with an initial configuration $\boldsymbol{x}^{C,(0)}$, and initialize linear elements in network H as $\boldsymbol{x}_\tau^{H,(0)} = \boldsymbol{x}^{H,(0)}$ with an initial configuration $\boldsymbol{x}^{H,(0)}$, for $\tau = 1, \ldots, H_\tau$.
2. set $i = 1$;
3. while $i \leq I$,
   - select at random the element type type among C and H: sample $U \sim \mathrm{Unif}(0, 1)$; if $U < 0.5$ then $\mathrm{type} = C$ else $\mathrm{type} = H$;
   - if $H_\tau > 1$ select a random the time step: $\tau \sim \mathrm{Unif}(\{1, \ldots, H_\tau\})$;
   - select at random one of the n^{type} object of network type: $J \sim \mathrm{Unif}(\{1, \ldots, n^{\mathrm{type}}\})$;
   - sample the new category for the selected element:

$$\tilde{x}_{J,\tau}^{\mathrm{type},(i)} \sim p\left(\tilde{x}_{J,\tau}^{\mathrm{type},(i)} | \boldsymbol{x}_{(-J)}^{\mathrm{type},(i)}\right)$$

     and denote the full configuration with the new category as $\tilde{\boldsymbol{x}}$;
   - increment $i \leftarrow i + 1$;
4. return the final configuration $\boldsymbol{x}^{(I)}$.

1.3. *Choice of burn-in period.* The landscape descriptors T_k are sufficient statistics in our models of *exponential family type* (Grelaud et al., 2009), i.e., they contain all the information on $\boldsymbol{\beta}$ that we can draw from an observation $\boldsymbol{x}$. Therefore, we can monitor the convergence of Markov chains to their stationary distribution by checking the m simulated series $T_k^{(j)}$, $k = 1, \ldots, m$, through trace plots, which further allows us to determine an appropriate burn-in period, and to analyze the mixing behavior of the Markov chains to fix the number $I - 1$ of intermediate states to be left out (see, e.g. Kiêu et al., 2013). In practice, we have found that the number of iterations needed for burn-in depends on the combination of size of the landscape and complexity of the model, and especially on the type of landscape descriptors involved. The running time necessary to simulate one landscape in one Markov chain for the examples discussed in this paper ranges from several seconds to several minutes.

For illustration, we here report trajectories of the landscape descriptors in a rather complex model for 50000 MCMC iterations with the small domain D1 in Figure 2, and for 1 million MCMC iterations with the large domain D3 in Figure 3, used to check the algorithm convergence.

2. Temporal landscape descriptor. In this section, we define the temporal landscape descriptor and give an example of temporal dynamics with configurations correlated over consecutive time steps, i.e., we evaluate temporal interactions. An example specification is:

$$T_{temp}^C(\boldsymbol{x}) = \sum_{i=1}^{n^C} \sum_{\tau=2}^{H_\tau} t(x_{i,\tau}^C, x_{i,\tau-1}^C). \tag{1}$$

Here, T_{temp}^C captures time dynamics for network C of crops over a horizon of H_τ discrete time steps.

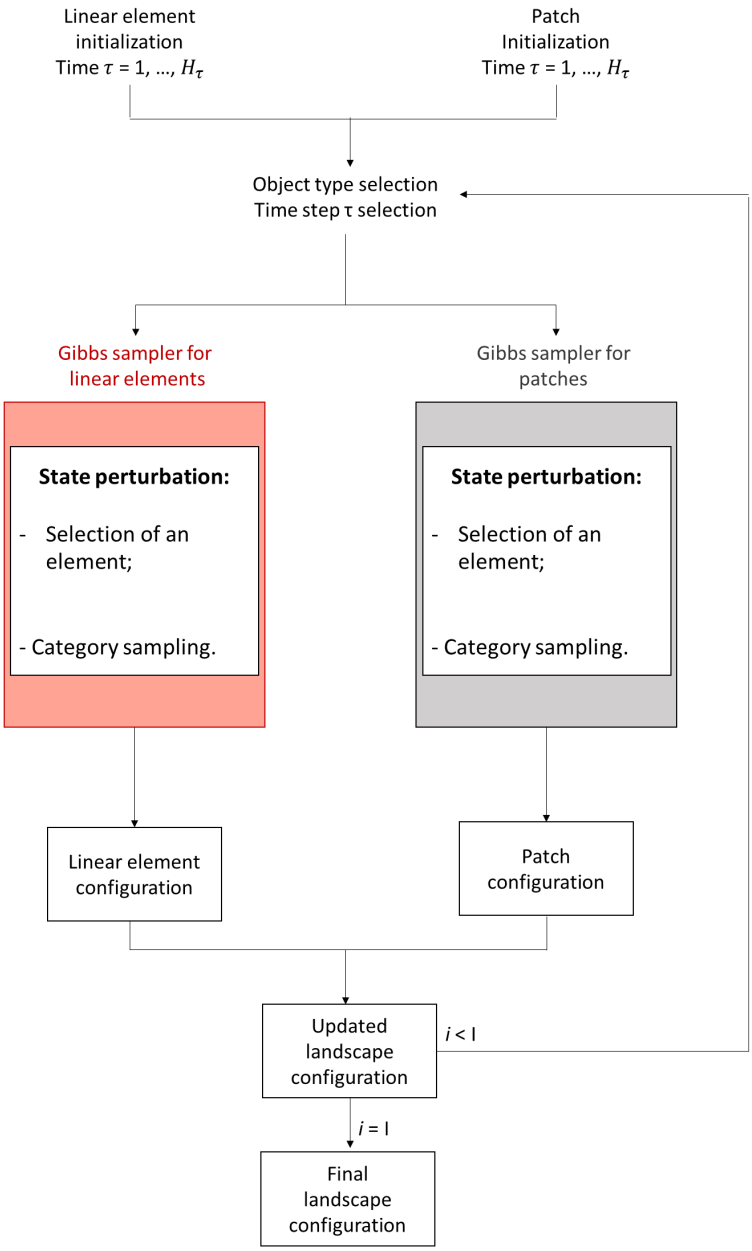

FIG 1. *Schematic representation of the Gibbs sampler. The index i indicatess the current iteration, I is the fixed number of iterations, τ is the current time, and H_τ is the time horizon.*

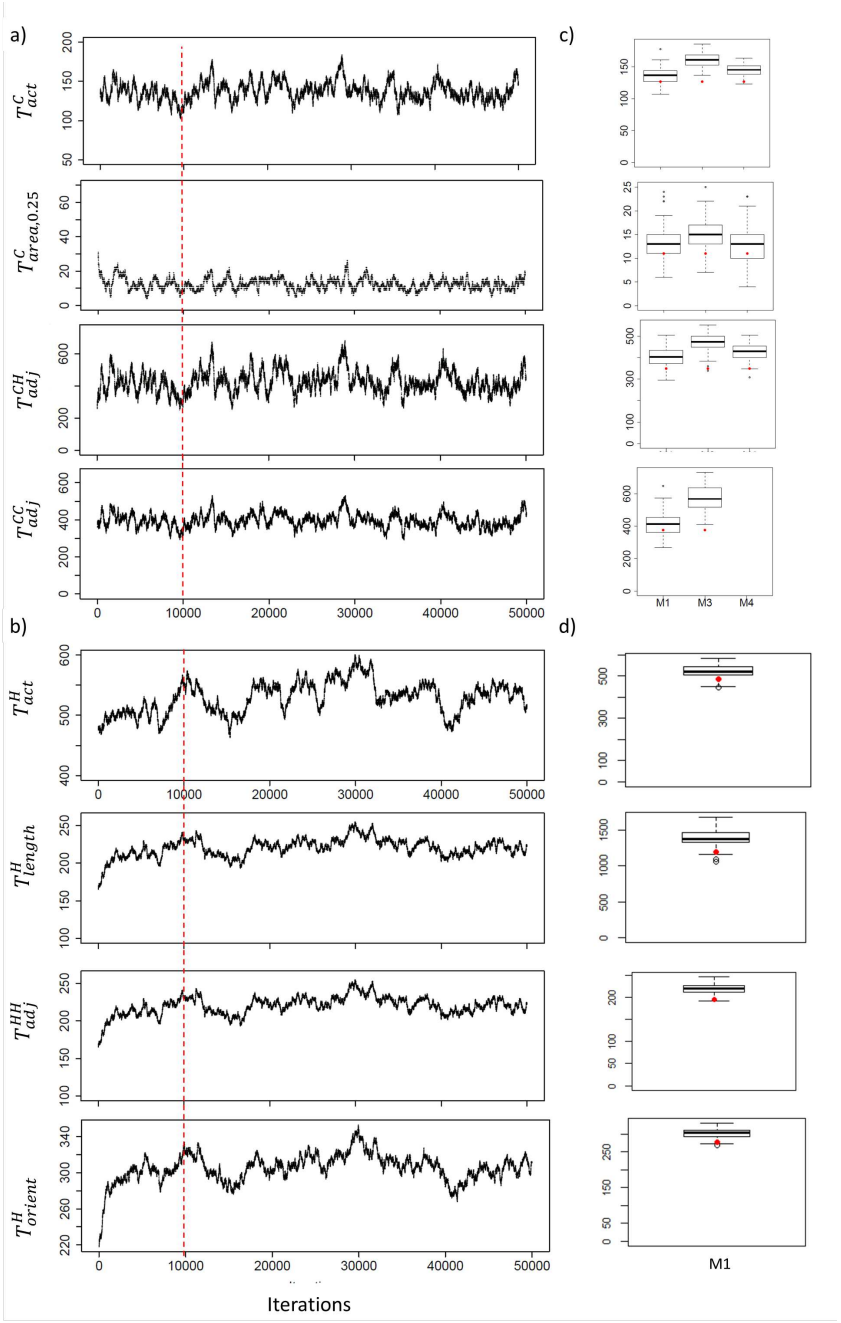

FIG 2. *MCMC simulation of a model for domain for D1. Convergence diagnostics in Panels a,b: trace plot examples for patch allocation with crop (a), and for linear segment allocation with hedges (b); the red dashed lines show the selected burn-in. Panels c, d: landscape descriptor values in domain D1 for 100 simulated landscapes (boxplots) and the real landscape (red dot) using models M1, M3 and M4 for crop and M1 for hedge; for patches (c) and linear elements (d). Descriptors in panels a,c from top to bottom: small crop area ($T^{C}_{\text{area},0.25}$), crop-hedge adjacency (T^{CH}_{adj}), crop-crop adjacency (T^{CC}_{adj}). Descriptors in panels b,d from top to bottom: long hedge allocation (T^{H}_{length}), hedge-hedge adjacency (T^{HH}_{adj}), allocation of horizontally oriented hedges (T^{H}_{orient}).*

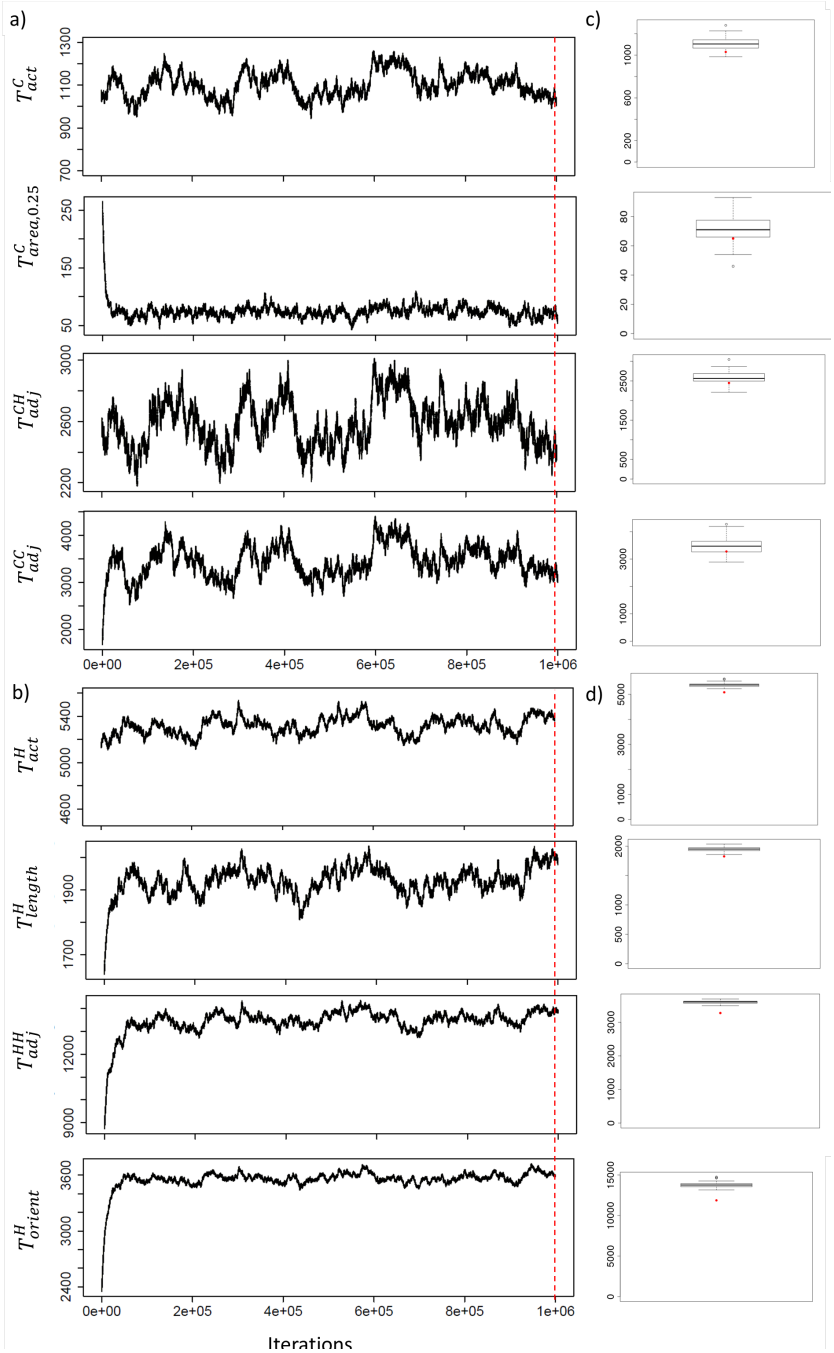

FIG 3. *Convergence diagnostic for D3 with model M1: trace plot for patch allocation with crop (a), linear segment allocation with hedges (b). The landscape descriptor values for the real landscape (red dot) and for the simulated ones (box plot) at the end of the iterations for patches (c) and linear elements (d). Panel a) and c) from top to bottom: small crop area ($T^C_{\text{area},0.25}$), crop-hedge adjacency (T^{CH}_{adj}), crop-crop adjacency (T^{CC}_{adj}). Descriptors in panels b,d from top to bottom: long hedge allocation (T^H_{length}), hedge-hedge adjacency (T^{HH}_{adj}), allocation of horizontally oriented hedges (T^H_{orient}).*

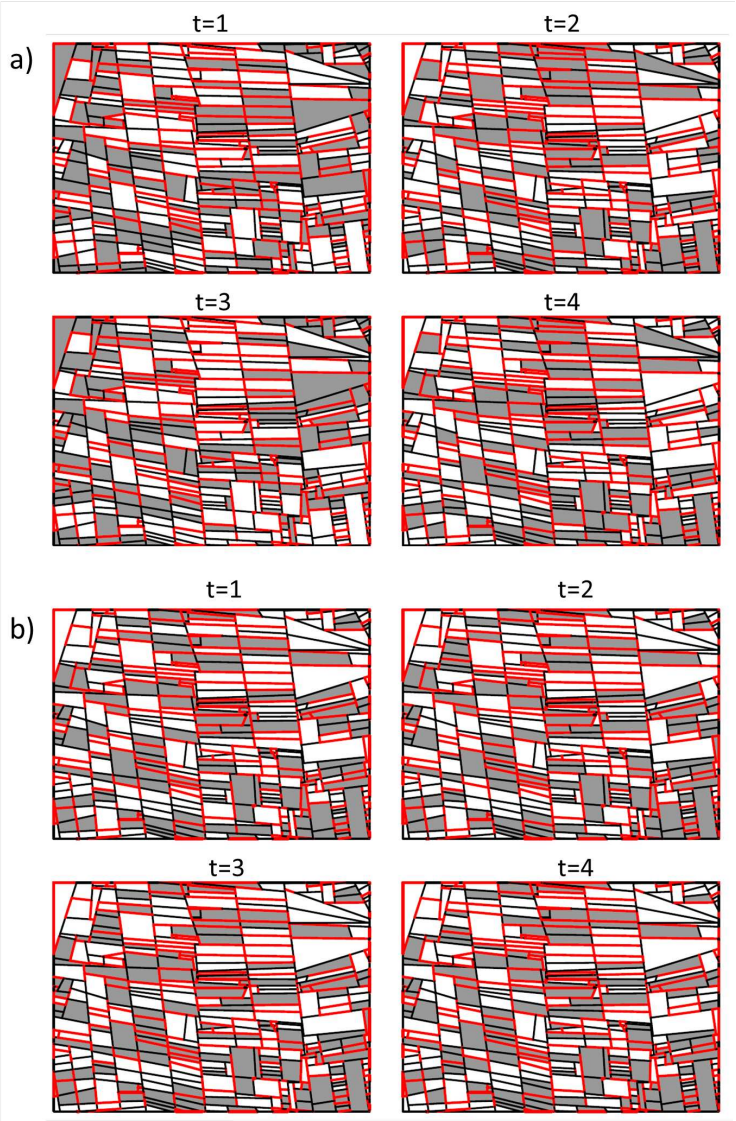

FIG 4. *Examples of crop rotation simulations with positive time correlation (Panel a) and negative time correlation (Panel b). Simulations are performed over four years. Gray boxes stand for crop ($x_i^C = 1$), white boxes stand for semi-natural habitat ($x_i^C = 0$). Red lines stand for hedges that are not influenced by rotation and are kept fixed.*

The specification of the temporal interaction among two objects of C aims to simulate crop rotation using 2 allocation categories (i.e., $x_i \in \{0, 1\}$) : *crop* ($x_i^C = 1$) or *natural habitat* ($x_i^C = 0$). Its formulation is given by:

$$t(x_{i,\tau}^C, x_{i,\tau-1}^C) = 1(x_{i,\tau-1}^C = x_{i,\tau}^C)$$

Simulation examples are presented in Figure 4.

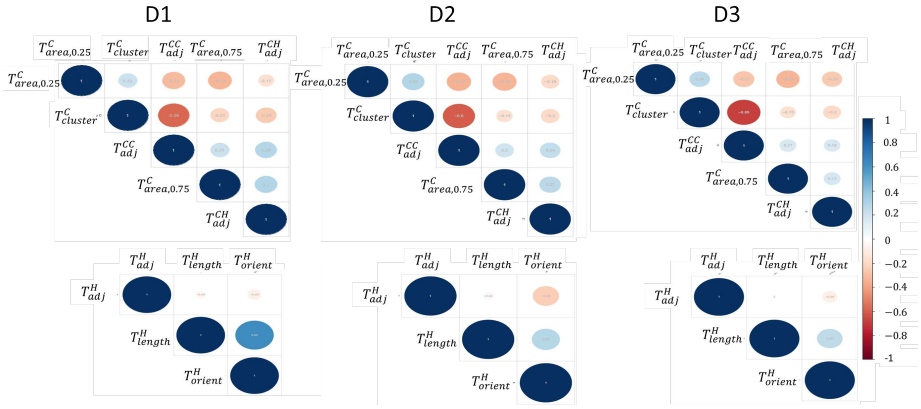

FIG 5. *Correlation of landscape descriptors for the spatial domains D1, D2, D3 for the crop network C (upper panel) and the hedge network H (lower panel).*

3. Landscape descriptor correlation. In order to avoid including strongly correlated landscape descriptors in a landscape model, we check the correlation among covariates arising in the logistic regression. In Figure 5 we display the correlation among all landscape descriptors for the three spatial domains.

4. Full results for variograms. To assess model diagnostics, we compute empirical variograms by transforming our landscapes in rasters. We contrast the variogram of the real landscape with the simulated ones. In Figure 6, variograms for each of the 3 spatial domains with model M1 are shown. They are discussed in the main text where we put focus on model comparison over the spatial domain D1.

5. Complete results for M1, M3 and M4 in the spatial domain D1. Here, we present all results of modelss M1, M3, M4 for the spatial domain D1. In Figure 7a, the boxplot of parameter estimate are shown for crop and hedge categories. In Figure 8, there is a focus on the crop category comparing estimated parameters for M1, M3 and M4. Specific values are reported and discussed in the main text in Table 4. For models M3 and M4, validation results related to network metrics are shown in Figure 9, while results for raster metrics are shown in Figure 10 and Figure 11 for M3 and M4, respectively. Lastly, in Figure 12 we show the variation of the residual standard deviation of model M1 to highlight the improvement achieved by the introduction of the large area landscape descriptor; more details are also provided in the main text.

6. Complete results for model M1 and all domains. In Figure 7 we report the boxplots for parameter estimates based on 100 simulations of the fitted model M1 for the three study domains.

6.1. *Model M1-D2.* The complete validation results for the network metrics in the study area D2 are reported in Figure 13. Figure 14 shows landscape metrics. Figure 17b illustrates the inter-connection metrics.

In Table 1, we report results for the Monte–Carlo pseudo p-values for network scale metrics and raster-based landscape metrics.

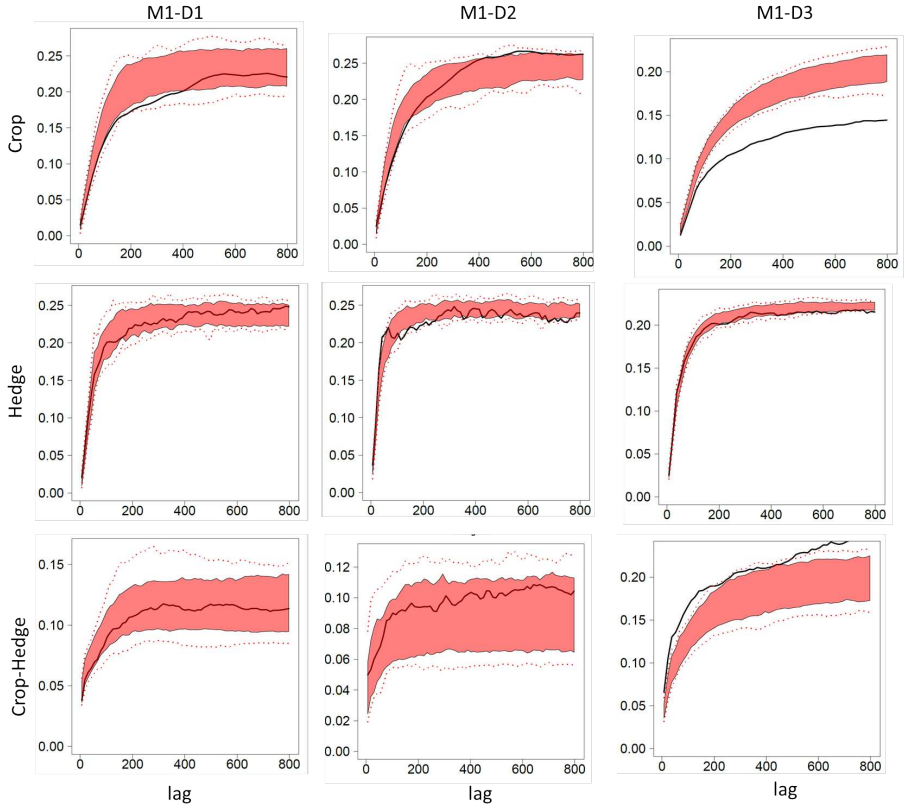

FIG 6. *Variograms for the* 3 *spatial domains D1, D2, D3.*

TABLE 1
Pseudo p-values obtained through the Monte–Carlo statistical test for the domain D2.

	Semi-natural	**Crop**	**Hedge**
Diameter	-	0.04	0.24
Efficiency	-	0.23	0.13
Cluster average	-	0.07	0
PLAND	0.09	0.10	0.11
PD	0	0.19	0.03
PARA_MN	0.04	0	0.12
ENN_MN	0.34	0	0.33
IJI	0.12	0.13	0.01
CLUMPY	0.13	0.21	0.03

6.2. *The model M1-D3.* The complete validation results for the network metrics in the study area D3 are reported in Figure 15. Figure 16 shows landscape metrics. Figure 17c illustrates the inter-connection metrics. The mean of the *Betweenness* distribution in the real landscape and in the simulations lies in the upper region of the boxplot, which is due to the presence of a small number of large outliers not shown in the boxplot.

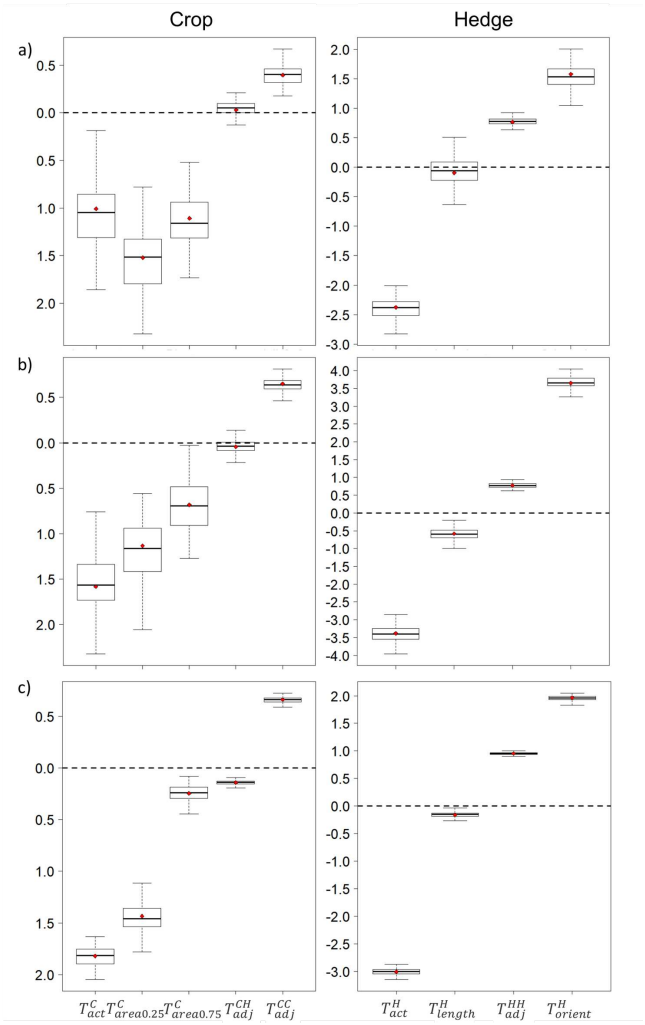

FIG 7. *Parameter estimation for study area D1 (Panel a), D2 (Panel b), D3 (Panel b) with model M1. Left: crop network; right: hedge network. Red dots represent the estimated value. Boxplots represent 100 simulations.*

In Table 2 we report results for the Monte–Carlo pseudo p-values for network-scale metrics and raster-based landscape metrics.

7. Pseudo-p-values for network metrics. The numbers in Table 3 report the proportion $p \in [0, 0.5]$ of the simulated metric values that are "more excentric" than the observed one; e.g., if the observed value is below the median and 26 among the 100 simulated values are even lower, we report 0.26. These *pseudo-p-values* imply that observed metrics for the crop network still appear realistic under the model. Overall, network-scale results indicate slightly stronger clustering of crop in the model as compared to reality, but still with similar order of magnitude for metric values. We also report pseudo-p-values for hedge network-scale metrics in Table 3, which show stronger discrepancy between observed and simulated values. Node-

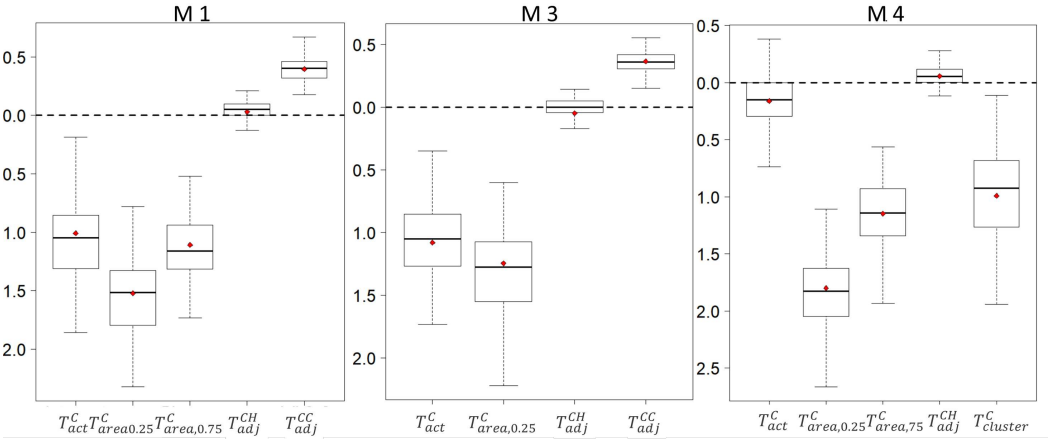

FIG 8. *Parameter estimation for the crop network in domain D1 with models M1, M3 and M4 (by columns). Red dots represent the estimated value. Boxplots represent 100 simulations.*

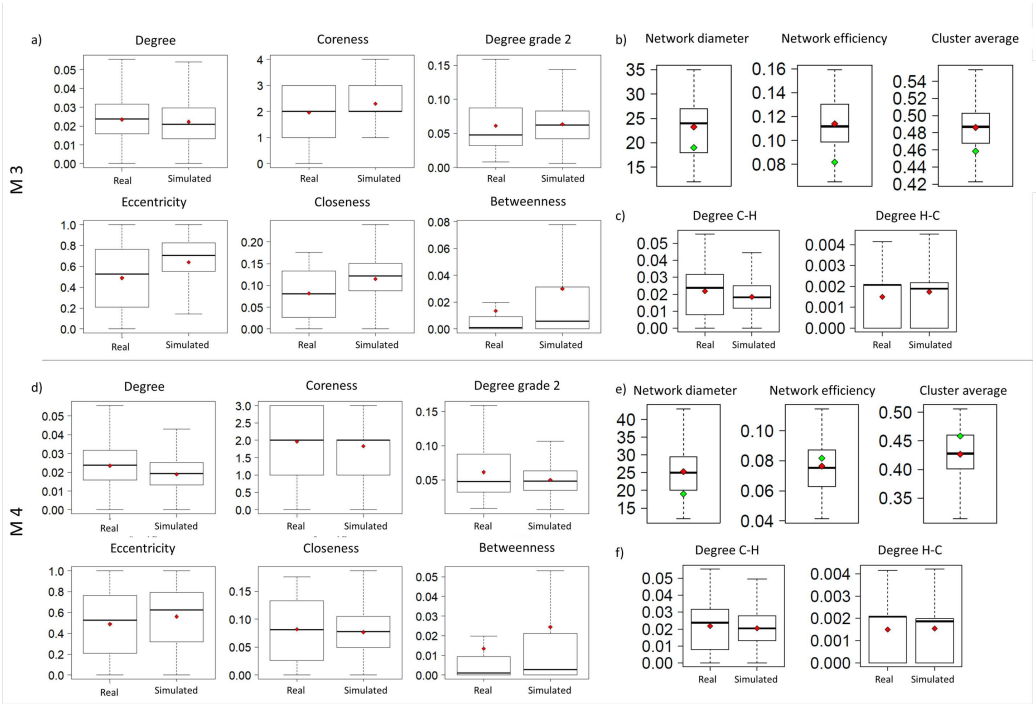

FIG 9. *Validation of crop network metrics in D1 with models M3 and M4 at node scale (panels a,d), at network scale (panels b,e) and for the degree among crop and hedges (panels c,f). In panels a,c,d,f, boxplots represent the distribution of the node metrics for the real landscape network (left boxplots) and the for the simulated landscapes (right boxplots). Red dots represent mean values of the node metric distribution of the real and simulated networks, resspectively. In panels b,e, boxplots represent distributions of the simulated landscapes; red dots represent mean values of the simulated landscapes; green dots represent the real landscape network values.*

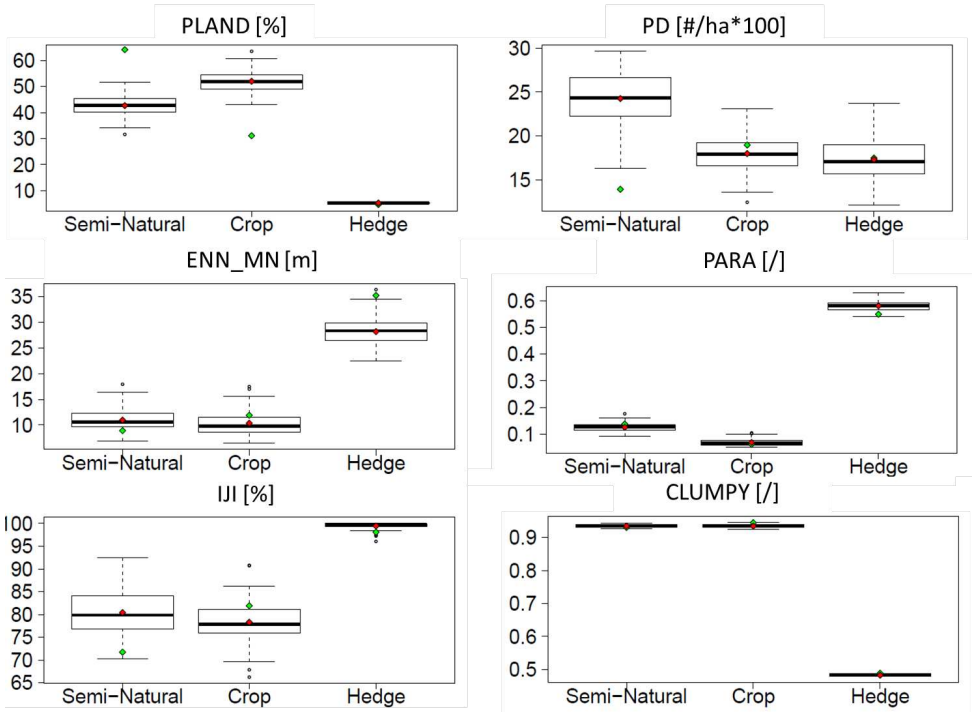

FIG 10. *Validation results for raster metrics in the domain D1 for model M3. Boxplots represent simulated landscapes transformed to raster format for the three habitats (i.e., semi-natural, crop, hedges). Red dots represent mean values of each habitat for simulated landscapes. Green dots represent values of each habitat for the real landscape.*

TABLE 2
Pseudo p-values obtained through the Monte–Carlo statistical test for the large domain D3.

	Semi-natural	**Crop**	**Hedge**
Diameter	-	0.30	0.15
Efficiency	-	0.35	0.15
Cluster average	-	0.34	0
PLAND	0	0	0
PD	0	0.01	0.41
PARA_MN	0	0	0
ENN_MN	0	0.01	0.16
IJI	0	0	0.05
CLUMPY	0.36	0	0

scale metrics for hedges, more directly controlled through the network descriptors included in our model, remain satisfying.

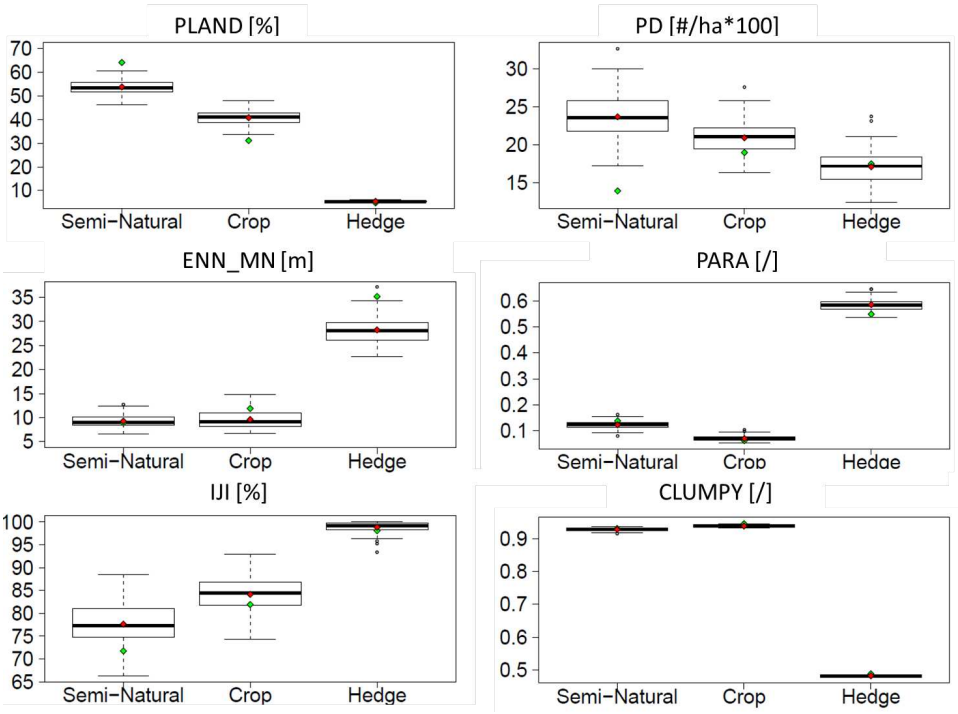

FIG 11. *Validation results for raster metrics in the domain D1 for model M4. Boxplots represent simulated landscapes transformed to raster format for the three habitat types (i.e., semi-natural, crop, hedges). Red dots represent mean values of each habitat for simulated landscapes. Green dots represent values of each habitat for the real landscape.*

TABLE 3
Pseudo-p-values of network-scale metrics and raster-based metrics for D1 and crop models M1, M3, M4.

	Semi-natural			**Crop**			**Hedge**
	M1	M3	M4	M1	M3	M4	M1
Diameter	-	-	-	0.57	0.26	0.15	0.19
Efficiency	-	-	-	0.56	0.06	0.38	0.23
Cluster average	-	-	-	0.16	0.13	0.28	0
PLAND	0.08	0	0	0.10	0	0	0
PD	0	0	0	0.44	0.26	0.19	0.37
PARA_MN	0.20	0.20	0.17	0.12	0.33	0.24	0.06
ENN_MN	0.49	0.11	0.43	0.30	0.24	0.14	0.01
IJI	0.45	0.02	0.09	0.47	0.19	0.28	0.47
CLUMPY	0.19	0.11	0.26	0.24	0.02	0.02	0

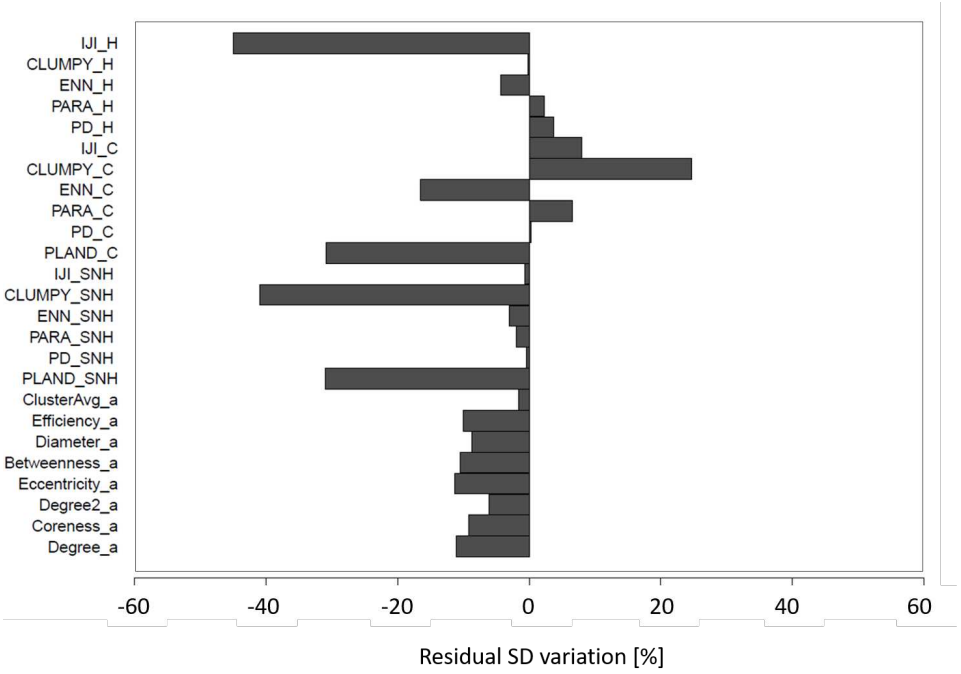

FIG 12. *Percentage variation of the residual standard deviation (SD) of model M1 in domain D1 with respect to model M3in domain D1. The letter a refers to the network patch network. Regarding raster metrics, SNH stands for Semi-natural habitat, C stands for Crop and H stands for hedges.*

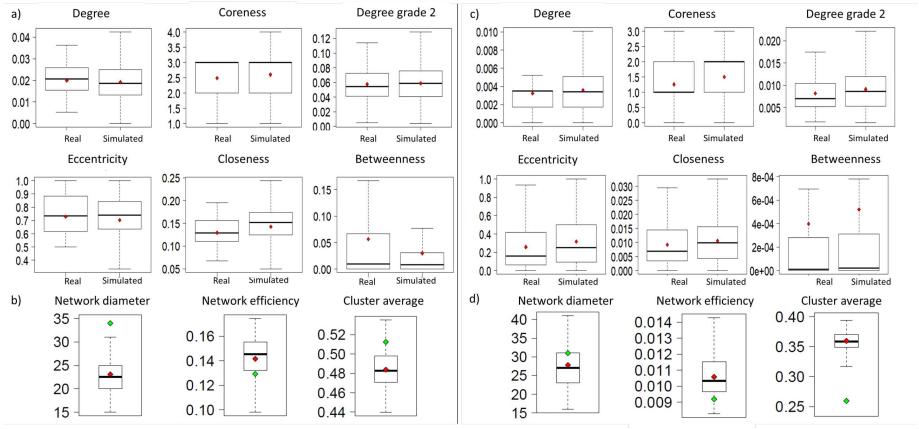

FIG 13. *Validation of network metrics for the domain D2. Validation at node scale (panels a,c), at network scale (panels b,d) for crop network (left) and hedge network (right), respectively. In panels a,c, boxplots represent distributions of node metrics for the real landscape network and for simulated landscapes. Red dots represent mean values of the node metric distribution of the real and simulated networks. In panels b,d, boxplots represent simulated landscapes. Red dots represent mean values of the simulated landscapes. Green dots represent the real landscape.*

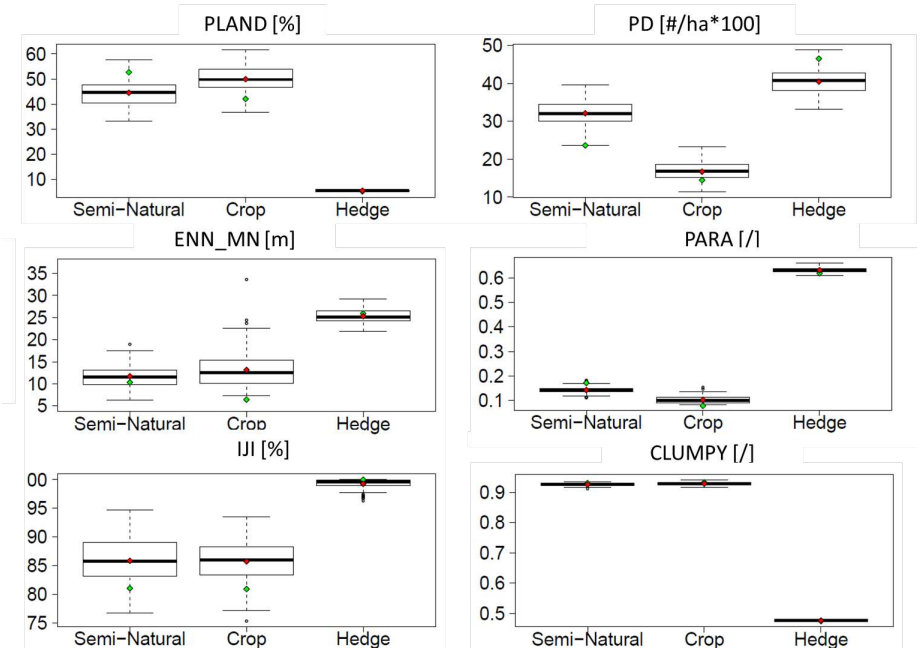

FIG 14. *Validation of raster metrics for the domain D2. Boxplots represent the simulated landscapes in raster format for the three habitat types (i.e., semi-natural, crop, hedge). Red dots represent mean values of each habitat for simulated landscapes. Green dots represent values of each habitat for the real landscape.*

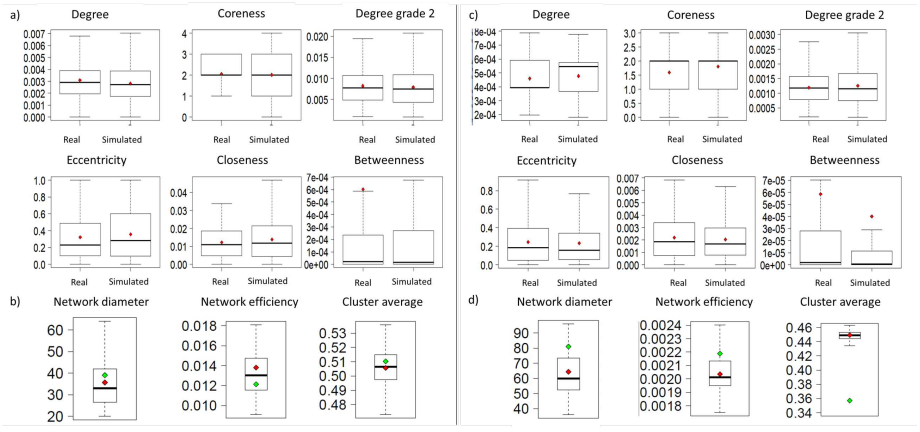

FIG 15. *Validation of network metrics for the domain D3. The description is the same as in Figure 13.*

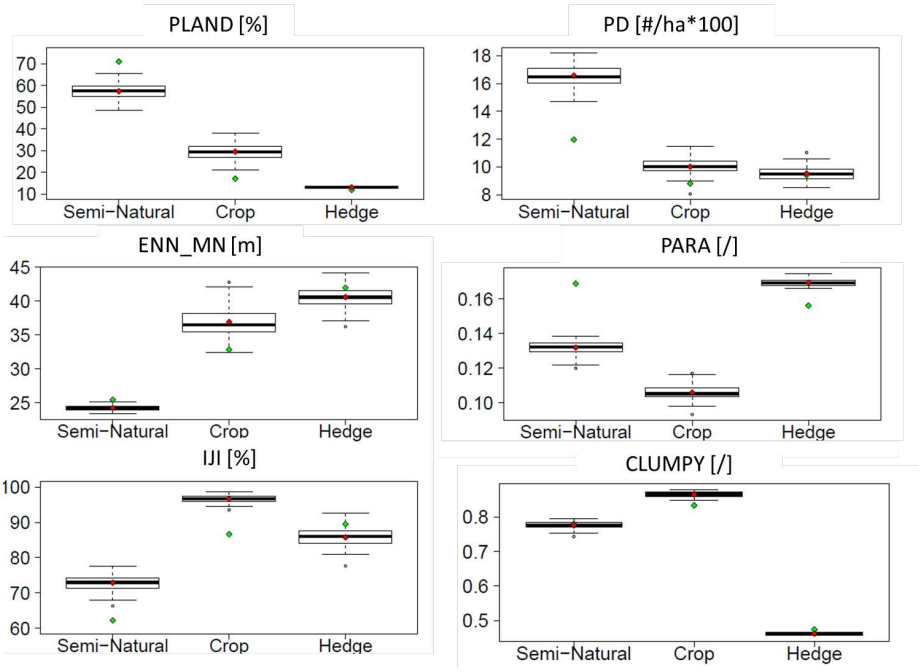

FIG 16. *Validation of landscape metrics for the domain D3. The description is the same as in Figure 14.*

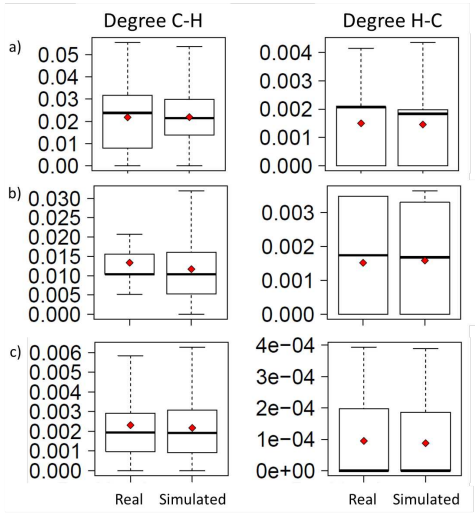

FIG 17. *Validation of network metrics for the three domains D1, D2 and D3 (panels a,b,c, respectively) related to inter-connections in the multi-layer network with model M1. In each display, boxplots show the distribution of the node metric for the real landscape (left boxplot) for the simulated landscapes (right boxplot) for the Crop-to-Hedge degree, which counts the number of links from crop patches to hedges (left column), and the Hedge-to-Crop degree, counting the number of links from hedges to crop patches (right column).*

REFERENCES

Casella, G. and George, E. I. (1992). Explaining the gibbs sampler. *The American Statistician*, 46(3):167–174.

Grelaud, A., Robert, C. P., Marin, J.-M., Rodolphe, F., Taly, J.-F., et al. (2009). ABC likelihood-free methods for model choice in Gibbs random fields. *Bayesian Analysis*, 4(2):317–335.

Kiêu, K., Adamczyk-Chauvat, K., Monod, H., and Stoica, R. S. (2013). A completely random T-tessellation model and Gibbsian extensions. *Spatial Statistics*, 6:118–138.

Supplement 2

,

S1 Supplementary Information of the paper: "More pests but less pesticide applications: ambivalent effect of landscape complexity on conservation biological control"

1. Description of the 2D/1D model for population dynamics in the landscape

Here, we detail the description of the dynamics of a species in a landscape defined as a 2D matrix crossed by 1D corridors, following the methodology developed in Roques & Bonnefon (2016). Here, we report some of the key information to understand the 2D/1D model for population dynamics for our analysis. More details can be found in the original paper Roques & Bonnefon (2016).

2D reaction-diffusion equations describe the dynamics in the matrix, and another set of 1D reaction-diffusion equations describe the dynamics in the corridors. The fluxes among the matrix and the corridors are described by coupling terms between the two sets of equations.

We consider a 2D matrix defined by a set $\Omega \subset R^2$, composed of finite mosaics i of polygonal disjoint 2D patches Ω_i separated by corridors (Fig 1). Patch boundary is denoted by $\delta\Omega_i$, each boundary consisting of a finite number of 1D edges λ_i^k . The edges can be classified as: interior edges (= the corridors), and exterior edges which belong to the boundary $\delta\Omega$ of Ω , for which no particular 1D dynamics are modelled. The population density is denoted by v_i in each patch Ω_i and by u_i^k in each corridor λ_i^k.

.

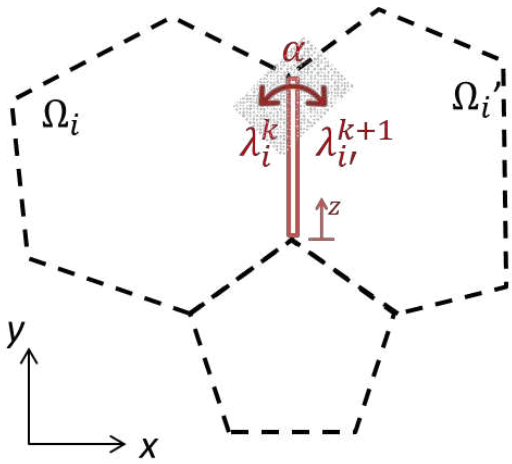

Fig. 1. Landscape representation. Patches $\boldsymbol{\Omega_i}$and edges $\boldsymbol{\lambda_i^k}$ at patch boundaries.

1.1 Dynamics in the 2D matrix

The population density is modelled by a reaction-diffusion equation:

$$\delta_t v_i = d\Delta v_i + f(v_i),$$

where d is the diffusion parameter that describes the mobility in the matrix 2D, and f is the growth function that describes the birth and death events in the patch Ω_i.

The exchanges among patch Ω_i and the surrounding corridors are described by the flux terms:

$$d\nabla v_i \, \boldsymbol{n} = \rho_{12} u_i^k(t,x,y) - \rho_{21} v_i \ (t,x,y),$$

where $\rho_{12} u_i^k(t,x,y)$ describes the flux of individuals leaving the corridor $\boldsymbol{\lambda_i^k}$ and entering the patch $\boldsymbol{\Omega_i}$ at time t and at the position (x,y), and $\rho_{21} v_i \ (t,x,y)$ describes the flux of individuals leaving the patch $\boldsymbol{\Omega_i}$ and entering the corridor $\boldsymbol{\lambda_i^k}$; finally, $\boldsymbol{n} = \boldsymbol{n}(\boldsymbol{x},\boldsymbol{y})$ denotes the outward unit normal to the boundary $\delta\Omega_i$. On the exterior boundary edges $\boldsymbol{\lambda_i^k} \in \delta\Omega_i$, standard reflecting boundary conditions are assumed: $d\nabla v_i \, \boldsymbol{n} = 0$. These boundary conditions mean that the individuals hitting the boundaries are reflected back inside the domain.

1.2 Dynamics in the corridors

Each corridor $\boldsymbol{\lambda_i^k}$ belongs to the common boundary of Ω_i and of another set, which is denoted by $\Omega_{i\prime}$, *i.e.*, $\boldsymbol{\lambda_i^k} = \boldsymbol{\lambda_{i\prime}^{k\prime}}$, where we model the 1D dynamics on each side of the corridor. The population densities in the corridor can be denoted by u_i^k and $u_{i\prime}^{k\prime}$ from the Ω_i and the $\Omega_{i,}$ sides, respectively, and we assumed that $u_i^k \neq u_{i\prime}^{k\prime}$, in general. The exchanges between the two sides of the corridor are taken into account through a permeability parameter $\alpha > 0$ (Fig. 1). To state the 1D equation for the dynamics in the corridors, we define an isometric transformation $z \rightarrow \big(x(z), y(z)\big)$, which maps any corridor $\boldsymbol{\lambda}$ into an interval $(0, L(\boldsymbol{\lambda}))$, where $L(\boldsymbol{\lambda})$ is the length of the corridor. Thus, the population density in the new coordinate $z \in L(\lambda)$ is defined by $\tilde{u}(t,z) = u(t,x,y)$. The population dynamics in each corridor $\boldsymbol{\lambda_i^k} = \boldsymbol{\lambda_{i\prime}^{k\prime}}$ separating two patches Ω_i and $\Omega_{i\prime}$ are described as follows:

$$\delta_t \tilde{u}_i^k = D\delta_{zz}\tilde{u}_i^k + \rho_{21} v_i \ \big(t, x(z), y(z)\big) - \rho_{12}\tilde{u}_i^k(t,z) - \alpha\tilde{u}_i^k(t,z) + \alpha\tilde{u}_{i\prime}^{k\prime}(t,z) + g\big(\tilde{u}_i^k\big),$$

$$t > 0, \qquad z \in \Big(0, L\big(\boldsymbol{\lambda_i^k}\big)\Big),$$

where g is the growth function in the corridor $\boldsymbol{\lambda_i^k}$; α is permeability parameter among the two side of the corridors, and D is the diffusion parameter on 1D corridor.

2. Predator and Pest dynamic

Here we show an example of the pest-predator dynamics resulting from the landscape configuration showed in Fig 2. Fig 3 illustrates snapshots for different time steps showing the pest and predator density in the whole landscape. Fig 4 shows temporal dynamics of pest and predator aggregated in space. In addition, we provide two video files of .gif type to show the whole spatio-temporal dynamics from the same simulation as in Figs 2,3,4 (See video in the supplement).

Fig. 2. Spatial configuration of crop (in grey) and hedges (in red).

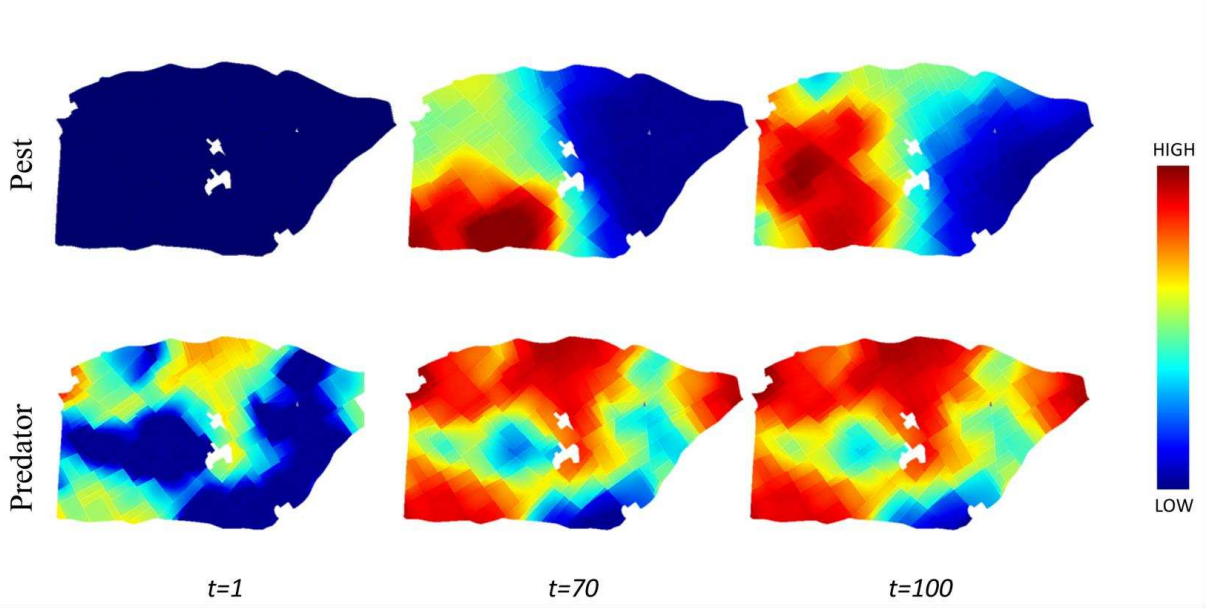

Fig. 3. Snapshots of pest and predator spatial dynamics. Simulation of predator-pest population dynamics at different time intervals *t={1, 70, 100}*. At the initial stage, the pest density (first line) is very low, followed by random introduction of pest. As time proceeds, the pest density increases (from left to right), and predator density (last line) also increases and diffuses to surrounding fields. At the final time step, high pest density arises where predators are absent. The temporal dynamic is shown in Fig 4.

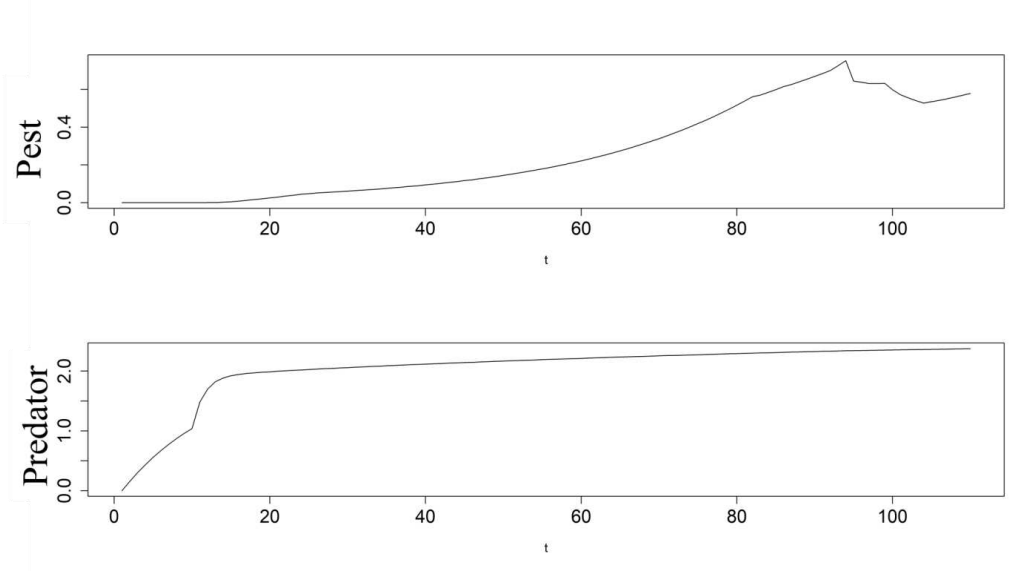

Fig. 4. Temporal dynamic of pest (first line) and predator (second line), aggregated over space.

3. Complete Sobol sensitivity analysis for predator and pest density and pesticide applications

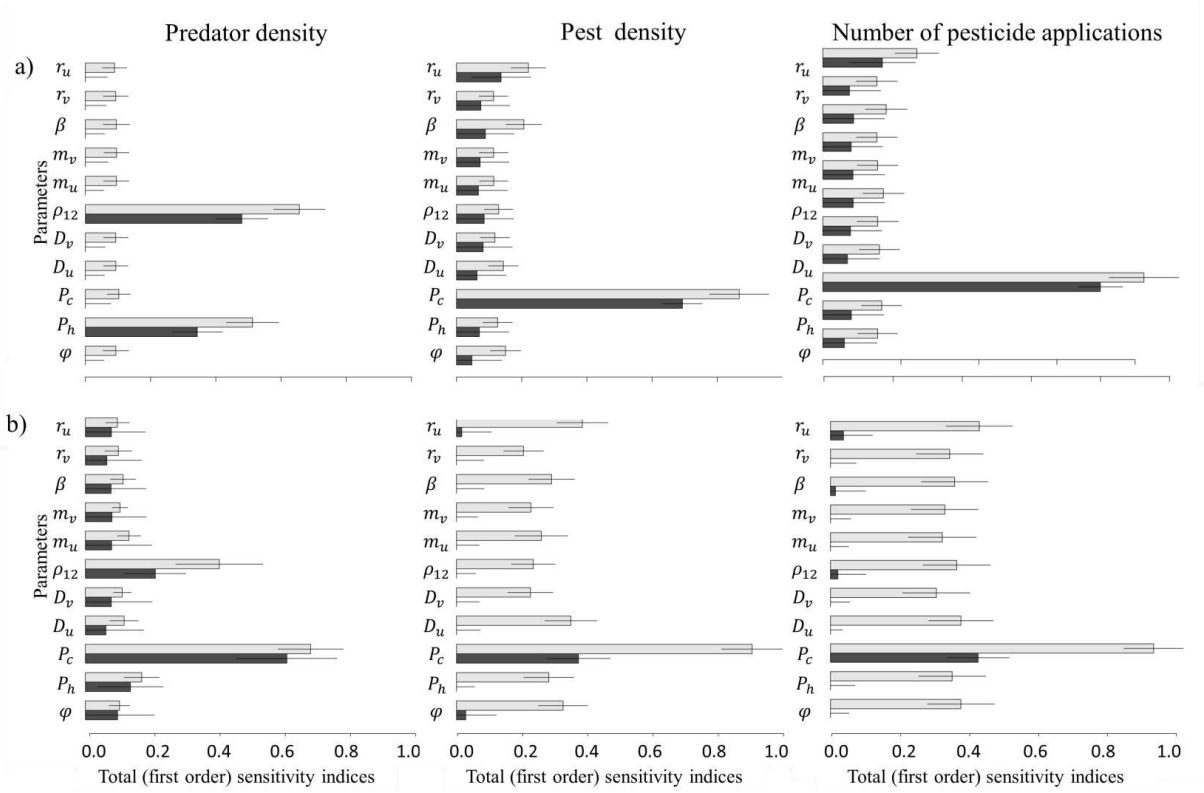

Fig. 5. Sobol sensitivity analysis. Total sensitivity indices (grey bar) and first-order sensitivity indices (black bar) of space-time averaged values for predator density, pest density and number of pesticide applications based on the mean (Panel a) or on the variance (Panel b) calculated over replicated simulations. The length of the bar indicates the mean of the sensitivity index, and the solid line indicates its 95% confidence interval.

3. Estimated effects of Generalized Linear Models (GLMs) for pest and predator densities, and for presence/absence and number of pesticide applications, and Generalized Linear Mixed-Effect Model for presence/absence and number of local pesticide applications.

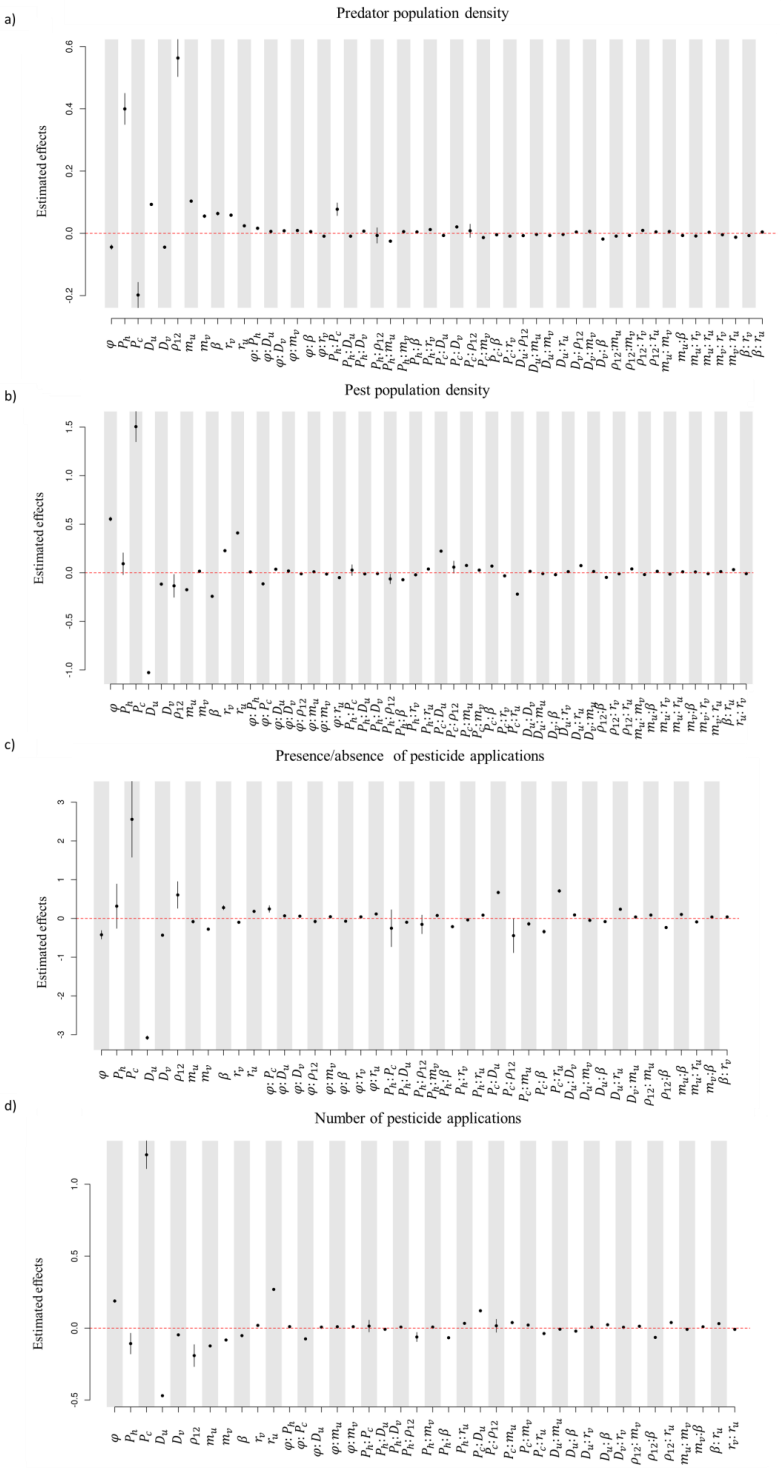
a)
Predator population density
Estimated effects
b)
Pest population density
Estimated effects
c)
Presence/absence of pesticide applications
Estimated effects
d)
Number of pesticide applications
Estimated effects

80

Fig. 6. GLM coefficient estimates. Effects of input parameters and their bivariate interactions on pest and predator population dynamics: Coefficient estimates (dots) and their confidence intervals (segments) for the parameters retained by the stepwise selection in the GLM for the predator density (a), the pest density (b), the presence/absence of pesticide applications (c) and the number of pesticide applications (d).

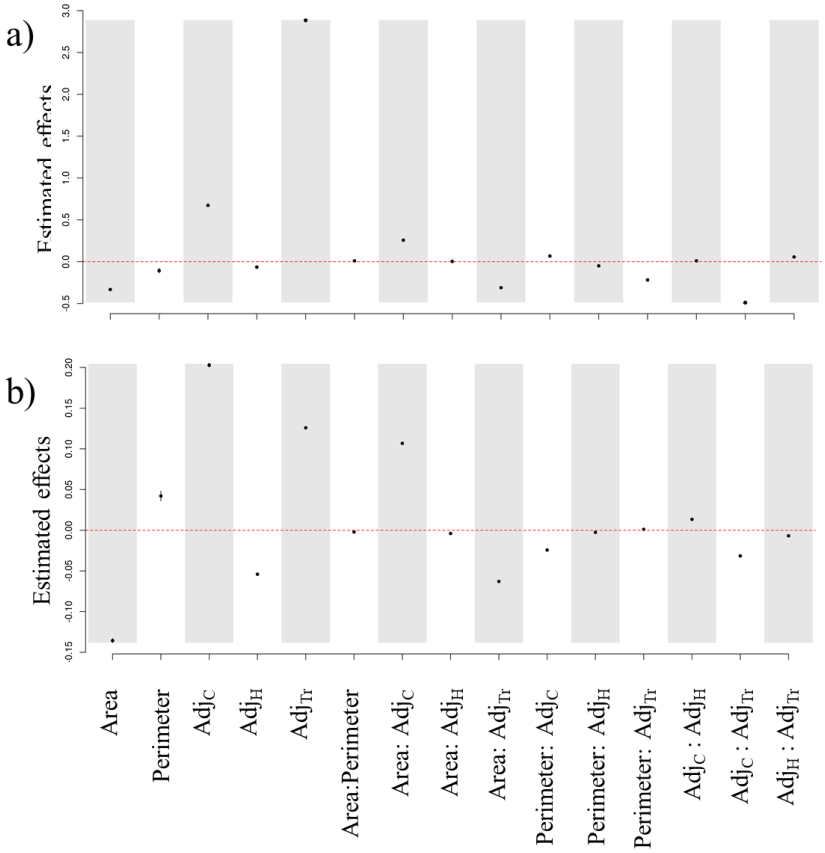

Fig. 7. Generalized Linear Mixed-Effect coefficient estimates. Estimated local effects (dots) and confidence intervals (segments) for the presence/absence of pesticide applications (a) and for the number of pesticide applications (b). The intercept values are not shown in this plot to better focus on the effects of the landscape covariables.

4.4 Sensitivity to pesticide application parameters

We test the sensitivity of our findings to pesticide applications when varying the pesticide efficacy and application threshold. We consider the following contrasted scenarios at landscape level:

- Scenario S1: a baseline scenario that considers an optimal pesticide efficacy (reduction of 99.5% of pest, $C_{it} = 0.1$ pests km^{-2} after application (See Table 2)) and a low application threshold (0.2 pests km^{-2});

- Scenario S2: sub-optimal pesticide efficacy (reduction of 70% of pest, $C_{it} = 6$ pests km^{-2} after application) and a low application threshold (0.2 pests km^{-2});

- Scenario S3: optimal pesticide efficacy (reduction of 99.5% of pest, $C_{it} = 0.1$ pests km^{-2} after application (See Table 2)) and a low application threshold (2 pests km^{-2}).

Scenario S1 depicts an ideal context for pesticide efficiency, while more realistic pesticide applications inflict about 70% mortality to pests (1,2). The pesticide application threshold controls the pesticide application frequency, which could be highly variable depending on the pest species and on the economic value of crops (3). Thus, a very low threshold generates a high pesticide application frequency, while a high threshold leads to more moderate pesticide utilisation.

We defined a smaller experimental setting where we vary only landscape parameters (aggregation (ϕ), crop proportion (Pc), hedge proportion (P_h)), and we perform a complete plan of 4 levels using the same ranges presented in Table 2 of the main text, with 15 repetitions each. We fixed population parameters (Table 2) to the median of the values considered in the main paper. For each scenario, we obtain 960 simulations.

To contrast the effects of these different scenarios on CBC, we applied GLMs considering the scenarios along with the landscape variables. Pest and predator densities, and pesticide application numbers (if different from 0), are analyzed as response variable by using the Gamma distribution with log-link function; presence/absence of pesticide applications during a simulation is analyzed using a GLM with binomial distribution. We use the same GLM formulas as those presented in the main text containing covariable interactions (see Table 2) up to 2nd order, and we also use a step-wise variable selection algorithm based on the Bayesian Information Criterion (BIC) in order to select the "best subset" of variables for each model.

Results are presented in Fig 8. In general, we observe that the directions of estimated effects are maintained across the scenarios, while the mean estimated effect has magnitude depending on the scenario. As expected, scenario S2 leads to an increase of pesticide applications, where covariates favoring pest outbreaks show a stronger effect than S1 (*e.g,* crop proportion for pest density (Fig. 8b) and presence/absence of pesticide applications (Fig. 8c)). Scenario S3 is expected to reduce the pesticide application frequency; therefore, for covariates favoring pest outbreaks, we observe that the estimated effect value is lower than S1 (*e.g,* spatial aggregation (ϕ) and crop proportion (Pc), for presence/absence of pesticide applications (Fig.8c)). Interestingly, S2 and S3 show remarkable effects provided by hedge proportion (Ph) for pest density: in S1, hedge proportion (Ph) is not significant, while in S2 and S3 hedge proportion (Ph) has a significant negative effect. Indeed, when pest reduction is lower due to low pesticide efficacy, or when pest reduction is slower due to an elevated pesticide application threshold on pest density, hedges may show a more relevant role in slowing down pest dynamics.

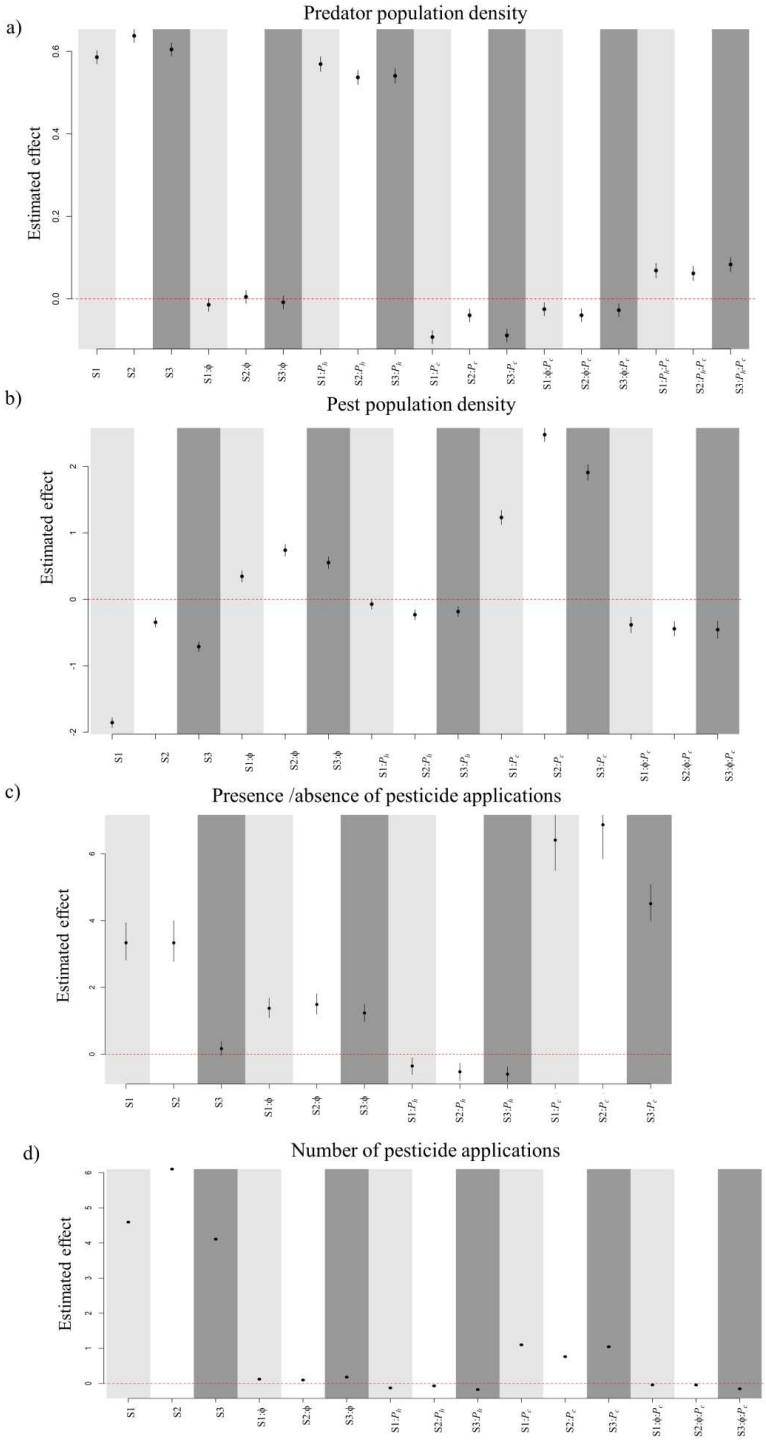
a)
Predator population density
Estimated effect
b)
Pest population density
Estimated effect
c)
Presence /absence of pesticide applications
Estimated effect
d)
Number of pesticide applications
Estimated effect

133

Fig. 8. GLM coefficient estimates for each scenario in the analysis of pesticide application sensitivity. Effects of input parameters and their bivariate interactions on pest and predator population dynamics: Coefficient estimates (dots) and their confidence intervals (segments) for the landscape parameters retained by the stepwise selection in the GLM, for the predator density (a), the pest density (b), the presence/absence of pesticide applications (c), and the number of pesticide applications (d). Scenarios S1, S2, S3 are indicated through different gray scales. All values are significant except for the following: *S1:* ϕ*, S2:* ϕ*, S3:* ϕ in a); *S1:*P_h in b).

Bibliography

1. Neil KA, Gaui SO, Mcrae KB. Control of the English grain aphid [Sitobion avenae (F.)] (Homoptera: Aphididae) and the oat-birdcherry aphid [Rhopalosiphum padi (L.)] (Homoptera: Aphididae) on winter cereals. Can Entomol. 1997;129(6):1079–91.
2. Abo El-Ghar GES, Abd AE. Impact of two synthetic pyrethroids and methomyl on management of the cabbage aphid, brevicoryne brassicae (L.) and its associated parasitoid, diaeretiella rapae (M'Intosh). Pestic Sci. 1989;25(1):35–41.
3. Bianchi FA, Ives AR, Schellhorn NA. Interactions between conventional and organic farming for biocontrol services across the landscape. Ecological Applications. 2013 Oct;23(7):1531-43.

Supplement 3

,

Supplementary material of: Spatio-temporal point processes as meta-models for population dynamics in heterogeneous landscapes

1 Exploratory spatio-temporal analysis

We give an example of the exploratory analysis of relevant behaviour and effects when we are close in both space and time to some reference or trigger event (*e.g.*, when studying what happens after an inoculation, or after a pest peak) and of relationships with the landscape structure. This analysis aims to highlight the importance of jointly considering the space and time dimensions in our analysis.

The spatio-temporal structure of pest peaks is explored by evaluating the pest peak occurrence intensity after a peak or after an inoculation. For each group of 15 repetitions of the 172,500 simulations, we select the first temporal pest peak or the first inoculation, and we then compute the spatial and temporal distances to all the other treatments later in time. Then, we use such distances as point in the xy plane and visualise the resulting cloud of points intensity. We run analyses where we either pull together all the simulations, or we run analysis on subsets of data by dividing them depending on key parameters. In Figure 1, we report the logarithm of the occurrence intensity of treatments with respect to the spatio-temporal distances among 1^{st}*peak-peaks* (Figure 1a) and 1^{st}*inoculation-peaks* (Figure 1b), where we consider the following data subsets: all the simulations together (first column); by splitting the simulations depending on the *% of crop* in the whole landscape (low and high in second and third columns, respectively); by splitting the simulations depending on *pest diffusion in crop* (low and high in forth and fifth columns, respectively).

The plots for 1^{st}*peak-peaks* allow us to assess how rapidly the pest dynamic is able to recover after the first peak and the associated application of a treatment within a patch to exceed again the treatment threshold at a later stage, which also involves the re-colonisation from the neighbouring patches (Figure 1a). When considering all the simulations, given a temporal distance, the peak intensity decreases moderately with short spatial distance and more rapidly as the spatial distance increases. On the other hand, given a spatial distance, there is a increasing trend of pest peak intensity until reaching a maximum value at a certain temporal distance, and then it decreases. The temporal range with high values is wider for shorter distances and shrinks as the spatial distance increases. In general, we observe a maximum intensity around the time step $t = 0.4$ at all spatial distances. This behaviour can be explained by the fact that pests need time to disperse and reach the threshold density above which the treatment is applied; and, at a short distance the pest threshold would be exceeded more quickly than at a longer distance. Given a temporal distance, pest density will be higher for shorter spatial distances. This behaviour changes when looking only at simulations with small % *of crop*, since pests have not a lot of space in their preferred habitat. Thus, they group in a small spatial range of suitable habitat. Consequently, the maximum intensity is reached at relatively short spatial and temporal distances. By contrast, for high *pest diffusion in crop*, we observe a larger temporal range at which the maximum pest peak intensity is observed, which is due to the fact that pests disperse rapidly, thus are able to spread in shorter time than on average for all simulations.

The plots for the 1^{st}*inoculation-peaks* analysis allow us to assess the capability of the pest population to develop and colonise the surrounding landscape (Figure 1b). For all the simulations, the maximum occurrence intensity of treatments depends mostly on the spatial distances with a decreasing trend at small to moderate spatial distances; therefore, the closer we are to the inoculation point, the more pest peaks above the treatment threshold will occur. More specifically for a small % *of crop*, the maximum occurrence intensity is always found for relatively small spatio-temporal distances, where for small temporal distances relatively high occurrence intensities persist over all spatial distances. This behaviour could be due to the fact that pests cannot disperse over larger surfaces and therefore may locally accumulate very fast. For high *pest diffusion in crop*, the trend is completely different; we note generally higher intensity values with respect

to the other cases, and the maximum intensity is realised for short spatial distances for all temporal distances. However, when the spatial distance increases and for short temporal distance, we observe relatively small pest peak occurrence intensities, due to the fact that pests spread quickly and may thus easily reach other habitats, which lowers the local pest density around the inoculation point and keeps it under the treatment threshold. At longer temporal distances, the pest propagation causes the threshold to be exceeded quite frequently.

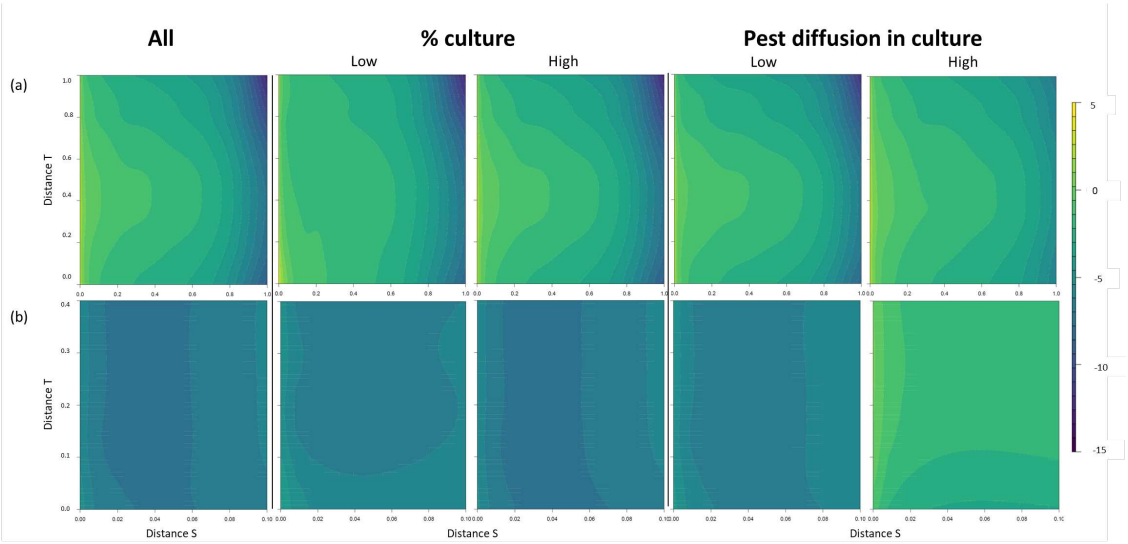

Figure 1: Spatio-temporal visualisation of pest peak occurrence intensity as a function of the spatial distance (x axis) and the temporal distance (y axis) with respect to the first pest peak in the simulation (Panel a) or with respect to the first inoculation in the simulation (Panel b); for all the simulations together (first column), or depending on low/high % *of crop* (second and third columns) and low/high *Pest diffusion in crop* (fourth and fifth columns). The colour bar displays the log-occurrence intensity.

2 Landscape model

We provide details about the landscape model, which was developed in Zamberletti et al. (2021). As fixed spatial support, we use an observed agricultural landscape and represent it through a vectorial approach by T-tessellation. It results in 188 polygons with a total of 577 edges. For simulating the spatial allocation of land-use categories in the T-tessellation, stationary Gaussian random fields (GRFs) are simulated in the landscape (with mean 0 and variance 1). We then fix a threshold on the values of the Gaussian field simulated at locations that represent the barycenter of a specific landscape element type (*e.g.*, polygons), and we allocate the landscape elements with one of two possible categories *e.g.*, crop, no crop) depending on the value of the GRF being below or above the threshold. The correlation parameters of the GRFs control the strength of spatial dependence, which, in turn, governs the clustering strength of landscape elements, such as surface elements and linear elements. The commonly used valid spatial correlation functions are restricted to nonnegative correlations, such that GRFs are useful to generate clustered or independent structures in space. It would be more difficult to obtain regular structures, *e.g.*, repulsive structures between neighboring elements. To simulate landscape configurations, GRFs are thresholded at a fixed quantile (*e.g.*, observed 70% quantile, where the probability level is one of the parameters of the model) to define presence (if above threshold) or absence (if below threshold) of crops or of hedges, respectively. For each type of elements of the landscape geometry (*i.e.*, , segments and polygons), a separate GRF is defined

to assign an land-use type controlling its spatial aggregation and proportion (*i.e.*, $W_1(s)$ and $W_2(s)$ for polygons and segments, with exponential correlation function given as $corr(s_1, s_2) = \exp(-\text{dist}(s_1, s_2)/\phi_i)$, $i = 1, 2$, respectively). Next, correlation between allocation of crop to patches and of hedges to edges can be generated by inducing correlation between their respective GRFs, here using the idea of a linear models of co-regionalization. Initially independent GRFs for landscape geometries can be linearly combined through correlation parameters (Equation 1, 2 and 3) to obtain the two dependent GRFs used to determine the final landscape configuration coupling surface and linear element allocation:

$$W_c(s) = \rho_c W_1(s) + \sqrt{1 - \rho_c^2} W_2(s) \tag{1}$$

$$W_h(s) = \rho_h W_1(s) + \sqrt{1 - \rho_h^2} W_2(s) \tag{2}$$

For a simpler and more parsimonious formulation, we fix $\rho_h = 1$ such that W_1 defines the GRF used for hedges, and we allow for $\rho_c \in [-1, 1]$ to control the correlation between W_h and W_c (Zamberletti et al., 2021). Moreover, we use the same spatial correlation range ϕ_1 in both of the initial fields. Then, the cross-correlation function between the GRFs for hedges and crops is as follows:

$$\text{Corr}(W_h(s_1), W_c(s_2)) = \rho_c \exp(-\text{dist}(s_1, s_2)/\phi_1) \tag{3}$$

Specifically, for correlation of hedges and crops at the same location x, we obtain $\text{Corr}(W_h(x), W_c(x)) = \rho_c$.

3 Population dynamics model

We report the population dynamics model to provide more details with respect to the narrative of the paper. The model is the same of Zamberletti et al. (2021). Population dynamics are described by a spatially explicit predator-pest model based on a system of partial differential equations. Our model is built on an earlier developed approach that considers both 2D diffusion on surface elements and 1D diffusion on linear elements (Roques and Bonnefon, 2016).

- Predator model structure:
  - 1D landscape elements:
    Linear 1D elements of the landscape matrix are denoted by h_i. A 1-dimensional reaction-diffusion model on linear elements is defined for the predator v_{h_i}:

$$\begin{cases} \partial_t v_{h_i} &= \partial_{xx} D_1^v v_{h_i} + r_v v_{h_i}(1 - \frac{v_{h_i}}{K_{h_i}}) & \text{if the edge } h_i \text{ carries a hedge,} \\ v_{h_i} &= 0 & \text{otherwise,} \end{cases} \tag{4}$$

    where D_1^v is the diffusion parameter of the predator along the hedges, r_v is the intrinsic growth rate of the predator, and K_{h_i} is the carrying capacity of the hedge i.
  - 2D landscape elements:
    Polygon-shaped 2D fields are denoted by Ω_i. The population density of predators v_{Ω_i} in each field is modelled by a reaction-diffusion equation with mobility parameter within field D_2, predation rate β, and mortality m:

$$\partial_t v_{\Omega_i} = \Delta D_2^v v_{\Omega_i} - m v_{\Omega_i} + \beta u_{\Omega_i} v_{\Omega_i}. \tag{5}$$

- Prey (i.e. pest) model structure:
  - 1D landscape elements:
    We make the assumption that edges do not host the pest u_{h_i}, and that they do not directly modify their population dynamics:

$$u_{h_i} = 0 \quad \text{for all } i. \tag{6}$$

– 2D landscape elements:
The pest u_{Ω_i} is assumed to live only in fields. In addition, the crop fields represent a source of pest, whereas the non-crop fields are a sink for the pest. In the absence of dispersal from fields hosting the crop, the pest population vanishes in fields hosting the non-crop type. A chemical treatment is applied to a given crop field when the pest population in that field reaches a given threshold. The bidimensional reaction-diffusion model is defined as follows:

$$\begin{cases} \partial_t u_{\Omega_i} &= \Delta D^v_{u_{\Omega_i}} u_{\Omega_i} + r_{u_{\Omega_i}}(1 - \frac{u_{\Omega_i}}{C_{it}}) - \beta u_{\Omega_i} v_{\Omega_i} & \text{for crop,} \\ \partial_t u_{\Omega_i} &= \Delta D^v_{u_{\Omega_i}} u_{\Omega_i} - m_{u_{\Omega_i}} - \beta u_{\Omega_i} v_{\Omega_i} & \text{for semi-natural,} \end{cases} \tag{7}$$

where the carrying capacity C_{it} of the field i can change in time due to chemical treatments: $C_{it} = K_{\Omega_i}$, if no chemical treatment is applied, and $C_{it} = \frac{200}{K_{\Omega_i}}$ for short period of time after the chemical treatment is applied.

The dynamics described by equations 4 to 7 are coupled to define predator-pest dynamics over landscapes. Moreover, the fluxes of individuals between 1D and 2D elements of the landscape are defined as follow:

- Edges (with or without a hedge) do not affect the pest population dynamics, *i.e.*, the pest perceives the landscape as a heterogeneous 2D environment without 1D effects of linear elements.
- Edges without a hedge do not affect the predator population dynamics, *i.e.*, two fields separated by an edge but without a hedge will be perceived as a unique (potentially heterogeneous) 2D element by the predator.
- The predator is attracted by hedges, thus migration from fields to hedges is relatively high.
- The predator could potentially have an aversion to move outside its natural habitat; therefore, migration from hedges to fields is always lower than migration from fields to hedges. Finally, we considered reflecting conditions on the boundaries of the landscape, meaning that in- and out-fluxes between the landscape and its surrounding environment are equal.

Dynamics among 1D and 2D elements are fully presented in (Roques and Bonnefon, 2016). The parameter that controls the predator movement between linear elements and fields is ρ_{12}. All the parameters of predator and pest dynamics are shown in Table 1.

Table 1: Parameters of the population dynamics model.

Parameters	Description	Range	Units
For landscape model			
ϕ	Aggregation of hedges and crops	$[5.55 \times 10^{-2} - 5.55]$	-
P_c	Proportion of crops	$[0 - 1]$	-
P_h	Proportion of hedges	$[0 - 1]$	-
ρ	Correlation between crops and hedges GRFs	0.5	-
Parameters for population dynamic model			
D_2^v	2D predator diffusion rate	$[0.0625 - 12]$	$km^2 d^{-1}$
m_v	Predator mortality rate	$[5 - 15]$	d^{-1}
β	Predation rate	$[1 - 10]$	d^{-1}
ρ_{21}	Predator migration rate from fields to hedges	5	-
D_1^1	1D predator diffusion rate	12	$km^2 d^{-1}$
r_v	Predator intrinsic growth rate	$[10 - 20]$	d^{-1}
K_{h_i}	Predator carrying capacity in hedge	1	-
ρ_{12}	Predator migration rate from hedge to field	$[0 - 5]$	-
D_2^u	2D pest diffusion rate	$[0.0625 - 12]$	$km^2 d^{-1}$
r_u	Pest intrinsic growth rate	$[10 - 20]$	d^{-1}
C_{it}	Pest carrying capacity in crop fields	$C_{it} = \begin{cases} 20 & \text{no treatment} \\ 0.1 & \text{after the treatment} \end{cases}$	-
m_u	Pest mortality rate	$[5 - 15]$	d^{-1}

4 Landscape discretisation for regression models

The spatial domain is discretised into small cells, different from the field polygons, and we assume a homogeneous point process intensity within each cell during each interval of time. Each combination of a spatial cell and a time unit represents a subset A as landscape elementary unit, where we count the events occurring within it and evaluate additional information (*i.e.*, spatio-temporal covariates) associated to each cell. The discretisation is achieved through a triangulation mesh of space, whose construction puts focus on the influence of landscape structure on pest-predator dynamics. We take into account the patch structure of the landscape by differentiating between three types of cells: cells where exactly two patches are adjacent (located around the patch edge midpoints, with half of the edge length contained within the cell, representing movement corridors between exactly two neighbouring patches), cells where three patches are adjacent (around the vertices of the T-tessellation, containing 1/4 of each of the neigbhouring edge lengths, representing movement corridors around hubs where more than 2 patches come together), and cells at the center of each patch (representing areas that are separated away from edges and hedges, representing the patch inner core). This kind of discretisation allows us to focus on the influence of linear landscape elements represented by patch boundaries where hedges could be allocated, and we assume that the intensity function of the space-time point process is homogeneous within each cell for a given time step. Due to the reflecting boundary conditions of the population dynamics model, we observed a relatively large number of pest density peaks occurring at the boundaries of the study region, and we decided to remove all the boundary cells from the analysis to avoid an overly high influence of the boundary behaviour on the CBC analysis.

5 Predictor variables for pest dynamics

We evaluate spatio-temporal, spatial and population trait covariates for each cell of the mesh to relate the spatio-temporal event patterns, landscape structure and population dynamics. The full list of covariates is summarised in Table 2. Spatio-temporal covariates (STC) refer to the number of pest peaks, treatments and introductions that have occurred in previous time steps in the same cell or in neighbouring cells. This allows identifying spatio-temporal dynamics driven by preceding events at local scale. For example, we consider the number of treatments in each cell occurring at the previous time step to characterise recent spatio-temporal dynamics. We also evaluate the number of cumulated events up to two time steps before the present one to assess the influence of the cell's full local temporal dynamics in the past. Spatial covariates (SC) refer to geometrical features of the landscape patch tessellation and the land use allocation to evaluate the effect of the configuration and composition of the landscape. For example, to evaluate landscape configuration properties, we consider a three-level categorical variable to indicate if the cell connects exactly two, or more than two patches, to assess its spatial position that could be important to assess fluxes among patches. We evaluate the landscape composition at local scale through a variable measuring the percentage of crop and hedge within a buffer centered on the centroid of each cell, and at global scale through a variable measuring the percentage of crop and hedge in the whole landscape. This enables an assessment of how the crop extent and the hedge network may locally and globally influence the population dynamics leading to the number of events within each cell. Specifically, since the buffer aims to characterise variables at local scale, the buffer diameter is adapted to pest growth rate $Rprey$ and dispersal $Dprey$, which determine the spreading speed of the population. The spreading speed can be evaluated as $v = 2\sqrt{Rprey * Dprey}$. Then, the travelled space (*i.e.*, the front of the population) is computed by the classical formulation $s = v \times t$, where s is the travelled space, identifying the front position, and t is the time, set equal to 0.01, as in the population dynamics model. Among all the possible simulated configurations of $Rprey$ and $Dprey$, resulting in highly different buffer sizes s, we group configurations in three classes defined by the $10\%-, 50\%-, 90\%-$percentile of the population front s. Then, the buffer diameter size is set equal to the population front s used as an approximation of the local range where the population could move during a time step starting from the center of a cell. The three resulting buffers have a diameter equal to 0.09, 0.19 and 0.26 Km for the $10\%-, 50\%-, 90\%-$percentile of s, respectively. To each pair of $Rprey$ and $Dprey$ is assigned the corresponding buffer, where we then calculate covariates of crop and hedge proportion. For population dynamics covariates (PDC), we select variables related to individual mobility, such as species dispersal in fields and spillover from hedge to fields. We select these species trait variables as they are directly related to the species' capability to move within the landscape.

Table 2: List of covariates of regression models.

Ref. ID	Covariate name	Spatial reference	Range	Unit	Description
Spatio-temporal (*STC*)					
1	tr_patch($t-1$)	patch	0-40	-	No. of treatments in the patch at $t-1$
2	tr_patch_cum($t-2$)	patch	0-97	-	No. of treatments in the patch cumulated up to $t-2$
3	tr_Nb.patch($t-1$)	patch	0-337	-	No. of treatments in neighbor patches at $t-1$
4	tr_Nb.patch_cum($t-2$)	patch	0-861	-	No. of treatments in neighbor patches cumulated up to $t-2$
5	pk_cell($t-1$)	cell	0-15	-	No. of pest density peaks at $t-1$
6	pk_cell_cum($t-2$)	cell	0-36	-	No. of pest density peaks cumulated up to $t-2$
7	pk_Nb.cell($t-1$)	cell	0-45	-	No. of pest density peaks in neighbor cells at $t-1$
8	pk_Nb.cell_cum($t-2$)	cell	0-97	-	No. of pest density peaks in neighbor cells cumulated up to $t-2$
9	int_cell($t-1$)	cell	0-30	-	No. of pest introduction in cell at $t-1$
10	int_cell_cum($t-2$)	cell	0-30	-	No. of pest introduction in cell cumulated up to $t-2$
11	int_Nb.cell($t-1$)	cell	0-30	-	No. of pest introduction in neighbor cells at $t-1$
12	int_Nb.cell_cum($t-2$)	cell	0-39	-	No. of pest introduction in neighbor cells cumulated up $t-2$
Spatial (*SC*)					
13	Area	cell	0-0.069	km^2	Cell dimension
14	cell_2patch	cell	0-1	-	Binary, it is = 1 if the cell is among 2 patches, 0 otherwise
15	cell_3patch	cell	0-1	-	Binary, it is = 1 if the cell is among 3 or more patches, 0 otherwise
16	%H_Buffer	buffer	0-1	%	Percentage of hedges within the buffer centered in the cell
17	%C_Buffer	buffer	0-1	%	Percentage of crops within the buffer centered in the cell
18	Aggr	landscape	0-5.54	-	Landscape crop and hedge aggregation
19	%C_Land	landscape	0-1	%	Landscape crop proportion
20	%H_Land	landscape	0-1	%	Landscape hedge proportion
Population dynamics (*PDC*)					
21	Dprey	landscape	0.06-12	km^2d^{-1}	Pest diffusion in crop patch
22	Dpred	landscape	0.07-12	km^2d^{-1}	Predator diffusion in crop patch
23	D12pred	landscape	0.1-1		Predator diffusion from hedge to crop

6 Correlation analysis of covariates

We assessed the correlations among the selected covariates defined for each cell of the domain and for each time step Figure 2. The main positive correlations arise for the covariate % of culture and % of hedge within the buffer, and the corresponding % of culture and hedge in the whole landscape, respectively. Other strong positive correlations are shown by the covariate evaluating the number of peaks and treatments at the previous time step or cumulated up to $(t-2)$ in the same cell or in the neighbouring ones. This highlights that locations favourable to high pest density will always experience pest outbreaks even after treatments.

7 Residual analysis of regression models

A residual analysis is performed to evaluate if the predicted values obtained by the GLMs are homogeneously distributed in tspace and time for the models of intensity peak occurrence and of peak value of pest density. Residuals are computed as the difference among the predicted values and the observed spatially explicit population model outcomes.

We analyse the residuals to check the residual homogeneity over space and the time (Figures 3, 4 and 5). We can conclude that the models defined for pest peak number and value are able to capture the variability of observed data (*i.e.*, population dynamic model outputs) in time and space (Figures 3) without any systematic biases. We can recognise the already discussed spatial trend depending on cell position: the first 200 cells are cells intersecting 3 patches, the cells among 200 and 600 are center cells. As to the model for peak number, higher intensity takes place in cells located over patch boundaries, while in the model for pest peak density value higher values take place in center cells. The temporal dynamics are very well captured and show a slow increasing trend for pest outbreak occurrence up to a maximum value at last time step, and a fast and drastic increasing trend for pest density values with respect to time. In Figure 4 and 5 a) and d), we can see that the residuals are relatively small and almost homogeneously distributed for both models in space (a) and time (d). This can be also verified in the map of the spatial domain discretised in cells where we visualise the error within each cell. Here, we remark that for the model of peak numbers, larger errors occur in cells intersecting 2 or more patches, where the intensity of occurrence is slightly overestimated. By contrast, in the model of peak valuse, larger errors occur in the relatively large cells centred in patches, where the pest density concentration tends to be slightly underestimated. In Figure 4 and 5 e), we report

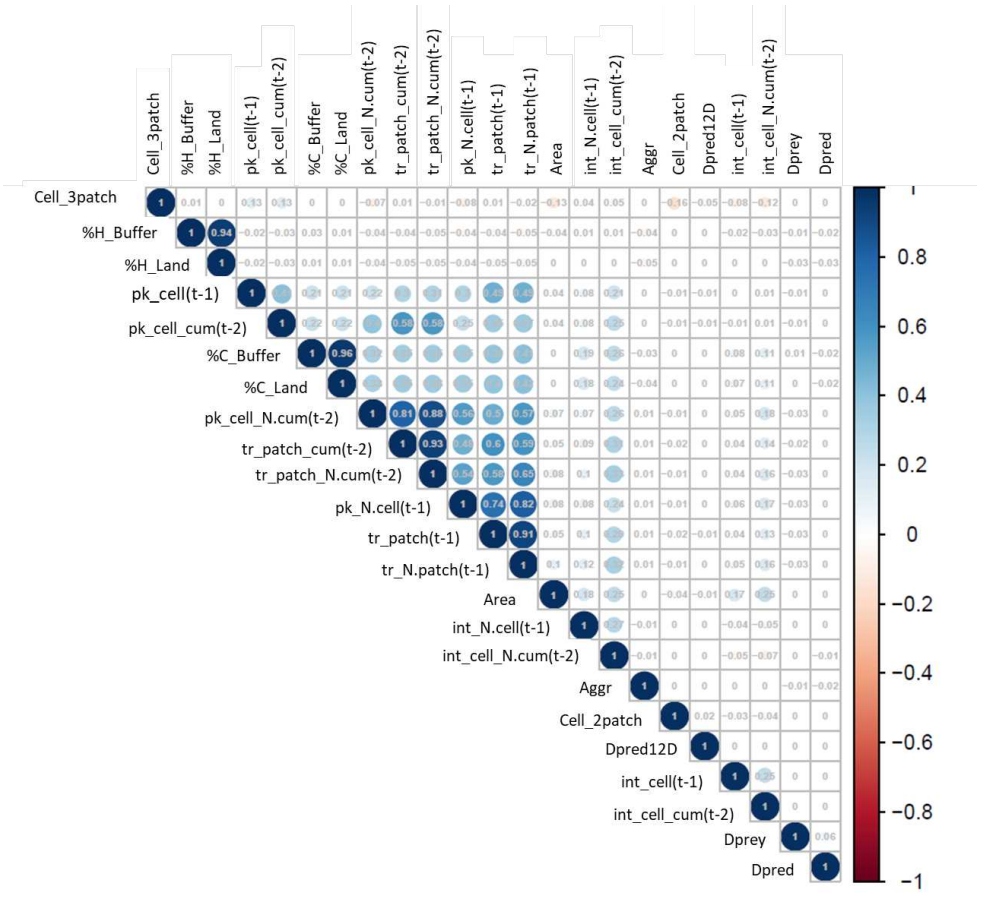

Figure 2: Empirical Pearson correlations among covariates selected for the occurrence intensity of pest density peaks and for the model for the peak value of the pest density.

the same plot as in Figures 3a but for each time step, in order to verify that also the dynamical behaviour is well captured for each time step, and not only on the temporal average. Lastly, the spatial variograms of residuals, 4 and 5 panels c), confirm that there is the same variability among cells over the distance, *i.e.*, there is no spatial structure left in the residuals.

Finally, we show the estimated temporal effect (*i.e.*, the intercept specific to each time interval) in the regression models for the occurrence intensity of pest density peaks (Figure 6a) and for the peak value of pest density (Figure 6b). We had introduced this temporal effect in order to better take into account and explain the temporal dynamics of the population, which were not fully explained by the other covariates. As for the occurrence intensity of pest density peaks (Figure 6a), the time-varying intercept is positive and it increases with time up to a constant value. This reflects that the number of pest outbreaks increases through time as the pest population grows and colonises the spatial domain. As for the peak value of pest density (Figure 6b), the time-varying intercept is negative and shows a relatively weak amplitude. It decreases with time, such that the maximum value of pest outbreaks occurs in the first time steps, probably when clusters of pest concentration arise that are not well homogenised over the spatial domain. Afterwards, when the pest population expands, there is a dilution effect that leads to a decrease in pest density peak values.

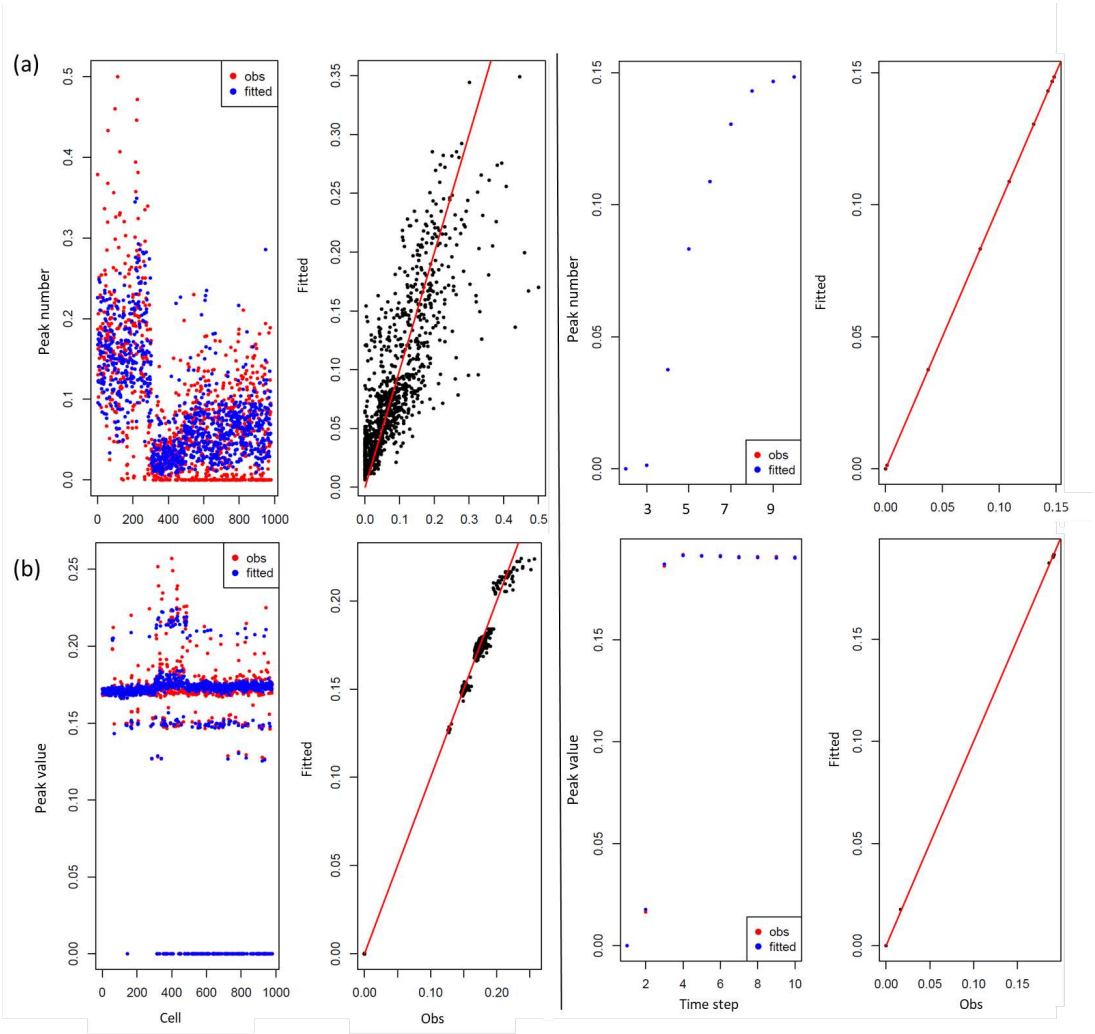

Figure 3: Residual analysis showing observations, *i.e.*, model output (red dots), with predicted (blue dots) occurrence of peaks (Panel a) and of peak maximum values (Panel b) over space (left panels, by averaging over time) and over time (right panels, by averaging over space).

References

Roques, L. and Bonnefon, O. (2016). Modelling population dynamics in realistic landscapes with linear elements: a mechanistic-statistical reaction-diffusion approach. *PloS one*, 11(3).

Zamberletti, P., Sabir, K., Opitz, T., Bonnefon, O., Gabriel, E., and Papaix, J. (2021). More pests but less treatments: ambivalent effect of landscape complexity on conservation biological control. *bioRxiv, 10.1101/2021.03.19.436155*.

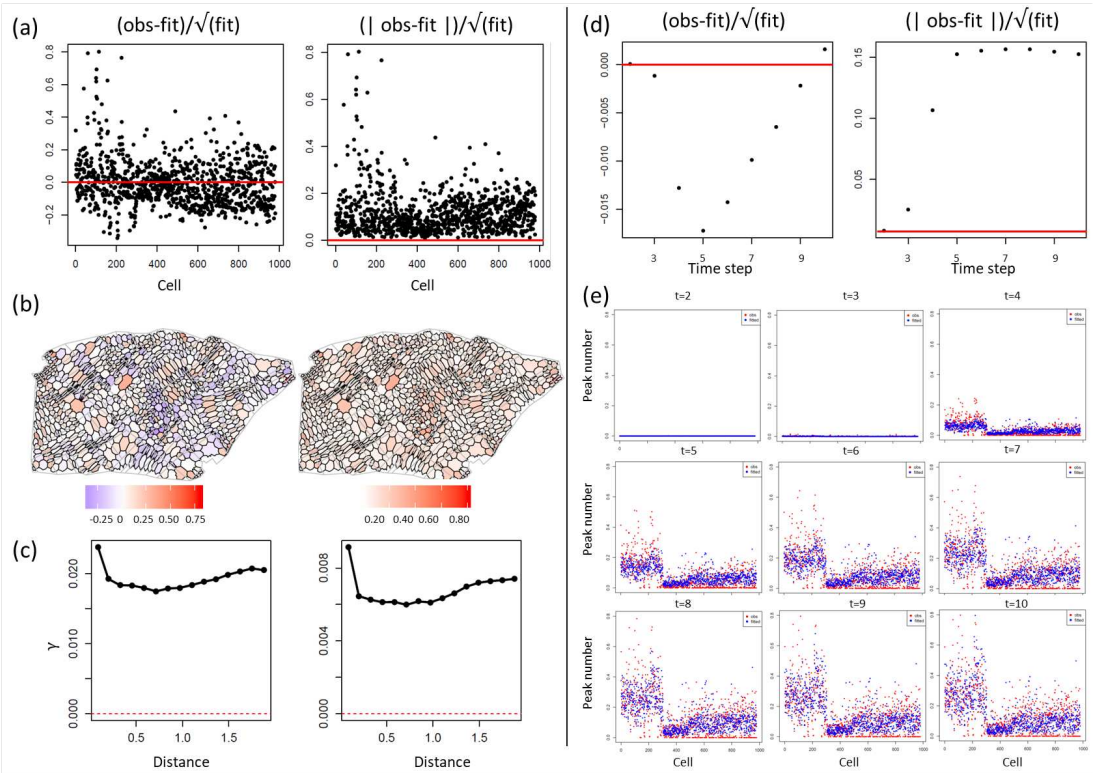

Figure 4: Residual analysis for the model of the occurrence intensity of peaks. Left: Spatial residual analysis. Panel a) Residuals scaled over the fitted values for each cell averaged over time steps; Panel b) Visualisation of the scaled residuals for each cell averaged over time steps; Panel c) Variogram of the scaled residuals. Right: Temporal analysis. Panel d) Residuals scaled over the fitted values for each time step averaged over cells; Panel e) Observations (red dots) and fitted values (blue values) for each time step.

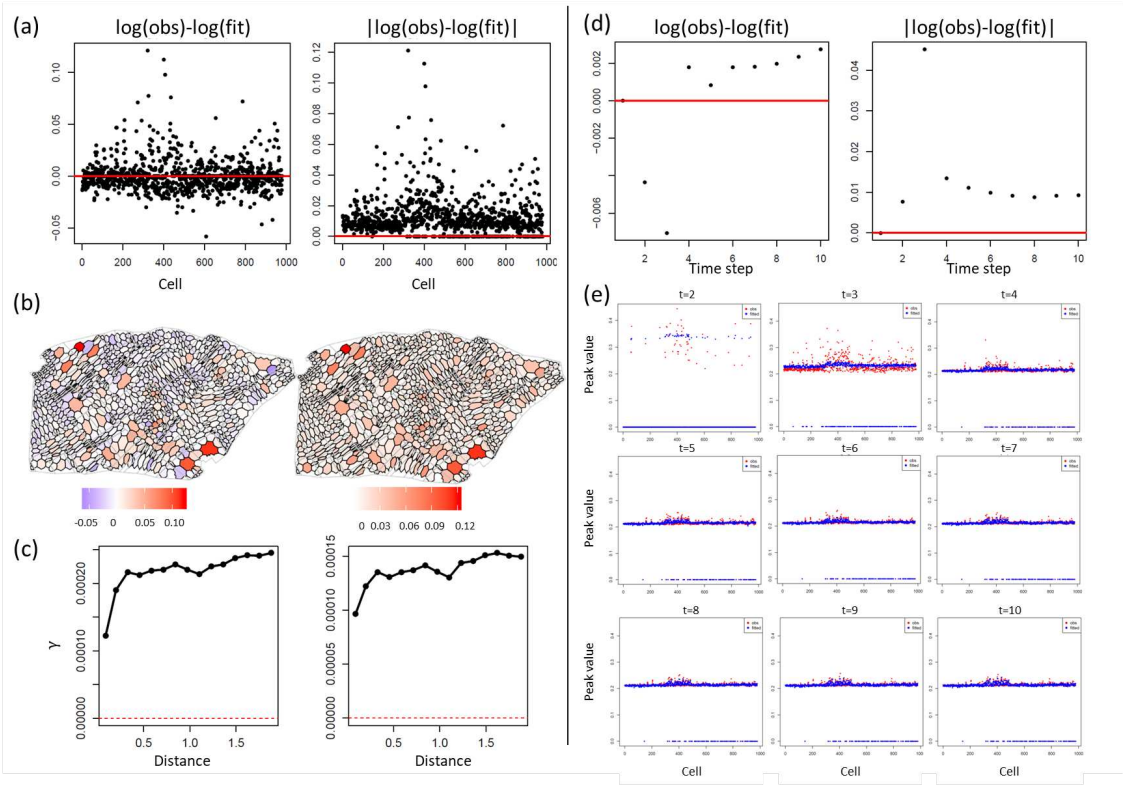

Figure 5: Residual analysis for the model of the peak values. The results presented follow the same structure as in Figure 4

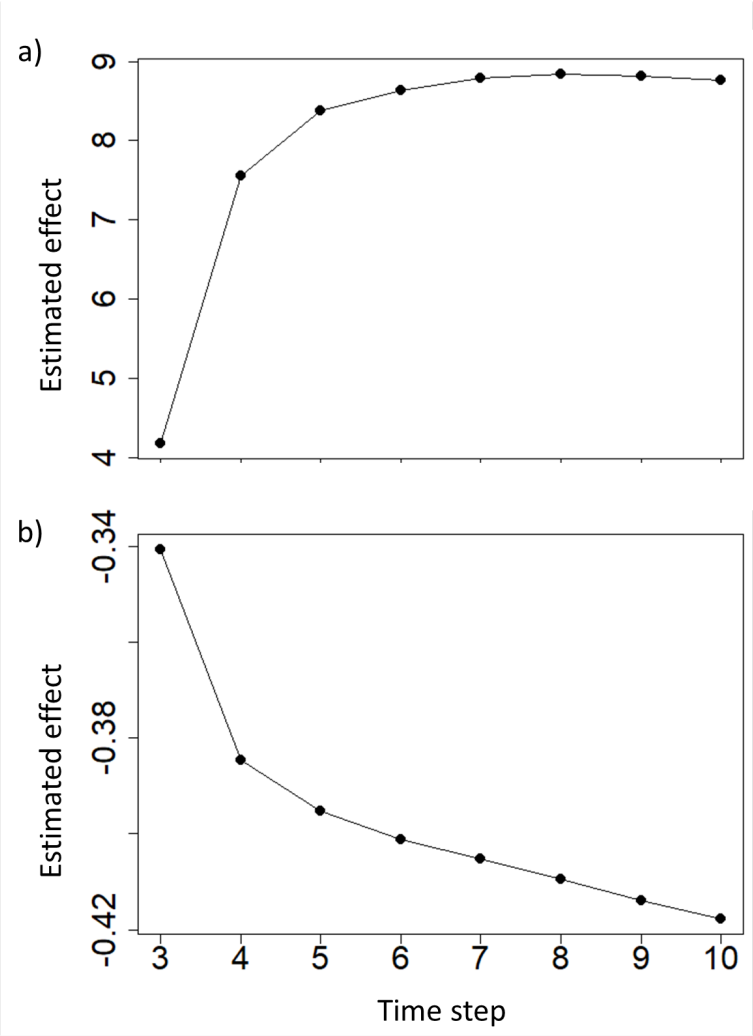

Figure 6: Estimated temporal effects for the occurrence intensity of pest density peaks (Panel a) and for the peak values of pest density (Panel b).

Supplement 4

Appendix A: Effect of mutation on the spreading speed

We simulate the model described in Equations 1 and 12 defined by only two phenotypes corresponding to $y = O_R$ and $y = O_D$ in order to compare our results with the ones of two morphs presented by Elliott and Cornell (2012) and Morris et al. (2019). Elliott and Cornell (2012) investigate numerically the effect of varying R and D on the spreading speed of the system and find that the propagation would be faster in the presence of both phenotypes than just one phenotype would be in the absence of mutation. We verify that we are in case expressed by Eq. (40) by Morris et al. (2019), since $D_h(O_D)/D_h(O_R) + R_h(O_D)/R_h(O_R) = R_h(O_R)/R_h(O_D) + R_h(O_D)/R_h(O_R) = (R_h(O_R)^2 + R_h(O_D)^2)/(R_h(O_D) * R_h(O_R)) >= (2 * R_h(O_R) * R_h(O_D))/(R_h(O_R) * R_h(O_D)) = 2$ (i.e. strict inequality as $R_h(O_R) \neq R_h(O_D)$). The spreading speed they derive is defined by the Eq. 13 in Elliott and Cornell (2012) and Eq. 7 in Morris et al. (2019), and in our case can be espressed as

$$v_f = \frac{|R_h(O_R)D_h(O_D) - R_h(O_D)D_h(O_D)|}{\sqrt{(R_h(O_R) - R_h(O_D)) - (D_h(O_D) - D_h(O_R))}} \tag{A1}$$

Here, we verify that, using the same parameter setting and fitness function as the phenotype continuous space, we obtain a value of spreading speed that corresponds to $v_f = 3$ for high specialisation (i.e. $d = 4$) with a low mutation value (i.e. $\mu = 0.01$). Moreover, we also test if the heterogeneity in R and D leads to a variation of spreading speed with 2 phenotypic traits with respect to the homogeneous v_f, see Table A1. In both cases $L \to \infty$ and $L \to 0$, in case of low mutation, the faster spreading speed corresponding to v_f appears for local and non-local system. For the scenario B (number 2 in Table A1), in case of low mutation, we find a spreading speed higher than the one without mutation, and, for $L \to \infty$, the trade-off is shifted in favour of O_R.

We verify and explain why, instead, the conditions do not hold true for having a faster spreading speed equal to v_f in case of low mutation when considering a continuous space of phenotypic traits. We evaluate the conditions expressed by Morris et al. (2019) for the appearance of v_f considering the fastest phenotype ($y = O_R$) with respect to all the other phenotypic traits $y \in (y_{\min}, y_{\max})$.

$$\frac{R_h(O_R)}{R_h(y)} + \frac{D_h(O_R)}{D_h(y)} > 2 \tag{A2}$$

and

$$\frac{R_h(y)}{R(_hO_R)} + \frac{D_h(y)}{D_h(O_R)} > 2 \tag{A3}$$

		$L \to \infty$				$L \to 0$			
		$\mu = 0$		$\mu = 0.01$		$\mu = 0$		$\mu = 0.01$	
		O_R	O_D	O_R	O_D	O_R	O_D	O_R	O_D
A	v_{th}	2.83	2.83	2.83	2.83	2.83	2.83	2.83	2.83
	v_L	2.86	2.76	2.98	2.87	2.86	2.76	2.98	2.87
	v_{NL}	2.85	0	2.98	0	2.85	0	2.98	0
B	v_{th}	2.91	3.08	2.91	3.08	2.83	2.83	2.83	2.83
	v_L	2.96	3	3.14	3.03	2.91	2.84	3.05	2.95
	v_{NL}	2.92	3	3.13	0	2.91	0	3.04	0
C	v_{th}	0.1	2.54	0.1	2.54	0.07	2.45	0.07	2.45
	v_L	0.43	2.46	2.36	2.45	0.2	2.41	1.2	2.39
	v_{NL}	0.25	2.46	2.43	2.44	0.24	2.43	2.4	2.4

Table A1 – Spreading speed of the system with only two phenotypic traits corresponding to the fastest ones ($y = O_R$ and $y = O_D$). In the first column: 1 stands for scenario A, 2 stands for scenario B, 3 stands for scenario C. In second column v_{th} is the spreading speed evaluated with analytical formulas, v_L is the numerical local spreading speed, v_{NL} is the numerical non-local spreading speed.

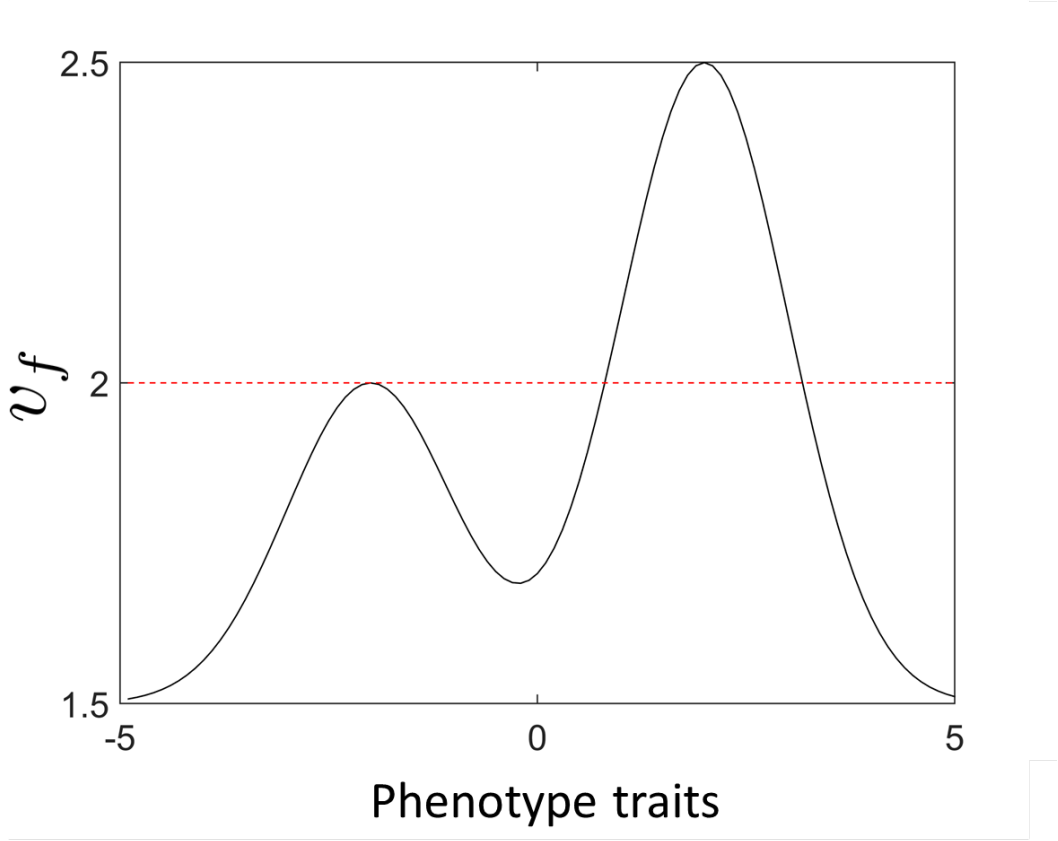

Figure A1 – Conditions for having a faster spreading speed v_f. The black line represents the minimum among the left term of conditions expressed in Eq. A2 and A3 and the dashed red curve the limit value beyond which v_f appears.

We draw the curve representing the minimum among the left term of conditions in Eq. (A2) and (A3) the limit equal to 2. A faster spreading speed appears when we are beyond the limit equal to 2, meaning that both conditions are verified (Figure A1). We find that a low step-wise mutation in a non-local system composed by a continuum phenotype space, is able to slow down the spreading speed that the system would have with only two phenotypic traits due to the mutation among the nearest neighbors and competition.

Appendix B: Spreading speed

Scenario A: ***Homogeneous case***

In the absence of mutation ($\mu = 0$), it is known that the spreading speed of the solution of (7.8) in the Homogeneous case (i.e. $R = R_h(y)$ and $D = D_h(y)$) associated with a phenotype y is $v(y) = 2\sqrt{R_h(y)\, D_h(y)}$ (Kolmogorov et al., 1937). Depending on d and σ (see (7.5)-(7.6)), there may be only one fastest phenotype y^* in 0 or two optima at $\pm d/2$.

Note that $D_h(y) = R_h(-y)$, thus:

$$(R_h(y)\, D_h(y))' = R_h'(y)R_h(-y) - R_h(y)R_h'(-y).$$

For $y = 0$, this quantity is equal to 0. Computing the second derivative, i.e., $(R_h\, D_h)''(y) = R_h''(y)R_h(-y) - 2\, R_h'(y)R_h'(-y) + R_h''(-y)R_h(y)$, at $y = 0$, yields $(R_h\, D_h)''(0) = 2(R_h''(0)R_h(0) - R_h'(0)^2)$. Thus, we observe that:

$$\begin{cases} (R_h\, D_h)''(0) > 0, & \text{if } d > 2\sigma\sqrt{1 + 2\, W\left(\frac{1}{2R_0}e^{-1/2}\right)}, \\ \\ (R_h\, D_h)''(0) < 0, & \text{if } d < 2\sigma\sqrt{1 + 2\, W\left(\frac{1}{2R_0}e^{-1/2}\right)}, \end{cases} \tag{B1}$$

with W the principal branch of the Lambert function. Thus, there exists a threshold on the optimum distance given by $d_{cr} = 2\sigma\sqrt{1 + 2\, W\left(\frac{1}{2R_0}e^{-1/2}\right)}$. When $d < d_{cr}$, 0 is a (local) maximum of the speed, while if $d > d_{cr}$, we conclude that the speed has two maxima, which are symmetric with respect to 0. As $(R_h\, D_h)'(d/2) < 0$, these maxima are reached in the region $(-d/2, d/2)$.

Scenario B: ***Heterogenous R, homogeneous D***

In the local equation (7.8), when the coefficient $R(x, y)$ is spatially heterogeneous and $L-$periodic, we adopt the formula given for the spreading speed in Berestycki and Hamel (2005). To state this formula, we first have to define a differential operator L_λ, acting on functions $\phi(x, y)$ which are $L-$periodic in x and satisfy no-flux boundary conditions at the boundaries $y = y_{\min}$, $y_{\max}$. For any $\lambda > 0$, this operator is defined by:

$$L_\lambda(\phi) := D(y)\, \partial_{xx}\phi + \mu\, \partial_{yy}\phi + 2\,\lambda\, D(y)\, \partial_x\phi + [\lambda^2 D(y) + R(x, y)]\phi. \tag{B2}$$

The spreading speed can then be computed by the Gärtner-Freidlin formula:

$$V = \min_{\lambda>0} \frac{k(\lambda)}{\lambda}, \tag{B3}$$

with $k(\lambda)$ the principal eigenvalue (the unique eigenvalue associated with a positive eigenfunction) of L_λ.
However, when $\mu = 0$, more tractable theoretical formulas can be obtained to determine the spreading speed $v(y)$ associated with a given phenotype y at the limit of rapidly varying and slowly varying environments (i.e. $(L \to 0)$ and $(L \to \infty)$, respectively).

1. **Rapidly varying environment** $L \to 0$

   We refer to El Smaily et al. (2009) work, where the spreading speed $v_0(y)$ of each phenotype is derived analytically:

   $$v_0(y) = 2\sqrt{D_h(y)\,\overline{R}_x(y)}, \tag{B4}$$

   with $\overline{R}_x(y)$ the mean value of the growth rate, averaged over space:

   $$\overline{R}_x(y) = \int_0^1 R(x,y)\,dx = R_h(y),$$

   as $R_s(x)$ has mean value 0. Finally, the speed is the same as in the homogeneous case $(R_s \equiv 0)$:

   $$v_0(y) = 2\sqrt{D_h(y)\,R_h(y)}.$$

2. **Slowly varying environment** $L \to +\infty$

   An explicit formula for the limit spreading speed $v_\infty(y)$ of each phenotype as $L \to +\infty$ can be derived analytically using the formulation of Hamel et al. (2010). It is given by the expression:

   $$v_\infty(y) = 4\sqrt{D_h(y)} \times \frac{(R^+(y))^2 + (R^-(y))^2 + (R^+(y) + R^-(y))\,\sqrt{\triangle(y)}}{(R^+(y) + R^-(y) + 2\sqrt{\triangle(y)})^{\frac{3}{2}}}$$

   with $R^+(y) = R_h(y) + R_0$, $R^-(y) = R_h(y) - R_0$ and $\triangle(y) = (R^+(y))^2 + (R^-(y))^2 - R^+(y)\,R^-(y)$.

Scenario C: ***Homogeneous R, heterogeneous D***

The Fokker-Planck diffusion term in the local equation (7.8), can be rewritten as:

$$\partial_{xx}(D(x,y)\,c(t,x,y)) = \partial_x(D(x,y)\,\partial_x c(t,x,y)) + \partial_x(c(t,x,y)\,\partial_x D(x,y)). \tag{B5}$$

The term $\partial_x(D(x,y)\,\partial_x c(t,x,y))$ corresponds to Fickian diffusion operator. Though both types of diffusion terms are found in the ecological literature, Fokker-Planck diffusion $\partial_{xx}(D(x,y)\,c(t,x,y))$ naturally emerges from Brownian motion with space-dependent mobility, and seems better adapted to describe individual movements (see Turchin, 1998; Roques, 2013), whereas Fickian diffusion emerges from flux considerations and seems more adapted to describe heat conduction in heterogeneous media. The main difference between these two operators is that Fickian diffusion tends to homogenize the density $c(t,x,y)$ (with respect to the diffusion variable x). The additional term $\partial_x(c(t,x,y)\,\partial_x D(x,y))$ in (B5) corresponds to a spatially-periodic transport term which is oriented towards the lower values of D. As the standard formula for the spreading speed with heterogeneous diffusion in (Berestycki and Hamel, 2005) and the formulas in the limiting cases (El Smaily et al., 2009; Hamel et al., 2011) are only available for Fickian diffusion operators, we used these formulas in Table **??** (Scenario C), thereby neglecting effect of the transport term $\partial_x(c(t,x,y)\,\partial_x D(x,y))$ on the spreading speeds $v(y)$. The corresponding equation, with mutation rate $\mu = 0$ is:

$$\partial_t c(t,x,y) = \partial_x(D(x,y)\,\partial_x c(t,x,y)) + c(t,x,y)\,(R(x,y) - \gamma\, c(t,x,y))\,. \tag{B6}$$

1. **Rapidly varying environment** $L \to 0$

   The spreading speed $v_0(y)$ of each phenotype can be derived from El Smaily et al. (2009):

   $$v_0(y) = 2\sqrt{R_h(y)\ <D>_H\ (y)},$$

   with $<D>_H\ (y) = \left(\int_0^1 \frac{1}{D(x,y)}\,dx\right)^{-1}$ the harmonic mean of $x \mapsto D(x,y)$.

2. **Slowly varying environment** $L \to +\infty$

   In this case, we use the results in Hamel et al. (2011), which show that:

   $$v_\infty(y) = 2\sqrt{R_h(y)}\ <\sqrt{D}>_H\ (y),$$

   with $<\sqrt{D}>_H\ (y) = \left(\int_0^1 \frac{1}{\sqrt{D(x,y)}}\,dx\right)^{-1}$ the harmonic mean of $x \mapsto \sqrt{D(x,y)}$.

Supplement 5

1. Parametrization of β_1 and β_2

We can relate β_1 and β_2 in order to reduce the number of parameter.

Relative order of magnitude of β_1 vs β_2: assume for simplicity that $U_1 + U_2$ is spatially constant. Set

$$N_{V_2}(t) = \int_\Omega V_2(t, \mathbf{x})\, d\mathbf{x},$$

the total population size of the predator 2. Integrating the equation satisfied by V_2 over Ω, we get:

$$N'_{V_2}(t) = N_{V_2}(t)\,(\beta_2\,(U_1 + U_2)(t) - m_V).$$

Consider now the first predator, and set

$$N^H_{V_1}(t) = \int_H v_1(t, x)\, dx \text{ and } N^\Omega_{V_1}(t) = \int_\Omega V_1(t, \mathbf{x})\, d\mathbf{x},$$

the population sizes of predator 1 in H and Ω, respectively. Integrating the equation (8.1) satisfied by v_1 over H, we get:

$$(N^H_{V_1})'(t) = \beta_1\, N^\Omega\,(U_1 + U_2) - m_H\, N^H + \rho_{21} \int_H V_1(t, x)\, dx - \rho_{12} N^H, \tag{B7}$$

and integrating (8.2) over Ω, using Green's formula and the boundary condition (given in the main text), we get:

$$(N^\Omega_{V_1})'(t) = -m_V\, N^\Omega - \rho_{21} \int_H V_1(t, x)\, dx + \rho_{12} N^H. \tag{B8}$$

Assume for simplicity that $V_1(t, \mathbf{x}) = \alpha(t)/D_{V_1}(\mathbf{x})$ for some $\alpha(t)$. Then,

$$N^\Omega_{V_1}(t) = \alpha(t) \int_\Omega \frac{1}{D_{V_1}(\mathbf{x})}\, d\mathbf{x},$$

and therefore

$$\alpha(t) = N^\Omega_{V_1}(t) \langle D_{V_1} \rangle \text{ with } \langle D_{V_1} \rangle = \frac{1}{\int_\Omega \frac{1}{D_{V_1}(\mathbf{x})}\, d\mathbf{x}}.$$

As, $D_{V_1}(\mathbf{x}) = a > 0$ for all $\mathbf{x} \in H$, we deduce that, on H,

$$\int_H V_1(t, x)\, dx = \frac{|H|\, N^\Omega_{V_1}(t)\, \langle D_{V_1} \rangle}{a}.$$

We can then solve explicitly the system (B7)-(B8), and we get that the exponential rate of

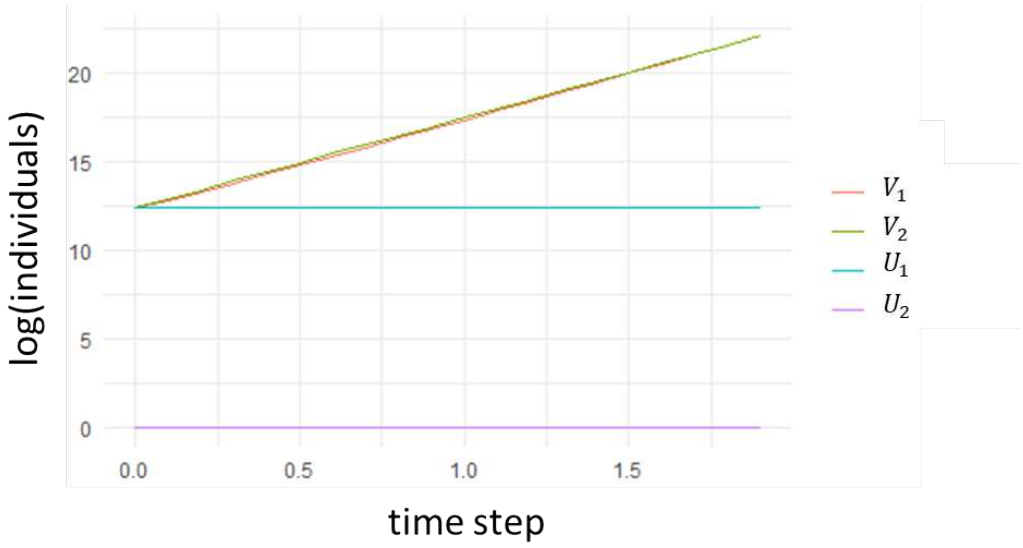

Figure 1 – Numerical calibration of β_1 and β_2.

growth of $N^{\Omega}_{V_1}(t)$ is:

$$-\frac{m_H + m_V + \rho(1+Z)}{2} + \frac{1}{2}\sqrt{(m_H - m_V + \rho\,(1-Z))^2 + 4\,\beta_1\,\rho\,(U_1+U_2)},$$

with $Z := |H|\langle D_{V_1}\rangle/a$ and assuming $\rho_{21} = \rho_{12} := \rho$. With the approximation $\langle D_{V_1}\rangle = a/|\Omega|$, we get $Z = |H|/|\Omega|$ (1D and 2D Lebesgue measures). For comparison, the growth rate of N_{V_2} is $(\beta_2\,(U_1+U_2)(t) - m_V)$. Finally, although the effect of $U_1 + U_2$ is different, a reasonable order of magnitude would be

$$\beta_1 = \beta_2^2/\rho.$$

However, in our application, we calibrate β_1 and β_2 by numerical simulation. We perform simulation where the prey abundance is kept constant (*i.e.*, we set mortality equal to 0) and we adjust the value of β_1 determining the population growth of V_1 in the 1D in order to matching the same exponential curve determined by the V_2 dynamic in the 2D. The result of the calibration is showed in Figure 1. The corresponding values for β_1 and β_2 are reported in Table 7.2 of the main text.

2. GLM results

We report all the coefficient estimated by the General Mixed Model (GLM) for the prey density, U_2 proportion, predator density, V_1 proportion.

Prey density (U_1 and U_2)	
Scenario 4	0.1983^{***}
Scenario 2	0.5267^{***}
Scenario 3	0.2124^{***}
Scenario 1	0.9422^{***}
Scenario 4:P_c	-0.0183^{***}
Scenario 2:P_c	-0.1212^{***}
Scenario 3:P_c	-0.0073^{***}
Scenario 1:P_c	0.0200^{***}
Scenario 4:P_h	-0.0028^{***}
Scenario 2:P_h	-0.0731^{***}
Scenario 3:P_h	0.0002
Scenario 1:P_h	-0.0000
Scenario 4:β_{adj}^{CC}	-0.0033^{***}
Scenario 2:β_{adj}^{CC}	-0.0155^{***}
Scenario 3:β_{adj}^{CC}	-0.0027^{***}
Scenario 1:β_{adj}^{CC}	0.0065^{***}
Scenario 4:β_{adj}^{CH}	-0.0026^{***}
Scenario 2:β_{adj}^{CH}	-0.0333^{***}
Scenario 3:β_{adj}^{CH}	-0.0002
Scenario 1:β_{adj}^{CH}	0.0007
Scenario 4:β_{adj}^{HH}	-0.0012^{**}
Scenario 2:β_{adj}^{HH}	0.0017^{***}
Scenario 3:β_{adj}^{HH}	-0.0002
Scenario 1:β_{adj}^{HH}	0.0008^{*}
Scenario 4:P_c:P_h	-0.0033^{***}
Scenario 2:P_c:P_h	-0.0240^{***}
Scenario 3:P_c:P_h	-0.0002
Scenario 1:P_c:P_h	-0.0003
Scenario 4:P_c:β_{adj}^{CC}	0.0017^{***}
Scenario 2:P_c:β_{adj}^{CC}	0.0083^{***}
Scenario 3:P_c:β_{adj}^{CC}	0.0017^{***}
Scenario 1:P_c:β_{adj}^{CC}	0.0014^{***}
Scenario 4:P_c:β_{adj}^{CH}	-0.0004
Scenario 2:P_c:β_{adj}^{CH}	0.0138^{***}
Scenario 3:P_c:β_{adj}^{CH}	0.0001
Scenario 1:P_c:β_{adj}^{CH}	0.0006
Scenario 4:P_c:β_{adj}^{HH}	-0.0001
Prey density (U_1 and U_2)	
Scenario 2:P_c:β_{adj}^{HH}	0.0042^{***}
Scenario 3:P_c:β_{adj}^{HH}	0.0003
Scenario 1:P_c:β_{adj}^{HH}	-0.0004
Scenario 4:P_h:β_{adj}^{CC}	0.0004
Scenario 2:P_h:β_{adj}^{CC}	-0.0039^{***}
Scenario 3:P_h:β_{adj}^{CC}	0.0004
Scenario 1:P_h:β_{adj}^{CC}	-0.0007
Scenario 4:P_h:β_{adj}^{CH}	0.0002
Scenario 2:P_h:β_{adj}^{CH}	0.0125^{***}
Scenario 3:P_h:β_{adj}^{CH}	-0.0002
Scenario 1:P_h:β_{adj}^{CH}	0.0006
Scenario 4:P_h:β_{adj}^{HH}	0.0002
Scenario 2:P_h:β_{adj}^{HH}	-0.0065^{***}
Scenario 3:P_h:β_{adj}^{HH}	0.0001
Scenario 1:P_h:β_{adj}^{HH}	-0.0004
Scenario 4:β_{adj}^{CC}:β_{adj}^{CH}	0.0006
Scenario 2:β_{adj}^{CC}:β_{adj}^{CH}	0.0041^{***}
Scenario 3:β_{adj}^{CC}:β_{adj}^{CH}	0.0006
Scenario 1:β_{adj}^{CC}:β_{adj}^{CH}	-0.0018^{***}
Scenario 4:β_{adj}^{CC}:β_{adj}^{HH}	0.0000
Scenario 2:β_{adj}^{CC}:β_{adj}^{HH}	0.0030^{***}
Scenario 3:β_{adj}^{CC}:β_{adj}^{HH}	0.0001
Scenario 1:β_{adj}^{CC}:β_{adj}^{HH}	0.0002
Scenario 4:β_{adj}^{CH}:β_{adj}^{HH}	-0.0006
Scenario 2:β_{adj}^{CH}:β_{adj}^{HH}	-0.0107^{***}
Scenario 3:β_{adj}^{CH}:β_{adj}^{HH}	-0.0001
Scenario 1:β_{adj}^{CH}:β_{adj}^{HH}	0.0003
AIC	-158315.2770
BIC	-157750.3006
Log Likelihood	79222.6385
Deviance	70.3188
Num. obs.	44000

$^{***}p < 0.001$; $^{**}p < 0.01$; $^{*}p < 0.05$

U_2 **proportion**	
Scenario 4	0.5288^{***}
Scenario 2	0.3996^{***}
Scenario 3	0.6065^{***}
Scenario 1	0.6197^{***}
Scenario 4:P_c	0.2597^{***}
Scenario 2:P_c	0.2179^{***}
Scenario 3:P_c	0.3054^{***}
Scenario 1:P_c	0.2916^{***}
Scenario 4:P_h	-0.0286^{***}
Scenario 2:P_h	-0.0698^{***}
Scenario 3:P_h	-0.0158^{***}
Scenario 1:P_h	-0.0137^{***}
Scenario 4:β_{adj}^{CC}	0.1150^{***}
Scenario 2:β_{adj}^{CC}	0.0938^{***}
Scenario 3:β_{adj}^{CC}	0.1109^{***}
Scenario 1:β_{adj}^{CC}	0.1045^{***}
Scenario 4:β_{adj}^{CH}	-0.0175^{***}
Scenario 2:β_{adj}^{CH}	-0.0203^{***}
Scenario 3:β_{adj}^{CH}	-0.0018
Scenario 1:β_{adj}^{CH}	0.0015
Scenario 4:β_{adj}^{HH}	-0.0015
Scenario 2:β_{adj}^{HH}	0.0047^{*}
Scenario 3:β_{adj}^{HH}	0.0033
Scenario 1:β_{adj}^{HH}	0.0035
Scenario 4:P_c:P_h	0.0091^{***}
Scenario 2:P_c:P_h	-0.0150^{***}
Scenario 3:P_c:P_h	0.0222^{***}
Scenario 1:P_c:P_h	0.0205^{***}
Scenario 4:P_c:β_{adj}^{CC}	-0.0716^{***}
Scenario 2:P_c:β_{adj}^{CC}	-0.0497^{***}
Scenario 3:P_c:β_{adj}^{CC}	-0.0743^{***}
Scenario 1:P_c:β_{adj}^{CC}	-0.0740^{***}
Scenario 4:P_c:β_{adj}^{CH}	0.0098^{***}
Scenario 2:P_c:β_{adj}^{CH}	0.0150^{***}
Scenario 3:P_c:β_{adj}^{CH}	0.0080^{***}
Scenario 1:P_c:β_{adj}^{CH}	0.0046^{*}
Scenario 4:P_h:β_{adj}^{CC}	-0.0228^{***}
Scenario 2:P_h:β_{adj}^{CC}	-0.0242^{***}
Scenario 3:P_h:β_{adj}^{CC}	-0.0231^{***}
Scenario 1:P_h:β_{adj}^{CC}	-0.0222^{***}
Scenario 4:P_h:β_{adj}^{CH}	0.0110^{***}
Scenario 2:P_h:β_{adj}^{CH}	0.0127^{***}
Scenario 3:P_h:β_{adj}^{CH}	0.0071^{***}
Scenario 1:P_h:β_{adj}^{CH}	0.0078^{***}
Scenario 4:β_{adj}^{CC}:β_{adj}^{CH}	-0.0279^{***}
Scenario 2:β_{adj}^{CC}:β_{adj}^{CH}	-0.0269^{***}
Scenario 3:β_{adj}^{CC}:β_{adj}^{CH}	-0.0252^{***}
Scenario 1:β_{adj}^{CC}:β_{adj}^{CH}	-0.0223^{***}
Scenario 4:β_{adj}^{CH}:β_{adj}^{HH}	0.0070^{**}
Scenario 2:β_{adj}^{CH}:β_{adj}^{HH}	0.0044^{*}
Scenario 3:β_{adj}^{CH}:β_{adj}^{HH}	0.0089^{***}
Scenario 1:β_{adj}^{CH}:β_{adj}^{HH}	0.0074^{***}
AIC	-6556.8242
BIC	-6096.1511
Log Likelihood	3331.4121
Deviance	2214.1858
Num. obs.	44000

$^{***}p < 0.001$; $^{**}p < 0.01$; $^{*}p < 0.05$

Predator density (V_1 and V_2)	
Scenario 4	0.1742^{***}
Scenario 2	0.2056^{***}
Scenario 3	0.1461^{***}
Scenario 4:P_c	0.0282^{***}
Scenario 2:P_c	0.0832^{***}
Scenario 3:P_c	0.0049^{***}
Scenario 4:P_h	0.0034^{***}
Scenario 2:P_h	0.0062^{***}
Scenario 3:P_h	0.0000
Scenario 4:β_{adj}^{CC}	0.0025^{***}
Scenario 2:β_{adj}^{CC}	0.0053^{***}
Scenario 3:β_{adj}^{CC}	0.0016^{***}
Scenario 4:β_{adj}^{CH}	0.0059^{***}
Scenario 2:β_{adj}^{CH}	0.0245^{***}
Scenario 3:β_{adj}^{CH}	0.0002
Scenario 4:β_{adj}^{HH}	0.0012^{***}
Scenario 2:β_{adj}^{HH}	-0.0040^{***}
Scenario 3:β_{adj}^{HH}	0.0002
Scenario 4:P_c:P_h	0.0043^{***}
Scenario 2:P_c:P_h	-0.0015^{***}
Scenario 3:P_c:P_h	-0.0001
Scenario 4:P_c:β_{adj}^{CH}	0.0019^{***}
Scenario 2:P_c:β_{adj}^{CH}	-0.0081^{***}
Scenario 3:P_c:β_{adj}^{CH}	0.0001
Scenario 4:P_c:β_{adj}^{HH}	-0.0004
Scenario 2:P_c:β_{adj}^{HH}	-0.0052^{***}
Scenario 3:P_c:β_{adj}^{HH}	-0.0001
Scenario 4:P_h:β_{adj}^{CH}	-0.0011^{***}
Scenario 2:P_h:β_{adj}^{CH}	-0.0096^{***}
Scenario 3:P_h:β_{adj}^{CH}	0.0002
Scenario 4:P_h:β_{adj}^{HH}	-0.0001
Scenario 2:P_h:β_{adj}^{HH}	0.0035^{***}
Scenario 3:P_h:β_{adj}^{HH}	-0.0001
Scenario 4:β_{adj}^{CC}:β_{adj}^{CH}	0.0000
Scenario 2:β_{adj}^{CC}:β_{adj}^{CH}	-0.0021^{***}
Scenario 3:β_{adj}^{CC}:β_{adj}^{CH}	-0.0004
Scenario 4:β_{adj}^{CH}:β_{adj}^{HH}	0.0011^{***}

Predator density (V_1 and V_2)	
Scenario 2:β_{adj}^{CH}:β_{adj}^{HH}	0.0049***
Scenario 3:β_{adj}^{CH}:β_{adj}^{HH}	0.0000
AIC	−151851.1239
BIC	−151514.9534
Log Likelihood	75965.5620
Deviance	19.3446
Num. obs.	33000

$^{***}p < 0.001$; $^{**}p < 0.01$; $^{*}p < 0.05$

Proportion of V_1	
(Intercept)	0.3574^{***}
P_c	0.2489^{***}
P_h	0.0531^{***}
β_{adj}^{CC}	0.0153^{***}
β_{adj}^{CH}	0.0517^{***}
β_{adj}^{HH}	0.0071^{***}
P_c:P_h	0.0517^{***}
P_c:β_{adj}^{CH}	-0.0042^{***}
P_c:β_{adj}^{HH}	-0.0051^{***}
P_h:β_{adj}^{CH}	-0.0134^{***}
β_{adj}^{CH}:β_{adj}^{HH}	0.0104^{***}
AIC	-15582.4484
BIC	-15494.7806
Log Likelihood	7803.2242
Deviance	155.8674
Num. obs.	11000

$^{***}p < 0.001$; $^{**}p < 0.01$; $^{*}p < 0.05$

3. Variance among replicates

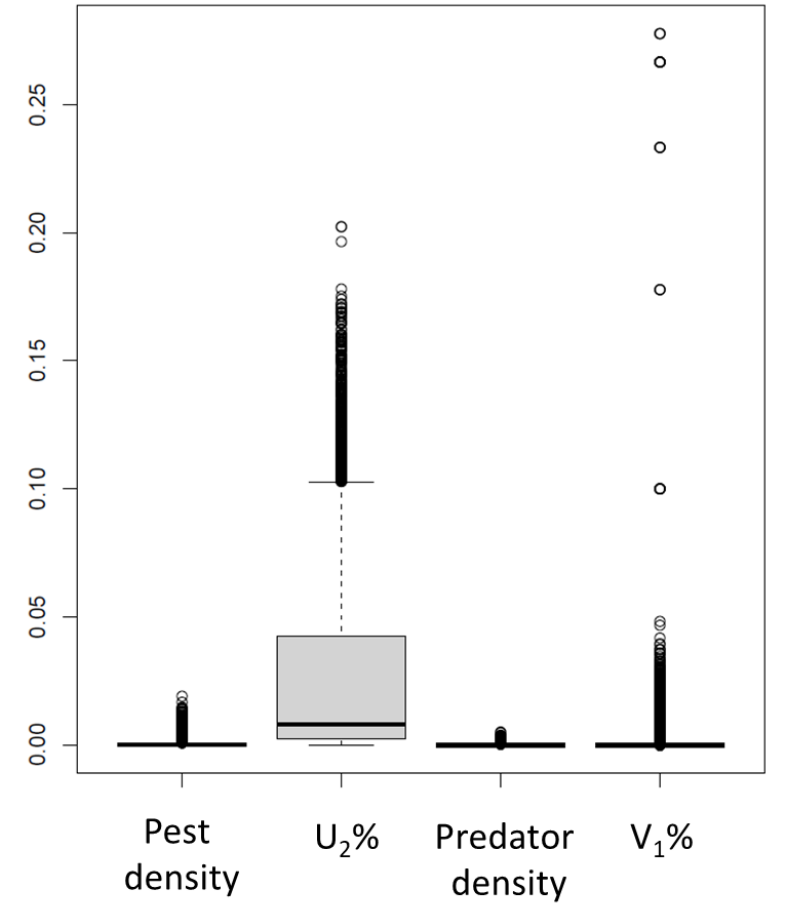

Figure 2 – Variance among replicates for the variables showed in Figures 8.4, 8.5, 8.6.

4. Predator composition additional results

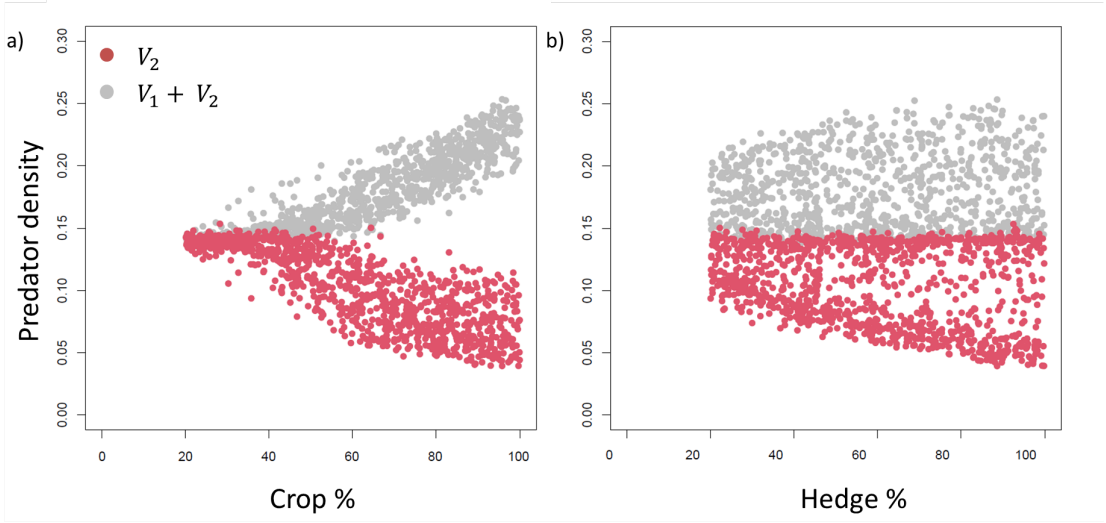

Figure 3 – Predator density and composition depending on crop and hedge proportion. Comparison of hedge predator V_1 and crop predator V_2 density with respect to crop proportion and hedge proportion. Density values are averaged over replicates.

Supplement 6

8.3.1 Undgraduate project report

Here, we attach the study report of the internship of Lingeshwari Ramlugon finalised at BioSP under my supervision. Ling's research focus on the relationships among landscape structures and landscape metrics. Her results are also used in the present work of thesis to define the study area and parameter range of Chapter 8. She applied the stochastic landscape generator model (Chapter 2.2) to perform parameter calibration and validation on a study region of the Lower Durance Valley. She computed the proposed ensemble of metrics vector and raster based. Then, she defined a complete simulation plan for which she simulated and generated landscape structures. Lastly, a Principal Component Analysis is realised to assess the relationship among parameters and generated pattern.

Étude sur les relations entre la structure du paysage et la dynamique multi-proies-prédateurs pour la lutte biologique

Lingeshwari Ramlugon

Sous la supervision de :

Patrizia Zamberletti
Julien Papaïx
Thomas Opitz
Edith Gabriel

Rapport de stage dans le cadre de la 3e année de Licence en Statistique et Informatique Décisionnelle à l'Université Toulouse III - Paul Sabatier

26 avril 2021 au 07 juillet 2021

Université Paul Sabatier, Faculté sciences et ingénierie, Bâtiment 3R1 b2 / 3e étage, 118 route de Narbonne, 31062 Toulouse cedex 09

Remerciements

Je tiens à remercier Edith Gabriel, Directrice de Recherche à INRAE et Patrizia Zamberletti, doctorante de m'avoir donné l'opportunité de faire mon stage dans l'unité BioSP.

Je remercie également Patrizia Zamberletti et Julien Papaïx, chercheur à l'unité BioSP de m'avoir guidé tout au long du stage et d'avoir répondu à mes innombrables questions.

Mes remerciements vont aussi à Thomas Opitz, chercheur à l'unité BioSP, de m'avoir éclairé lorsque j'en avais besoin.

Je souhaite aussi remercier Adrien Mazoyer, mon professeur de statistiques à l'Université de Toulouse III – Paul Sabatier d'avoir clarifié mes doutes.

Résumé

Dans le cadre de mon cursus en 3e année de Licence en Statistique et Informatique Décisionnelle à l'Université de Toulouse III – Paul Sabatier, j'ai réalisé mon stage de fin d'études dans l'unité BioSP (Biostatistique et Processus Spatiaux) de l'Institut Nationale de Rercherche en Agronomie et Environnement (INRAE). J'ai été encadrée par Patrizia Zamberletti, doctorante en biostatistique. L'objectif de ce stage est d'étudier la relation entre la structure d'un paysage et la dynamique des ravageurs et prédateurs qui s'y trouvent. En effet, la structure d'un paysage affecte la diversité, l'abondance et le mouvement de ses prédateurs. Pour étudier la dynamique des proie-prédateurs, deux modèles ont été couplés : un modèle qui vise à simuler les paysages pour la définition du support spatial et un modèle proie-prédateur qui simule la dynamique dans les paysages. Dans ce stage, je me concentre sur la première étape de modélisation. On utilise un modèle pour simuler différents paysages qui se rapprochent statistiquement du paysage réel. Le paysage étudié est un sous-domaine de la Basse Vallée de la Durance, situé près d'Avignon en France. Pour étudier ce paysage, on le représente comme un pavage avec des polygones et des segments. On modélise l'allocation comme étant binaire : un polygone peut contenir une culture ou autre ; un segment peut contenir une haie ou autre en utilisant un modèle de type "famille exponentielle". Le modèle utilise des paramètres qui peuvent être estimés sur le paysage réel ou sélectionnés parmi une plage de valeurs pour générer d'autres paysages avec des configurations et compositions différentes. Ce rapport résume donc le travail effectué pour faire l'estimation des paramètres sur le paysage réel de la Basse Vallée de la Durance et, en suite, pour analyser la sensibilité du modèle avec un jeu de paramètres différent. Le travail consiste à estimer les paramètres du modèle par la méthode de vraisemblance composite qui revient à faire une régression logistique ; vérifier que les paramètres estimés ne contiennent pas de biais en les comparant avec des paramètres calculés sur des paysages simulés selon un échantillonneur de Gibbs ; calculer des métriques paysagères pour une représentation vectorisée et en raster du paysage pour le paysage réel et les paysages simulés et comparer ces métriques ; établir différentes combinaisons de paramètres (configurations) et simuler des répétitions d'allocation pour chaque configuration et calculer des métriques sur chaque paysage simulé ; réaliser une analyse en composantes principales où les variables correspondent aux métriques et les individus aux configurations ; étudier le lien entre les différentes configurations et la structure de leurs paysages. On conclut en indiquant comment certains paramètres de descripteurs affectent la structure du paysage.

Table des matières

1 Introduction

Les stratégies de régulation des ravageurs des cultures basées sur la biodiversité de leurs prédateurs naturels présentent des avantages environnementaux en réduisant les pertes de rendement sans les conséquences environnementales négatives qui résultent de l'utilisation de produits phytosanitaires. Le rôle fonctionnel de chaque espèce dans l'écosystème est déterminé par les traits morphologiques, comportementaux ou physiologiques d'un organisme, et est également influencé par le contexte paysager(Bianchi et al., 2006). En effet, la structure d'un paysage affecte la diversité et l'abondance des prédateurs dans un paysage. Un paysage complexe ou hétérogène avec plusieurs éléments (forêts, haies, bordures de champs, rivières, cultures, etc.) peut donc soutenir une plus grande diversité de prédateurs (Poggi et al., 2021).

L'hétérogénéité d'un paysage est définie par sa composition et sa configuration(Langhammer et al., 2019). La composition fait référence à l'occupation du sol, c'est-à-dire aux différents habitats présents (forêts, haies, rivières, cultures, etc.) et à leur proportion. La configuration fait référence à la taille, à la forme et à la disposition spatio-temporelle de ces éléments. Afin d'étudier les effets de l'hétérogénéité des paysages agricoles sur les dynamiques écologiques, des générateurs stochastiques son utilisés pour simuler des scénarios de paysages et s'affranchir ainsi d'un contexte spécifique à une région donnée. Ces paysages virtuels sont construits en contrôlant des propriétés comme la proportion d'un type de culture ou d'habitat semi-naturel ou l'agrégation des habitats. Les modèles de paysage existants utilisent une représentation vectorielle (c'est-à-dire une collection d'objets géométriques, comme des polygones ou segments) ou une représentation en raster (c'est-à-dire une discrétisation de l'espace en cellules auxquelles une occupation du sol est donnée). La majorité des modèles utilisent une représentation en raster ; cependant, les paysages agricoles sont souvent caractérisés par des parcelles en forme de polygones, et des éléments linéaires tels que les haies. Une approche vectorielle semble donc préférable pour bien représenter la disposition spatiale de ces structures géométriques sur un support continu. En se basant sur l'approche développée par Zamberletti et al. (2021), l'objectif de ce travail est d'estimer les paramètres d'un modèle de paysage en l'ajustant à un paysage réel, puis de le valider en évaluant sa capacité à reproduire des caractéristiques du paysage, et enfin de tester la sensibilité du modèle aux différents paramètres.

Les travaux réalisés dans ce rapport sont basés sur une représentation vectorielle d'un sous-domaine de la Basse Vallée de la Durance situé près d'Avignon en France. Le modèle mathématique utilisé est un modèle paramétrique probabiliste de type "famille exponentielle" qui simule l'allocation des parcelles (p. ex. culture vs. espace semi-naturel) et des segments (p. ex. présence/absence de haie). Pour les tests effectués sur le modèle, on adopte une approche de type "Monte–Carlo" en simulant n paysages avec des allocations différentes grâce à un échantillonneur de Gibbs. Le rapport est organisé suivant les différentes étapes menées : (i) estimation des paramètres du modèle et test de leur significativité (chapitre 3), (ii) calcul des métriques paysagères pour une représentation vectorisée et une représentation rastérisée du paysage (chapitre 4) et (iii) étude de la sensibilité du modèle (chapitre 5).

2 Domaine d'étude

Les données de paysage agricole réel sont obtenues à travers des prises de vues satellitaires ou aériennes. Dans cette étude, on se base sur le paysage agricole de la Basse Vallée de la Durance (qu'on note BVD dans la suite) dans le sud-est de la France. Ce paysage agricole s'étend sur plus de $163km^2$ et est principalement caractérisé par une activité agricole (87%) et des zones urbanisées, avec pour principales cultures des espaces ouverts (46%) et des vergers de pommiers/poiriers (24%).

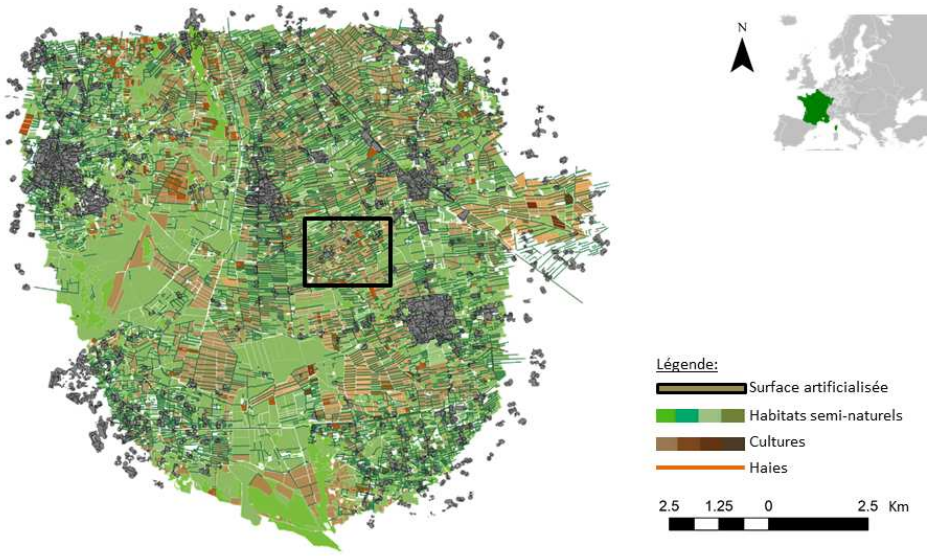

FIGURE 1: Basse Vallée de la Durance

La région cumule un total de $1146km$ de haies, qu'on représentera par la suite comme des segments dont la longueur moyenne est de $105m$. Une particularité de la région est la prédominance de haies orientées est-ouest, dont la fonction est de briser les vents forts (Mistral) qui soufflent du nord.

Pour l'ajustement des modèles aux données, un sous-domaine de la région d'étude a été sélectionné (Figure 1 encadré en noir). Pour étudier ce sous-domaine de la BVD, ce paysage est représente comme un pavage, ou tessellation, définissant une partition de l'espace géographique.

3 Modélisation d'un paysage réel

Une approche vectorielle est utilisée pour la représentation du paysage, où les éléments du paysage sont définis comme des objets géométriques : les parcelles (tels que les surfaces cultivées ou les prairies) sont représentées par des polygones, et les éléments linéaires (tels que les haies, les bordures de champ fleuries, ou les rivières) sont représentés par des segments. La tessellation du sous-domaine contient 263 parcelles et 814 segments.

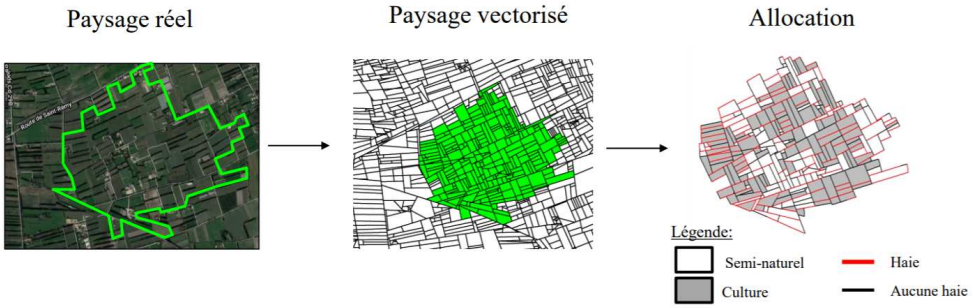

Les objets sont notés comme l'ensemble $O = \{O_1, ..., O_n\}$ avec n étant le nombre total d'objets dans le paysage (Figure 2a). De manière générale, chaque objet a la structure suivante : $O_i = (X_i, Z_i)$. (Z_i) contient des informations géométriques tel que l'aire ou les coordonnées, considéré comme étant fixé dans notre modélisation. (X_i) contient une information qualitative que nous cherchons à modéliser et à simuler, telle que la catégorie d'usage de sol (allocation). Pour les parcelles, les catégories d'allocations possibles sont les suivantes : habitat semi-naturel $(X_i = 2)$, culture $(X_i = 1)$ ou autre $(X_i = 0)$. Pour les segments, la catégorie d'allocation est un segment avec une haie $(X_i = 1)$ ou non $(X_i = 0)$. Ici, nous simplifions l'approche en choisissant une modélisation se basant sur une allocation binaire : pour les segments, l'allocation peut être une haie $(X_i = 1)$ ou autre $(X_i = 0)$; pour les parcelles, l'allocation peut être une culture $(X_i = 1)$ ou autre $(X_i = 0)$.

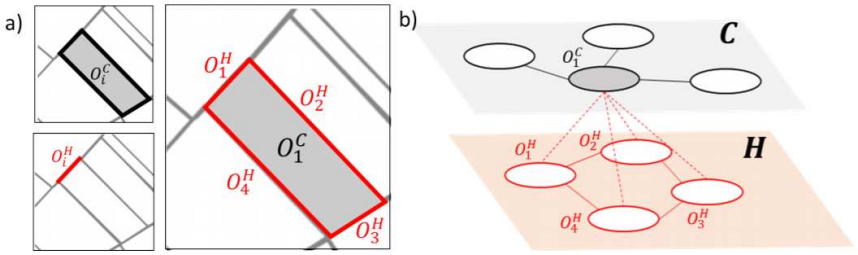

FIGURE 2: Représentation du paysage. a) Les polygones gris sont les parcelles, et les éléments linéaires rouges sont les segments. b) Réseau multicouche. La couche C représente le réseau des parcelles et la couche H représente le réseau des segments. Les liens entre le réseau C et H représentent les liens entre les parcelles et les segments.

Pour modéliser les éléments du paysage et leur structure spatiale, on définit un réseau multicouche. Un réseau est composé d'objets représentés par des noeuds (ou sommets), et l'interaction entre ces objets (telle que l'adjacence spatiale entre objets) est représentée par des liens entre les noeuds (Urban et al., 2009; Lü et al., 2016). Par exemple, deux polygones sont considérés comme étant adjacents s'ils partagent un de leurs cotés. Un réseau multi-couche est un ensemble de plusieurs réseaux avec des liaisons entre les noeuds appartenant à différents réseaux (Figure 2). Dans cette étude, le réseau multi-couche représente la liaison faite entre le réseau de parcelles (C) et le réseau de segments (H). Pour illustration, considérons une parcelle (O_C^1) qui est entourée par 4 haies $(O_H^1, O_H^2, O_H^3, O_H^4)$. D'abord, on établit le réseau des parcelles. Si deux parcelles sont

adjacentes, on trace le lien entre les deux noeuds. On fait la même chose pour les segments. Enfin on lie les objets adjacents des deux réseaux (voir les arêtes en pointillés dans la Figure 2b), où les haies $(O_H^1, O_H^2, O_H^3, O_H^4)$ sont adjacentes à la parcelle (O_C^1). Un réseau multi-couche est mathématiquement défini par sa matrice d'adjacence. Les entrées de la matrice d'adjacence indiquent si deux objets sont adjacents ou non. Si deux objets sont adjacents, le coefficient de la matrice vaudra 1 ; dans le cas contraire, le coefficient vaudra 0. La diagonale est toujours nulle car, pour des raisons de modélisation, nous supposons que les objets ne sont pas adjacents à eux-mêmes. Pour chaque paysage, on construit 3 matrices d'adjacence pour l'adjacence entre parcelles (A_C), entre segments (A_H) et entre parcelles et segments (A_{CH}).

3.1 Le modèle d'allocation

Dans ce travail, on vise a générer des paysages virtuels en simulant l'allocation des catégories d'usage de sol binaire. L'allocation des catégories dans le paysage est représentée par un modèle stochastique et paramétrique, construit comme un modèle de Gibbs, de type "famille exponentielle" pour pouvoir facilement estimer les paramètres. Étant donné $z = \{z_1, ..., z_n\} \in Z^n$, $\boldsymbol{x} = \{x_1, \ldots, x_n\} \in X^n$, la probabilité d'allouer une configuration $\boldsymbol{x}$ au paysage est définie comme suit :

$$p(\boldsymbol{x}) = \frac{1}{c(\boldsymbol{\beta})} \exp\left(-\sum_{k=1}^{m} \beta_k T_k(\boldsymbol{x})\right), \quad \boldsymbol{x} \in \mathcal{X}, \quad \boldsymbol{\beta} \in \mathbb{R}^m. \tag{1}$$

T_k sont m fonctions, appelées des descripteurs de paysages, $X \to (-\infty, +\infty)$, $k = 1, ..., m$ qui évaluent la valeur $T_k(\boldsymbol{x})$ représentant des statistiques d'intérêt pour guider l'allocation $\boldsymbol{x}$; $c(\beta) > 0$ est une constante de normalisation inconnue ; β est le vecteur des coefficients dont le rôle est de favoriser ou de pénaliser les fortes valeurs $T_k(\boldsymbol{x}) > 0$.

3.2 Les descripteurs du paysage

Les descripteurs de paysages, notés T_k, ont pour but de représenter les caractéristiques importantes du paysage. Ces caractéristiques peuvent représenter la composition (caractéristiques des objets) ou les interactions spatiales, temporelles, ou spatio-temporelles des objets dans le paysage. Dans ce travail, en terme de composition, nous considérons deux termes d'activité (pour contrôler la proportion d'éléments avec $X_i = 1$ pour les polygones et les segments), qui intègrent l'information de la surface d'une parcelle et de la longueur d'un segment. En terme d'interactions, on tient compte seulement des interactions spatiales entre les paires d'objets, et les descripteurs considérés sont basés sur adjacence entre les parcelles, l'adjacence entre les segments et l'adjacence entre les parcelles et les segments. Les descripteurs pour les parcelles sont notés T_k^C, et ceux pour les segments T_k^H. Un total de 9 descripteurs $(m = 9)$ pour notre modèle (équation 1) a été considéré :

Pour les parcelles, on a :
T_{act}^C : descripteur du terme d'activité, équivalent au nombre de parcelles ayant une culture ;
$T_{area,0.25}^C$: descripteur indiquant si une parcelle de culture est petite ou non. Une parcelle est considérée comme petite si son aire est inférieure au 1er quartile ;
$T_{area,0.75}^C$: descripteur indiquant si une parcelle de culture est grande ou non. Une parcelle est considérée comme grande si son aire est supérieure au 3e quartile ;
T_{adj}^{CH} : descripteur du nombre de haies adjacentes à chaque parcelle ;
T_{adj}^{CC} : descripteur du nombre de cultures adjacentes à chaque parcelle.

Pour les segments, on a :
T_{act}^H : descripteur du terme d'activité équivalent au nombre de segments ayant une haie ;
T_{length}^H : descripteur indiquant si une haie est longue ou non. Une haie est considérée comme longue si elle est supérieure à la médiane des haies du paysage ;
T_{orient}^H : descripteur indiquant si une haie est horizontale ou non. Une haie est considérée comme horizontale si son angle à partir d'un axe horizontal appartient à l'intervalle $[0, \frac{\pi}{6}] \cup [\frac{5\pi}{6}, 2\pi]$;
T_{adj}^{HH} : descripteur indiquant le nombre de haie adjacentes, cumulées pour tous les segments.

C	H
T^C_{act}, $T^C_{area,0.25}$, $T^C_{area,0.75}$, T^{CH}_{adj}, T^{CC}_{adj}	T^H_{act}, T^H_{length}, T^H_{orient}, T^{HH}_{adj}

Tableau 1: Résumé des descripteurs de notre modèle pour les parcelles (C) et les segments (H).

3.3 Estimation des paramètres

Dans cette partie, on aborde les méthodes utilisées pour estimer les paramètres $\beta_k, k \in \{1, ..., m\}$ et tester leur significativité. Le premier objectif est l'estimation des paramètres sur le paysage observé, pour ensuite pouvoir simuler des paysages différents mais partageant certaines caractéristiques avec le paysage observé.

Pour l'estimation des paramètres, idéalement, on utiliserait la méthode du maximum de vraisemblance , mais la constante de normalisation $c(\beta)$ ne peut pas être calculée facilement du fait du grand nombre de configurations $|\mathcal{X}|$ avait été plus limité, on aurait pu évaluer la constante $c(\beta)$. Au lieu de la vraisemblance classique, nous avons ici recours à la méthode de la vraisemblance composite (Besag, 1974), basée sur les probabilités conditionnelles d'allocation selon l'équation 2 :

$$p(x_i \mid \boldsymbol{x}_{-i}) = \frac{p(\boldsymbol{x})}{\sum_{y \in \mathcal{X}_i} p(\boldsymbol{x}_{-i}, x)} = \frac{\exp\left(-\sum_{k=1}^{m} \beta_k T_k(\boldsymbol{x})\right)}{\sum_{x \in \mathcal{X}_i} \exp\left(-\sum_{k=1}^{m} \beta_k T_k(\boldsymbol{x}_{-i}, x)\right)}, \tag{2}$$

La probabilité conditionnelle correspond à la probabilité d'allouer $x_i \in \{0; 1\}$ sachant l'allocation x_{-i} de tous les autres objets. La vraisemblance composite est définie comme le produit des probabilités conditionnelles,

$$\ell(\boldsymbol{\beta}) = \prod_{i=1}^{n} p(x_i \mid \boldsymbol{x}_{-i}), \tag{3}$$

où la constante $c(\beta)$ est éliminée. Dans le cas d'une allocation binaire, la vraisemblance composite est équivalente à la régression logistique suivante pour estimer les $\beta_k \in k = \{1, ..., m\}$ grâce à la fonction glm() du logiciel R :

$$\log \frac{p(x_i \mid \boldsymbol{x}_{-i})}{1 - p(x_i \mid \boldsymbol{x}_{-i})} = \sum_{k=1}^{m} \beta_k \left(T_k(\boldsymbol{x}) - T_k(\tilde{\boldsymbol{x}})\right). \tag{4}$$

Après l'estimation des paramètres, il est opportun de vérifier que l'estimation à l'aide de la vraisemblance composite n'induit pas de biais d'estimation des paramètres. Pour ce faire, on utilise la méthode du bootstrap paramétrique, qui consiste à simuler n allocations de paysage (par exemple $n = 100$) à partir du modèle estimé, et à ré-estimer les paramètres pour les simulations. Donc, on simule d'abord les vecteurs d'allocations des parcelles et segments. La simulation d'allocation dépend des paramètres estimés sur le paysage réel. L'algorithme utilisé pour simuler les allocations pour les parcelles et les segments est un échantillonneur de Gibbs, une variante de Monte-Carlo par chaînes de Markov (MCMC) (Fienberg, 2010).

Nous utilisons également l'approche de simulation pour tester la significativité de chaque paramètre (i.e. $\beta_k, k \in \{1, ..., m\}$ où m est le nombre de descripteurs) avec un test bilatéral de type Monte-Carlo. Le test est basé sur une variante du bootstrap paramétrique. L'hypothèse nulle (H_0) indique que le paramètre qu'on cherche à tester est égal à 0, et l'hypothèse alternative indique que le paramètre est différent de zéro. Un paramètre à la fois est testé en le mettant à zéro dans le modèle simulé, tandis que les autres paramètres gardent leurs valeurs estimés sur le paysage réel. Nous avons simulé n fois l'allocation avec le paramètre à tester avec la technique MCMC, et nous estimons à nouveau les paramètres à partir des paysages simulés. Pour le test statistique, nous étudions la probabilité que la valeur absolue du paramètre estimé sur un paysage simulé (avec le paramètre à tester mis à zéro) soit inférieure au paramètre absolu estimé sur le paysage réel ou n'ait pas le même signe. Si cette proportion est supérieure à $0,95$ alors on rejette l'hypothèse nulle pour conclure que le paramètre est significativement différent

de 0. Si la proportion est inférieure à $0,95$ alors on conserve H0, et on ne peut pas conclure sur la significativité du paramètre. Par exemple, pour tester la significativité du paramètre β^C_{act} (paramètre associé au descripteur T^C_{act}) les hypothèses établies sont :

$$H_0 : \beta^C_{act} = 0$$
$$H_1 : \beta^C_{act} \neq 0$$

On met β^C_{act} (dont la valeur estimée sur le paysage réel est -0,348) à 0, et on garde $\beta^C_{area,0.25}$ = -1.304 ; $\beta^C_{area,0.75}$ = 0.209 ; β^{CH}_{adj} = -0.254 ; β^{CC}_{adj} = 0.408. On simule n paysages et on estime les paramètres sur chaque paysage simulé. On obtient n estimations du paramètre étudiés. On calcule la proportion de β^C_{act} estimés qui sont supérieur à -0.348, et on prend une décision en fonction de cette proportion.

3.4 Estimation et validation du modèle

3.4.1 Résultats des estimations des paramètres

β^C_{act}	$\beta^C_{area,0.25}$	$\beta^C_{area,0.75}$	β^{CH}_{adj}	β^{CC}_{adj}
-0,348	-1,304	0,209	-0,254	0,408

Tableau 2: Les paramètres estimés des parcelles

Le descripteur $T^C_{area,0.25}$ indique si une parcelle de culture est petite ou pas. Le paramètre $\beta^C_{area,0.25}$ est négatif, donc les parcelles qui contiennent des cultures ont tendance à avoir une aire supérieure au 1er quartile. Le descripteur $T^C_{area,0.75}$ indique si une parcelle est grande (une aire supérieur au 3e quartile), $\beta^C_{area,0.75}$ positif indique donc que les parcelles avec des cultures ont tendance à être grande. Le descripteur T^{CH}_{adj} indique le nombre de haies adjacentes pour une parcelle et on a β^{CH}_{adj} qui est négatif. Cela veut dire que dans notre paysage, les haies ont tendances à être là où il n'y a pas de cultures. Le descripteur T^{CC}_{adj} indique l'adjacence des cultures, et le paramètre β^{CC}_{adj} est positif, ce qui signifie que les cultures ont tendance à former des agrégats.

β^H_{act}	β^H_{length}	β^{HH}_{adj}	β^H_{orient}
-3,649	-0,550	0,857	3,820

Tableau 3: Les paramètres estimés des segments

Le descripteur T^H_{length} indique si une haie est longue ou pas. Le fait que β^H_{length} soit négatif signifie que les haies ont tendance à être courtes. β^{HH}_{adj} et β^H_{orient} sont positifs. Le descripteur T^{HH}_{adj} indique le nombre de haies adjacentes, le paramètre β^{HH}_{adj} étant positif, les haies ont tendance à être adjacentes. Le descripteur T^H_{orient} indique la position (horizontale ou verticale des haies), et β^H_{orient} est positif donc les haies ont tendance à être horizontales.

3.4.2 Biais d'estimation et significativité des paramètres

On représente la distribution des paramètres estimés sur les paysages simulés et la valeur estimée sur le paysage réel à travers des boîtes à moustache. Ceci permet de visualiser la distribution des valeurs et de voir si les paramètres des paysages simulés coïncident avec ceux du paysage réel.

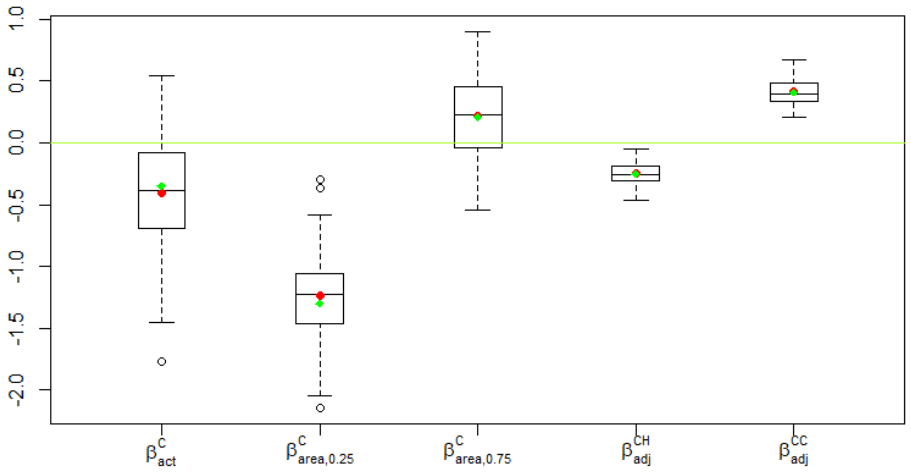

FIGURE 3: Distribution des paramètres pour les parcelles. Le point vert représente β estimé sur le paysage réel, le point rouge représente la moyenne des β estimés sur les 100 paysages simulés

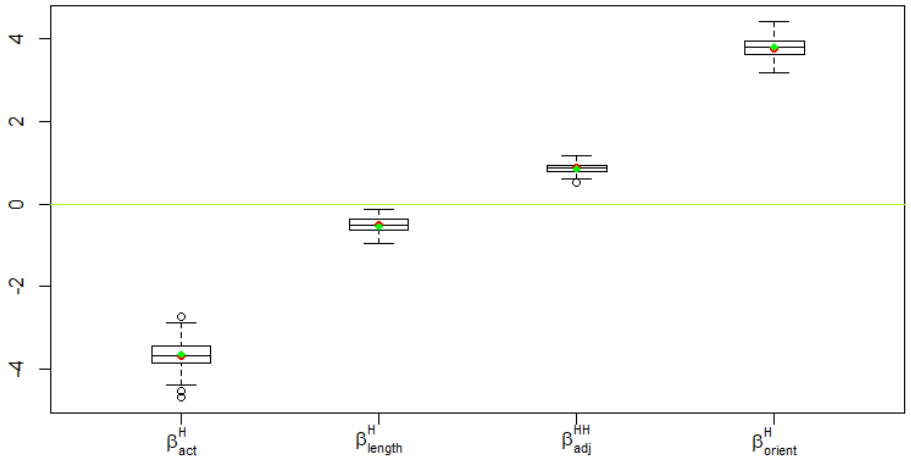

FIGURE 4: Distribution des paramètres pour les segments. Le point vert représente β estimé sur le paysage réel, le point rouge représente la moyenne des β estimés sur les 100 paysages simulés

Si on compare les Figures 3 et 4, nous remarquons que les paramètres des parcelles ont une distribution plus dispersée car il y a moins de parcelles que de segments ce qui augmente la variabilité des estimations. Pour tous les paramètres (parcelles et segments) la distribution des simulations coïncident avec la valeur estimée sur le paysage réel. Cela montre que le modèle

n'est pas biaisé et que les simulations réalisées avec les paramètres estimés reproduisent les caractéristiques du paysage réel.

β^C_{act}	$\beta^C_{area,0.25}$	$\beta^C_{area,0.75}$	β^{CH}_{adj}	β^{CC}_{adj}
0,83	**1**	0,73	**0,96**	**1**

Tableau 4: Statistique de test (probabilité) pour chaque paramètre des parcelles.

Selon le Tableau 4, les paramètres $\beta^C_{area,0.25}$, β^{CH}_{adj} et β^{CC}_{adj} sont significatifs, ce qui n'est pas le cas pour $\beta^C_{area,0.75}$. Ce résultat est cohérent avec la distribution de ce paramètre présenté dans la Figure 3. En effet la distribution pour ce paramètre contient les valeurs nulles, alors que les distributions de $\beta^C_{area,0.25}$, $\beta^C_{area,0.75}$ et β^{CC}_{adj} n'incluent pas zéro.

β^H_{act}	β^H_{length}	β^{HH}_{adj}	β^H_{orient}
1	**1**	**1**	**1**

Tableau 5: Statistique de test (probabilité) pour chaque paramètre des segments.

Pour les haies, les probabilités confirment les résultats des boîtes à moustaches : tous les paramètres sont significativement différent de 0 (Tableau 5).

4 Métriques de validation

Selon la représentation, en vecteur ou en raster, d'un paysage, des métriques paysagères différentes existent. Les métriques sont des fonctions qui visent à synthétiser les propriétés et les caractéristiques des paysages. Dans le cas présent, elles nous permettrons de vérifier que les paysages simulés se rapprochent du paysage réel. Les métriques peuvent être à l'échelle globale, auquel cas nous avons une métrique pour tout le paysage, ou à l'échelle locale, auquel cas nous avons plusieurs valeurs pour un même paysage (i.e. une valeur pour chaque élément du paysage considéré).

Les métriques fréquemment utilisées requièrent une représentation sous forme d'un réseau du paysage, ce qui est notre cas (cf chapitre 3). Il existe aussi des métriques pour les paysages représentés en raster (McGarigal, 1995), et dans ce travail, on cherche à voir si le modèle réussi à capturer la compléxité d'un paysage rasterisé. Etant donné que les données initiales se présentent sous forme d'un paysage vectorisé, pour utiliser une représentation en raster, on transforme le paysage vectorisé en un raster avec une resolution 100 x 100 pixels. Les métriques utilisées sont décrites dans le Tableau 6.

Nom	Description	Support	Plage de valeurs	Références
Degré*	Nombre de noeuds connectés	noeud	[0 ;1]	[1],[2]
Coreness	Décomposition k-core de l'influence d'un noeud	noeud	[0 ;∞[	[1],[2]
Degré 2e niveau*	Nombre de noeuds connectés à au plus 2 pas	noeud	[0 ;1]	[1],[2]
Excentricité*	Nombre de liens nécessaire pour relier le noeud le plus distant	noeud	[0 ;1]	[1],[2]
Proximité	Inverse de la distance géodésique entre les noeuds	noeud	[0 ;∞[	[1],[2]
Intermédiarité*	Utilité du noeud dans la transmission d'information sur le réseau	noeud	[0 ;1]	[1],[2]
Diamètre	Chemin le plus long	réseau	[0 ;∞[	[1]
Efficacité	Efficacité d'échange d'informations	réseau	[0 ;∞[	[2],[3]
Coefficient de clustering	Probabilité que deux noeuds soient connectés sachant qu'ils ont un voisin en commun	réseau	[0 ;1]	[2],[3]
PLAND [%]	Proportion d'une catégorie dans un paysage	raster	[0 ;100]	[4],[5]
PD [# / ha 100]	Densité d'une catégorie	raster	[0 ;∞[	[4],[5]
ENN [m]	Distance entre plus proche voisins	raster	[0 ;∞[	[4],[5]
PARA [/]	Rapport périmètre-aire d'une catégorie	raster	[0 ;∞[	[4],[5]
IJI [/]	Index mesurant la mixité spatiale des catégories	raster	[0 ;100]	[4],[5]
CLUMPY [/]	Index mesurant si la distribution d'une catégorie est aléatoire	raster	[-1 ;1]	[4],[5]

Tableau 6: Métriques des paysages. L'étoile (*) indique que les métriques ont été normalisées par le nombre de noeuds. Une métrique peut être de type noeud ou de type réseau (Lü et al., 2016; McGarigal, 1995; Latora and Marchiori, 2001; Urban et al., 2009; Cushman et al., 2008).

4.1 Les métriques des réseaux

On représente le paysage vectorisé sous forme d'un réseau avec des liens entre les objets (cf. chapitre 3). Par conséquent, les métriques sont établies soit à l'échelle des noeuds soit à l'échelle du réseau (ensemble de tous les noeuds et liens). On rappelle qu'un noeud est un objet (parcelles, segments). Dans la suite, on calcule donc les métriques pour le réseau des parcelles avec une culture et le réseau des segments avec une haie.

Les métriques à l'échelle des noeuds sont les suivantes :

1. La **centralité de degré** (*degree centrality* en anglais) ou tout simplement le **degré** est le nombre de liens depuis un sommet. Cette centralité est normée en la rapportant au nombre de sommets moins un.
2. Le **coreness** est une mesure permettant d'identifier les noeuds fortement interconnectés sur un réseau. Elle ressemble au degré, mais le coreness tient aussi compte de la position du noeud sur le réseau. Ceci est du fait qu'il est probable qu'un noeud situé au centre soit plus influent dans la transmission d'information qu'un noeud situé sur la périphérie du réseau. Cette mesure est calculée selon une décomposition en k-core. (cf. section 2.1.4, Lü et al. (2016)). Un noeud avec un coreness élevé correspond à un objet qui est entouré par plusieurs objets de la même catégorie et qui est au centre du réseau.
3. La **centralité de degré de 2e niveau** ou **degré 2e niveau** (*degree grade 2* en anglais) ressemble au degré mais tient aussi compte du degré des voisins d'un noeud. En d'autres termes, dans un réseau non-orienté, le degré 2e niveau d'un noeud est le nombre de liens connectés à ce noeud à deux pas plus loin. Cette centralité est normée en la rapportant au nombre de sommets moins un.

4. L'**excentricité** (*eccentricity* en anglais) d'un noeud correspond au nombre de liens nécessaires pour relier le noeud le plus distant. Plus l'excentricité d'un noeud est faible, plus le noeud est considéré comme influent. Pour comparer l'excentricité dans différents réseaux, cette métrique est normalisée. (cf section 2.2.1, Lü et al. (2016)). Un noeud avec une faible excentricité correspond à un objet adjacent à plusieurs objets de la même catégorie.
5. La **centralité de proximité** ou **proximité** (*closeness* en anglais) d'un noeud est l'inverse de la distance géodésique (chemin le plus court) entre ce noeud et tous les autres noeuds. La centralité de proximité d'un noeud est élevée quand sa distance à tous les autres noeuds est faible. Le noeud le plus central est "proche" de toute l'information dans le réseau.
6. La **centralité d'intermédiarité** ou **intermédiarité** (*betweenness* en anglais) mesure l'utilité d'un noeud dans la transmission de l'information au sein du réseau. Le noeud joue un rôle central si beaucoup de plus courts chemins entre deux sommets doivent emprunter ce noeud.

Les métriques de centralité (degré, degré 2e niveau, proximité, intermédiarité) avec une valeur élevée correspondent à des objets entourés par beaucoup d'objets de la même catégorie.

À l'échelle du réseau les métriques sont les suivantes :

7. Le **diamètre** (*diameter* en anglais) d'un graphe est la plus grande distance géodésique possible qu'il puisse exister entre deux sommets. Un réseau avec un grand diamètre indique que les objets ont une forte connectivité, mais n'indique pas forcément si ces objets forment des agrégats.
8. L'**efficacité** (*efficiency* en anglais) d'un graphe est une mesure de l'efficacité d'échange d'informations sur un réseau. L'éfficacité entre deux noeuds est l'inverse de la distance géodésique entre ces noeuds. L'éfficacité globale d'un graphe correspond à la moyenne des efficacités entre chaque paire de noeuds. Un réseau avec une grande efficacité indique que les objets de même catégorie ont tendance à être adjacents.
9. Le **coefficient de clustering** (*cluster average* en anglais) d'un graphe (aussi appelé **coefficient d'agglomération**, **de connexion**, **de regroupement**, **d'aggrégation**) est une mesure du regroupement des noeuds dans un réseau. Plus précisément, ce coefficient est la probabilité que deux noeuds soient connectés, sachant qu'ils ont un voisin en commun. Le coefficient de clustering est calculé en faisant le rapport entre le nombre de triangle (connexion entre trois noeuds) formés dans un graphe au nombre total de triangles possibles. Un coefficient de clustering élevé indique que les objets de même catégorie ont tendance à former des agrégats.

Les métriques des réseaux sont basés sur la théorie des graphes. De ce fait, certaines métriques tiennent compte de la transmission de l'information. Dans notre cas la transmission correspondrait à la dynamique proie-prédateur.

4.2 Les métriques basées sur une représentation en raster des paysages

Un paysage représenté par un raster est composé de cellules (ou pixels) qui contiennent de l'information géographiques (i.e. les coordonnées) et l'information que le raster vise à représenter. Ici, l'information que nous représentons correspond à la catégorie d'allocation d'usage de sol du pixel. Le paysage rasterisé contient trois catégories d'allocations possibles : habitat semi-naturel, culture ou haie. Un ensemble de pixels adjacents de la même catégorie est appelé une tache (de l'anglais "*patch*"). On calcule les métriques suivantes à l'échelle des catégories d'allocation :

1. La **proportion (PLAND)** correspond à la proportion d'une catégorie d'allocation dans le paysage.
2. La **densité des habitats (PD)** correspond au nombre de tache d'une catégorie
3. La **distance des voisinages (ENN)** est la distance (en ligne droite) la plus courte entre une tache et son voisin le plus proche de la même catégorie.
4. Le **rapport périmètre-aire (PARA)** est le rapport entre le périmètre et la surface d'une catégorie de tache, dans lequel la forme de de la tache est confondue avec sa taille ; si la forme est constante, une augmentation de la taille de la tache entraînera une diminution du rapport périmètre-aire.

5. L'**index d'interspersion et de juxtaposition (IJI)** est un index qui mesure la mixité des habitats. Cet index indique si un habitat a tendance à être adjacent à un seul ou plusieurs habitats. Un index IJI avec une grande valeur indique une forte mixité.
6. L'**agrégation (CLUMPY)** (*clumpiness* en anglais) est un index calculé en fonction de la matrice d'adjacence qui indique la fréquence à laquelle deux habitats de catégories différentes sont adjacents. Cette index mesure si la distribution d'un habitat a tendance à être aléatoire ou agrégé. Si la valeur de cet index est élevée, cela veut dire que ce type d'habitat a tendance à être groupé.

4.3 Résultats de la validation

On souhaite évaluer si les paysages simulés arrivent à capturer les caractéristiques du paysage réel sur des métriques qui ne sont pas considérées dans le modèle, c'est-à-dire sur des caractéristiques paysagères qui ne sont pas prises en compte lors de l'estimation des paramètres. On commence par visualiser la distribution des métriques calculées sur les paysages simulés et on les compare aux métriques calculées sur le paysage réel. Ensuite, on réalise un test pour évaluer la pertinence des métriques à l'échelle du réseau.

Pour tester la pertinence d'une métrique, pour chaque catégorie d'élément (parcelles, segments), on teste l'égalité de cette métrique à la valeur réelle (valeur estimée sur la paysage réel).

Nous faisons les hypothèses suivantes :

L'hypothèse nulle (H_0) indique que la métrique que l'on cherche à tester est égale à la valeur réelle contre l'hypothèse alternative indiquant que la métrique est différente de valeur réelle.

Il y a deux statistiques de tests pour vérifier H_0 que l'on appelle dans la suite p-valeur :

(i) Si la moyenne de la métrique sur les 100 simulations est inférieure à la valeur réelle, alors la p-valeur c'est la proportion des simulations où cette métrique est supérieur à la valeur réelle. On ne rejette pas H0 si la p-valeur est supérieur à 0,05.
(ii) Si la moyenne de la métrique sur les 100 simulations est supérieur à la valeur réelle, alors la p-valeur c'est la proportion des simulations où cette métrique est inférieur à la valeur réelle. On ne rejette pas H0 si la p-valeur est supérieur à 0,05.

4.3.1 Validation des métriques du réseau

Un paysage représenté comme un réseau est composé de plusieurs noeuds. Par conséquent, pour chaque paysage (simulé ou le paysage réel) on a un ensemble de valeurs pour chaque métrique à l'échelle des noeuds. On a une seule valeur pour chaque métrique à l'échelle de tout le réseau.

Etant donné les 100 simulations de paysage, on a une distribution pour chaque métrique. Pour les métriques à l'échelle des noeuds, la distribution des simulations correspond à tous les noeuds des 100 simulations et la distribution du paysage réel correspond à tous les noeuds du paysage. Pour les métriques à l'échelle du réseau, la distribution des simulations correspond à la métrique calculée sur chaque paysage simulé.

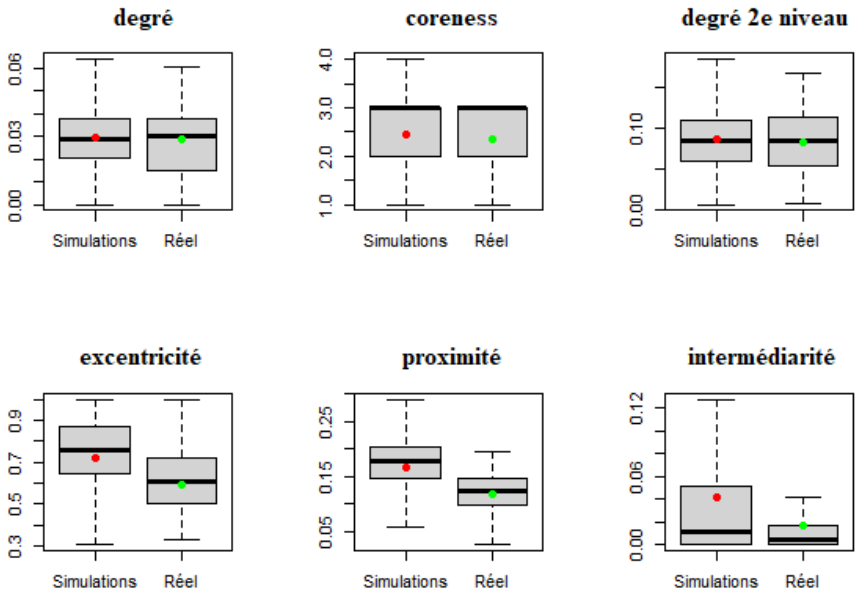

FIGURE 5: Distribution des métriques à l'échelle des noeuds pour le réseau des cultures. A gauche, les boîtes à moustaches des métriques pour les paysages simulés. A droite, les boîtes à moustaches des métriques pour le paysage réel. Le point rouge représente la moyenne de la métrique des paysages simulés et le point vert représente la moyenne de la métrique du paysage réel.

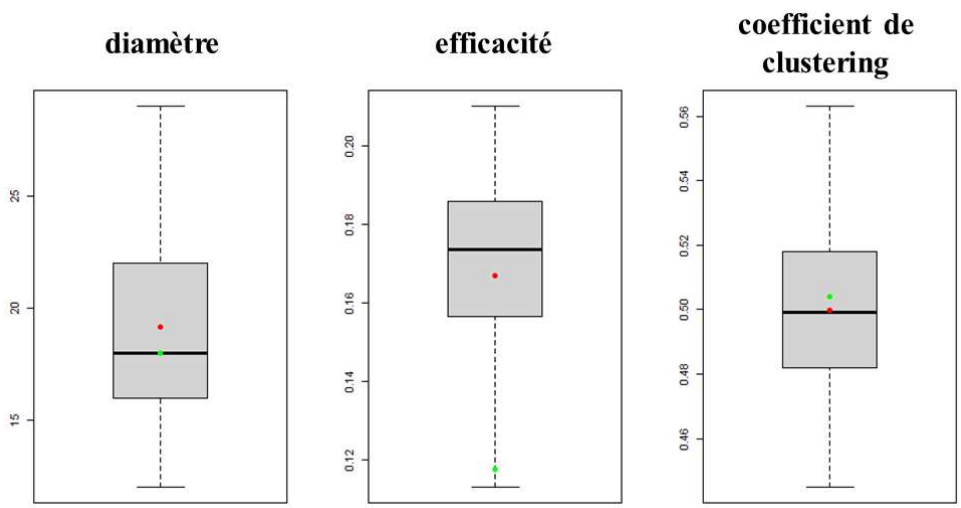

FIGURE 6: Distribution des métriques à l'échelle du réseau pour le réseau des parcelles. Le point vert représente la valeur du paysage réel, le point rouge représente la moyenne de la métrique des paysages simulés.

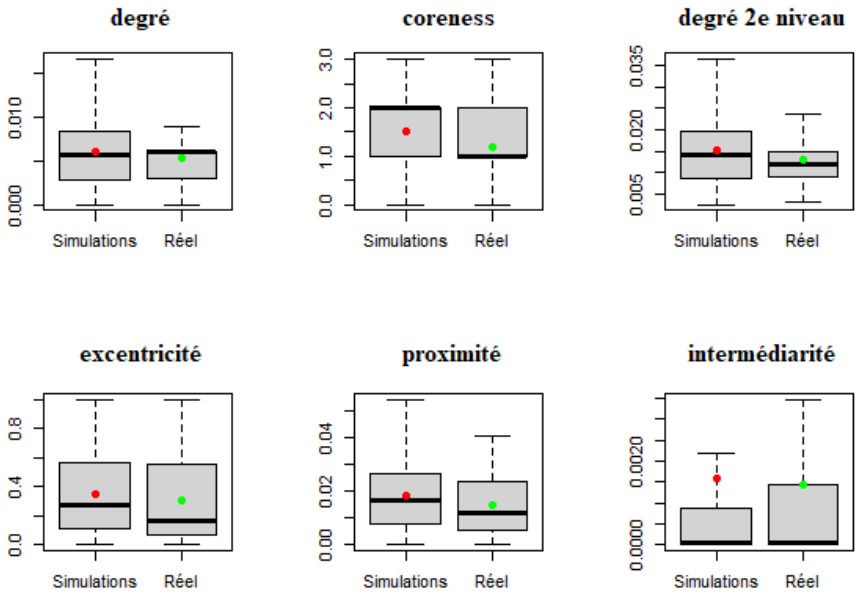

FIGURE 7: Distribution des métriques à l'échelle des noeuds pour le réseau des segments. A gauche, les boîtes à moustaches des métriques pour les paysages simulés. A droite, les boîtes à moustaches des métriques pour le paysage réel. Le point rouge représente la moyenne de la métrique des paysages simulés et le point vert représente la moyenne de la métrique du paysage réel.

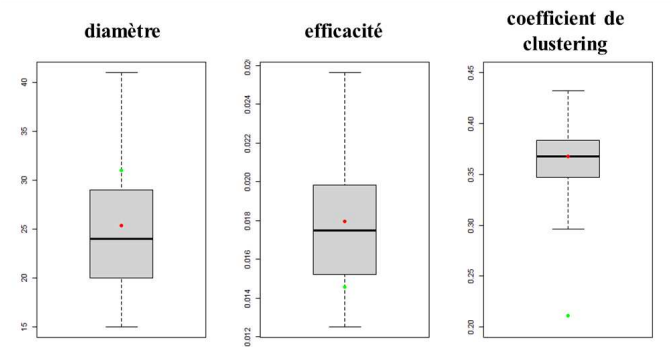

FIGURE 8: Distribution des métriques à l'échelle du réseau pour le réseau des segments. Le point vert représente la valeur du paysage réel, le point rouge représente la moyenne de la métrique des paysages simulés.

	Culture	Haie
Diamètre	**0,42**	**0,18**
Efficacité	**0,06**	**0,12**
Coefficient de clustering	**0,44**	0,00

Tableau 7: Statistique de test (p-valeur) pour chaque métrique.

Selon le Tableau 7, on a les p-valeurs du diamètre, de l'efficacité et du coefficient de clustering qui sont supérieures à 0,05 pour le réseau des parcelles. On ne peut donc pas conclure qu'il y a une différence significative entre la métrique calculée sur les simulations et la métrique calculée sur le paysage réel. On ne peut pas rejeter l'hypothèse que l'allocation des parcelles dans les paysages simulés se rapprochent à celle du paysage réel.

Pour les segments, le diamètre et l'efficacité ont des p-valeurs supérieures à 0,05 qui ne permettent pas de conclure d'une différence significative entre la métrique calculée sur les simulations et la métrique calculée sur le paysage réel. Cependant la p-valeur du coefficient de clustering est nulle est on rejette l'hypothèse d'égalité. On peut conclure que le coefficient de clustering calculé sur les simulations ne correspond pas à la réalité. Ceci étant dit, sachant que cette métrique varie entre 0,30 et 0,43 selon les simulations et vaut 0,20 selon le paysage réel, les ordres de grandeurs sont conservés entre les paysages simulés et le paysage réel.

4.3.2 Validation des métriques des paysages

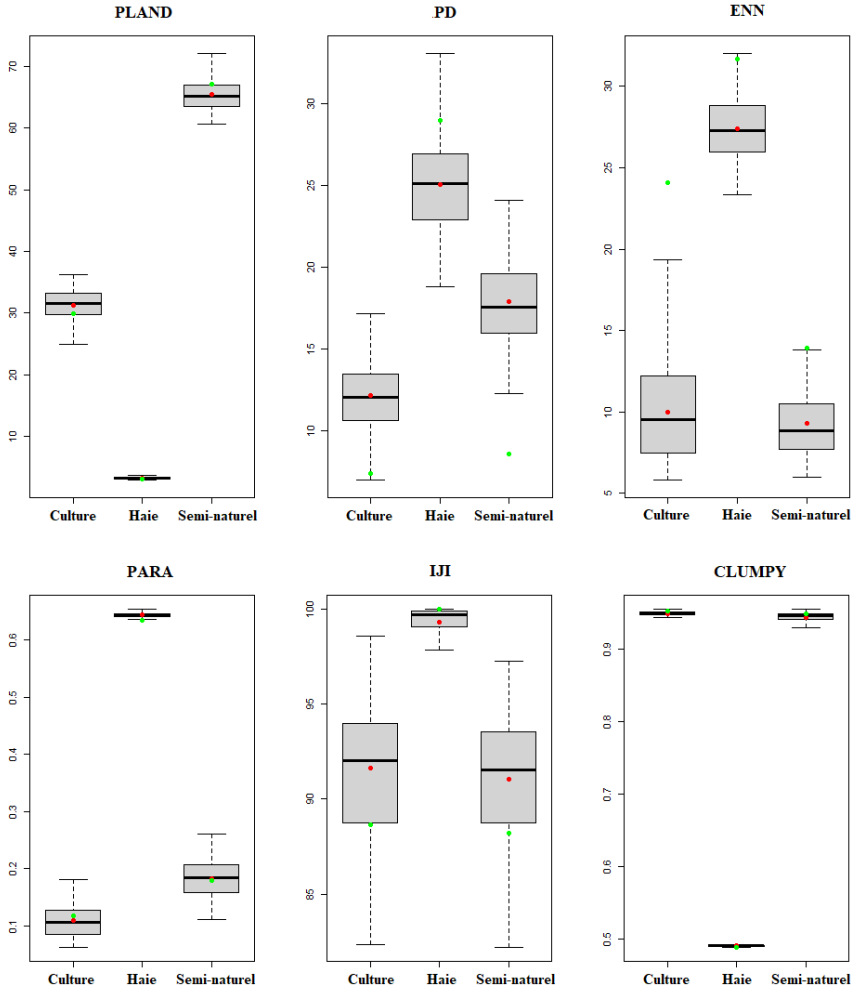

FIGURE 9: Distribution des métriques des paysages selon chaque catégorie d'allocation (culture, haie, habitat semi-naturel

	Semi-naturel	Culture	Haie
PLAND	**0,25**	**0,25**	**0,12**
PD	0,00	0,03	**0,06**
ENN_MN	0,03	0,00	0,02
PARA	**0,45**	**0,37**	0,00
IJI	**0,19**	**0,24**	**0,11**
CLUMPY	**0,24**	**0,09**	0,02

Tableau 8: Statistique de test (p-valeur) pour chaque métrique de chaque catégorie d'allocation.

Selon le Tableau 8, on ne peut pas conclure qu'il y a une différence significative entre la valeur réelle des métriques PLAND et IJI et la valeur calculée sur les paysages simulés. On peut dire que le modèle arrive à bien reproduire le pourcentage des habitats et la mixité du paysage réel dans les simulations. La densité des habitats de type haie du paysage réel arrive à être reproduite dans les simulations (p-valeur=0,06). Ceci est aussi le cas pour rapport perimètre-aire et l'agrégation des habitats de type semi-naturel ou culture.

5 Analyse de sensibilité

Dans cette partie, on cherche à évaluer la sensibilité du modèle aux paramètres d'interaction : (1) adjacence entre parcelles, (2) adjacence entre segments et (3) adjacence entre parcelles et segments. Cette analyse permettra de comprendre le lien entre ces trois paramètres et les structures paysagères simulées par le modèle en étudiant comment différentes configurations de paramètres affectent l'allocation des cultures et des haies dans les paysages simulés. Les paramètres de l'adjacence entre parcelles (T_{adj}^{CC}), l'adjacence entre segments (T_{adj}^{HH}) et l'adjacence entre parcelles et segments (T_{adj}^{CH}) varient sur l'intervalle [-5 ;5] avec un pas de 1 alors que les autres paramètres (cf. Tableau 1) sont fixés. Ceci amène à 1331 configurations de paramètres possibles. Pour chaque configuration, on simule 50 répétitions des paysages pour chaque configuration des paramètres et on calcule les métriques (cf chapitre 4.1, 4.2) sur chaque simulation.

On décide de faire varier les paramètres sur l'intervalle [-5 ;5], car cet intervalle contient toutes les valeurs des paramètres estimées sur le paysage réel. Selon les figures 3 et 4, on a un intervalle entre [-2 ;1] pour les paramètres des descripteurs des parcelles et un intervalle entre [-4,5 ;4,5] pour les paramètres des descripteurs des segments. Le choix de simuler 50 répétitions des paysages repose sur le fait que la variance des paramètres estimés se stabilise autour de 50 simulations lorsque calculée sur un nombre croissant de simulations.

Etant donné que pour chaque paysage il y a un ensemble de valeurs pour les métriques à l'échelle des noeuds, on décide de moyenner ces métriques sur tous les noeuds du paysage afin de se retrouver avec une métrique par simulation. Pour chaque paysage simulé, on a donc les métriques suivantes à l'échelle du réseau :

1. Le diamètre ;
2. l'efficacité ;
3. le coefficient de clustering ;
4. la degré moyen ;
5. le coreness moyen ;
6. le degré 2e niveau moyen ;
7. l'excentricité moyenne ;
8. la proximité moyenne ;
9. l'intermédiarité moyenne.

et pour les métriques qui basées sur une représentation en raster des paysages, on a les mêmes que celles du tableau 6.

Nous réalisons une analyse en composantes principales (ACP), qui nous permet d'explorer les liaisons entre les métriques (nos variables) et les configurations des paramètres.

Dans une ACP, les variables d'entrée sont remplacées par de nouvelles variables qui sont des combinaisons des variables initiales. Ces nouvelles variables sont appelées **composantes principales** (CP) ou **axes principaux**. Pour savoir quelles composantes principales utiliser pour l'analyse, on se réfère à leurs variances. Seules les composantes principales dont la variance excède 1 sont retenues (critère de Kaiser). En calculant la contribution de chaque composante principale, on peut trouver la part d'information initiale conservée par les axes choisies, qui est égale à la somme des contributions des axes qu'on conserve.

Pour voir le lien entre les variables initiales et les composantes principales, on utilise un tableau des corrélations. On analyse ensuite les variables initiales qui sont significativement corrélées aux composantes principales conservées (i.e. corrélations supérieures ou égales à 0.7 ou inférieurs ou égales à -0.7). On réalise l'ACP pour sur les métriques du réseau et les métriques du raster séparément. Pour les métriques du réseaux, on réalise deux ACP. Dans la première ACP, les variables initiales sont les moyennes (sur les 50 répétitions) des métriques listées dans le chapitre 5. Dans la deuxième ACP, les variables initiales sont les variances des mêmes métriques. Pour

les métriques des raster, on réalise trois ACP, une pour chaque catégorie (habitat semi-naturel, culture, haie). Pour identifier l'effet des descripteurs (T_{adj}^{CC}, T_{adj}^{HH} et T_{adj}^{CH}) sur l'ensemble des metriques, on réalise une régression linéaire des composantes principales en fonction des trois descripteurs. On indique le coefficient estimé (ce), l'erreur type (ErT) et la p-valeur (p).

5.1 ACP sur le réseau des parcelles

5.1.1 Analyse des moyennes entre répétitions

	CP1	CP2	CP3	CP4	CP5	CP6	CP7	CP8	CP9
Contribution	0,76	0,17	0,05	0,01	0,01	0,00	0,00	0,00	0,00
Variance	**6,86**	**1,52**	0,42	0,13	0,05	0,02	0,01	0,00	0,00

Tableau 9: Contributions et variances des composantes principales.

	CP1	CP2	CP3	CP4	CP5	CP6	CP7	CP8	CP9
Diamètre	-0,34	**0,91**	0,15	-0,16	-0,09	-0,02	-0,01	0,00	0,00
Efficacité	**-0,98**	-0,05	-0,19	-0,04	0,04	-0,01	-0,04	0,00	0,00
Coefficient de clustering	**-0,83**	-0,10	0,53	0,01	0,10	0,00	-0,01	0,00	0,00
Degré moyen	**-0,91**	-0,38	0,10	-0,02	-0,11	0,06	0,02	0,01	0,00
Coreness moyen	**-0,97**	-0,20	-0,05	-0,09	0,02	-0,08	0,05	0,00	0,00
Degré 2e niveau moyen	**-0,93**	-0,35	-0,02	-0,03	-0,09	0,02	-0,01	-0,02	0,00
Excentricité moyenne	**-0,88**	0,37	-0,02	0,30	-0,05	-0,03	0,00	0,00	0,00
Proximité moyenne	**-0,98**	-0,05	-0,19	-0,04	0,04	-0,01	-0,04	0,00	0,00
Intermédiarité moyenne	**-0,85**	0,49	-0,15	-0,01	0,10	0,08	0,03	0,00	0,00

Tableau 10: Corrélations entre les métriques moyennées et les composantes principales.

La régression de la CP1 en fonction des descripteurs indique que seul le paramètre contrôlant l'adjacence entre parcelles a un effet significatif (*ce=2,687e-01 ; ErT=7,751e-03 ; p<2e-16*). Ce résultat est cohérent avec le fait que ce descripteur affecte directement les métriques du réseau des parcelles. Au contraire, la régression de la CP2 en fonction des descripteurs montre que c'est le paramètre contrôlant l'adjacence entre parcelles et segments qui affecte cet axe (*ce=2,687e-01 ; ErT=7,751e-03 ; p<2e-16*). La CP2 étant liée essentiellement au diamètre du réseau nous pouvons dire ici que ce dernière augmente avec l'augmentation de l'adjacence entre les parcelles et segments. Le diamètre évalue la connectivité des cultures dans le paysage et quand on a un grand diamètre cela signifie que toutes les cultures sont bien connectées et le paysage n'est pas fragmenté (i.e. chaque culture est adjacente à au moins une autre culture). Vu que les haies sont placées sur la bordure des parcelles, l'adjacence entre les cultures et haies favorise aussi l'adjacence entre les deux parcelles qui partagent la haie.

5.1.2 Analyse de la variance entre répétitions

Dans cette partie nous étudions comment la variance entre les réplications peut être expliquée par les différentes configurations de paramètres. Cette variance reflète la stochasticité du générateur de paysage. Contrairement à l'analyse des moyennes (chapitre 5.1.1), nous nous intéressons ici à comprendre en quoi une même configuration de paramètres peut amener à des paysages différents. Selon le Tableau 11, les trois premières composantes principales conservent 81% de l'information initiale et leurs variances respectives sont supérieures à 1.

	CP1	CP2	CP3	CP4	CP5	CP6	CP7	CP8	CP9
Contribution	0,42	0,24	0,15	0,07	0,07	0,03	0,01	0,01	0,00
Variance	**3,78**	**2,15**	**1,31**	0,65	0,64	0,31	0,10	0,06	0,00

Tableau 11: Contributions et variances des composantes principales.

	CP1	CP2	CP3	CP4	CP5	CP6	CP7	CP8	CP9
Diamètre	-0,60	-0,57	0,05	-0,16	-0,49	0,16	0,13	0,07	0,00
Efficacité	**-0,92**	0,15	0,23	0,08	0,18	-0,16	0,05	0,06	0,00
Coefficient de clustering	0,09	**-0,74**	-0,54	-0,05	-0,05	-0,39	0,02	-0,03	0,00
Degré moyen	-0,66	0,03	**-0,71**	-0,03	0,05	0,13	-0,16	0,10	0,00
Coreness moyen	0,14	0,69	-0,23	0,48	-0,45	-0,12	0,02	0,02	0,00
Degré 2e niveau moyen	-0,69	0,45	-0,50	-0,09	0,10	0,11	0,13	-0,15	0,00
Excentricité moyenne	0,17	**0,73**	0,02	-0,60	-0,20	-0,17	-0,02	0,04	0,00
Proximité moyenne	**-0,92**	0,15	0,23	0,08	0,18	-0,16	0,05	0,06	0,00
Intermédiarité moyenne	**-0,86**	-0,14	0,34	0,00	-0,28	-0,05	-0,17	-0,13	0,00

Tableau 12: Corrélations entre les variances des métriques et les composantes principales.

Selon le Tableau 12, les variances de l'efficacité, de la proximité moyenne et de l'intermédiarité moyenne sont négativement corrélés à la CP1. La variance du coefficient de clustering est négativement corrélé à la CP2 alors que la variance de l'excentricité moyenne est positivement corrélée à la CP2. La variance du degré moyen est négativement corrélé à la CP3. Ainsi l'axe 1 peut être interprété comme les configurations qui simule des paysages où l'adjacence des cultures varie faiblement (valeurs positives) ; l'axe 2 comme les configurations où l'agrégation des cultures varie faiblement mais l'adjacence est différente (valeurs positives) et l'axe 3 comme les configurations où l'adjacence varie faiblement (valeurs positives).

La régression de la CP1 en fonction des descripteurs indique que les paramètres contrôlant l'adjacence entre parcelles (*ce= -8,902e-02 ; ErT=1,629e-02 ; p=5,58e-08*) et entre parcelles et segments (*ce=1,319e-01 ; ErT=1,629e-02 ; p =1,28e-15*) ont un effet significatif. La régression de la CP2 en fonction des descripteurs montre que les paramètres de l'adjacence entre parcelles (*ce=3,030e-01 ; ErT=8,949e-03 ; p<2e-16*) et de l'adjacence entre parcelles et segments (*ce=-1,311e-01 ; ErT=8,949e-03 ; pp<2e-16*) ont un effet significatif. Pour la régression de la CP3, on a aussi l'adjacence entre parcelles (*ce=1,056e-01 ; ErT=7,974e-03 ; p<2e-16*) et entre parcelles et segments (*ce=1,882e-01 ; ErT=7,974e-03 ; p<2e-16*) qui ont un effet significatif. Ce résultat est cohérent avec le fait que ces descripteurs affectent directement les métriques liées à l'adjacence des cultures.

5.2 ACP sur le réseau des segments

5.2.1 Analyse des moyennes entre répétitions

	CP1	CP2	CP3	CP4	CP5	CP6	CP7	CP8	CP9
Contribution	0,94	0,04	0,02	0,00	0,00	0,00	0,00	0,00	0,00
Variance	**8,43**	0,34	0,21	0,01	0,01	0,00	0,00	0,00	0,00

Tableau 13: Contributions et variances des composantes principales.

On a les deux premières composantes principales qui conservent 98% de l'information initiale. Et seule la première composante principale à une variance supérieure à 1.

	CP1	CP2	CP3	CP4	CP5	CP6	CP7	CP8	CP9
Diamètre	**-0,99**	-0,04	0,04	0,08	0,01	-0,01	0,01	0,00	0,00
Efficacité	**-0,99**	0,11	-0,01	-0,02	0,04	0,00	0,00	0,00	0,00
Coefficient de clustering	**-0,88**	-0,29	-0,37	-0,01	-0,01	0,00	0,00	0,00	0,00
Degré moyen	**-0,98**	-0,12	0,12	-0,01	-0,02	0,03	0,01	0,00	0,00
Coreness moyen	**-0,98**	-0,16	0,13	0,01	-0,01	0,01	-0,02	0,00	0,00
Degré 2e niveau moyen	**-1,00**	-0,06	0,08	-0,02	0,01	0,02	0,01	-0,01	0,00
Excentricité moyenne	**-0,99**	0,02	0,11	-0,03	-0,03	-0,04	0,00	0,00	0,00
Proximité moyenne	**-0,99**	0,11	-0,01	-0,02	0,04	0,00	0,00	0,00	0,00
Intermédiarité moyenne	**-0,89**	0,43	-0,15	0,01	-0,03	0,01	0,00	0,00	0,00

Tableau 14: Corrélations entre les métriques moyennées et les composantes principales.

Selon le tableau 14, toutes les métriques sont négativement corrélées à la première composante principale (CP1). L'axe 1 peut être interprété comme les configurations avec un réseau où les haies ont tendance à être dispersées (valeurs positives). De plus, le diamètre corrélé négativement indique que les haies ont aussi tendance à être isolées (valeurs positives).

La régression de la CP1 en fonction des descripteurs indique que seul le paramètre contrôlant l'adjacence entre segments (*ce=-7,165e-01 ; ErT=1,575e-02 ; p<2e-16*) a un effet significatif. Ce résultat est cohérent avec le fait que ce descripteur affecte directement les métriques du réseau des segments.

5.2.2 Analyse de la variance entre répétitions

	CP1	CP2	CP3	CP4	CP5	CP6	CP7	CP8	CP9
Contribution	0,76	0,13	0,05	0,02	0,02	0,02	0,01	0,00	0,00
Variance	**6,86**	**1,15**	0,43	0,19	0,15	0,12	0,08	0,03	0,00

Tableau 15: Contributions et variances des composantes principales.

Les deux premières composantes principales conservent 89% de l'information initiale et se sont les seules à avoir une variance supérieure à 1.

	CP1	CP2	CP3	CP4	CP5	CP6	CP7	CP8	CP9
Diamètre	**-0,93**	-0,11	0,14	0,04	0,23	0,21	-0,03	0,05	0,00
Efficacité	**-0,91**	-0,37	-0,09	0,04	-0,09	-0,06	-0,09	0,03	0,00
Coefficient de clustering	**0,78**	-0,40	-0,41	-0,23	0,10	0,05	-0,02	0,00	0,00
Degré moyen	**-0,86**	0,35	-0,30	-0,02	-0,12	0,08	0,15	0,06	0,00
Coreness moyen	**-0,78**	0,52	-0,21	0,00	0,20	-0,18	-0,06	-0,01	0,00
Degré 2e niveau moyen	**-0,96**	0,17	-0,11	-0,02	-0,08	0,14	-0,07	-0,12	0,00
Excentricité moyenne	**-0,89**	0,03	0,28	-0,35	-0,03	-0,06	0,03	0,00	0,00
Proximité moyenne	**-0,91**	-0,37	-0,09	0,04	-0,09	-0,06	-0,09	0,03	0,00
Intermédiarité moyenne	**-0,82**	-0,53	-0,02	0,08	0,09	-0,08	0,18	-0,06	0,00

Tableau 16: Corrélations entre les variances des métriques et les composantes principales.

Selon le Tableau 16, toutes les métriques sont négativement corrélées à la première composante principale (CP1) sauf le coefficient de clustering qui est positivement corrélé à la CP1. L'axe 1 peut être interprété comme les configurations qui simule des paysages où l'adjacence des haies varie faiblement mais la tendance à former des agrégats varie significativement.
La régression de la CP1 en fonction des descripteurs indique que seul le paramètre contrôlant l'adjacence entre segments (*ce=-5,803e-01 ; ErT=1,622e-02 ; p<2e-16*) a un effet significatif. Ce

résultat est cohérent avec le fait que ce descripteur affecte directement les métriques du réseau des segments.

5.3 ACP sur la représentation en raster du paysage

Dans cette partie, on réalise une ACP pour chaque catégorie (habitat semi-naturel, culture, haie) en analysant les moyennes et variances des métriques selon 50 simulations.

5.3.1 Analyse des moyennes entre répétitions

		CP1	CP2	CP3	CP4	CP5	CP6
Semi-naturel	Contribution	0,52	0,31	0,11	0,04	0,02	0,01
	Variance	**3,12**	**1,85**	0,64	0,25	0,10	0,04
Culture	Contribution	0,69	0,16	0,10	0,04	0,01	0,01
	Variance	**4,14**	0,93	0,58	0,24	0,07	0,04
Haie	Contribution	0,73	0,17	0,08	0,02	0,00	0,00
	Variance	**4,39**	**1,00**	0,46	0,14	0,02	0,00

Tableau 17: Contributions et variances des composantes principales pour chaque catégorie

		CP1	CP2	CP3	CP4	CP5	CP6
Semi-naturel	PLAND	**-0,79**	-0,57	0,08	-0,11	-0,05	0,14
	PD	-0,52	0,54	-0,65	-0,05	-0,09	0,01
	PARA	0,48	**-0,75**	-0,39	-0,21	0,14	-0,02
	ENN	**0,81**	0,42	0,16	-0,36	-0,10	0,03
	CLUMPY	**0,90**	0,33	-0,13	0,18	0,10	0,12
	IJI	**-0,72**	0,63	0,14	-0,16	0,22	0,01
Culture	PLAND	**0,89**	0,22	0,31	0,21	0,17	0,04
	PD	**-0,85**	0,44	-0,21	-0,16	0,10	0,11
	PARA	**0,74**	0,28	-0,57	0,21	-0,05	0,01
	ENN	-0,68	-0,65	-0,25	0,17	0,12	0,01
	CLUMPY	**0,88**	-0,43	0,02	-0,10	-0,06	0,14
	IJI	**-0,91**	0,10	0,24	0,30	-0,12	0,07
Haie	PLAND	**0,92**	0,01	0,29	0,27	-0,04	0,00
	PD	**-1,00**	-0,01	0,00	0,00	-0,07	-0,02
	PARA	**-0,91**	0,00	-0,34	0,25	0,04	0,00
	ENN	**0,87**	0,02	-0,49	-0,01	-0,07	0,01
	CLUMPY	**0,99**	0,01	-0,16	-0,01	0,05	-0,03
	IJI	0,04	**-1,00**	-0,01	0,00	0,00	0,00

Tableau 18: Corrélations entre les métriques moyennées pour chaque catégorie et les composantes principales

Selon le Tableau 17, le pourcentage d'information initiale conservé par les deux premières composantes principales est de 83% pour les habitats semi-naturels, 85% pour les cultures et 90% pour les haies. On obtient une variance supérieure à 1 pour la première composante principale des cultures et pour les deux premières composantes principales des habitats semi-naturels et des haies.

Dans le Tableau 18, pour les habitats semi-naturels, on a la proportion et l'index IJI qui sont négativement corrélés à la CP1 et la distance des voisinages et l'index d'agrégation positivement corrélés à la CP1. Les métriques de l'axe 1 reflètent donc la proportion et l'agrégation de cette catégorie dans le paysage. Les configurations avec une valeur positive sur l'axe 1 renvoient

des paysages avec une proportion faible d'habitats semi-naturels qui ont tendance à être adjacents et à former des agrégats. Ce résultat peut être expliqué par les effets des paramètres de la régression en fonction de l'adjacence entre haies (*ce=3,308e-01 ; ErT=1,033e-02 ; p=0,001*), l'adjacence entre culture et haies (*ce=1,204e-01 ; ErT=1,033e-02 ; p<2e-16*) et l'adjacence entre cultures (*ce=-3,932e-01 ; ErT=1,033e-02 ; p<2e-16*). Si le paramètre d'adjacence entre cultures augmente, on a plus d'agrégats de cultures et donc moins de possibilité pour les habitats semi-naturels d'être agrégés, car l'allocation de l'habitat semi-naturel est conditionné à l'espace qui reste dans le paysage après l'allocation des haies et des cultures. Les interactions des descripteurs d'adjacence entre cultures et haies et d'adjacence entre haies, ont un effet inverse de l'adjacence des cultures. En effet, si les cultures et haies ou les haies entre elles-mêmes ont tendance être agrégés, les habitats semi-naturels seront agrégés aussi. Ceci est dû à la représentation des haies comme séquence de pixels, par conséquent, l'adjacence des haies ne limite pas trop l'espace alloué à l'habitat semi-naturel. Ensuite, on a le rapport périmètre-aire qui est négativement corrélé à la CP2. L'axe 2 indique la complexité géométrique des taches. Ainsi, des valeurs positives sur l'axe 2 désigne des habitats semi-naturels ayant une géométrie plus simple. De la régression, on observe que l'adjacence entre haies (*ce=8,717e-02 ; ErT=7,522e-03 ; p<2e-16*), l'adjacence entre cultures et haies (*ce=3,021e-01 ; ErT=7,522e-03 ; p<2e-16*) et l'adjacence entre cultures (*ce=1,045e-01 ; ErT=7,522e-03 ; p<2e-16*) ont tous un effet positif et significatif. On s'attend que à l'augmentation des interactions des cultures et haies, on ait des formes plus régulières pour les taches d'habitats semi-naturels.

Pour les cultures, on a la proportion, le rapport périmètre-aire et l'indice d'agrégation qui sont positivement corrélés à la CP1, alors que la densité de l'habitat et l'index IJI y sont négativement corrélés. Les métriques liées à cet axe indiquent donc la proportion, l'agrégation et la mixité des cultures dans le paysage. Si une configuration est positive sur l'axe 1, ceci signifie qu'elle simule des paysages avec une grande proportion de cultures qui ont tendance à être agrégées. La variation de l'axe 1 peut être expliquée par une régression en fonction de l'adjacence entre haies (*ce=-6,894e-02 ; ErT=1,154e-02 ; p= 2,97e-09*), l'adjacence entre culture et haies (*ce=-6,146e-02 ; ErT=1,154e-02 ; p=1,18e-07*) et l'adjacence entre cultures (*ce=4,776e-01 ; ErT=1,154e-02 ; p<2e-16*). Comme attendu, l'adjacence des cultures est le plus influant pour CP1, favorisant des structures où le cultures sont agrégées, avec une forme plus régulière et avec une proportion plus élevée. Si on a les haies qui ont tendance à être agrégées entre elles ou si les cultures ont tendance à être entourées de haies, il sera moins possible pour les cultures d'être agrégées entre elles. Le fait que la disposition des haies est un effet significatif sur l'agrégation des cultures est cohérent avec le fait que l'allocation se fait d'abord pour les haies et après pour les cultures.

Pour les haies, on a la proportion, la distance des voisinages et l'indice d'agrégation qui sont positivement corrélés à la CP1. La densité de l'habitat et et le rapport périmètre-aire sont négativement corrélé à cet axe. Les métriques de l'axe 1 résume donc l'agrégation des haies ainsi que la géométrie et le nombre de tache de cette catégorie. Les configurations ayant une valeur positive sur cet axe simulent des paysages où les haies ont tendance à former des agrégats qui sont grands, peu nombreux et d'une complexité géométrique simple. Le seule paramètre contrôlant ce résultat est celui de l'adjacence entre haies (*ce=5,996e-01 ; ErT=7,702e-03 ; p<2e-16*). Ce résultat est cohérent avec le fait que l'allocation des haies est indépendante des autres types d'éléments. Si le paramètre d'adjacence entre les haies augmente, on s'attend effectivement à avoir plus d'agrégats de haies dans le paysage. La complexité géométrique simple est expliquée du fait que les haies sont des éléments linéaires dont la forme est constante. L'index IJI est négativement corrélé à la CP2. L'axe 2 reflète donc la mixité des taches de type haie dans les paysages. Des valeurs positives sur cet axe indiquent une faible mixité des haies. Ce résultat peut être expliqué par les effets des paramètres de la régression en fonction de l'adjacence entre cultures (*ce=-2,157e-01 ; ErT=5,154e-03 ; p<2e-16*) et l'adjacence entre cultures et haies (*ce=-1,342e-01 ; ErT=5,154e-03 ; p<2e-16*). On s'attend à ce que des paysages où les cultures sont peu agrégées entre elles ou des paysages où les cultures faiblement entourées de haies aient des haies qui sont très peu entourées par des taches de catégories différentes.

5.3.2 Analyse des variances entre répétitions

		CP1	CP2	CP3	CP4	CP5	CP6
Semi-naturel	Contribution	0,39	0,28	0,11	0,09	0,07	0,06
	Variance	**2,32**	**1,71**	0,66	0,55	0,43	0,34
Culture	Contribution	0,39	0,28	0,11	0,10	0,08	0,04
	Variance	**2,35**	**1,68**	0,68	0,59	0,48	0,22
Haie	Contribution	0,54	0,17	0,16	0,06	0,05	0,02
	Variance	**3,24**	**1,01**	0,95	0,38	0,29	0,13

Tableau 19: Contributions et variances des composantes principales pour chaque catégorie

		CP1	CP2	CP3	CP4	CP5	CP6
Semi-naturel	PLAND	0,06	**0,85**	-0,26	0,31	-0,26	-0,22
	PD	0,61	0,39	0,65	-0,14	-0,19	0,00
	PARA	**-0,78**	0,20	-0,03	-0,54	-0,11	-0,23
	ENN	**-0,85**	0,15	0,09	0,11	-0,29	0,39
	CLUMPY	0,31	**0,80**	-0,21	-0,25	0,28	0,27
	IJI	**-0,72**	0,36	0,36	0,25	0,39	-0,12
Culture	PLAND	0,21	**-0,74**	0,54	0,33	0,05	-0,08
	PD	**0,76**	-0,30	-0,10	-0,08	-0,57	0,06
	PARA	**-0,86**	-0,31	0,01	0,14	-0,13	0,35
	ENN	**-0,76**	-0,14	0,30	-0,49	-0,20	-0,15
	CLUMPY	0,43	**-0,71**	-0,11	-0,43	0,32	0,14
	IJI	-0,48	-0,66	-0,52	0,16	-0,03	-0,21
Haie	PLAND	-0,10	**0,90**	-0,41	0,03	0,06	0,00
	PD	**-0,88**	0,03	-0,09	-0,06	-0,45	-0,07
	PARA	**0,90**	0,08	0,03	0,26	-0,26	0,21
	ENN	**0,93**	0,07	0,05	0,18	-0,08	-0,29
	CLUMPY	**0,84**	0,11	0,02	-0,53	-0,10	0,02
	IJI	0,24	-0,42	**-0,87**	0,00	0,00	0,00

Tableau 20: Corrélations entre les variances des métriques pour chaque catégorie et les composantes principales

Selon le Tableau 19, le pourcentage d'information initiale conservé par les deux premières composantes principales est de 67% pour les habitats semi-naturels, 67% pour les cultures et 71% pour les haies. Les deux composantes principales ont une variance supérieure à 1 pour toutes les catégories.

Dans le Tableau 20, pour les habitats semi-naturels, le rapport périmètre-aire, la distance des voisinages et l'index IJI sont négativement corrélés à la CP1. Les métriques de l'axe 1 reflètent la variance de la complexité géométrique, de la distance entre voisinages et de la mixité de cette catégorie dans les paysages. Les configurations ayant des valeurs positives sur l'axe 1 correspondent à des configurations qui simulent des paysages où pour cette catégorie, la géométrie des taches, la distance entre les taches et la mixité des taches varient faiblement. Ce résultat peut être expliqué par l'effet des paramètres de la régression en fonction de l'adjacence entre haies (*ce=1,313e-01 ; ErT=1,047e-02 ; p<2e-16*), l'adjacence entre culture et haies (*ce=1,558e-01 ; ErT=1,047e-02 ; p<2e-16*) et l'adjacence entre cultures (*ce=-2,107e-01 ; ErT=1,047e-02 ; p<2e-16*). Si les haies sont adjacentes ou si elles entourent des cultures, on s'attend à avoir des paysages où la géométrie des taches, la distance entre les taches et la mixité des taches varient faiblement. Inversement, on a des paysages avec ces métriques qui varient considérablement si les cultures ont tendance à être adjacentes. On a la proportion et l'agrégation qui sont positivement corrélées à la CP2. L'axe 2 indique des paysages où la proportion et l'agrégation des taches

semi-naturelles varient considérablement. Cette variation peut être expliquée par une régression de cet axe en fonction de l'adjacence entre haies (*ce=8,717e-02 ; ErT=7,522e-03 ; p<2e-16*), l'adjacence entre culture et haies (*ce=3,021e-01 ; ErT=7,522e-03 ; p<2e-16*) et l'adjacence entre cultures (*ce=1,045e-01 ; ErT=7,522e-03 ; p<2e-16*). Si l'adjacence entre cultures, l'adjacence entre haies et l'adjacence entre culture et haies augmente, on a tendance à avoir les paysages où la proportion et l'agrégation des taches semi-naturelles sont significativement différentes.

Pour les cultures, la densité est positivement corrélée à la CP1 alors que le rapport périmètre-aire et la distance des voisinages sont négativement corrélés à cet axe. L'axe 1 correspond à la variance de la densité, de la complexité géométrique et de la distance entre voisins de cette catégorie. Les valeurs positives sur l'axe 1 correspondent à des paysages où le nombre de taches varie considérablement, mais où les taches ont presque la même complexité et les mêmes distances entre voisins. Ce résultat peut être expliqué par une régression de cet axe en fonction des descripteurs de l'adjacence entre haies (*ce=1,592e-01 ; ErT=1,169e-02 ; p<2e-16*), de l'adjacence entre culture et haies (*ce=9,573e-01 ; ErT=1,169e-02 ; p<2e-16*) et de l'adjacence entre cultures (*ce=-1,378e-01 ; ErT=1,169e-02 ; p<2e-16*). Si on augmente l'adjacence entre haies et l'adjacence entre les cultures et les haies, on se retrouve avec des paysages où le nombre de taches de cette catégorie varie faiblement mais où la complexité géométrique et de la distance entre voisins varie considérablement. Inversement, la complexité géométrique et la distance entre voisins varie faiblement alors que le nombre de taches de type culture varie considérablement lorsque l'adjacence entre cultures augmente. Ce résultat est cohérent avec le fait que ce descripteur affecte directement la densité et l'agrégation des cultures. On a que la proportion et l'agrégation sont négativement corrélées à la CP2. Les valeurs positives sur l'axe 2 reflètent les paysages où la proportion et l'agrégation des taches semi-naturelles varient faiblement. Cette variation peut être expliquée par l'adjacence entre haies (*ce=8,717e-02 ; ErT=7,522e-03 ; p<2e-16*), l'adjacence entre culture et haies (*ce=3,021e-01 ; ErT=7,522e-03 ; p<2e-16*) et l'adjacence entre cultures (*ce=1,045e-01 ; ErT=7,522e-03 ; p<2e-16*). Plus on augmente les paramètres d'interactions des éléments du paysage, de moins en moins varie la proportion et l'agrégation des taches la catégorie culture dans les paysages.

Pour les haies, la densité est négativement corrélée à la CP1 alors que le rapport périmètre-aire, la distance des voisinages et l'agrégation sont positivement corrélés à cet axe. Les configurations ayant une valeur positive sur cet axe renvoient des paysages où le nombre de taches de cette catégorie varie peu, mais où la complexité géométrique, la distance entre voisins, et l'agrégation varie considérablement. Ce résultat peut être expliqué par l'adjacence entre haies (*ce=4,351e-01 ; ErT=1,000e-02 ; p<2e-16*), l'adjacence entre culture et haies (*ce=9,573e-01 ; ErT=1,000e-02 ; p=0,047*) et l'adjacence entre cultures (*ce=-1,990e-01 ; ErT=1,000e-02 ; p=0,004*). Si on augmente l'interaction des haies entre elles ou avec des cultures, on se retrouve avec des paysages où le nombre de taches de type haie varie faiblement, mais où la complexité géométrique, la distance entre voisins, et l'agrégation varie considérablement. Inversement, augmenter l'interaction entre les cultures, renvoie à des paysages où le nombre de taches de haies varie plus et la complexité géométrique, la distance entre voisins, et l'agrégation varie moins. On a la proportion qui est positivement corrélée à la CP2. Les valeurs positives de cet axe reflètent des paysages où la proportion de haies varie de manière significative. Ceci peut être expliqué par la régression de l'axe en fonction de l'adjacence entre culture et haies (*ce=6,497e-02 ; ErT=8,289e-03 ; p=9,25e-15*) et l'adjacence entre cultures (*ce=7,763e-02 ; ErT=8,289e-03 ; p<2e-16*). Lorsque l'on augmente l'adjacence entre les cultures et les haies ou l'adjacence entre les cultures, on a des paysages où la proportion de haies varie significativement. Ce résultat semble cohérent, car augmenter ces interactions implique d'augmenter le nombre de taches de cultures. On a aussi que l'indice IJI est négativement corrélé à la CP3. L'axe 3 reflète donc des paysages avec des mixités des haies plus (valeurs positives) ou moins (valeurs négatives) différentes. Ce résultat peut être expliqué par la régression de l'axe en fonction de l'adjacence entre haies (*ce=1,974e-02 ; ErT=6,166e-03 ; p=0,001*), l'adjacence entre culture et haies (*ce=1,519e-01 ; ErT=6,166e-03 ; p<2e-16*) et l'adjacence entre cultures (*ce=1,438e-01 ; ErT=6,166e-03 ; p<2e-16*). Si on augmente l'interaction entre les éléments, on a logiquement que la mixité des taches de type haies qui varie plus.

6 Conclusion

Dans ce travail, l'objectif était de modéliser différentes compositions et configurations des paysages. Le paysage est représenté avec une approche vectorielle qui nous a permis de distinguer des éléments parcellaires et linéaires et de tenir compte des interactions entre eux. Les éléments et leur structure spatiale sont définis avec un réseau multi-couche, où les nœuds représentent des éléments et les liens représentent les interactions entre ces éléments. L'allocation de catégories d'usage de sol est réalisée par un modèle stochastique de type "famille exponentielle". Nous avons considéré une allocation binaire où on tient compte de la présence de cultures dans les parcelles et de haies dans les éléments linéaires. Le modèle considère neuf descripteurs. On a estimé leurs valeurs sur le paysage réel de la Basse Vallée de la Durance et on a testé leur significativité. On a trouvé que dans ce domaine d'étude on a une tendance à ne pas avoir des cultures dans des petites parcelles et à ne pas avoir de haies qui entourent les cultures. En revanche, on trouve que les cultures ont une tendance à former des agrégats. Les haies sont plutôt courtes, avec une orientation est-ouest et une tendance à être regroupées. De plus, les estimateurs ne sont pas biaisés et les paysages simulés capturent les caractéristiques du paysage réel sur des métriques qui ne sont pas considérées dans le modèle d'allocation. Pour les métriques basées sur une représentation en réseau du paysage, on a trouvé qu'il n'y avait pas de différence significative entre les simulations et la réalité. Dans les cas où on trouve qu'il y a une différence significative, les ordres de grandeur sont conservés. Pour les métriques basées sur une représentation en raster du paysage, on a conclu qu'il n'y avait pas de différence significative entre les simulations et la réalité pour la majorité d'entre elles. Sinon, les ordres de grandeurs sont tout de même conservés dans tous les cas. On a observé que les métriques des réseaux réussissent à mieux capturer l'agrégation des éléments du paysage que les métriques basées sur une représentation en raster, et cela particulièrement pour les haies. On a réalisé une analyse de sensibilité du modèle par analyse en composantes principales en faisant varier les paramètres des descripteurs d'adjacence entre cultures, d'adjacence entre haies et d'adjacence entre cultures et haies. Pour chaque configuration on a simulé des répétitions des paysages et nos variables pour l'ACP étaient les moyennes et les variances des métriques. On a trouvé que pour les métriques moyennées, diminuer les paramètres liés à l'adjacence des éléments de même type correspondait à des paysages avec des métriques de centralité plus faible pour les réseaux, et des métriques d'agrégation plus faibles pour la représentation en raster. Ce résultat correspond à des paysages où l'allocation des éléments est plus dispersée. Contrairement aux métriques moyennées, la variance des métriques paysagères n'a pas de tendance spécifique. Les travaux réalisés permettent d'établir la relation entre la disposition spatiale des objets du paysage et comment cette disposition affecte les métriques paysagères. Ceci permettra de contrôler avec aisance l'adjacence des éléments du paysages pour simuler des paysages très divers, et afin d'étudier, par la suite, la dynamique des proie-prédateurs.

Sources

https://www.ibm.com/docs/fr/i2-anb/9.2.1?topic=measures-k-core
https://groupefmr.hypotheses.org/2324
https://www.irit.fr/~Umberto.Grandi/teaching/raisonnement/2reseauxsociaux.pdf
https://www.tandfonline.com/doi/full/10.1016/j.akcej.2015.06.001
https://www.umass.edu/landeco/research/fragstats/documents/Metrics/Contagion%20-%20Interspersion%20Metrics/Metrics/C115%20-%20CLUMPY.htm
https://www150.statcan.gc.ca/n1/pub/12-001-x/2013002/article/11887/section4-fra.htm

Références

Besag, J. (1974). Spatial interaction and the statistical analysis of lattice systems. Journal of the Royal Statistical Society : Series B (Methodological), 36(2) :192–225.

Bianchi, F. J., Booij, C., and Tscharntke, T. (2006). Sustainable pest regulation in agricultural landscapes : a review on landscape composition, biodiversity and natural pest control. Proceedings of the Royal Society B : Biological Sciences, 273(1595) :1715–1727.

Cushman, S. A., McGarigal, K., and Neel, M. C. (2008). Parsimony in landscape metrics : strength, universality, and consistency. Ecological indicators, 8(5) :691–703.

Fienberg, S. E. (2010). Introduction to papers on the modeling and analysis of network data. The Annals of Applied Statistics, pages 1–4.

Langhammer, M., Thober, J., Lange, M., Frank, K., and Grimm, V. (2019). Agricultural landscape generators for simulation models : A review of existing solutions and an outline of future directions. Ecological Modelling, 393 :135–151.

Latora, V. and Marchiori, M. (2001). Efficient behavior of small-world networks. Physical review letters, 87(19) :198701.

Lü, L., Chen, D., Ren, X.-L., Zhang, Q.-M., Zhang, Y.-C., and Zhou, T. (2016). Vital nodes identification in complex networks. Physics Reports, 650 :1–63.

McGarigal, K. (1995). FRAGSTATS : spatial pattern analysis program for quantifying landscape structure, volume 351. US Department of Agriculture, Forest Service, Pacific Northwest Research Station.

Poggi, S., Vinatier, F., Hannachi, M., Sanz Sanz, E., Rudi, G., Zamberletti, P., et al. (2021). How can models foster the transition towards future agricultural landscapes. The Future of Agricultural Landscapes, Part II, page 305.

Urban, D. L., Minor, E. S., Treml, E. A., and Schick, R. S. (2009). Graph models of habitat mosaics. Ecology letters, 12(3) :260–273.

Zamberletti, P., Papaïx, J., Gabriel, E., and Opitz, T. (2021). Landscape allocation : stochastic generators and statistical inference. Annals of Applied Statistics (in press ; arXiv preprint arXiv :2003.02155).